

Bio-based polyesters from cyclic monomers derived from carbohydrates

Ph.D. Thesis presented by Cristina Lavilla Aguilar

Directed by Prof. Sebastián Muñoz Guerra

Barcelona, September 2013

*Tesi presentada per obtenir el títol de Doctor per la Universitat Politècnica de Catalunya
Doctorat en Polímers i Biopolímers*



Departament d'Enginyeria Química

Escola Tècnica Superior d'Enginyeria Industrial de Barcelona

Universitat Politècnica de Catalunya

Abstract

Polyesters are extremely versatile polymers which can be used in a wide variety of applications ranging from high performance materials to recyclable and degradable polymers. The preparation of polyesters from renewable feedstock is currently receiving increasing attention in both industrial and academic research. This Thesis is specifically addressed to the development of aliphatic and aromatic polyesters with enhanced properties made from carbohydrate-based cyclic acetalized monomers, *i.e.* a bicyclic acetalized aldaric acid derived from D-galactose, bicyclic acetalized alditols derived from D-galactose and D-mannose, and a cyclic acetalized alditol derived from L-tartaric acid.

The novel aliphatic polyesters derived from bicyclic acetalized galactaric acid and D-mannitol, which are biodegradable materials, are distinguished by presenting an enhanced rigidity compared to the aliphatic polyesters commonly used so far, which invariably influences their whole thermal and mechanical behavior.

Bicyclic acetalized carbohydrate-based compounds are also used as comonomers in the preparation of random poly(alkylene terephthalate) copolyesters by melt polycondensation (MP). Since linear α,ω -alkanediols with varying length are employed, and the copolymerizations with bicyclic monomers are carried out for a wide range of compositions, a detailed structure-properties study is described. The effect of the presence of the carbohydrate-based comonomer on thermal and mechanical properties of the polyester is largely dependant on which unit, the diol or the diacid, is replaced. The incorporation of acetalized alditols increases the thermal stability, the glass-transition temperature and the mechanical modulus. On the contrary, these parameters are diminished when the terephthalate units are replaced by bicyclic acetalized galactaric acid. Also the hydrolytic and enzymatic degradability depends on the units introduced into the polyester backbone.

The incorporation of cyclic acetalized carbohydrate-based alditols into the amorphous phase of poly(butylene terephthalate) by the solid-state modification (SSM) technique is reported, which leads to increases in glass-transition temperature. The resulting SSM-prepared copolyesters have a unique block-like chemical microstructure that endows them with superior thermal properties when compared to their random counterparts obtained by MP.

Given the structural proximity between isosorbide and bicyclic acetalized alditols, as well as their common potential use as polycondensation monomers, a comparative evaluation of their suitability for the synthesis of aromatic polyesters is carried out in this Thesis. The greater facility of bicyclic acetalized alditols compared to isosorbide to react under the conditions employed is highlighted. Also the influence of the symmetry and stiffness of the bicyclic structure on the thermal behavior of the copolyesters is discussed.

Key words: polyester, carbohydrates, bio-based, cyclic acetalized monomers, D-galactose, D-mannose, L-tartaric acid, random copolyesters, block-like copolyesters

Resumen

Los poliésteres son polímeros extremadamente versátiles que se usan en una amplia variedad de aplicaciones, desde materiales de altas prestaciones a polímeros reciclables o degradables. La preparación de poliésteres a partir de fuentes renovables genera cada vez más interés, tanto en la industria como en el mundo académico. En esta Tesis se emplean fuentes naturales para desarrollar nuevos poliésteres alifáticos y aromáticos con propiedades mejoradas, a partir de monómeros cíclicos derivados de carbohidratos, *i.e.* un ácido aldárico acetalizado bicíclico derivado de D-galactosa, alditoles acetalizados bicíclicos derivados de D-galactosa y D-manosa, y un alditol acetalizado cíclico derivado de ácido L-tartárico.

Los nuevos poliésteres alifáticos derivados de ácido galactárico y D-mannitol acetalizado bicíclico, que son materiales biodegradables, destacan por presentar una rigidez mejorada respecto a los poliésteres alifáticos comúnmente usados hasta ahora, hecho que influencia invariablemente sus propiedades térmicas y mecánicas.

También se reporta el uso de monómeros bicíclicos acetalizados derivados de carbohidratos para la preparación de copoliésteres poli(alquilen tereftalato)s con microestructura al azar, mediante policondensación en fundido (MP). Se emplean α,ω -alcanodiolos lineales con diferentes longitudes, y las copolimerizaciones con monómeros bicíclicos se llevan a cabo en un amplio rango de composiciones, lo que permite desarrollar un estudio estructura-propiedades detallado. El efecto de la unidad renovable en las propiedades térmicas y mecánicas del poliéster depende de qué unidad no renovable, diol o diácido, reemplaza. La incorporación de alditoles acetalizados aumenta la estabilidad térmica, la temperatura de transición vítrea y el módulo elástico. Por contra, estos parámetros disminuyen cuando las unidades tereftálicas se reemplazan por ácido galactárico acetalizado bicíclico. Las unidades renovables introducidas afectan también a la degradabilidad hidrolítica y enzimática de los poliésteres.

Mediante la técnica de modificación en estado sólido (SSM), se incorporan alditoles cíclicos acetalizados a la fase amorfa del poli(butilen tereftalato), lo cual conlleva a un aumento de su temperatura de transición vítrea. Los copoliésteres resultantes presentan una microestructura en bloques, que los dota de propiedades térmicas superiores respecto a los copoliésteres análogos con microestructura al azar preparados mediante MP.

En esta Tesis también se comparan las características y propiedades del monómero isosorbide y los alditos acetalizados bicíclicos para la síntesis de poliésteres aromáticos, debido a su proximidad estructural, así como a su uso potencial como monómeros en policondensaciones. Se destaca la mayor facilidad de reacción en las condiciones empleadas de los alditos acetalizados bicíclicos comparados con isosorbide. También se estudia la influencia de la simetría y rigidez de la estructura bicíclica en las propiedades térmicas de los copoliésteres.

Palabras clave: poliéster, carbohidratos, fuentes naturales, monómeros cíclicos acetalizados, D-galactosa, D-manosa, ácido L-tartárico, copoliésteres al azar, copoliésteres en bloque

Resum

Els polièsters són polímers extremadament versàtils que s'usen en una àmplia varietat d'aplicacions, des de materials d'altres prestacions a polímers reciclables o degradables. La preparació de polièsters a partir de fonts renovables genera cada vegada més interès, tant a la indústria com al món acadèmic. En aquesta Tesi s'utilitzen fonts naturals per desenvolupar nous polièsters alifàtics i aromàtics amb propietats millorades, a partir de monòmers cíclics derivats de carbohidrats, *i.e.* un àcid aldàric acetalitzat bicíclic derivat de D-galactosa, alditols acetalitzats bicíclics derivats de D-galactosa i D-manosa, i un alditol acetalitzat cíclic derivat d'àcid L-tartàric.

Els nous polièsters alifàtics derivats d'àcid galactàric i D-mannitol acetalitzat bicíclic, que són materials biodegradables, destaquen per presentar una rigidesa millorada respecte als polièsters alifàtics comunament usats fins al dia d'avui, fet que influencia invariablement les seves propietats tèrmiques i mecàniques.

També es reporta l'ús de monòmers bicíclics acetalitzats derivats de carbohidrats per a la preparació de copolièsters poli(alquilen tereftalat)s amb microestructura a l'atzar, mitjançant policondensació en estat fos (MP). S'utilitzen α,ω -alcanodiols lineals de diferents longituds, i les polimeritzacions amb monòmers bicíclics es duen a terme en un ampli rang de composicions, fets que permeten desenvolupar un estudi estructura-propietats detallat. L'efecte de la unitat renovable en les propietats tèrmiques i mecàniques del polièster depèn de quina unitat no renovable, diol o diàcid, substitueix. La incorporació d'alditols acetalitzats augmenta l'estabilitat tèrmica, la temperatura de transició vítria i el mòdul elàstic. D'altra banda, aquests paràmetres disminueixen quan les unitats tereftàliques es substitueixen per àcid galactàric acetalitzat bicíclic. Les unitats renovables introduïdes afecten també la degradabilitat hidrolítica i enzimàtica dels polièsters.

Mitjançant la tècnica de modificació en estat sòlid (SSM), s'incorporen alditols cíclics acetalitzats a la fase amorfa del poli(butilen tereftalat), fet que augmenta la seva temperatura de transició vítria. Els copolièsters resultants presenten una microestructura en blocs, que els proporciona unes propietats tèrmiques superiors respecte als copolièsters anàlegs amb microestructura a l'atzar preparats mitjançant MP.

En aquesta Tesi també es comparen les característiques i propietats del monòmer isosorbide i els alditols acetalitzats bicíclics per a la síntesi de polièsters

aromàtics, degut a la seva proximitat estructural, així com el seu ús potencial com a monòmers en policondensacions. Es destaca la major facilitat de reacció en les condicions estudiades dels alditols acetalitzats, i també s'avalua la influència de la simetria i la rigidesa de l'estructura bicíclica en les propietats tèrmiques dels copolièsters.

Paraules clau: polièster, carbohidrats, fonts naturals, monòmers cíclics acetalitzats, D-galactosa, D-manosa, àcid L-tartàric, copolièsters a l'atzar, copolièsters en bloc

Table of Contents

Chapter 1. Aim and outline of this Thesis	1
Chapter 2. Polyesters: Traditional products and present bio-based tendencies	13
2.1. Introduction	14
2.2. Types and applications of thermoplastic polyesters	16
2.2.1. Aliphatic polyesters	16
2.2.2. Aromatic polyesters	18
2.2.3. Aliphatic-aromatic copolyesters	20
2.2.4. Fully aromatic polyesters	21
2.2.5. Thermoplastic elastomers	22
2.3. Synthetic methods	23
2.3.1. Melt polymerization	23
2.3.2. Solid-state polymerization	25
2.3.3. Solution polymerization from diacyl dichlorides	27
2.3.4. Ring-opening polymerization	27
2.3.5. Enzymatic polymerization	28
2.4. Bio-based polyesters	29
2.4.1. Polyesters partially or totally produced by bacteria	29
2.4.1.1. Polylactic acid (PLA)	29
2.4.1.2. Polyhydroxyalkanoates (PHAs)	30
2.4.2. Alternative routes from renewable sources to conventional monomers	31
2.4.3. Polyesters from carbohydrate-derived monomers with modified properties	33
2.4.3.1. Unprotected alditols and aldaric acids	33
2.4.3.2. Acyclic O-protected alditols and aldaric acids	34
2.4.3.3. 2,5-Furandicarboxylic acid (FDCA)	36
2.4.3.4. Dianhydrohexitols and derivatives	38
2.4.3.5. Cyclic acetalized alditols, aldonic and aldaric acids	47
2.5. References	49

Chapter 3. Aliphatic polyesters from cyclic acetalized carbohydrate-based monomers	59
3.1. Aim and scope of this Chapter	61
3.2. Carbohydrate-based polyesters made from bicyclic acetalized galactaric acid	63
3.2.1. Introduction	64
3.2.2. Experimental section	66
3.2.2.1. Materials	66
3.2.2.2. General methods	66
3.2.2.3. Polymer synthesis	67
3.2.2.4. Hydrolytic and enzymatic degradation procedures	70
3.2.3. Results and discussion	71
3.2.3.1. Synthesis and characterization	71
3.2.3.2. Thermal and mechanical properties	75
3.2.3.3. Hydrolytic degradation and biodegradation	81
3.2.4. Conclusions	86
3.2.5. References	86
3.3. Carbohydrate-based copolyesters made from bicyclic acetalized galactaric acid	89
3.3.1. Introduction	90
3.3.2. Experimental section	92
3.3.2.1. Materials	92
3.3.2.2. General methods	92
3.3.2.3. Polymer synthesis	93
3.3.3. Results and discussion	94
3.3.3.1. Synthesis and chemical structure	94
3.3.3.2. Thermal properties	99
3.3.3.3. Crystal structure	108
3.3.3.4. Stress-strain behavior	110
3.3.4. Conclusions	111
3.3.5. References	112
3.4. High T_g bio-based aliphatic copolyesters from bicyclic D-mannitol	115
3.4.1. Introduction	116
3.4.2. Experimental section	118
3.4.2.1. Materials	118

3.4.2.2. General methods	119
3.4.2.3. Polymer synthesis	120
3.4.2.4. Biodegradation and hydrolytic degradation	122
3.4.3. Results and discussion	122
3.4.3.1. Synthesis and chemical structure	122
3.4.3.2. Thermal and mechanical properties	126
3.4.3.3. Biodegradation and hydrolytic degradation	136
3.4.3.4. Main features of PManxS polyester	141
3.4.4. Conclusions	142
3.4.5. References	142
Chapter 4. Poly(alkylene terephthalate) copolyesters from cyclic acetalized carbohydrate-based monomers	145
4.1. Aim and scope of this Chapter	147
4.2. Biodegradable aromatic copolyesters made from bicyclic acetalized galactaric acid	149
4.2.1. Introduction	150
4.2.2. Experimental section	152
4.2.2.1. Materials	152
4.2.2.2. General methods	152
4.2.2.3. Polymer synthesis	153
4.2.2.4. Hydrolytic and enzymatic degradation procedures	155
4.2.3. Results and discussion	155
4.2.3.1. Synthesis and chemical structure	155
4.2.3.2. Thermal properties	158
4.2.3.3. Crystal structure and stress-strain behavior	164
4.2.3.4. Hydrolytic degradation and biodegradation	167
4.2.4. Conclusions	173
4.2.5. References	173
4.3. PET copolyesters from a D-mannitol-derived bicyclic diol	175
4.3.1. Introduction	176
4.3.2. Experimental section	177
4.3.2.1. Materials	177
4.3.2.2. General methods	178
4.3.2.3. Polymer synthesis	178
4.3.2.4. Hydrolytic and enzymatic degradation procedures	180

4.3.3. Results and discussion	181
4.3.3.1. Synthesis and chemical structure	181
4.3.3.2. Thermal and mechanical properties	185
4.3.3.3. Degradability	188
4.3.4. Conclusions	190
4.3.5. References	190

Chapter 5. Poly(butylene terephthalate) copolyesters from cyclic acetalized carbohydrate-based monomers	193
5.1. Aim and scope of this Chapter	195
5.2. Bio-based poly(butylene terephthalate) copolyesters containing bicyclic diacetalized galactitol and galactaric acid: Influence of composition on properties	197
5.2.1. Introduction	198
5.2.2. Experimental section	200
5.2.2.1. Materials	200
5.2.2.2. General methods	200
5.2.2.3. Polymer synthesis	201
5.2.3. Results and discussion	205
5.2.3.1. Synthesis and chemical structure	205
5.2.3.2. Thermal properties	211
5.2.3.3. Isothermal crystallization	216
5.2.3.4. Crystal structure and stress-strain behavior	221
5.2.4. Conclusions	224
5.2.5. References	224
5.3. Biodegradation and hydrolytic degradation of poly(butylene terephthalate) copolyesters containing cyclic sugar units	227
5.3.1. Introduction	228
5.3.2. Experimental section	229
5.3.2.1. Materials	229
5.3.2.2. General methods	230
5.3.2.3. Hydrolytic and enzymatic degradation procedures	230
5.3.3. Results and discussion	231
5.3.3.1. PBT copolyesters containing galactitol units	232
5.3.3.2. PBT copolyesters containing galactarate units	237
5.3.3.3. Stability of the diacetal structure	241
5.3.4. Conclusions	242

5.3.5. References	243
5.4. Bio-based aromatic polyesters from a bicyclic diol derived from D-mannitol	245
5.4.1. Introduction	246
5.4.2. Experimental section	247
5.4.2.1. Materials	247
5.4.2.2. General methods	248
5.4.2.3. Monomer synthesis	249
5.4.2.4. Polymer synthesis	250
5.4.3. Results and discussion	252
5.4.3.1. Monomer synthesis and conformation	252
5.4.3.2. Polymer synthesis and chemical structure	255
5.4.3.3. Thermal properties	258
5.4.3.4. Isothermal crystallization	262
5.4.3.5. Crystal structure and stress-strain behavior	265
5.4.4. Conclusions	267
5.4.5. References	268

Chapter 6. SSM-prepared poly(butylene terephthalate) copolyesters from cyclic acetalized carbohydrate-based monomers **271**

6.1. Aim and scope of this Chapter	273
6.2. Solid-state modification of PBT with cyclic acetalized galactitol and D-mannitol: Influence of composition and chemical microstructure on thermal properties	275
6.2.1. Introduction	276
6.2.2. Experimental section	278
6.2.2.1. Materials	278
6.2.2.2. General methods	278
6.2.2.3. Solution preparation of physical mixtures	279
6.2.2.4. Solid-state modification (SSM) of PBT	280
6.2.3. Results and discussion	282
6.2.3.1. Polymer synthesis	282
6.2.3.2. Chemical microstructure	286
6.2.3.3. Thermal properties	289
6.2.4. Conclusions	296
6.2.5. References	297
6.3. Carbohydrate-based PBT copolyesters from a cyclic diol derived from naturally occurring tartaric acid: A comparative study regarding melt polycondensation and	

solid-state modification	301
6.3.1. Introduction	302
6.3.2. Experimental section	304
6.3.2.1. Materials	304
6.3.2.2. General methods	304
6.3.2.3. Polymer synthesis	305
6.3.2.4. Hydrolytic degradation procedures	307
6.3.3. Results and discussion	308
6.3.3.1. Polymer synthesis	308
6.3.3.2. Chemical microstructure	312
6.3.3.3. Thermal properties	314
6.3.3.4. Isothermal crystallization	319
6.3.3.5. Hydrolytic degradation	321
6.3.4. Conclusions	323
6.3.5. References	324
Chapter 7. Cyclic acetalized alditols compared to isosorbide as comonomers for terephthalate copolyesters	327
7.1. Aim and scope of this Chapter	329
7.2. Sugar-based aromatic copolyesters: A comparative study regarding isosorbide and diacetalized alditols as sustainable comonomers	331
7.2.1. Introduction	332
7.2.2. Experimental section	335
7.2.3. Results and discussion	336
7.2.3.1. Synthesis: Molecular weight and composition	336
7.2.3.2. Thermal properties	341
7.2.4. Conclusions	345
7.2.5. References	345
General conclusions	349
Annex A	353
Annex B	355
Annex C	360
Annex D	374
Annex E	382
Annex F	390

Annex G	394
Annex H	398
Annex I	404
Acknowledgements	412
The Author	414
List of publications	415

Glossary

a	Mark-Houwink parameter
Ad	Dimethyl adipate
Ar	2,3,4-Tri-O-methyl-L-arabinitol
ArH	Aromatic proton
Ar-OMe	2,3,4-Tri-O-methyl-L-arabinitol
asym st	Asymmetric stretching vibration
ATR	Attenuated total reflectance
B	1,4-Butylene units
BISHET	Bis-(2-hydroxyethyl) terephthalate
bs	Broad singlet
COSY	2D ^1H - ^1H Homonuclear NMR spectra
d	Doublet
DBTO	Dibutyl tin oxide
dd	Doublet of doublets
DFT	Density functional theory
d_{hkl}	Bragg spacings
DMF	<i>N,N</i> -Dimethyl formamide
DMSO	Dimethyl sulfoxide
DMT	Dimethyl terephthalate
DSC	Differential scanning calorimetry
\bar{D}	Polydispersity
δ	Chemical shift (ppm)
ΔH_c	Crystallization enthalpy
ΔH_{cc}	Cold crystallization enthalpy
ΔH_m	Melting enthalpy
ΔH_m^0	Melting enthalpy of a 100% crystalline polymer
ΔT	'Undercooling' values required for crystallization ($\Delta T = T_m - T_c$)
E	Elastic modulus
E	1,2-Ethylene units
ϵ	Elongation at break
Endo	Secondary hydroxyl groups (1,4:3,6-dianhydrohexitols) or methylol groups (bicyclic acetalized alditols) oriented inside the bicyclic structure
EG	Ethylene glycol
EtOH	Ethanol
Et₂O	Diethyl ether
Exo	Secondary hydroxyl groups (1,4:3,6-dianhydrohexitols) or methylol groups (bicyclic acetalized alditols) oriented outside the bicyclic structure
F	Furfural
FA	Furfuryl alcohol
FDCA	2,5-Furandicarboxylic acid
FTIR	Fourier transform infrared spectroscopy

Galx	Acetalized bicyclic non-fused 2,3:4,5-di- <i>O</i> -methylene structure with <i>D-galacto</i> configuration
GPC	Gel permeation chromatography
HETCOR	2D ^{13}C - ^1H Heteronuclear shift correlation NMR spectra
HFIP	1,1,1,3,3,3-Hexafluoroisopropanol
HMF	Hydroxymethylfuraldehyde
HMW	High molecular weight
HPLC	High performance liquid chromatography
$[\eta]$	Intrinsic viscosity
ICI	Imperial Chemical Industries
IIDCA	1-Carbon extended isoidide derivative with dicarboxylic functionality (chain extension at C2 and C5 of the isohexide skeleton), namely isoidide dicarboxylic acid
IIDML	1-Carbon extended isoidide derivative with two primary hydroxyl groups (chain extension at C2 and C5 of the isohexide skeleton), namely isoidide hydroxymethylene diol
IR	Infrared spectroscopy
Is	Isosorbide; 1,4:3,6-dianhydro- <i>D</i> -glucitol
Isoidide	1,4:3,6-Dianhydro- <i>L</i> -iditol
Isomannide	1,4:3,6-Dianhydro- <i>D</i> -mannitol
Isosorbide	1,4:3,6-Dianhydro- <i>D</i> -glucitol
<i>J</i>	Coupling constant
<i>k</i>	Avrami kinetic constant
<i>K</i>	Mark-Houwink constant
LA	Lactic acid
LC	Liquid crystalline
LDH	Lactate deshydrogenase
Lit.	Literature
LMW	Low molecular weight
LNP	Liquid nitrogen pump
<i>m</i>	In NMR spectra, multiplet peak; in WAXD measurements, medium intensity
MAF	Mobile amorphous fraction
Manx	Acetalized bicyclic fused 2,4:3,5-di- <i>O</i> -methylene structure with <i>D-manno</i> configuration
M_n	Number-average molecular weight
M_p	Peak molecular weight
m.p.	Melting point
MP	Melt polycondensation
$^{\text{MP}}\text{PB}_x\text{Th}_y\text{T}$	Random copolyesters poly(butylene terephthalate-co- 2,3-di- <i>O</i> -methylene- <i>L</i> -threitol terephthalate)s, prepared by melt polycondensation
M_v	Viscosimetric molecular weight
M_w	Weight-average molecular weight
<i>N</i>	Relative molar amount of the dyads as obtained from ^{13}C NMR

<i>n</i>	In isothermal crystallization studies, Avrami exponent; in chemical microstructure analysis by ¹³ C NMR, number average sequence lengths
NaTFA-HFIP	0.05 M sodium trifluoroacetate-hexafluoroisopropanol
n.d.	Not determined
NMP	<i>N</i> -Methyl-2-pyrrolidone
NMR	Nuclear magnetic resonance
NOE	Nuclear Overhauser effect
NOESY	Nuclear Overhauser effect spectroscopy
PBF	Poly(butylene 2,5-furandicarboxylate)
PBGalx	Poly(butylene 2,3:4,5-di- <i>O</i> -methylene-galactarate)
PBS	Poly(butylene succinate)
PBT	Poly(butylene terephthalate)
PBT_xGalx_y	Random copolyesters poly(butylene terephthalate-co- butylene 2,3:4,5-di- <i>O</i> -methylene-galactarate)s, prepared by melt polycondensation
PB_xGalx_yT	Random copolyesters poly(butylene terephthalate-co- 2,3:4,5-di- <i>O</i> -methylene-galactitol terephthalate)s, prepared by melt polycondensation
PB_xIs_yT	Random copolyesters poly(butylene terephthalate-co- isosorbide terephthalate)s, prepared by melt polycondensation
PB_xManx_yS	Random copolyesters poly(butylene succinate-co-2,4:3,5-di- <i>O</i> -methylene- <i>D</i> -mannitol succinate)s, prepared by melt polycondensation
PB_xManx_yT	Random copolyesters poly(butylene terephthalate-co- 2,4:3,5-di- <i>O</i> -methylene- <i>D</i> -mannitol terephthalate)s, prepared by melt polycondensation
PCL	Poly(ϵ -caprolactone)
PDGalx	Poly(dodecamethylene 2,3:4,5-di- <i>O</i> -methylene-galactarate)
PDT	Poly(dodecamethylene terephthalate)
PDT_xGalx_y	Random copolyesters poly(dodecamethylene terephthalate-co-dodecamethylene 2,3:4,5-di- <i>O</i> -methylene-galactarate)s, prepared by melt polycondensation
PEF	Poly(ethylene 2,5-furandicarboxylate)
PEI	Poly(ethylene isophthalate)
PE-<i>n</i>Ad	Poly(alkylene adipate)s, the <i>n</i> being the number of methylenes
PE-<i>n</i>Ad_xGalx_y	Random copolyesters poly(alkylene adipate-co- alkylene 2,3:4,5-di- <i>O</i> -methylene-galactarate)s, the <i>n</i> being the number of methylenes, prepared by melt polycondensation
PE-<i>n</i>Galx	Poly(alkylene 2,3:4,5-di- <i>O</i> -methylene-galactarate)s, the <i>n</i> being the number of methylenes
PET	Poly(ethylene terephthalate)
PE_xManx_yT	Random copolyesters poly(ethylene terephthalate-co- 2,4:3,5-di- <i>O</i> -methylene- <i>D</i> -mannitol terephthalate)s, prepared by melt polycondensation
PGA	Poly(glycolic acid)
PGalxT	Poly(2,3:4,5-di- <i>O</i> -methylene-galactitol terephthalate)

PHAs	Polyhydroxyalkanoates
PHB	Poly(3-hydroxybutyrate)
PHF	Poly(hexamethylene 2,5-furandicarboxylate)
PHGalx	Poly(hexamethylene 2,3:4,5-di-O-methylene-galactarate)
PHH	Poly(3-hydroxyhexanoate)
PHT	Poly(hexamethylene terephthalate)
PHT_xGal_y	Random copolyesters poly(hexamethylene terephthalate-co-hexamethylene 2,3:4,5-di-O-methylene-galactarate)s, prepared by melt polycondensation
PHV	Poly(3-hydroxyvalerate)
PIsT	Poly(isosorbide terephthalate)
PLA	Poly(lactic acid)
PLLA	Isotactic poly(L-lactic acid)
PManxS	Poly(2,4:3,5-di-O-methylene-D-mannitol succinate)
PManxT	Poly(2,4:3,5-di-O-methylene-D-mannitol terephthalate)
PMMA	Poly(methyl methacrylate)
POF	Poly(octamethylene 2,5-furandicarboxylate)
Poly(HB-co-HH)	Copolyester poly(3-hydroxybutyrate-co- 3-hydroxyhexanoate)
Poly(HB-co-HV)	Copolyester poly(3-hydroxybutyrate-co- 3-hydroxyvalerate)
POM	Polarizing optical microscopy
PPF	Poly(propylene 2,5-furandicarboxylate)
PTA	Purified terephthalic acid
PThxT	Poly(2,3-di-O-methylene-L-threitol terephthalate)
PTT	Poly(trimethylene terephthalate)
py	Pyridine
θ	Contact angle in degrees (°)
R	Randomness index of copolyesters statistically calculated on the basis of the ¹³ C NMR analysis
RAF	Rigid amorphous fraction
R_c	Randomness index of the amorphous fraction of copolyesters
rock	Rocking vibration
ROP	Ring-opening polymerization
s	In NMR spectra, singlet peak; in WAXD measurements, strong intensity
S	Sugar-based units
σ	Tensile strength
SA	Succinic acid
SEC	Size-exclusion chromatography
SEM	Scanning electron microscopy
SSM	Solid-state modification
^{SSM}PB_xGal_yT	Block-like copolyesters poly(butylene terephthalate-co- 2,3:4,5-di-O-methylene-galactitol terephthalate)s, prepared by solid-state modification of PBT

^{SSM}PB_xMan_yT	Block-like copolyesters poly(butylene terephthalate-co- 2,4:3,5-di-O-methylene-D-mannitol terephthalate)s, prepared by solid-state modification of PBT
^{SSM}PB_xThx_yT	Block-like copolyesters poly(butylene terephthalate-co- 2,3-di-O-methylene-L-threitol terephthalate)s, prepared by solid-state modification of PBT
SSP	Solid-state polycondensation
st	Stretching vibration
Sym st	Symmetric stretching vibration
t	Triplet peak
T	Terephthalate units
t₀	Onset crystallization time
t_{1/2}	Half-crystallization time
°T_{5%}	In TGA, temperature at which 5% weight loss was observed
TBT	Titanium (IV) tetrabutoxide
T_c	Crystallization temperature
T_{cc}	Cold crystallization temperature
T_d or ^{max}T_d	In TGA, temperature for maximum degradation rate
TFA	Trifluoroacetic acid
TFA-<i>d</i>	Deuterated trifluoroacetic acid
T_g	Glass-transition temperature
TGA	Thermogravimetry
THF	Tetrahydrofuran
Th-OMe	2,3-Di-O-methyl-L-threitol
Thx	Acetalized cyclic 2,3-di-O-methylene structure with L-tartaric acid configuration
T_m	Melting temperature
TMS	Tetramethylsilane
TPEs	Thermoplastic elastomers
t_{SSM}	SSM reaction time
U	One unit (U) was defined as that amount of enzyme which catalyzed the release of fatty acid from triglycerides at the rate of 1 μmol·min ⁻¹ .
ν	Wavenumber (cm ⁻¹)
w	In WAXD measurements, weak intensity
W	In TGA, remaining weight at 600 °C
WAXD	Wide angle X-ray diffraction
X	Molar composition determined by ¹ H NMR
X_c	Crystallinity index
Xy	2,3,4-Tri-O-methylxylitol
Xy-OBn	2,3,4-Tri-O-benzylxylitol
XRD	X-Ray diffraction

CHAPTER 1

AIM AND OUTLINE OF THIS THESIS

Introduction

The development of bio-based polymers is nowadays attracting a great deal of interest, due to the high price and future depletion of fossil fuel stocks, together with concerns regarding environmental sustainability. However, this approach is not new; bio-based polymers have a history of more than a century, much longer than petrochemical polymers. In the 19th century, natural raw materials such as casein, shellac, gum, natural rubber, and cellulose were chemically modified to convert them into useful polymers with new properties. An important objective was to convert the infusible and frequently insoluble natural stocks into materials capable of being processed. The first horn-like plastic material was galalith, produced by reacting casein from milk with formaldehyde to form a stiff thermoset resin resembling stone. Although the biodegradable and water-soluble galalith was not moldable, sheets could be produced, thus enabling dyeing and machining. The latex of Brazilian rubber trees was collected, coagulated, dried, and vulcanized with sulfur to produce industrial rubber for making tires. When the highly flammable and explosive nitrocellulose, obtained by nitration of cellulose and used as smokeless gunpowder, was plasticized with camphor, it was rendered thermoplastic. Bio-based nitrocellulose, marketed as Parkesine and Celluloid, was rather hazardous owing to its explosive character. Nevertheless, moldable nitrocellulose became a successful substitute for ivory and was used for making billiard balls, thus saving the lives of thousands of elephants. Photographic films were possible at those times thanks to the use of nitrocellulose as supporting film for the silver nitrate emulsion, although they represented a severe fire and safety hazard for cinemas.

Since then, numerous new compounds derived from renewable resources have been developed. One example is ethylene which was synthesized by the dehydration of bio-based ethanol in the 1940s. Also in that time the protein casein was used for paints and glues and later on, in formulation with formaldehyde, as plastic used for products like buttons, knives and letter openers. Soy protein was reacted with formaldehyde and co-condensed with phenol and urea; these soy plastics were used to produce several

automotive parts such as steering wheels, glove-box doors and interior trim. Shellac was produced by extraction of the natural polymer excreted by the shell louse, and was used for paints and varnish next to small solid articles. Also regenerated cellulose, e.g. in the form of cellophane film or man-made cellulose fibers, was developed in those times and has been used in a wide range of applications, such as apparel, food (e.g. for sausages) and non-plastics (e.g. varnishes). However, many of the inventions in the 1930s and 1940s stayed in laboratory and were never used for commercial production. The main reason was the large-scale industrial use of petrochemical feedstock to manufacture a great variety of synthetic polymers since 1950s. Exploitation of oil and gas as fossil raw materials for the chemical industry and polymer production greatly improved cost-effectiveness and simplified manufacturing of macromolecular materials. The attractive combination of low cost with facile processing represented the key feature of petrochemical polymers. Also some bio-based products, such as man-made cellulose fibers, continued being produced but their production did not grow at the rate of the newly emerging petrochemical products. On the other hand, starch derivatives used as paper and textile auxiliaries had a long period of growth and are still used nowadays.

The oil price shocks of the 1970s led to renewed interest into the possibilities offered by non-petrochemical feedstock. However, some time after the interest in petrochemical polymers continued growing. Driven by concerns about rapidly increasing amounts of waste, in the 1990s new recycling technologies enabled effective reuse of polymer products that had completed their first lifecycle.

Bio-based polymers have experienced a renaissance in the last few decades. Many new polymers from bio-based feedstock have been developed, e.g. polylactic acid (PLA) from carbohydrates. Today, public concerns about environment, climate change and limited fossil fuel resources have become more important drivers. The utilization of fossil fuels in the manufacture of plastics accounts today for about 7% of worldwide oil and gas. It is anticipated that this resource will be depleted in the coming decades; furthermore, the price of oil has increased rapidly in recent years, and it is subject to unpredictable socio-political influences. While the use of fossil reserves for transportation and heating is certainly the most serious concern, the chemical industry will also be faced with the problematic issue associated to the use of an essentially non-renewable feedstock for the majority of their products. Polymers based on renewable resources are very attractive, not only for coming from natural feedstock, but also for the benefits they provide from waste treatment point of view. In fact, many of the products derived from

renewable resources can be degraded in the presence of microorganisms, therefore being able to battle against the problem of increasing amounts of waste and limited landfill capacity. In addition, polymers derived from natural sources not only provide important environmental benefits, but in some cases are also biocompatible materials, property essential for its application in biomedicine.

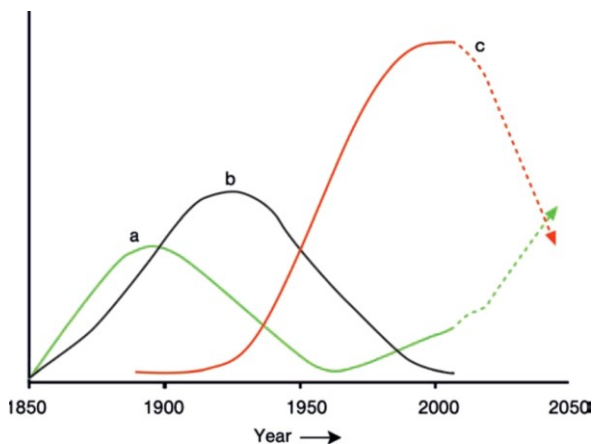


Figure 1.1. Raw materials used by the chemical industry in hystorical perspective. Renewable feedstock (a); coal (b); oil and gas (c). Source: Lichtenthaler, F.W. *Carbohydrates as Organic Raw Materials*. Ullmann's Encyclopedia of Industrial Chemistry, 2010.

Carbohydrates are the most abundant natural organic compounds in plants, originated as product of photosynthesis, an endothermic reaction reducing carbon dioxide which requires the energy of the light and the pigment chlorophyll. Carbohydrates are an important source of metabolic energy, both for humans and animals. Nature produces annually about $140 \cdot 10^9$ tons of carbohydrates from carbon dioxide and water, making these compounds the most abundant organic material on earth. Humanity only uses 4% of this huge amount for food and non-food purposes. They can be looked therefore as an extraordinary source of chemicals capable of providing a wide diversity of building blocks for polycondensation polymers. Thus, the development of carbohydrate-based polymers has the potential to reduce the amount of petroleum consumed in the chemical industry and also to open new high-value-added markets to agriculture. However, there are only a few examples of carbohydrate-derived plastics commercially available, which is mostly due to the still high cost of these materials compared to petroleum-based counterparts. Another severe limitation in the use of carbohydrates as a source for monomers for the synthesis of linear polycondensates is their inherent multifunctionality; certain previous

treatments are usually required to avoid the formation of highly cross-linked polymers. The most commonly used strategy is blocking the exceeding functional chemical groups with stable protecting groups, and thus retaining only two reactive functional groups to carry out linear polycondensation. Protection of the exceeding hydroxyl groups as methoxy ethers has led to obtaining hydrophilic linear polyesters, which in some cases were also biodegradable. However, given the flexibility of the acyclic molecular structure of these carbohydrate-based monomers, the resulting polyesters have a glass-transition temperature, mechanical strength and stiffness generally restricted. Isosorbide, along with their two less accessible 1,4:3,6-dianhydrohexitol stereoisomers isomannide and isoidide, are currently drawing a great interest in the polymer science field as bio-based monomers able to provide enhanced stiffness into the polymer chain they are incorporated. These three isohexides are composed of two fused tetrahydrofuran rings, with two secondary hydroxyl groups remaining free for reaction. Because of their fused bicyclic structure, 1,4:3,6-dianhydrohexitols are able to increase the glass-transition temperature of common aliphatic and aromatic polyesters. Nevertheless, the main shortcoming of isosorbide and its isomers is the limited reactivity of their secondary hydroxyl groups; in fact, this feature seriously hampers the polycondensation reaction in the melt, so polyesters from 1,4:3,6-dianhydrohexitols obtained by this method display rather limited molecular weights.

Aim and scope of this Thesis

In this Thesis, the potential use of cyclic carbohydrate-based monomers to prepare polyesters is highlighted. Polyesters are extremely versatile polymers which can be used in a wide variety of applications ranging from high performance materials to recyclable and degradable polymers. The preparation of polyesters from renewable feedstock is currently receiving increasing attention in the industry and academia. For instance, bio-based succinic acid for aliphatic polyester preparation is industrially produced nowadays by anaerobic fermentation using various types of microorganisms and natural substrates. Also the bicyclic diol monomer isosorbide, which is prepared by dehydration of D-glucose coming from cereal starch, is already available at industrial scale today.

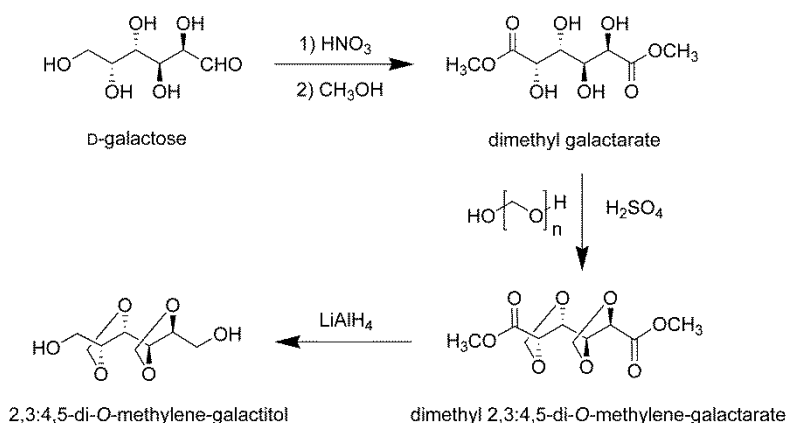
This Thesis is specifically addressed to the development of aliphatic and aromatic polyesters with enhanced properties made from carbohydrate-based cyclic

acetalized monomers. The main advantage of cyclic acetalized diols compared to 1,4:3,6-dihydrohexitols is that in the former case, the two hydroxyl groups free for reaction are primary and thus display enhanced reactivity compared to those of 1,4:3,6-dihydrohexitols. The aim of the Thesis is to prepare, characterize and evaluate the basic properties of linear aliphatic and aromatic polyesters made from cyclic acetalized monomers derived from carbohydrates, namely a bicyclic acetalized aldarcic acid derived from D-galactose, bicyclic acetalized alditols derived from D-galactose and D-mannose, and a cyclic acetalized alditol derived from L-tartaric acid.

An aldaric acid is an aldose derivative which has both the primary hydroxyl and the carbonyl groups oxidized to carboxylic groups. Aldaric acids are useful to obtain linear polyesters by reaction with diols provided that all the secondary hydroxyl groups are duly protected. In this work, the secondary hydroxyl groups are protected as methylene acetals, leading to carbohydrate-based diacids with a cyclic structure.

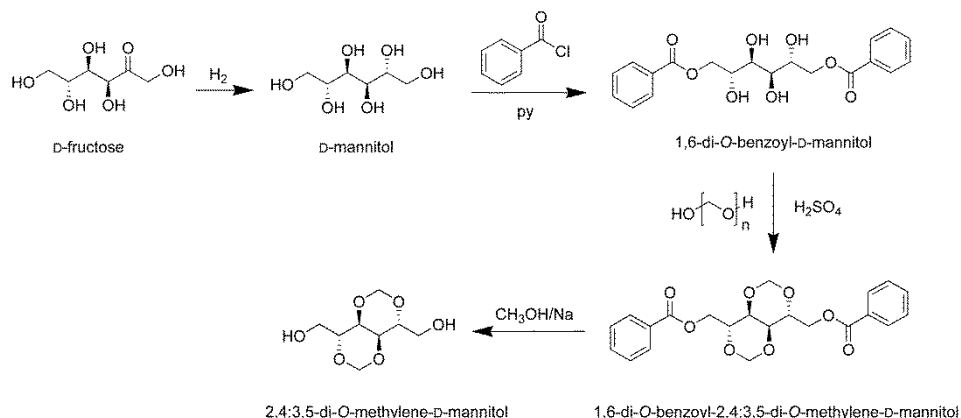
An alditol is an aldose derivative which has the carbonyl group reduced to hydroxyl group. The protection of the secondary hydroxyl groups, leaving the two primary hydroxyl groups free for reaction, makes alditols usable as monomers for the production of linear polyesters by reaction with dicarboxylic acids. In this work, the secondary hydroxyl groups are protected as methylene acetals, leading to carbohydrate-based diols with a cyclic structure.

The synthetic procedures followed for the preparation of the four carbohydrate-based monomers used in this Thesis are depicted in Schemes 1.1, 1.2 and 1.3, summarized below and further detailed in Annex A.



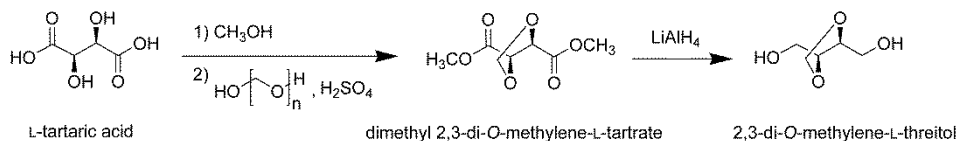
Scheme 1.1. Synthesis of dimethyl 2,3:4,5-di-O-methylene-galactarate and 2,3:4,5-di-O-methylene-galactitol from D-galactose.

The bicyclic monomers dimethyl 2,3:4,5-di-*O*-methylene-galactarate and 2,3:4,5-di-*O*-methylene galactitol were synthesized from commercially available mucic acid (galactaric acid), which in turn is produced from naturally occurring *D*-galactose or *D*-galactose containing compounds by oxidation with nitric acid. Mucic acid was first esterified to obtain the dimethyl ester derivative, which was subsequently acetalized with paraformaldehyde to obtain the bicyclic compound dimethyl 2,3:4,5-di-*O*-methylene-galactarate. Subsequent reduction led to the preparation of the bicyclic diol 2,3:4,5-di-*O*-methylene galactitol. Both *galacto* derivatives dimethyl 2,3:4,5-di-*O*-methylene-galactarate and 2,3:4,5-di-*O*-methylene-galactitol are composed of two non-fused 1,3-dioxolane rings, bearing two carboxylate or two primary hydroxyl groups, respectively, free for reaction. These two compounds are centrosymmetric, thus the two reactive groups display the same reactivity since they are spatially undistinguishable.



Scheme 1.2. Synthesis of 2,4:3,5-di-*O*-methylene-*D*-mannitol from *D*-fructose.

The bicyclic diol 2,4:3,5-di-*O*-methylene-*D*-mannitol was synthesized from commercially available *D*-mannitol, which in turn is produced from naturally occurring *D*-fructose by hydrogenation. The primary hydroxyl groups of *D*-mannitol were first protected to form the benzoxy derivative; thus 2,4:3,5-di-*O*-methylene-*D*-mannitol was obtained by acetalization of 1,6-di-*O*-benzoyl-*D*-mannitol with paraformaldehyde, followed by hydrolysis of the benzoxy groups. 2,4:3,5-di-*O*-methylene-*D*-mannitol consists of two fused 1,3-dioxane rings and possesses a twofold axis of symmetry, hence its two primary hydroxyl groups display the same reactivity.



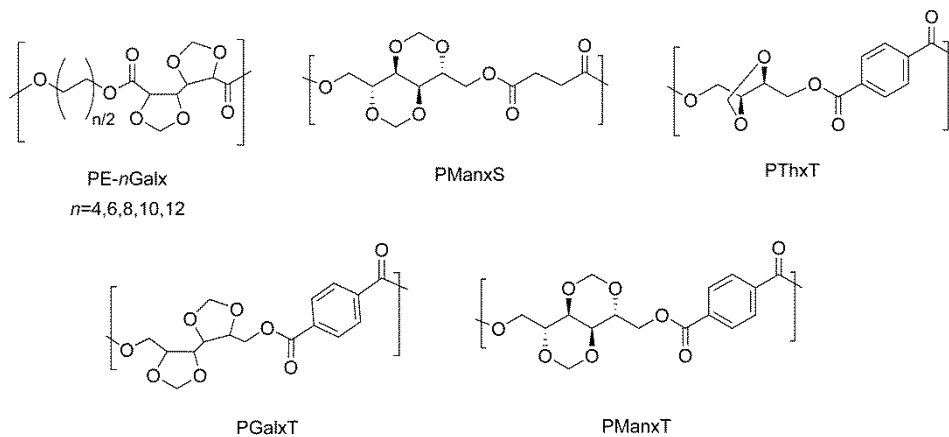
Scheme 1.3. Synthesis of 2,3-di-O-methylene-L-threitol from L-tartaric acid.

The cyclic diol 2,3-di-O-methylene-L-threitol was synthesized from commercially available tartaric acid, a dihydroxy dicarboxylic acid occurring in many plants and fermented grape juice. This cyclic diol was produced by a synthetic route which involved esterification, acetal formation and reduction of the carboxylate groups to hydroxyl groups. This monomer also possesses a twofold axis of symmetry, thus its two primary hydroxyl groups display the same reactivity.

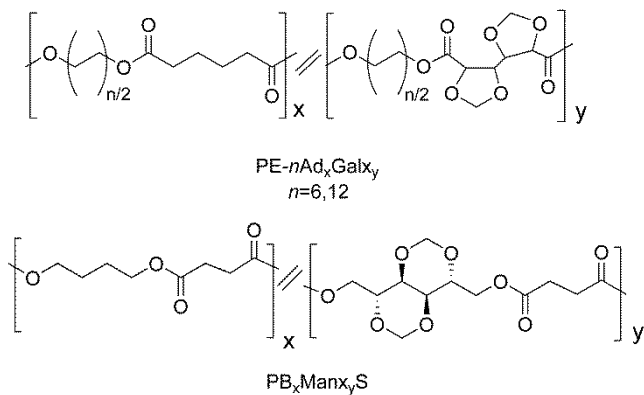
In this Thesis, cyclic carbohydrate-based dimethyl esters have been polymerized with a wide variety of diols, such as 1,4-butanediol, 1,6-hexanediol, 1,8-octanediol, 1,10-decanediol and 1,12-dodecanediol, and also copolymerized with the dimethyl esters of adipic acid and terephthalic acid. Cyclic carbohydrate-based diols have been polymerized with the dimethyl esters of succinic acid and terephthalic acid, and copolymerized with ethylene glycol and 1,4-butanediol. Some of these monomers can also be potentially derived from biomass, as described in Chapter 2.

The polymerizations of the four carbohydrate-based cyclic acetalized monomers with the selected carboxylic or diol compounds have rendered a collection of aliphatic and aromatic homopolyesters and copolyesters covering a good diversity of structures and properties. Two techniques have been used, *viz.* melt polymerization (MP) and solid-state modification (SSM). Copolyesters with a random chemical microstructure have been obtained by melt polymerization, whereas the latter technique has allowed preparing block-like copolyesters.

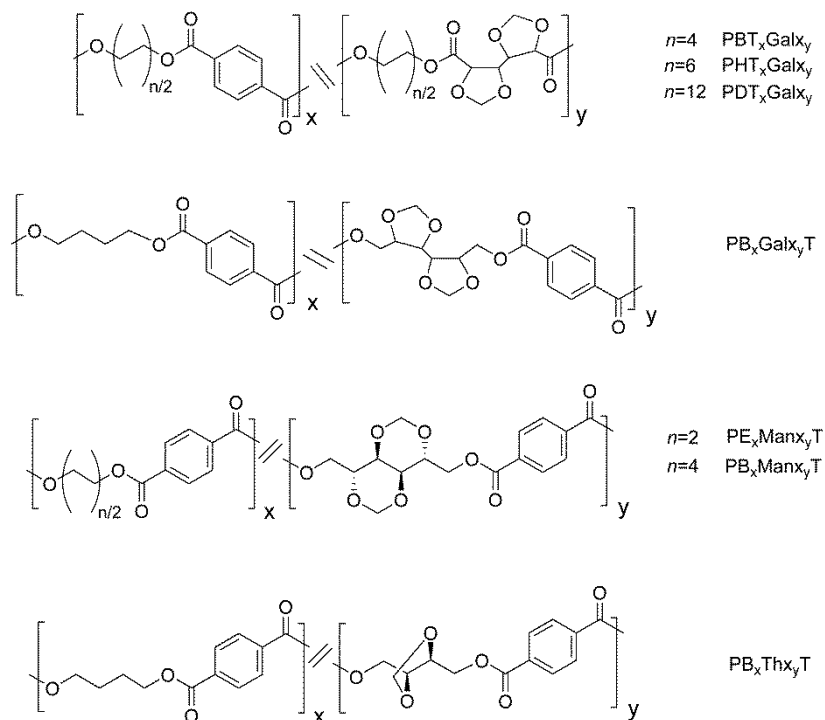
The chemical structures of the polyesters studied in this Thesis are depicted in Schemes 1.4, 1.5, 1.6 and 1.7.



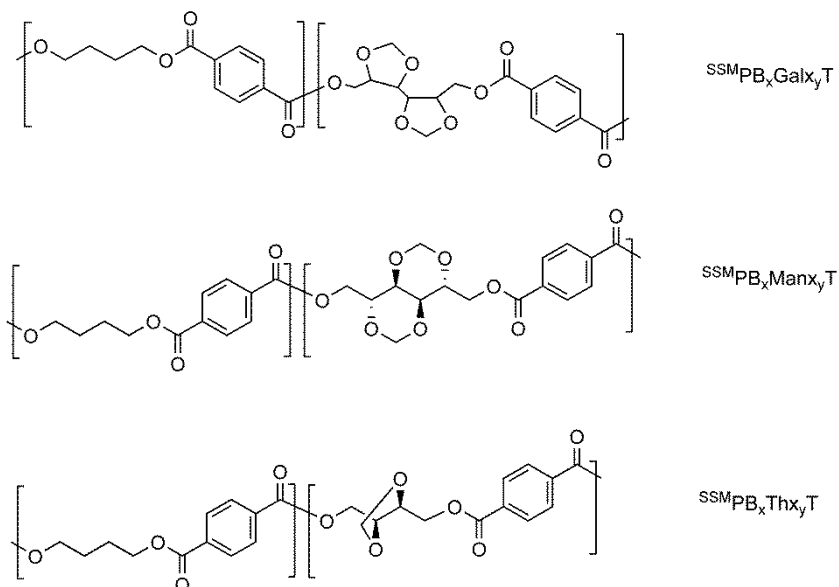
Scheme 1.4. Homopolyesters studied in this Thesis which were prepared by melt polymerization.



Scheme 1.5. Random aliphatic copolyesters studied in this Thesis which were prepared by melt polymerization.



Scheme 1.6. Random aromatic copolyesters studied in this Thesis which were prepared by melt polymerization.



Scheme 1.7. Block-like copolyesters studied in this Thesis which were prepared by solid-state modification.

Structure of the Thesis

This Thesis consists of seven Chapters followed by a summary of the conclusions drawn from the whole work.

Chapter 1 is a general introduction of the Thesis which includes its aims and organization.

Chapter 2 is a review of some aspects of polyesters, such as their main synthetic methods, types and applications, with emphasis on the present bio-based tendencies regarding polyester preparation. Polyesters partially or totally produced by bacteria, and alternative routes from renewable sources to obtain conventional monomers are described. The latter approach entails no differences in terms of material properties between bio-based polyesters and their petrochemical counterparts, since they share the same chemical structure. Furthermore, the use so far of carbohydrate-based monomers to produce polyesters with modified properties is reviewed. This includes acyclic monomers as well as cyclic monomers such as 2,5-furandicarboxylic acid and 1,4:3,6-dianhydrohexitols.

Chapter 3 describes the synthesis and characterization of aliphatic polyesters from bicyclic acetalized monomers derived from D-galactose and D-mannose. These novel polyesters, which are biodegradable materials, are distinguished by presenting an enhanced rigidity compared to the aliphatic polyesters commonly used so far, which invariably influences their whole thermal and mechanical behavior.

In **Chapter 4**, bicyclic acetalized carbohydrate-based compounds are used as comonomers in the preparation of poly(alkylene terephthalate) copolyesters. Since linear α,ω -alkanediols with varying length (with 2, 6 or 12 carbon atoms) are employed, and the copolymerizations with bicyclic monomers are carried out for the whole range of compositions, a detailed structure-properties study is described in this Chapter. These copolyesters are found to be more hydrolytically and enzymatically degradable than the parent PET, PHT and PDT homopolyesters.

In **Chapter 5**, the focus is on several series of poly(butylene terephthalate) copolyesters obtained by replacing either the diol or the diacid with bicyclic acetalized carbohydrate-based diols or diacids. The effect of the presence of the carbohydrate-based comonomer on thermal and mechanical properties is opposite according to which

unit, the diol or the diacid, is replaced. The incorporation of acetalized diols increases the thermal stability, the glass-transition temperature and the mechanical moduli. On the contrary, these parameters are diminished when the terephthalate units are the replaced ones. Also the hydrolytic and enzymatic degradability depends on which is the carbohydrate-based monomer used in the melt copolymerization.

Chapter 6 describes the incorporation of cyclic acetalized carbohydrate-based diols into the amorphous phase of poly(butylene terephthalate) by the solid-state modification (SSM) technique. Glass-transition temperatures increase upon incorporation of the rigid bio-based diols. The resulting copolyesters have a unique block-like chemical microstructure that endows them with superior thermal properties when compared to their random counterparts obtained by melt copolymerization. The materials prepared by SSM display higher melting points, crystallization temperatures and crystallinity, due to the presence of long PBT sequences in the copolyester.

Chapter 7 presents a comparative study regarding the use of isosorbide and two bicyclic acetalized diols for the preparation of terephthalate copolyesters. Given the structural proximity between isosorbide and diacetalized alditols, as well as their common potential use as polycondensation monomers, it is encouraging to make a comparative evaluation of their suitability for the synthesis of polyesters. The greater facility of diacetalized alditols compared to isosorbide to react under the conditions employed is highlighted. Also the influence of the symmetry and stiffness of the bicyclic structure on the thermal behavior of the copolyesters is discussed.

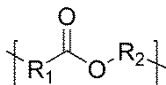
CHAPTER 2

POLYESTERS: TRADITIONAL PRODUCTS AND PRESENT BIO-BASED TENDENCIES

Summary: Polyester is the general name given to a family of polymers which contain the ester group in their constitutional repeating unit. Since the pioneering experiments of Carothers in the 1930s, polyesters have found extensive use in a wide range of applications, including engineering plastics, high performance materials, and recyclable and degradable polymers, due to the enormous variety of structures and properties which constitute the polyester family. This introductory chapter reviews some aspects of polyesters, such as their main types and applications as well as their synthetic methods. It also describes the present bio-based tendencies regarding polyester preparation. Alternative routes from natural feedstock to produce monomers which are conventionally obtained from petrochemical sources are described; this approach entails no differences in terms of material properties between bio-based polyesters and their petrochemical counterparts since they share the same chemical structure. Finally, the use so far of carbohydrate-derived monomers to produce polyesters with modified properties is reviewed; this includes acyclic monomers as well as cyclic monomers such as 2,5-furandicarboxylic acid and 1,4:3,6-dianhydrohexitols.

2.1. Introduction

Polyesters are polymers in which the main chain is composed of aliphatic or aromatic moieties R_1 and R_2 linked together by ester groups (Scheme 2.1).



Scheme 2.1. General formula of polyesters.

The polyester family is extremely large and, depending on the nature of R_1 and R_2 , exhibits an enormous variety of structures, properties and therefore, applications. It has been known since the early 19th century that heating carboxylic polyacids with glycerol resulted in resinous compounds. In the 1910-1920s, the General Electric Company led extensive research on the chemistry of phthalic anhydride-glycerol reaction and developed the technology of alkyd resins (glyptal resins), which are essentially polyesters of phthalic anhydride, glycerol, and monocarboxylic unsaturated fatty acids. These resins are still used in coatings, varnishes and paints. However, the modern history of polyesters began when Carothers performed experimental studies on reactions between aliphatic diacids and diols and established the relationships between degree of polymerization, conversion, functionality and gel point, that is, the base relationships of step-growth polymerization (Carothers, 1929, 1931 and 1936; Carothers and Arvin, 1929; Carothers and Dorough, 1930; Carothers *et al.*, 1932). However, these polyesters had low melting point and were sensitive to hydrolysis, and therefore they could not compete with aliphatic polyamides (nylons), also discovered in the 1930s by Carothers at the DuPont Company.

To increase the polyester melting point and to approach the thermomechanical properties obtained by nylons, it was necessary to stiffen the polyester chain by using rigid aromatic monomers instead of flexible aliphatic ones. In the early 1940s, high melting point fiber-forming polyesters from terephthalic acid and aliphatic diols were synthesized by Whinfield in the laboratories of the Calico Printers Association in the United Kingdom. After World War II the patent rights on these aromatic polyesters were shared between Imperial Chemical Industries (ICI) and DuPont, and several members of this family became, and are still today, major commercial polymers (Whinfield and Dickson, 1946). Poly(ethylene terephthalate) (PET) is now one of the most produced

polymers, primarily for textile and packaging applications. Poly(butylene terephthalate) (PBT) finds uses as solid-state molding resin. Poly(trimethylene terephthalate) (PTT), although was described in Whinfield's original patent, is a newcomer in the commercial polyester family and has found its first applications in the textile industry.

A new type of thermosetting resin, based on unsaturated polyesters, was developed at the end of the 1930s (Ellis, 1937). Unsaturated polyesters were synthesized by reacting mixtures of saturated and unsaturated diacids or anhydrides with aliphatic diols. The thermosetting resin was obtained by dissolving these polyesters in an unsaturated monomer, such as styrene, capable of undergoing free-radical copolymerization with the unsaturations in polyester chains. The liquid resin was transformed into a rigid and insoluble cross-linked polymer network after radical polymerization in the presence of heat or catalysts. Unsaturated polyester resins found their first applications in combination with glass fibers for protective radar domes during World War II, and are now one of the most important matrix resins for glass-fiber-reinforced composite materials (Fradet and Tessier, 2003).

In the late 1950s and the 1960s, low-molecular weight ($M_n = 1,000-3,000 \text{ g}\cdot\text{mol}^{-1}$) hydroxyl-ended aliphatic polyesters were used as macromonomers in the synthesis of polyurethane elastomers and flexible foams by reaction with diisocyanates. Although aliphatic polyesters were the first step-growth polymers fully characterized, they did not find commercial applications until then. In the 1970s, polyesterether block copolymers were commercialized by Dupont under the tradename Hytrel; these copolymers exhibited the characteristics of thermoplastic elastomers (Holden *et al.*, 1996). During this period attention was also focused on high-performance fully aromatic polyesters; the commercial introduction of the first one, the amorphous poly(bisphenol-A isophthalate-terephthalate) (Union Carbide's Ardel), took place in the mid 1970s (Dean *et al.*, 1989). Despite their high cost, liquid crystalline thermotropic polyesters, such as poly(6-hydroxy-2-naphthoic acid-co-4-hydroxybenzoic acid) (Ticona's Vectra), described at the end of the 1970s (Calundann, 1977), found and still have a number of applications in high-technology markets.

In the 1990s, environmental concerns began to be gaining ground (Lichtenthaler, 2010). The versatility of the ester linkage, able to undergo hydrolysis in some conditions, makes polyesters the polymers of choice to fulfill the increasing demand for recyclable and biodegradable polymers (Albertsson and Varma, 2003). This has resulted in a renewed interest in aliphatic polyesters, such as poly(lactones), poly(lactides) or

copolyesters containing aliphatic moieties. PET production is also strongly driven by the demand of recyclable polymers.

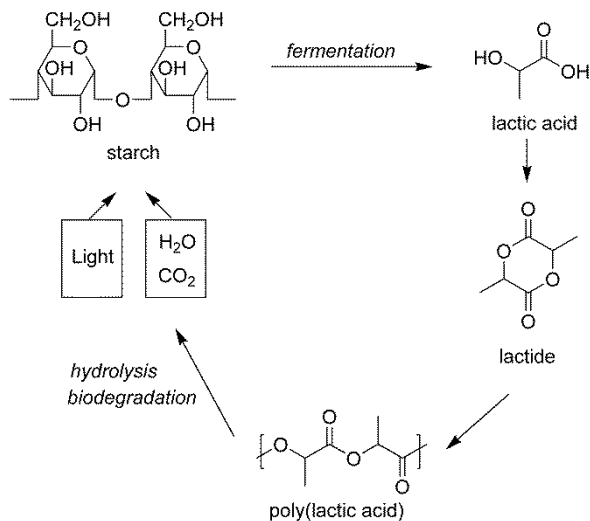
2.2. Types and applications of thermoplastic polyesters

Polyesters are one of the most versatile classes of polymers ever produced, covering a wide range of properties and applications. As described above, polyester polyols are used in the synthesis of polyurethane elastomers and flexible foams by reaction with diisocyanates; they are also used for other applications such as coatings, paints, sealants and adhesives. Unsaturated polyesters have found extensive use to yield thermosetting polyester resins with a wide range of properties, and can be also reinforced with glass fibers or filled with large amounts of low-cost fillers. Furthermore, thermoplastic polyesters are used as fibers, engineering thermoplastics and high-performance polymers. The main properties and applications of thermoplastic polyesters which have a closer relation with this Thesis are discussed below.

2.2.1. Aliphatic polyesters

The ester linkage can be easily cleaved by hydrolysis under alkaline, acid, or enzymatic catalysis. This feature makes aliphatic polyesters very attractive for those applications which require degradation of the polymers, *i.e.* biomedical devices and environmentally degradable polyesters.

Poly(lactic acid) (PLA) is an aliphatic polyester whose monomer is produced from carbohydrates and is degraded by microorganisms to generate ultimately CO₂ and H₂O. This polymer can be therefore considered fully environmentally-friendly and it is an excellent representative of what is today so-called a *green polymer* (Scheme 2.2). PLA has found use in medical applications and it is receiving interest as a material suitable for replacing conventional commodity plastics in a wide diversity of applications (Tokiwa and Jarerat, 2004).

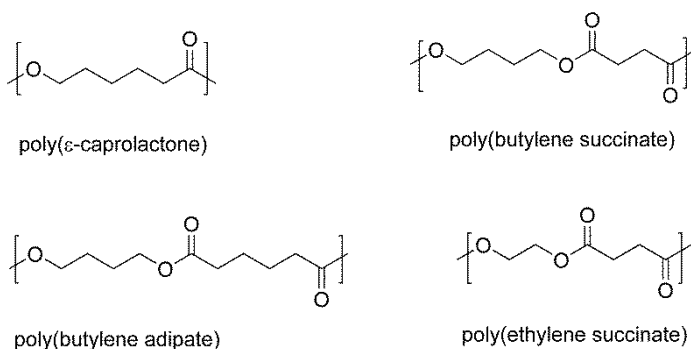


Scheme 2.2. Cycle of poly(lactic acid).

Bioresorbable implants, for instance orthopedic fixations or sutures, are devices designed to slowly degrade in the body after implantation, so that a second surgical intervention is not required for implant removal after healing. Polyesters and copolyesters of lactic acid and glycolic acid have been used as bioresorbable sutures since the 1960s. These polyesters give no toxic or inflammatory response, can be sterilized, and are slowly and completely hydrolyzed into natural metabolic by-products that are eliminated by the body. Other aliphatic polyesters such as poly(ϵ -caprolactone), poly(dioxanone) and poly(trimethylene carbonate) have also been used for this application (Middleton and Tipton, 2000). Bioresorbable polymers can be processed by conventional methods such as injection-molding, compression-molding and extrusion, and sterilization is achieved by irradiation or by exposure to ethylene oxide. They are used in wound closure (sutures, staples), osteosynthetic materials (pins, screws, rods, bone plates), cardiovascular surgery (stents, grafts), and intestinal surgery (anastomosis rings) (Ikada and Tsuji, 2000). They also find application as matrix materials for implanted drug release devices or drug-containing microspheres or microcapsules (Arshady, 1991).

The use of environmentally biodegradable harmless polymers, which disappear after a few weeks or months in soil, is an elegant way of dealing with solid waste disposal problem. Poly(ϵ -caprolactone) has been proposed as a soil-degraded container material, with applications for growing and transplanting trees as a thin-walled tree seedling container (Raghavan, 1995). In addition, its blends with starch and derivatives have been

used in shopping bags (Darwis *et al.*, 1998). During the last few years, a number of companies have put biodegradable polymers on the market; almost all these polymers are polyesters or copolyesters. For instance, copolyesters of poly(butylene succinate), poly(butylene adipate) and poly(ethylene succinate) have been commercialized under the trade mark of Bionolle. The potential applications of aliphatic polyesters in injection-molded articles (cutlery, brushes), tubular films (composting bags, shopping bags), flexible packaging, food tray, cosmetic bottles and beverage bottles have been proposed, although for some of these applications the performance of the existing grades should be improved. The chemical structures of some commonly used aliphatic polyesters are depicted in Scheme 2.3.

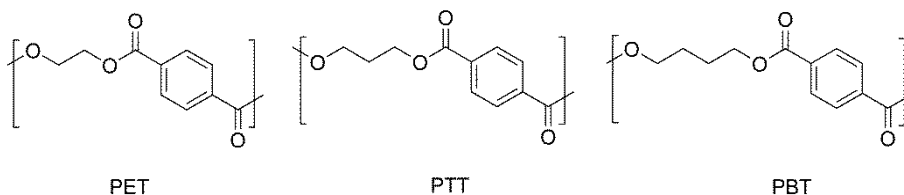


Scheme 2.3. Chemical structure of some common aliphatic polyesters.

2.2.2. Aromatic polyesters

In terms of volume and economic importance, thermoplastic polyesters are dominated by poly(ethylene terephthalate) (PET); this polyester accounts for 8% of the global polymer production (Rappaport, 2010). The chemical structure of PET, together with other aromatic polyesters, is depicted in Scheme 2.4. PET has experienced an enormous development in fibers and molding resins, and has found extensive use in food packaging and bottle markets for glass replacement, where its capability of being recycled is a supplementary force driving PET consumption. Fibers are the largest end use for PET; the world production of PET fibers surpassed that of nylon fibers in the beginning of the 1970s and has reached a level close to that of cotton (Altun and Ulcay, 2004). The growth of PET fibers production has been caused by its low production costs and their ability to be blended with natural fibers such as cotton. PET resins, which

constitute the second largest application of PET, are mainly used for the packaging field, in reheat stretch blow-molded bottles for carbonated and non-carbonated soft drinks and water, and in food and cosmetics containers. PET resins are also used in sheet thermoforming applications, and as glass-fiber reinforced resin for injection-molding applications. Due to a slow crystallization rate in the unoriented state but rapid crystallization upon orientation, PET is very suitable for the biaxial film orientation process. In this process the amorphous film obtained after extrusion and quenching is successively drawn in two orthogonal directions, leading to stress-induced crystallization with biaxial orientation of polymer chains in the film plane. The resulting transparent film has approximately 50% crystallinity and exhibits excellent thermal, mechanical and electrical properties (Fradet and Tessier, 2003). PET film is the base film for some photographic films and magnetic tapes; it is also used as dielectric film in capacitors.



Scheme 2.4. Chemical structure of some common aromatic polyesters.

Poly(butylene terephthalate) (PBT) is mainly used as glass-fiber reinforced engineering thermoplastic, although PBT fibers can also be made. PBT crystallizes much more rapidly than PET and does not require nucleating agents for extrusion and injection molding applications; PBT crystallizes rapidly in mold at room temperature. Moreover, due to a lower melting point than PET, it can be molded at comparatively lower temperature (Gallucci and Patel, 2004). This permits fast processing and rapid production cycles. However, larger volumes and lower prices make PET a serious PBT competitor for resin applications.

Poly(trimethylene terephthalate) (PTT) was already mentioned in Whinfield's original patent that described PET and PBT (Whinfield and Dickson, 1946). However, no economically viable route to 1,3-propanediol monomer was available until the 1990s when Shell developed a route based on ethylene oxide hydroformylation (Drent, 1992) and Degussa a route based on acrolein hydration/hydrogenation (Breitkopf, 1991). PTT fibers present a combination of properties, including resilience, softness of touch and

dyeability which makes them very attractive for the fabric, carpet and apparel markets. PTT is intended to compete for film and engineering thermoplastic applications with PET, PBT and polyamides.

2.2.3. Aliphatic-aromatic copolyesters

Aliphatic polyesters can be degraded under relatively mild conditions, and are biodegradable products. However, their thermal and mechanical properties are often limited and exclude these materials from many applications. On the contrary, aromatic polyesters are distinguished by displaying an excellent pattern of physical properties; nevertheless, they are strongly resistant to hydrolysis as well as to bacterial and fungal attack, and usually remain unaltered in the environment. Trying to combine both the excellent material properties of aromatic polyesters and the potential biodegradability of the aliphatic ones, a large number of aliphatic-aromatic copolyesters have been developed during the last decades, and some products have been recently commercialized on a scale of a few thousand tons per year (Müller, 2005).

A variety of random copolyesters made from a mixture of terephthalic acid and several aliphatic diacids with different diols have been prepared by melt polycondensation (Witt *et al.*, 1994, 1996 and 1997; Atfani and Brisse, 1999; Nagata *et al.*, 2000; Ki and Park, 2001). In the range between 40 and 50 mol% of terephthalic acid (referred to the acid components), random copolyesters combine sufficient biodegradability with adequate technical properties (Müller, 2005).

Furthermore, reactive blending of homopolymers is another method to produce aliphatic-aromatic copolyesters with intermediate properties. Aromatic homopolyesters such as PET and PBT have been reacted by this technique with aliphatic homopolyesters like poly(butylene succinate), poly(butylene adipate), poly(ϵ -caprolactone), poly(lactic acid) and poly(glycolic acid) (Tokiwa and Suzuki, 1981; Chiellini *et al.*, 1996; Iwamoto and Towika, 1994; Kim and Park, 1999; Kint *et al.*, 2003). The aliphatic-aromatic copolyesters obtained by heating the homopolyesters in the molten state have a blocky chemical microstructure.

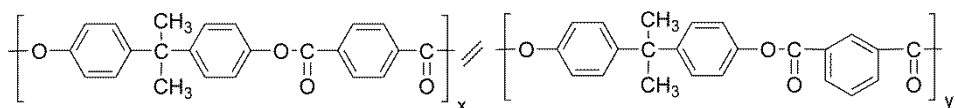
Several aliphatic-aromatic copolyesters are nowadays commercialized by different companies. Ecoflex, produced by BASF (Warzelhan *et al.*, 1996a and 1996b), and Eastar Bio, produced by Eastman (Ohta *et al.*, 1995), are copolyesters from

terephthalic acid, adipic acid and 1,4-butanediol. These materials are suitable for biowaste bags and films for horticulture, agriculture, food packaging and household applications. Biomax (DuPont) is, according to the producer, a standard PET with addition of special monomers to allow degradation to take place, with applications in paper coatings, disposable cutlery, thermoformable cups and trays, and films (Gallagher *et al.*, 1992a, 1992b and 1995). Ire Chemicals produces aliphatic-aromatic copolyesters made from terephthalic acid, adipic acid, succinic acid, ethylene glycol and/or 1,4-butanediol, with applications such as agricultural films and plastic bags (Chung *et al.*, 2000, 2001a and 2001b).

2.2.4. Fully aromatic polyesters

This class comprises amorphous high- T_g copolyesters, known as amorphous polyarylates, and semicrystalline polyesters that often exhibit anisotropic liquid crystalline melts.

Copolyesters of bisphenol A and iso- and terephthalic acid (Scheme 2.5) are amorphous engineering thermoplastics with excellent heat and ultraviolet light resistance (Dean *et al.*, 1989). Their amorphous morphology imparts on them properties of transparency and dimensional stability (Mahajan *et al.*, 1996). Amorphous polyarylates find applications for injection-molded parts in automotive, electronics, safety and building equipment; for example, headlight housings, fire helmets, face shields, and transparent exterior parts such as solar energy components and glazing.



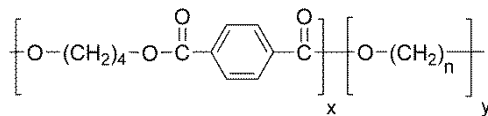
Scheme 2.5. Chemical structure of random copolyesters of bisphenol A and iso- and terephthalic acid.

Liquid crystalline (LC) polyesters are made from rigid para-oriented monomers such as 4-hydroxybenzoic acid, hydroquinone, terephthalic acid, or 2,6-dihydroxynaphthoic acid (Calundann, 1977). They exhibit a LC mesophase in the molten state, usually a nematic one; due to high stiffness, polymer chains tend to line up parallel to each other, instead of forming random coils and isotropic melts. This structure is retained in the

semicrystalline solid forming materials termed as self-reinforced thermoplastic resins. LC polyesters offer a combination of properties which makes them suitable for precision molding of small parts, *i.e.* extremely high melting fluidity, high heat resistance and dimensional stability, exceptional tensile strength and modulus in the flow direction (Jackson, 1980; Schmidt and Guo, 1988). Their major market is electronics, for example they find use in miniature connectors; other applications comprise precision parts for audiovisual equipment and for automotive industry.

2.2.5. Thermoplastic elastomers

Thermoplastic elastomers (TPEs) are polymers which present the typical mechanical properties of rubber and the processing ease of thermoplastics. Polyester TPEs are multiblock copolymers containing blocks of amorphous low- T_g polyether covalently bonded to blocks of semicrystalline PBT polyester (Scheme 2.6). At service temperature, the material exhibits biphasic morphology with microphase separation between a low- T_g polyether-rich phase and a semicrystalline PBT-rich phase (Fakirov *et al.*, 1991). The semicrystalline microphase acts as physical cross-links for the amorphous low- T_g regions imparting the material the properties of an elastomer.



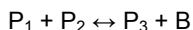
Scheme 2.6. Chemical structure of block PBT-polyether copolymers.

At processing temperature, the PBT phase melts, allowing the polyester TPE to be processed by conventional methods such as extrusion or injection-molding. A typical member of this class of polyesters is Dupont's Hytrel, a poly(oxytetramethylene)-*block*-poly(butylene terephthalate) obtained by replacing some of the 1,4-butanediol by dihydroxy-poly(oxytetramethylene) polyether in PBT synthesis. Depending on the polyether:PBT ratio, polyester TPE properties range from those of the rubbery polymers to those of engineering thermoplastics. They are used in industrial and automotive hydraulic tubing, hoses, gaskets and bellows; autoclavable medical tubing; and jacketing for electrical and fiber-optics cable (Holden *et al.*, 1996).

2.3. Synthetic methods

2.3.1. Melt polymerization

The synthesis of polyesters is carried out by a stoichiometric stepwise reaction between bifunctional reactants, which is accompanied by the formation of a low molecular weight condensate. There is an equilibrium such as:



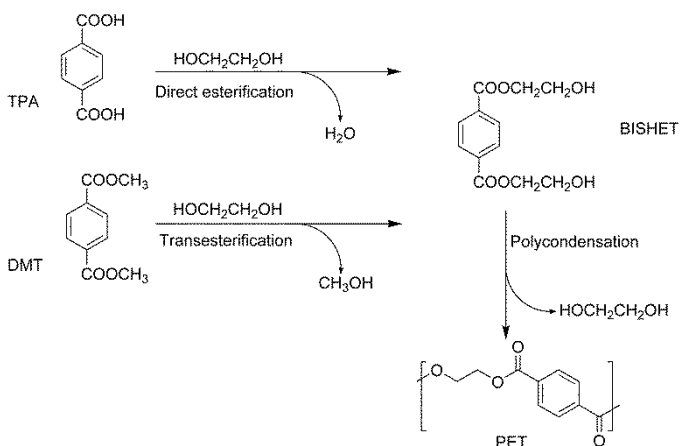
where P_1 and P_2 are monomer molecules or polymer chains which combine to form P_3 (a longer chain), and B is a small molecule by-product. Since polyesterifications are step-growth processes, the synthesis of high-molecular weight polyesters requires maintaining proper end-group stoichiometry and the removal of the condensate to prevent depolymerization. Side reactions, which may cause imbalance of the reactive groups and limit the molecular weight or may lead to the formation of undesired changes in polymer structure, must also be carefully controlled (Vouyiouka *et al.*, 2005).

Polyesters are typically manufactured by two routes: direct esterification of a diacid with a diol, followed by polycondensation to form the polymer; or transesterification of a dimethyl ester with a diol, followed by polycondensation (Pang *et al.*, 2006). Direct esterification and transesterification polymerizations are rather slow at low temperature and must be carried out at high temperature and high end-group concentration, preferably in the bulk. Vacuum is generally applied during the last steps of reaction to distill off reaction condensate (*i.e.* water in direct polyesterification or methanol in transesterification polymerizations from a dimethyl ester and a diol), and to continuously shift the reaction toward the formation of high-molecular weight polyester. Monomer excess adventitiously or deliberately introduced in the reaction mixture can be eliminated at high temperature and under vacuum during the last steps of the reaction. The presence of a catalyst is usually required for the preparation of high-molecular weight polyesters. Metal salts and oxides, such as zinc acetate and diantimony trioxide, and organometallic compounds, mainly titanium and zirconium alkoxides, are the preferred catalysts for bulk polyesterifications carried out in the 160-290 °C temperature range (Fradet and Maréchal, 1982).

The hydroxy-carboxy reaction (direct esterification) is the most straightforward method of polyester synthesis. It was first reported in the 1930s by Carothers (Carothers,

1931) and is still a very widely used method for the synthesis of polyesters from diacids and diols, or from hydroxyacids. As an example, PET synthesis by direct polyesterification in bulk from purified terephthalic acid (PTA) and ethylene glycol (EG) is described, and the synthetic process is depicted in Scheme 2.7. The reaction is performed in two stages. In the first stage, PTA is reacted with excess EG (approximately 1: 1.5-3 ratio) at 240-260 °C with elimination of water, yielding bis-(2-hydroxyethyl) terephthalate (BISHET). The medium is then heated to 270-290 °C under a progressively reduced pressure until EG is removed and relatively high-molecular weight PET is obtained (Pang *et al.*, 2006). The molecular weight of PET can be further increased by a solid-state postpolymerization under inert gas flow or under vacuum at 220-250 °C (see Section 2.3.2).

Hydroxy-ester interchange (transesterification) reactions play a predominant role in most industrial preparations of aliphatic and aromatic polyesters. Regarding the synthesis of PET, the monomers for the transesterification reaction are dimethyl terephthalate (DMT) and ethylene glycol (EG). The reactor is charged with DMT and EG with a 1: 2.1-2.3 molar ratio. The reaction is carried out in two stages. During the transesterification stage, a low stream of nitrogen is passed through the apparatus and the reaction temperature should be 170-210 °C; methanol is collected and bis-(2-hydroxyethyl) terephthalate (BISHET) is obtained. The second stage is usually carried out at 270-290 °C, and vacuum is applied at the end of the reaction until EG is removed and relatively-high molecular weight PET is obtained (Pang *et al.*, 2006). Also in this case, often solid-state postpolymerization is applied in order to increase the molecular weight of the resulting PET.



Scheme 2.7. PET polymerization process from TPA or DMT and EG.

2.3.2. Solid-state polymerization

In solid-state polymerization (SSP), starting materials are heated to a temperature higher than the glass-transition temperature (T_g), but lower than the melting temperature (T_m) so that the end groups are mobile enough to react. Polycondensation progresses through chain end reactions in the amorphous phase of the semicrystalline polymer, which in most cases is in the form of flakes (mean diameter > 1.0 mm) or powder (mean diameter < 100 μm) (Vouyiouka *et al.*, 2005; Papaspyrides and Vouyiouka, 2009). The advantages of SSP include the use of low temperatures, which restrain side reactions and thermal degradation of the product. The increase in molecular weight during SSP is accompanied by increased crystallinity and crystal perfection (Srinivasan *et al.*, 1994) while drying the polymer, which is important because moisture content may influence processability. Disadvantages of SSP focus on low reaction rates compared to melt polycondensation, and possible agglomeration of particles, especially at high temperatures (Kampouris and Papaspyrides, 1985).

SSP may be carried out in glass tubes, fluidized and fixed bed reactors, rotating flasks, tumbler dryers, etc. Mechanical agitation is usually provided in SSP systems, in order to facilitate good heat and mass transfer, and to prevent agglomeration, especially for reaction temperatures above 200 °C (Fortunato *et al.*, 1981; Chang *et al.*, 1983). During SSP processes, by-products are removed by application of vacuum or through convection caused by passing inert gas, usually at atmospheric pressure. Although reaction usually proceeds faster in vacuum than under a nitrogen sweep (Ma *et al.*, 2003), if a high vacuum is used, the subsequent return to atmospheric pressure may result in oxidation and discoloration of the polymer. The use of an inert gas in SSP systems serves three principal objectives: to remove the condensate, to inhibit polymer oxidation by excluding oxygen from the reactor atmosphere, and to heat the reacting mass. The inert gases used most often in SSP processes are nitrogen, carbon dioxide, helium and supercritical carbon dioxide (Mallon *et al.*, 1998; Gross *et al.*, 1999 and 2000; Shi *et al.*, 2001).

SSP progress involves both chemical and physical steps, since it is controlled by reaction kinetics, chain-end mobility in the amorphous phase, and condensate removal through diffusion. The reaction temperature emerges as the most important parameter of SSP rate variation, due to its influence on all aspects of the reaction progress. An increase of the SSP temperature accelerates the overall rate of the process, as a result of speeding up the chemical reaction, the mobility of the functional end groups and the by-

product diffusion (Chang, 1970; Srinivasan *et al.*, 1998). It is generally accepted that a smaller size of prepolymer particles can lead to an increased SSP rate, due to the shorter diffusion distance and the larger particle area per unit volume (Duh, 2001). In addition, the surface by-product diffusion is influenced by the flow of the inert gas. Acceleration in the gas flow can increase the mass and heat transfer rates in the gas-solid system and decrease the resistance to the diffusion of the by-product from the particle surface into the bulk of the gas phase (Gao *et al.*, 1997; Yao *et al.*, 2001). It is reported that, at a given reaction temperature, increasing the gas flow velocity in the SSP of small-sized PET sample results in changing the limitation step from surface diffusion control to chemical reaction control (Huang and Walsh, 1998). However the effect of gas flow rate is not very significant in cases where the diffusion of condensate inside the particles is the controlling step. Generally, refinement in reacting particle size distribution and morphology, in conjunction with high gas flow rates, increases the interfacial area per unit volume and the effectiveness of by-product elimination. SSP has been used to produce very high molecular weight ($M_n > 30,000 \text{ g}\cdot\text{mol}^{-1}$) PET for injection or blow molding applications; the solid-state polymerization of PET is carried out at around 220-230 °C for 10-30 h (Duh, 2001 and 2002).

Solid-state modification (SSM) is a recently developed variant of SSP which consists of making to react a comonomer with a semicrystalline polymer in the solid state, under an inert gas flow or vacuum at 20-30 °C below the T_m of the polymer but well above its T_g (Jansen *et al.*, 2005 and 2006). The SSM technique takes advantage of the molecular mobility in the amorphous phase of the polymer above T_g to insert the comonomer into the mobile amorphous phase of the polyester, whereas the chain segments in the rigid amorphous fraction and the crystalline phase do not participate in the transesterification reactions. Thus, SSM allows for the exclusive modification of the properties concerning the amorphous phase and hence, the crystallization behavior of the resulting copolymers should be quite comparable with that of the starting material. Furthermore, under these relatively mild conditions, side or thermal degradation reactions are minimized or even effectively suppressed. This approach has been used to incorporate sever comonomers into the amorphous phase of PBT (Jansen *et al.*, 2005, 2006, 2007 and 2008; Sablong *et al.*, 2008 and Gubbels *et al.*, 2013a).

2.3.3. Solution polymerization from diacyl dichlorides

Since some diols involved in the polyester preparation are not reactive enough under melt polycondensation conditions, often they are made to react with a more active diacid derivative, *i.e.* a chloride. The reaction between diacyl dichlorides and aliphatic diols or diphenolic compounds commonly takes place in solution and at low to moderate temperatures (-10 to 100 °C) (Kwolek and Morgan, 1964). High temperature solution reactions have also been reported for less soluble aromatic polyesters (Liaw *et al.*, 2000). Solution polymerization from diacyl dichlorides and diols or diphenols is usually carried out in the presence of tertiary amines such as triethylamine or pyridine, which play a role of both reaction catalyst and HCl acceptor (Vasnes *et al.*, 1990). The by-product (HCl) precipitates in the form of its quaternary ammonium salt and cannot participate in the reverse reaction. This also prevents possible H⁺-catalyzed side reactions during polymerization or polymer processing. The existence of such side reactions is the reason why high-temperature bulk processes involving acid chlorides, although possible, are not commonly applied to polyester synthesis. However, the extensive use of solvents and environmentally unfriendly reagents makes solution polymerization not suitable to be applied at industrial scale (Fradet and Tessier, 2003).

2.3.4. Ring-opening polymerization

The ring-opening polymerization (ROP) of cyclic esters, mainly lactones and lactides, is a convenient method of preparation of degradable aliphatic polyesters. Poly(lactic acid) (PLA) and poly(glycolic acid) (PGA) and their copolymers are usually synthesized by the ring-opening polymerization of their cyclic dimers, lactide and glycolide, respectively. Poly(ϵ -caprolactone) (PCL), other poly(lactones), and their copolymers have also been synthesized by the ROP of the corresponding lactones (Thomas, 2010). An initiator is required for ROP reactions; a wide range of initiators have been proposed, mainly salts or organocompounds of tin, titanium, zinc, aluminum and lanthanides (Pang *et al.*, 2006).

2.3.5. Enzymatic polymerization

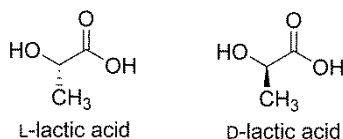
Polyesters can be also obtained by enzyme-catalyzed polymerization. Enzymes are proteins which exhibit a high catalytic efficiency and specificity for a given chemical reaction. Lipases and esterases belong to a class of enzymes referred to as hydrolyases which specifically catalyze the *in vivo* hydrolysis of esters. These enzymes, mainly lipases, were also found to catalyze a number of *in vitro* esterification and polyesterification reactions in organic medium (Kobayashi, 1999). Enzyme-catalyzed polyesterifications are carried out at 20-80 °C in solution or in the bulk using free or immobilized enzymes, which are usually removed from reaction medium at the end of the reaction. Solvent hydrophobicity plays an important role in enzymatic activity, particularly for lipases which normally act at oil-water interfaces in living cells (Brady *et al.*, 1990). The best reactivity is usually found for hydrophobic solvents such as hexane, toluene, diisopropylether or diphenylether. Hydrophilic polar solvents such as DMSO or methanol lead to significant modifications in enzyme conformation and therefore to a dramatic decrease in enzyme activity (Lalot *et al.* 1996). Polyesters have been obtained in organic medium by polyesterification of hydroxy acids (Shuai *et al.*, 1999), hydroxy esters (Gutman *et al.*, 1997), stoichiometric mixtures of diols and diacids (Binns *et al.*, 1998 and 1999), diols and diesters (Mezoul *et al.*, 1995 and 1996; Berkane *et al.*, 1997) and cyclic anhydrides (Kobayashi and Uyama, 1993). Since lipases also catalyze the reverse reaction (*i.e.* hydrolysis or alcoholysis of polyester), lipase-catalyzed polyesterifications can be regarded as equilibrium polycondensations. Various methods have been employed to remove the reaction by-product, water or alcohol, in order to displace the equilibrium toward the formation of polyester: addition of molecular sieves, Dean-Stark distillation of toluene-water azeotrope, or bubbling inert gas in reaction medium. In the case of reactions carried out without solvent, vacuum can be applied to distill off the by-product, *i.e.* water or alcohol. The use of vinyl esters is a convenient way to displace esterification equilibrium, since the theoretical by-product, vinyl alcohol, tautomerizes into acetaldehyde, which cannot participate in the reverse reaction (Uyama *et al.*, 1999). Activated esters such as 2,2,2-trifluoroethyl, 2-chloroethyl and 2,2,2-trichloroethyl esters have been reported to yield high-molecular weight polyesters (Linko *et al.*, 1995; Wang *et al.*, 1996). The enzymatic synthesis of polyesters is mainly used for the preparation of soluble or low-melting point polyesters, mainly aliphatic ones. Although the synthesis of some aromatic polyesters of isophthalic acid has also been reported, lipases exhibit a very low catalytic activity for rigid aromatic monomers such as terephthalates or diphenols (Wu *et al.*, 1998; Rodney *et al.*, 1999).

2.4. Bio-based polyesters

2.4.1. Polyesters partially or totally produced by bacteria

2.4.1.1. Polylactic acid (PLA)

Poly(lactic acid) (PLA) is an aliphatic polyester used in biomedical applications such as sutures, stents, dental implants, vascular grafts, bone screws and pins (Albertsson and Varma, 2003). It has also been investigated as a vector for drug delivery, for example in the long-term delivery of antimicrobial drugs, contraceptives and prostate cancer treatments, and as a scaffold material to support cell and tissue growth (Williams, 2007). Moreover it is also used for food packaging and bottle packaging of milk, water and juices. For the PLA industry, lactic acid (LA) with high optical purity of over 98-99% of L-LA is required; D-LA is not desirable for food, drink and biomedical applications due to the metabolic problems that D-LA may cause. The chemical structures of L-LA and D-LA are depicted in Scheme 2.8. Isotactic poly(L-lactic acid) (PLLA) is a semicrystalline polymer with a glass-transition temperature near 60 °C and a melting temperature near 180 °C (Tang *et al.*, 2004).



Scheme 2.8. Chemical structure of L- and D-lactic acid.

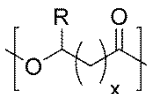
Lactic acid can be produced via either chemical synthesis or microbial fermentation. However, the chemical processes produce a racemic (50:50) mixture of D-LA and L-LA (D,L-LA). Glucose is transformed to pyruvic acid through the glycolysis pathway. Many bacteria contain an enzyme called lactate dehydrogenase (LDH) which converts pyruvic acid to lactic acid. Depending on the bacterial species and its LDH specificity, the lactic acid fermentation process can produce very pure D-LA or L-LA or a mixture of them. Molecular biology tools have been employed to delete the D-LDH genes to enhance the optical purity of its L-LA synthesis (Jem *et al.*, 2010). Under high temperature (> 100 °C), D-LA or L-LA may be converted to each other through a racemization process, which eventually results in a racemic mixture with inferior optical

properties (Benninga, 1990). Therefore, processing at elevated temperature should be avoided.

Polymerization of lactic acid can be conducted either by direct polycondensation of LA, or by a ring-opening polymerization of the lactide, a cyclic dimer of LA. The direct polycondensation process dehydrates LA to form oligomers which are further polymerized to PLA under simultaneous dehydration to avoid the degradation of polymer in the presence of moisture. Removal of water generated by the LA condensation is usually very difficult during the final stage of polymerization as the diffusion of moisture in a highly viscous polymeric melt is very slow. The residual water trapped will reduce PLA molecular weights. The direct polymerization process is reported to be used only by Tonji and Mitsui Chemicals companies (Chen and Patel, 2012). Most industrial PLA production processes employ the conversion of lactides to PLA via a ring-opening polymerization (ROP) catalyzed by organometallic catalysts (Du *et al.*, 2007 and Pang *et al.*, 2008). During the process, LA is dehydrated and condensed into its oligomers at high temperature under vacuum to remove moisture. Subsequently lactide is obtained from catalytic depolymerization of these short polylactic acid chains under reduced pressure. Residual LA is removed from lactide via distillation or crystallization. The purified lactide is polymerized into PLA at temperatures above the melting point of lactide and below the degradation temperatures of PLA.

2.4.1.2. Polyhydroxyalkanoates (PHAs)

Whereas PLA production is a two-stage process (fermentation to monomer followed by a conventional polymerization step), polyhydroxyalkanoates (PHAs) are the only bioplastics completely synthesized by microorganisms. PHA can be synthesized by over 30% of soil inhabiting bacteria (Chen and Patel, 2012).



Scheme 2.9. Chemical structure of polyhydroxyalkanoates.

The generic chemical structure for PHAs is depicted in Scheme 2.9, where x is 1 for all commercially relevant polymers and R can be either hydrogen or hydrocarbon chains. Poly(3-hydroxybutyrate) (PHB), with R =methyl, poly(3-hydroxyvalerate) (PHV), with R =ethyl, and poly(3-hydroxyhexanoate) (PHH), with R =propyl, are some of the most widely known PHAs. The bacteria can be fed a range of different carbon sources; for instance, *E. coli* fed with a range of oils produces different compositions of poly(HB-co-HH), whereas *R. eutropha* fed with a combination of glucose and propionate produces poly(HB-co-HV). Homopolymers, random copolymers and block copolymers of PHAs can be produced depending on the bacterial species and growth conditions (Gao, 2011). PHAs with T_g ranging from -50 to 4 °C, and T_m between 60 and 170 °C have been developed. Such diversity has allowed the development of a range of applications including environmentally friendly biodegradable plastics for packaging purposes, fibers, biodegradable and biocompatible implants and controlled drug release carriers (Wu *et al.*, 2000).

2.4.2. Alternative routes from renewable sources to conventional monomers

In this section, alternative routes from renewable sources to produce monomers which are currently obtained from petrochemical feedstock are described. The use of these bio-based monomers does not entail differences in terms of material properties between partially bio-based polyesters and their petrochemical counterparts, since they have exactly the same chemical structure.

Succinic acid. Bio-based succinic acid may be produced by anaerobic fermentation using various types of microorganisms. For example, succinic acid can be produced from glucose by the rumen organism *Actinobacillus succinogenes*; and can also be produced by *Anarobiospirillum succiniproducens* using glucose or even lactose, sucrose, maltose or fructose as carbon sources (Ryu *et al.*, 1999; Lee *et al.*, 2003). Feedstocks including corn starch, corn steep liquor, whey, cane molasses, glycerol, lignocelluloses, cereals, and straw hydrolases could be utilized for succinic acid production (Xu and Guo, 2010). The French starch and starch derivative producer Roquette and the Dutch chemical company DSM have built a demonstration plant in France for production of several hundred tons of succinic acid per year from starch using fermentation technology. Also BASF and the Dutch company Purac are jointly pursuing succinic acid production.

Mitsubishi Japan has also attempted to industrialize succinic acid microbial production (Chen and Patel, 2012).

Adipic acid. The bio-based adipic acid is still in its nascent state and it is not commercially available nowadays. However, companies as Verdezyne and Rennovia are developing bio-based routes to produce adipic acid. The bio-based process carried out by Verdezyne uses genetically modified enzymes to ferment glucose to adipic acid. On the other hand, Rennovia uses air oxidation to convert glucose to glucaric acid, followed by hydrodeoxygenation to convert glucaric acid to adipic acid (IHS Chemical Process Economics Program, 2012).

Terephthalic acid. Terephthalic acid has been reported as potentially being made from bio-based *p*-xylene produced by depolymerization of lignin (Bozell *et al.*, 2007). Recently, the production of terephthalic acid from limonene has been patented. In this case bio-based terephthalic acid is produced by the hydrogenation of limonene to *p*-cymene using zeolites and the subsequent oxidation of this compound (Berti *et al.*, 2010). This technology needs, however, further development and does not offer an economically viable production route for the short to midterm, mainly due to the difficult accessibility of limonene.

Ethylene glycol. Microbial ethanol for application as biofuel is being produced at the multimillion ton scale, from starch and from sugar. Bioethanol can be catalytically dehydrated to ethylene with activated clay, phosphoric acid, sulfuric acid, activated alumina, metal oxides and zeolites as catalysts (Huang *et al.*, 2008). Using bio-based ethylene, bio-based ethylene glycol can be produced via the conventional route of direct oxidation to ethylene oxide followed by thermal hydrolysis (Rebsdatt and Mayer, 2000). The large beverage company Coca-Cola Co. introduced in 2009 the PlantBottle as the first recyclable PET bottle using up to 30% bio-based monomers; bio-based ethylene glycol and recycled PET are employed in PET production. PepsiCo developed the first 100% bio-based bottle in 2011 (PepsiCo, 2011). It has also been announced a new generation of 100% bio-based PlantBottle from Coca-Cola Co. (Coca-Cola Co., 2011).

1,3-Propanediol. The production of bio-based 1,3-propanediol has been developed and commercialized by the joint venture DuPont Tate & Lyle LLC, with an annual capacity of 45,000 tons. Bio-based 1,3-propanediol is produced via the fermentation of glucose. There is a fermentation pathway in nature which consists of two steps: naturally occurring yeasts first ferment glucose to glycerol and then microbes ferment glycerol to 1,3-

propanediol. In the patented industrial bioprocess, glucose derived from wet-milled corn is metabolized by genetically engineered microorganism *E. coli*; this microorganism converts glucose to 1,3-propanediol in a single step (DuPont, 2013).

1,4-Butanediol. Genomatica Inc. developed a sucrose-based process for the manufacture of 1,4-butanediol by an engineered microorganism (Chen and Patel, 2012). On the other hand, 1,4-butanediol can also be produced from bio-based succinic acid involving three steps: corn-derived glucose is fermented to succinic acid, succinic acid is then purified by electrodialysis and it is finally reduced catalytically to 1,4-butanediol. Recently, an aqueous-phase hydrogenation of biomass-based succinic acid to 1,4-butanediol over supported bimetallic catalysts was reported (Minh *et al.*, 2010). However, most 1,4-butanediol is still produced from chemical processes.

1,10-Decanediol. By reacting castor oil with NaOH or KOH at elevated temperatures and in the presence of catalysts, sebacic acid and 2-octanol are formed preferably. Then sebacic acid can be converted to 1,10-decanediol via hydrogenation. Thus, 1,10-decanediol has been reported as a potential bio-based derivative of the castor oil (Mutlu and Meier, 2010).

2.4.3. Polyesters from carbohydrate-derived monomers with modified properties

2.4.3.1. Unprotected alditols and aldaric acids

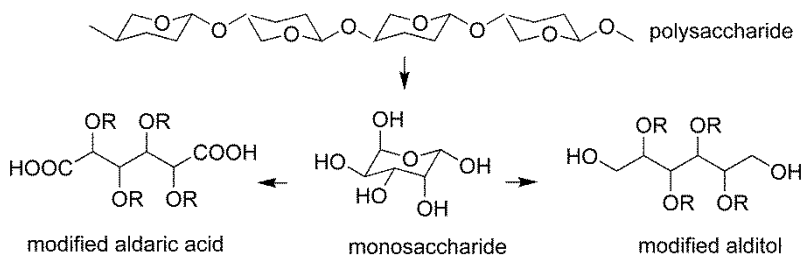
Linear polycondensation of monomers derived from carbohydrates is not straightforward. Carbohydrate-based compounds usually possess an excess of functional groups that upon polycondensation would lead to undesirable cross-linking reactions unless special precautions are taken. Nevertheless, some linear polycondensates have been synthesized using sugar-derived monomers bearing free hydroxyl groups by a solution polycondensation approach (Kiely *et al.*, 1994 and 2000).

Lipases have been reported to provide regioselectivity during esterification reactions of alditols at mild temperatures. In 2000, the first example of an alditol used as monomer in enzyme-catalyzed polymerization was described; D-glucitol was polymerized through its positions C-1 and C-6 with divinyl sebacate in CH₃CN (Uyama *et al.*, 2000). The preparation of polyesters from 1,8-octanediol, adipic acid and several unprotected alditols, such as erythritol, xylitol, ribitol, D-mannitol, D-glucitol and galactitol, has also

been reported. Polymerizations were carried out under vacuum, using the immobilized Lipase B from *Candida antarctica* (Novozyme 435) as catalyst (Hu *et al.*, 2006).

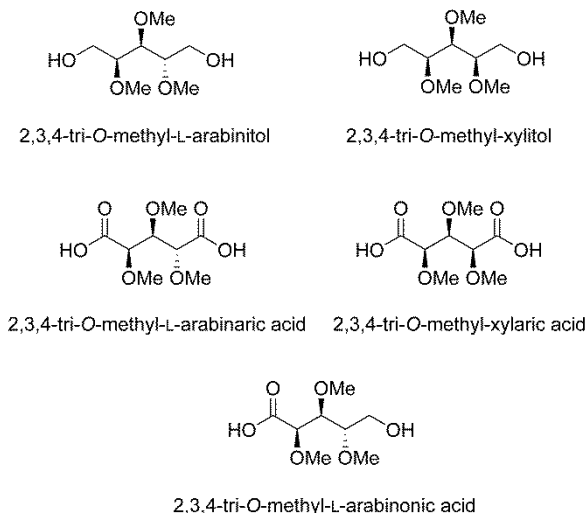
2.4.3.2. Acyclic *O*-protected alditols and aldaric acids

Although some syntheses leading to linear polyesters have been realized using sugar-derived monomers with free hydroxyl groups (see above), most of them are carried out with derivatives in which the secondary hydroxyl groups have been appropriately blocked (Scheme 2.10).



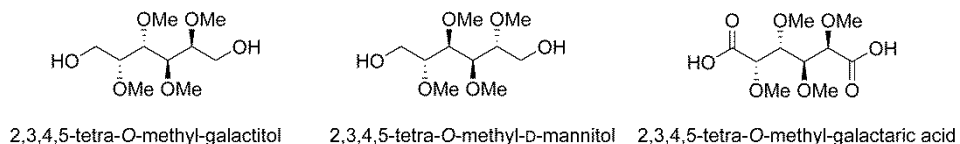
Scheme 2.10. Modification of carbohydrates leading to *O*-protected alditols and aldaric acids.

The pioneering work of Drew and Haworth in the 1920s described the polycondensation of 2,3,4-tri-*O*-methyl-*L*-arabinonic acid to give an oligomeric material not completely characterized (Drew and Haworth, 1927). Also in the field of aliphatic polyesters from acyclic *O*-protected carbohydrate-based monomers, several poly(alkylene dicarboxylates) have been recently obtained by polycondensation reaction of the alditols 2,3,4-tri-*O*-methyl-*L*-arabinitol and 2,3,4-tri-*O*-methyl-xylitol, and aldaric acids 2,3,4-tri-*O*-methyl-*L*-arabinaric acid and 2,3,4-tri-*O*-methyl-xylaric acid (García-Martín *et al.*, 2006). The chemical structures of these *O*-protected carbohydrate-based monomers are depicted in Scheme 2.11. 1,4-Butanediol and adipic acid were also used as comonomers.



Scheme 2.11. Chemical structure of some monomers derived from L-arabinose and D-xylose.

The synthesis of aromatic polyesters, specifically of poly(phthalate)s, using carbohydrate-based acyclic O-protected monomers has also been explored. Thus poly(ethylene terephthalate) (PET), poly(ethylene isophthalate) (PEI) and poly(butylene terephthalate) (PBT) have been chemically modified by insertion of different O-methyl alditols (Galbis and García-Martín, 2008 and 2010). Firstly, a series of PET copolyesters containing 2,3-di-O-methyl-L-threitol were prepared and duly characterized (Kint *et al.*, 2001). Later PET and PEI analogues with total replacement of the ethylene glycol units by 2,3,4,5-tetra-O-methyl-hexitols having either D-*manno* or *galacto* configurations were synthesized (Zamora *et al.*, 2005a). Polyesters analogous to PET, PEI and PBT have also been prepared by using 2,3,4-tri-O-methyl-L-arabinitol and 2,3,4-tri-O-methyl-xylitol (Zamora *et al.*, 2005b; Alla *et al.*, 2006). The 2,3,4-tri-O-benzyl ethers of L-arabinitol and xylitol were also used to synthesize polyesters analogous to PET and PBT (Zamora *et al.*, 2008). Butylene copolyesters based on O-methyl aldaric acids as L-arabinaric and galactaric acids, and terephthalic acid were also prepared and characterized (Zamora *et al.*, 2009). The chemical structures of some of these O-protected carbohydrate-based monomers are depicted in Scheme 2.12.

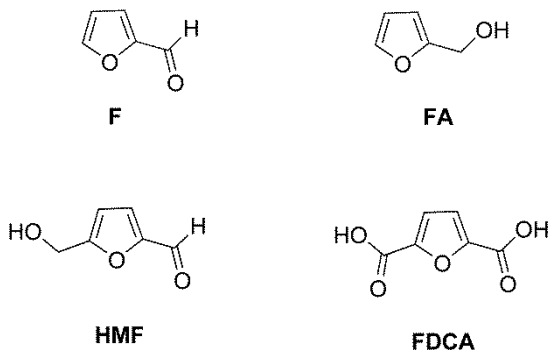


Scheme 2.12. Chemical structure of some monomers derived from D-galactose and D-mannose.

The hydrolytic degradation of a series of homo- and copolyesters analogous to PET and PEI based on *O*-methyl protected L-arabinitol, xylitol, D-mannitol and galactitol was relatively fast at temperatures 10 °C above their respective T_g . The hydrolysis of copolyesters took place preferentially by cleavage of the ester groups of the sugar units (Zamora *et al.*, 2006). The hydrolytic degradation of PBT copolyesters containing up to 50% of *O*-methyl protected pentitols derived from L-arabinose and D-xylose was also studied (Alla *et al.*, 2006). It was shown that these copolyesters were much more sensitive to hydrolysis than was PBT.

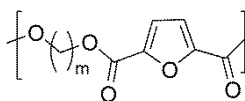
2.4.3.3. 2,5-Furandicarboxylic acid (FDCA)

The research strategy related to furan polymers relies on the use of two furan derivatives, *i.e.* furfural (F) and hydroxymethylfuraldehyde (HMF), as starting building blocks from which two sets of monomers can be synthesized: those containing double bonds suitable for chain polymerizations and copolymerizations, and those with carboxyl or hydroxyl functionalities associated with step-growth mechanisms (Gandini and Belgacem, 1997; Gandini, 2010 and 2011). Furfural (F) is produced as an industrial commodity, with a yearly production close to 300,000 tons. Its precursors are pentoses present in corn, rice, sugar and cotton, among others. Furfural production is based on the acid catalyzed hydrolytic depolymerization of C5 hemicelluloses, particularly xylenes. Most of the furfural is today converted into furfuryl alcohol (FA), which is extensively employed as a precursor to a variety of resins for several applications. The second furan derivative which can be prepared from the appropriate C6 polysaccharides is hydroxymethylfuraldehyde (HMF). The chemical structures of these furan-based products are depicted in Scheme 2.13. The acid-catalyzed dehydration of fructose to HMF can be performed in high-boiling polar solvents, in supercritical acetone and water, or by addition of phase modifiers (Moreau *et al.*, 2004; Román-Leshkov *et al.*, 2006; Zhao *et al.*, 2007).



Scheme 2.13. Chemical structure of furfural (F), furfuryl alcohol (FA), hydroxymethylfuraldehyde (HMF) and 2,5-furandicarboxylic acid (FDCA).

Especially 2,5-furandicarboxylic acid (FDCA), as a HMF derivative, has gained particular attention as a suitable monomer for step-growth polymerization. Moore and Kelly initially explored the scope and limitations of FDCA in polycondensation reactions and synthesized a series of polyesters based on FDCA and several diols (Moore and Kelly, 1978 and 1979). However, due to the limited availability of high-purity FDCA, the research interest in this field declined in the following years. Recent developments in the catalytic routes toward high-purity FDCA allowed the preparation of larger amounts of this compound, and led to a significant increase in the amount of research carried out towards FDCA polycondensates. The use of this compound to obtain bio-based polyesters has been extensively studied in the last years (Gandini *et al.*, 2009a and 2009b; Jiang *et al.*, 2011; Wu *et al.*, 2012a; Gubbels *et al.*, 2013b). The general chemical structure of the furan-based polyesters obtained upon polycondensation of FDCA with linear aliphatic diols is depicted in Scheme 2.14, and the thermal properties of this family of compounds are shown in Table 2.1.



Scheme 2.14. Chemical structure of furan-based polyesters obtained upon polycondensation of FDCA with linear aliphatic diols.

FDCA was used in conjunction with ethylene glycol to synthesize poly(ethylene 2,5-furandicarboxylate) (PEF), *i.e.* the furan analog of PET. The replacement of the terephthalate ring by the furan counterpart led to a decrease in melting temperature compared to PET, whereas maintained its glass-transition temperature (Gomes *et al.*,

2011). The same considerations apply to the homologous polymer with 1,4-butanediol units, *i.e.* PBF and PBT (Zhu *et al.*, 2013). The angle between the carboxylic acid groups, which determines the degree of linearity of the monomer, is 180° in terephthalic acid, whereas is significantly smaller for FDCA, ranging from 129.4° (X-ray diffraction) to 133.6° (DFT) and hence closer to the value of 120° found for isophthalic acid (Wu *et al.*, 2011). Although the use of both terephthalic acid and FDCA results in a similar T_g of their corresponding polyesters, such a difference in angles has significant effects on crystallinity (van Es, 2013).

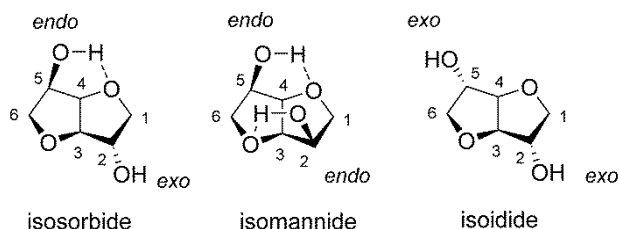
Table 2.1. Thermal properties and molecular weights of FDCA-based polyesters.

Polymer	Diol	Thermal properties		Molecular weights		Ref.
		T_g (°C)	T_m (°C)	M_n (g·mol ⁻¹)	M_w (g·mol ⁻¹)	
PEF	ethylene glycol	80	215	22,400	44,500	Gomes <i>et al.</i> , 2011
PPF	1,3-propanediol	50	174	21,600	27,600	Gomes <i>et al.</i> , 2011
PBF	1,4-butanediol	39	172	21,300	49,000	Zhu <i>et al.</i> , 2013
PHF	1,6-hexanediol	28	148	32,100	66,700	Jiang <i>et al.</i> , 2011
POF	1,8-octanediol	22	133	20,700	47,500	Jiang <i>et al.</i> , 2011

2.4.3.4. Dianhydrohexitols and derivatives

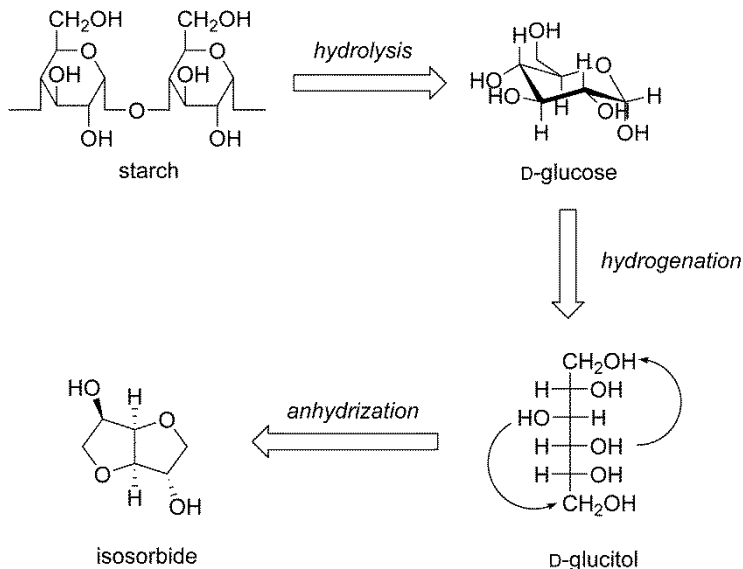
The first research on the synthesis and structure of 1,4:3,6-dianhydrohexitols was conducted in the 1950s. Depending on the chirality, three isomers of the 1,4:3,6-dianhydrohexitols exist: isosorbide (1,4:3,6-dianhydro-D-glucitol), isomannide (1,4:3,6-dianhydro-D-mannitol) and isoidide (1,4:3,6-dianhydro-L-iditol). The 1,4:3,6-

dianhydrohexitols are composed of two *cis*-fused tetrahydrofuran rings, nearly planar and V-shaped with a 120° angle between rings. The secondary hydroxyl groups are situated at carbons 2 and 5 and positioned either inside (*endo*) or outside (*exo*) the V-shaped molecule. Isoidide has two *exo* hydroxyl groups, whereas for isomannide they are both *endo*, and for isosorbide there is one *exo* and one *endo* hydroxyl group (Scheme 2.15). *Exo* and *endo* hydroxyl groups exhibit different reactivities since they are more or less accessible depending on the steric requirements of the studied reaction (Matheson and Angyal, 1952; Cope and Shen, 1956). The reactivity also depends on the existence of hydrogen bonds (Buck *et al.*, 1966).



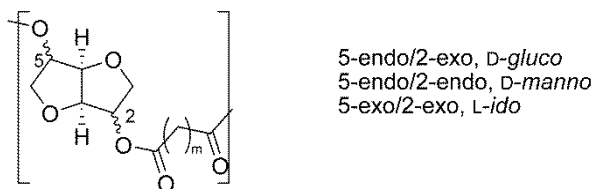
Scheme 2.15. Chemical structure of isosorbide, isomannide and isoidide.

Starch extracted from cereals is first degraded to D-glucose and D-mannose by an enzymatic process. The hydrogenation of these two sugars gives D-sorbitol and D-mannitol, respectively, which can be subsequently dehydrated to obtain isosorbide and isomannide (Scheme 2.16). However, isomannide is less studied because of its low reactivity; isosorbide is the sole product produced at industrial scale (Fenouillot *et al.* 2010). Isoidide is the most reactive 1,4:3,6-dianhydrohexitol, but it is derived from L-idose which rarely exists in nature and cannot be extracted from vegetal biomass. As alternative synthetic routes, the isomerizations from isosorbide or isomannide have been proposed (Wright and Brandner, 1962).



Scheme 2.16. Preparation of isosorbide.

Numerous aliphatic polyesters have been synthesized from 1,4:3,6-dianhydrohexitols. The chemical structure and the thermal properties of some of these polyesters are presented in Scheme 2.17 and in Table 2.2, respectively. Due to the low reactivity of their secondary hydroxyl groups, the use of dicarboxylic acid chlorides as polycondensation comonomers is usually required. Braun and Bergmann first described the preparation in the molten state at 80 °C of a series of low-molecular weight polyesters based on isosorbide and isomannide and several dicarboxylic acid chlorides (Braun and Bergmann, 1992). Okada *et al.* studied the biodegradability of aliphatic polyesters prepared by polycondensation of chloride diacids with 1,4:3,6-dianhydrohexitols in bulk at 140-160 °C. They observed that the polymers obtained from isosorbide degraded faster than the ones based on isomannide (Okada *et al.*, 1995, 1996 and 2000; Okada and Aoi, 2002).



Scheme 2.17. Chemical structure aliphatic polyesters from 1,4:3,6-dianhydrohexitols.

Table 2.2. Thermal properties and molecular weights of aliphatic polyesters from 1,4:3,6-dianhydrohexitols.

Diol	Diacid	Thermal properties		Molecular weights		Ref.
		T_g (°C)	T_m (°C)	M_n (g·mol ⁻¹)	M_w (g·mol ⁻¹)	
isosorbide	succinic	65	-	7,500	10,800	Braun and Bergmann, 1992
		36	-	8,000	14,400	Okada <i>et al.</i> , 1996
		57	-	2,400	4,300	Noordover <i>et al.</i> , 2006
isosorbide	glutaric	68	-	3,100	5,000	Noordover <i>et al.</i> , 2006
		28	-	20,000	34,000	Okada <i>et al.</i> , 1996
isosorbide	adipic	25	-	13,000	25,000	Braun and Bergmann, 1992
		40	-	26,000	39,000	Okada <i>et al.</i> , 1996
isosorbide	suberic	11	-	20,000	49,000	Braun and Bergmann, 1992
isosorbide	sebacic	0	-	23,000	60,000	Braun and Bergmann, 1992
		-10	-	34,000	40,800	Okada <i>et al.</i> , 1996
isosorbide	1,12-dodecanoic	-2	-	15,000	28,000	Braun and Bergmann, 1992
isosorbide	1,14-tetradecanedioic	-4	53/67/79 ^a	14,700	31,300	Braun and Bergmann, 1992
isomannide	succinic	75	175	9,000	16,200	Okada <i>et al.</i> , 1996
isomannide	glutaric	37	-	11,000	17,600	Okada <i>et al.</i> , 1996
		30	-	8,800	15,000	Braun and Bergmann, 1992
isomannide	adipic	28	-	20,000	30,000	Okada <i>et al.</i> , 1996

Table 2.2. Thermal properties and molecular weights of aliphatic polyesters from 1,4:3,6-dianhydrohexitols.

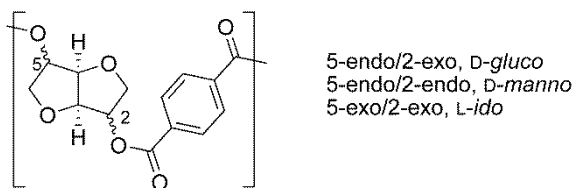
Diol	Diacid	Thermal properties		Molecular weights		Ref.
		T_g (°C)	T_m (°C)	M_n (g·mol ⁻¹)	M_w (g·mol ⁻¹)	
isomannide	sebacic	0	-	13,700	26,000	Braun and Bergmann, 1992
		-8	-	18,000	25,200	Okada <i>et al.</i> , 1996
isoidide	glutaric	50	181	18,000	30,600	Okada <i>et al.</i> , 1996
isoidide	adipic	45	164	34,000	44,200	Okada <i>et al.</i> , 1996
isoidide	sebacic	0	134	28,000	39,200	Okada <i>et al.</i> , 1996

^a Multiple melting peak.

In some applications of aliphatic polyesters, low-molecular weights are needed. For example, for powder-coating resins, M_n values between 2,000 and 6,000 g·mol⁻¹ are required. Moreover, powder-coating resins need to have a sufficiently high glass-transition temperature (*i.e.*, $T_g > 45$ °C) to provide good storage stability and processability. Isosorbide was polymerized with renewable diacid monomers such as succinic acid and citric acid and copolymerized with renewable diol monomers, like 2,3-butanediol, 1,3-propanediol and neopentylglycol (Noordover *et al.*, 2006 and 2007; van Haveren *et al.*, 2007). Titanium (IV) tetrabutoxide (TBT) was used as catalyst. The polycondensation was carried out in bulk at a maximum temperature of 250 °C, and relatively low-molecular weights were obtained ($M_n = 2,000$ -4,600 g·mol⁻¹). The glass-transition temperature (T_g) could be easily adjusted between 20 and 65 °C by varying the proportions of the different components and the molecular weight of the polymer.

On the other hand, Thiem and Lüders prepared low-molecular weight poly(terephthalate)s by polycondensation of terephthalic acid dichloride and 1,4:3,6-dianhydrohexitols in the melt at 180 °C (Scheme 2.18). For poly(isosorbide terephthalate) and poly(isoidide terephthalate) having molecular weights (determined by vapour pressure osmometry) of 3,000 and 3,800 g·mol⁻¹, respectively, the glass-transition temperatures were 155 °C and 153 °C, respectively. Concerning poly(isomannide

terephthalate), the formation of cross-linked polymers was reported, suggesting that under such polymerization conditions the anhydro ring in isosorbide might be partially ruptured (Thiem and Lüders, 1984a and 1984b). Storbeck *et al.* reinvestigated the synthesis and characterization of these poly(terephthalate)s using acyl chlorides in solution. The reaction conditions were optimized, and pyridine was found to be the most useful acceptor of the generated hydrogen chloride. The glass-transition temperature of the synthesized poly(isosorbide terephthalate) with ($M_n = 14,200 \text{ g}\cdot\text{mol}^{-1}$) was reported to be $197 \text{ }^\circ\text{C}$ (Storbeck *et al.*, 1993). Recently, Kricheldorf *et al.* explored the melt transesterification of dimethyl terephthalate with isosorbide in bulk at a maximum temperature of $250 \text{ }^\circ\text{C}$, with titanium (IV) tetrabutoxide (TBT) as catalyst (Kricheldorf *et al.*, 2007). However, it was noticed that the reaction was slow and the inherent viscosity of the resulting polyester was very low ($0.11 \text{ dL}\cdot\text{g}^{-1}$). This result highlights the difficulty to reach high molecular weights in a bulk polycondensation involving esterification or transesterification. Since the two secondary hydroxyl groups of 1,4:3,6-dianhydrohexitols display reduced reactivity under melt polycondensation conditions with either a diacid or a diester, in most cases reported in the literature terephthaloyl chloride is used as comonomer, either for melt polycondensation or in solution. With the use of the diacid chloride, higher molecular weights are produced, three to ten times greater than those obtained from conventional bulk polymerization starting with terephthalic acid or dimethyl terephthalate (Fenouillot *et al.*, 2010).



Scheme 2.18. Chemical structure of poly(terephthalate)s obtained from 1,4:3,6-dianhydrohexitols.

Also aromatic copolyesters from isosorbide and either poly(ethylene terephthalate) (PET) or poly(butylene terephthalate) (PBT) have been extensively studied and their applications well defined: packaging (bottles, films) and molded parts (Fenouillot *et al.*, 2010). For bottles, an increase of the T_g and more generally of the thermomechanical resistance could open the field of hot-filled and pasteurized-container applications. Another objective could be to reduce the weight of the packaging. For high contents in isosorbide, T_g higher than $120 \text{ }^\circ\text{C}$ are feasible and competition with polycarbonate could be possible.

Storbeck and Ballauff performed polycondensation of terephthaloyl chloride with isosorbide and ethylene glycol. Intrinsic viscosities of up to $0.46 \text{ dL}\cdot\text{g}^{-1}$ were obtained. They studied the entire range of diol proportions, and found that isosorbide-based PET copolyesters were amorphous above 20 mol% of isosorbide (Storbeck and Ballauff, 1996). The classical industrial melt polycondensation from terephthalic acid or dimethyl terephthalate were covered by patent (Charbonneau *et al.*, 1999). The content of isosorbide in the feed was not totally incorporated into the polyester chains; significant amounts of isosorbide were lost by distillation during the esterification or during the transesterification step. Fenouillot *et al.* performed also studies on melt polycondensation of such copolyesters to quantify the actual proportion of isosorbide inserted into the polyester chains, and found that about 25% of isosorbide was lost (Fenouillot *et al.*, 2010).

Kricheldorf *et al.* studied polycondensation of 1,4-butanediol with isosorbide and either dimethyl terephthalate in bulk using TBT as catalyst, or terephthaloyl chloride in solution using pyridine as catalyst and HCl acceptor (Kricheldorf *et al.*, 2007). Copolyesters with very low molecular weights, *i.e.* inherent viscosities between 0.08 and $0.37 \text{ dL}\cdot\text{g}^{-1}$, were obtained by transesterification in the melt. However higher inherent viscosities, with values of up to $0.74 \text{ dL}\cdot\text{g}^{-1}$, could be attained by using polycondensation in solution with terephthaloyl chloride. Isosorbide-based PBT copolyesters were found to be amorphous for isosorbide contents above 32 mol%.

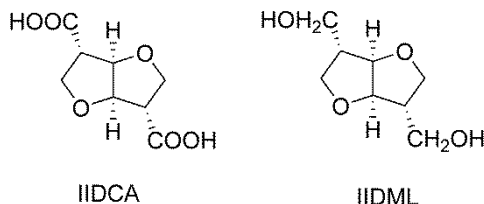
The industrial applications of copolyesters containing low to moderate proportions of isosorbide are that of classical of PET or PBT taking advantage of the increased glass-transition temperature. Numerous patents described isosorbide-based PET and PBT copolyesters; some of them claimed the method of polymerization while several claimed specific polyester applications. For instance, the addition of isosorbide into PET to produce bottles able to resist hot-fill process (Charbonneau and Johnson, 1999) and thermoformable sheets where a low rate of crystallization is required (Khanarian *et al.*, 2000) have been patented. Also fibers, films and polymer blends were cited (Khanarian *et al.*, 2002). Furthermore, the incorporation of isosorbide by transesterifying poly(ethylene terephthalate) with poly(isosorbide terephthalate) oligomers in bulk at $285 \text{ }^\circ\text{C}$ was also patented (Adelman *et al.*, 2003). In this way they could incorporate 24 mol% of isosorbide relative to the total diol content, and the polymer obtained was amorphous with $T_g = 139 \text{ }^\circ\text{C}$ and an inherent viscosity of $0.57 \text{ dL}\cdot\text{g}^{-1}$. In this case the aim was not to compete with PET but rather with polycarbonate (PC) or

poly(methyl methacrylate) (PMMA). At this point it should be stated that all aromatic copolyesters containing isosorbide are yellowish, an important flaw for certain applications. The sensitivity of isosorbide to thermooxidation at the high temperatures needed to polymerize polyesters is the cause of yellowing. The efforts for solving this problem were highlighted in a recent patent from Charbonneau on poly(ethylene-co-isosorbide terephthalate); the synthetic routes cited were the typical PTA or DMT synthesis but with the observation that oxygen should absolutely be avoided in the reactive medium. Moreover, two antioxidants were added just before polycondensation: the primary one was a hindered phenol and the secondary one was a trivalent phosphorous compound (Charbonneau, 2006).

Recently, Sablong *et al.* studied the incorporation of isosorbide into PBT by solid-state modification (SSM). Experiments using SSM for the direct incorporation of isosorbide into PBT were unsuccessful; isosorbide could not be incorporated under such conditions, due to the relatively low reactivity of its two secondary hydroxyl. The synthesis of a macrodiol bearing two primary hydroxyl groups, from isosorbide, terephthaloyl chloride and 1,4-butanediol was necessary to incorporate isosorbide into the PBT chain. Very high molecular weights ($M_n = 80,000\text{--}140,000 \text{ g}\cdot\text{mol}^{-1}$) could be attained by using this technique (Sablong *et al.*, 2008).

Isosorbide and isoidide have also been polymerized with the dichloride derivative of 2,5-furandicarboxylic acid in solution. Amorphous polyesters with high glass-transition temperatures, *i.e.* 180 °C for poly(isosorbide 2,5-furandicarboxylate) ($M_n = 13,700 \text{ g}\cdot\text{mol}^{-1}$) and 140 °C for poly(isoidide 2,5-furandicarboxylate) ($M_n = 5,700 \text{ g}\cdot\text{mol}^{-1}$), were obtained (Gomes *et al.*, 2011).

The low reactivity of the secondary hydroxyl groups of the 1,4:3,6-dianhydrohexitols explains why the synthesis of more reactive derivatives such as amines (Thiem and Lüders, 1986; Bachmann *et al.*, 1998; Jasinska *et al.*, 2011) or isocyanates (Pfeffer *et al.*, 2011a and 2011b), has been considered. Regarding polyester synthesis from isohexide-derived monomers with enhanced reactivity, another strategy is based on chain extension at C2 and C5 of the isohexide skeleton. Very recently the synthesis of a 1-carbon extended isohexide derivative with dicarboxylic functionality, namely isoidide dicarboxylic acid (IIDCA), and a 1-carbon extended diol with primary hydroxyl groups, namely isoidide hydroxymethylene diol (IIDML), has been reported (Wu *et al.*, 2011). Their chemical structures are depicted in Scheme 2.19.



Scheme 2.19. Chemical structure of the 1-carbon extended isohexide derivatives IIDCA and IIDML.

The main properties of polyesters based on these 1-carbon extended isohexide derivatives are presented in Table 2.3. Aliphatic polyesters with M_w in the 13,000-34,000 $\text{g}\cdot\text{mol}^{-1}$ range were obtained by melt polycondensation from the dimethyl ester of IIDCA and aliphatic diols with 2 to 12 methylene groups (Wu *et al.*, 2012b). These aliphatic polyesters were semicrystalline, with T_m values in the 40-125 °C range. The glass-transition temperatures were between -33 °C and 18 °C. The synthesis of a series of fully isohexide-based polyesters has been recently reported (Wu *et al.*, 2013). The combination of the dimethyl ester of the IIDCA with isosorbide, isomannide or isidide resulted in semicrystalline low molecular weight polyesters ($M_w = 1,700\text{-}3,600 \text{ g}\cdot\text{mol}^{-1}$) with T_m in the 80-170 °C range. T_g values were 73, 30 and 85 °C for polyesters obtained from the dimethyl ester of IIDCA and isosorbide, isomannide or isidide, respectively. Also a fully isohexide-based polyester from the dimethyl ester of IIDCA and the extended diol IIDML was prepared using the same melt polycondensation conditions. An increase in the reactivity of the extended diol bearing two primary hydroxyl groups with respect to the secondary hydroxyl groups of isidide was reported; the M_w of this IIDCA-IIDML polyester being 10,400 $\text{g}\cdot\text{mol}^{-1}$. This polyester was semicrystalline and its glass-transition temperature was 48 °C (Wu *et al.*, 2013). However the 1-carbon extension resulted in a significant decrease in T_g of the resulting polyesters compared to incorporation of the parent isohexide; the IIDCA-isidide polyester showed a T_g value of 85 °C despite having lower molecular weight. When compared to the polyester from terephthalic acid and isidide, the analogous polyester containing the extended isidide diol IIDML also showed a dramatic drop in T_g of approx. 100 °C (209 °C vs. 105 °C) (Wu, 2012; van Es, 2013).

Table 2.3. Thermal properties and molecular weights of polyesters from monomers based on chain extension at C2 and C5 of the isohexide skeleton.

Diol	Diacid	Thermal properties		Molecular weights		Ref.
		T_g (°C)	T_m (°C)	M_n (g·mol ⁻¹)	M_w (g·mol ⁻¹)	
ethylene glycol	IIDCA	18	125	6,100	13,100	Wu <i>et al.</i> , 2012b
1,4-butanediol	IIDCA	0	47/62 ^a	14,100	34,100	Wu <i>et al.</i> , 2012b
1,6-hexanediol	IIDCA	-20	54	10,200	22,800	Wu <i>et al.</i> , 2012b
1,8-octanediol	IIDCA	-30	43/51/55 ^a	10,000	17,100	Wu <i>et al.</i> , 2012b
1,10-decanediol	IIDCA	-33	43/54 ^a	11,800	24,600	Wu <i>et al.</i> , 2012b
1,12-dodecanediol	IIDCA	-30	57/64 ^a	8,800	18,000	Wu <i>et al.</i> , 2012b
isosorbide	IIDCA	73	125/168 ^a	2,600	3,300	Wu <i>et al.</i> , 2013
isomannide	IIDCA	30	89	1,200	1,700	Wu <i>et al.</i> , 2013
isoidide	IIDCA	85	109/143 ^a	2,500	3,600	Wu <i>et al.</i> , 2013
IIDML	IIDCA	48	118/150 ^a	5,400	10,400	Wu <i>et al.</i> , 2013
IIDML	terephthalic	105	268/277/ 296 ^a	7,700	17,700	Wu, 2012

^a Multiple melting peak.

2.4.3.5. Cyclic acetalized alditols, aldonic and aldaric acids

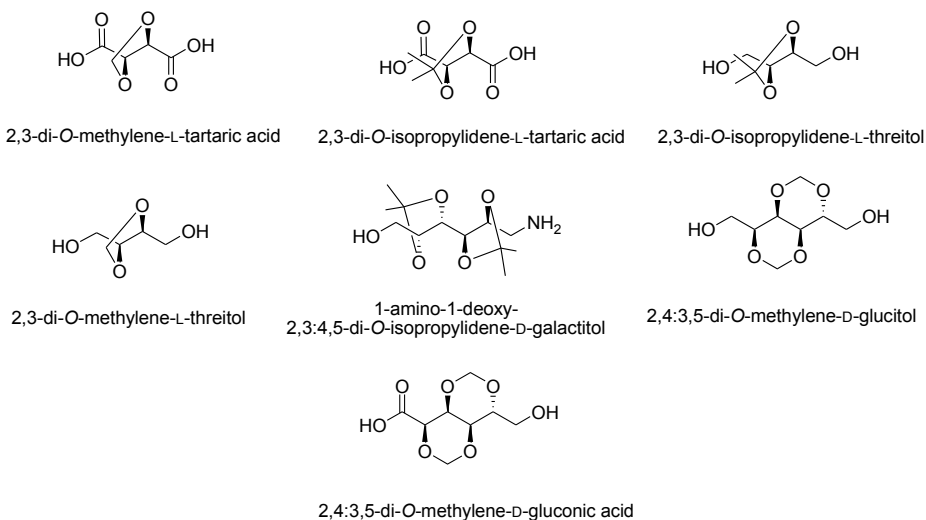
The use of cyclic acetalized alditols, aldonic and aldaric acid derivatives as building blocks for the synthesis of polycondensates is not new, but very few cases have been reported so far:

- The synthesis and crystal structure of linear polyamides from 2,3-di-O-methylene-L-tartaric acid and several diamines have been described (Rodríguez-Galán *et al.*, 1992; Iribarren *et al.*, 2000), and their biodegradability has been tested (Kimura *et*

al., 1999). The incorporation of the dimethyl ester derivative into polyesters has been recently reported (Japu *et al.*, 2013a).

- Low molecular weight polyesters made from 2,3-di-*O*-isopropylidene-*L*-tartaric acid and linear alkanediols and from 2,3-di-*O*-isopropylidene-*L*-threitol and aliphatic diacids have been reported (Dhamaniya and Jacob, 2010 and 2012).
- Polyurethanes have been synthesized from 2,3-di-*O*-isopropylidene-*L*-threitol and from 2,3-di-*O*-methylene-*L*-threitol (Marín and Muñoz-Guerra, 2008).
- In the 1950s, Mehlretter and Mellies reported on the polymerization of 2,4:3,5-di-*O*-methylene-*D*-gluconic acid in an attempt to benzoylate this compound with an equivalent amount of benzoyl chloride or benzoic anhydride in pyridine solution (Mehlretter and Mellies, 1955).
- Polyurethanes from 1-amino-1-deoxy-2,3:4,5-di-*O*-isopropylidene-*D*-galactitol have been prepared (Gómez and Varela, 2009).
- 2,4:3,5-di-*O*-methylene-*D*-glucitol has been used as monomer for the preparation of polyurethanes (Marín and Muñoz-Guerra, 2009), and its incorporation into polyesters is currently being studied in another PhD thesis in our research group (Japu *et al.*, 2012 and 2013b).

The chemical structure of these cyclic acetalized alditols, aldonic and aldaric acids are depicted in Scheme 2.20.



Scheme 2.20. Chemical structure of cyclic acetalized alditols, aldonic and aldaric acids being studied so far.

2.5. References

- Adelman, D.J.; Charbonneau, L.F.; Ung, S. *US Patent* 6656577 (to E.I. du Pont de Nemours and Co.), **2003**.
- Albertsson, A.-C.; Varma, I.K. *Biomacromolecules* **2003**, *4*, 1466-1486.
- Alla, A.; Hakkou, K.; Zamora, F.; Martínez de Ilarduya, A.; Galbis, J.A.; Muñoz-Guerra, S. *Macromolecules* **2006**, *39*, 1410-1416.
- Altun, S.; Ulcay, Y. *J. Polym. Environ.* **2004**, *12*, 231-237.
- Arshady, R. *J. Control. Release* **1991**, *17*, 1-21.
- Atfani, M.; Brisse, F. *Macromolecules* **1999**, *32*, 7741-7752.
- Bachmann, F.; Reimer, J.; Ruppenstein, M.; Thiem, J. *Macromol. Rapid Commun.* **1998**, *19*, 21-26.
- Benninga, H.A. *History of Lactic Acid Making: A Chapter in the History of Biotechnology*; Kluwer: Dordrecht, Boston and London, **1990**.
- Berkane, C.; Mezoul, G.; Lalot, T.; Brigodiot, M.; Maréchal, E. *Macromolecules* **1997**, *30*, 7729-7734.
- Berti, C.; Binassi, E.; Colonna, M.; Fiorini, M.; Kannan, G.; Karanam, S.; Mazzacurati, M.; Odeh, I.; Vannini, M. *US Pat. Appl. Publ.* 20100168371 (to SABIC-IP), **2010**.
- Binns, F.; Harffey, P.; Roberts, S.M.; Taylor, A. *J. Polym. Sci., Polym. Chem.*, **1998**, *36*, 2069-2079.
- Binns, F.; Harffey, P.; Roberts, S.M.; Taylor, A. *J. Chem. Soc., Perkin Trans. 1*, **1999**, *19*, 2671-2676.
- Bozell, J.J.; Holladay, J.E.; Johnson, D.; White, J.F. *Top Value Added Chemicals from Biomass - Volume II: Results of Screening for Potential Candidates from Biorefinery Lignin*. Report PNNL-16983., Pacific Northwest National Laboratory (PNNL) and National Renewable Energy Laboratory (NREL), **2007**,
http://www.pnl.gov/main/publications/external/technical_reports/PNNL-16983.pdf
[Accessed on May 2, 2013]
- Brady, L.; Brzozowski, A.M.; Derewenda, Z.S.; Dodson, E.; Dodson, G.; Tolley, S.; Turkenburg, J.P.; Christiansen, L.; Høge-Jensen, B.; Nørskov, L.; Thim, L.; Menge, U. *Nature* **1990**, *343*, 767-770.
- Braun, D.; Bergmann, M. *J. Prakt. Chem.* **1992**, *334*, 298-310.
- Breitkopf, N.; Dämbkes, G.; Bach, H. *US Patent* 5008473 (to Ruhrchemie Aktiengesellschaft), **1991**.
- Buck, K.W.; Duxbury, J.M.; Foster, A.B.; Perry, A.R.; Webber, J.M. *Carbohydr. Res.* **1966**, *2*, 122-131.

- Calundann, G.W. *US Patent* 4161470 (to Celanese Corp.), **1977**.
- Carothers, W.H. *J. Am. Chem. Soc.* **1929**, *51*, 2548-2559. (1929a)
- Carothers, W.H.; Arvin, J.A. *J. Am. Chem. Soc.* **1929**, *51*, 2560-2570. (1929b)
- Carothers, W.H.; Dorough, G.L. *J. Am. Chem. Soc.* **1930**, *52*, 711-721.
- Carothers, W.H. *Chem. Rev.* **1931**, *8*, 353-426.
- Carothers, W.H.; Dorough, G.L.; van Natta, F.J. *J. Am. Chem. Soc.* **1932**, *54*, 761-772.
- Carothers, W.H.; *Trans. Faraday. Soc.* **1936**, *32*, 39-53.
- Chang, T. *Polym. Eng. Sci.* **1970**, *10*, 364-368.
- Chang, S.; Sheu, M.; Chen, S. *J. Appl. Polym. Sci.* **1983**, *28*, 3289-3300.
- Charbonneau, L.F.; Johnson, R.E.; Witteler, H.B.; Khanarian, G. *US Patent* 5959066 (to HNA Holdings, Inc.), **1999**.
- Charbonneau, L.F.; Johnson, R.E. *WO Patent* 9954533 (to HNA Holdings, Inc.), **1999**.
- Charbonneau, L.F. *WO Patent* 2006032022 (to E.I. du Pont de Nemours and Co.), **2006**.
- Chen, G.Q.; Patel, M.K. *Chem. Rev.* **2012**, *112*, 2082-2089.
- Chiellini, E.; Corti, A.; Giovannini, A.; Narducci, P.; Paparella, M.; Solaro, R. *J. Environ. Polym. Degrad.* **1996**, *4*, 37-50.
- Chung, H.S.; Lee, J.W.; Kim, D.H.; Jun, J.N.; Lee, S.W. *WO Patent* 0011063 (to Ire Chemical Ltd.), **2000**.
- Chung, H.S.; Lee, J.W.; Kim, D.H.; Jun, J.N.; Lee, S.W. *EP Patent* 1106640A2 (to Ire Chemical Ltd.), **2001**. (2001a)
- Chung, H.S.; Lee, J.W.; Kim, D.H.; Jun, J.N.; Lee, S.W. *EP Patent* 1108737A2 (to Ire Chemical Ltd.), **2001**. (2001b)
- Coca-Cola Co., **2011**.
<http://www.coca-colacompany.com/stories/plant-bottle-basics> [Accessed on May 2, 2013]
- Cope, A.C.; Shen, T.Y. *J. Am. Chem. Soc.* **1956**, *78*, 3177-3182.
- Darwis, D.; Mitomo, H.; Enjoji, T.; Yoshii, F.; Makuuchi, K. *Polym. Degrad. Stabil.* **1998**, *62*, 259-265.
- Dean, B.D.; Matzner, M.; Tibbitt, J.M. *The Synthesis, Characterization, Reactions and Applications of Polymers*. In: Allen, G.; Bevington, J.C.; Eds. *Comprehensive Polymer Science*, Vol 5; Pergamon: Oxford, **1989**, p. 317.
- Dhamaniya, S.; Jacob, J. *Polymer* **2010**, *51*, 5392-5399.
- Dhamaniya, S.; Jacob, J. *Polym. Bull.* **2012**, *68*, 1287-1304.

Drent, E. *Eur. Patent* 478850A1 (to Shell Oil Company), **1992**.

Drew, H.D.K.; Haworth, W.N. *J. Chem. Soc.* **1927**, 775-779.

Du, H.Z.; Pang, X.; Yu, H.Y.; Zhuang, X.L.; Chen, X.S.; Cui, D.M.; Wang, X.H.; Jing, X.B. *Macromolecules* **2007**, *40*, 1904-1913.

Duh, B. *J. Appl. Polym. Sci.* **2001**, *81*, 1748-1761.

Duh, B. *Polymer* **2002**, *43*, 3147-3154.

DuPont. *DuPont Renewable Sourced Materials website*, **2013**

http://www2.dupont.com/Renewably_Sourced_Materials/en_US/procbuildingblocks.html
[Accessed on May 2, 2013]

Ellis, C. *US Patent* 2225313 (to Ellis-Foster Co.), **1937**.

Fakirov, S.; Fakirov, C.; Fischer, E.W.; Stamm, M. *Polymer* **1991**, *32*, 1773-1180.

Fenouillot, F.; Rosseau, A.; Colomines, G.; Saint-Loup, R.; Pascault, J.-P. *Prog. Polym. Sci.* **2010**, *35*, 578-622.

Fortunato, B.; Pilati, F.; Manaresi, P. *Polymer* **1981**, *22*, 655-657.

Fradet, A.; Maréchal, E. *Adv. Polym. Sci.* **1982**, *43*, 51-142.

Fradet, A.; Tessier, M. *Polyesters*. In: Rogers, M.E.; Long, T.E.; Eds. *Synthetic Methods in Step-Growth Polymers*; John Wiley & Sons: Hoboken, **2003**, pp. 17-134.

Galbis, J.A.; García-Martín, M.G. *Sugars as Monomers*. In: Belgacem, M.N.; Gandini, A.; Eds. *Monomers, Polymers and Composites from Renewable Resources*; Elsevier: Oxford, **2008**, 89-114.

Galbis, J.A.; García-Martín, M.G. *Chem. Curr. Top.* **2010**, *295*, 147-176.

Gallagher, F.G.; Hamilton, C.J.; Hansen, S.M.; Shin, H.; Huynkook; Tietz, R.F. *US Patent* 5171308 (to DuPont De Nemours and Co.), **1992**. (1992a)

Gallagher, F.G.; Hamilton, C.J.; Hansen, S.M.; Shin, H.; Huynkook; Tietz, R.F. *US Patent* 5171309 (to DuPont De Nemours and Co.), **1992**. (1992b)

Gallagher, F.G.; Gray, D.S.; Hamilton, C.J.; Tietz, R.F.; Wallenberger, F.T. *WO Patent* 9514740 (to DuPont De Nemours and Co.), **1995**.

Gallucci, R.R.; Patel, B.R. *Poly(butylene terephthalate)*. In: Scheirs, J.; Long, T.E.; Eds. *Modern Polyesters, Chemistry and Technology of Polyesters and Copolyesters*; John Wiley & Sons: Chichester, **2004**, pp. 293-321.

Gandini, A.; Belgacem, M.N. *Prog. Polym. Sci.* **1997**, *22*, 1203-1397.

Gandini, A.; Silvestre, A.J.D.; Pascoal Neto, C.; Sousa, A.F.; Gomes, M. *J. Polym. Sci., Polym. Chem.* **2009**, *47*, 295-298. (2009a)

Gandini, A.; Coelho, D.; Gomes, M.; Reis, B.; Silvestre, A. *J. Mater. Chem.* **2009**, *19*, 8656-8664. (2009b)

Gandini, A. *Monomers and Macromonomers from Renewable Resources*. In: Loos, K.; Ed. *Biocatalysis in Polymer Chemistry*; Wiley-VCH: Weinheim, **2010**.

Gandini, A. *Green Chem.* **2011**, *13*, 1061-1083.

Gao, Q.; Nan-Xun, H.; Zhi-Lian, T.; Gerking, L. *Chem. Eng. Sci.* **1997**, *52*, 371-376.

Gao, X.; Chen, J.C.; Wu, Q.; Chen, G.Q. *Curr. Opin. Biotechnol.* **2011**, *22*, 768-774.

García-Martín, M.G.; Ruiz Pérez, R.; Benito Hernández, E.; Galbis, J.A. *Macromolecules* **2006**, *39*, 7941-7949.

Gomes, M.; Gandini, A.; Silvestre, A.J.D.; Reis, B. *J. Polym. Sci., Polym. Chem.* **2011**, *49*, 3759-3768.

Gómez, R.; Varela, O. *Macromolecules* **2009**, *42*, 8112-8117.

Gross, S.; Flowers, D.; Roberts, G.; Kiserow, D.; DeSimone, J. *Macromolecules* **1999**, *32*, 3167-3169.

Gross, S.; Roberts, G.; Kiserow, D.; DeSimone, J. *Macromolecules* **2000**, *33*, 40-45.

Gubbels, E.; Jasinska-Walc, L.; Hermida Merino, D.; Goossens, H.; Koning, C. *Macromolecules* **2013**, *46*, 3975-3984. (2013a)

Gubbels, E.; Jasinska-Walc, L.; Koning, C. *J. Polym. Sci., Polym. Chem.* **2013**, *51*, 890-898. (2013b)

Gutman, A.L.; Knaani, D.; Bravdo, T. *Macromol. Symp.* **1997**, *122*, 39-44.

Holden, G.; Legge, N.R.; Quirk, R.; Schroeder, H.E. *Thermoplastic Elastomers*; Carl Hanser Verlag: Munich, **1996**.

Hu, J.; Gao, W.; Kulshrestha, A.; Gross, R.A. *Macromolecules* **2006**, *39*, 6789-6792.

Huang, B.; Walsh, J. *Polymer* **1998**, *39*, 6991-6999.

Huang, Y.M.; Li, H.; Huang, X.J.; Hu, Y.C.; Hu, Y. *Chin. J. Bioprocess Eng.* **2008**, *6*, 1-6.

IHS Chemical Process Economics Program (PEP) Report #284 *Bio-Based Adipic Acid*, **2012**.

<http://www.ihs.com/products/chemical/technology/pep/bio-based-adipic-acid.aspx>
[Accessed on May 2, 2013]

Ikada, Y.; Tsuji, H. *Macromol. Rapid Commun.* **2000**, *21*, 117-132.

Iribarren, J. I.; Martínez de Ilarduya, A.; Alemán, C.; Oraison, J. M.; Rodríguez-Galán, A.; Muñoz-Guerra, S. *Polymer* **2000**, *41*, 4869-4879.

Iwamoto, A.; Tokiwa, Y. *Polym. Degrad. Stabil.* **1994**, *45*, 205-213.

- Jackson, W.J. *Br. Polym. J.* **1980**, *12*, 154-162.
- Jansen, M.A.G.; Goossens, J.G.P.; de Wit, G.; Bailly, C.; Schick, C.; Koning, C.E. *Macromolecules* **2005**, *38*, 10658-10666.
- Jansen, M.A.G.; Goossens, J.G.P.; de Wit, G.; Bailly, C.; Koning, C.E. *Anal. Chim. Acta* **2006**, *557*, 19-30.
- Jansen, M.A.G.; Wu, L.H.; Goossens, J.G.P.; de Wit, G.; Bailly, C.; Koning, C.E. *J Polym. Sci., Polym. Chem.* **2007**, *45*, 882-899.
- Jansen, M.A.G.; Wu, L.H.; Goossens, J.G.P.; de Wit, G.; Bailly, C.; Koning, C.E.; Portale, G. *J Polym. Sci., Polym. Chem.* **2008**, *46*, 1203-1217.
- Japu, C.; Alla, A.; Martínez de Ilarduya, A.; García-Martín, M.G.; Benito, E.; Galbis, J.A.; Muñoz-Guerra, S. *Polym. Chem.* **2012**, *3*, 2092-2101.
- Japu, C.; Martínez de Ilarduya, A.; Alla, A.; Muñoz-Guerra, S. *Polymer* **2013**, *54*, 1573-1582. (2013a)
- Japu, C.; Martínez de Ilarduya, A.; Alla, A.; García-Martín, M.G.; Galbis, J.A.; Muñoz-Guerra, S. *Polym. Chem.* **2013**, *4*, 3524-3536. (2013b)
- Jasinska, L.; Villani, M.; Wu, J.; Van Es, D.; Klop, E.; Rastogi, S.; Koning, C. E. *Macromolecules* **2011**, *44*, 3458-3466.
- Jem, K.J.; van der Pol, J.F.; de Vos, S. *Plastics from Bacteria, Natural Functions and Applications*; Springer: Heidelberg, **2010**, pp. 323-346.
- Jiang, M.; Liu, Q.; Zhang, Q.; Ye, C.; Zhou, G. *J. Polym. Sci., Polym. Chem.* **2011**, *50*, 1026-1036.
- Kampouris, E.; Papaspyrides, C. *Polymer* **1985**, *26*, 413-417.
- Khanarian, G.; Charbonneau, L.F.; Johnson, R.E.; Witteler, H.B.; Lee, R.G.; Sandor, R.B. *US Patent* 6025061 (to HNA Holdings, Inc.), **2000**.
- Khanarian, G.; Charbonneau, L.F.; Witteler, H.B. *US Patent* 6359070 (to E.I. Du Pont de Nemours and Co.), **2002**.
- Ki, H.C.; Park, O.O. *Polymer* **2001**, *42*, 1849-1861.
- Kiely, D.E.; Chen, L.; Lin, T.-H. *J. Am. Chem. Soc.* **1994**, *116*, 571-578.
- Kiely, D.E.; Chen, L.; Lin, T.-H. *J. Polym. Sci., Polym. Chem.* **2000**, *38*, 594-603.
- Kim, Y.J.; Park, O.O. *J. Appl. Polym. Sci.* **1999**, *72*, 945-951.
- Kimura, H.; Yoshinari, T.; Takeishi, M. *Polym. J.* **1999**, *31*, 388-392.

- Kint, D.P.R.; Wigstrom, E.; Martínez de Ilarduya, A.; Alla, A.; Muñoz-Guerra, S. *J. Polym. Sci., Polym. Chem.* **2001**, *39*, 3250-3262.
- Kint, D.P.R.; Alla, A.; Deloret, E.; Campos, J.L.; Muñoz-Guerra, S. *Polymer* **2003**, *44*, 1321-1330.
- Kobayashi, S. *J. Polym. Sci., Polym. Chem.* **1999**, *37*, 3041-3056.
- Kobayashi, S.; Uyama, H. *Makromol. Chem. Rapid. Commun.* **1993**, *14*, 841-844.
- Kricheldorf, H.R.; Behnken, G.; Sell, M. *J. Macromol. Sci. Part A: Pure Appl. Chem.* **2007**, *44*, 679-684.
- Kwolek, S.L.; Morgan, P.W. *J. Polym. Sci., Polym. Chem.* **1964**, *2*, 2693-2703.
- Lalot, T.; Brigodiot, M.; Maréchal, E. *Polymer Properties*. In: Allen, G.; Aggarwal, S.L.; Russo, S.; Eds. *Comprehensive Polymer Science*, Vol. 2; Pergamon: Oxford, **1996**, p. 29.
- Lee, P.C.; Lee, S.Y.; Hong, S.H.; Chang, H.N. *Bioprocess Biosyst. Eng.* **2003**, *26*, 63-67.
- Liaw, D.-J.; Liaw, B.-Y.; Hsu, J.-J.; Cheng, Y.-C. *J. Polym. Sci., Polym. Chem.* **2000**, *38*, 4451-4456.
- Lichtenthaler, F.W. *Carbohydrates as Organic Raw Materials*. Ullmann's Encyclopedia of Industrial Chemistry, **2010**. DOI: 10.1002/14356007.n05_n07
- Linko, Y.-Y.; Wang, Z.-L.; Seppala, J. *Enz. Microb. Technol.* **1995**, *17*, 506-511.
- Ma, Y.; Agarwal, U.; Sikkema, P.; Lemstra, P. *Polymer* **2003**, *44*, 4085-4096.
- Mahajan, S.S.; Idage, B.B.; Chavan, N.N.; Sivaram, S. *J. Appl. Polym. Sci.* **1996**, *61*, 2297-2304.
- Mallon, F.; Beers, K.; Ives, A.; Ray, W. *J. Appl. Polym. Sci.* **1998**, *69*, 1789-1791.
- Marín, R.; Muñoz-Guerra, S. *J. Polym. Sci., Polym. Chem.* **2008**, *46*, 7996-8012.
- Marín, R.; Muñoz-Guerra, S. *J. Appl. Polym. Sci.* **2009**, *114*, 3723-3736.
- Matheson, N.K.; Angyal, S.J. *J. Chem. Soc.* **1952**, 1133-1138.
- Mehlretter, C.L.; Mellies. *J. Am. Chem. Soc.* **1955**, *77*, 427-428.
- Mezoul, G.; Lalot, T.; Brigodiot, M.; Maréchal, J. *J. Polym. Sci., Polym. Chem.* **1995**, *33*, 2691-2698.
- Mezoul, G.; Lalot, T.; Brigodiot, M.; Maréchal. *Polym. Bull.* **1996**, *36*, 541-548.
- Middleton, J.C.; Tipton, A.J. *Biomaterials* **2000**, *21*, 2335-2346.
- Minh, D.P.; Besson, M.; Pinel, C.; Fuertes, P.; Petitjean, C. *Top. Catal.* **2010**, *53*, 1270-1273.
- Moore, J.A.; Kelly, J.E. *Macromolecules* **1978**, *11*, 568-573.

- Moore, J.A.; Kelly, J.E. *Polymer* **1979**, *20*, 627-628.
- Moreau, C.; Belgacem, M.N.; Gandini, A. *Topic. Catal.* **2004**, *27*, 11-30.
- Müller, R.J. *Aliphatic-aromatic polyesters*. In: Bastioli, C.; Ed. *Handbook of Biodegradable Polymers*; Rapra Technology: Shawbury, **2005**, pp. 303-337.
- Mutlu, H.; Meier, M.A.R. *Eur. J. Lipid Sci. Technol.* **2010**, *112*, 10-30.
- Nagata, M.; Goto, H.; Sakai, W.; Tsutsumi, N. *Polymer* **2000**, *41*, 4373-4376.
- Noordover, B.A.J.; van Staalduinen, V.G.; Duchateau, R.; Koning, C.E.; van Benthem, R.A.T.M.; Mak, M. *Biomacromolecules* **2006**, *7*, 3406-3416.
- Noordover, B.A.J.; Duchateau, R.; van Benthem, R.A.T.M.; Ming, W.; Koning, C.E. *Biomacromolecules* **2007**, *8*, 3860-3870.
- Ohta, M.; Obuchi, S.; Yoshida, Y. *US Patent* 5444143 (to Mitsui Toatsu Chemicals, Inc.), **1995**.
- Okada, M.; Okada, Y.; Aoi, K. *J. Polym. Sci., Polym. Chem.* **1995**, *33*, 2813-2820.
- Okada, M.; Okada, Y.; Tao, A.; Aoi, K. *J. Appl. Polym. Sci.* **1996**, *62*, 2257-2265.
- Okada, M.; Tsunoda, K.; Tachikawa, K.; Aoi, K. *J. Appl. Polym. Sci.* **2000**, *77*, 338-346.
- Okada, M.; Aoi, K. *Current Trends Polym. Sci.* **2002**, *7*, 57-70.
- Pang, K.; Kotek, R.; Tonelli, A. *Prog. Polym. Sci.* **2006**, *31*, 1009-1037.
- Pang, X.; Du, H.Z.; Chen, X.S.; Wang, X.H.; Jing, X.B. *Chem. Eur. J.* **2008**, *14*, 3126-3136.
- Papaspyrides, C.D.; Vouyiouka, S.N. *Fundamentals of Solid State Polymerization*. In: Papaspyrides, C.D.; Vouyiouka, S.N.; Eds. *Solid State Polymerization*; John Wiley & sons: Hoboken, **2009**, pp 2-28.
- PepsiCo, **2011**.
<http://www.pepsico.com/PressRelease/PepsiCo-Develops-Worlds-First-100-Percent-Plant-Based-Renewably-Sourced-PET-Bott03152011.html> [Accessed on May 2, 2013]
- Pfeffer, J.; Ortel, M.; Spyrou, E.; Haas, T.; Korek, U.; Schmidt, H.; Dingerdissen, U. *WO Patent* 2011000585, **2011**. (2011a)
- Pfeffer, J.; Ortel, M.; Spyrou, E.; Haas, T.; Korek, U.; Schmidt, H.; Dingerdissen, U. *WO Patent* 2011000586, **2011**. (2011b)
- Raghavan, D. *Polym.-Plast. Technol. Eng.* **1995**, *34*, 41-63.
- Rappaport, H. *Outlook on Blow Molding Resins*, in the 26th Annual Blow Molding Conference, Atlanta, **2010**.
- Rebsdat, S; Mayer, D. *Ethylene Glycol, Ullmann's Encyclopedia of Industrial Chemistry*; Wiley-VCH: Weinheim, **2000**.

Rodney, R.L., Allinson, B.T.; Beckman, E.J.; Russell, A.J. *Biotechnol. Bioeng.* **1999**, *65*, 485-489.

Román-Leshkov, Y.; Chheda, J.N.; Dumesic, J.A. *Science* **2006**, *312*, 1933-1937.

Rodríguez Galán, A.; Bou, J.J.; Muñoz-Guerra, S. *J. Polym. Sci., Polym. Chem.* **1992**, *30*, 713-721.

Ryu, H.W.; Kang, K.H.; Yun, J.S. *Appl. Biochem. Biotechnol.* **1999**, *78*, 511-520.

Sabloug, R.; Duchateau, R.; Koning, C.E.; de Wit, G.; van Es, D.; Koelewijn, R.; van Haveren, J. *Biomacromolecules* **2008**, *9*, 3090-3097.

Schmidt, H.-W.; Guo, D. *Makromol. Chem.* **1988**, *189*, 2029-2037.

Shi, C.; Gross, S.; DeSimone, J.; Kiserow, D.; Roberts, G. *Macromolecules* **2001**, *34*, 2062-2064.

Shuai, X.; Jedlinski, Z.; Kowalczyk, M.; Rydz, J.; Tan, H. *Eur. Polym. J.* **1999**, *35*, 721-725.

Srinivasan, R.; Desai, P.; Abhiraman, A.; Knorr, R. *J. Appl. Polym. Sci.* **1994**, *53*, 1731-1743.

Srinivasan, R.; Almonacil, C.; Narayan, S.; Desai, P.; Abhiraman, A. *Macromolecules* **1998**, *31*, 6813-6821.

Storbeck, R.; Rehahn, M.; Ballauff, M. *Makromol. Chem.* **1993**, *194*, 53-64.

Storbeck, R.; Ballauff, M. *J. Appl. Polym. Sci.* **1996**, *59*, 1199-1202.

Tang, Z.Y.; Chen, X.S.; Pang, X.; Yang, Y.K.; Zhang, X.F.; Jing, J.P. *Biomacromolecules* **2004**, *5*, 965-970.

Thiem, J.; Lüders, H. *Polym. Bull.* **1984**, *11*, 365-369. (1984a)

Thiem, J.; Lüders, H. *Starch/Stärke* **1984**, *36*, 170-176. (1984b)

Thiem, J.; Lüders, H. *Makromol. Chem.* **1986**, *187*, 2775-2785.

Thomas, C.M. *Chem. Soc. Rev.* **2010**, *39*, 165-173.

Tokiwa, Y.; Suzuki, T. *J. Appl. Polym. Sci.* **1981**, *26*, 441-448.

Tokiwa, Y.; Jarerat, A. *Biotechnol. Lett.* **2004**, *26*, 771-777.

Uyama, H.; Yaguchi, S.; Kobayashi, S. *J. Polym. Sci., Polym. Chem.* **1999**, *37*, 2737-2745.

Uyama, H.; Klegraf, E.; Wada, S.; Kobayashi, S. *Chem. Lett.* **2000**, *29*, 800-801.

van Es, D.S. *J. Renew. Mater.* **2013**, *1*, 61-72.

van Haveren, J.; Oostveen, E.A.; Micciche, F.; Noordover, B.A.J.; Koning, C.E.; van Benthem, R.A.T.M. *J. Coat. Technol. Res.* **2007**, *4*, 177-186.

van Natta, F.J.; Hill, J.W.; Carothers, W.H. *J. Am. Chem. Soc.* **1934**, *56*, 455-457.

Vasnes, V.A.; Ignatov, V.N.; Vinogradova, S.V.; Tseitlin, H.M. *Makromol. Chem.* **1990**, *191*, 1759-1763.

Vouyiouka, S.N.; Karakatsani, E.K.; Papaspyrides, C.D. *Prog. Polym. Sci.* **2005**, *30*, 10-37.

Wang, Z.-L.; Hiltunen, K.; Orava, P.; Seppala, J.; Linko, Y.-Y. *J. Macromol. Sci. Pure Appl. Chem.* **1996**, *A33*, 599-612.

Warzelhan, V.; Pipper, G.; Seeliger, U.; Bauer, P.; Pagga, U.; Yamamoto, M. *WO Patent* 9625446 (to BASF AG), **1996**. (1996a)

Warzelhan, V.; Pipper, G.; Seeliger, U.; Bauer, P.; Beimborn, D.B.; Yamamoto, M. *WO Patent* 9625448 (to BASF AG), **1996**. (1996b)

Whinfield, J.R.; Dickson, J.T. *British Patent* 578079 (to ICI), **1946**.

Williams, C.K. *Chem. Soc. Rev.* **2007**, *36*, 1573-1580.

Witt, U.; Müller, R.J.; Augusta, J.; Widdecke, H.; Deckwer, W.D. *Macromol. Chem. Phys.* **1994**, *195*, 793-802.

Witt, U.; Müller, Deckwer, W.D. *J. Macromol. Sci. Pure Appl. Chem.* **1996**, *A32*, 851-856.

Witt, U.; Müller, Deckwer, W.D. *J. Environ. Polym. Degrad.* **1997**, *5*, 81-89.

Wright, L.W.; Brandner, J.D. *US Patent* 3023223 (to Atlas Chemical Industries, Inc.), **1962**.

Wu, X.Y.; Linko, Y.-Y.; Seppala, J.; Leisola, M.; Linko, P. *J. Ind. Microbiol. Biotechnol.* **1998**, *20*, 328-332.

Wu, Q.; Sun, S.Q.; Yu, P.H.F.; Chen, A.X.Z.; Chen, G.Q. *Acta. Polym. Sin.* **2000**, *6*, 751-756.

Wu, J.; Eduard, P.; Thiyagarajan, T.; van Haveren, J.; van Es, D.; Koning, C.E.; Lutz, M.; Foseca Guerra, C. *Chem. Sus. Chem.* **2011**, *4*, 599-603.

Wu, L.; Mincheva, R.; Xu, Y.; Raquez, J.-M.; Dubois, P. *Biomacromolecules* **2012**, *13*, 2973-2981. (2012a)

Wu, J.; Eduard, P.; Thiyagarajan, S.; Jasinska-Walc, L.; Rozanski, A.; Fonseca Guerra, C.; Noordover, B.A.J.; van Haveren, J.; van Es, D.S.; Koning, C.E. *Macromolecules* **2012**, *45*, 5069-5080. (2012b)

Wu, J. *Carbohydrate-based Building Blocks and Step-growth Polymers: Synthesis, Characterization and Structure-property relations*. PhD thesis, Eindhoven Technical University, **2012**.

Wu, J.; Eduard, P.; Jasinska-Walc, L.; Rozanski, A.; Noordover, B.A.J.; van Es, D.S.; Koning, C.E. *Macromolecules* **2013**, *46*, 384-394.

Xu, J.; Guo, B.H. *Plastics from Bacteria, Natural Functions and Applications*; Springer: Heidelberg, **2010**, pp. 347-388.

Yao, K.; McAuley, K.; Berg, D.; Marchildon, E. *Chem. Eng. Sci.* **2001**, *56*, 4801-4814.

Zamora, F.; Hakkou, K.; Alla, A.; Rivas, M.; Roffé, I.; Mancera, M.; Muñoz-Guerra, S.; Galbis, J.A. *J. Polym. Sci., Polym. Chem.* **2005**, *43*, 4570-4577. (2005a)

Zamora, F.; Hakkou, K.; Alla, A.; Espartero, J. L.; Muñoz-Guerra, S.; Galbis, J.A. *J. Polym. Sci., Polym. Chem.* **2005**, *43*, 6394-6410. (2005b)

Zamora, F.; Hakkou, K.; Alla, A.; Muñoz-Guerra, S.; Galbis, J.A. *Polym. Degr. Stabil.* **2006**, *91*, 2654-2659.

Zamora, F.; Hakkou, K.; Alla, A.; Marín-Bernabé, R.; De Paz, M.V.; Martínez de Ilarduya, A.; Muñoz-Guerra, S.; Galbis, J.A. *J. Polym. Sci., Polym. Chem.* **2008**, *46*, 5167-5179.

Zamora, F.; Hakkou, K.; Alla, A.; Rivas, M.; Martínez de Ilarduya, A.; Muñoz-Guerra, S.; Galbis, J. A. *J. Polym. Sci., Polym. Chem.* **2009**, *47*, 1168-1177.

Zhao, H.; Holladay, J.E.; Brown, H.; Zhang, Z.C. *Science* **2007**, *316*, 1597-1600.

Zhu, J.; Cai, J.; Xie, W.; Chen, P.-H.; Gazzano, M.; Scandola, M.; Gross, R.A. *Macromolecules* **2013**, *46*, 796-804.

CHAPTER 3

ALIPHATIC POLYESTERS FROM CYCLIC ACETALIZED CARBOHYDRATE-BASED MONOMERS

3.1. Aim and scope of this Chapter

Driven by increasing concerns on sustainable development and minimizing the impact of materials on the environment, biodegradable polymers have attracted a great deal of interest in the last decades. Among synthetic biodegradable polymers, aliphatic polyesters are the most widely studied and largely used. Aliphatic polyesters such as poly(butylene succinate) (PBS), poly(L-lactic acid) (PLA), poly(ϵ -caprolactone) (PCL) and poly(3-hydroxy butyrate) (PHB) have found intensive use in a broad variety of medical applications such as bioresorbable surgical sutures, prosthesis, dental implants, bone screw and plates for temporary internal fracture fixation, and controlled drug delivery systems. Aliphatic polyesters are also receiving attention as materials suitable for replacing conventional commodity plastics in injection-molded articles (cutlery, brushes), tubular films (composting bags, shopping bags), packaging and food tray. However, most of them have a glass-transition temperature (T_g) not high enough for its use in those applications where stiffness and thermal resistance are priority requisites. In this regard, various approaches such as blending and copolymerization with aromatic polyesters as poly(butylene terephthalate) (PBT) and poly(ethylene terephthalate) (PET) have been explored. The interest for cyclic monomers arises from their capacity for adding stiffness to the polymer chain with the subsequent increase in T_g ; the disadvantage of using aromatic units for such purpose is that they are originated from fossil feedstocks and are reluctant to biodegradation.

The use of carbohydrate-based monomers with a cyclic structure constitutes a scarcely explored approach for the preparation of renewable aliphatic polyesters with improved physical properties, especially those related to polymer chain stiffness. Moreover, carbohydrate-derived polycondensates typically display enhanced hydrophilicity, lower toxicity and higher susceptibility to hydrolytic degradation and biodegradation than those coming from petrochemical feedstocks.

1,4:3,6-Dianhydro-D-glucitol, known as isosorbide, along with their two less accessible stereoisomers isomannide and isoidide, are currently drawing an enormous interest in the polymer science field as bio-based monomers able to provide enhanced stiffness into the polymer chain they are incorporated. Nevertheless, the main shortcoming of isosorbide and its isomers is the limited reactivity of their secondary hydroxyl groups; in fact, this feature seriously hampers the polycondensation reaction in the melt, so aliphatic polyesters from 1,4:3,6-dianhydrohexitols and aliphatic dicarboxylic

acids or dicarboxylic esters obtained by this method display rather limited molecular weights. Higher molecular weights are achievable via polycondensation with aliphatic dicarboxylic chlorides, but this method is not appropriate for industrial application.

In this Chapter, aliphatic polyesters from bicyclic acetalized carbohydrate-based monomers will be obtained by polycondensation in the melt and in the total absence of solvents, to imitate as far as possible the conditions usually applied in the industry. The characterization of the new polyesters, the evaluation of their thermal and mechanical properties and their degradability and biodegradability will be reported.

3.2. Carbohydrate-based polyesters made from bicyclic acetalized galactaric acid

Summary: The dimethyl ester of 2,3:4,5-di-O-methylene-galactaric acid (Galx) was made to react in the melt with 1,n-alkanediols $\text{HO}(\text{CH}_2)_n\text{OH}$ containing even numbers of methylenes (n from 6 to 12) to produce linear polycyclic polyesters. Two sets of poly(alkylene 2,3:4,5-di-O-methylene-galactarate) polyesters (PE-nGalx) with weight-average molecular weights in the $\sim 5,000$ - $10,000$ and $\sim 35,000$ - $45,000 \text{ g}\cdot\text{mol}^{-1}$ ranges were obtained using TBT and DBTO catalysts, respectively. For comparative purposes a set of poly(alkylene adipate) polyesters (PE-nAd) was also synthesized with molecular weights in the higher range using a similar procedure. The thermal stability of PE-nGalx was greater than that of PE-nAd although it notably decayed as molecular weight decreased. The replacement of Ad by Galx in the polyesters caused increases in T_g of up to $70 \text{ }^\circ\text{C}$, and almost doubled the tensile mechanical parameters. All PE-nGalx were semicrystalline but only those made from 1,12-dodecanediol were able to crystallize from the melt with a crystallization rate that diminished as the molecular weight increased. In general, the galactarate containing polyesters displayed higher solubility and wettability than polyadipates, they hydrolyzed faster and exhibited comparable sensitivity to the action of lipases.

Publication derived from this work:

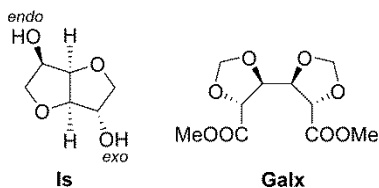
Lavilla, C.; Alla, A.; Martínez de Ilarduya, A.; Benito, E.; García-Martín, M.G.; Galbis, J.A.; Muñoz-Guerra, S. *Biomacromolecules* **2011**, *12*, 2642-2652.

3.2.1. Introduction

The development of bio-based polymers today is drawing an enormous amount of interest for their potential to reduce the utilization of petrochemicals and to increase the added-value of agriculture products and wastes (Wool and Sun, 2005). Among the renewable naturally-occurring sources, carbohydrates stand out in a privileged position due to their huge abundance and because they are inexhaustible and readily available. A good assortment of monomers based on carbohydrates has been recently explored for making different classes of polymers (Wang *et al.*, 2002; Bou *et al.*, 1996; Kricheldorf, 1997; Galbis and García-Martín, 2008). The hydroxyl and carboxylic rich functionality of these compounds makes them mostly appropriate for polycondensation in spite of the fact that certain chemical handling for group protection will be required if linear polymers are searched. Carbohydrate-based polycondensates may be provided with a great diversity of chemical structures and unusual properties; they typically display enhanced hydrophilicity, less toxicity, and higher susceptibility to biodegradation than petrochemical-based polycondensates, offering therefore a wide possibility of applications in food packaging and medical devices (García-Martín *et al.*, 2005; Haider and Williams, 2008).

Among the wide diversity of sugar-derived monomers that have been recently explored, 1,4:3,6-dianhydrohexitols have drawn particular attention for the synthesis of linear polycondensates (Fenouillot *et al.*, 2010; Galbis and García-Martín, 2010). In these hexitols, the four exceeding hydroxyl groups are blocked by intramolecular etherification leading to a bicyclic structure with the secondary 2- and 5-hydroxyl groups standing free for reaction. The interest for monomers having a cyclic structure arises from their capacity for adding stiffness to the polymer chain with the subsequent increasing in the T_g . 1,4:3,6-Dianhydro-D-glucitol known as isosorbide (Is) is the only dianhydrohexitol industrially available today because it can be produced from cereal starch through an economically acceptable process. It is composed of two *cis*-fused nearly planar tetrahydrofuran rings with a dihedral angle of 120° and the 2- and 5-hydroxyl groups in *endo* and *exo* positions, respectively (Scheme 3.1). Isosorbide has been extensively investigated in the last decades as a convenient building block for diverse polycondensates (Chatti *et al.*, 2006; Caouthar *et al.*, 2007; Sablong *et al.*, 2008; Noordover *et al.*, 2008; Marín and Muñoz-Guerra, 2009). In this line, special attention is given to aromatic polyesters and copolyesters (Thiem and Lüders, 1984; Storbeck *et al.*, 1993, Quintana *et al.*, 2011), in

which Is has proven to replace successfully petrochemical diols without detriment, or even with improvement, of their properties.



Scheme 3.1. Chemical structures of 1,4:3,6-dianhydrosorbitol (isosorbide, Is) and dimethyl 2,3:4,5-di-O-methylene galactarate (Galx).

In this work we present a new bicyclic carbohydrate-based monomer useful for the preparation of linear polycondensates, specifically for the synthesis of aliphatic polyesters. Dimethyl 2,3:4,5-di-O-methylene-galactarate (Scheme 3.1), abbreviated as Galx, is the dimethyl ester of galactaric acid with the hydroxyl groups acetalized with formaldehyde. This compound is readily synthesized in one step from commercially available mucic acid (galactaric acid) which in turn is produced from naturally-occurring D-galactose or D-galactose-containing compounds by oxidation with nitric acid (Butler *et al.*, 1958). Contrary to isosorbide, Galx is centrosymmetric and therefore does not generate *regicity* in the growing polymer chain, and its two carboxyl groups display the same reactivity because they are spatially undistinguishable.

The use of acetalized aldaric acid derivatives as building blocks for the synthesis of polycondensates is not new, but most of the cases reported so far refer to polyamides and polyesters derived from acetalized tartaric acid, which contain a dioxolane ring forming part of the polymer backbone. Thus, Muñoz-Guerra *et al.* have described the synthesis and crystal structure of linear polyamides from di-O-methylene L-tartaric acid and several diamines (Rodríguez-Galán *et al.*, 1992; Iribarren *et al.*, 2000), and Kimura *et al.* studied their biodegradability (Kimura *et al.*, 1999). More recently, low molecular weight polyesters made from di-O-isopropylidene L-tartaric acid and alkanediols have been reported (Dhamaniya and Jacob, 2010). To our knowledge, bicyclic acetalized aldaric acid derivatives have not been explored for the synthesis of polycondensates to date. It should be mentioned however that 1-deoxy-1-isocyanate-2,3:4,5-di-O-isopropylidene-D-galactitol has been synthesized and used as monomer for the preparation of $[n]$ -polyurethanes (Gómez and Varela, 2009).

3.2.2. Experimental section

3.2.2.1. Materials

Dimethyl 2,3:4,5-di-O-methylene-galactarate was synthesized following the procedure reported by Stacey *et al.* (Butler *et al.*, 1958). The reagents 1,6-hexanediol (97%), 1,8-octanediol (98%), 1,10-decanediol (98%), 1,12-dodecanediol (99%), dimethyl adipate (> 99%), and the catalysts titanium (IV) tetrabutoxide (TBT, 98%) and dibutyl tin oxide (DBTO, 98%) were purchased from Sigma-Aldrich. Solvents used for purification and characterization, as chloroform, methanol and diethyl ether, and solvents used in the solubility essays, were purchased from Panreac and were all of either technical or high-purity grade. The enzymes used in biodegradation experiments, lipase from porcine pancreas (activity 15-35 U·mg⁻¹, pH 8.0, 37 °C) and Amano lipase from *Pseudomonas fluorescens* (activity ≥ 20 U·mg⁻¹, pH 8.0, 55 °C) were also purchased from Sigma-Aldrich. One unit (U) was defined as that amount of enzyme which catalyzed the release of fatty acid from triglycerides at the rate of 1 μmol·min⁻¹. All the reagents and solvents were used as received without further purification.

3.2.2.2. General methods

¹H and ¹³C NMR spectra were recorded on a Bruker AMX-300 spectrometer at 25.0 °C operating at 300.1 and 75.5 MHz, respectively. Polyesters and water degradation products were dissolved in deuterated chloroform or deuterated water, and spectra were internally referenced to tetramethylsilane (TMS) or the sodium salt of 3-(trimethylsilyl)-propanesulfonic acid. About 10 and 50 mg of sample dissolved in 1 mL of solvent were used for ¹H and ¹³C NMR, respectively. A total of 64 scans were acquired for ¹H and 1000-10000 for ¹³C, with 32 and 64-K data points as well as relaxation delays of 1 and 2 s, respectively. Elemental analyses were determined in the Microanalysis Laboratories of the CSIC, Barcelona, Spain. FTIR measurements were carried out in a Jasco 4100 FTIR spectrophotometer, coupled with an ATR accessory Specac MKII, with a single reflection Golden Gate diamond, ZnSe lenses and a high stability temperature driver West6100+. The absorbance of the sample was recorded in the range of 4000-550 cm⁻¹ accumulating 32 scans for each run. Intrinsic viscosities of polyesters dissolved in chloroform were measured in an Anton Paar AMVn Automated Micro Viscosimeter at 25.00±0.01 °C, using the VisioLab for AMVn software. Gel permeation chromatograms were acquired at 35.0 °C with a Waters equipment provided with a refraction-index detector. The samples were chromatographed with 0.05 M sodium trifluoroacetate-hexafluoroisopropanol

(NaTFA-HFIP) using a polystyrene-divinylbenzene packed linear column with a flow rate of $0.5 \text{ mL}\cdot\text{min}^{-1}$. Chromatograms were calibrated against poly(methyl methacrylate) (PMMA) monodisperse standards. The thermal behavior of polyesters was examined by DSC using a Perkin Elmer DSC Pyris 1. DSC data were obtained from 3 to 5 mg samples at heating/cooling rates of $10 \text{ }^\circ\text{C}\cdot\text{min}^{-1}$ under a nitrogen flow of $20 \text{ mL}\cdot\text{min}^{-1}$. Indium and zinc were used as standards for temperature and enthalpy calibration. The glass-transition temperatures were determined at a heating rate of $20 \text{ }^\circ\text{C}\cdot\text{min}^{-1}$ from rapidly melt-quenched polymer samples. The treatment of the samples for isothermal crystallization experiments was the following: the thermal history was removed by heating the sample up to $150 \text{ }^\circ\text{C}$ and left at this temperature for 5 min, and then it was cooled at $20 \text{ }^\circ\text{C}\cdot\text{min}^{-1}$ to the selected crystallization temperature, where it was left to crystallize until saturation. Isothermal crystallization under the same conditions was also carried out in an Olympus BX51 Polarizing Optical Microscope coupled to a THMS LINKAM heating plate and a cooling system LNP (Liquid Nitrogen Pump). Thermogravimetric analyses were performed under a nitrogen flow of $20 \text{ mL}\cdot\text{min}^{-1}$ at a heating rate of $10 \text{ }^\circ\text{C}\cdot\text{min}^{-1}$, within a temperature range of 30 to $600 \text{ }^\circ\text{C}$, using a Perkin Elmer TGA 6 equipment. Sample weights of about 10-15 mg were used in these experiments. Films for mechanical testing and contact angle measurements were prepared with a thickness of $\sim 200 \text{ }\mu\text{m}$ by casting from a chloroform solution at a concentration of $100 \text{ g}\cdot\text{L}^{-1}$. For evaluating mechanical properties, the films were cut into strips with a width of 3 mm, while the distance between testing marks was 10 mm. The tensile strength, elongation at break and Young's modulus were measured at a stretching rate of $30 \text{ mm}\cdot\text{min}^{-1}$ on a Zwick 2.5/TN1S testing machine coupled with a compressor Dalbe DR 150, at $23 \text{ }^\circ\text{C}$. Contact angles between liquid and polyester film surfaces were measured by means of a Krüss DSA 100 contact angle measuring system. Angle values were registered after 3 min of dropping $15 \text{ }\mu\text{L}$ of either water or ethylene glycol onto the polyester surface at $23 \text{ }^\circ\text{C}$. Scanning electron microscopy (SEM) images were taken with a field-emission JEOL JSM-7001F instrument (JEOL, Japan) from uncoated samples.

3.2.2.3. Polymer synthesis

Synthesis of poly(alkylene 2,3:4,5-di-O-methylene galactarate)s (PE-*n*Galx). PE-*n*Galx polyesters were obtained from an aliphatic α,ω -diol (1,6-hexanediol, 1,8-octanediol, 1,10-decanediol or 1,12-dodecanediol) and dimethyl 2,3:4,5-di-O-methylene-galactarate.

Procedure A. A mixture of dimethyl 2,3:4,5-di-*O*-methylene-galactarate and the corresponding diol at a molar ratio of 1/1 was prepared in a round-bottom flask, and several cycles of argon and vacuum were applied. The temperature was raised to 135 °C for 30 min with stirring until homogenization of the mixture, and then TBT catalyst (0.5% mol respect to monomers) was added. Transesterification reactions were carried out under argon at heating at 140 °C for 4 h followed by two periods of 1 h at 150 and 160 °C, respectively. Polycondensation reactions were performed for 2 h at 175 °C under vacuum (0.6-1.3 mbar). The polymerized mixture was then dissolved in dichloromethane, and the solution was poured dropwise into diethyl ether while stirring. The precipitated solid was filtered, washed with diethyl ether, and dried under vacuum.

Procedure B. The reaction was performed in a three-necked, cylindrical-bottom flask equipped with a mechanical stirrer, a nitrogen inlet and a vacuum distillation outlet. A 1/1 molar ratio of the diol to dimethyl 2,3:4,5-di-*O*-methylene-galactarate and dibutyl tin oxide (DBTO) as catalyst (0.4% mol respect to monomers) were used. The apparatus was vented with nitrogen several times at room temperature to remove the air and avoid oxidation during the polymerization. Transesterification reactions were carried out under a low nitrogen flow for a period of 3 h at 140 °C. Polycondensation reactions were left to proceed for 5 h at 140 °C, under a 0.03-0.06 mbar vacuum. Then, the reaction mixture was cooled to room temperature, and the atmospheric pressure was recovered with nitrogen to prevent degradation. Polymers obtained were dissolved in chloroform and precipitated in excess of methanol to remove unreacted monomers and remaining oligomers. Finally, the polymer was collected by filtration, extensively washed with methanol and diethyl ether, and dried under vacuum.

PE-6Galx. IR (film), ν (cm⁻¹): 1734 (C=O st), 1260 (C-O asym st, ester), 1165 (C-O sym st, ester), 1093 (C-O asym st, acetal), 799 (C-O sym st, acetal), 724 (CH₂ rock). ¹H NMR (300.1 MHz, CDCl₃), δ (ppm): 5.25 and 5.08 (2 s, 4H, 2CH₂), 4.61 (m, 2H, 2CH), 4.27 (m, 2H, 2CH), 4.20 (t, 4H, 2CH₂), 1.70 (m, 4H, 2CH₂), 1.40 (m, 4H, 2CH₂). ¹³C (75.5 MHz, CDCl₃), δ (ppm): 170.3 (CO), 96.8, 79.0, 75.3, 65.6, 28.4, 25.4. Anal. Calcd for C₁₄H₂₀O₈·0.25 H₂O: C, 52.40; H, 6.37. Found: C, 52.08; H, 6.44.

PE-8Galx. IR (film), ν (cm⁻¹): 1733 (C=O st), 1259 (C-O asym st, ester), 1167 (C-O sym st, ester), 1092 (C-O asym st, acetal), 796 (C-O sym st, acetal), 719 (CH₂ rock). ¹H NMR (300.1 MHz, CDCl₃), δ (ppm): 5.26 and 5.08 (2s, 4H, 2CH₂), 4.61 (m, 2H, 2CH), 4.28 (m, 2H, 2CH), 4.20 (t, 4H, 2CH₂), 1.68 (m, 4H, 2 CH₂), 1.34 (m, 8H, 4CH₂). ¹³C (75.5 MHz,

CDCl_3), δ (ppm): 170.3 (CO), 96.8, 79.0, 75.2, 65.8, 29.0, 28.5, 25.7. Anal. Calcd for $\text{C}_{16}\text{H}_{24}\text{O}_8 \cdot 0.25 \text{H}_2\text{O}$: C, 55.09; H, 7.08. Found: C, 55.08; H, 7.02.

PE-10Galx. IR (film), ν (cm^{-1}): 1734 (C=O st), 1259 (C-O asym st, ester), 1168 (C-O st sym, ester), 1093 (C-O asym st, acetal), 797 (C-O sym st, acetal), 719 (CH_2 rock). ^1H NMR (300.1 MHz, CDCl_3), δ (ppm): 5.25 and 5.07 (2s, 4H, 2 CH_2), 4.60 (m, 2H, 2CH), 4.28 (m, 2H, 2CH), 4.19 (t, 4H, 2 CH_2), 1.67 (m, 4H, 2 CH_2), 1.30 (m, 12H, 6 CH_2). ^{13}C (75.5 MHz, CDCl_3), δ (ppm): 170.3 (CO), 96.8, 79.0, 75.2, 65.9, 29.4, 29.1, 28.5, 25.7. Anal. Calcd for $\text{C}_{18}\text{H}_{28}\text{O}_8 \cdot 0.25 \text{H}_2\text{O}$: C, 58.05; H, 7.58. Found: C, 57.47; H, 7.47.

PE-12Galx. IR (film), ν (cm^{-1}): 1734 (C=O st), 1259 (C-O asym st, ester), 1168 (C-O sym st, ester), 1095 (C-O asym st, acetal), 801 (C-O sym st, acetal), 719 (CH_2 rock). ^1H NMR (300.1 MHz, CDCl_3), δ (ppm): 5.25 and 5.07 (2s, 4H, 2 CH_2), 4.60 (m, 2H, 2CH), 4.28 (m, 2H, 2CH), 4.19 (t, 4H, 2 CH_2), 1.67 (m, 4H, 2 CH_2), 1.27 (m, 16H, 8 CH_2). ^{13}C (75.5 MHz, CDCl_3), δ (ppm): 170.3 (CO), 96.8, 79.0, 75.1, 65.9, 29.5, 29.4, 29.2, 28.5, 25.8. Anal. Calcd for $\text{C}_{20}\text{H}_{32}\text{O}_8 \cdot 0.25 \text{H}_2\text{O}$: C, 59.32; H, 8.09. Found: C, 58.60; H, 8.07.

Synthesis of poly(alkylene adipate)s (PE-*n*Ad). Dimethyl adipate and the corresponding aliphatic α,ω -diol (1,6-hexanediol, 1,8-octanediol, 1,10-decanediol or 1,12-dodecanediol) were introduced in a three-necked, cylindrical-bottom flask equipped with a mechanical stirrer, a nitrogen inlet and a vacuum distillation outlet. A molar excess of 16, 11, 3 and 2% of diol was used for 1,6-hexanediol, 1,8-octanediol, 1,10-decanediol and 1,12-dodecanediol, respectively. The apparatus was vented with nitrogen several times at room temperature, heated at 180 °C under stirring until homogeneization of the mixture, and then titanium (IV) butoxide (TBT) catalyst (0.5% mol respect to dimethyl adipate) was added. Transesterification reactions were carried out under a low nitrogen flow for a period of 3 h at 180 °C. The temperature was then increased to 200 °C, and polycondensation reactions were performed at this temperature for 3 h, under a 0.03-0.06 mbar vacuum. After that, the reaction mixture was cooled to room temperature, and atmospheric pressure was recovered with nitrogen to prevent degradation. The solid mass was dissolved in chloroform, and the polymer was precipitated with methanol, collected by filtration, extensively washed with methanol and diethyl ether, and dried under vacuum.

PE-6Ad. IR (film), ν (cm^{-1}): 1724 (C=O st), 1256 (C-O asym st, ester), 1162 (C-O st sym ester), 733 and 725 (CH_2 rock). ^1H NMR (300.1 MHz, CDCl_3), δ (ppm): 4.06 (t, 4H, 2 CH_2), 2.32 (t, 4H, 2 CH_2), 1.64 (m, 8H, 4 CH_2), 1.38 (m, 4H, 2 CH_2). ^{13}C (75.5 MHz, CDCl_3), δ

(ppm): 173.4 (CO), 64.3, 33.9, 28.5, 25.6, 24.4. Anal. Calcd for C₁₂H₂₀O₄: C, 63.14; H, 8.83. Found: C, 62.46; H, 8.84.

PE-8Ad. IR (film), ν (cm⁻¹): 1721 (C=O st), 1257 (C-O asym st, ester), 1165 (C-O sym st, ester), 733 and 725 (CH₂ rock). ¹H NMR (300.1 MHz, CDCl₃), δ (ppm): 4.05 (t, 4H, 2CH₂), 2.32 (t, 4H, 2CH₂), 1.65 (m, 8H, 4CH₂), 1.32 (m, 8H, 4CH₂). ¹³C (75.5 MHz, CDCl₃), δ (ppm): 173.4 (CO), 64.5, 33.9, 29.1, 28.6, 25.8, 24.4. Anal. Calcd for C₁₄H₂₄O₄: C, 65.60; H, 9.44. Found: C, 65.06; H, 9.55.

PE-10Ad. IR (film), ν (cm⁻¹): 1726 (C=O st), 1257 (C-O asym st, ester), 1164 (C-O sym st, ester), 732 and 723 (CH₂ rock). ¹H NMR (300.1 MHz, CDCl₃), δ (ppm): 4.05 (t, 4H, 2CH₂), 2.32 (t, 4H, 2CH₂), 1.62 (m, 8H, 4CH₂), 1.30 (m, 12H, 6CH₂). ¹³C (75.5 MHz, CDCl₃), δ (ppm): 173.4 (CO), 64.5, 34.0, 29.4, 29.2, 28.6, 25.9, 24.5. Anal. Calcd for C₁₆H₂₈O₄: C, 67.57; H, 9.92. Found: C, 67.29; H, 9.98.

PE-12Ad. IR (film), ν (cm⁻¹): 1728 (C=O st), 1259 (C-O asym st, ester), 1162 (C-O sym st, ester), 733 and 724 (CH₂ rock). ¹H NMR (300.1 MHz, CDCl₃), δ (ppm): 4.06 (t, 4H, 2CH₂), 2.32 (t, 4H, 2CH₂), 1.64 (m, 8H, 4CH₂), 1.28 (m, 16H, 8CH₂). ¹³C (75.5 MHz, CDCl₃), δ (ppm): 173.4 (CO), 64.5, 34.0, 29.5, 29.4, 29.2, 28.5, 25.9, 24.4. Anal. Calcd for C₁₈H₃₂O₄: C, 69.19; H, 10.32. Found: C, 69.22; H, 10.39.

3.2.2.4. Hydrolytic and enzymatic degradation procedures

For hydrolytic and enzymatic degradation studies, films of polyesters with a thickness of ~200 μ m were prepared by casting from a chloroform solution ($c=100$ g·L⁻¹). The films were cut into 10 mm diameter, 20 to 30 mg weight disks and dried under vacuum to a constant weight. For hydrolytic degradation, samples were immersed in vials containing 10 mL of sodium phosphate buffer (pH 7.4), sodium carbonate buffer (pH 10.5) or citric acid buffer (pH 2.0) at 23 °C. After incubation for the scheduled period of time, the samples were rinsed thoroughly with distilled water and dried to a constant weight. The enzymatic degradation was carried out at 37 °C in vials containing 10 mL of the enzymatic medium, consisting of a pH 7.4 buffered sodium phosphate solution containing either lipase from porcine pancreas (10 mg) or Amano lipase from *Pseudomonas fluorescens* (10 mg). The buffered enzyme solution was replaced every 72 h to maintain the enzyme activity. At the end of the scheduled incubation periods, the disks were withdrawn from the incubation medium, washed thoroughly with distilled water

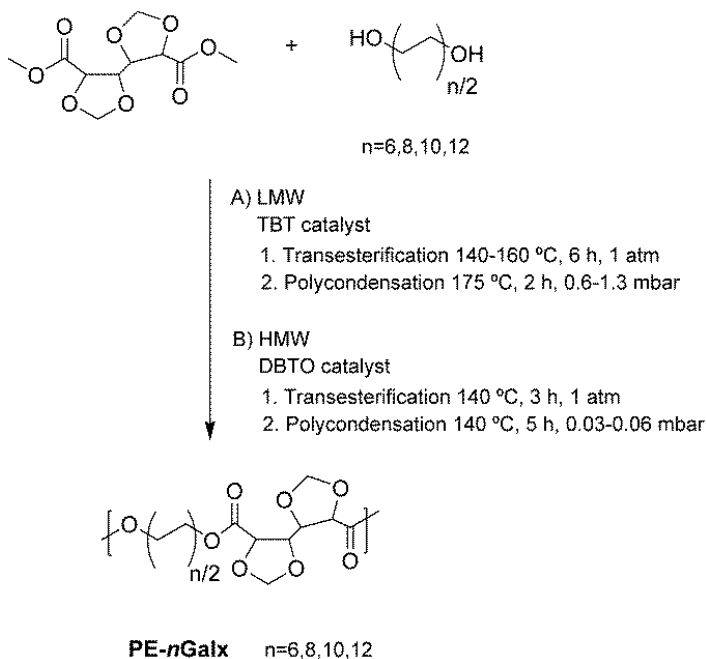
and dried to constant weight and analyzed by GPC chromatography and NMR spectroscopy.

3.2.3. Results and discussion

3.2.3.1. Synthesis and characterization

The synthesis of polygalactarates (PE-*n*Galx) and polyadipates (PE-*n*Ad) studied in this work was carried out by reaction of linear 1,*n*-alkanediols with the dimethyl ester of either 2,3:4,5-di-*O*-methylene-galactaric or adipic acid, respectively. Reactions were invariably performed in the melt and in the total absence of solvents to imitate as far as possible the conditions usually applied in the industrial practice. They were conducted in two successive stages at temperatures between 140 and 200 °C and under a progressively diminishing reaction pressure to facilitate the removal of released by-products. For the synthesis of polyadipates, the reaction was carried out at 180-200 °C using the familiar TBT catalyst and a small excess of diol with regard to the diester to compensate for the loss of volatiles. The resulting PE-*n*Ad polyesters had M_w between 38,000 and 42,000 g·mol⁻¹, with polydispersities close to 2. When this procedure was applied to the synthesis of polygalactarates, nonsoluble products were invariably obtained, suggesting the occurrence of cross-linking reactions involving the acetal group. It is noteworthy to mention in this regard that the opening of the tetrahydrofuran rings of isomannide has been reported to take place in the polycondensation of this compound with terephthalic acid (Thiem and Lüders, 1984). To circumvent such undesirable side reactions, some modifications were explored in this work. As a result, two slightly different procedures, which are detailed in Scheme 3.2, leading to linear polyesters with dissimilar molecular weights, were finally applied for obtaining PE-*n*Galx. In procedure A, polycondensation was carried out within the 140-175 °C temperature range with TBT catalyst and under a minimum pressure of 0.6 mbar; in this case, the resulting polyesters attained relatively small molecular weights, with M_w confined in the ~5,000-10,000 g·mol⁻¹ interval and intrinsic viscosities ranging between 0.19 and 0.23 dL·g⁻¹. In procedure B, TBT was replaced by the more active DBTO catalyst, temperature was maintained at 140 °C along the whole process, and pressure in the second step was lowered down to hundredths of a mbar; under these conditions, PE-*n*Galx with intrinsic viscosities above 0.5 dL·g⁻¹ and M_w comprised in the ~35,000-45,000 g·mol⁻¹ range were obtained. The polymer size features of the three sets of polyesters are compared in Table 3.1. In

addition to GPC, the M_n of the polyesters were also estimated by end-group analysis carried out by NMR, and an acceptable concordance was found between values provided by the two techniques; with the exception of PE-10Galx obtained by procedure A, the polydispersity of the polyesters in the three series was not far from 2, as it is usually found in linear polycondensates.



Scheme 3.2. Polymerization reactions leading to PE-*n*Galx polyesters.

The composition of polygalactarates obtained by procedure B as well as of polyadipates was ascertained by combustion analysis. It was noticed that a better correspondence between theoretical and experimental values could be attained if calculations were made assuming that one-fourth of a mol of water per mol of polyester was present in PE-*n*Galx. This approach is habitually used with carbohydrate-based polycondensates to take into account the high water affinity exhibited by these compounds (Bueno *et al.*, 1995). Infrared spectra of PE-*n*Galx were very similar for the whole series showing the typical carboxylate (~ 1730 , ~ 1260 and ~ 1170 cm^{-1}) and cyclic acetal (~ 1090 cm^{-1} and ~ 800 cm^{-1}) stretching absorptions as well as the methylene stretching (3000 - 2850 cm^{-1}), bending (~ 1470 cm^{-1}) and rocking (~ 720 cm^{-1}) bands, with

intensities increasing steadily with the value of n . The same absorption bands were observed in the infrared spectra recorded from the PE- n Ad series but with the logical absence of those arising from the acetal group. The precise wavenumber values observed for each polymer are given in Section 3.2.2, and the IR spectra of the three sets of polyesters are provided in Annex B. NMR spectroscopy confirmed definitely the chemical structure of PE- n Galx, giving an account of all the groups contained in the repeating unit of every polyester, with signals exhibiting the expected area and multiplicity, whereas no trace of any other signal was detected in the spectra. A detailed description of the NMR spectra of all PE- n Galx as well as those recorded from PE- n Ad is given in Section 3.2.2; for illustration, both ^1H and ^{13}C spectra of PE-8Galx are shown in Figure 3.1.

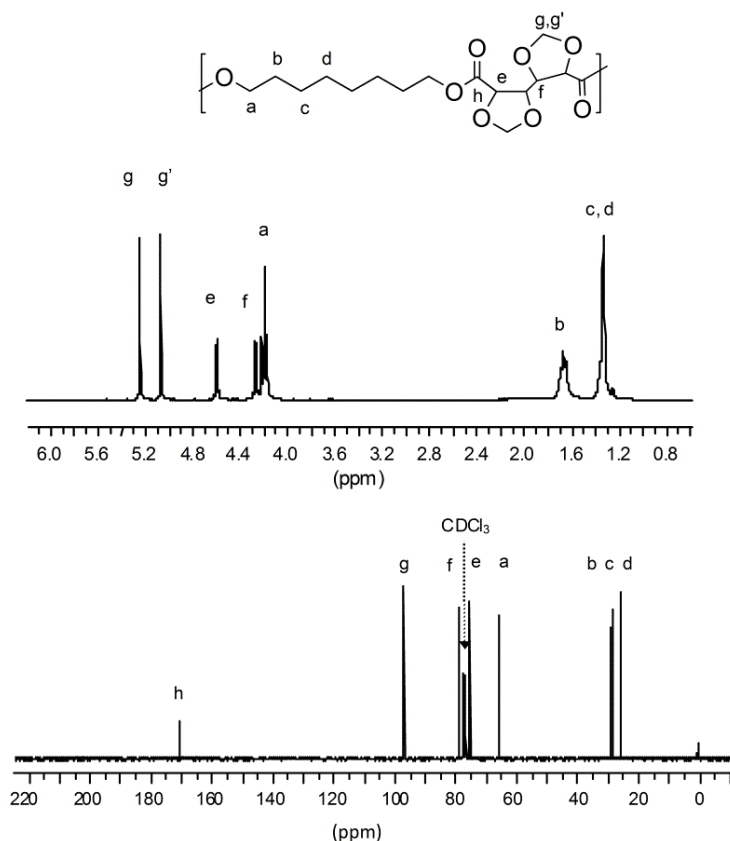


Figure 3.1. ^1H (top) and ^{13}C NMR (bottom) spectra of PE-8Galx (HMW).

Table 3.1. Molecular weights, solubility and wettability of PE-*n*Galx and PE-*n*Ad polyesters.

Polyester	Molecular weight					Solubility ^d					Contact angle ^e	
	$[\eta]^a$	M_n^b	M_n^c	M_w^c	\mathcal{D}^c	H ₂ O EtOH	Et ₂ O DMSO	NMP DMF	THF CHCl ₃	HFIP TFA	θ_{water} (deg)	θ_{EG} (deg)
LMW												
PE-6Galx	0.19	4,400	2,800	5,100	1.8	-	-	+	+	+	n.d.	n.d.
PE-8Galx	0.22	4,700	3,800	11,100	2.9	-	-	+	+	+	n.d.	n.d.
PE-10Galx	0.22	4,600	2,900	11,400	3.9	-	-	+	+	+	n.d.	n.d.
PE-12Galx	0.23	4,700	3,300	7,300	2.2	-	-	+	+	+	n.d.	n.d.
HMW												
PE-6Galx	0.51	16,800	15,100	34,700	2.3	-	-	+	+	+	82.4	57.6
PE-8Galx	0.62	18,000	17,200	43,100	2.5	-	-	+	+	+	84.9	56.5
PE-10Galx	0.53	17,100	15,600	34,900	2.2	-	-	+	+	+	88.1	65.1
PE-12Galx	0.59	16,200	15,200	38,100	2.5	-	-	+	+	+	88.6	67.1
PE-6Ad	0.68	23,800	21,700	42,200	1.9	-	-	-	+	+	102.8	73.2
PE-8Ad	0.59	16,400	15,500	35,300	2.3	-	-	-	+	+	104.4	77.8
PE-10Ad	0.62	18,000	15,700	36,600	2.3	-	-	-	+	+	109.6	84.3
PE-12Ad	0.66	16,000	16,900	38,000	2.2	-	-	-	+	+	112.5	75.1

^a Intrinsic viscosity in dL·g⁻¹ measured in chloroform at 25 °C.

^b Number-average molecular weight in g·mol⁻¹ determined by ¹H NMR end group analysis.

^c Number and weight-average molecular weights in g·mol⁻¹ and dispersities measured by GPC in HFIP against PMMA standards.

^d (-) Insoluble, (+) soluble.

^e Static measurement in water and ethylenglycol after 3 min of dropping. n.d: not determined.

Due to the absence of strong intermolecular interactions, aliphatic polyesters distinguish among polycondensates by exhibiting a relative good solubility in organic solvents. The solubility of both PE-*n*Galx and PE-*n*Ad was assessed in an assortment of representative solvents, and results are compared in Table 3.1. Solubility appears to be nonsensitive to the length of the diol polymethylene segment in none of the two series, and the incorporation of the acetalized galactarate unit in the polyester only produces a slight increase in solubility so that PE-*n*Galx become additionally soluble in NMP and DMF. It is also observed that none of the polyesters becomes water-soluble, although the sugar residue introduces certain hydrophilic character in the polymer chain. This effect was quantitatively evaluated by measuring the wettability of the polyester films by the contact angle technique at short times of contact with water and ethylene glycol as liquids, and results are compared in Table 3.1. It was found that the contact angle continuously increased with the value of *n* within each series revealing a progressive decreasing in the polarity of the polymer chain, as expected. Comparison of the two series shows that PE-*n*Galx afford much lower angle values than PE-*n*Ad indicating a larger wettability, as corresponds to the higher polarity provoked by the presence of the diacetalized sugar unit.

3.2.3.2. Thermal and mechanical properties

Galx is a thermally fairly stable solid compound that starts to volatilize above 100 °C and displays a sublimation temperature of 255 °C without perceivable decomposition. The thermal stability of polyesters made from this compound was evaluated by thermogravimetry under inert atmosphere and compared with that displayed by polyadipates. TGA traces obtained for the high molecular weight PE-*n*Galx and for PE-*n*Ad are depicted in Figure 3.2, and thermal data provided by this analysis for the three sets of polyesters under study are presented in Table 3.2. The weight loss profiles generated in all cases reveal a thermal degradation mechanism involving one main step occurring at 350-400 °C and leaving a final residue almost negligible for PE-*n*Ad, but that amounts to 10-20% of the initial weight in the case of PE-*n*Galx. The overview of the collected TGA data leads to the general appreciation that all these polyesters display a more than satisfactory resistance to heat with the onset decomposition temperatures around 300 °C, which is very comparable to the thermal behavior displayed by aliphatic polyesters made from isosorbide. Although there is not a steady correlation of the decomposition temperatures with *n* in none of the three sets, the ranges of values observed for each of them allow to evaluate comparatively their thermal stability. Thus,

there is a clear indication that the resistance to heat of PE-*n*Galx increases with molecular weight, and that the thermal stability of these polyesters is 20-30 °C higher than that of PE-*n*Ad having similar *n* and molecular weight values. The valuable conclusion drawn from this thermogravimetric study is that the insertion of Galx units in aliphatic polyesters instead of reducing their thermal stability contributes to a significant increase in their decomposition temperatures.

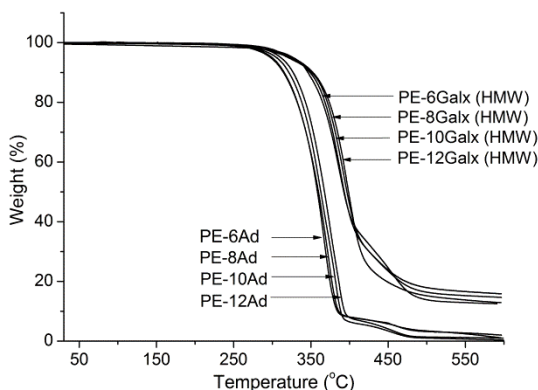


Figure 3.2. TGA traces of PE-*n*Galx (HMW) and PE-*n*Ad.

Linear aliphatic polyesters without substituents are characterized by displaying low glass-transition temperatures. Our DSC T_g measurements of PE-*n*Ad polyesters (Table 3.2) confirm indeed such general observation; these polyesters are so flexible and tend to crystallize so fast that T_g could be only determined for the relatively less flexible PE-6Ad which displayed a value as low as -61 °C. The replacement of the adipate unit by the Galx unit in PE-*n*Ad increased T_g of PE-6Ad by almost 70 °C and renders values for the HMW series of PE-*n*Galx comprised in the -17 to 6 °C range. It is well-known that the incorporation of rigid structures such as aromatic or aliphatic cyclic units in a polyester chain gives rise to a dramatic increase in T_g (Brandrup *et al.*, 1999). Polyesters with M_n in the 10,000-23,000 g·mol⁻¹ range made from isosorbide and aliphatic dicarboxylic acids with lengths similar to the alkanediols used in this work are reported to have T_g between -10 and 10 °C (Braun and Bergmann, 1992), which are perfectly comparable to those displayed by HMW PE-*n*Galx. It seems therefore that Galx exerts a similar effect as Is on T_g , which is rather striking because a higher stiffness should be expected for the almost planar fused five-membered tetrahydrofuran rings than for the puckered and conformationally interconvertible 5,5'-bis(1,3-dioxolane) structure.

Table 3.2. Thermal and mechanical properties of PE-*n*Galx and PE-*n*Ad polyesters.

Polyester	TGA			DSC											Tensile test		
				First heating ^e				Cooling ^e		Second heating ^e							
	$T_{5\%}^a$ (°C)	T_d^b (°C)	W^c (%)	T_g^d (°C)	T_m (°C)	ΔH_m (J·g ⁻¹)	X_c^g	T_c (°C)	ΔH_c (J·g ⁻¹)	T_c (°C)	ΔH_c (J·g ⁻¹)	T_m (°C)	ΔH_m (J·g ⁻¹)	X_c^g	E (MPa)	σ (MPa)	ε (%)
LMW																	
PE-6Galx	280	356	18	-4	61/73 ^f	34.8		-	-	-	-	-	-	-	n.d.	n.d.	n.d.
PE-8Galx	315	385	13	-17	52/66/74 ^f	44.3		-	-	-	-	-	-	-	n.d.	n.d.	n.d.
PE-10Galx	294	375	12	-22	57/75 ^f	48.5		-	-	31	30.4	78	31.8	-	n.d.	n.d.	n.d.
PE-12Galx	276	369	10	-19	77	42.7		46	28.6	-	-	79	28.2	-	n.d.	n.d.	n.d.
HMW																	
PE-6Galx	325	398	13	6	51/70/73 ^f	15.7		-	-	-	-	-	-	-	154	13	55
PE-8Galx	320	392	15	-8	52/69/73 ^f	24.5		-	-	-	-	-	-	-	157	12	50
PE-10Galx	323	387	16	-13	53/77/81 ^f	25.0		-	-	40	20.1	81	20.2	-	151	13	60
PE-12Galx	327	387	13	-17	86	28.9		35	26.3	-	-	86	26.9	-	153	13	60
PE-6Ad	300	367	1	-61	56	100.5	0.60	40	69.8	-	-	57	73.1	0.44	100	7	201
PE-8Ad	297	372	2	n.d.	67	108.4	0.68	46	84.6	-	-	68	85.3	0.53	88	8	210
PE-10Ad	305	363	1	n.d.	73	109.2	0.70	58	99.2	-	-	74	99.7	0.64	95	7	203
PE-12Ad	311	375	1	n.d.	75	118.8	0.71	63	102.5	-	-	75	109.1	0.65	87	6	215

^aTemperature at which 5 % weight loss was observed. ^bTemperature for maximum degradation rate. ^cRemaining weight at 600 °C. ^dGlass-transition temperature taken as the inflection point of the heating DSC traces of melt-quenched samples recorded at 20 °C·min⁻¹. ^eMelting (T_m) and crystallization (T_c) temperatures, and melting (ΔH_m) and crystallization (ΔH_c) enthalpies measured by DSC at heating/cooling rates of 10 °C·min⁻¹. ^fMultiple melting peak.

^gCrystallinity index based on 100 % crystalline polyester: ΔH_m^o PE-6Ad = 38.1 KJ·mol⁻¹; ΔH_m^o PE-8Ad = 41.0 KJ·mol⁻¹; ΔH_m^o PE-10Ad = 44.0 KJ·mol⁻¹; ΔH_m^o PE-12Ad = 52.0 KJ·mol⁻¹ (Maglio *et al.*, 1979).

It seems that the relatively elongated shape of Galx will allow a closer packing of the polymer chains, which implies less free volume and accordingly a higher T_g . With regard to the influence of the constitution of PE-*n*Galx on T_g , the effects observed were those according to expectations; T_g of the LMW set were around 10 °C lower than of HMW set, and within each set, it decreased almost steadily with increasing values of *n*.

The melting-crystallization behavior of the polyesters was characterized by DSC and the collected data are gathered in Table 3.2. PE-*n*Ad polyesters are highly crystalline polymers displaying melting temperatures between 56 and 75 °C and melting enthalpies greater than 100 J·g⁻¹ which correspond to crystallinity indexes of 0.6-0.7, both parameters increasing steadily with the value of *n*. These unsubstituted polyesters crystallized very fast when cooled from the melt with a recovery of about 70-90% of their initial crystallinity and almost exact replication of their melting temperatures. PE-*n*Galx are also crystalline but they show remarkable differences compared to PE-*n*Ad that evidence the detrimental influence exerted by the diacetalized galactarate residue on crystallinity and crystallizability. The heating DSC traces of PE-*n*Galx (HMW) are depicted in Figure 3.3. Those obtained from samples coming directly from synthesis displayed wide endotherms consisting of several melting peaks indicative of a defective crystallization of the polyester. Traces with similar profiles were obtained from PE-*n*Galx (LMW), which are not shown here but can be inspected on Annex B. Annealing of pristine samples of PE-*n*Galx (HMW) at temperatures between 60 and 75 °C for 12 h homogenized the crystalline morphology; in fact, melting of the annealed polymer took place sharply and at high temperatures, as corresponds to a single population of crystallites of well-definite size. T_m of PE-*n*Galx (measured on annealed samples) are within the 70-85 °C range, which is not far from the PE-*n*Ad melting temperature range, with values increasing regularly with the value of *n*. Whereas neither molecular weight nor constitution seem to notably affect melting temperatures, their influence on melting enthalpy appears to be very remarkable. As can be seen in Table 3.2, ΔH_m of PE-*n*Galx (HMW) polymers are several times smaller than those of PE-*n*Ad and approximately the half of the values observed for PE-*n*Galx (LMW). Lastly, just to note that, with regard to polyesters made from isosorbide reported in the literature (Okada *et al.*, 2000), melting of PE-*n*Galx takes place at higher temperatures but with similar associated enthalpies.

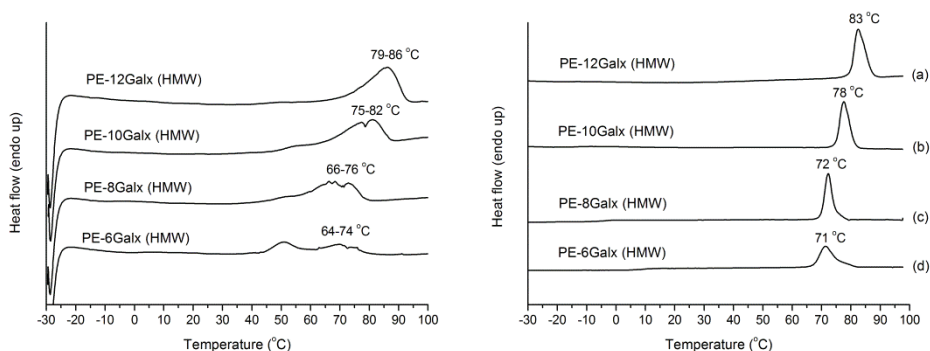


Figure 3.3. DSC melting traces of samples of PE-*n*Galx (HMW) coming directly from synthesis (left) and annealed (right) at (a) 75 °C for 12 h, (b) 70 °C for 12 h, (c) 65 °C for 12 h and (d) 60 °C for 12 h.

Table 3.3. Isothermal crystallization data for LMW and HMW PE-12Galx.

Polyester	T_c (°C)	t_0 (min)	$t_{1/2}$ (min)	n	$-\log k$	T_m (°C)
PE-12Galx (LMW)	50	0.28	2.08	2.28	0.75	78.2
	55	0.38	3.16	2.51	1.27	78.5
	60	0.41	5.16	2.96	2.14	79.2
PE-12Galx (HMW)	50	0.35	2.36	2.80	1.04	81.9
	55	0.40	3.74	2.92	1.76	82.5
	60	0.45	8.66	2.99	2.90	83.1

At difference with PE-*n*Ad, PE-*n*Galx are in general unable to crystallize from the melt. In fact, only PE-12Galx, both LMW and HMW, which is the highest flexible PE-*n*Galx, showed exothermal crystallization peaks at the cooling DSC traces; the crystallized polymers display similar T_m but significantly lower ΔH_m than their respective pristine samples. Given the extreme relevance of this property regarding polymer processing, the isothermal crystallization of LMW and HMW PE-12Galx was kinetically analyzed at different temperatures by using the Avrami approach to appraise quantitatively the effect of molecular weight on crystallizability. The relative crystallinity vs. time plot as well as the double logarithmic plot for both low and high molecular weight PE-12Galx are compared in Figure 3.4, and kinetics data extracted from these results are gathered in Table 3.3. The conclusions that may be drawn from the kinetics study are according to expectations. LMW PE-12Galx crystallized much faster than HMW PE-

12Galx, and in both cases crystallization rate diminished as temperature increased revealing that within the studied temperature range, the process is dominated by nucleating effects. Furthermore, the influence of temperature on crystallization rate is more pronounced in the case of high molecular weight PE-12Galx.

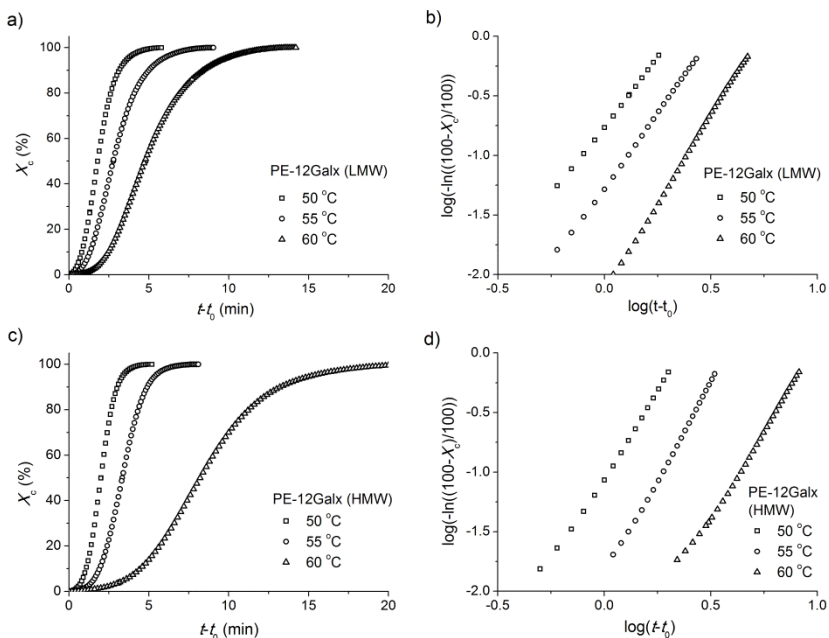


Figure 3.4. Isothermal crystallization of PE-12Galx at the indicated temperatures. a) Relative crystallinity vs. time plot for PE-12Galx (LMW). b) Log-log plot for PE-12Galx (LMW). c) Relative crystallinity vs. time plot for PE-12Galx (HMW). d) Log-log plot for PE-12Galx (HMW).

A preliminary evaluation of the mechanical behavior of PE-*n*Galx (HMW) compared to PE-*n*Ad was made by tensile testing at room temperature. The obtained stress-strain curves are depicted in Figure 3.5, and the mechanical parameters extracted from them are listed in Table 3.2. The elastic modulus values of PE-*n*Galx oscillate in the 150-160 MPa range, whereas PE-*n*Ad have moduli in the 85-100 MPa range. Tensile strengths reach values of 12-13 MPa and 6-8 MPa for PE-*n*Galx and PE-*n*Ad, respectively, whereas elongations at break are around 50 and 200%. The higher rigidity and lower ductility observed for PE-*n*Galx seem to be the logical consequence of the higher T_g displayed by these polyesters compared to PE-*n*Ad, which doubtless is due to the presence of the bicyclic acetal structure in the polymer chain. However, no correlation between the mechanical parameters and the length of polymethylene segment becomes

apparent, the small observed differences falling within the acceptable experimental error limit.

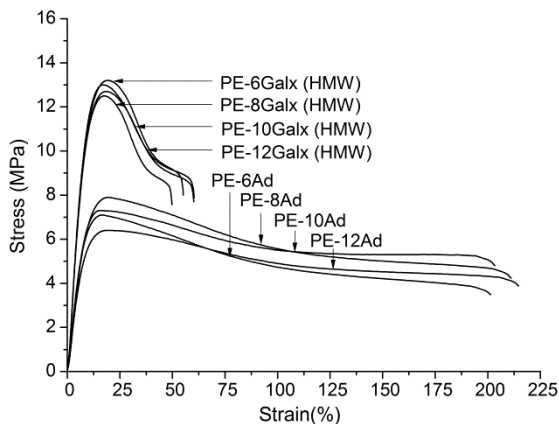


Figure 3.5. Stress-strain curves for PE-*n*Galx (HMW) and PE-*n*Ad.

3.2.3.3. Hydrolytic degradation and biodegradation

It is well-known that polycondensates of synthetic origin are resistant to hydrolysis or even apparently inert for long time intervals when incubated under physiological conditions. It has been repeatedly shown that the incorporation of sugar residues in polyesters, polyamides or polyurethanes enhances the susceptibility of the polymer to hydrolysis (Ruiz-Donaire *et al.*, 1995; Zamora *et al.*, 2006; De Paz *et al.*, 2007). Both aliphatic and aromatic polyesters containing isosorbide were reported to be hydrolyzed at higher rates than their unsubstituted analogous when incubated under similar conditions. Okada *et al.* focused on the biodegradability of polyesters made from aliphatic dicarboxylic acids and 1,4:3,6 dianhydrohexitols (Okada *et al.*, 1996, 1997 and 1999), and concluded that all of them were biodegraded to an extent that largely depended on the configuration of the anhydroalditol. To evaluate the effect of Galx on the hydrolysis of aliphatic polyesters, a comparative study using PE-8Ad and PE-8Galx was carried out in this work. Samples of the two polymers were incubated in aqueous buffers at pH 2.0, 7.4 and 10.5 at room temperature for two months, and the evolution of the degradation process was followed by measuring the weight loss and the molecular weight of the residual polymer. The results of this comparative study are presented in Figure 3.6. The profiles obtained for PE-8Ad indicate that there is no loss of mass and that the decrease in molecular weight is practically negligible at any pH. On the contrary, PE-8Galx showed an appreciable weight loss that was minimum (~4%) at pH 7.4 and

maximum (~15%) at pH 2.0, as well as a significant decreasing of both M_w and M_n , whereas polydispersity remained almost constant.

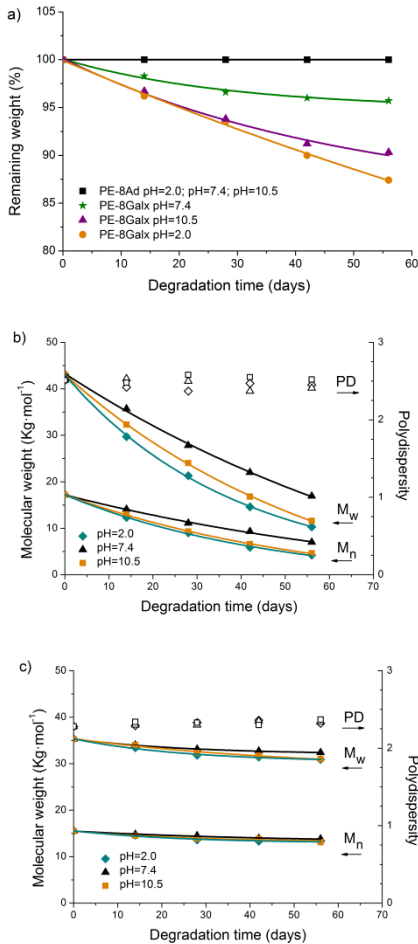


Figure 3.6. a) Remaining weight vs. hydrolytic degradation time for PE-8Galx (HMW) and PE-8Ad at pH 2.0, 7.4 and 10.5. (b) Changes in M_w and M_n (solid symbols) and polydispersity index (empty symbols) vs. incubation time for PE-8Galx. (c) Changes in M_w and M_n (solid symbols) and polydispersity index (empty symbols) vs. incubation time for PE-8Ad.

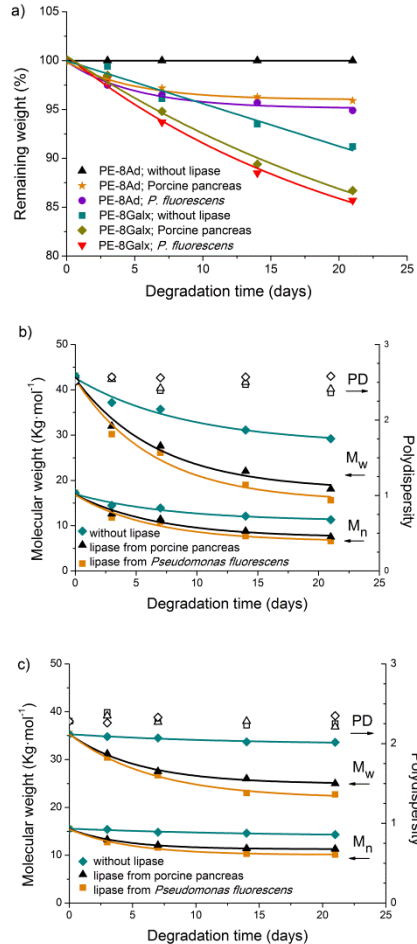


Figure 3.7. Degradation of PE-8Galx (HMW) and PE-8Ad in the presence of lipases from *Pseudomonas fluorescens* and porcine pancreas, and without lipase. (a) Remaining weight vs. degradation time. (b) Changes in M_w and M_n (solid symbols) and polydispersity index (empty symbols) vs. incubation time for PE-8Galx. (c) Changes in M_w and M_n (solid symbols) and polydispersity index (empty symbols) vs. incubation time for PE-8Ad.

A similar study was then performed with PE-8Ad and PE-8Galx but adding either *P.fluorescens* or porcine pancreas lipases to the incubation medium at pH 7.4, and results obtained over an incubation period of three weeks at 37 °C are presented in Figure 3.7. In the presence of lipases, both PE-8Ad and PE-8Galx showed appreciable greater weight losses and molecular weight reductions than in the absence of enzymes indicating that the hydrolysis of both polyesters was speeded by lipases. The activity of the two lipases was not noteworthy different as neither was the sensitivity of the two polymers to the enzymatic action; in fact, a comparison of the plots in Figure 3.7 clearly reveals that the greater degree of biodegradation apparently observed for PE-8Galx is the only consequence of its lower intrinsic stability against hydrolysis.

The changes taking place in the micromorphology of PE-8Ad and PE-8Galx due to the degradation process were revealed by SEM analysis as it is illustrated in Figure 3.8. The surface of a fresh fractured pristine sample of PE-8Ad exhibited a spherulitic texture, which became more vivid after incubation in water at pH 2.0, probably due to the removal of some intra- and interspherulitic amorphous material. Upon incubation in the presence of porcine pancreas lipase, the surface became smoother and developed some small cracks, indicating that a certain degradation in bulk happened. The results obtained in the parallel analysis carried out on PE-8Galx were clearly different. In this case, the initial surface did not display any feature of crystalline morphology, and after incubation in acidic water, plenty of holes and grooves appeared delineating what seems to be a texture made of relatively small impinging spherulites. In the presence of lipase, large cracks causing the total fracture of the material became apparent. The SEM pictures support the conclusion that PE-8Galx becomes more severely degraded than PE-8Ad, both in the presence and in the absence of lipases, and that the degradation process does not follow the same mechanism in each case.

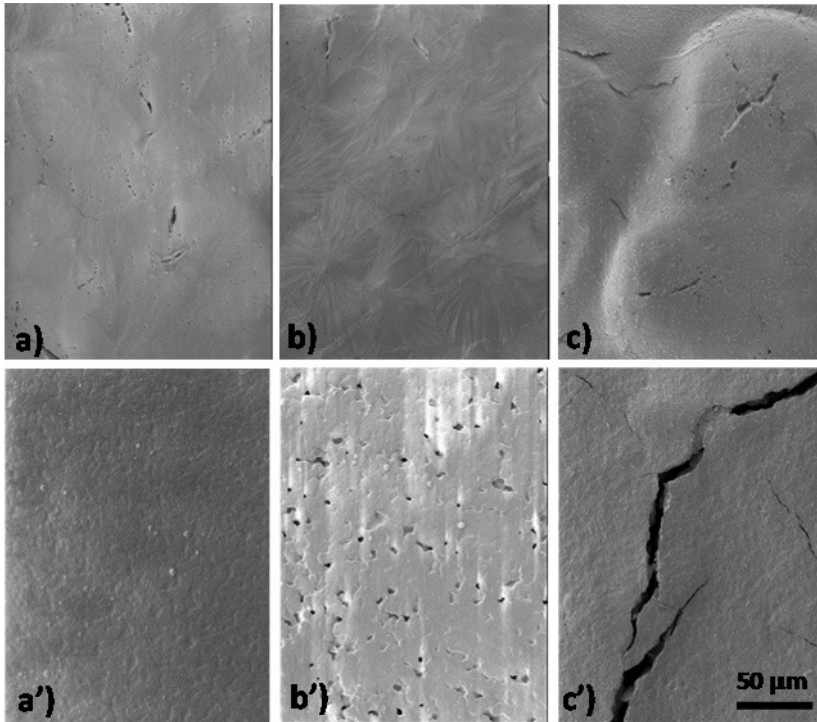


Figure 3.8. SEM micrographs of PE-8Ad (top) and PE-8Galx (HMW) (bottom). (a, a') Initial sample. (b, b') After incubation at pH=2.0 for 56 days. (c, c') After incubation in the presence of lipase from porcine pancreas at pH=7.4 for 21 days.

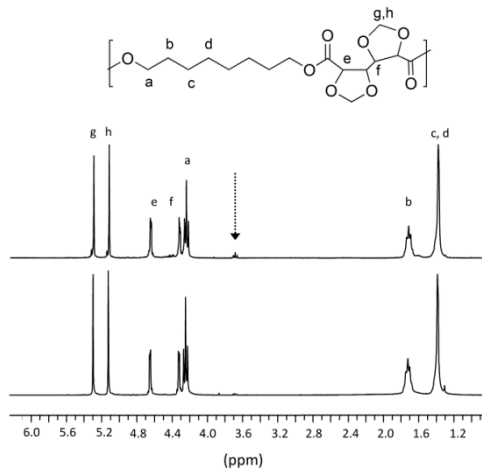


Figure 3.9. Compared ¹H NMR spectra for PE-8Galx (HMW) after incubation at pH=2.0 for 56 days (top) and initial sample (bottom). The arrow indicates the signal arising from -CH₂OH end groups that appear upon hydrolysis of the main chain ester group.

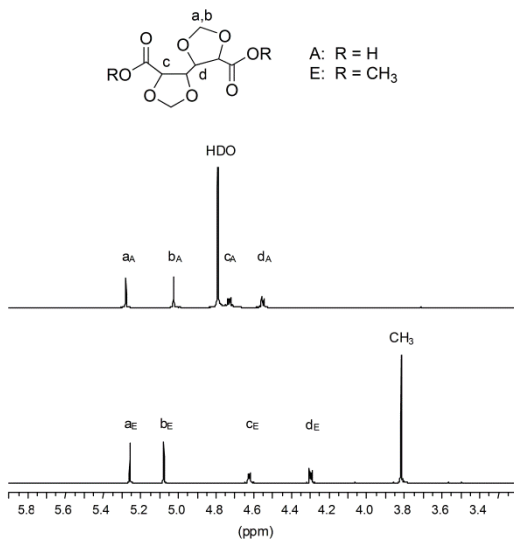


Figure 3.10. ^1H NMR spectra in D_2O of the product resulting after incubation of dimethyl 2,3:4,5-di-O-methylene galactarate at pH 2.0 for three months at room temperature (top) and of initial sample in CDCl_3 (bottom).

Finally, a NMR study was made to explore how the polyester chain is degraded at the molecular level. The changes taking place in the ^1H NMR spectrum of a sample of PE-8Galx upon incubation in aqueous buffer at pH 2.0 are shown in Figure 3.9. All the signals present in the original spectrum remained unaltered after degradation, and the only changes observed after incubation was the appearing of a small signal corresponding to hydroxymethyl group at 3.6 ppm. ^1H NMR spectra of PE-8Galx samples incubated at pH 7.4 and 10.5 afforded similar results, indicating that degradation proceeded by splitting of the relatively weak ester group without modification of the polymer chain structure. The result is rather striking since the acetal group is known to be sensitive to acidic conditions (Smith and March, 2007) and the opening of the dioxolane rings should have therefore been expected to happen in some extent. To check the stability of the diacetal structure, dimethyl 2,3:4,5-di-O-methylene-galactarate was incubated at room temperature in aqueous buffer at pH 2.0, 7.4 and 10.5. The initial powdered nonsoluble sample dissolved as degradation proceeded, and the NMR analysis of the solution after three months revealed that hydrolysis of the ester groups had happened almost quantitatively at both pH 2.0 and 10.5, whereas at pH 7.4 about 5% of the initial diester was still remaining. What was really remarkable is that the acetal group stayed intact after the treatment with whatever were the incubation conditions. The

^1H NMR spectrum of the incubating medium at pH 2.0 is depicted in Figure 3.10, showing all the expected signals due to the protons of the dioxolane ring with their right relative areas. It is concluded therefore that the methylene diacetal of galactaric unit is extremely resistant to hydrolysis. This result dissipates possible concerns about instability of PE-*n*Galx due to uncontrolled opening of the acetal rings and allows to anticipate a satisfactory behavior of these polyesters in processing and handling.

3.2.4. Conclusions

The bicyclic acetalized dimethyl 2,3:4,5-di-*O*-methylene-galactarate compound was successfully used as monomer for the synthesis of linear polyesters PE-*n*Galx by polycondensation in the melt with alkanediols. The use of DBTO instead of TBT as catalyst allowed to proceed at lower temperature without increasing reaction times, which led to attaining higher molecular weights. PE-*n*Galx displayed solubility similar to their homologous linear nonsubstituted polyesters PE-*n*Ad, but they were more hydrophilic. The presence of the diacetal unit in the polyester slightly improved the thermal stability, increased notably T_g , increased slightly T_m , and repressed partially the crystallizability of the polyesters. Due to their higher T_g , PE-*n*Galx appeared to be stiffer and less ductile than PE-*n*Ad. The polyesters containing Galx units were degraded by water through splitting of the ester group, whereas the acetal group remained stable against hydrolysis. Hydrolysis of PE-*n*Galx took place at a higher rate than for PE-*n*Ad, and in both cases degradation was speeded by enzymes with a similar effect.

3.2.5. References

- Bou, J.; Rodríguez-Galán, A.; Muñoz-Guerra, S. *Biodegradable optically active polyamides*. In: Salamone, E.; Ed. *The Polymeric Materials Encyclopedia*, vol. 1; CRC Press: Boca Raton, **1996**, pp. 561-569.
- Brandrup, J.; Immergut, E.H.; Grulke, E.A. *Polymer Handbook*; Wiley: New York, **1999**.
- Braun, D.; Bergmann, M. *J. Prakt. Chem.* **1992**, 334, 298-310.
- Bueno, M.; Galbis, J.A.; García-Martín, M.G.; DePaz, M.V.; Zamora, F.; Muñoz-Guerra, S. *J. Polym. Sci., Polym. Chem.* **1995**, 33, 299.
- Butler, K.; Lawrance, D.R.; Stacey, M. *J. Chem. Soc.* **1958**, 740-743.
- Caouthar, A.; Roger, P.; Tessier, M.; Chatti, S.; Blais, J.C.; Bortolussi, M. *Eur. Polym. J.* **2007**, 43, 220-230.

- Chatti, S.; Schwarz, G.; Kricheldorf, H.R. *Macromolecules* **2006**, *39*, 9064-9070.
- De Paz, M.V.; Marín, R.; Zamora, F.; Hakkou, K.; Alla, A.; Galbis, J.A.; Muñoz-Guerra, S. *J. Polym. Sci., Pol. Chem.* **2007**, *45*, 4109-4117.
- Dhamaniya, S.; Jacob, J. *Polymer* **2010**, *51*, 5392-5399.
- Fenouillot, F.; Rousseau, A.; Colomines, G.; Saint-Loup, R.; Pascault, J.-P. *Prog. Polym. Sci.* **2010**, *35*, 578-622.
- Galbis, J.A.; García-Martín, M.G. *Sugars as Monomers*. In: Belgacem, M.N.; Gandini, A.; Eds. *Monomers, Polymers and Composites from Renewable Resources*; Elsevier: Oxford, **2008**, 89-114.
- Galbis, J.A.; García-Martín, M.G. *Chem. Curr. Top.* **2010**, *295*, 147-176.
- García-Martín, M.G.; Pérez, R.R.; Hernández, E.B.; Espartero, J.L.; Muñoz-Guerra, S.; Galbis, J.A. *Macromolecules* **2005**, *38*, 8664-8670.
- Gómez, R.; Varela, O. *Macromolecules* **2009**, *42*, 8112-8117.
- Haider, A.F.; Williams, C.K. *J. Polym. Sci., Polym. Chem.* **2008**, *46*, 2891-2896.
- Iribarren, J. I.; Martínez de Ilarduya, A.; Alemán, C.; Oraison, J. M.; Rodríguez-Galán, A.; Muñoz-Guerra, S. *Polymer* **2000**, *41*, 4869-4879.
- Kimura, H.; Yoshinari, T.; Takeishi, M. *Polym. J.* **1999**, *31*, 388-392.
- Kricheldorf, H. R. *J. Macromol. Sci.* **1997**, *C37*, 599-631.
- Marín, R.; Muñoz-Guerra, S. *J. Appl. Polym. Sci.* **2009**, *114*, 3723-3736.
- Maglio, G.; Marchetta, C.; Botta, A.; Palumbo, R.; Pracella, M. *Eur. Polym. J.* **1979**, *15*, 695-699.
- Noordover, B.A.J.; van Staalduinen, V.G.; Duchateau, R.; Koning, C.E.; van Benthem, R.A.T.M.; Mak, M.; Heise, A.; Frissen, A.E.; van Haveren, J. *Biomacromolecules* **2008**, *7*, 3406-3416.
- Okada, M.; Okada, Y.; Tao, A.; Aoi, K. *J. Appl. Polym. Sci.* **1996**, *62*, 2257-2265.
- Okada, M.; Tachikawa, K.; Aoi, K. *J. Polym. Sci., Pol. Chem.* **1997**, *35*, 2729-2737.
- Okada, M.; Tachikawa, K.; Aoi, K. *J. Appl. Polym. Sci.* **1999**, *74*, 3342-3350.
- Okada, M.; Tsunoda, K.; Tachikawa, K.; Aoi, K. *J. Appl. Polym. Sci.* **2000**, *77*, 338-346.
- Quintana, R.; Martínez de Ilarduya, A.; Alla, A.; Muñoz-Guerra, S. *J. Polym. Sci., Polym. Chem.* **2011**, *49*, 2252-2260.
- Rodríguez-Galán, A.; Bou, J.J.; Muñoz-Guerra, S. *J. Polym. Sci., Polym. Chem.* **1992**, *30*, 713-721.

Ruiz-Donaire, P.; Bou, J.; Muñoz-Guerra, S.; Rodríguez-Galán, A. *J. Appl. Polym. Sci.* **1995**, *58*, 41–54.

Sablong, R.; Duchateau, R.; Koning, C.E.; de Wit, G.; van Es, D.; Koelewijn, R.; van Haveren, J. *Biomacromolecules* **2008**, *9*, 3090-3097.

Smith, M.B.; March, J. *March's Advanced Organic Chemistry*; Wiley: Hoboken, **2007**, pp. 523,1270.

Storbeck, R.; Rehahn, M.; Balluff, M. *Makromol. Chem.* **1993**, *194*, 53-64.

Thiem, J.; Lüders, H. *Polym. Bull.* **1984**, *11*, 365-369.

Wang, Q.; Dordick, J.S.; Linhardt, R.J. *Chem. Mater.* **2002**, *14*, 3232-3244.

Wool, R.; Sun, S. *Biobased Polymers and Composites*; Academic Press: New York, **2005**.

Zamora, F.; Hakkou, K.; Muñoz-Guerra, S.; Galbis, J.A. *Polym. Degrad. Stabil.* **2006**, *91*, 2654-2659.

3.3. Carbohydrate-based copolyesters made from bicyclic acetalized galactaric acid

Summary: Mixtures of the dimethyl esters of adipic acid and 2,3:4,5-di-O-methylene-galactaric acid (Galx) were made to react in the melt with either 1,6-hexanediol or 1,12-dodecanediol to produce linear polycyclic copolyesters with aldarate units contents varying from 10 up to 90 mole-%. The copolyesters had weight-average molecular weights in the $\sim 35,000$ - $45,000 \text{ g}\cdot\text{mol}^{-1}$ range and a random microstructure, and were thermally stable up to near $300 \text{ }^\circ\text{C}$. They displayed T_g in the -50 to $-7 \text{ }^\circ\text{C}$ range with values largely increasing with the content in galactarate units. All the copolyesters were semicrystalline with T_m between 20 and $90 \text{ }^\circ\text{C}$ but only those made from 1,12-dodecanediol were able to crystallize from the melt at a crystallization rate that decreased as the contents in the two comonomers approach to each other. Copolyesters containing minor amounts of galactarate units adopted the crystal structure characteristic of aliphatic polyesters but a new crystal polymorph was formed when the cyclic sugar units became the majority. Stress-strain parameters were sensitively affected by composition of the copolyesters with the mechanical behavior changing from flexible/ductile to stiff/brittle with the replacement of adipate units by the galactarate units.

Publication derived from this work:

Lavilla, C.; Alla, A.; Martínez de Iarduya, A.; Benito, E.; García-Martín, M.G.; Galbis, J.A.; Muñoz-Guerra, S. *J. Polym. Sci., Polym. Chem.* **2012**, *50*, 1591-1604.

3.3.1. Introduction

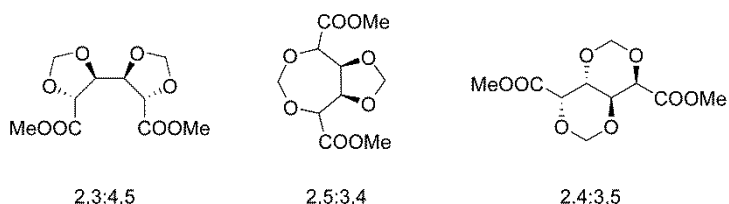
Due to the increasing demand on bio-based plastics, polymers made from monomers derived from naturally-occurring compounds are gaining interest. The use of renewable sources for building-blocks of polymers not only contributes to reduce their dependence on petrochemicals but also increases the added-value of agriculture products and wastes (Wool and Sun, 2005; Belgacem and Gandini, 2008; Pillai, 2010; Gandini, 2011). Carbohydrates are very prevalent and readily available compounds that may afford a wide variety of monomers suitable for making different classes of polymers (Kricheldorf, 1997; Varela, 2000; Okada, 2001; Varma *et al.*, 2004; Galbis and García-Martín, 2010). Carbohydrate derived monomers are particularly appropriate for polycondensation due to the occurrence in them of highly reactive hydroxyl groups. However, although some examples of polycondensates prepared from unprotected sugar based monomers have been reported (Kiely *et al.*, 1994; Chen and Kiely, 1996), the multifunctionality usually present in these compounds requires specific group protection if linear polymers with high molecular weight are desired. Carbohydrate-based polycondensates may typically display enhanced hydrophilicity, lower toxicity and higher susceptibility to biodegradation than those coming from petrochemical feedstock.

Recently, the bicyclic 1,4:3,6-dianhydrohexitols (Fenouillot *et al.*, 2010), and specifically 1,4:3,6-dianhydro-D-glucitol known as isosorbide (Is) (Thiem and Lüders, 1984; Chatti *et al.*, 2006a and 2006b; Noordover *et al.*, 2006; Juais *et al.*, 2010), have deserved particular consideration for the synthesis of linear polycondensates. These compounds have four hydroxyl groups blocked by intramolecular etherification leaving those at the 2 and 5 positions free for reaction. Their interest as building blocks in polycondensation relies on that they add stiffness to the polymer chain with the subsequent increasing in T_g . In this regard, great attention is given to aromatic polyesters and copolyesters (Storbeck *et al.*, 1993; Sablong *et al.*, 2008; Quintana *et al.*, 2011), where Is has proven to replace petrochemical diols without detriment, or even with improvement, of their properties.

The use of intramolecularly acetalized sugars constitutes another interesting option for the synthesis of bio-based polycondensates containing cyclic structures in the main chain. Thus, a variety of polyamides and polyesters derived from di-O-methylene L-threitol and L-tartaric acid, which distinguish in containing the 1,3-dioxolane ring forming part of the polymer backbone, have been described and their crystal structure and a number of their properties studied in certain cases (Rodríguez-Galán *et al.*, 1992; Kimura

et al., 1999; Iribarren *et al.*, 2000; Kint *et al.*, 2001). More recently low molecular weight polyesters made from di-*O*-isopropylidene-*L*-tartaric acid and alkanediols have been also reported (Dhamaniya and Jacob, 2010). However, the use in polycondensation of bicyclic acetalized alditols or aldaric acids derived from hexoses appears to be much more limited. To our knowledge the use of bicyclic acetalized alditols is restricted to a few exploratory cases that were reported long time ago (Beaman *et al.*, 1959; Bird *et al.*, 1960, 1961 and 1963; Black *et al.*, 1963), and the only case concerning aldaric acids is the synthesis of polygalactarates homopolymers recently reported by us (Lavilla *et al.*, 2011 -Subchapter 3.2-), in a pioneer paper in this topic which should be taken as the predecessor of the present one. It should be mentioned also that, although not as strict polycondensation monomers, 1-deoxy-1-isocyanate-2,3,4,5-di-*O*-isopropylidene-*D*-galactitol and 2,4:3,5-di-*O*-methylene-glucitol have been synthesized and used as monomers for the preparation of linear polyurethanes (Gómez and Varela, 2009; Marín and Muñoz-Guerra, 2009).

In this work we describe the synthesis, characterization and some properties of copolyesters PE-6Ad_xGal_y and PE-12Ad_xGal_y. They are prepared from 1,6-hexanediol or 1,12-dodecanediol respectively, and mixtures of dimethyl adipate and dimethyl 2,3:4,5-di-*O*-methylene-galactarate, the latter abbreviated as Galx. Three constitutional isomers differing in the arrangement of the two acetal rings are feasible in the acid catalyzed methylenation of dimethyl galactarate with formaldehyde (Scheme 3.3). The 2,3:4,5-di-*O*-methylene galactarate (Galx) is the main product of the reaction which is obtained along with the 2,5:3,4 isomer at a 1 to 2 ratio approximately. The 2,4:3,5 isomer seems not to be formed under such reaction conditions (Burden and Stoddart, 1975). Since Galx is a centrosymmetric compound, the two carboxyl groups are spatially undistinguishable and they display therefore the same reactivity. Consequently, it does not generate *regicity* in the growing polymer chain.



Scheme 3.3. The three isomeric bicyclic structures feasible for the di-*O*-methylene acetal of dimethyl galactarate. The 2,3:4,5 isomer (Galx) is used in this work.

3.3.2. Experimental section

3.3.2.1. Materials

Dimethyl 2,3:4,5-di-O-methylene-galactarate was synthesized following the procedure reported by Stacey *et al.* (Butler *et al.*, 1958). The reagents 1,12-dodecanediol (99%), 1,6-hexanediol (97%) and dimethyl adipate (> 99%), and the catalyst dibutyl tin oxide (DBTO, 98%) were purchased from Sigma-Aldrich. Solvents used for purification and characterization, as chloroform and methanol, as well as solvents used in the solubility essays, were purchased from Panreac and they all were of either technical or high-purity grade. All the reagents and solvents were used as received without further purification.

3.3.2.2. General methods

^1H and ^{13}C NMR spectra were recorded on a Bruker AMX-300 spectrometer at 25.0 °C operating at 300.1 and 75.5 MHz, respectively. Polyesters were dissolved in deuterated chloroform or in deuterated benzene, and spectra were internally referenced to tetramethylsilane (TMS). About 10 and 50 mg of sample dissolved in 1 mL of solvent were used for ^1H and ^{13}C NMR, respectively. Sixty-four scans were acquired for ^1H and 1,000-10,000 for ^{13}C with 32 and 64-K data points as well as relaxation delays of 1 and 2 s, respectively. FTIR measurements were carried out in a Jasco 4100 FTIR spectrophotometer, coupled with an ATR accessory Specac MKII, with a single reflection Golden Gate diamond, ZnSe lenses and a high stability temperature driver West6100+. The absorbance of the sample was recorded in the range of 4000-550 cm^{-1} accumulating 32 scans for each run. Intrinsic viscosities of polyesters dissolved in chloroform were measured in an Anton Paar AMVn Automated Micro Viscosimeter at 25.00±0.01 °C, using the VisioLab for AMVn software. Gel permeation chromatograms were acquired at 35.0 °C with a Waters equipment provided with a refraction-index detector. The samples were chromatographed with 0.05 M sodium trifluoroacetate-hexafluoroisopropanol (NaTFA-HFIP) using a polystyrene-divinylbenzene packed linear column with a flow rate of 0.5 $\text{mL}\cdot\text{min}^{-1}$. Chromatograms were calibrated against poly(methyl methacrylate) (PMMA) monodisperse standards. The thermal behavior of polyesters was examined by DSC using a Perkin Elmer DSC Pyris 1. DSC data were obtained from 3 to 5 mg samples at heating/cooling rates of 10 $^{\circ}\text{C}\cdot\text{min}^{-1}$ under a nitrogen flow of 20 $\text{mL}\cdot\text{min}^{-1}$. Indium and zinc were used as standards for temperature and enthalpy calibration. The glass-

transition temperatures were determined at a heating rate of $20\text{ }^{\circ}\text{C}\cdot\text{min}^{-1}$ from rapidly melt-quenched polymer samples. The treatment of the samples for isothermal crystallization experiments was the following: the thermal history was removed by heating the sample up to $150\text{ }^{\circ}\text{C}$ and left at this temperature for 5 min, and then it was cooled at $20\text{ }^{\circ}\text{C}\cdot\text{min}^{-1}$ to the selected crystallization temperature, where it was left to crystallize until saturation. For morphological study, isothermal crystallizations under the same conditions were carried out in an Olympus BX51 Polarizing Optical Microscope coupled to a THMS LINKAM heating plate and a cooling system LNP (Liquid Nitrogen Pump). Thermogravimetric analyses were performed under a nitrogen flow of $20\text{ mL}\cdot\text{min}^{-1}$ at a heating rate of $10\text{ }^{\circ}\text{C}\cdot\text{min}^{-1}$, within a temperature range of 30 to $600\text{ }^{\circ}\text{C}$, using a Perkin Elmer TGA 6 equipment. Sample weights of about 10-15 mg were used in these experiments. Films for mechanical testing measurements were prepared with a thickness of $\sim 200\text{ }\mu\text{m}$ by casting from chloroform solution at a polymer concentration of $100\text{ g}\cdot\text{L}^{-1}$; the films were then cut into strips with a width of 3 mm while the distance between testing marks was 10 mm. The tensile strength, elongation at break and Young's modulus were measured at a stretching rate of $30\text{ mm}\cdot\text{min}^{-1}$ on a Zwick 2.5/TN1S testing machine coupled with a compressor Dalbe DR 150, at $23\text{ }^{\circ}\text{C}$. Powder X-ray diffraction patterns were recorded on the INEL CPS-120 diffractometer in Debye-Scherrer configuration using the $\text{Cu-K}\alpha$ radiation of wavelength 0.1542 nm from powdered samples coming directly from synthesis. Wide-angle X-ray scattering of anisotropic samples was performed in the synchrotron beamline A2 at HASYLAB, Hamburg, Germany. Scattering patterns were collected by a two-dimensional position sensitive marccd 165 detector. Series of scattering patterns were recorded at 30 s cycle times including 20 s of exposure.

3.3.2.3. Polymer synthesis

The homopolyesters PE-12Galx, PE-12Ad, PE-6Galx and PE-6Ad were synthesized following the procedure recently reported by Lavilla *et al.* (Lavilla *et al.*, 2011 -Subchapter 3.2-). PE- $n\text{Ad}_x\text{Gal}_y$ copolyesters were obtained from the chosen aliphatic α,ω -diol (either 1,6-hexanediol or 1,12-dodecanediol) and a mixture of dimethyl 2,3:4,5-di-*O*-methylene-galactarate and dimethyl adipate with the selected composition. The reaction was performed in a three-necked, cylindrical-bottom flask equipped with a mechanical stirrer, a nitrogen inlet and a vacuum distillation outlet. A 5% molar excess of diol to the diester mixture, and dibutyl tin oxide (DBTO) as catalyst (0.8% w/w respect to monomers) were used. The apparatus was vented with nitrogen several times at room

temperature in order to remove the air and avoid oxidation during the polymerization. The transesterification reaction was carried out under a low nitrogen flow at 140 °C for 3 h. The polycondensation reaction was left to proceed at 140 °C for 5 h, under a 0.03-0.06 mbar vacuum. Then, the reaction mixture was cooled to room temperature, and the atmospheric pressure was recovered with nitrogen to prevent degradation. The resulting polymers were dissolved in chloroform and precipitated in excess of methanol in order to remove unreacted monomers and formed oligomers. Finally, the polymer was collected by filtration, extensively washed with methanol, and dried under vacuum.

PE-12Ad_xGalx_y. IR (film), ν (cm⁻¹): 1730 (C=O st), 1260 (C-O asym st, ester), 1160 (C-O sym st, ester), 1095 (C-O asym st, acetal), 800 (C-O sym st, acetal), 730 and 720 (CH₂ rock). ¹H NMR (300.1 MHz, CDCl₃), δ (ppm): 5.25 and 5.05 (2s, Galx, 2CH₂), 4.60 (m, Galx, 2CH), 4.28 (m, Galx, 2CH), 4.19 (t, Galx, 2CH₂), 4.06 (t, Ad, 2CH₂), 2.32 (t, Ad, 2CH₂), 1.65 (m, Ad, Galx, 6CH₂), 1.28 (m, Ad, Galx, 16CH₂). ¹³C NMR (75.5 MHz, C₆D₆), δ (ppm): 172.6 (CO), 170.3 (CO), 97.1, 79.9, 76.3, 65.6, 64.3, 34.1, 29.9, 29.8, 29.6, 29.5, 29.2, 28.9, 26.4, 26.1, 24.9.

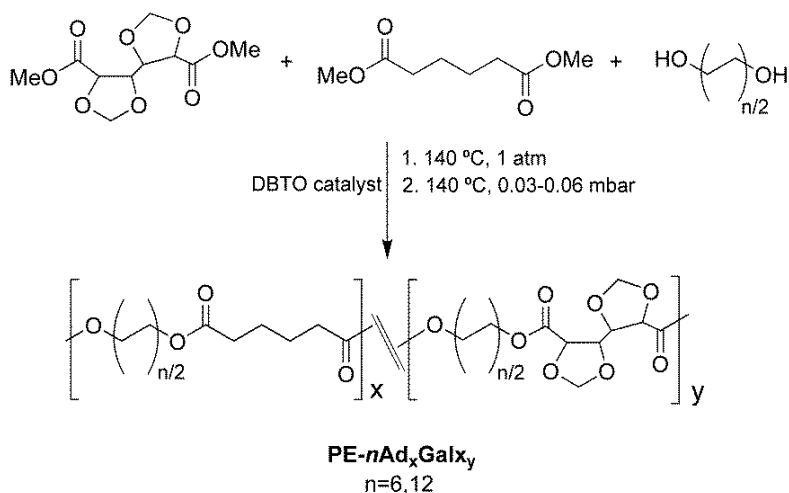
PE-6Ad_xGalx_y. IR (film), ν (cm⁻¹): 1730 (C=O st), 1260 (C-O asym st, ester), 1160 (C-O sym st, ester), 1095 (C-O asym st, acetal), 800 (C-O sym st, acetal), 730 and 720 (CH₂ rock). ¹H NMR (300.1 MHz, CDCl₃), δ (ppm): 5.25 and 5.05 (2s, Galx, 2CH₂), 4.60 (m, Galx, 2CH), 4.28 (m, Galx, 2CH), 4.20 (t, Galx, 2CH₂), 4.06 (t, Ad, 2CH₂), 2.32 (t, Ad, 2CH₂), 1.65 (m, Ad, Galx, 6CH₂), 1.39 (m, Ad, Galx, 4CH₂). ¹³C NMR (75.5 MHz, CDCl₃), δ (ppm): 173.4 (CO), 170.3 (CO), 96.8, 79.0, 75.3, 65.6, 64.3, 33.9, 28.5, 28.4, 25.5, 25.4, 24.4.

3.3.3. Results and discussion

3.3.3.1. Synthesis and chemical structure

The synthesis of PE-12Ad_xGalx_y and PE-6Ad_xGalx_y copolyesters was carried out by reacting mixtures of dimethyl adipate and Galx in the selected proportions, with 1,12-dodecanediol or 1,6-hexanediol respectively, as depicted in Scheme 3.4. Polycondensation conditions were similar to those previously applied by us in the synthesis of PE-*n*Ad and PE-*n*Galx homopolyester series, which included the two pairs of parent homopolyesters (PE-12Ad/PE12Galx and PE-6Ad/PE-6Galx) used in this work as

references. Thus, reactions were performed in the melt and in the total absence of solvents, and under a progressively diminishing reaction pressure in order to facilitate the releasing of volatile by-products. As before, the catalyst DBTO was used instead of the more familiar TBT, which allowed to keep the temperature at 140 °C along the whole polycondensation process minimizing the decomposition of thermally sensitive sugar compounds. By these means, copolyesters could be prepared as white powders with acceptable molecular weights in yields close to 90%. The synthesis results obtained for the two copolyester series are gathered in Table 3.4 together with data previously reported for their corresponding parent homopolyesters.



Scheme 3.4. Polymerization reactions leading to PE-*n*Ad_{*x*}Gal_{*y*} copolyesters.

The intrinsic viscosities of the copolyesters oscillate between 0.5 and 0.8 dL·g⁻¹, with the lower values being generally observed for the PE-6 series. The GPC analysis afforded *M_n* values comprised in the ~14,000-16,000 g·mol⁻¹ range with polydispersities between 2 and 3. In addition to GPC, the *M_n* of the polyesters was estimated by ¹H NMR (end-group analysis) and a very good agreement was found between values provided by the two techniques. The chemical constitution and composition of the resulting polycondensates were ascertained by infrared and ¹H NMR spectroscopies. Infrared spectra were very similar for the two series showing the typical carboxylate (~1730, ~1260 and ~1170 cm⁻¹) and cyclic acetal (~1095 and ~800 cm⁻¹) stretching absorptions as well as the methylene stretching (3000-2850 cm⁻¹), bending (~1470 cm⁻¹) and rocking (~730-720 cm⁻¹) bands with intensities according to compositions.

Table 3.4. Molecular weights and compositions of PE-12Ad_xGalx_y and PE-6Ad_xGalx_y copolyesters.

Copolyester	Yield (%)	Molecular weight					Molar composition				Solubility ^e				
		$[\eta]^a$	M_n^b	M_n^c	M_w^c	\mathcal{D}^c	Feed		Copolyester ^d		H ₂ O EtOH	Et ₂ O DMSO	NMP DMF	THF CHCl ₃	HFIP TFA
							X _{Ad}	X _{Galx}	X _{Ad}	X _{Galx}					
PE-12Ad	91	0.66	16,000	16,900	38,000	2.2	100	0	100	0	-	-	-	+	+
PE-12Ad ₉₀ Galx ₁₀	90	0.73	15,200	14,200	37,000	2.6	90	10	89.6	10.4	-	-	-	+	+
PE-12Ad ₇₀ Galx ₃₀	88	0.76	16,900	16,300	45,600	2.8	70	30	68.2	31.8	-	-	+	+	+
PE-12Ad ₅₀ Galx ₅₀	89	0.68	15,500	14,300	38,700	2.7	50	50	48.6	51.4	-	-	+	+	+
PE-12Ad ₃₀ Galx ₇₀	89	0.72	16,300	15,500	42,000	2.7	30	70	28.2	71.8	-	-	+	+	+
PE-12Ad ₁₀ Galx ₉₀	90	0.69	15,800	14,500	37,800	2.6	10	90	9.6	90.4	-	-	+	+	+
PE-12Galx	91	0.81	20,400	16,400	41,200	2.5	0	100	0	100	-	-	+	+	+
PE-6Ad	92	0.68	23,800	21,700	42,200	1.9	100	0	100	0	-	-	-	+	+
PE-6Ad ₉₀ Galx ₁₀	90	0.80	18,600	16,200	45,300	2.8	90	10	89.0	11.0	-	-	-	+	+
PE-6Ad ₇₀ Galx ₃₀	88	0.67	17,900	15,100	39,400	2.6	70	30	68.2	31.8	-	-	+	+	+
PE-6Ad ₅₀ Galx ₅₀	89	0.52	16,500	15,400	35,000	2.3	50	50	48.3	51.7	-	-	+	+	+
PE-6Ad ₃₀ Galx ₇₀	88	0.53	16,900	16,000	36,200	2.3	30	70	28.1	71.9	-	-	+	+	+
PE-6Ad ₁₀ Galx ₉₀	91	0.62	17,200	15,300	38,100	2.5	10	90	11.7	88.3	-	-	+	+	+
PE-6Galx	90	0.51	16,800	15,100	34,700	2.3	0	100	0	100	-	-	+	+	+

^aIntrinsic viscosity in dL·g⁻¹ measured in chloroform at 25 °C. ^bNumber-average molecular weight in g·mol⁻¹ determined by ¹H NMR end group analysis. ^cNumber and weight-average molecular weights in g·mol⁻¹ and dispersities measured by GPC in HFIP against PMMA standards. ^dMolar composition determined by integration of the ¹H NMR spectra. ^e(-) Insoluble, (+) soluble.

The ^1H NMR spectra corroborated the chemical structure of the copolyesters with all signals being correctly assigned to the different protons contained in their repeating units (Figure 3.11). No significant traces of other signals indicative of impurities were detected in these spectra. Furthermore, integration of the proton signals arising from Ad and Galx units led to quantify the composition of the copolyesters in such units. Data provided by this analysis are given in Table 3.4, where it can be seen that the copolyesters compositions are essentially similar to those of their respective feeds. A close comparison of the composition values reveals however, that the content of the copolymers in adipic units is slightly lower than in their corresponding feed in most cases. Such preferential incorporation of the Galx units may be attributed to slight losses of the relatively volatile dimethyl adipate taking place during polycondensation.

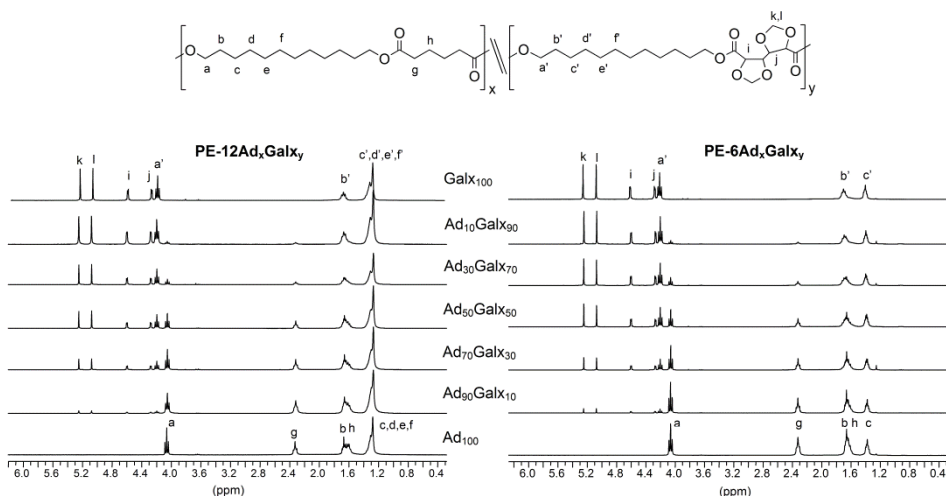


Figure 3.11. Compared ^1H NMR spectra of PE-12Ad $_x$ Gal $_y$ and PE-6Ad $_x$ Gal $_y$ copolyesters.

The microstructure of PE-12Ad $_x$ Gal $_y$ copolyesters was determined by ^{13}C NMR analysis and the spectrum registered from PE-12Ad $_{50}$ Gal $_{50}$ is shown in Figure 3.12 for illustration. The signals of all the magnetically different carbons contained in the repeating units of the copolyesters appear well resolved in the ^{13}C NMR spectra and in particular those arising from the methylene carbons of the diol, which come out to be sensitive to sequence effects at the dyad level. As shown in Figure 3.13 for the case of the PE-12Ad $_x$ Gal $_y$, series, each resonance of the two δ -methylene carbons appears split so that four peaks are seen in the 29.4-29.7 ppm chemical shift interval corresponding to the three types of dyads (AdAd, AdGalx and GalxAd, GalxGalx) that are feasible along the copolyester chain. The dyad contents were determined by area integration provided that

relaxation times of the involved carbon atoms are comparable. The plot of the content in each type of dyad as a function of the copolyesters composition reveals that the microstructure of the copolyesters is clearly statistical and randomness was calculated to be quite near unity in all cases. The statistical values obtained from this microstructure analysis are given in Table 3.5. Similar experimental results (not shown) were obtained in the analysis of the PE-6Ad_xGal_y, so the same conclusions regarding microstructure were drawn for this series.

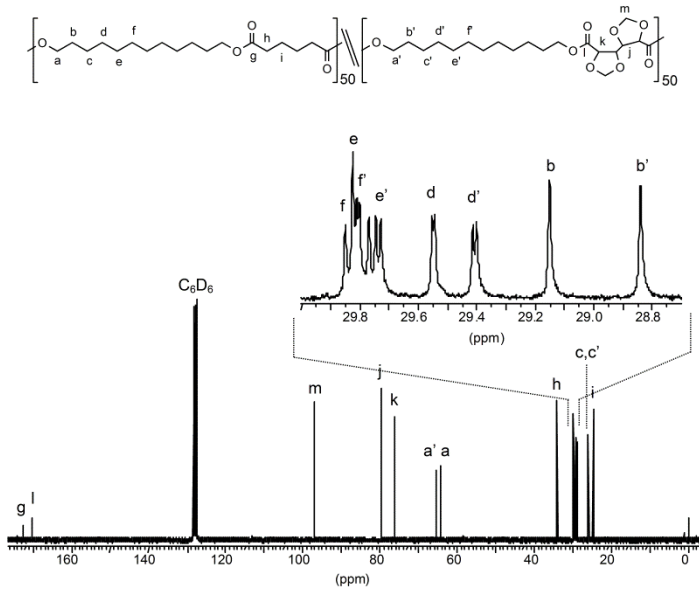


Figure 3.12. ¹³C NMR spectrum of PE-12Ad₅₀Gal₅₀ copolyester.

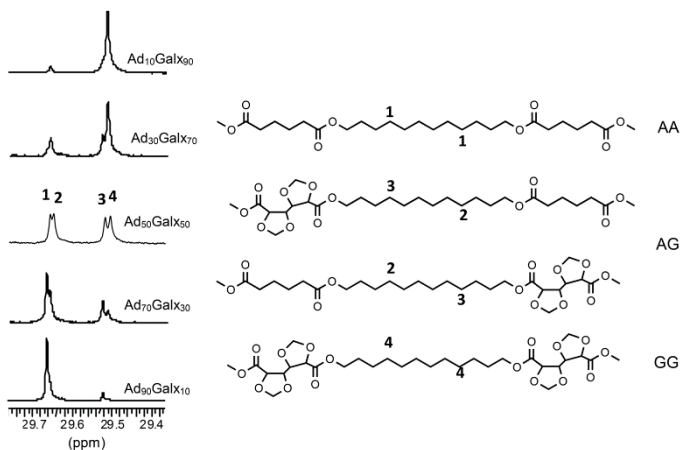


Figure 3.13. ¹³C NMR signals used for the microstructure analysis of PE-12Ad_xGal_y copolyesters (left) with indication of the dyads to which they are assigned (right).

Table 3.5. Microstructure analysis of PE-12Ad_xGal_y copolyesters.

Copolyester	Dyads (mol %)			Number Average Sequence Lengths		Randomness
	AA	AG/GA	GG	n_{Ad}	n_{Galx}	R
PE-12Ad ₉₀ Gal ₁₀	81.17	17.34	1.50	10.36	1.17	0.95
PE-12Ad ₇₀ Gal ₃₀	48.15	39.98	11.87	3.41	1.59	0.92
PE-12Ad ₅₀ Gal ₅₀	22.71	51.43	25.86	1.88	2.01	1.03
PE-12Ad ₃₀ Gal ₇₀	9.97	37.06	52.97	1.54	3.85	0.91
PE-12Ad ₁₀ Gal ₉₀	2.30	15.28	82.42	1.30	11.79	0.85

3.3.3.2. Thermal properties

The thermal behavior of both PE-12Ad_xGal_y and PE-6Ad_xGal_y copolyesters has been systematically studied by TGA and DSC taking as reference their parent homopolyesters containing exclusively adipate or 2,3:4,5-di-*O*-methylene galactarate units. Firstly, the thermal stability was evaluated by TGA under an inert atmosphere. The weight loss vs. temperature plots registered for the two series are shown in Figure 3.14 evidencing the similitude of behavior among the members of each series. As it is illustrated in Figure 3.15 for the specific cases of PE-12Ad₇₀Gal₃₀ and PE-12Ad₁₀Gal₉₀, the thermal decomposition happens through two or three steps depending on the copolyester composition. In all cases the main step takes place with a maximum rate T_d located in the 350–400 °C temperature range with values roughly increasing with the content in Gal_x units, and involving weight losses up to 90% of the initial weight. A second decomposition step taking place at temperatures around 450 °C and involving weight losses of 30% as maximum is invariably accompanying the main peak. The copolyesters highly enriched in Gal_x units as well as Gal_x homopolyesters still show a third decomposition step near below 350 °C with weight losses less than 15%. The concluding remark that can be drawn from the TGA analysis is that in general the replacement of adipate by Gal_x units increases the thermal stability of the polyesters in the two series. Such a trend is not applicable however to copolyesters with very high contents in sugar units ($\geq 90\%$), which start to decompose at temperatures below 350 °C, apparently due to the presence of long sequences of Gal_x units.

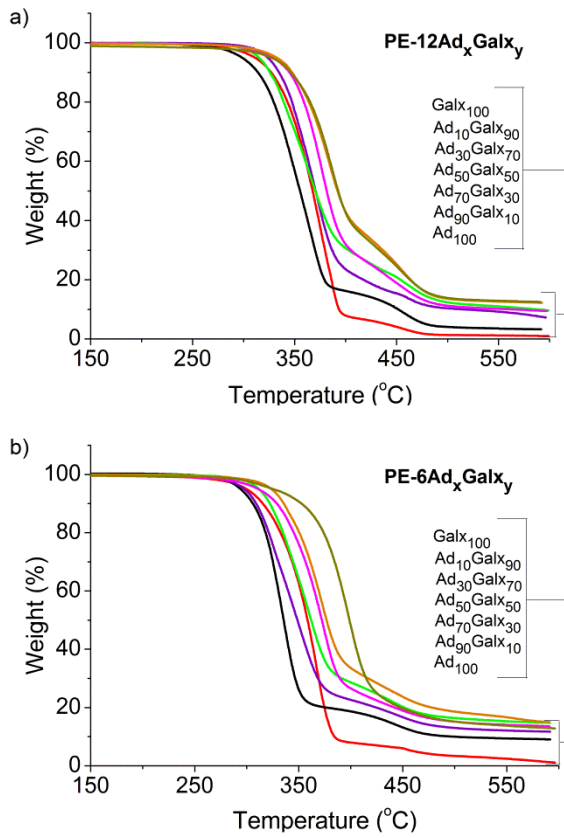


Figure 3.14. TGA traces of PE-12Ad_xGal_x_y (a) and PE-6Ad_xGal_x_y (b) copolyesters.

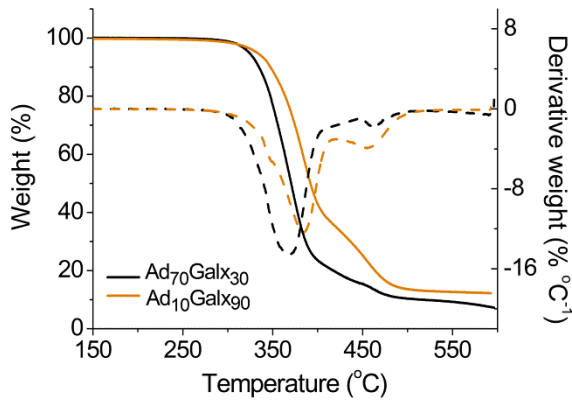


Figure 3.15. TGA traces (solid lines) and derivative curves (dashed lines) of PE-12Ad₇₀Gal_x₃₀ and PE-12Ad₁₀Gal_x₉₀ copolyesters.

The DSC analysis revealed significant changes in the melting and glass-transitions of PE-12Ad and PE-6Ad polyesters upon the incorporation of cyclic acetalized galactaric units. Glass-transition and melting temperatures, and melting enthalpies measured in the DSC analysis of both pristine samples and samples crystallized from the melt are given in Table 3.6. A remarkable feature of Galx homopolyesters is that they have considerably higher T_g than their analogues made of Ad. Accordingly, the T_g of the copolyesters within each series increases steadily with the content in Galx units with minimum and maximum values corresponding to their respective reference homopolyesters (Figure 3.16). The trend observed for T_g with the copolyester composition is in full agreement with what should be expected from the stiffness/bulkiness of the bicyclic sugar unit compared to the relative flexible/slender tetramethylene segment of the adipic acid, once it is provided that the microstructure of the copolyesters is statistical.

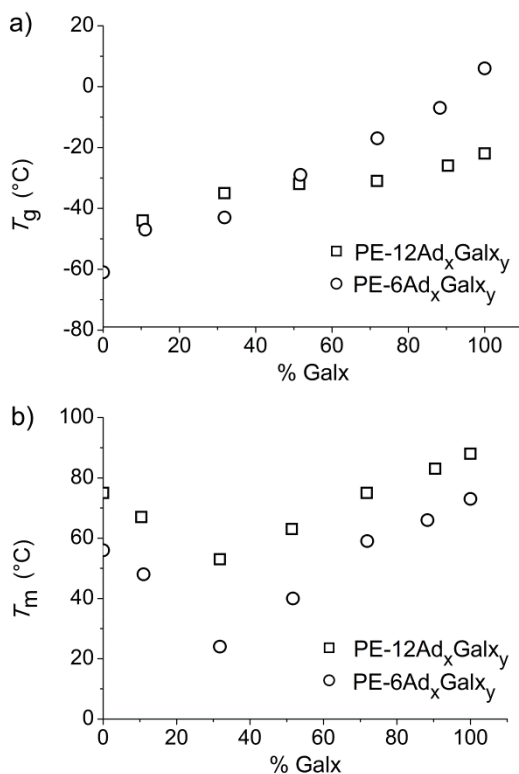


Figure 3.16. Glass-transition temperature (a) and melting temperature (b) vs. composition plots for PE-12Ad_xGalx_y and PE-6Ad_xGalx_y.

Table 3.6. Thermal properties of PE-12Ad_xGal_y and PE-6Ad_xGal_y copolyesters.

Copolyester	TGA			DSC								
	°T _{5%} ^a (°C)	T _d ^b (°C)	W ^c (%)	First heating ^e			Cooling ^e		Second heating ^e			
				T _g ^d (°C)	T _m (°C)	ΔH _m (J·g ⁻¹)	T _c (°C)	ΔH _c (J·g ⁻¹)	T _c (°C)	ΔH _c (J·g ⁻¹)	T _m (°C)	ΔH _m (J·g ⁻¹)
PE-12Ad	311	375	1	n.d.	75	118.8	63	102.5	-	-	75	109.1
PE-12Ad ₉₀ Gal _{x10}	299	365	3	-44	67	108.5	56	80.6	-	-	68	87.9
PE-12Ad ₇₀ Gal _{x30}	325	369	7	-35	53	68.5	39	47.8	-	-	53	43.4
PE-12Ad ₅₀ Gal _{x50}	315	365	10	-32	43/63 ^f	41.2	20	40.4	-	-	36/61 ^f	31.8
PE-12Ad ₃₀ Gal _{x70}	328	376	10	-31	75	37.8	26	33.8	-	-	75	29.1
PE-12Ad ₁₀ Gal _{x90}	332	383	12	-26	83	32.1	36	29.6	-	-	82	27.0
PE-12Gal _x	329	388	13	-22	88	43.7	45	35.8	-	-	88	35.2
PE-6Ad	300	367	1	-61	56	100.5	40	69.8	-	-	57	73.1
PE-6Ad ₉₀ Gal _{x10}	294	334	9	-47	48	61.1	25	49.9	-	-	43/47 ^f	49.4
PE-6Ad ₇₀ Gal _{x30}	297	346	12	-43	24	20.5	-6	15.5	-6	9.7	26	26.0
PE-6Ad ₅₀ Gal _{x50}	311	359	13	-29	40	10.9	-	-	-	-	-	-
PE-6Ad ₃₀ Gal _{x70}	311	373	13	-17	43/59 ^f	20.4	-	-	-	-	-	-
PE-6Ad ₁₀ Gal _{x90}	324	373	13	-7	45/66 ^f	20.4	-	-	-	-	-	-
PE-6Gal _x	325	398	13	6	51/70/73 ^f	15.7	-	-	-	-	-	-

^aTemperature at which 5 % weight loss was observed. ^bTemperature for maximum degradation rate. ^cRemaining weight at 600 °C. ^dGlass-transition temperature taken as the inflection point of the heating DSC traces of melt-quenched samples recorded at 20 °C·min⁻¹; n.d.: not determined.

^eMelting (T_m) and crystallization (T_c) temperatures, and melting (ΔH_m) and crystallization (ΔH_c) enthalpies measured by DSC at heating/cooling rates of 10 °C·min⁻¹. ^fMultiple melting peak.

As it is shown in Figure 3.17, the heating DSC traces registered from samples of homopolyesters and copolyesters coming directly from synthesis display in all cases endothermic peaks characteristic of melting and reveal therefore that all they are crystalline. The melting temperatures and enthalpies measured by DSC are listed in Table 3.6. The homopolyesters PE-12Galx and PE-6Galx display T_m higher than their corresponding analogues PE-12Ad and PE-6Ad but involve smaller ΔH_m indicative of lower crystallinity. As it is depicted in Figure 3.16, the variation of T_m of the copolyesters with the degree of replacement of Ad by Galx does not follow the continuous trend observed for T_g but it falls into a minimum for intermediate copolyesters compositions. Such behavior suggests the occurrence of two different crystal structures in each series according to which unit, Ad or Galx, is predominant in the copolyester. On the other hand the melting enthalpy values reveal that crystallinity tends to decrease with increasing contents in Galx units exception made for the homopolyester PE-12Galx which displays an ΔH_m higher than their copolyesters containing minor amounts of Ad.

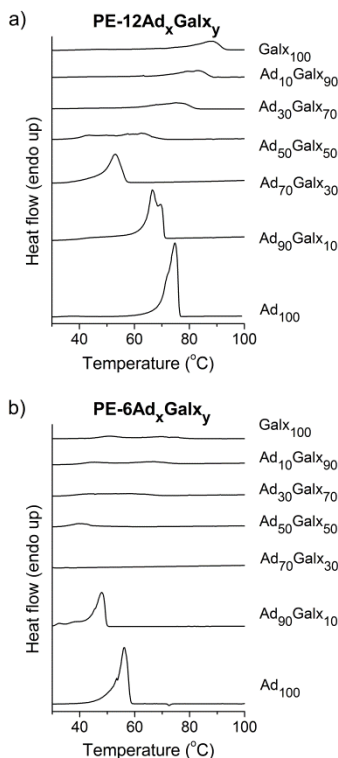


Figure 3.17. DSC melting traces of PE-12Ad_xGalx_y, (a) and PE-6Ad_xGalx_y, (b) coming directly from synthesis.

The cooling DSC traces obtained from molten samples revealed that the polyesters made from 1,12-dodecanediol crystallize easier than those made from 1,6-hexanediol, which makes much sense given the higher flexibility of the dodecamethylene segment. In fact, while PE-12Ad_xGal_y were able to crystallize for the whole range of compositions, PE-6Ad_xGal_y crystallized only for contents in Gal_x units below 30%. In both series the material crystallized from the melt displayed similar melting temperatures but significantly smaller enthalpies than the original samples indicating that a lower degree of crystallinity was reached. A comparative inspection of melting enthalpy data given in Table 3.6 brings into evidence the hindering effect of the Gal_x unit on crystallizability as far as copolyesters enriched in Ad units are concerned. To evaluate quantitatively the effect of composition on crystallizability, the isothermal crystallization in the 35-70 °C temperature range of the whole PE-12Ad_xGal_y series including the parent homopolyesters, was comparatively studied. Unfortunately, not all members could be compared at the same T_c due to the large differences in crystallization rates displayed by them and to the short ranges of temperatures at which crystallization evolution is measurable by DSC. Nevertheless, crystallization conditions were chosen as close as possible in order to draw out meaningful conclusions. The Weeks-Hofmann plot of T_m vs. T_c showed a good correlation (Figure 3.18) and provides the equilibrium melting temperatures, which continue displaying the same trend with composition as was observed for the values measured for non-isothermally crystallized samples.

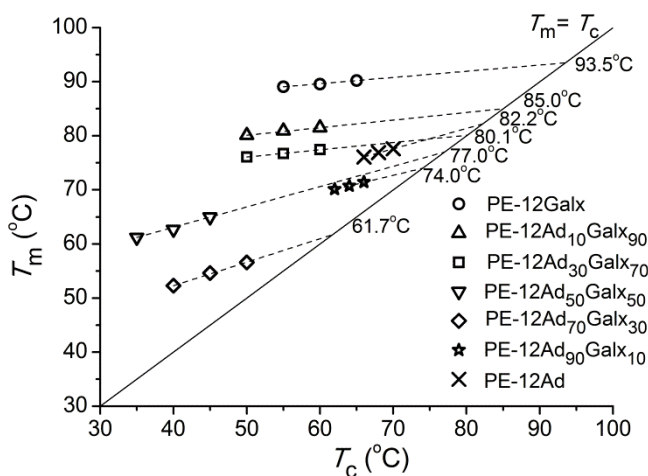


Figure 3.18. Hoffman-Weeks plot for isothermally crystallized PE-12Ad_xGal_y copolyesters.

Table 3.7. Isothermal crystallization data for PE-12Ad_xGal_y.

Copolyester	T_c (°C)	t_0 (min)	$t_{1/2}$ (min)	n	$-\log k$	T_m (°C)
PE-12Galx	55	0.07	0.38	2.28	-1.03	89.1
	60	0.22	0.94	2.42	-0.18	89.6
	65	0.37	2.23	2.76	0.88	90.2
PE-12Ad ₁₀ Gal _{x90}	50	0.23	1.12	2.31	0.07	80.1
	55	0.37	2.21	2.73	0.88	80.9
	60	0.42	5.75	2.96	2.31	81.5
PE-12Ad ₃₀ Gal _{x70}	50	0.45	2.80	2.84	1.25	76.1
	55	0.71	6.94	2.94	2.66	76.7
	60	1.09	23.44	3.00	4.16	77.4
PE-12Ad ₅₀ Gal _{x50}	35	0.33	2.56	2.30	1.31	61.2
	40	2.06	10.35	2.32	3.10	62.7
	45	14.42	33.69	2.34	5.17	65.0
PE-12Ad ₇₀ Gal _{x30}	40	0.06	0.23	2.44	-2.00	52.3
	45	0.27	1.12	2.46	0.03	54.6
	50	0.73	9.05	2.55	2.52	56.6
PE-12Ad ₉₀ Gal _{x10}	62	0.33	2.57	2.59	1.13	70.1
	64	0.53	4.82	2.67	1.98	70.7
	66	2.40	19.35	2.80	4.19	71.4
PE-12Ad	66	0.18	0.43	2.85	-1.18	76.1
	68	0.38	1.90	3.28	0.73	76.9
	70	1.55	6.19	3.59	2.59	77.6

Kinetic data afforded by the Avrami analysis of the results obtained at the selected crystallization temperatures are gathered in Table 3.7. The evolution of the relative crystallinity with crystallization time for PE-12Galx, PE-12Ad₁₀Gal_{x90} and PE-12Ad₃₀Gal_{x70} at T_c of 55 and 60 °C measured by DSC are depicted in Figure 3.19. The spherulitic growth rate measured by optical microscopy on thin films at cooling from the melt and the morphological appearance of the crystallized material are shown in Figures 3.20 and 3.21. It is seen that for every polyester the crystallization half-time as well as the Avrami exponent n increase with temperature, and that the material crystallized in spherulites displaying a fibrillar texture that not changed significantly with temperature. It

can be inferred therefore that the crystallization rate of these copolyesters is governed by the diffusion factor, and since the n values oscillate in the 2.2-3.6 range, the process should be initiated mainly by instantaneous nucleation. The double logarithmic plot of crystallinity vs. time used for the Avrami analysis (Figure 3.19) indicates that only primary crystallization takes place in the selected time intervals. From these plots as well as from data given in Table 3.7, it can be certainly concluded that the incorporation of Ad units in the PE-12Galx depress the crystallizability. On the other hand, comparison of Avrami data for the PE-12Ad and PE-12Ad₉₀Galx₁₀ indicates that crystallization is largely delayed by the presence of Galx units. Furthermore, comparison of $t_{1/2}$ for PE-12Ad₇₀Galx₃₀ and PE-12Ad₅₀Galx₅₀ leads to the same conclusion although in this case crystallization took place at significantly lower temperatures. The conclusion derived from this analysis is that crystallization rate is maximum for the homopolyesters PE-12Ad and PE-12Galx and that it decays in both cases upon incorporation of the second comonomer to fall into a minimum for intermediate compositions.

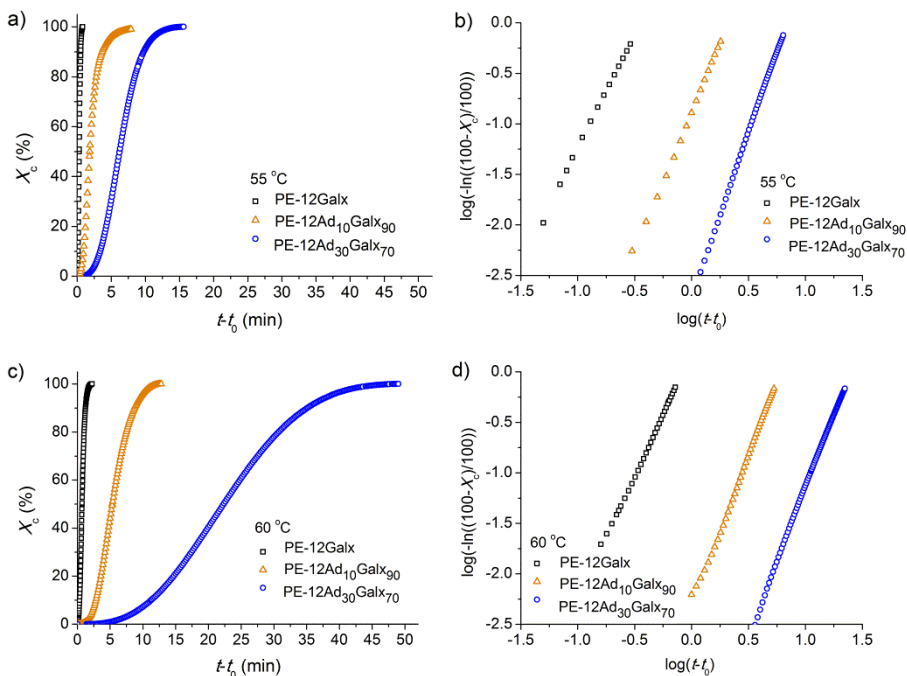


Figure 3.19. Isothermal crystallization of PE-12Galx, PE-12Ad₁₀Galx₉₀ and PE-12Ad₃₀Galx₇₀ at the indicated temperatures. (a) Relative crystallinity vs. time plot at 55°C. (b) Log-log plot at 55°C. (c) Relative crystallinity vs. time plot at 60°C. (d) Log-log plot at 60°C.

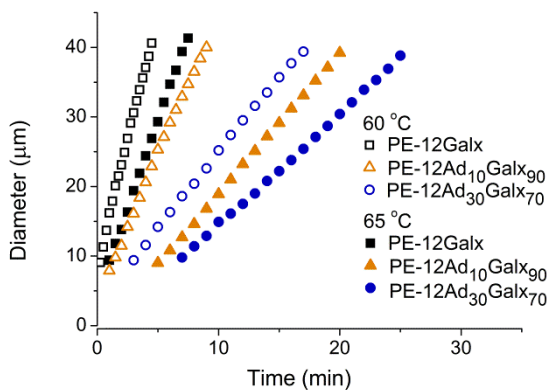


Figure 3.20. Spherulitic diameter vs. time plot for isothermally crystallized PE-12Galx, PE-12Ad₁₀Galx₉₀ and PE-12Ad₃₀Galx₇₀ at 60°C and 65°C.

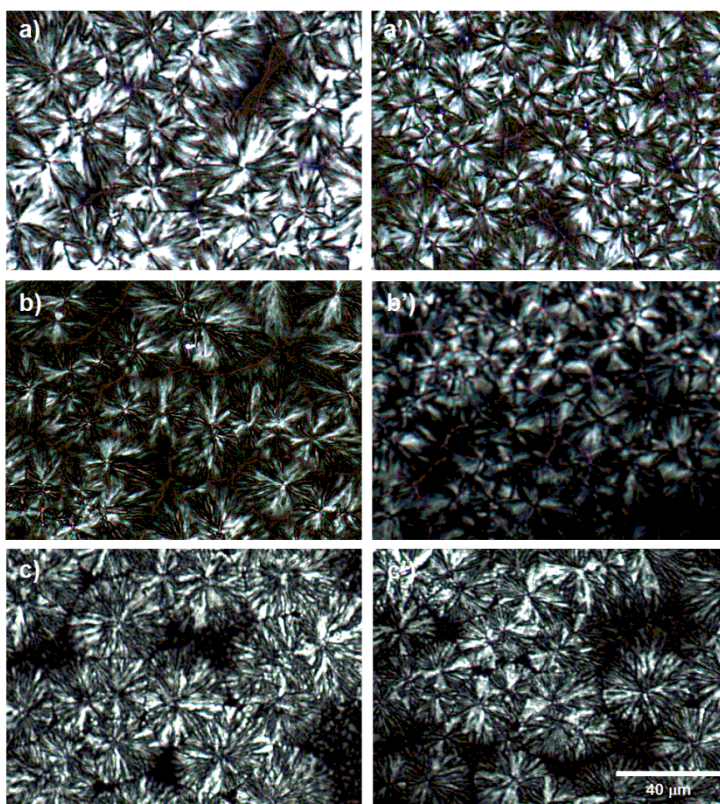


Figure 3.21. Polarized optical micrographs of samples isothermally crystallized at the indicated temperatures: PE-12Galx at 65 °C (a) and 60 °C (a'), PE-12Ad₁₀Galx₉₀ at 65°C (b) and 60 °C (b'), PE-12Ad₃₀Galx₇₀ at 65°C (c) and 60°C (c'). The scale bar corresponds to 40 μm.

3.3.3.3. Crystal structure

It is known that the insertion of sugar units bearing side groups in linear polyamides and polyesters create bulky heterogeneities in the polymer hindering the close chain packing required for crystallization. The behavior usually observed is that both aliphatic and aromatic random copolyesters with minor amounts of sugar units, *i.e.* below ~30%, are able to crystallize retaining the crystal structure of the parent homopolyester with rejection of the sugar units from the crystalline phase. Whereas homopolyesters entirely made of sugar units are able to crystallize adopting specific crystal structures, the copolyesters enriched in sugar units are usually amorphous (Zamora *et al.*, 2005; Alla *et al.*, 2006 and 2008). DSC has shown that both PE-12Ad_xGalx_y and PE-6Ad_xGalx_y copolyesters are crystalline for the whole range of compositions which is a rather unusual behavior. The X-ray diffraction analysis corroborated the DSC results since, as it is shown in Figure 3.22, discrete scattering profiles indicative of semicrystalline material were recorded for the whole series. The Bragg spacings and crystallinity indexes measured on such profiles are compared in Table 3.8. It is seen that homopolymer PE-12Ad and the copolymers PE-12Ad₉₀Galx₁₀ and PE-12Ad₇₀Galx₃₀ display the same diffraction pattern which is distinguished by the presence of two prominent reflections at 4.2 and 3.7 Å. Such a pattern is characteristic of poly(alkylene dicarboxylate) polyesters which are known to crystallize usually in an orthorhombic or monoclinic lattice with chains adopting a quasi *all-trans* conformation (Armelin *et al.*, 2001). Accordingly, the two observed reflections should be related with the side-by-side packing of the chains and indexed therefore as *hk0*, and the absence of higher spacing reflections, which would arise from planes with $l \neq 0$, may be interpreted as the result of the balancing shift of the chains along the *c* direction of the structure.

A different pattern containing three sharp reflections at 4.0, 4.3 and 4.6 Å along with another broad one at 17-18 Å was recorded for PE-12Ad_xGalx_y copolyesters with 50% or more of Galx units as well as for the homopolyester PE-12Galx. It is clear that a new crystal structure is adopted when the content in Galx units becomes the majority. The X-ray diffraction pattern shown in Figure 3.22, which is illustrative of the whole set, was recorded from a fiber of PE-12Ad₁₀Galx₉₀ obtained by stretching from the melt. The reflections at 4.0 and 4.6 Å are equatorially placed and interpreted therefore to arise from *hk0* plane whereas the in-between one at 4.3 Å is off-meridional and should be related with the azimuthal arrangement of the chains. On the other hand, the reflection at 17.9 Å is observed in the fiber pattern at an off-meridian position (inset of Figure 3.22b). This

reflection may be indexed as either $hk0$ or $hk1$ for a crystal structure made of almost extended chains which are progressively or regularly shifted along the c -axis, respectively. Since the repeating unit length calculated for PE-12Ad $_x$ Gal $_y$ with the chain in *all-trans* conformation is 24 Å, it is concluded that the shifting of the chains must be around 3 Å.

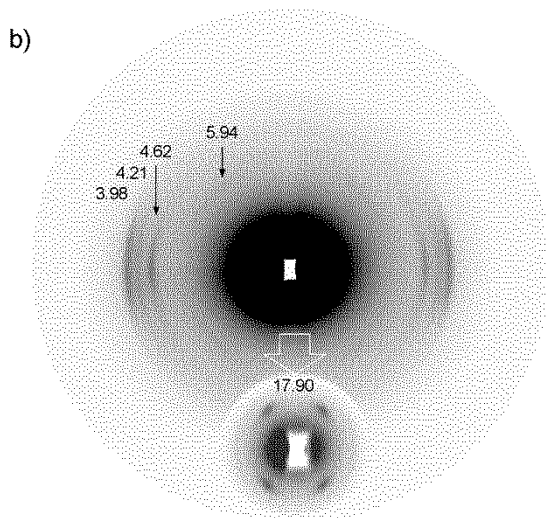
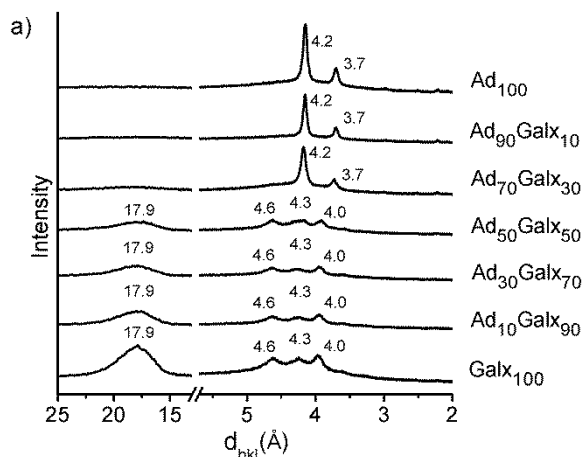


Figure 3.22. a) Powder WAXD profiles of PE-12Ad $_x$ Gal $_y$ copolyesters. b) Fiber pattern of PE-12Ad $_{10}$ Gal $_{90}$ (fiber axis vertical), Inset: Inner region showing medium-angle reflections.

Table 3.8. Powder X-ray diffraction data and mechanical properties of PE-12Ad_xGalx_y copolyesters.

Copolyester	X-ray diffraction data			Mechanical Properties		
	d^a (Å)		X_c^b	Elastic modulus (MPa)	Tensile strength (MPa)	Elongation at break (%)
PE-12Ad	4.2 s	3.7 m	0.51	87 ± 5	6 ± 1	215 ± 9
PE-12Ad ₉₀ Galx ₁₀	4.2 s	3.7 m	0.48	98 ± 4	7 ± 1	110 ± 8
PE-12Ad ₇₀ Galx ₃₀	4.2 s	3.7 m	0.47	100 ± 4	8 ± 1	92 ± 7
PE-12Ad ₅₀ Galx ₅₀	17.9 s 4.6 s 4.3 s 4.0 s		0.46	107 ± 3	9 ± 1	90 ± 8
PE-12Ad ₃₀ Galx ₇₀	17.9 s 4.6 s 4.3 s 4.0 s		0.44	129 ± 5	10 ± 1	78 ± 8
PE-12Ad ₁₀ Galx ₉₀	17.9 s 4.6 s 4.3 s 4.0 s		0.43	140 ± 5	12 ± 1	67 ± 6
PE-12Galx	17.9 s 4.6 s 4.3 s 4.0 s		0.42	155 ± 4	13 ± 1	59 ± 4

^a Bragg spacings measured in powder diffraction patterns for samples coming directly from synthesis. Intensities visually estimated as follows: m, medium; s, strong; w, weak.

^b Crystallinity index calculated as the quotient between crystalline area and total area. Crystalline and amorphous areas were quantified using PeakFit v4.12 software.

3.3.3.4. Stress-strain behavior

Aliphatic polyesters are known to display meager mechanical properties, which together with their rather low melting temperature, constitute one of the main reasons that have hampered their industrial expansibility. This has also restricted their use in biomedical applications in spite of their good biocompatibility and biodegradability. In this regard it is interesting to evaluate the effect of the replacement of the alkylene dicarboxylate by the galactarate units on the mechanical behavior of polyadipates. For this aim, comparative tensile essays of the PE-12Ad_xGalx_y series were carried out using thin films prepared by casting from chloroform solution. The traces registered in these essays are shown in Figure 3.23 and the mechanical parameters values extracted from such traces are given in Table 3.8. The evolution followed by the stress-strain curves with the content in Galx units clearly illustrates their influence on the mechanical compliance. It is noteworthy how the behavior changes from flexible/ductile typical of semicrystalline aliphatic polyesters to stiff/brittle when adipate units are entirely replaced by Galx units; the elastic modulus becomes almost doubled and the elongation to break is reduced to near one fourth of its value. The copolyesters with intermediate compositions show a steadily changing stress-strain behavior with mechanical parameters spanning between those of the two homopolyesters. As expected, the observed changes in the stress-strain behavior closely follow the changes in T_g ; both effects are the logical consequence of the

increasing stiffness of the polyester chain that is motivated by the progressive replacement of Ad by Galx.

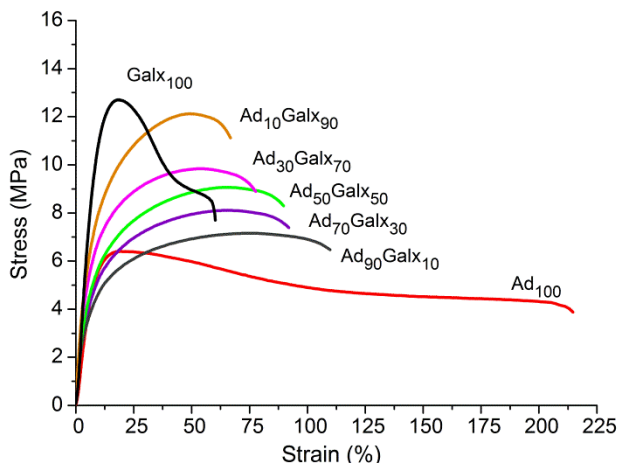


Figure 3.23. Stress-strain curves for PE-12Ad_xGal_y copolyesters.

3.3.4. Conclusions

The bicyclic diester dimethyl 2,3:4,5-di-*O*-methylene galactarate (Galx) was successfully copolymerized in the melt with dimethyl adipate and alkanediols (1,6-hexanediol and 1,12-dodecanediol) to obtain bio-based polycyclic random copolyesters covering the full range of compositions. The Galx containing copolyesters had agreeable molecular weights and were thermally stable and semicrystalline for all compositions. The enriched adipate copolyesters take up the crystal structure typical of aliphatic linear polyesters while a second crystal form seems to be adopted for high contents in sugar units. The melting temperature of the copolyesters changes with composition according to a power function that goes to the minimum as the contents in the two comonomers approach to each other. Copolyesters made from 1,12-dodecanediol were able to crystallize from the melt at a rate depending on composition. The incorporation of the Galx unit in the polyadipate chain increased the T_g as well as the modulus of rigidity and the stress yield whereas diminished the ductility of the polymer. The suitability of the bicyclic acetalized dimethyl galactarate to prepare bio-based aliphatic copolyesters with overall satisfying properties and increased T_g has been demonstrated.

3.3.5. References

Alla, A.; Hakkou, K.; Zamora, F.; Martínez de Ilarduya, A.; Galbis, J.A.; Muñoz-Guerra, S. *Macromolecules* **2006**, *39*, 1410-1416.

Alla, A.; Hakkou, K.; Zamora, F.; Martínez de Ilarduya, A.; Galbis, J.A.; Muñoz-Guerra, S. *J Polym. Sci., Polym. Chem.* **2008**, *46*, 5167–5179.

Armelin, E.; Casas, M.T.; Puiggali, J. *Polymer* **2001**, *42*, 5695-5699.

Beaman, R.G.; Morgan, P.W.; Koller, C.R.; Wittbecker, E.L.; Magat, E.E. *J. Polym. Sci.*, **1959**, *40*, 329-336.

Belgacem, M.N.; Gandini, A. *Monomers, Polymers and Composites from Renewable Resources*; Elsevier: Oxford, **2008**.

Bird, T.P.; Black, A.P.; Dewar, E.T.; Rutherford, D. *Chem. Ind.* **1960**, 1331-1332.

Bird, T.P.; Black, W.A.P.; Dewar, E.T.; Hare, J.B. *Chem. Ind.* **1961**, 1077.

Bird, T.P.; Black, W.A.P.; Dewar, E.T.; Hare, J.B. *J. Chem. Soc.* **1963**, 1208-1212.

Black, W.A.P.; Dewar, E.T.; Hare, J.B. *J. Chem. Soc.* **1963**, 5724-5727.

Burden, I.; Stoddart, J. F. *J. Chem. Soc. Perkin I* **1975**, 675-682.

Butler, K.; Lawrance, R.L.; Stacey, M. *J. Chem. Soc.* **1958**, 740-743.

Chatti, S.; Schwarz, G.; Kricheldorf, H.R. *Macromolecules* **2006**, *39*, 9064-9070. (2006a)

Chatti, S.; Kricheldorf, H.R.; Schwarz, G. *J. Polym. Sci., Polym. Chem.* **2006**, *44*, 3616-3628. (2006b)

Chen, L.; Kiely, D.E. *J. Org. Chem.* **1996**, *61*, 5847-5851.

Dhamaniya, S.; Jacob, J. *Polymer* **2010**, *51*, 5392-5399.

Fenouillot, F.; Rousseau, A.; Colomines, G.; Saint-Loup, R.; Pascault, J.P. *Prog. Polym. Sci.* **2010**, *35*, 578-622.

Gómez, R.; Varela, O. *Macromolecules* **2009**, *42*, 8112-8117.

Galbis, J.A.; García-Martín, M.G. *Top. Curr. Chem.* **2010**, *295*, 147–176.

Gandini, A. *Green Chem.* **2011**, *13*, 1061-1083.

Iribarren, J.I.; Martínez de Ilarduya, A.; Alemán, C., Oraison, J.M., Rodríguez-Galán, A., Muñoz-Guerra, S. *Polymer* **2000**, *41*, 4869–4879.

Juais, D.; Naves, A.F.; Li, C.; Gross, R.A.; Catalani, L.H. *Macromolecules* **2010**, *43*, 10315-10319.

Kiely, D.E.; Chen, L.; Lin, T.H. *J. Amer. Chem. Soc.* **1994**, *116*, 571-578.

- Kimura, H.; Yoshinari, T.; Takeishi, M. *Polym. J.* **1999**, *31*, 388-392.
- Kint, D.P.R.; Wingström, E.; Martínez de Ilarduya, A.; Alla, A.; Muñoz-Guerra, S. *J. Polym. Sci., Polym. Chem.* **2001**, *39*, 3250-3262.
- Kricheldorf, H.R. *J. Macromol. Sci., Rev. Macromol. Chem. Phys.* **1997**, *C37*, 599-631.
- Lavilla, C.; Alla, A.; Martínez de Ilarduya, A.; Benito, E.; García-Martín, M.G.; Galbis, J.A.; Muñoz-Guerra, S. *Biomacromolecules* **2011**, *12*, 2642-2652. **-Subchapter 3.2-**
- Marín, R.; Muñoz-Guerra, S. *J. Appl. Polym. Sci.* **2009**, *114*, 3723-3736.
- Noordover, B.A.J.; van Staaldin, V.G.; Duchateau, R.; Koning, C.E.; van Benthem, R.A.T.M.; Mak, M.; Heise, A.; Frissen, A.E.; van Haveren, J. *Biomacromolecules* **2006**, *7*, 3406-3416.
- Okada, M. *Prog. Polym. Sci.* **2001**, *26*, 67-104.
- Pillai, C.K.S. *Design. Monom. Polym.* **2010**, *13*, 87-121.
- Quintana, R.; Martínez de Ilarduya, A.; Alla, A.; Muñoz-Guerra, S. *J. Polym. Sci., Polym. Chem.* **2011**, *49*, 2252-2260.
- Rodríguez-Galán, A.; Bou, J.; Muñoz-Guerra, S. *J. Polym. Sci., Polym. Chem.* **1992**, *30*, 713-721.
- Sablong, R.; Duchateau, R.; Koning, C.E.; de Wit, G.; van Es, D.; Koelewijn, R.; van Haveren, J. *Biomacromolecules* **2008**, *9*, 3090-3097.
- Storbeck, R.; Rehahn, M.; Balluff, M. *Makromol. Chem.* **1993**, *194*, 53-64.
- Thiem, J.; Lüders, H. *Polym. Bull.* **1984**, *11*, 365-369.
- Varela, O. *Adv. Carbohydr. Chem. Biochem.* **2000**, *55*, 137-174.
- Varma, A.J.; Kennedy, J.F.; Galgali, P.Q. *Carbohydr. Polym.* **2004**, *56*, 429-445.
- Wool, R.; Sun, S. *Biobased Polymers and Composites*; Academic Press: New York, **2005**.
- Zamora, F.; Hakkou, K.; Alla, A.; Espartero, J.L.; Muñoz-Guerra, S.; Galbis, J.A. *J. Polym. Sci., Polym. Chem.* **2005**, *43*, 6394-6410.

3.4. High T_g bio-based aliphatic polyesters from bicyclic D-mannitol

Summary: The carbohydrate-based diol 2,4:3,5-di-O-methylene-D-mannitol (Manx) has been used to obtain aliphatic polyesters. Manx is a symmetric bicyclic compound consisting of two fused 1,3-dioxane rings and bearing two primary hydroxyl groups. In terms of stiffness it is comparable to the widely known isosorbide but it affords the additional advantages of being much more reactive in polycondensation and capable of producing stereoregular polymers with fairly high molecular weights. A fully bio-based homopolyester (PManxS) has been synthesized by polycondensation in the melt from dimethyl succinate and Manx. The high thermal stability of PManxS, its relatively high glass-transition temperature ($T_g = 68$ °C) and elastic modulus, and its enhanced sensitivity to the action of lipases point to PManxS as a polyester of exceptional interest for those applications where biodegradability and molecular stiffness are priority requirements. In addition, random copolyesters (PB_xMan_xS) covering a broad range of compositions have been obtained using mixtures of Manx and 1,4-butanediol in the reaction with dimethyl succinate. All PB_xMan_xS were semicrystalline and displayed T_g values from -29 to +51 °C steadily increasing with the content in Manx units. The stress-strain behavior of these copolyesters largely depended on their content in Manx and they were enzymatically degraded faster than PBS.

Publication derived from this work:

Lavilla, C.; Alla, A.; Martínez de Ilarduya, A.; Muñoz-Guerra, S. *Biomacromolecules* **2013**, *14*, 781-793.

3.4.1. Introduction

Due to increasing concerns on sustainable development and minimizing the impact of materials on the environment, biodegradable polymers have attracted a great deal of interest in the last decades (Engelberg and Kohn, 1991; Albertsson and Varma, 2002; Okada, 2002; Nair and Laurencin, 2007). Aliphatic polyesters such as poly(butylene succinate) (PBS), poly(L-lactic acid), poly(ϵ -caprolactone) and poly(3-hydroxy butyrate) among others, constitute a distinguished bunch of biodegradable polymers that are commercially available in several forms. Some of these aliphatic polyesters have found intensive use in a broad variety of medical applications such as bioresorbable surgical sutures, prosthesis, dental implants, bone screw and plates for temporary internal fracture fixation, and controlled drug delivery systems (Wang *et al.*, 2012; Coutinho *et al.*, 2012). Nowadays PBS is receiving exceptional attention as a polymeric material suitable for replacing conventional commodity plastics in injection-molded articles (cutlery, brushes), tubular films (composting bags, shopping bags), flexible packaging and food tray since it has a melting temperature similar to that of low density polyethylene, satisfactory mechanical properties and can be processed with the conventional equipments commonly used for polyolefins (Papageorgiou and Bikiaris, 2007; Gualandi *et al.*, 2012). However, PBS has a glass-transition temperature (T_g) of -37 °C, not high enough for its use in rigid packaging and cosmetic and beverage bottles where stiffness and thermal resistance are priority requisites. In this regard, various approaches such as blending and copolymerization with aromatic polyesters as poly(butylene terephthalate) (PBT) and poly(ethylene terephthalate) (PET) have been recently explored (Deng *et al.*, 2004; Li *et al.*, 2012). The interest for cyclic monomers arises from their capacity for adding stiffness to the polymer chain with the subsequent increase in T_g ; the disadvantage of using aromatic units for such purpose is that they are originated from fossil feedstocks and are reluctant to biodegradation.

The use of carbohydrate-based monomers with a cyclic structure constitute a scarcely explored approach for the preparation of renewable aliphatic polyesters with improved physical properties, especially those related to polymer chain stiffness (Galbis and García-Martín, 2010; Gandini, 2011). Moreover, carbohydrate-derived polycondensates typically display enhanced hydrophilicity, lower toxicity and higher susceptibility to hydrolytic degradation and biodegradation than those coming from petrochemical feedstocks. Thus 2,3-O-isopropylidene-L-tartaric acid (Dhamaniya and Jacob, 2010 and 2012) and 2,5-furandicarboxylic acid (Gandini *et al.*, 2009; Gomes *et al.*,

2011; Wu *et al.*, 2012a) have been polymerized with several diols to obtain bio-based aliphatic cyclic polyesters. 1,4:3,6-Dianhydro-D-glucitol, known as isosorbide, which is prepared by dehydration of D-glucose coming from cereal starch, is the only bicyclic carbohydrate-based monomer industrially available today. Isosorbide, along with their two less accessible stereoisomers isomannide and isoidide, are currently drawing an enormous interest in the polymer science field as bio-based monomers able to provide enhanced stiffness into the polymer chain they are incorporated (Fenouillot *et al.*, 2010). These three isohexides are composed of two fused tetrahydrofuran rings, with two secondary hydroxyl groups remaining free for reaction. Due to their fused bicyclic structure, 1,4:3,6-dianhydrohexitols and their diacid derivatives are able to increase the glass-transition temperature of common aliphatic polyesters (Braun and Bergmann, 1992; Okada *et al.*, 1996 and 2000; Noordover *et al.*, 2006; Wu *et al.*, 2012b). Nevertheless, the main shortcoming of isosorbide and its isomers is the limited reactivity of their secondary hydroxyl groups; in fact, this feature seriously hampers the polycondensation reaction in the melt, so aliphatic polyesters from 1,4:3,6-dianhydrohexitols and aliphatic dicarboxylic acids or dicarboxylic esters obtained by this method display rather limited molecular weights (Braun and Bergmann, 1992; Noordover *et al.*, 2006). Higher molecular weights are achievable via polycondensation with aliphatic dicarboxylic chlorides (Okada *et al.*, 1996 and 2000), but this method is not appropriate for industrial application (Fradet and Tessier, 2003).

Recently, we have reported the synthesis and characterization of aliphatic polyesters made from dimethyl 2,3:4,5-di-O-methylene-galactarate (Galx), which is a bicyclic monomer obtained by internal acetalization of galactaric acid (Lavilla *et al.*, 2011 -Subchapter 3.2- and 2012a -Subchapter 3.3-). This monomer has been shown to be very suitable to prepare aliphatic polyesters by polycondensation with aliphatic diols in the melt, since it is able to react at a rate similar to that of other acyclic conventional monomers. At difference with dianhydrohexitols, Galx is composed of two independent 1,3-dioxolane rings linked by a single C-C bond, and thence they were found to confer lower rigidity to the polyester backbone than a fused bicyclic structure is able to do. To our knowledge, the bicyclic diester Galx is the only bicyclic diacetalized carbohydrate-based monomer that has been used up to date to obtain aliphatic polyesters.

In this work bicyclic 2,4:3:5-di-O-methylene-D-mannitol, abbreviated as Manx, has been used to obtain aliphatic polyesters. Manx is obtained by internal acetalization of D-mannitol in a similar way to the bicyclic diester Galx is obtained from mucic acid.

Nevertheless, at difference with Galx, Manx is a rigid structure composed of two fused 1,3-dioxane rings, which will confer to the polymer chain higher stiffness than the two non-fused rings of Galx. Manx is therefore a diol very adequate for the synthesis of bio-based aliphatic polyesters with T_g much higher than usually found in these compounds; in fact, too low T_g is widely recognized to be one of the main shortcomings of most of common aliphatic polyesters. At difference with isosorbide, which has been previously exploited with the same purpose, the use of Manx as a monomer or comonomer for polyesters will lead to stereoregular chains because of the twofold axis of symmetry present in the molecule. Furthermore the high reactivity of the two primary hydroxyl groups of Manx, which are able to react more efficiently than the secondary hydroxyl groups of isosorbide, will be able to render higher molecular weight polyesters. Here we present a fully bio-based polysuccinate (PManxS) made from the renewable diol Manx and the dimethyl ester of succinic acid (SA), which has been synthesized by melt polycondensation; its thermal and mechanical properties and its ability to be biodegraded have been evaluated and compared with those displayed by PBS. We also present an exploratory account of new bio-based aliphatic copolyesters obtained by partially replacing 1,4-butanediol in PBS by Manx. An assortment of products with properties grading between those of PBS and PManxS have been obtained and characterized. These copolyesters are called PB_xManx_yS , with the subscripts x and y standing for their molar contents in butanediol and Manx units, respectively. The combination of Manx with SA has been proven to be satisfactory to afford bio-based polysuccinates with T_g much higher than most of those known so far and comparable to those prepared from isosorbide.

3.4.2. Experimental section

3.4.2.1. Materials

2,4:3,5-Di-O-methylene-D-mannitol was synthesized following the procedure recently reported by Lavilla *et al.* (Lavilla *et al.*, 2012b -Subchapter 5.4-). Dimethyl succinate (98+%) was purchased from Merck-Schuchardt. 1,4-butanediol (99%) and the catalyst dibutyl tin oxide (DBTO, 98%) were purchased from Sigma-Aldrich. Solvents used for purification and characterization were purchased from Panreac and they all were of either technical or high-purity grade. All the reagents and solvents were used as received without further purification.

3.4.2.2. General methods

^1H and ^{13}C NMR spectra were recorded on a Bruker AMX-300 spectrometer at 25.0 °C operating at 300.1 and 75.5 MHz, respectively. Samples were dissolved in a mixture of deuterated chloroform and trifluoroacetic acid (9:1) or in deuterated water, and spectra were internally referenced to tetramethylsilane (TMS). About 10 and 50 mg of sample dissolved in 1 mL of solvent were used for ^1H and ^{13}C NMR, respectively. Sixty-four scans were acquired for ^1H and 1,000-10,000 for ^{13}C with 32 and 64-K data points as well as relaxation delays of 1 and 2 s, respectively. 2D ^1H - ^1H homonuclear (COSY) and ^{13}C - ^1H heteronuclear shift correlation (HETCOR) spectra were recorded by means of the *cosy* and *hxcO*, respectively, pulse sequences implemented in the Bruker NMR instrument package. Intrinsic viscosities of polyesters dissolved in chloroform were measured in an Anton Paar AMVn Automated Micro Viscosimeter at 25.00±0.01 °C, using the VisioLab for AMVn software. Gel permeation chromatograms were acquired at 35.0 °C with a Waters equipment provided with a refraction-index detector. Samples were chromatographed with 0.05 M sodium trifluoroacetate-hexafluoroisopropanol (NaTFA-HFIP) using a polystyrene-divinylbenzene packed linear column with a flow rate of 0.5 mL·min⁻¹. Chromatograms were calibrated against poly(methyl methacrylate) (PMMA) monodisperse standards. The thermal behavior of polyesters was examined by DSC using a Perkin Elmer DSC Pyris 1. DSC data were obtained from 3 to 5 mg samples at heating/cooling rates of 10 °C·min⁻¹ under a nitrogen flow of 20 mL·min⁻¹. Indium and zinc were used as standards for temperature and enthalpy calibration. The glass-transition temperatures were determined at a heating rate of 20 °C·min⁻¹ from rapidly melt-quenched polymer samples. The treatment of the samples for isothermal crystallization experiments was the following: the thermal history was removed by heating the sample up to 200 °C and left at this temperature for 5 min, and then it was cooled at 20 °C·min⁻¹ to the selected crystallization temperature, where it was left to crystallize until saturation. For morphological study, isothermal crystallizations conducted under the same conditions were carried out in an Olympus BX51 Polarizing Optical Microscope coupled to a THMS LINKAM heating plate and a cooling system LNP (Liquid Nitrogen Pump). Thermogravimetric analyses were performed under a nitrogen flow of 20 mL·min⁻¹ at a heating rate of 10 °C·min⁻¹, within a temperature range of 30 to 600 °C, using a Perkin Elmer TGA 6 equipment. Sample weights of about 10-15 mg were used in these experiments. Films for mechanical testing and contact angle measurements were prepared with a thickness of ~200 μm by casting from chloroform solution at a polymer concentration of 100 g·L⁻¹. For tensile essays the films were then cut into strips with a

width of 3 mm while the distance between testing marks was 10 mm. The tensile strength, elongation at break and Young's modulus were measured at a stretching rate of 30 mm·min⁻¹ on a Zwick 2.5/TN1S testing machine coupled with a compressor Dalbe DR150, at 23 °C. Contact angles were measured in an equipment OCA 20 (DataPhysics Instruments GmbH, Filderstadt) provided with the SCA20 software for image and data treatment. Angle values were registered after 45 s of dropping 1.5 µL of water onto the polyester surface at 23 °C. X-ray diffraction patterns were recorded on the PANalytical X'Pert PRO MPD θ/θ diffractometer using the Cu-K α radiation of wavelength 0.1542 nm from powdered samples coming from synthesis. Scanning electron microscopy (SEM) images were taken with a field-emission JEOL JSM-7001F instrument (JEOL, Japan) from platinum/palladium coated samples.

3.4.2.3. Polymer synthesis

PManxS homopolyester was obtained from 2,4:3,5-di-O-methylene-D-mannitol and dimethyl succinate. PB_xMan_yS copolyesters were obtained from a mixture of 1,4-butanediol, 2,4:3,5-di-O-methylene-D-mannitol and dimethyl succinate with the selected composition. PBS was obtained from 1,4-butanediol and dimethyl succinate. The reactions were performed in a three-necked, cylindrical-bottom flask equipped with a mechanical stirrer, a nitrogen inlet and a vacuum distillation outlet. An excess of diol mixture to dimethyl succinate was used and dibutyl tin oxide (DBTO, 0.6% molar respect to monomers) was the catalyst of choice. The apparatus was vented with nitrogen several times at room temperature in order to remove air and avoid oxidation during the polymerization. Transesterification reactions were carried out under a low nitrogen flow at the selected temperature. Polycondensation reactions were left to proceed at the selected temperature under a 0.03-0.06 mbar vacuum. Then, the reaction mixture was cooled to room temperature, and the atmospheric pressure was recovered with nitrogen to prevent degradation. The resulting polymers were dissolved in chloroform and precipitated in excess of methanol in order to remove unreacted monomers and formed oligomers. Finally, the polymer was collected by filtration, extensively washed with methanol, and dried under vacuum. These powdered samples coming directly from synthesis, *i.e.* without any further treatment other than reprecipitation and washing, were throughout used for the characterization performed in this work unless otherwise stated.

PManxS homopolyester. 5% molar excess of 2,4:3,5-di-O-methylene-D-mannitol to dimethyl succinate. Transesterification reactions at 160 °C for 3 h under a low nitrogen

flow. Polycondensation reactions at 160 °C for 5 h under a 0.03-0.06 mbar vacuum. ^1H NMR (300.1 MHz, CDCl_3/TFA), δ (ppm): 5.1-4.9 (m, 4H, OCH_2O), 4.6-4.4 (m, 4H, OCH_2CH), 4.6-4.4 (m, 2H, OCH_2CH), 4.3-4.1 (m, 2H, OCH_2CHCH), 2.8 (s, 4H, $\text{COCH}_2\text{CH}_2\text{CO}$). ^{13}C NMR (75.5 MHz, CDCl_3/TFA), δ (ppm): 175.2 (CO), 88.5, 71.6, 66.7, 63.9, 29.2.

PBS homopolyester. 20% molar excess of 1,4-butanediol to dimethyl succinate. Transesterification reactions at 160 °C for 2.5 h and at 180 °C for 0.5 h under a low nitrogen flow. Polycondensation reactions at 180 °C for 3.5 h under a 0.03-0.06 mbar vacuum. ^1H NMR (300.1 MHz, CDCl_3/TFA), δ (ppm): 4.2 (t, 4H, $\text{OCH}_2\text{CH}_2\text{CH}_2$), 2.8 (s, 4H, $\text{COCH}_2\text{CH}_2\text{CO}$), 1.8 (t, 4H, $\text{OCH}_2\text{CH}_2\text{CH}_2$). ^{13}C NMR (75.5 MHz, CDCl_3/TFA), δ (ppm): 175.7 (CO), 66.3, 29.6, 25.2.

$\text{PB}_x\text{Man}_y\text{S}$ copolyesters. The copolyesters were obtained by a similar procedure, with polymerization conditions slightly differing for each composition feed.

$\text{PB}_{95}\text{Man}_5\text{S}$ and $\text{PB}_{90}\text{Man}_{10}\text{S}$. 5% molar excess of the diol mixture to dimethyl succinate. Transesterification reactions at 160 °C for 2.5 h and at 180 °C for 0.5 h and under a low nitrogen flow. Polycondensation reactions at 180 °C for 3.5 h under a 0.03-0.06 mbar vacuum.

$\text{PB}_{80}\text{Man}_{20}\text{S}$ and $\text{PB}_{70}\text{Man}_{30}\text{S}$. 5% molar excess of the diol mixture to dimethyl succinate. Transesterification reactions at 160 °C for 2.5 h and at 170 °C for 0.5 h and under a low nitrogen flow. Polycondensation reactions at 170 °C for 4 h under a 0.03-0.06 mbar vacuum.

$\text{PB}_{50}\text{Man}_{50}\text{S}$ and $\text{PB}_{30}\text{Man}_{70}\text{S}$. 5% molar excess of the diol mixture to dimethyl succinate. Transesterification reactions at 160 °C for 3 h and under a low nitrogen flow. Polycondensation reactions at 160 °C for 5 h under a 0.03-0.06 mbar vacuum.

NMR characterization of $\text{PB}_x\text{Man}_y\text{S}$ copolyesters. ^1H NMR (300.1 MHz, CDCl_3/TFA), δ (ppm): 5.1-4.9 (m, $y\cdot 4\text{H}$, OCH_2O), 4.6-4.4 (m, $y\cdot 4\text{H}$, OCH_2CH), 4.6-4.4 (m, $y\cdot 2\text{H}$, OCH_2CH), 4.3-4.1 (m, $y\cdot 2\text{H}$, OCH_2CHCH), 4.2 (t, $x\cdot 4\text{H}$, $\text{OCH}_2\text{CH}_2\text{CH}_2$), 2.8 (s, 4H, $\text{COCH}_2\text{CH}_2\text{CO}$), 1.8 (t, $x\cdot 4\text{H}$, $\text{OCH}_2\text{CH}_2\text{CH}_2$). ^{13}C NMR (75.5 MHz, CDCl_3/TFA), δ (ppm): 175.7 (CO), 175.2 (CO), 88.5, 71.6, 66.7, 66.3, 63.9, 29.6, 29.2, 25.2.

3.4.2.4. Biodegradation and hydrolytic degradation

Films for polyester biodegradation and hydrolytic degradation studies were prepared with a thickness of ~200 μm by casting from chloroform solution at a polymer concentration of $100 \text{ g}\cdot\text{L}^{-1}$. The films were cut into 10 mm diameter, 20 to 30 mg weight disks and dried in vacuum to constant weight. For hydrolytic degradation, samples were immersed in vials containing 10 mL of either citric acid buffer (pH 2.0) or sodium phosphate buffer (pH 7.4) at 37 °C. After incubation for the scheduled period of time, the samples were rinsed thoroughly with distilled water and dried to constant weight. The enzymatic degradation was carried out at 37 °C in vials containing 10 mL of the enzymatic medium, consisting of a pH 7.4 buffered sodium phosphate solution containing lipase from porcine pancreas (10 mg). The buffered enzyme solution was replaced every 72 h to maintain the enzyme activity. At the end of the scheduled incubation periods, the disks were withdrawn from the incubation medium, washed thoroughly with distilled water, dried to constant weight and analyzed by GPC chromatography, NMR spectroscopy and SEM microscopy.

For hydrolytic degradation studies of 2,4:3,5-di-O-methylene-D-mannitol, samples of this diol (80 mg) were immersed in NMR tubes containing 1 mL of citric acid buffer (pH 2.0), sodium phosphate buffer (pH 7.4) or sodium carbonate buffer (pH 10.5), all of them prepared in D_2O , and were incubated at 37 °C for 12 weeks. The residue left after incubation was analyzed by NMR spectroscopy.

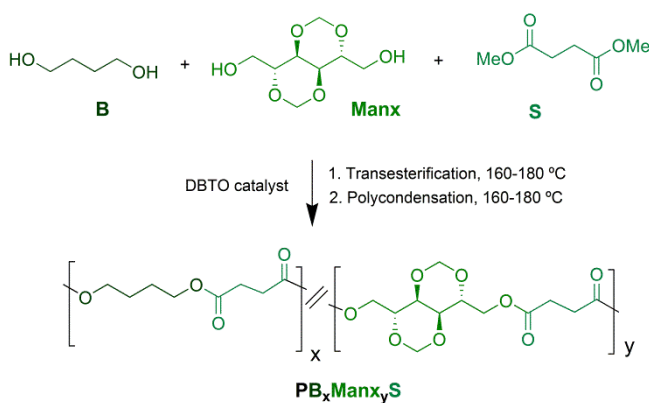
3.4.3. Results and discussion

3.4.3.1. Synthesis and chemical structure

The synthesis of the bio-based homopolyester PManxS was carried out by reaction of 2,4:3,5-di-O-methylene-D-mannitol (Manx) with the dimethyl ester of succinic acid. The reaction was performed in the melt and in the total absence of solvents to imitate as far as possible the conditions usually applied in the industry, in two successive stages at 160 °C and under a progressively diminishing reaction pressure to facilitate the removal of released by-products. Dibutyl tin oxide (DBTO) was the catalyst of choice instead of the commonly used titanium (IV) tetrabutoxide (TBT); our previous results in the synthesis of aliphatic homopolyesters from the bicyclic non-fused diester dimethyl

2,3:4,5-di-O-methylene-galactarate demonstrated the higher activity of DBTO catalyst compared to TBT (Lavilla *et al.*, 2011 -Subchapter 3.2-), which allowed to proceed at lower temperatures without increasing reaction times. Using mild conditions for polymerization, decomposition of thermally sensitive sugar compound was minimized and higher molecular weights could be attained. The M_w of the resulting PManxS homopolymer was higher than 30,000 g·mol⁻¹, with a 2.3 dispersity value. It is worthy to note that M_w of PManxS here obtained by melt polycondensation from the bicyclic diol Manx and succinic dimethyl ester is much higher than those reported for melt polycondensation of 1,4:3,6-dianhydrohexitols with aliphatic diesters or diacids (Braun and Bergmann, 1992; Noordover *et al.*, 2006). The higher reactivity of the primary hydroxyl groups of acetalized alditols compared to the secondary hydroxyl groups of 1,4:3,6-dianhydrohexitols is doubtlessly the reason for the observed differences. In fact, a recent study carried out by us comparing aromatic polyesters made from either acetalized alditols or alditol dianhydrides showed a much easier synthesis of the formers when obtained by melt polycondensation (Lavilla and Muñoz-Guerra, 2013 -Subchapter 7.2-).

The synthesis of PB_xMan_yS copolyesters were carried out from 1,4-butanediol, 2,4:3,5-di-O-methylene-D-mannitol and dimethyl succinate also by a two-step melt polycondensation process, at temperatures between 160 and 180 °C (Scheme 3.5); lower temperatures and longer reaction times were used for copolyesters with higher contents in Manx units. The homopolymer PBS, used in this study for comparison purposes, was prepared from 1,4-butanediol and dimethyl succinate following a similar procedure. The resulting PB_xMan_yS copolyesters had M_w in the 33,000 to 48,000 g·mol⁻¹ range, with dispersities between 2.3 and 2.5, and intrinsic viscosities ranging from 0.6 to 0.9 dL·g⁻¹ (Table 3.9).



Scheme 3.5. Polymerization reactions leading to PB_xMan_yS copolyesters.

Table 3.9. Molar composition, molecular weight, microstructure and contact angle.

Copolyester	Yield (%)	Molar composition				Molecular weight				Microstructure				Contact angle ^e		
		Feed		Copolyester ^a		$[\eta]^b$	M_n^c	M_w^c	\mathcal{D}^c	Dyads		Number Average Sequence Lengths			Randomness ^d	
		X_B	X_{Manx}	X_B	X_{Manx}					BB	BManx/ManxB	ManxManx	n_B			n_{Manx}
PBS	90	100	0	100	0	0.97	19,500	49,100	2.5							113±4
PB ₉₅ Manx ₅ S	87	95	5	94.3	5.7	0.90	19,900	47,800	2.4	87.9	11.4	0.7	16.4	1.1	0.96	114±5
PB ₉₀ Manx ₁₀ S	89	90	10	88.7	11.3	0.72	16,900	39,100	2.3	78.0	20.5	1.5	8.6	1.1	0.99	114±4
PB ₈₀ Manx ₂₀ S	88	80	20	80.7	19.3	0.69	14,600	35,200	2.4	66.3	30.8	3.0	5.3	1.2	1.03	117±3
PB ₇₀ Manx ₃₀ S	86	70	30	69.1	30.9	0.70	14,200	35,000	2.5	47.0	44.3	8.8	3.1	1.4	1.04	113±2
PB ₅₀ Manx ₅₀ S	87	50	50	51.1	48.9	0.61	13,900	33,400	2.4	26.1	50.0	24.0	2.0	2.0	1.00	114±4
PB ₃₀ Manx ₇₀ S	89	30	70	29.7	70.3	0.60	13,500	33,500	2.5	8.4	43.4	48.2	1.4	3.2	1.03	116±8
PManxS	85	0	100	0	100	0.56	13,300	30,800	2.3							74±7

^a Molar composition determined by integration of the ¹H NMR spectra. ^b Intrinsic viscosity in dL·g⁻¹ measured in chloroform at 25 °C. ^c Number and weight-average molecular weights in g·mol⁻¹ and dispersities measured by GPC in HFIP against PMMA standards. ^d Randomness index of copolyesters statistically calculated on the basis of the ¹³C NMR analysis. ^e Contact angle measured after 45 seconds of dropping 1.5 μL of water.

Both the ^1H and ^{13}C NMR analysis ascertained the chemical constitution and composition of the polyesters. They are detailed in Section 3.4.2, and a selection of the illustrative spectra is provided in Annex C. The assignment of the signals arising from the sugar units was supported by COSY and HETCOR spectra, which are included in Annex C. Integration of the proton signals arising from B and Manx units led to quantify the composition of the copolyesters in such units, which appeared to be very close to those of their respective feeds (Table 3.9). The microstructure of $\text{PB}_x\text{Man}_y\text{S}$ copolyesters was determined by ^{13}C NMR analysis. As it is depicted in Figure 3.24, the ^{13}C NMR spectra of copolyesters show one of the succinic signals with resolution enough as to make possible the elucidation of the copolyester microstructure as far as distribution of B and Manx units along the copolyester chain is concerned. As a consequence of the occurrence of different dyad types (BB, BManx, ManxB and ManxManx), this signal appears split into four peaks that spread within the 29.2-29.7 ppm chemical shift interval. By integration of these peaks, the dyad contents, the number-average sequence lengths and the degree of randomness were estimated (Table 3.9), leading to the conclusion that the microstructure of the copolyesters was random in all cases.

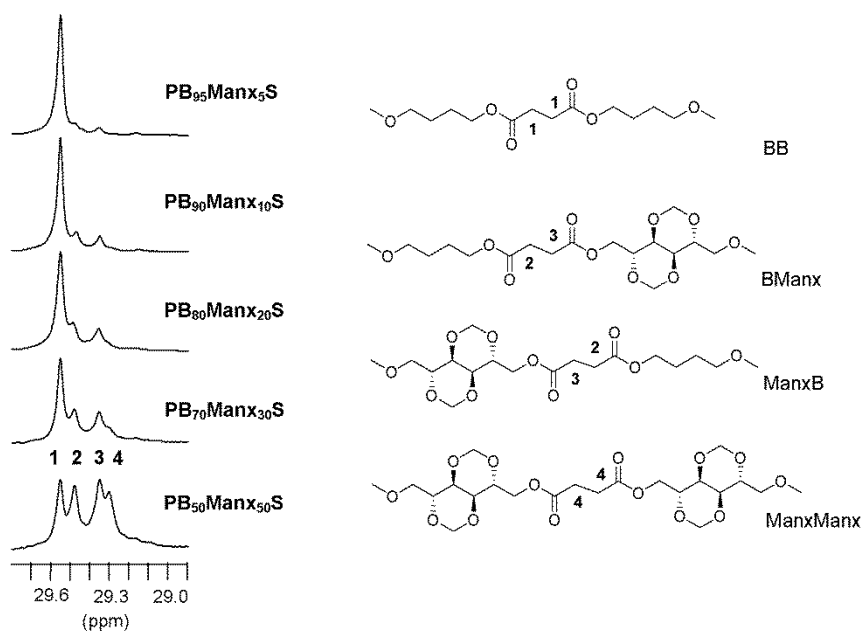


Figure 3.24. ^{13}C NMR signals used for the microstructure analysis of $\text{PB}_x\text{Man}_y\text{S}$ copolyesters with indication of the dyads to which they are assigned.

The solvent affinity of Manx containing polysuccinates was similar to that displayed by PBS. All they continue to be non-soluble in water but readily soluble in chloroform. The contact angle between water and polyester films was measured to estimate their hydrophilicity (Table 3.9); no significant differences were observed in the θ_{water} of PBS ($\sim 113^\circ$) with the incorporation of Manx units except for the case of the homopolyester where the contact angle decreased to near 75° indicating the much higher hydrophilic character of this compound.

3.4.3.2. Thermal and mechanical properties

The thermal behavior of PManxS homopolyester and $\text{PB}_x\text{Man}_y\text{S}$ copolyesters has been comparatively studied by TGA and DSC; the thermal parameters resulting from these analyses are given in Table 3.10, where the corresponding data for the homopolyester PBS are also included for reference. First, the thermal stability was evaluated by TGA under inert atmosphere. The TGA traces of PManxS and PBS homopolyesters together with their derivative curves are shown in Figure 3.25a, and those recorded from the whole set of $\text{PB}_x\text{Man}_y\text{S}$ copolyesters are comparatively depicted in Figure 3.25b. Thermal decomposition of PManxS occurs in a single stage with maximum rate taking place at 413°C ($^{\text{max}}T_d$), and only 5% of the initial weight remains at 600°C ; the maximum decomposition rate of PBS homopolyester occurs at 384°C ($^{\text{max}}T_d$), the residual weight left upon heating at 600°C being 4%. Decomposition of $\text{PB}_x\text{Man}_y\text{S}$ copolyesters takes place also in one stage, at temperatures ranging between $^{\text{max}}T_d$ of their two corresponding homopolyesters PBS and PManxS and steadily increasing as butanediol units are replaced by Manx units. The valuable conclusion drawn from this comparative thermogravimetric study is that the insertion of Manx in aliphatic polyesters instead of reducing their decomposition temperatures contributes significantly to increasing their thermal stability, which can broaden even more the application window of aliphatic polyesters. Since the melting in these copolyesters decreases with composition, a wider range of temperatures between melting and decomposition exists, allowing a more comfortable melt processing.

Table 3.10. Thermal properties.

Copolyester	TGA			DSC								
	$^{\circ}T_{5\%}^a$	T_d^b	W^c	T_g^d	First heating ^e		Cooling ^e		Second heating ^e			
					T_m	ΔH_m	T_c	ΔH_c	T_c	ΔH_c	T_m	ΔH_m
($^{\circ}C$)	($^{\circ}C$)	(%)	($^{\circ}C$)	($^{\circ}C$)	($^{\circ}C$)	($J \cdot g^{-1}$)	($^{\circ}C$)	($J \cdot g^{-1}$)	($^{\circ}C$)	($J \cdot g^{-1}$)	($^{\circ}C$)	($J \cdot g^{-1}$)
PBS	320	384	4	-37	111/114 (113)	75.0 (103.1)	81	60.7	-	-	113	61.1
PB ₉₅ Man ₅ S	320	386	6	-29	107 (107)	62.9 (69.3)	64	59.5	-	-	107	60.7
PB ₉₀ Man ₁₀ S	322	387	5	-20	94 (93)	45.3 (48.4)	42	16.9	35	18.7	95	36.2
PB ₈₀ Man ₂₀ S	323	410	4	-8	50/74/84 (51/82)	44.7 (47.3)	-	-	59	16.0	85	16.1
PB ₇₀ Man ₃₀ S	322	413	4	3	52/64 (49/63)	30.1 (38.7)	-	-	-	-	-	-
PB ₅₀ Man ₅₀ S	323	413	4	26	64/85 (62/80)	10.1 (10.9)	-	-	-	-	-	-
PB ₃₀ Man ₇₀ S	321	413	5	51	91 (90)	3.8 (4.6)	-	-	-	-	-	-
PMan _x S	320	413	5	68	- (125) ^f	- (14.0) ^f	-	-	-	-	-	-

^aTemperature at which 5% weight loss was observed. ^bTemperature for maximum degradation rate. ^cRemaining weight at 600 $^{\circ}C$. ^dGlass-transition temperature taken as the inflection point of the heating DSC traces of melt-quenched samples recorded at 20 $^{\circ}C \cdot min^{-1}$. ^eMelting (T_m) and crystallization (T_c) temperatures, and melting (ΔH_m) and crystallization (ΔH_c) enthalpies measured by DSC at heating/cooling rates of 10 $^{\circ}C \cdot min^{-1}$ of powdered samples coming directly from synthesis (without parentheses) and of films prepared by casting from solution (in parentheses). ^fAfter annealing for 1h at 60 $^{\circ}C$, T_m increased to 127 $^{\circ}C$ and ΔH_m to 21.5 $J \cdot g^{-1}$.

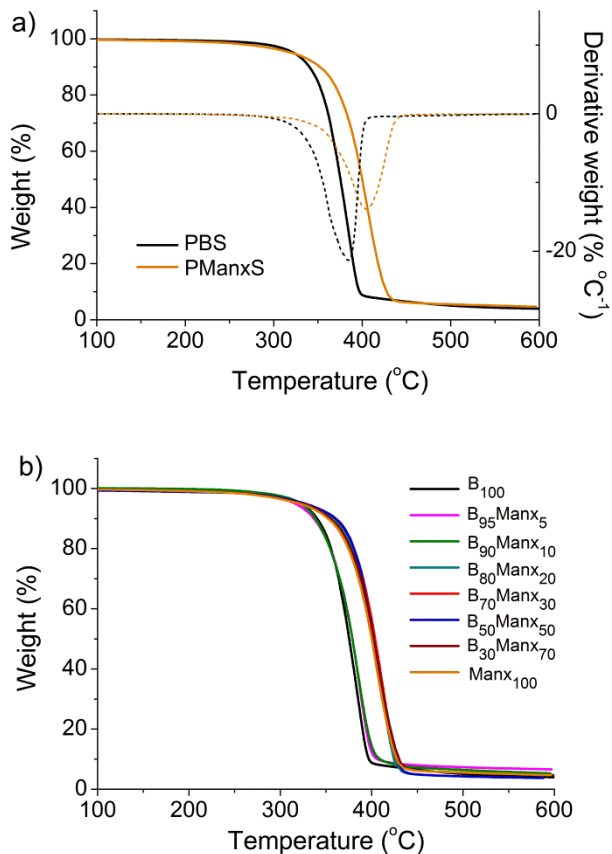


Figure 3.25. (a) TGA traces (solid lines) and derivative curves (dashed lines) of PBS and PManxS homopolyesters. (b) TGA traces of PB_xManx_yS copolyesters.

Another thermal property of prime importance in connection with the potential application of these polyesters is the glass-transition temperature (T_g). For instance, an increase in the T_g of aliphatic polyesters such as PBS could open their use in the rigid packaging field. The DSC analyses revealed that the T_g steadily increased as butanediol was replaced by Manx units going from -29 °C for PB₉₅Manx₅S up to 51 °C for PB₃₀Manx₇₀S (Figure 3.26a). These results are fully consistent with the T_g values of -37 °C and 68 °C observed for the PBS and PManxS homopolyesters, respectively, provided that the microstructure of the copolyesters is random. Such a remarkable positive effect of the incorporation of Manx on T_g makes this compound a bio-based comonomer very suitable for the preparation of aliphatic polyesters with enhanced T_g .

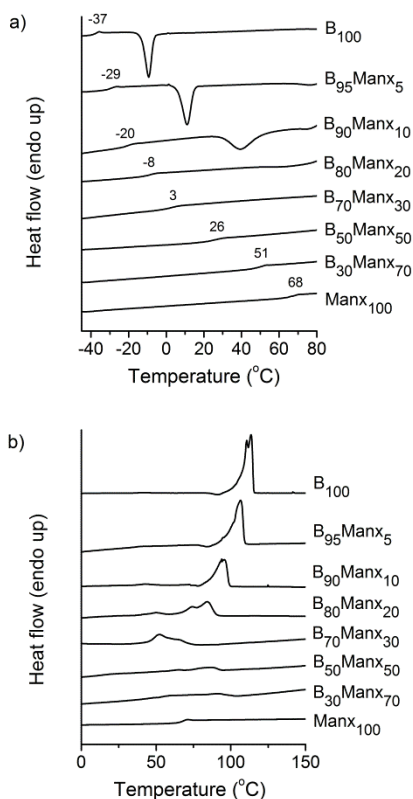


Figure 3.26. (a) DSC heating traces of PB_xMan_xS copolyesters quenched from the melt. (b) DSC heating traces of PB_xMan_xS copolyesters coming directly from synthesis.

DSC traces of polyesters coming directly from synthesis are depicted in Figure 3.26b. All PB_xMan_yS copolyesters as well as PBS homopolyester gave heating traces with melting endotherms indicating that they were semicrystalline, whereas PManxS appeared to be amorphous. Comparison of melting temperatures and enthalpies of PB_xMan_yS copolyesters with that of PBS leads to the conclusion that the insertion of Manx units gives place to a significant decrease in both T_m and ΔH_m . The T_m did not follow a continuous trend with composition but it fell into a minimum for copolyester compositions around 30% of Manx units (Figure 3.27). This behavior suggested the occurrence of two different crystal structures depending on the unit, butanediol or Manx, that is predominant in the copolyester.

To complement DSC data, powder X-ray diffraction analyses were performed for PB_xMan_yS copolyesters as well as for PBS and PManxS homopolyesters coming directly

from synthesis. The X-ray diffraction profiles recorded from powders are compared in Figure 3.28, and the most prominent Bragg spacings present therein are listed in Table 3.11. Essentially the same diffraction pattern regarding both spacing and intensities is shared by PBS homopolymer and copolymers containing up to 30% of Manx units. This pattern is distinguished by the presence of three sharp strong reflections at 4.5, 4.1 and 3.9 Å indicating that the monoclinic crystal structure of PBS (Ihn *et al.*, 1995) is retained in such copolymers. It must be assumed that the bicyclic structure in these copolymers is segregated from the crystal lattice which is made of homogeneous sequences of butylene succinate units. Since the average length of these sequences diminishes with the content in Manx, the crystallite thickness decreases and consequently T_m goes down. Conversely, both PB₅₀Man₅₀S and PB₃₀Man₇₀S produced a scattering profile with a clearly different shape where the three most prominent reflections corresponding now to 4.7, 4.5 and 4.0 Å which also coincides with that exhibited by the PManxS homopolymer. The larger values observed for these spacings, which presumably arise from the interplanar distances that are defined by the side-by-side packing of the chains, are consistent with the bigger size of Manx compared to butanediol. In addition, several weaker reflections are observed at higher spacings in the 6-8 Å range, which might be associated to the axial repeat of the polyester chain. Apparently a second crystal form different from that of PBS, which is able to accommodate the bicyclic structure in the lattice, seems to be adopted by both the homopolymer and the copolymers containing major amounts of Manx. In this case the butylene succinate would be the unit that is segregated from the crystalline phase; accordingly, the T_m in the Manx-enriched interval should be expected to increase with the content in Manx, as it is experimentally observed.

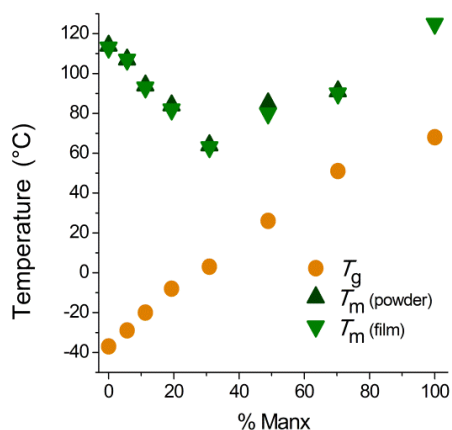


Figure 3.27. Glass-transition and melting temperatures versus composition plot for PB_xMan_x,S copolymers.

Table 3.11. Powder X-ray diffraction data and mechanical properties.

Copolyester	X-ray diffraction data												Mechanical Properties					
	d^a (Å)												X_c^b	Elastic modulus (MPa)	Tensile strength (MPa)	Elongation at break (%)		
PBS														2.6 w	0.52	351±11	20±2	19±4
PB ₉₅ Manx ₅ S														2.6 w	0.48	355±13	22±2	14±3
PB ₉₀ Manx ₁₀ S														2.6 w	0.45	372±14	22±2	9±2
PB ₈₀ Manx ₂₀ S														2.6 w	0.43	403±15	24±2	7±3
PB ₇₀ Manx ₃₀ S														2.6 w	0.37	428±12	24±3	5±2
PB ₅₀ Manx ₅₀ S	7.0 w	6.2 w	5.6 w	4.7 s	4.5 m	4.2 w	4.0 m	3.4 w	3.1 w	2.9 w	2.8 w			0.28		471±15	26±2	3±1
PB ₃₀ Manx ₇₀ S	7.0 w	6.2 w	5.6 w	4.7 s	4.5 m	4.2 w	4.0 m	3.4 w	3.1 w	2.9 w	2.8 w			0.17		515±14	28±3	2±1
PManxS	(7.0 w)	(6.2 w)	(5.6 w)	(4.7 s)	(4.5 m)	(4.2 w)	(4.0 m)	(3.4 w)	(3.1 w)	(2.9 w)	(2.8 w)			(0.31)		573±15	31±3	2±1

^a Bragg spacings measured in powder diffraction patterns. Intensities visually estimated as follows: m, medium; s, strong; w, weak. Data from samples coming directly from synthesis (without parentheses) and from PManxS film annealed for 1h at 60 °C (in parentheses). ^b Crystallinity index calculated as the quotient between crystalline area and total area quantified in the X-ray diffraction profiles using the PeakFit v4.12 software.

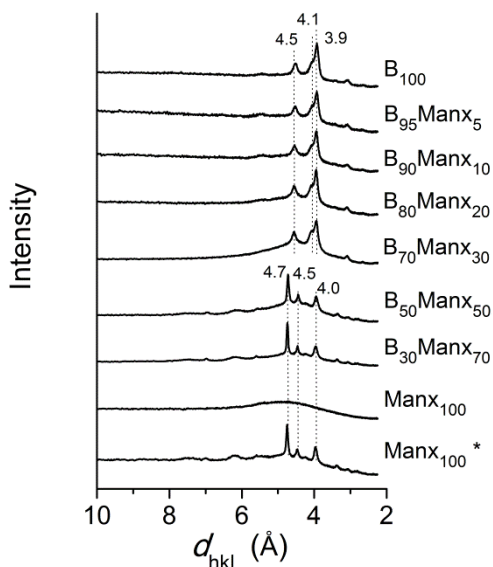


Figure 3.28. Powder WAXD profiles of PBS, PManxS and $PB_x\text{Manx}_y\text{S}$ copolyesters coming directly from synthesis. *The PManxS profile at the bottom was obtained from a film casted from chloroform that was annealed for 1 h at 60 °C.

Crystallinity was found however to decay steadily along the whole series as the content in Manx units increased, to the point that no discrete scattering could be detected for the homopolyester PManxS coming directly from synthesis. These observations are in full agreement with DSC results and reveal the depressing influence that the bicyclic structure has on crystallizability, which may be due to the opposite effect that it has on T_m and T_g . Increasing amounts of Manx led to polyesters with narrower crystallization window ($T_m - T_g$) and therefore exhibiting less crystallinity because the melt becomes frozen before the chains can crystallize upon supercooling. Nevertheless, PManxS was able to crystallize by casting from a chloroform solution. After annealing the cast film showed a melting peak at 127 °C with an enthalpy of 21.5 J·g⁻¹, and produced a WAXD profile identical to those recorded from the enriched Manx copolyesters (Figure 3.28). These results suggest that rather than hampering the close side-by-side packing of the polyester chains required to form the crystal lattice, the main repressing effect of Manx on crystallization should be due to the restricted mobility that the presence of the bicyclic structure confers to the polyester chain. This is in full agreement with the high delay that is observed in the isothermal crystallization time of $PB_x\text{Manx}_y\text{S}$ for slight rises in Manx contents, more than tenfold for a 5% of increment in Manx (see below).

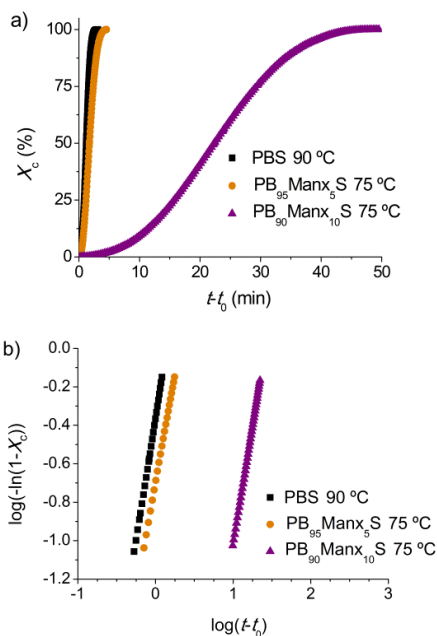


Figure 3.29. Isothermal crystallization of PBS, PB₉₅Man₅S and PB₉₀Man₁₀S at the indicated temperatures. Relative crystallinity versus time plot (a) and log-log plot (b).

The cooling DSC traces obtained from molten samples revealed that PB_xMan_yS copolyesters with molar contents in Man_x below or equal to 10%, as well as PBS homopolyester, were able to crystallize from the melt. After crystallization upon cooling at a constant rate of 10 °C·min⁻¹, PBS homopolyester and PB₉₅Man₅S copolyester recovered about 80-97% of their initial crystallinity and displayed almost the same melting temperatures. Conversely PB₉₀Man₁₀S copolyester crystallized under such conditions recovering only 37% of its original crystallinity. However, it presented cold crystallization at the second heating run with recovering about 80% of the initially crystallized material, and melting at nearly the same initial temperature. Given the relevance of the ability for crystallizing from the melt regarding polymer processing, the isothermal crystallization of PB₉₅Man₅S and PB₉₀Man₁₀S copolyesters and PBS homopolyester was comparatively studied in the 70-100 °C interval. Unfortunately, not all of them could be compared at exactly the same crystallization temperature due to large differences in crystallization rates displayed by them; nevertheless, crystallization conditions were chosen as close as possible in order to be able to draw out meaningful conclusions. Avrami $\log[-\ln(1-X_c)]$ versus $\log(t-t_0)$ data plots and the evolution of the relative crystallinity, X_c , versus

crystallization time for some illustrative crystallization experiments are shown in Figure 3.29. Data afforded by the experiments carried out are gathered in Table 3.12, where the observed onset and half-crystallization times, as well as the corresponding calculated Avrami parameters, are given for each case. It is seen that for each copolyester the crystallization half-time as well as the Avrami exponent n increase with temperature, the values of the latter being in the 2.2-2.8 range corresponding to a complex axialitic-spherulitic crystallization as was observed by polarizing optical microscopy (illustrative pictures shown in Annex C). The double-logarithmic plot indicates that only primary crystallization takes place in the selected time intervals and that the presence of Manx units depresses the crystallizability in succinate copolyesters. The valuable conclusion that can be drawn from this study is that PB₉₅Manx₅S and PB₉₀Manx₁₀S copolyesters continue displaying the ability of crystallizing from the melt although at lower crystallization rates than their parent homopolyester PBS.

Table 3.12. Isothermal crystallization data.

Copolyester	T_c (°C)	t_0 (min)	$t_{1/2}$ (min)	n	$-\log k$	T_m (°C)
PBS	90	0.17	1.37	2.44	0.37	111.9
	95	0.59	5.24	2.69	1.99	113.0
	100	0.95	20.33	2.76	3.73	113.8
PB ₉₅ Manx ₅ S	75	0.29	2.03	2.22	0.70	105.0
	80	0.53	4.82	2.65	1.85	105.9
PB ₉₀ Manx ₁₀ S	70	0.73	8.98	2.41	2.35	95.8
	75	1.21	23.54	2.46	3.48	96.6

Mechanical tests and biodegradation essays of PManxS and PB_xManx_yS copolyesters were performed on films prepared by casting from solution as described in the Section 3.4.2. For comparison purposes, PBS was tested as well. DSC analysis were also carried out on these films to evaluate if great differences regarding thermal properties exist between powdered and film samples. DSC data recorded for films showed that melting enthalpies from PBS and all PB_xManx_yS films were slightly higher than those displayed by powdered samples coming directly from synthesis (Table 3.10), with values steadily decreasing with the increasing content of the copolyester in Manx units. On the contrary, no significant differences in melting temperature were observed between films and powdered samples. The case of PManxS deserves particular mention since it was amorphous when coming directly from synthesis but able to crystallize by

casting. In fact the DSC trace of the PManxS film showed a melting peak at 125 °C and a melting enthalpy of 14.0 J·g⁻¹, which is higher than those observed for films of PB₅₀Manx₅₀S and PB₃₀Manx₇₀S copolyesters. These results bring out the capability of the homopolyester to crystallize under conditions favoring chain mobility.

The stress-strain curves resulted from tensile essays are depicted in Figure 3.30, and the mechanical parameters measured in these tests are compared in Table 3.11. PManxS homopolyester displayed higher modulus and tensile strength than PBS and accordingly PB_xManx_yS copolyesters present a nearly steady trend consisting of a continuous increase in both elastic modulus and tensile strength and a decrease in ductility when their content in Manx units increase. This behavior is in full accordance with what should be expected from the trend observed for glass-transition temperatures along the polyester series. It should be noticed however that the molecular weight of polyesters decreases steadily with the Manx content along the series whereas chain stiffness increases. For a rigorous comparison of their mechanical properties, longer chain lengths would be required for stiffer polyesters in order to undergo comparable entanglement effects upon stretching. It is probably therefore that the differences observed in the mechanical parameters would become even greater if Manx-rich polyesters with higher molecular weights were used for this comparative study.

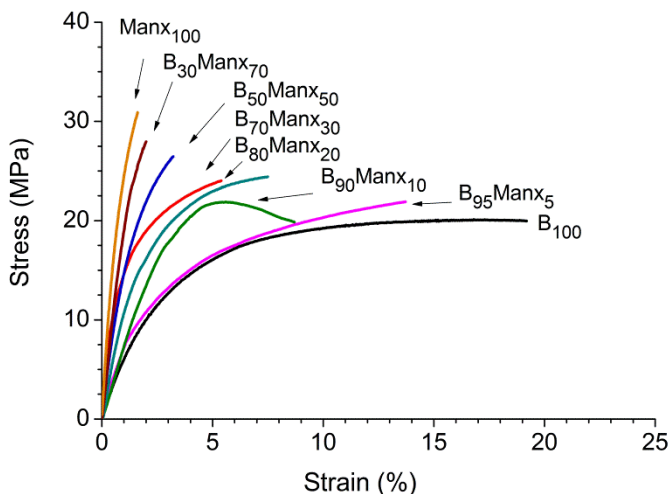


Figure 3.30. Stress-strain curves of PB_xManx_yS copolyesters.

3.4.3.3. Biodegradation and hydrolytic degradation

To evaluate the effects that the incorporation of Manx units exerts on biodegradability and hydrolytic degradability of aliphatic polyesters, PManxS homopolyester and PB₇₀Manx₃₀S copolyester were incubated under a variety of conditions. For comparison purposes, PBS was also tested in parallel. First, they were incubated in pH 7.4 buffer at 37 °C, both in the presence and in the absence of porcine pancreas lipase. The changes taking place in sample weight and molecular weight of PBS, PB₇₀Manx₃₀S and PManxS polyesters at increasing incubation times under these conditions are presented in Figure 3.31.

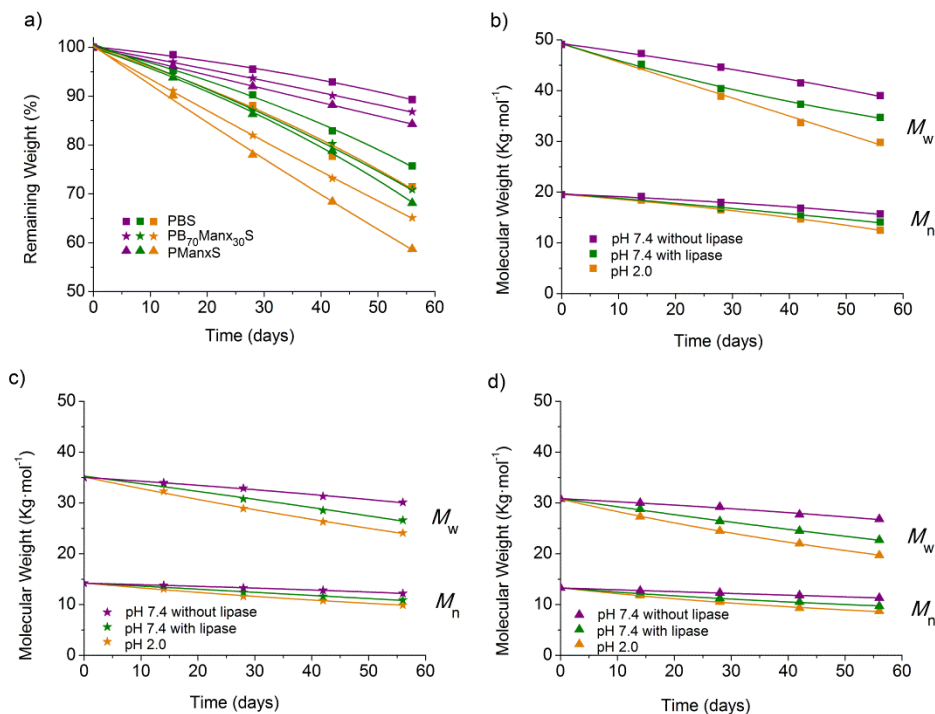


Figure 3.31. Degradation of PBS, PB₇₀Manx₃₀S and PManxS at pH 2.0 (orange) and at pH 7.4 at 37 °C with (green) and without (purple) porcine pancreas lipase. Remaining weight (a) and molecular weight of PBS (b), PB₇₀Manx₃₀S (c) and PManxS (d) versus degradation time.

Upon 8 weeks of incubation with enzymes, PManxS lost 32% of the initial weight, whereas the weight loss undergone by PBS was 24%. Under such conditions PB₇₀Manx₃₀S lost 29% of weight, a value intermediate between those observed for the two homopolyesters. Conversely, the weight losses observed for these polyesters when

incubated in the absence of lipase was only between 10 and 15%. Accordingly, a slight decay in M_w and M_n was observed for the three polyesters when incubated without enzymes, whereas changes were much more noticeable in the presence of lipase. Melting enthalpies displayed by PBS, PB₇₀Manx₃₀S and PManxS polyesters after incubation are compared in Figure 3.32. It was noteworthy to observe that crystallinity of the three polyesters increased as degradation proceeded, and that the raise in crystallinity was higher when samples were incubated in the presence of lipase. Such increase in crystallinity is indicative that hydrolysis has taken place preferably in the more permeable amorphous phase, as it is usually observed in semicrystalline polymers.

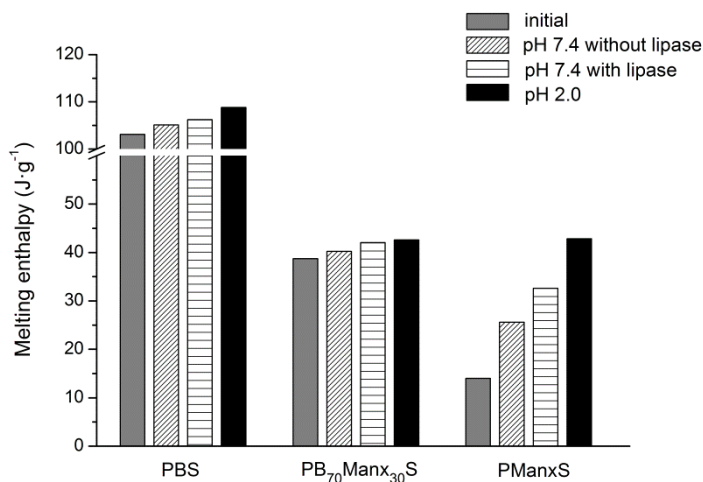


Figure 3.32. Melting enthalpies of PBS, PB₇₀Manx₃₀S and PManxS after 56 days of incubation and initial samples.

Selected SEM micrographs of PBS, PB₇₀Manx₃₀S and PManxS polyesters before and after incubation are shown in Figure 3.33 and a wider selection of is afforded in Annex C. This morphological analysis confirmed that the surface of the three polyesters displayed apparent physical alterations when they were incubated in the presence of lipase, whereas much less perceivable changes took place after incubation without enzymes. The conclusion derived from these observations is that degradation of PManxS and PB₇₀Manx₃₀S polyesters under physiological conditions was clearly enhanced by the action of enzymes, a property that points to Manx as a potential comonomer for the preparation of biodegradable aliphatic polyesters.

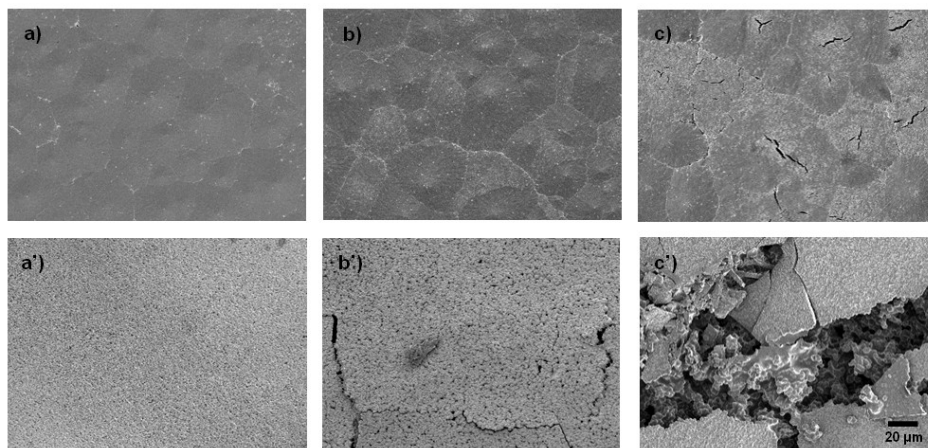


Figure 3.33. SEM micrographs of PB₇₀Man₃₀S (top) and PManxS (bottom): Initial sample (a,a'). After incubation at pH 7.4 for 56 days without (b,b') and with (c,c') porcine pancreas lipase.

In order to get insight into the degradation of the polyester chain at the molecular level, PBS, PB₇₀Man₃₀S and PManxS polyesters were incubated at 37 °C in aqueous buffer at pH 2.0. Under these conditions, the hydrolysis process will be speeded and the detailed analysis of both releasing fragments and residual polymer will be feasible within reasonable periods of time. Changes taking place in sample weight, M_w and M_n of the three polyesters upon hydrolysis are depicted in Figure 3.31. The weight losses undergone by PBS, PB₇₀Man₃₀S and PManxS were 30-40% after 8 weeks of incubation. A substantial decrease in M_w and an increase in melting enthalpy were also observed under such conditions (Figure 3.32), and SEM analysis showed very apparent alterations in the surfaces of the three polyesters (see Annex C). According to the relatively greater changes observed in sample weight, molecular weight and morphology in these essays as compared to those observed at pH 7.4, it is concluded that the hydrolytic degradation of PB_xMan_yS copolyesters and homopolyesters was boosted under acidic conditions.

¹H NMR spectra of the products released to the aqueous medium and the residual polymer resulting after 8 weeks of incubation in acidic water are depicted in Figure 3.34 and in Annex C. All the spectra recorded from the supernatant solution showed signals corresponding to succinic acid and soluble oligomers, in addition to either 1,4-butanediol or 2,4:3,5-di-O-methylene-D-mannitol signals for PBS and PManxS, respectively. On the contrary, and as it could be expected, signals of both diols were seen for the PB₇₀Man₃₀S copolyester. The spectra recorded from the residue of the three cases displayed, in addition to the signals characteristic of the polymer, another one

arising from CH_2OH end groups; this signal is indicative of the presence of reduced molecular weight fragments in full agreement with data provided by the GPC analysis.

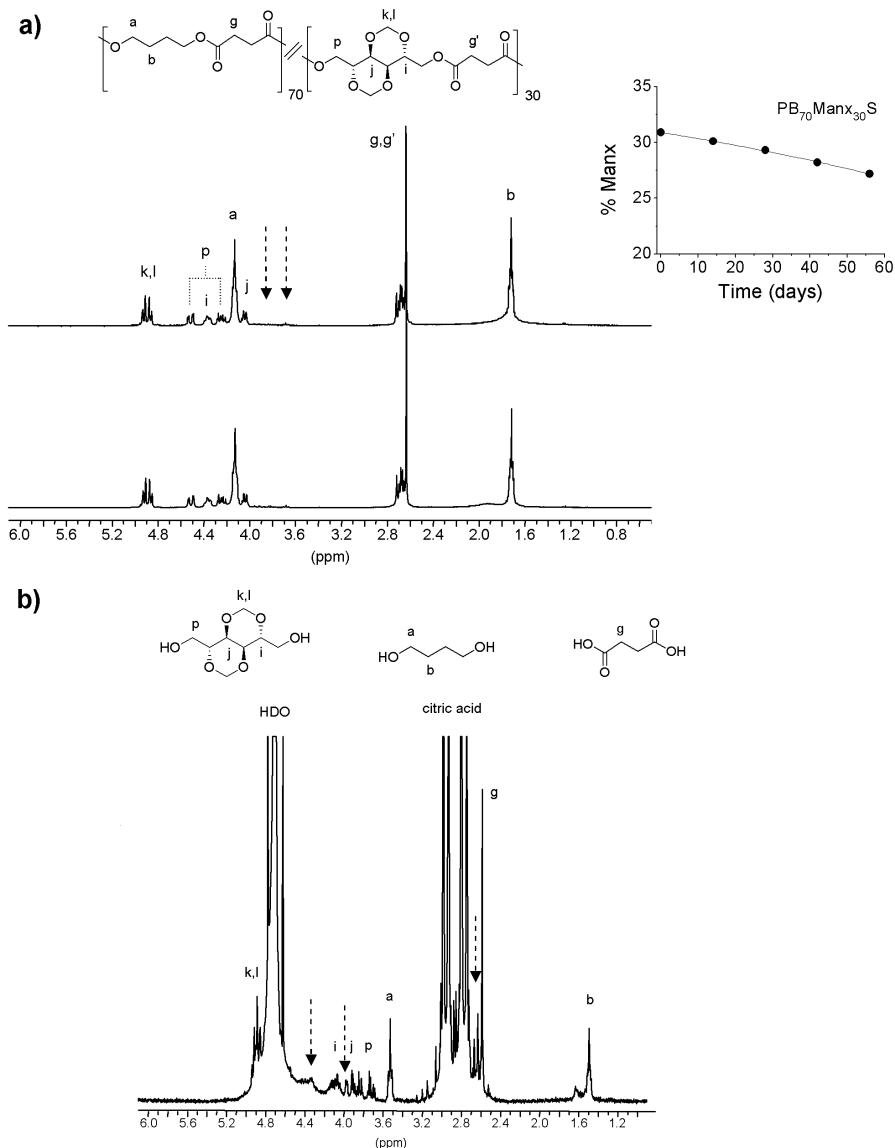


Figure 3.34. (a) Compared ^1H NMR spectra in CDCl_3 of $\text{PB}_{70}\text{Manx}_{30}\text{S}$ after incubation at pH 2.0 for 56 days (top) and initial sample (bottom); the arrows indicate the signals arising from $-\text{CH}_2\text{OH}$ end groups that appear upon hydrolysis of the main chain ester group. The evolution of the content in Manx units of the residual polyester along incubation time is represented on the right. (b) ^1H NMR spectrum in D_2O of the products released to the aqueous medium after incubation. The arrows indicate signals corresponding to oligomers generated upon hydrolysis of the main chain ester group.

The NMR analysis of the residual polymer afforded in addition two remarkable indications: a) A progressive decrease in the Manx to B ratio in the PB₇₀Man₃₀S copolyester along the degradation process, which was estimated by integration of the corresponding NMR signals. b) A full stability of the bicyclic structure against hydrolysis as it could be inferred from the total absence in the spectra of any signal indicative of hydrolysis of the acetal group. NMR results have demonstrated therefore that PManxS and PB₇₀Man₃₀S polyesters were degraded by water through splitting of the ester group, preferably through that involving the sugar diol, whereas the acetal group remained stable against hydrolysis. This result is really striking because acetals are known to be sensitive to acidic conditions (Smith and March, 2007) and the opening of the dioxane rings might be therefore expected to happen in some extent. In order to corroborate the stability of the bicyclic dioxane structure against hydrolysis observed in Manx containing copolyesters, compound 2,4:3,5-di-O-methylene-D-mannitol was incubated in aqueous buffer at pH 2.0, 7.4 and 10.5 for 12 weeks. The spectra recorded at the end of incubation period are shown in Figure 3.35; all they correspond to the structure of the original diol without exhibiting any sign indicative of hydrolysis of the acetal group.

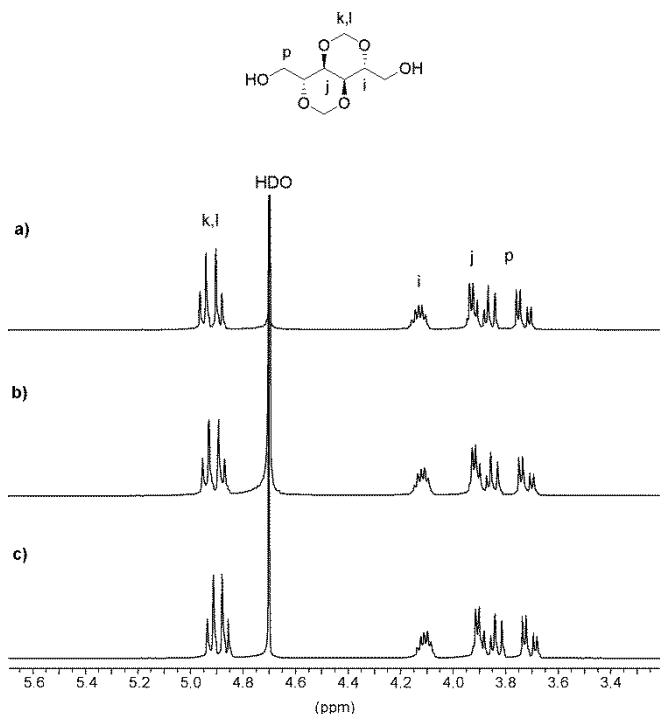
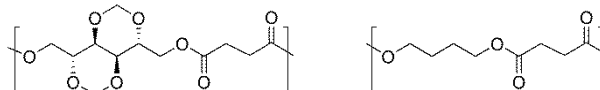


Figure 3.35. ¹H NMR spectra in D₂O of 2,4:3,5-di-O-methylene-D-mannitol after incubation for 90 days at pH 2.0 (a), 7.4 (b) and 10.5 (c).

3.4.3.4. Main features of PManxS polyester

PManxS is a singular polyester since it is fully bio-based, is more stable to heating than PBS, displays a T_g comparable to aromatic polyesters and is semicrystalline. The chemical structure of PManxS is depicted in Scheme 3.6.



Scheme 3.6. Chemical structure of PManxS (left) and PBS (right) polyesters.

The onset decomposition temperature of PManxS is around 320 °C and its maximum decomposition rate happens at 413 °C, about 30 °C above that of PBS. It is able to crystallize by casting from solution showing a $T_m = 125$ °C. Its glass-transition temperature is quite high ($T_g = 68$ °C), especially if compared with that of PBS ($T_g = -37$ °C). As expected from the bicyclic structure of the Manx unit, the T_g of PManxS is higher than those of the polyesters made from 1,4-butanediol and the cyclic diacids 2,3-O-isopropylidene-L-tartrate (Dhamaniya and Jacob, 2010) and 2,5-furandicarboxylic acid (Wu *et al.*, 2012a), whose T_g are -9 and 45 °C, respectively. Since the two rings of Manx are fused, the T_g of PManxS is even higher than that of the polyester made from 1,4-butanediol and the bicyclic non-fused dimethyl 2,3:4,5-di-O-methylene-galactarate ($T_g = 18$ °C) (Lavilla *et al.*, 2012c -Subchapter 5.2-; Lavilla and Muñoz-Guerra, 2012 -Subchapter 5.3-); in fact, it is much higher than that of the polyester made from 1,4-butanediol and bicyclic fused isoidide dicarboxylic acid ($T_g = 0$ °C) (Wu *et al.*, 2012b). Regarding 1,4:3,6-dianhydrohexitols, the T_g reported for the polyester from succinic acid and isomannide ($T_g = 75$ °C) (Okada *et al.*, 1996) is very close to that of PManxS, whereas T_g values ranging from 36 to 68 °C have been reported for polyesters obtained from succinic acid and isosorbide (Okada *et al.*, 1996 and 2000; Noorderver *et al.*, 2006). The main advantage of PManxS over polysuccinates made from dianhydrohexitols is that, having nearly the same T_g , it is obtained more easily by melt polycondensation. PManxS is a biodegradable polyester which exhibits a sensitivity to the action of lipases comparable to the commonly used PBS. PManxS is degraded through splitting of the relatively weak ester group and without alteration of the diacetal group forming part of the carbohydrate-based Manx unit.

The renewable origin of PManxS polyester, its good thermal stability, its biodegradability, and its relatively high glass-transition temperature make it a bio-based

polyester of exceptional interest as an potential alternative to PBS in those applications where thermal and mechanical properties are matters of utmost importance.

3.4.4. Conclusions

Fully and partially bio-based aliphatic polyesters have been obtained from the bicyclic carbohydrate-based diol 2,4:3:5-di-*O*-methylene-*D*-mannitol (Manx) and succinic acid. The synthesis of the homopolyester PManxS was carried out by polycondensation in the melt to imitate as far as possible the conditions usually applied in the industry, and using DBTO as catalyst. This novel polyester melts at 127 °C and its T_g is 68 °C, which is more than 100 degrees higher than the T_g of PBS and comparable to those displayed by aliphatic polyesters obtained from 1,4:3,6-dianhydrohexitols; the advantage of PManxS is that it can be obtained more easily and with higher molecular weight by melt polycondensation. The higher reactivity of primary hydroxyl groups of the diol Manx compared to the secondary ones of 1,4:3,6-dianhydrohexitols is responsible for such benefit. PB_xManx_yS copolyesters made from Manx, 1,4-butanediol and dimethyl succinate were semicrystalline with melting temperatures lower than that of the parent homopolyester PBS. Since the thermal stability increases with the content in Manx, a wider range of temperatures between melting and decomposition exists in these copolyesters. Their T_g and consequently their elastic modulus and tensile strength increased with the content in Manx units. Hydrolytic degradation of Manx containing polyesters happened through hydrolysis of the main chain ester group without modification of the diacetal structure. Degradation of both PManxS and the copolyester PB₇₀Manx₃₀S under physiological conditions was clearly favored by the action of enzymes. This exploratory study of Manx containing polyesters and copolyesters points to 2,4:3:5-di-*O*-methylene-*D*-mannitol as a potential comonomer for obtaining biodegradable aliphatic polyesters with enhanced T_g .

3.4.5. References

- Albertsson, A.C.; Varma, I.K. *Adv. Polym. Sci.* **2002**, *157*, 1-40.
- Braun, D.; Bergmann, M. J. *Prakt. Chem.* **1992**, *334*, 298-310.

Coutinho, D.F.; Gomes, M.E.; Neves, N.M.; Reis, R.L. *Acta Biomater.* **2012**, *8*, 1490-1497.

Deng, L.M.; Wang, Y.Z.; Yang, K.K.; Wang, X.L.; Zhou, Q.; Ding, S.D. *Acta Mater.* **2004**, *52*, 5871-5878.

Dhamaniya, S.; Jacob, J. *Polymer* **2010**, *51*, 5392-5399.

Dhamaniya, S.; Jacob, J. *Polym. Bull.* **2012**, *68*, 1287-1304.

Engelberg, I.; Kohn, J. *Biomaterials* **1991**, *12*, 292-304.

Fenouillot, F.; Rousseau, A.; Colomines, G.; Saint-Loup, R.; Pascault, J.P. *Prog. Polym. Sci.* **2010**, *35*, 578-622.

Fradet, A.; Tessier, M. *Polyesters*. In: Rogers, M.E.; Long, T.E.; Eds. *Synthetic Methods in Step-Growth Polymers*; John Wiley & Sons: Hoboken, **2003**, pp. 17-134.

Galbis, J.A.; García-Martín, M.G. *Top. Curr. Chem.* **2010**, *295*, 147-176.

Gandini, A.; Coelho, D.; Gomes, M.; Reis, M.; Silvestre, A.J.D. *J. Mater. Chem.* **2009**, *19*, 8656-8664.

Gandini, A. *Green Chem.* **2011**, *13*, 1061-1083.

Gomes, M.; Gandini, A.; Silvestre, A.J.D.; Reis, B. *J. Polym. Sci., Polym. Chem.* **2011**, *49*, 3759-3768.

Gualandi, C.; Soccio, M.; Saino, E.; Focarete, M.L.; Lotti, N.; Munari, A.; Moroni, L.; Visai, L. *Soft Matter* **2012**, *8*, 5466-5476.

Ihn, K.J.; Yoo, E.S.; Im, S.S. *Macromolecules* **1995**, *28*, 2460-2464.

Lavilla, C.; Alla, A.; Martínez de Ilarduya, A.; Benito, E.; García-Martín, M.G.; Galbis, J.A.; Muñoz-Guerra, S. *Biomacromolecules* **2011**, *12*, 2642-2652. **-Subchapter 3.2-**

Lavilla, C.; Alla, A.; Martínez de Ilarduya, A.; Benito, E.; García-Martín, M.G.; Galbis, J.A.; Muñoz-Guerra, S. *J. Polym. Sci., Polym. Chem.* **2012**, *50*, 1591-1604. (2012a) **-Subchapter 3.3-**

Lavilla, C.; Martínez de Ilarduya, A.; Alla, A.; García-Martín, M.G.; Galbis, J.A.; Muñoz-Guerra, S. *Macromolecules* **2012**, *45*, 8257-8266. (2012b) **-Subchapter 5.4-**

Lavilla, C.; Alla, A.; Martínez de Ilarduya, A.; Benito, E.; García-Martín, M.G.; Galbis, J.A.; Muñoz-Guerra, S. *Polymer* **2012**, *53*, 3432-3445. (2012c) **-Subchapter 5.2-**

Lavilla, C.; Muñoz-Guerra, S. *Polym. Degrad. Stabil.* **2012**, *97*, 1762-1771. **-Subchapter 5.3-**

Lavilla, C.; Muñoz-Guerra, S. *Green Chem.* **2013**, *15*, 144-151. **-Subchapter 7.2-**

Li, W.D.; Zeng, J.B.; Lou, X.J.; Zhang, J.J.; Wang, Y.Z. *Polym. Chem.* **2012**, *3*, 1344-1353.

Nair, L.S.; Laurencin, C.T. *Prog. Polym. Sci.* **2007**, *32*, 762-798.

Noordover, B.A.J.; van Staalduinen, V.G.; Duchateau, R.; Koning, C.E.; van Benthem, R.A.T.M.; Mak, M.; Heise, A.; Frissen, A.E.; van Haveren, J. *Biomacromolecules* **2006**, *7*, 3406-3416.

Okada, M.; Okada, Y.; Tao, A.; Aoi, K. *J. Appl. Polym. Sci.* **1996**, *62*, 2257-2265.

Okada, M.; Tsunoda, K.; Tachikawa, K.; Aoi, K. *J. Appl. Polym. Sci.* **2000**, *77*, 338-346.

Okada, M. *Prog. Polym. Sci.* **2002**, *27*, 87-133.

Papageorgiou, G.Z.; Bikiaris, D.N. *Biomacromolecules* **2007**, *8*, 2437-2449.

Smith, M.B.; March, J. *March's Advanced Organic Chemistry*; Wiley: Hoboken, **2007**, pp. 523,1270.

Wang, H.Y.; Xu, M.; Wu, Z.W.; Zhang, W.; Ji, J.H.; Chu, P.K. *ACS Appl. Mater. Interfaces* **2012**, *4*, 4380-4386.

Wu, L.; Mincheva, R.; Xu, Y.; Raquez, J.M.; Dubois, P. *Biomacromolecules* **2012**, *13*, 2973-2981. (2012a)

Wu, J.; Eduard, P.; Thiyagarajan, S.; Jasinska-Walc, L.; Rozanski, A.; Fonseca Guerra, C.; Noordover, B.A.J.; van Haveren, J.; van Es, D.S.; Koning, C.E. *Macromolecules* **2012**, *45*, 5069-5080. (2012b)

CHAPTER 4

POLY(ALKYLENE TEREPHTHALATE) COPOLYESTERS FROM CYCLIC ACETALIZED CARBOHYDRATE-BASED MONOMERS

4.1. Aim and scope of this Chapter

Aromatic polyesters are massively used in diverse applications; they are high performance thermoplastic materials with good mechanical and thermal properties. However, they are markedly hydrophobic and more resistant to hydrolysis than usually needed in many of its most common applications. Thus, different strategies to obtain modified aromatic polyesters able to be chemically degraded under smooth conditions or biologically degraded are currently drawing an enormous interest. Furthermore, despite being innocuous for humans, aromatic polyesters are considered not to be environmentally friendly materials because of their non-renewable origin. In this regard, great efforts are being made nowadays to incorporate bio-based units into poly(terephthalate)s.

Among the renewable naturally occurring sources, carbohydrates stand out in a privileged position due to their huge abundance and because they are inexhaustible and readily available. Recently several examples of poly(terephthalate) copolyesters containing acyclic sugar-derived units have been described in the literature, and particular attention has been paid to the sensitivity displayed by these carbohydrate-based polyesters to degradability. Hydrolytic degradation experiments revealed that aromatic copolyesters made from pentitols and hexitols with acyclic *O*-protected groups degraded significantly faster than their parent homopolyesters, and that degradation rate depended on the configuration of the sugar units. Conversely no evaluation of their biodegradability was reported.

Carbohydrate-derived monomers with a cyclic structure are distinguished by providing polyesters and copolyesters with improved properties, especially those related to polymer chain stiffness. In this Chapter, bicyclic acetalized carbohydrate-based compounds are used as comonomers in the preparation of poly(alkylene terephthalate) copolyesters. The copolymerizations with bicyclic monomers are carried out over the entire range of compositions, in order to develop a detailed structure-properties study. Furthermore, several linear α,ω -alkanedioles (with 2, 6 or 12 carbon atoms) are employed. The large difference in length between the alkanedioles will be noticeably reflected in the properties exhibited by their respective copolyesters, which will allow a comparative study within the structure-property relationship frame. The hydrolytic and enzymatic degradability of the resulting carbohydrate-based aromatic copolyesters will also be comparatively evaluated and discussed.

4.2. Biodegradable aromatic copolyesters made from bicyclic acetalized galactaric acid

Summary: *Random poly(hexamethylene terephthalate-co-galactarate)s and poly(dodecamethylene terephthalate-co-galactarate)s copolyesters covering the whole range of compositions were obtained with weight-average molecular weights of ~30,000-50,000 g·mol⁻¹ by melt polycondensation. They were thermally stable above 300 °C, and displayed T_g in the +20 to -20 °C range with values steadily decreasing with the content in galactarate units. All the copolyesters were semicrystalline with T_m between 50 and 150 °C and those made from dodecanediol were able to crystallize from the melt at a crystallization rate depending on composition. Copolyesters containing up to 50% of galactaric units retained the crystal structure of their respective polyterephthalate homopolyesters, whereas they adopted the structure of the respective polygalactarates when the content in Galx units reached 70%. Stress-strain essays revealed a decay in the mechanical parameters as the aromatic units were replaced by Galx. Incubation in aqueous buffer revealed that hydrolysis of the polyesters was largely enhanced by copolymerization and evidenced the capacity of the Galx unit for making aromatic polyesters susceptible to biodegradation. A detailed NMR analysis complemented by SEM observations indicated that hydrolysis took place by preferred splitting of galactarate ester bonds with releasing of alkanediol and Galx-diacid.*

Publication derived from this work:

Lavilla, C.; Alla, A.; Martínez de Iarduya, A.; Benito, E.; García-Martín, M.G.; Galbis, J.A.; Muñoz-Guerra, S. *J. Polym. Sci., Polym. Chem.* **2012**, *50*, 3393-3406.

4.2.1. Introduction

Nowadays great attention is given to the development of bio-based and biodegradable polymers, in order to reduce the amount of petroleum that is consumed in the industry as well as to minimize the impact of the use of plastics on the environment (Wool and Sun, 2005; Mathers and Meier, 2011). Aromatic polyesters are high performance thermoplastic materials with excellent mechanical and thermal properties that are massively used in diverse applications. Despite being innocuous for humans, they are considered unfriendly compounds because of their great resistance to degradation by atmospheric and biological agents. Thus, different strategies to obtain modified aromatic polyesters able to be chemically degraded under smooth conditions or biologically degraded are currently drawing an enormous interest (Maeda *et al.*, 2000; Müller *et al.*, 2001; Marten *et al.*, 2005; Rychter *et al.*, 2010).

The incorporation of carbohydrate moieties in polycondensation polymers, such as polyamides and polyesters, is an interesting approach to yield novel sustainable and biodegradable materials (Galbis and García-Martín, 2008). The use of carbohydrates as polymer building blocks is motivated by several features: they are easily available, even coming from agricultural wastes, they are found in a very rich variety of structures with large stereochemical diversity, and they constitute a renewable source with good accessibility everywhere. Nevertheless, linear polycondensation of monomers derived from carbohydrates is not straightforward. Carbohydrate-based compounds usually possess an excess of functional groups that upon polycondensation would lead to undesirable cross-linking reactions unless special precautions are taken. Although some linear polycondensates have been synthesized using sugar-derived monomers bearing free hydroxyl groups (Kiely *et al.*, 1994 and 2000), most synthesis have been carried out with derivatives in which the exceeding functional groups have been appropriately blocked (Kricheldorf, 1997; Okada, 2002; Williams, 2007; Metzke and Guan, 2008).

Recently several examples of aromatic polyesters and copolyesters containing sugar derived units have been described in the literature. Poly(ethylene terephthalate) (PET), poly(ethylene isophthalate) (PEI) and poly(butylene terephthalate) (PBT) were chemically modified by the insertion of different alditols and aldaric acids having *D-manno*, *galacto*, *L-arabino*, and *xylo* configurations with the secondary hydroxyl groups protected as methyl ether (Alla *et al.*, 2006; Zamora *et al.*, 2006). Particular attention was paid to the sensitivity displayed by these carbohydrate-based polyesters to degradability. Hydrolytic degradation experiments revealed that PET, PEI and PBT analogs made from

pentitols and hexitols degraded significantly faster than their parent homopolyesters at rates depending on the configuration of the sugar units. Conversely no evaluation of their biodegradability was reported. The state-of-art in this regard is that whereas a fair number of aromatic-aliphatic copolyesters displaying biodegradability have been created along these last decades (Marten *et al.*, 1995a, 1995b and 2005; Papageorgiou *et al.*, 2008 and 2010), no case of biodegradable aromatic copolyester containing sugar residues has been reported so far. On the other hand, carbohydrate-based monomers with a cyclic structure constitute an interesting approach to the preparation of polycondensates with improved physical properties, especially those related to polymer chain stiffness (Fenouillot *et al.*, 2010). The use of these cyclic monomers has been however scarcely investigated with most of the work carried out up to date having been devoted to bicyclic 1,4:3,6 dianhydroalditols, specifically those made from D-glucitol, D-mannitol and D-iditol. The former, which is known as isosorbide and that is prepared from D-glucose coming from cereal starch, has been by far the most studied dianhydroalditol. Thus PET and PBT copolyesters containing isosorbide have been synthesized over the entire range of compositions. As the proportion of isosorbide increased, the copolyesters were less prone to crystallize and their melting temperature steadily decreased. In fact, PET and PBT copolyesters became amorphous for isosorbide contents above 20% and 30%, respectively (Storbeck and Ballauff, 1996; Kricheldorf *et al.*, 2007).

In this work we report on novel aromatic copolyesters based on dimethyl 2,3:4,5-di-O-methylene-galactarate, abbreviated as Galx. Galx is a bicyclic carbohydrate-based monomer generated by intramolecular acetalization of commercially available mucic acid (galactaric acid), which in turn is produced from naturally-occurring D-galactose or D-galactose-containing compounds by oxidation with nitric acid. Up to now, Galx has only been used for the preparation of aliphatic polyesters and copolyesters (Lavilla *et al.*, 2011 -Subchapter 3.2- and 2012 -Subchapter 3.3-). Aliphatic polyesters containing Galx units were found to be degraded by water through splitting of the ester group, whereas the acetal group remained stable against hydrolysis in acidic, neutral and basic media. Furthermore, these polyesters were hydrolyzed much faster in the presence of lipases revealing the beneficial effect of the Galx units regarding biodegradability. A second interesting characteristic of Galx is that its incorporation in a polyester does not alter significantly the crystallizability in spite of being a bulky compound. In fact, copolyesters made of alkanediols, Galx and adipic acid were found to be semicrystalline over the entire range of compositions. Contrary to isosorbide, Galx is centrosymmetric and does not

generate therefore regioisomerism in the growing polymer chain, and its two carboxyl groups display the same reactivity since they are spatially undistinguishable.

The diols chosen for this study are 1,6-hexanediol and 1,12-dodecanediol; the polyesters derived from these long diols are expected to display relatively low T_m making feasible polycondensation at lower temperatures, which is very desirable given the high sensitivity of sugar-derived monomers to heat. Furthermore, the large difference in length between the two diols will be noticeably reflected in the properties exhibited by their respective copolyesters which will allow a comparative study within the structure-property relationship frame.

4.2.2. Experimental section

4.2.2.1. Materials

Dimethyl 2,3:4,5-di-O-methylene-galactarate was synthesized following the procedure reported by Stacey *et al.* (Butler *et al.*, 1958). The reagents 1,6-hexanediol (97%), 1,12-dodecanediol (99%), dimethyl terephthalate (99+%), and the catalyst dibutyl tin oxide (DBTO, 98%) were purchased from Sigma-Aldrich. Solvents used for purification and characterization, as chloroform and methanol, as well as solvents used in the solubility essays, were purchased from Panreac and were all of either technical or high-purity grade. The enzyme used in biodegradation experiments, lipase from porcine pancreas (activity 15-35 U·mg⁻¹, pH 8.0, 37 °C) was also purchased from Sigma-Aldrich. One unit (U) was defined as that amount of enzyme which catalyzed the release of fatty acid from triglycerides at the rate of 1 μmol·min⁻¹. All the reagents and solvents were used as received without further purification.

4.2.2.2. General methods

¹H and ¹³C NMR spectra were recorded on a Bruker AMX-300 spectrometer at 25.0 °C operating at 300.1 and 75.5 MHz, respectively. Polyesters and water degradation products were dissolved in deuterated chloroform or in deuterated water, and spectra were internally referenced to tetramethylsilane (TMS) or the sodium salt of 3-(trimethylsilyl)-propanesulfonic acid. About 10 and 50 mg of sample dissolved in 1 mL of solvent were used for ¹H and ¹³C NMR, respectively. Sixty-four scans were acquired for ¹H and 1,000-10,000 for ¹³C with 32 and 64-K data points as well as relaxation delays of

1 and 2 s, respectively. Intrinsic viscosities of polyesters dissolved in chloroform were measured in an Anton Paar AMVn Automated Micro Viscosimeter at 25.00 ± 0.01 °C, using the VisioLab for AMVn software. Gel permeation chromatograms were acquired at 35.0 °C with a Waters equipment provided with a refraction-index detector. The samples were chromatographed with 0.05 M sodium trifluoroacetate-hexafluoroisopropanol (NaTFA-HFIP) using a polystyrene-divinylbenzene packed linear column with a flow rate of $0.5 \text{ mL} \cdot \text{min}^{-1}$. Chromatograms were calibrated against poly(methyl methacrylate) (PMMA) monodisperse standards. The thermal behavior of polyesters was examined by DSC using a Perkin Elmer DSC Pyris 1. DSC data were obtained from 3 to 5 mg samples at heating/cooling rates of $10 \text{ }^\circ\text{C} \cdot \text{min}^{-1}$ under a nitrogen flow of $20 \text{ mL} \cdot \text{min}^{-1}$. Indium and zinc were used as standards for temperature and enthalpy calibration. The glass-transition temperatures were determined at a heating rate of $20 \text{ }^\circ\text{C} \cdot \text{min}^{-1}$ from rapidly melt-quenched polymer samples. The treatment of the samples for isothermal crystallization experiments was the following: the thermal history was removed by heating the sample up to 200 °C and left at this temperature for 5 min, and then it was cooled at $20 \text{ }^\circ\text{C} \cdot \text{min}^{-1}$ to the selected crystallization temperature, where it was left to crystallize until saturation. Thermogravimetric analyses were performed under a nitrogen flow of $20 \text{ mL} \cdot \text{min}^{-1}$ at a heating rate of $10 \text{ }^\circ\text{C} \cdot \text{min}^{-1}$, within a temperature range of 30 to 600 °C, using a Perkin Elmer TGA 6 equipment. Sample weights of about 10-15 mg were used in these experiments. Films for mechanical testing measurements were prepared with a thickness of $\sim 200 \text{ }\mu\text{m}$ by casting from a chloroform solution at a concentration of $100 \text{ g} \cdot \text{L}^{-1}$. The films were cut into strips with a width of 3 mm while the distance between testing marks was 10 mm. The tensile strength, elongation at break and Young's modulus were measured at a stretching rate of $30 \text{ mm} \cdot \text{min}^{-1}$ on a Zwick 2.5/TN1S testing machine coupled with a compressor Dalbe DR 150, at 23 °C. X-ray diffraction patterns were recorded on the PANalytical X'Pert PRO MPD θ/θ diffractometer using the Cu-K α radiation of wavelength 0.1542 nm from powdered samples coming directly from synthesis. Scanning electron microscopy (SEM) images were taken with a field-emission JEOL JSM-7001F instrument (JEOL, Japan) from Pt/Pd coated samples.

4.2.2.3. Polymer synthesis

PHT $_x$ Gal $_y$ and PDT $_x$ Gal $_y$ copolyesters as well as PHT, PDT, PHGal $_x$ and PDGal $_x$ homopolyesters were obtained from the chosen aliphatic α,ω -diol (either 1,6-hexanediol or 1,12-dodecanediol) and a mixture of dimethyl 2,3:4,5-di-O-methylene-galactarate and dimethyl terephthalate with the selected composition. The reaction was

performed in a three-necked, cylindrical-bottom flask equipped with a mechanical stirrer, a nitrogen inlet and a vacuum distillation outlet. With regard to $\text{PHT}_x\text{Galx}_y$ and $\text{PDT}_x\text{Galx}_y$ copolyesters as well as PHGalx and PDGalx homopolyesters, 5% molar excess of diol to the diester mixture, and dibutyl tin oxide (DBTO) as catalyst (0.8%-mol respect to monomers) were used. The apparatus was vented with nitrogen several times at room temperature in order to remove the air and avoid oxidation during the polymerization. The transesterification reaction was carried out under a low nitrogen flow at 140 °C for 3 h. The polycondensation reaction was left to proceed at 140 °C for 5 h, under a 0.03-0.06 mbar vacuum. Then, the reaction mixture was cooled to room temperature, and the atmospheric pressure was recovered with nitrogen to prevent degradation. The resulting polymers were dissolved in chloroform and precipitated in excess of methanol in order to remove unreacted monomers and formed oligomers. Finally, the polymer was collected by filtration, extensively washed with methanol, and dried under vacuum. Since dimethyl terephthalate is not as thermally sensitive as Galx, shorter periods of time combined with higher temperatures were used for the preparation of both PHT and PDT. A 10% molar excess of the diol to dimethyl terephthalate and DBTO as catalyst was used in this case to compensate expected larger losses of the volatile diol at these higher temperatures. Transesterification reactions were carried out at 180 °C for a period of 3 h under a low nitrogen flow, whereas polycondensation reactions took place for 3 h at 200 °C under vacuum. Polyesters were dissolved in chloroform, precipitated and washed with methanol, and dried under vacuum.

$\text{PHT}_x\text{Galx}_y$. ^1H NMR (300.1 MHz, CDCl_3), δ (ppm): 8.09 (s, T, 4CH), 5.25 and 5.05 (2s, Galx, 2 CH_2), 4.60 (m, Galx, 2CH), 4.36 (t, T, 2 CH_2), 4.27 (m, Galx, 2CH), 4.20 (t, Galx, 2 CH_2), 1.83 (m, T, 2 CH_2), 1.69 (m, Galx, 2 CH_2), 1.54 (m, T, 2 CH_2), 1.39 (m, Galx, 2 CH_2). ^{13}C NMR (75.5 MHz, CDCl_3), δ (ppm): 170.3 (CO), 165.8 (CO), 134.1, 129.5, 96.8, 79.0, 75.2, 65.6, 65.3, 28.6, 28.4, 25.7, 25.5.

$\text{PDT}_x\text{Galx}_y$. ^1H NMR (300.1 MHz, CDCl_3), δ (ppm): 8.09 (s, T, 4CH), 5.25 and 5.05 (2s, Galx, 2 CH_2), 4.60 (m, Galx, 2CH), 4.33 (t, T, 2 CH_2), 4.27 (m, Galx, 2CH), 4.19 (t, Galx, 2 CH_2), 1.77 (m, T, 2 CH_2), 1.66 (m, Galx, 2 CH_2), 1.28 (m, Galx, T, 16 CH_2). ^{13}C NMR (75.5 MHz, CDCl_3), δ (ppm): 170.3 (CO), 165.8 (CO), 134.3, 129.4, 96.8, 79.0, 75.4, 65.7, 65.4, 29.4, 29.2, 29.1, 28.7, 28.5, 25.9, 25.7.

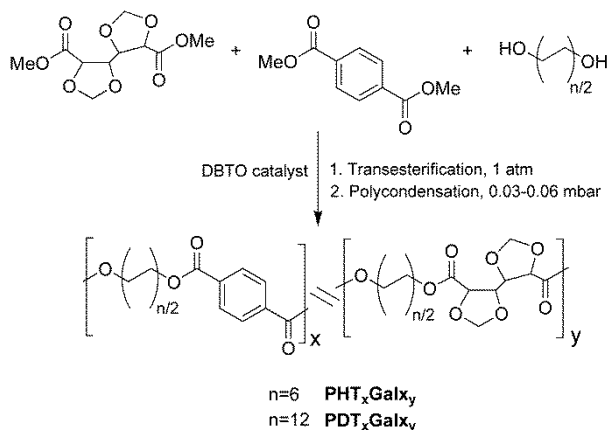
4.2.2.4. Hydrolytic and enzymatic degradation procedures

For hydrolytic and enzymatic degradation studies, films of polyesters with a thickness of ~ 200 μm were prepared by casting from a chloroform solution ($c=100$ $\text{g}\cdot\text{L}^{-1}$). The films were cut into 10-mm diameter, 20 to 30-mg weight disks and dried in vacuum to constant weight. For hydrolytic degradation, samples were immersed in vials containing 10 mL of citric acid buffer (pH 2.0) at 80 °C and 23 °C. After incubation for the scheduled period of time, the samples were rinsed thoroughly with distilled water and dried to constant weight. The enzymatic degradation was carried out at 37 °C in vials containing 10 mL of the enzymatic medium, consisting of a pH 7.4 buffered sodium phosphate solution containing lipase from porcine pancreas (10 mg). The buffered enzyme solution was replaced every 72 h to maintain the enzyme activity. At the end of the scheduled incubation periods, the disks were withdrawn from the incubation medium, washed thoroughly with distilled water, dried to constant weight, and analyzed by GPC chromatography and NMR spectroscopy.

4.2.3. Results and discussion

4.2.3.1. Synthesis and chemical structure

Aromatic copolyesters from dimethyl terephthalate, dimethyl 2,3:4,5-di-O-methylene galactarate, and either 1,6-hexanediol (PHT_xGal_y copolyesters) or 1,12-dodecanediol (PDT_xGal_y copolyesters) at the entire range of molar galactaric/terephthalic compositions were prepared by a two-step melt-polycondensation process as indicated in Scheme 4.1, using DBTO as catalyst. Transesterification reactions were performed under a low nitrogen flow for a period of 3 h at 140 °C. Polycondensation reactions were carried out for 5 h at the same temperature in order to minimize the decomposition of thermally sensitive sugar compounds, and under vacuum to facilitate the removal of volatile by-products. When polymerizations were ended, the reaction mixtures were dissolved in chloroform and precipitated in methanol to obtain the copolyesters as white powders in yields close to 90%. The chemical constitution and composition of the resulting copolyesters were ascertained by ¹H NMR (see Annex D), and their molecular weights were estimated by GPC and viscosimetry. Data provided by these analyses are given in Table 4.1, where it can be seen that the copolyesters had compositions essentially similar to those of their corresponding feeds.



Scheme 4.1. Polymerization reactions leading to PHT_xGal_y and PDT_xGal_y copolyesters.

Intrinsic viscosities of polyesters and copolyesters were between 0.6 and 1.0 dL·g⁻¹, with the higher values being generally observed for the whole series of PDT_xGal_y and for PHT_xGal_y with low content in galactaric units. The weight-average molecular weights of copolyesters were found to be within the 30,000–48,000 g·mol⁻¹ range, with dispersities between 2.0 and 2.8. The M_n were estimated by both GPC and ¹H-NMR (end group analysis) and a very good concordance was found between values provided by the two techniques. Nevertheless, the NMR-based M_n -values were always higher than those obtained by GPC, which could be in principle attributed to the use of GPC standards leading to underestimated molecular weights. On the other hand, the presence of endless macrocyclic chains would result in an overestimation of the M_n values calculated by end-group analysis, and could be also a reason for the observed differences; however the occurrence of these macrocycles in the polycondensated product cannot be ascertained since they are undistinguishable from linear chains by NMR.

The microstructure of copolyesters was determined by ¹³C NMR analysis. Complex signals were observed for the carbon atoms of diol units, indicating that these units are sensitive to sequence distribution effects. Thus, as shown in Figure 4.1, the resonance of the *c* and *c'* carbon atoms of diol units appeared as four signals in the 25.3–25.8 ppm chemical shift interval corresponding to the four types of dyads (TT, GT, TG and GG) that are possible along the copolyester chain. The plot of the content in each type of dyad as a function of the copolyester composition reveals that the microstructure of the copolyester is clearly statistical, with randomness quite near unity in all cases. The statistical values obtained from this microstructure analysis are shown in Table 4.2. Similar results were obtained for the PDT_xGal_y series.

Table 4.1. Molecular weights and compositions of PHT_xGal_y and PDT_xGal_y copolyesters.

Copolyester	Yield (%)	Molar composition				Molecular weight					Solubility ^e					
		Feed		Copolyester ^a		[η] ^b	M_n^c	M_n^d	M_w^d	\mathcal{D}^d	H ₂ O EtOH	Et ₂ O DMSO	DMF	NMP THF	CHCl ₃	HFIP TFA
		X _{Galx}	X _T	X _{Galx}	X _T											
PHT	91	0	100	0	100	0.95	23,500	17,100	47,900	2.8	-	-	-	-	+	+
PHT ₉₀ Gal ₁₀	90	10	90	11.0	89.0	0.67	16,500	14,500	30,500	2.1	-	-	-	-	+	+
PHT ₇₀ Gal ₃₀	90	30	70	29.1	70.9	0.76	18,500	15,100	41,500	2.7	-	-	-	+	+	+
PHT ₅₀ Gal ₅₀	92	50	50	49.6	50.4	0.68	17,100	13,800	35,800	2.8	-	-	+	+	+	+
PHT ₃₀ Gal ₇₀	89	70	30	70.9	29.1	0.66	15,600	13,000	33,000	2.5	-	-	+	+	+	+
PHT ₁₀ Gal ₉₀	91	90	10	89.8	10.2	0.69	19,100	16,200	41,300	2.7	-	-	+	+	+	+
PHGalx	90	100	0	100	0	0.60	17,900	16,300	40,300	2.3	-	-	+	+	+	+
PDT	92	0	100	0	100	1.06	22,700	16,100	37,200	2.3	-	-	-	-	+	+
PDT ₉₀ Gal ₁₀	91	10	90	9.9	90.1	0.84	18,300	15,600	30,500	2.0	-	-	-	-	+	+
PDT ₇₀ Gal ₃₀	90	30	70	29.6	70.4	0.99	15,800	14,500	33,800	2.3	-	-	-	+	+	+
PDT ₅₀ Gal ₅₀	93	50	50	51.0	49.0	0.92	16,900	15,300	38,700	2.5	-	-	+	+	+	+
PDT ₃₀ Gal ₇₀	92	70	30	70.3	29.7	0.74	17,500	15,200	31,700	2.1	-	-	+	+	+	+
PDT ₁₀ Gal ₉₀	93	90	10	89.9	10.1	0.77	16,100	14,700	30,800	2.1	-	-	+	+	+	+
PDGalx	91	100	0	100	0	0.81	20,400	16,400	41,200	2.5	-	-	+	+	+	+

^a Molar composition determined by integration of the ¹H NMR spectra. ^b Intrinsic viscosity in dL·g⁻¹ measured in chloroform at 25 °C. ^c Number-average molecular weight in g·mol⁻¹ determined by ¹H NMR end group analysis. ^d Number and weight-average molecular weights in g·mol⁻¹ and dispersities measured by GPC in HFIP against PMMA standards. ^e (-) Insoluble, (+) soluble.

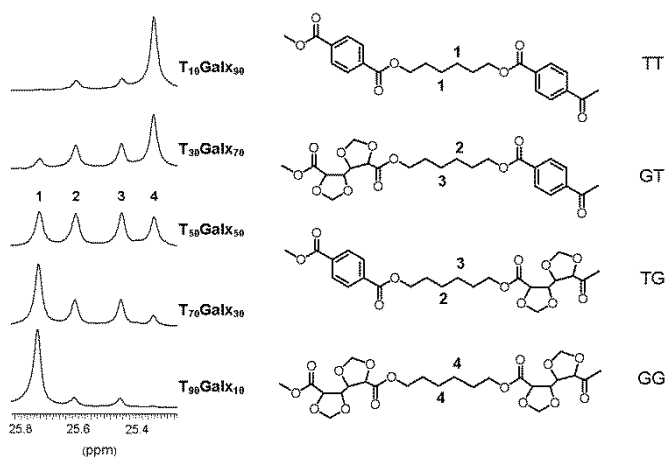


Figure 4.1. ^{13}C NMR signals used for the microstructure analysis of PHT_xGal_y copolyesters (left) with indication of the dyads to which they are assigned (right).

Table 4.2. Microstructure analysis of PHT_xGal_y copolyesters.

Copolyester	Dyads (mol %)			Number Average Sequence Lengths		Randomness R
	TT	TG/GT	GG	n_T	n_{Galx}	
$\text{PHT}_{90}\text{Gal}_{10}$	80.9	17.6	1.6	10.2	1.2	0.95
$\text{PHT}_{70}\text{Gal}_{30}$	49.7	41.5	8.7	3.4	1.4	0.99
$\text{PHT}_{50}\text{Gal}_{50}$	26.8	50.8	22.4	2.1	1.9	1.02
$\text{PHT}_{30}\text{Gal}_{70}$	9.1	43.5	47.4	1.4	3.2	1.02
$\text{PHT}_{10}\text{Gal}_{90}$	1.4	23.6	75.0	1.1	7.4	1.03

The solubility of both PHT_xGal_y and PDT_xGal_y copolyesters was assessed in an assortment of representative solvents, and results are compared in Table 4.1. Solubility appears to be nonsensitive to the length of the diol polymethylene segment, and the incorporation of the acetalized galactarate unit in the polyester only produces a slight increase in solubility so that PHT_xGal_y and PDT_xGal_y copolyesters become additionally soluble in DMF, NMP and THF. All of them are invariably insoluble in water, ethanol, diethyl ether and DMSO, and soluble in chloroform, HFIP and TFA.

4.2.3.2. Thermal properties

Thermal data of both PHT_xGal_y and PDT_xGal_y copolyesters were recorded by TGA and DSC and they are shown in Table 4.3, where the corresponding data for the parent homopolyesters PHT, PHGalx, PDT and PDGalx are also included for comparison.

Table 4.3. Thermal properties of PHT_xGal_y and PDT_xGal_y copolyesters.

Copolyester	TGA			DSC								
	$^{\circ}T_{5\%}^a$	T_d^b	W^c	T_g^d	First heating ^e		Cooling ^e		Second heating ^e			
					T_m	ΔH_m	T_c	ΔH_c	T_c	ΔH_c	T_m	ΔH_m
($^{\circ}C$)	($^{\circ}C$)	(%)	($^{\circ}C$)	($^{\circ}C$)	($J \cdot g^{-1}$)	($^{\circ}C$)	($J \cdot g^{-1}$)	($^{\circ}C$)	($J \cdot g^{-1}$)	($^{\circ}C$)	($J \cdot g^{-1}$)	
PHT	370	408	3	18	142	34.4	106	28.9	-	-	136/143 ^f	25.9
PHT ₉₀ Gal ₁₀	362	408	5	9	126/133 ^f	33.1	98	27.5	-	-	124/134 ^f	24.8
PHT ₇₀ Gal ₃₀	343	358/406	8	5	100	17.9	-	-	56	16.9	100	15.2
PHT ₅₀ Gal ₅₀	335	354/406	10	1	48/65 ^f	13.9	-	-	-	-	-	-
PHT ₃₀ Gal ₇₀	333	368/408	10	0	50	12.6	-	-	-	-	-	-
PHT ₁₀ Gal ₉₀	327	351/397/451	12	0	44/56/71 ^f	13.3	-	-	-	-	-	-
PHGal _x	327	350/398/450	13	0	51/71/73 ^f	16.2	-	-	-	-	-	-
PDT	373	411	1	-6	119	56.8	94	54.4	-	-	117	53.6
PDT ₉₀ Gal ₁₀	363	413	2	-9	116	54.1	88	50.2	-	-	112	47.0
PDT ₇₀ Gal ₃₀	347	360/413	4	-18	99	36.4	72	32.8	-	-	99	32.5
PDT ₅₀ Gal ₅₀	336	365/415	8	-19	80	35.3	47	29.9	-	-	81	28.9
PDT ₃₀ Gal ₇₀	334	383/417	10	-19	69	33.4	17	9.5	11	16.8	71	26.5
PDT ₁₀ Gal ₉₀	333	354/388/462	12	-22	82	41.2	42	35.3	-	-	82	34.6
PDGal _x	329	352/387/459	13	-22	88	43.7	45	36.8	-	-	88	35.2

^aTemperature at which 5 % weight loss was observed. ^bTemperature for maximum degradation rate. ^cRemaining weight at 600 $^{\circ}C$. ^dGlass-transition temperature taken as the inflection point of the heating DSC traces of melt-quenched samples recorded at 20 $^{\circ}C \cdot min^{-1}$. ^eMelting (T_m) and crystallization (T_c) temperatures, and melting (ΔH_m) and crystallization (ΔH_c) enthalpies measured by DSC at heating/cooling rates of 10 $^{\circ}C \cdot min^{-1}$.

^fMultiple melting peak.

The TGA traces of PHT_xGal_y and PDT_xGal_y copolyesters registered under an inert atmosphere are comparatively depicted in Figure 4.2, evidencing the similar behavior among the members of the two series. Decomposition of aromatic homopolyesters PHT and PDT took place in a single step which initiated above 350 °C, and attained the maximum rate at 410 °C. Both carbohydrate-based homopolyesters PHGalx and PDGalx were decomposed in three different stages, the first one with a maximum rate around 350 °C involving a weight loss of 15%; the second stage at 390-400 °C with a weight loss of 45%, and the final stage at 450-460 °C involving a weight loss of 25-30%, leaving a residual weight of 13% at 600 °C. With regard to PHT_xGal_y and PDT_xGal_y copolyesters, those with galactaric/terephthalic compositions between 30-70% showed an intermediate mechanism involving two different stages with maximum decomposition rates at 360 and 410 °C, respectively, leaving a final residue of 4-10% of the initial weight. The copolyesters containing amounts of the second comonomer below 10% decomposed by a mechanism similar to those of their respective parent homopolyesters. The residual weight at 600 °C of both PHT_xGal_y and PDT_xGal_y copolyesters invariably increased with their content in Galx units.

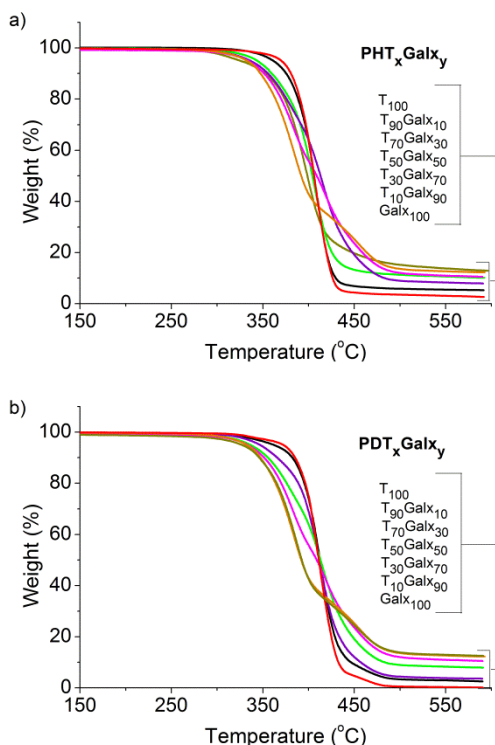


Figure 4.2. TGA traces of PHT_xGal_y (a) and PDT_xGal_y (b) copolyesters.

The DSC analysis of samples quenched from the melt revealed the occurrence of a unique T_g for these copolyesters, with a value decreasing with the content in Galx units, and confined between those of their respective parent homopolyesters. DSC traces of PHT_xGalx_y and PDT_xGalx_y copolyesters registered at first heating are depicted in Figure 4.3. All copolyesters coming directly from synthesis, as well as their parent homopolyesters, gave heating traces with melting endotherms indicating that all of them were semicrystalline. The trend followed by T_m as a function of the copolyester composition is shown in Annex D. In each series, the aromatic homopolyester displayed T_m and ΔH_m higher than their corresponding carbohydrate-based homopolyester. Regarding copolyesters, The T_m did not follow a continuous trend with composition but it fell into a minimum for copolyester compositions around 70% of Galx units. This behavior suggested the occurrence of two different crystal structures in each series according to which unit, galactaric or terephthalic, is predominant in the copolyester. Melting enthalpies displayed a similar behavior to melting temperatures, also falling into a minimum for intermediate compositions.

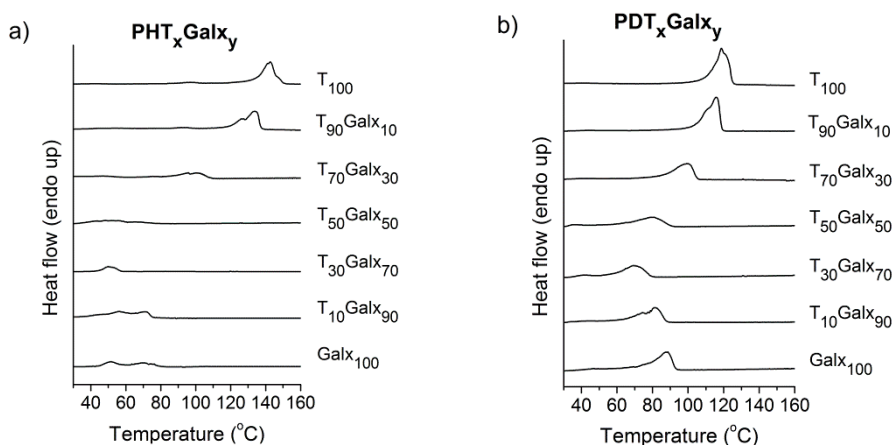


Figure 4.3. DSC melting traces of PHT_xGalx_y (a) and PDT_xGalx_y (b) coming directly from synthesis.

All PDT_xGalx_y copolyesters and their respective parent PDT and PDGalx homopolyesters were able to crystallize upon cooling from the melt. On the contrary, in the PHT_xGalx_y series, only $PHT_{90}Galx_{10}$ crystallized from the melt, although $PHT_{70}Galx_{30}$ presented cold crystallization. Moreover PHT crystallized from the melt, whereas PHGalx did not present such behavior. The different results found between the two series regarding crystallization were in accordance with the higher flexibility of the

dodecamethylene segment. The copolyesters crystallized from the melt recovered about 75-90% of their initial crystallinity and displayed almost the same melting temperatures. To evaluate quantitatively the effect of composition on crystallizability, the isothermal crystallization of PDT_xGalx_y copolyesters in the whole range of compositions was comparatively studied in the 50-105 °C interval. Unfortunately, not all the copolyesters could be compared at the same isothermal crystallization temperature due to large differences in their crystallization rates. Nevertheless, crystallization temperatures were selected as close as possible so that meaningful conclusions could be drawn. For comparative purposes, the isothermal crystallization of $PHT_{90}Galx_{10}$ and its parent homopolymer PHT were also examined. PDT_xGalx_y equilibrium melting temperatures provided by the Hoffman-Weeks plot of T_m vs. T_c (Annex D) displayed the same trend with composition as the copolyester samples coming directly from synthesis.

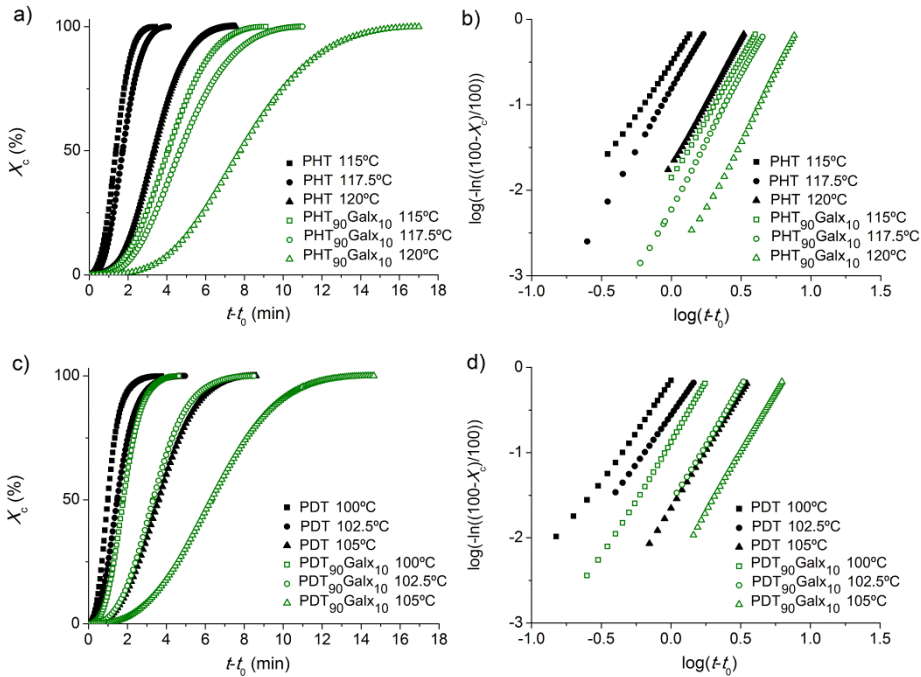


Figure 4.4. Isothermal crystallization of PHT, $PHT_{90}Galx_{10}$, PDT and $PDT_{90}Galx_{10}$ at the indicated temperatures. Relative crystallinity vs. time plot (a, a') and log-log plot (b, b').

Avrami ($\log[-\ln((100-X_c)/100)]$) vs. $\log(t - t_0)$ plots and the evolution of the relative crystallinity, X_c , vs. crystallization time for some illustrative crystallization experiments are depicted in Figure 4.4. Data afforded by the experiments carried out are gathered in Table 4.4, where the observed onset and half-crystallization times, as well as the

corresponding calculated Avrami parameters, are given for each case. For each copolyester, an increase in temperature caused a delay in the onset of crystallization, as well as in the crystallization rate. Avrami exponents oscillated in the 2.1-3.2 range, with values increasing with temperature for each copolyester. The influence of replacing the terephthalate units by Galx in the aromatic homopolyester chain was studied for both PHT and PDT and it was observed that the presence of Galx units in minor amounts depressed the crystallizability in terephthalate copolyesters. On the other hand, comparison of PDGalx, PDT₁₀Galx₉₀ and PDT₃₀Galx₇₀ isothermally crystallized at 60 °C revealed that the crystallization of Galx enriched copolyesters was largely delayed by the presence of terephthalate units. The conclusion derived from this study is that crystallization rate is maximum for the homopolyesters PDT and PDGalx and that it decays in both cases upon incorporation of a second comonomer to fall into a minimum for intermediate copolyester compositions

Table 4.4. Isothermal crystallization data for PHT_xGalx_y and PDT_xGalx_y copolyesters.

Copolyester	T_c (°C)	t_0 (min)	$t_{1/2}$ (min)	n	$-\log k$	T_m (°C)
PHT	115	0.27	1.64	2.42	0.51	139.6
	117.5	0.29	2.01	2.88	0.82	140.6
	120	0.31	3.65	2.99	1.73	141.3
PHT ₉₀ Galx ₁₀	115	0.38	4.44	2.82	1.88	132.2
	117.5	0.44	5.13	3.07	2.19	133.0
	120	0.61	8.39	3.23	3.04	133.9
PDT	100	0.23	1.23	2.27	0.18	118.7
	102.5	0.28	1.77	2.31	0.56	119.4
	105	0.42	4.01	2.69	1.65	120.3
PDT ₉₀ Galx ₁₀	100	0.31	2.10	2.72	0.87	115.4
	102.5	0.38	3.70	2.76	1.60	116.2
	105	0.86	6.91	2.80	2.39	117.3
PDT ₇₀ Galx ₃₀	80	0.26	1.47	2.50	0.37	100.7
	85	0.41	3.08	2.79	1.34	102.2
	90	1.41	10.58	2.83	2.85	104.9
PDT ₅₀ Galx ₅₀	72	0.20	1.12	2.06	0.06	87.1
	74	0.30	1.30	2.13	0.14	88.0
	76	0.45	2.32	2.25	0.73	89.4
PDT ₃₀ Galx ₇₀	50	0.33	2.58	2.12	0.96	74.2
	55	0.56	6.54	2.75	2.25	75.5
	60	0.94	9.86	3.08	3.03	76.4
PDT ₁₀ Galx ₉₀	55	0.13	0.64	2.31	-0.53	84.9
	60	0.26	1.16	2.49	0.06	85.4
	65	0.45	2.58	2.78	1.07	86.0
PDGalx	55	0.07	0.38	2.28	-1.03	89.1
	60	0.22	0.94	2.42	-0.18	89.6
	65	0.37	2.23	2.76	0.88	90.2

4.2.3.3. Crystal structure and stress-strain behavior

DSC results have shown that both PHT_xGal_y and PDT_xGal_y copolyesters are semicrystalline for the whole range of compositions and suggested the existence of two different structures depending on which unit, galactaric or terephthalic, is predominant in the copolyester. In order to complement DSC data, powder X-ray diffraction analyses were performed for both PHT_xGal_y and PDT_xGal_y copolyesters. Powder X-ray diffraction patterns are presented in Figure 4.5, and most Bragg spacings present in such patterns are listed in Table 4.5. Homopolymer PDT and PDT₉₀Gal₁₀, PDT₇₀Gal₃₀ and PDT₅₀Gal₅₀ copolyesters produced the same diffraction pattern which was distinguished by the presence of four prominent reflections at 5.5, 5.0, 4.3 and 3.8 Å. On their turn, PHT and PHT₉₀Gal₁₀, PHT₇₀Gal₃₀ and PHT₅₀Gal₅₀ copolyesters displayed the same diffraction pattern with five prominent reflections at 5.0, 4.8, 4.3, 4.0 and 3.6 Å only differing in the degree of sharpness. On the other hand, PDT₃₀Gal₇₀ and PDT₁₀Gal₉₀ displayed the same reflection pattern as homopolymer PDGalx, with three prominent reflections at 4.6, 4.3 and 4.0 Å, whereas PHT₃₀Gal₇₀ and PHT₁₀Gal₉₀ displayed the same reflection pattern as PHGalx, with three prominent reflections at 5.0, 4.3 and 4.0 Å. The valuable conclusion that can be drawn from these results is that PHT_xGal_y and PDT_xGal_y copolyesters containing up to 50% of galactaric units must share the same crystal structure as PHT and PDT, respectively, whereas they retain the structure of PHGalx and PDGalx homopolymers, respectively, when the content in Galx units arrive to be 70% as minimum.

To evaluate the influence of the presence of Galx units in the terephthalate polyesters, tensile essays of both PHT_xGal_y and PDT_xGal_y series were carried out using thin films prepared by casting from chloroform solution. The recorded stress-strain curves are shown in Figure 4.6, and the mechanical parameters measured in such essays are listed in Table 4.5. PHT was the polyester which presented the highest elastic modulus and tensile strength with a steadily reduction in these parameters as the terephthalate units were replaced by Galx units, so that all the copolyester values span between those of PHT and PHGalx homopolymers. The same trend was observed for PDT_xGal_y copolyesters, with elastic modulus comprised between 430 and 150 MPa and tensile strength values located in the 13-18 MPa range.

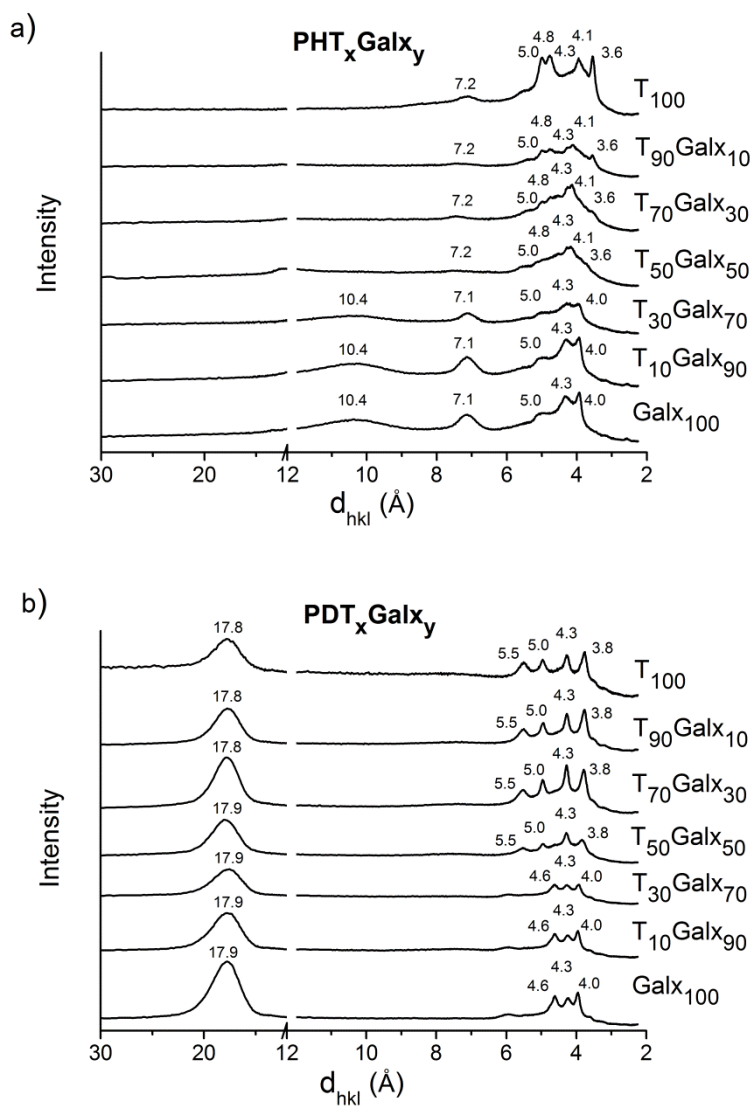


Figure 4.5. Powder WAXD profiles of PHT_xGal_y (a) and PDT_xGal_y (b) copolyesters.

Table 4.5. Powder X-ray diffraction data and mechanical properties of PHT_xGal_y and PDT_xGal_y copolyesters.

Copolyester	X-ray diffraction data							Mechanical Properties			
			d^a (Å)				X_c^b	Elastic modulus (MPa)	Tensile strength (MPa)	Elongation at break (%)	
PHT		7.2 m	5.0 s	4.8 s	4.3 w	4.0 s	3.6 s	0.41	610±15	24±2	14±2
PHT ₉₀ Gal ₁₀		7.2 m	5.0 s	4.8 s	4.3 m	4.1 s	3.6 s	0.40	563±12	22±1	21±3
PHT ₇₀ Gal ₃₀		7.2 m	5.0 m	4.8 m	4.3 m	4.1 m	3.6 m	0.37	451±9	19±2	25±3
PHT ₅₀ Gal ₅₀		7.2 m	5.0 m	4.8 w	4.3 m	4.1 m	3.6 w	0.34	327±9	17±1	188±7
PHT ₃₀ Gal ₇₀	10.4 m	7.1 s	5.0 s		4.3 s	4.0 s		0.30	260±7	15±1	147±6
PHT ₁₀ Gal ₉₀	10.4 m	7.1 s	5.0 s		4.3 s	4.0 s		0.33	176±5	14±1	49±4
PHGalx	10.4 m	7.1 s	5.0 s		4.3 s	4.0 s		0.34	158±4	13±1	54±5
PDT	17.8 s		5.5 s	5.0 s	4.3 s	3.8 s		0.50	432±11	18±2	24±3
PDT ₉₀ Gal ₁₀	17.8 s		5.5 s	5.0 s	4.3 s	3.8 s		0.48	389±8	17±2	26±3
PDT ₇₀ Gal ₃₀	17.8 s		5.5 s	5.0 s	4.3 s	3.8 s		0.45	317±8	16±1	28±4
PDT ₅₀ Gal ₅₀	17.9 s		5.5 s	5.0 s	4.3 s	3.8 s		0.43	261±6	16±1	283±12
PDT ₃₀ Gal ₇₀	17.9 s				4.6 s	4.3 s	4.0 s	0.40	220±6	15±1	245±9
PDT ₁₀ Gal ₉₀	17.9 s				4.6 s	4.3 s	4.0 s	0.41	172±5	14±1	33±5
PDGalx	17.9 s				4.6 s	4.3 s	4.0 s	0.42	155±4	13±1	59±4

^a Bragg spacings measured in powder diffraction patterns for samples coming directly from synthesis. Intensities visually estimated as follows: m, medium; s, strong; w, weak. ^b Crystallinity index calculated as the quotient between crystalline area and total area. Crystalline and amorphous areas in the X-ray diffraction pattern were quantified using PeakFit v4.12 software.

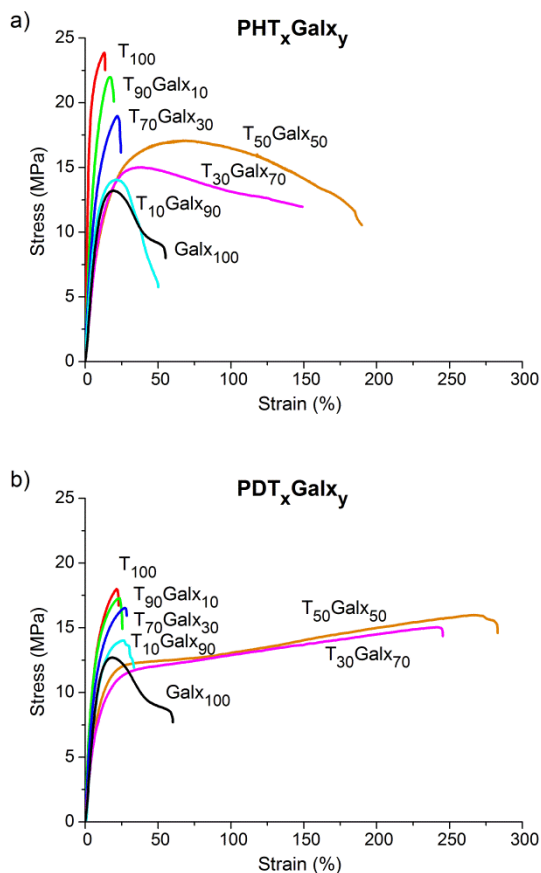


Figure 4.6. Stress-strain curves for PHT_xGal_y (a) and PDT_xGal_y (b) copolyesters.

4.2.3.4. Hydrolytic degradation and biodegradation

The difficulty in hydrolyzing and biodegrading aromatic polyesters is a well-known fact (Maeda *et al.*, 2000; Müller *et al.*, 2001; Marten *et al.*, 2005; Rychter *et al.*, 2010). On the other hand, previous studies on the degradability of polyesters containing sugar moieties have revealed that the presence of these units increases the hydrophilicity of polyesters and enhances the attack by water (Alla *et al.*, 2006; Zamora *et al.*, 2006; Lavilla *et al.*, 2011 -Subchapter 3.2-). To investigate the influence of the incorporation of Galx on hydrodegradation and biodegradation of polyterephthalates, a comparative study

of the two homopolyesters PDT and PDGalx and the intermediate PDT₅₀Galx₅₀ copolyester was made under a variety of conditions.

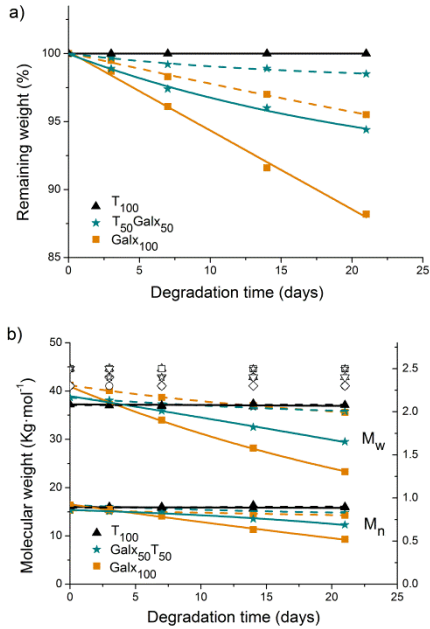


Figure 4.7. Degradation of PDT, PDT₅₀Galx₅₀ and PDGalx at pH 7.4 in the presence of lipase from porcine pancreas (solid lines) and without lipase (dashed lines) at 37 °C. (a) Remaining weight vs. degradation time. (b) Changes in M_w and M_n (solid symbols) and polydispersity index (empty symbols) vs. incubation time.

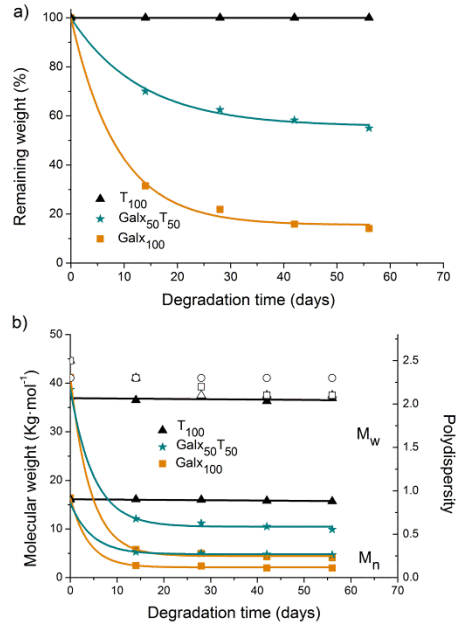


Figure 4.8. Degradation of PDT, PDT₅₀Galx₅₀ and PDGalx at pH 2.0 at 80 °C. (a) Remaining weight vs. degradation time. (b) Changes in M_w and M_n (solid symbols) and polydispersity index (empty symbols) vs. incubation time.

Degradation results obtained for the copolyester PDT₅₀Galx₅₀, as well as for its parent homopolyesters upon incubation in aqueous pH 7.4 buffer at 37 °C, with and without porcine pancreas lipase, are presented in Figure 4.7. The changes taking place in sample weight, M_w , M_n and polydispersity were followed as a function of the incubation time. According to the invariance observed for these parameters in the case of PDT homopolyester, it was concluded that no detectable degradation took place in this polymer, neither in the presence nor in the absence of lipase. On the contrary, the results obtained for both PDT₅₀Galx₅₀ and PDGalx were much more stirring. A substantial decay in sample weight, M_w and M_n was observed for both polyesters when they were incubated in the aqueous buffer, which was more pronounced as the content in Galx increased. Nonetheless what is really remarkable in this study is the fact that degradation was

significantly more noticeable when incubation was made adding lipases to the degradation medium. This result evidences the capacity of Galx unit for making aromatic polyester susceptible to biodegradation. Given the random nature of the copolyesters and assuming that aliphatic moieties are firstly degraded, the remaining aromatic residues will be composed of a few repeating units (their average length will depend on the copolyesters composition). Earlier studies carried out by us on the degradability of building blocks of aromatic polyesters showed that DMT and BISHET were readily degraded by bacteria (Cerdà-Cuellar *et al.*, 2004). It should be reasonably expected therefore that the aromatic fragments resulting in the earlier biodegradation stages of these copolyesters will be fully degraded at the end of the process.

In a previous study carried out on aliphatic polyesters containing Galx it was observed that such polyesters appeared to be more susceptible to hydrolytic degradation in acid than in either basic or neutral medium (Lavilla *et al.*, 2011 -Subchapter 3.2-). To evaluate the ability of Galx containing aromatic copolyesters to be degraded by water in acidic medium under mild conditions, copolyester PDT₅₀Galx₅₀ as well as the parent homopolyesters PDT and PDGalx were then incubated in parallel in aqueous pH 2.0 buffer at room temperature. The changes taking place in sample weight, M_w , M_n and polydispersity at increasing incubation times are shown in Annex D. Hydrolysis of both PDT₅₀Galx₅₀ copolyester and PDGalx homopolyester appeared to be enhanced by acid whereas PDT homopolyester remained unchanged upon incubation in the acidic medium. Nevertheless, the weight loss undergone by PDT₅₀Galx₅₀ and PDGalx when incubated at in the acidic medium for 8 weeks was only about 5% and 10% of initial weight, respectively.

In order to estimate the hydrodegradability of these copolyesters in a more aggressive medium, copolyester PDT₅₀Galx₅₀ as well as the parent homopolyesters PDT and PDGalx were incubated at 80 °C in water at pH 2.0. Results are compared in Figure 4.8, which clearly reveals a notable influence of the Galx units under such conditions. A fast weight loss of PDT₅₀Galx₅₀ and PDGalx samples took place during the first period of incubation, which slowed down in the later stages. In fact, the weight that was lost upon 8 weeks of incubation was about 40% and 85% for PDT₅₀Galx₅₀ and PDGalx, respectively; whereas the weight of PDT homopolyester was maintained unchangeable through all the process. Even more remarkable was the decrease in molecular weight, particularly if compared with the invariance observed for PDT. In accordance to changes observed in sample weight, M_w remained invariable corroborating that PDT is fully resistant to the

aqueous attack. On the contrary, the decrease in M_w of PDT₅₀Galx₅₀ and PDGalx became apparent from the beginning to reach a final value of 11,000 and 5,000 g·mol⁻¹, respectively, after 8 weeks of incubation.

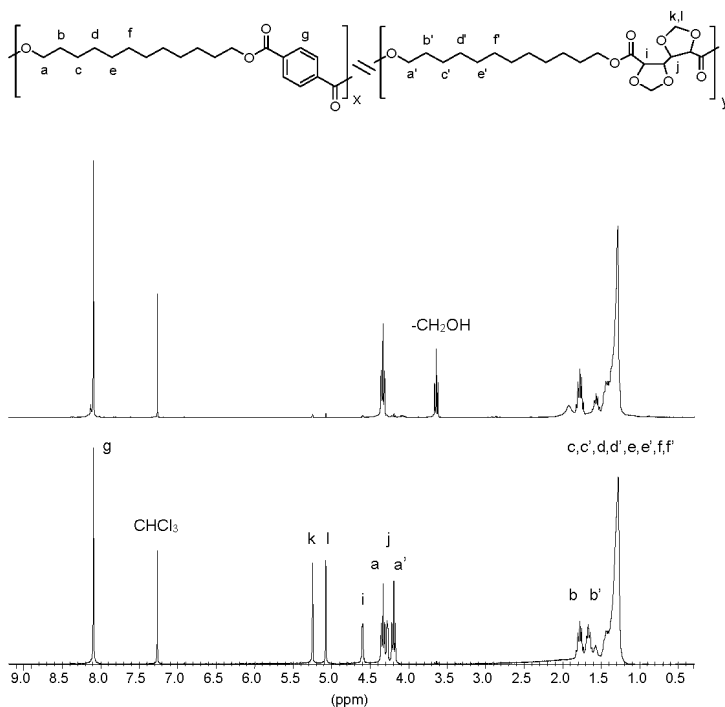


Figure 4.9. Compared ¹H NMR spectra PDT₅₀Galx₅₀ after incubation at pH 2.0 at 80 °C for 56 days (top) and initial sample (bottom).

A NMR study was undertaken to deep insight the degradation of the polyester chain at the molecular level. ¹H NMR spectra of the products released to the aqueous medium and the residual material resulting after 8 weeks of incubation in acidic water at 80 °C are depicted in Figure 4.9 and in Annex D. As expected, PDT spectra of both the aqueous medium and the residual material did not show differences with the initial spectra. By contrast, the PDGalx spectrum of the incubation medium showed signals corresponding to the released Galx diacid. The fact that no signals corresponding to 1,12-dodecanediol were detected was probably due to the insolubility of 1,12-dodecanediol in water. Furthermore the NMR spectrum of the residual material showed -CH₂OH signals of terminal groups of both oligomers and 1,12-dodecanediol, which probably crystallized after being released to the aqueous medium (see SEM results described below). On the

other hand, the NMR analysis of the incubation medium of PDT₅₀Galx₅₀ showed only signals characteristic of Galx diacids and the spectrum of residual polymer contained -CH₂OH signals of both oligomers and 1,12-dodecanediol in addition to those arising from aromatic COOH end-groups of oligomers. Integration of galactaric and terephthalic signals indicated that the residual material contained 2.0% of Galx and 98.0% of terephthalic units. Comparison with the ¹H NMR spectrum of initial PDT₅₀Galx₅₀ leads to conclude that degradation of this copolyester occurs mainly by splitting of the Galx ester groups with release of water-soluble Galx diacid and water-insoluble 1,12-dodecanediol to the medium. The residual copolyester showed a continuous reduction in molecular weight and an increase in the terephthalate content as degradation proceeded.

The analysis by SEM (Figure 4.10 and Annex D) of the surface of the incubated material revealed the changes taking place in the micromorphology of the copolyester PDT₅₀Galx₅₀, as well as the parent homopolyesters PDT and PDGalx due to degradation. The SEM analysis confirmed that the smooth surface of PDT remained unaltered after being incubated under any applied condition confirming the reluctance of this polyester to be hydrolyzed. The surface of the initial sample of PDGalx exhibited a spherulitic texture, which became plenty of cracks after being incubated under physiological conditions in the presence of lipase, a feature that was absent when incubation was carried out in the absence of enzymes. However, when PDGalx was incubated in acidic water at room temperature, some little cracks were also developed; indicating that hydrodegradation was more active in acidic than in neutral medium. After being incubated at 80 °C in water at pH 2.0, the spherulites of PDGalx were almost destroyed, and a second phase was deposited on them, which is thought to be composed of 1,12-dodecanediol that crystallized after being released to the medium. With regard to PDT₅₀Galx₅₀, SEM micrographs of samples incubated at 80 °C in water at pH 2.0 showed almost destruction of the polymer surface with features similar to that happening with PDGalx. On the other hand, when PDT₅₀Galx₅₀ was incubated in the presence of lipase, plenty of tiny holes and cracks appeared in the surface evidencing again a degradation process similar to that undergone by PDGalx. The important conclusion derived from this study is that degradation of PDT₅₀Galx₅₀ copolyester under physiological conditions was due to the action of lipase, a property that points to these carbohydrate-based aromatic copolyesters as interesting biodegradable materials.

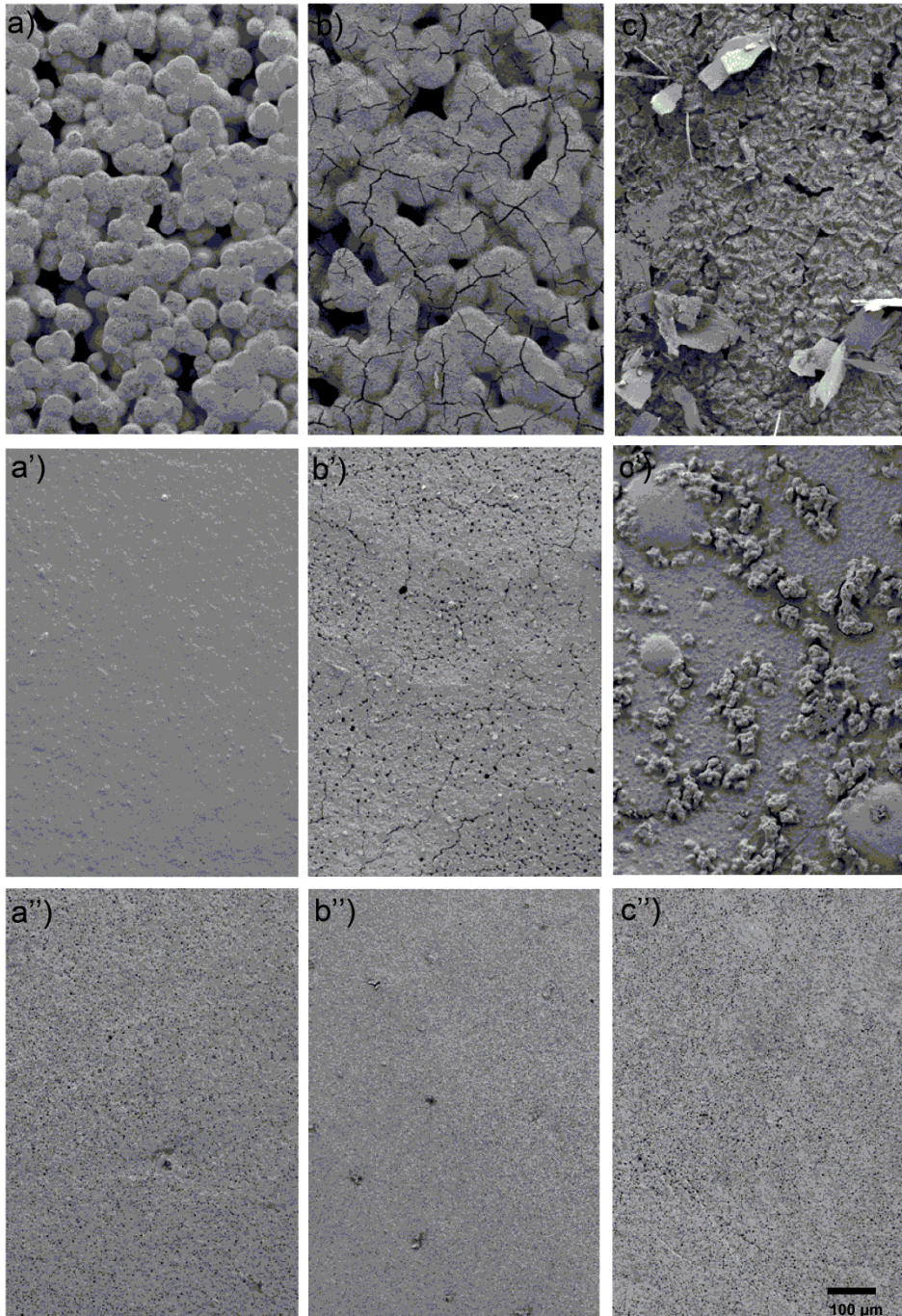


Figure 4.10. SEM micrographs of PDGalx (top), PDT₅₀Galx₅₀ (center) and PDT (bottom). (a, a', a'') Initial sample. (b, b', b'') After incubation in the presence of lipase from porcine pancreas at pH 7.4 at 37 °C for 21 days. (c, c', c'') After incubation at pH 2.0 at 80 °C for 56 days.

4.2.4. Conclusions

The bicyclic diacetal dimethyl 2,3:4,5-di-*O*-methylene galactarate Galx has been successfully used as comonomer of dimethyl terephthalate to produce random copolyesters by melt polycondensation with either 1,6-hexanediol or 1,12-dodecanediol. Two sets of galactarate-terephthalate copolyesters, each one covering the whole range of compositions and with a random microstructure, were obtained. The copolyesters were thermally stable and semicrystalline with melting temperatures and enthalpies slightly decreasing as the content in the second comonomer increased and falling into a minimum for intermediate compositions, in accordance with the existence of two different crystal structures in each series. The copolyesters made of dodecanediol were able to crystallize from the melt although the crystallization rate was significantly delayed by the presence of Galx. Also the glass-transition temperature of the parent terephthalate homopolyesters diminished with the replacement of the aromatic units by the sugar units. The Galx containing copolyesters displayed an accentuated hydrodegradability when compared to the fully aromatic homopolyesters, and which is most remarkable, they appeared to be sensitive to enzymatic action showing a significant hydrolytic degradability under physiological conditions in the presence of lipases. The hydrolysis of the copolyesters took place mainly by breaking of the galactarate ester bonds. It is concluded therefore that the incorporation of the acetalized galactarate units in aromatic polyesters makes them not only more easily degradable but also biodegradable while retaining their thermal and mechanical properties at acceptable values.

4.2.5. References

- Alla, A.; Hakkou, K.; Zamora, F.; Martínez de Ilarduya, A.; Galbis, J.A.; Muñoz-Guerra, S. *Macromolecules* **2006**, *39*, 1410-1416.
- Butler, K.; Lawrance, R.L.; Stacey, M. *J. Chem. Soc.* **1958**, 740-743.
- Cerdà-Cuellar, M.; Kint, D.P.R.; Muñoz-Guerra, S.; Marqués-Calvo, M.S. *Polym. Deg. Stab.* **2004**, *85*, 865-871.
- Fenouillot, F.; Rousseau, A.; Colomines, G.; Saint-Loup, R.; Pascault, J.-P. *Prog. Polym. Sci.* **2010**, *35*, 578-622.
- Galbis, J.A.; García-Martín, M.G. *Sugars as Monomers*. In: Belgacem, M.N.; Gandini, A.; Eds. *Monomers, Polymers and Composites from Renewable Resources*; Elsevier: Oxford, **2008**, 89-114.
- Kiely, D.E.; Chen, L.; Lin, T-H. *J. Am. Chem. Soc.* **1994**, *116*, 571-578.

- Kiely, D.E.; Chen, L.; Lin, T-H. *J. Polym. Sci., Polym. Chem.* **2000**, *38*, 594-603.
- Kricheldorf, H. R. *J. Macromol. Sci.* **1997**, *C37*, 599-631.
- Kricheldorf, H.R.; Behnken, G.; Sell, M. *J. Macromol. Sci. Part A Pure Appl. Chem.* **2007**, *44*, 679-684.
- Lavilla, C.; Alla, A.; Martínez de Ilarduya, A.; Benito, E.; García-Martín, M.G.; Galbis, J.A.; Muñoz-Guerra, S. *Biomacromolecules* **2011**, *12*, 2642-2652. **-Subchapter 3.2-**
- Lavilla, C.; Alla, A.; Martínez de Ilarduya, A.; Benito, E.; García-Martín, M.G.; Galbis, J.A.; Muñoz-Guerra, S. *J. Polym. Sci., Polym. Chem.* **2012**, *50*, 1591-1604. **-Subchapter 3.3-**
- Maeda, Y.; Maeda, T.; Yamaguchi, K.; Kubota, S.; Nakayama, A.; Kawasaki, N.; Yamamoto, N.; Aiba, S. *J. Polym. Sci., Polym. Chem.* **2000**, *38*, 4478-4489.
- Marten, E.; Müller, R.J.; Deckwer, W.D. *J. Macromol. Sci. Part A Pure Appl. Chem.* **1995**, *A32*, 851-856. (1995a)
- Marten, E.; Müller, R.J.; Deckwer, W.D. *J. Environ. Polym. Degrad.* **1995**, *3*, 215-223. (1995b).
- Marten, E.; Müller, R.J. Deckwer, W.-D. *Polym. Degrad. Stabil.* **2005**, *88*, 371-381.
- Mathers, R.T.; Meier, M.A.R. *Green Polymerization Methods*; Wiley-VCH: Weinheim, **2011**.
- Metzke, M.; Guan, Z. *Biomacromolecules* **2008**, *9*, 208-215.
- Müller, R.J.; Kleebert, I.; Deckwer, W.D. *J. Biotechnol.* **2001**, *86*, 87-95.
- Okada, M. *Prog. Polym. Sci.* **2002**, *27*, 87-133.
- Papageorgiou, G.Z.; Vassiliou, A.A.; Karavelidis, V.D.; Koumbis, A.; Bikiaris, D.N. *Macromolecules* **2008**, *41*, 1675-1684.
- Papageorgiou, G.Z.; Nanaki, S.G.; Bikiaris, D.N. *Polym. Degrad. Stabil.* **2010**, *95*, 627-637.
- Rychter, P.; Kawalec, M.; Sobota, M.; Kurcok, P.; Kowalczyk, M. *Biomacromolecules* **2010**, *11*, 839-847.
- Storbeck, R.; Ballauff, M. *J. Appl. Polym. Sci.* **1996**, *59*, 1199-1202.
- Williams, C.K. *Chem. Soc. Rev.* **2007**, *36*, 1573-1580.
- Wool, R.; Sun, S. *Biobased Polymers and Composites*; Academic Press: New York, **2005**.
- Zamora, F.; Hakkou, K.; Muñoz-Guerra, S.; Galbis, J.A. *Polym. Degrad. Stabil.* **2006**, *91*, 2654-2659.

4.3. PET copolyesters from a D-mannitol-derived bicyclic diol

Summary: *The carbohydrate-based bicyclic diol 2,4:3,5-di-O-methylene-D-mannitol (Manx) was made to react in the melt with ethylene glycol and dimethyl terephthalate to produce random PE_xMan_xT copolyesters covering the whole range of molar compositions. The copolyesters had weight-average molecular weights in the 33,000-41,000 $g \cdot mol^{-1}$ interval and were thermally stable up to nearly 380 °C. They displayed T_g in the 81 to 137 °C range with values largely increasing with the content in Manx units. Copolyesters containing minor amounts of Manx were semicrystalline whereas those with contents equal or more than 30% of Manx were amorphous. Stress-strain parameters were affected by composition, increasing tensile strength and elastic modulus and reducing elongation at break when introducing Manx units. These bio-based PET copolyesters showed enhanced susceptibility to hydrolysis.*

Publication derived from this work:

Lavilla, C.; Martínez de Ilarduya, A.; Alla, A.; Muñoz-Guerra, S. *Polym. Chem.* **2013**, *4*, 282-289.

4.3.1. Introduction

Poly(ethylene terephthalate) (PET) is a linear aromatic polyester of exceptional importance for its large number of applications in a wide variety of domestic, industrial and technological fields (Turner *et al.*, 2003). PET displays an excellent pattern of basic properties such as high mechanical strength, good thermal stability and low permeability to gases in addition to an exceptional transparency. Nevertheless, there is currently a growing interest in increasing the glass-transition temperature (T_g) of PET to extend its use to new demanding applications such as the hot-filled and pasteurized-container fields (Bouma *et al.*, 2000; Hibbs *et al.*, 2004; Lotti *et al.*, 2013). Moreover, PET is markedly hydrophobic and more resistant to hydrolysis than usually needed in many of its most common applications. Despite being innocuous for humans, it is considered not to be an environmentally friendly material because its non-renewable origin. In this regard, great efforts are being made nowadays to incorporate degradable and renewable units into PET (Salhi *et al.*, 2004; Olewnik *et al.*, 2007; Kondratowicz and Ukielski, 2009).

Among the renewable naturally occurring sources, carbohydrates stand out in a privileged position due to their huge abundance and because they are inexhaustible and readily available. However, they possess an excess of functional groups that upon polycondensation would lead to undesirable cross-linking reactions unless special precaution are taken. Although some linear polycondensates have been synthesized using carbohydrate-based monomers bearing free hydroxyl groups (Kiely *et al.*, 1994 and 2000), most of linear polycondensations have been carried out with derivatives in which the exceeding functional groups have been appropriately protected (Okada, 2002; Williams, 2007; Metzke and Guan, 2008). With regard to PET, carbohydrate-derived acyclic alditols with the secondary hydroxyl groups protected as methyl ether and benzyl ether have been used to replace ethylene glycol (Kint *et al.*, 2001; Zamora *et al.*, 2005 and 2008). The resulting copolyesters displayed enhanced hydrophilicity when compared to PET, although the introduction of these acyclic units induced also a significant decrease in the T_g . Diacid and diol monomers with a cyclic structure stand out for providing polyesters and copolyesters with improved properties, especially those related to polymer chain stiffness. Among carbohydrate-derived cyclic monomers, 2,5-furandicarboxylic acid has been reported as a potential alternative to replace terephthalic acid for the preparation of aromatic polyesters based on renewable sources (Gandini *et al.*, 2009; Gomes *et al.*, 2011). 1,4:3,6-Dianhydro-D-glucitol, known as isosorbide, which is prepared by dehydration of D-glucose, is the only bicyclic carbohydrate-based

monomer industrially available today. Isosorbide along with other less accessible dianhydrohexitols derivatives are receiving recently a great deal of attention as building blocks for the synthesis of aromatic copolyesters with increased T_g (Sablong *et al.*, 2008; Fenouillot *et al.*, 2010; Quintana *et al.*, 2011; Wu *et al.*, 2012). The two free hydroxyl groups of isosorbide are secondary and, due to their different spatial position in the molecule, they display different reactivity. These features seriously hamper the polycondensation reaction in the melt, so isosorbide polyesters obtained by this method display rather limited molecular weights and are prone to display discoloration (Storbeck and Ballauff, 1996; Kricheldorf *et al.*, 2007). Another type of carbohydrate-based bicyclic monomers is that obtained by internal acetalization of alditols and aldaric acids. This type of monomers has been shown to be very suitable to prepare polyesters by polycondensation in the melt since they are able to react at a rate similar to that of other acyclic conventional monomers (Lavilla *et al.*, 2011 -Subchapter 3.2-, 2012a -Subchapter 3.3-, 2012b -Subchapter 4.2-, 2012c -Subchapter 5.2- and 2012d -Subchapter 5.4-; Japu *et al.*, 2012).

In this paper we present an exploratory account of PET copolyesters that are obtained by replacing partially ethylene glycol by 2,4:3,5-di-O-methylene-D-mannitol, abbreviated as Manx, a bicyclic diol obtained by internal acetalization of D-mannitol. Contrary to isosorbide, the two hydroxyl groups of Manx remaining free for reaction are primary and, since Manx possess a twofold axis of symmetry, they display the same reactivity; moreover, the use of Manx as comonomer leads to stereoregular PET copolyesters because only one position is feasible for these units in the polymer chain.

4.3.2. Experimental section

4.3.2.1. Materials

2,4:3,5-di-O-methylene-D-mannitol was synthesized following the procedure recently reported by Lavilla *et al.* (Lavilla *et al.*, 2012d -Subchapter 5.4-). The reagents ethylene glycol (99+%) and dimethyl terephthalate (99+%), and the catalyst dibutyl tin oxide (DBTO, 98%) were purchased from Sigma-Aldrich. Solvents used for purification and characterization were purchased from Panreac and they all were of either technical or high-purity grade. All the reagents and solvents were used as received without further purification.

4.3.2.2. General methods

^1H and ^{13}C NMR spectra were recorded on a Bruker AMX-300 spectrometer at 25.0 °C operating at 300.1 and 75.5 MHz, respectively. Samples were dissolved in a mixture of deuterated chloroform and trifluoroacetic acid (9:1), and spectra were internally referenced to tetramethylsilane (TMS). About 10 and 50 mg of sample dissolved in 1 mL of solvent were used for ^1H and ^{13}C NMR, respectively. Sixty-four scans were acquired for ^1H and 1,000-10,000 for ^{13}C with 32 and 64-K data points as well as relaxation delays of 1 and 2 s, respectively. Intrinsic viscosities of polymers dissolved in dichloroacetic acid were measured in an Ubbelohde viscosimeter thermostated at 25.0 ± 0.1 °C. Gel permeation chromatograms were acquired at 35.0 °C using a Waters equipment provided with a refraction-index detector. The samples were chromatographed with 0.05 M sodium trifluoroacetate-hexafluoroisopropanol (NaTFA-HFIP) using a polystyrene-divinylbenzene packed linear column with a flow rate of $0.5 \text{ mL} \cdot \text{min}^{-1}$. Chromatograms were calibrated against poly(methyl methacrylate) (PMMA) monodisperse standards. The thermal behavior of polyesters was examined by DSC using a Perkin Elmer DSC Pyris 1. DSC data were obtained from 3 to 5 mg samples at heating/cooling rates of $10 \text{ }^\circ\text{C} \cdot \text{min}^{-1}$ under a nitrogen flow of $20 \text{ mL} \cdot \text{min}^{-1}$. Indium and zinc were used as standards for temperature and enthalpy calibration. The glass-transition temperatures were determined at a heating rate of $20 \text{ }^\circ\text{C} \cdot \text{min}^{-1}$ from rapidly melt-quenched polymer samples. Thermogravimetric analyses were performed under a nitrogen flow of $20 \text{ mL} \cdot \text{min}^{-1}$ at a heating rate of $10 \text{ }^\circ\text{C} \cdot \text{min}^{-1}$, within a temperature range of 30 to 600 °C, using a Perkin Elmer TGA 6 equipment. Sample weights of about 10-15 mg were used in these experiments. Films for mechanical testing measurements were prepared with a thickness of $\sim 200 \text{ }\mu\text{m}$ by casting from solution ($100 \text{ g} \cdot \text{L}^{-1}$) in either chloroform or a mixture of chloroform and hexafluoroisopropanol (5:1); the films were then cut into strips with a width of 3 mm while the distance between testing marks was 10 mm. The tensile strength, elongation at break and Young's modulus were measured at a stretching rate of $30 \text{ mm} \cdot \text{min}^{-1}$ at 23 °C on a Zwick 2.5/TN1S testing machine coupled with a compressor Dalbe DR 150. Scanning electron microscopy (SEM) images were taken with a field-emission JEOL JSM-7001F instrument (JEOL, Japan) from platinum/palladium coated samples.

4.3.2.3. Polymer synthesis

$\text{PE}_x\text{Man}_y\text{T}$ copolyesters were obtained from a mixture of ethylene glycol, 2,4:3,5-di-O-methylene-D-mannitol and dimethyl terephthalate with the selected composition. PET and PMan_xT homopolyesters were obtained by reacting dimethyl

terephthalate with ethylene glycol and 2,4:3,5-di-O-methylene-D-mannitol, respectively. The reactions were performed in a three-necked, cylindrical-bottom flask equipped with a mechanical stirrer, a nitrogen inlet and a vacuum distillation outlet. An excess of diol mixture to dimethyl terephthalate was used and dibutyl tin oxide (DBTO, 0.6% molar respect to monomers) was the catalyst of choice. Antioxidants Irganox 1010 (0.1% w/w) and Irgafos 126 (0.3% w/w) were added to the reaction mixture. Transesterification reactions were carried out under a low nitrogen flow at the selected temperature. Polycondensation reactions were left to proceed at the selected temperature under a 0.03-0.06 mbar vacuum. Then, the reaction mixture was cooled to room temperature, and the atmospheric pressure was recovered with nitrogen to prevent degradation. The resulting polymers were dissolved in chloroform or in a mixture of chloroform and trifluoroacetic acid (9:1) and precipitated in excess of methanol in order to remove unreacted monomers and formed oligomers. Finally, the polymer was collected by filtration, extensively washed with methanol, and dried under vacuum. The copolyesters obtained are abbreviated PE_xMan_yT , where x and y are the mole percentages (mol%) of ethylene glycol and 2,4:3,5-di-O-methylene-D-mannitol, respectively, in the resulting copolyester.

PET homopolymer. 120% molar excess of ethylene glycol to dimethyl terephthalate. Transesterification reactions at 220 °C for 3 h. Polycondensation reactions at 260 °C for 2 h under a 0.03-0.06 mbar vacuum. 1H NMR (300.1 MHz, $CDCl_3/TFA$), δ (ppm): 8.13 (s, 4H, ArH), 4.79 (s, 4H, CH_2). ^{13}C NMR (75.5 MHz, $CDCl_3/TFA$), δ (ppm): 167.5 (CO), 133.5, 130.1, 63.9.

PE_xMan_yT copolyesters. 1H NMR (300.1 MHz, $CDCl_3/TFA$), δ (ppm): 8.1 (s, 4H, ArH), 5.2-5.0 (m, y -4H, OCH_2O), 4.9-4.5 (m, y -4H, OCH_2CH), 4.8 (s, x -4H, OCH_2CH_2O), 4.7 (m, y -2H, OCH_2CH), 4.3 (m, y -2H, OCH_2CHCH). ^{13}C NMR (75.5 MHz, $CDCl_3/TFA$), δ (ppm): 167.7 (CO), 167.6 (CO), 133.7-133.2, 130.2, 88.3, 71.3, 66.5, 64.2, 64.0.

$PE_{86}Man_{14}T$. 50% molar excess of the diol mixture to dimethyl terephthalate. Transesterification reactions at 160 °C for 1 h and at 225 °C for 2 h under a low nitrogen flow. Polycondensation reactions at 255 °C for 1.5 h under a 0.03-0.06 mbar vacuum.

$PE_{69}Man_{31}T$. 50% molar excess of the diol mixture to dimethyl terephthalate. Transesterification reactions at 160 °C for 1 h and at 225 °C for 2 h under a low nitrogen flow. Polycondensation reactions at 250 °C for 2 h under a 0.03-0.06 mbar vacuum.

PE₅₆Manx₄₄T and PE₄₄Manx₅₆T. 50% molar excess of the diol mixture to dimethyl terephthalate. Transesterification reactions at 160 °C for 1 h and at 225 °C for 2 h under a low nitrogen flow. Polycondensation reactions at 240 °C for 2.5 h under a 0.03-0.06 mbar vacuum.

PE₃₁Manx₆₉T. 50% molar excess of the diol mixture to dimethyl terephthalate. Transesterification reactions at 160 °C for 1 h and at 225 °C for 2 h under a low nitrogen flow. Polycondensation reactions at 230 °C for 3 h under a 0.03-0.06 mbar vacuum.

PE₁₅Manx₈₅T. 50% molar excess of the diol mixture to dimethyl terephthalate. Transesterification reactions at 160 °C for 1 h and at 210 °C for 2 h under a low nitrogen flow. Polycondensation reactions at 210 °C for 4 h under a 0.03-0.06 mbar vacuum.

PManxT homopolyester. 5% molar excess of 2,4:3,5-di-O-methylene-D-mannitol to dimethyl terephthalate. Transesterification reactions at 160 °C for 1 h and at 180 °C for 2 h under a low nitrogen flow. Polycondensation reactions at 180 °C for 5 h under a 0.03-0.06 mbar vacuum. ¹H NMR (300.1 MHz, CDCl₃/TFA), δ (ppm): 8.1 (s, 4H, ArH), 5.2-5.0 (m, 4H, OCH₂O), 4.9-4.5 (m, 4H, OCH₂CH), 4.7 (m, 2H, OCH₂CH), 4.3 (m, 2H, OCH₂CHCH). ¹³C NMR (75.5 MHz, CDCl₃/TFA), δ (ppm): 167.5 (CO), 133.5, 130.3, 88.6, 71.4, 66.7, 64.4.

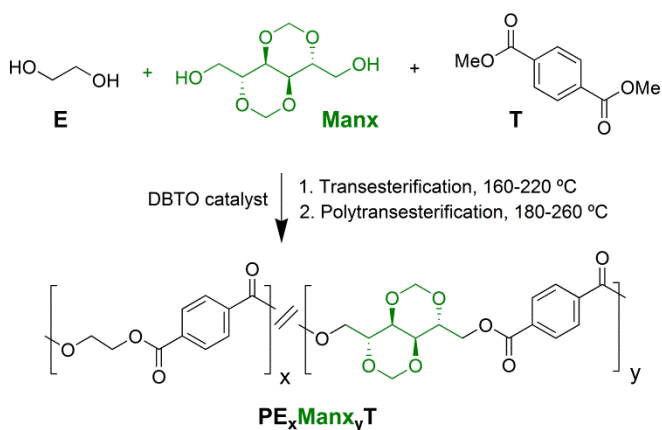
4.3.2.4. Hydrolytic and enzymatic degradation procedures

Films for polyester hydrolytic and enzymatic degradation studies were prepared with a thickness of ~200 μm by casting from solution (100 g·L⁻¹) in either chloroform or a mixture of chloroform and hexafluoroisopropanol (5:1). The films were cut into 10-mm diameter, 20 to 30-mg weight disks and dried in vacuum to constant weight. For hydrolytic degradation, samples were immersed in vials containing 10 mL of citric acid buffer (pH 2.0) at 80 °C. After incubation for the scheduled period of time, the samples were rinsed thoroughly with distilled water and dried to constant weight. The enzymatic degradation was carried out at 37 °C in vials containing 10 mL of the enzymatic medium, consisting of a pH 7.4 buffered sodium phosphate solution containing lipase from porcine pancreas (10 mg). The buffered enzyme solution was replaced every 72 h to maintain the enzyme activity. At the end of the scheduled incubation periods, the disks were withdrawn from the incubation medium, washed thoroughly with distilled water, dried to constant weight and analyzed by GPC chromatography, NMR spectroscopy and SEM microscopy.

4.3.3. Results and discussion

4.3.3.1. Synthesis and chemical structure

PE_xMan_yT copolyesters from ethylene glycol, 2,4:3,5-di-O-methylene-D-mannitol (Man_x) and dimethyl terephthalate within the entire range of molar ethylene glycol/Man_x compositions were prepared by a two-step melt-polycondensation process as depicted in Scheme 4.2, using DBTO as catalyst and in the total absence of solvents in order to imitate as far as possible the conditions usually applied in the industrial practice. PMan_xT and PET homopolyesters were obtained by a similar procedure. An excess of the diol mixture to dimethyl terephthalate was used in all cases to ensure that the growing chains were hydroxyl ended at any polymerization stage. Transesterification reactions were initiated at mild temperature to minimize the volatilization of the diols at the beginning of the process, and progressively increased to avoid crystallization of incipient oligomers. Polycondensation reactions were performed under vacuum to facilitate the removal of methanol and the excess of diols, and at temperatures in the 180-260 °C range; lower temperatures and longer reaction times were used for copolyesters with higher contents in Man_x to prevent the decomposition of the sugar-based compounds. Polyesters were obtained in yields close to 85-90% after purification, which was performed by dissolving the reaction mass in either chloroform or a mixture of chloroform and trifluoroacetic acid and precipitating the polymer with methanol. The chemical constitution and composition of the resulting copolyesters were ascertained by ¹H NMR, and their molecular weights were estimated by both GPC and viscosimetry. Data provided by these analyses are given in Table 4.6.



Scheme 4.2. Polymerization reactions leading to PE_xMan_yT copolyesters.

Table 4.6. Molar composition, molecular weight and microstructure of PE_xMan_yT copolyesters.

Copolyester	Yield (%)	Molar composition				Molecular weight					Microstructure					
		Feed		Copolyester ^a		M_n^b	M_w^b	\bar{D}^b	$[\eta]^c$	M_v^d	Dyads			Number Average Sequence Lengths		Randomness ^e
		X_E	X_{Manx}	X_E	X_{Manx}						EE	EManx/ ManxE	Manx Manx	n_E	n_{Manx}	
PET	90	100	0	100	0	14,400	33,600	2.3	0.67	18,000	-	-	-			
PE ₈₆ Man ₁₄ T	87	90	10	85.7	14.3	16,400	41,600	2.5	0.80	26,300	70.6	25.7	3.7	6.5	1.3	0.93
PE ₆₉ Man ₃₁ T	88	80	20	68.8	31.2	16,500	39,700	2.4	0.75	22,900	46.0	43.2	10.8	3.1	1.5	0.99
PE ₅₆ Man ₄₄ T	85	70	30	55.7	44.3	14,700	36,300	2.5	0.70	19,800	28.4	51.2	20.4	2.1	1.8	1.03
PE ₄₄ Man ₅₆ T	86	60	40	43.6	56.4	14,100	34,500	2.4	0.66	17,500	18.2	48.2	33.6	1.8	2.4	0.99
PE ₃₁ Man ₆₉ T	87	50	50	31.4	68.6	14,300	34,700	2.4	0.68	18,600	10.6	40.1	49.3	1.5	3.5	0.94
PE ₁₅ Man ₈₅ T	85	30	70	15.4	84.6	13,300	33,100	2.5	0.60	14,300	4.9	24.7	70.4	1.4	6.7	0.87
PManxT	85	0	100	0	100	12,900	30,200	2.3	0.51	10,100	-	-	-			

^a Molar composition determined by integration of the ¹H NMR spectra. ^b Number and weight-average molecular weights in g·mol⁻¹ measured by GPC in HFIP against PMMA standards. ^c Intrinsic viscosity in dL·g⁻¹ measured in dichloroacetic acid at 25 °C. ^d Viscosimetric molecular weight in g·mol⁻¹ determined using the Mark-Houwink parameters $K=6.7 \cdot 10^{-3}$ and $a=0.47$, reported for PET (Moore and Sanderson, 1968). ^e Degree of randomness of copolyesters calculated on the basis of the ¹³C NMR analysis.

The ^1H NMR spectra corroborated the chemical structure of the copolyesters with all signals being properly assigned to the different protons contained in their repeating units (Figure 4.11). Integration of the proton signals arising from E and Manx units led to quantify the composition of the copolyesters in such units. The content of the copolyesters in Manx units was found to be in all cases higher than in their corresponding feeds; such preference may be attributed to losses of the more-volatile ethylene glycol provided that Manx and ethylene glycol react at a similar rate. It is worthy to note that in the case of PET copolyesters made from isosorbide (Fenouillot *et al.*, 2010; Quintana *et al.*, 2011), compositions of the copolyesters differed also significantly to those of their feeds, but in this case the losses were in sugar-based comonomer. This opposite behavior in the preferential incorporation of the comonomers could be attributed to the higher reactivity of the primary hydroxyl groups of Manx compared to the secondary hydroxyl groups of isosorbide.

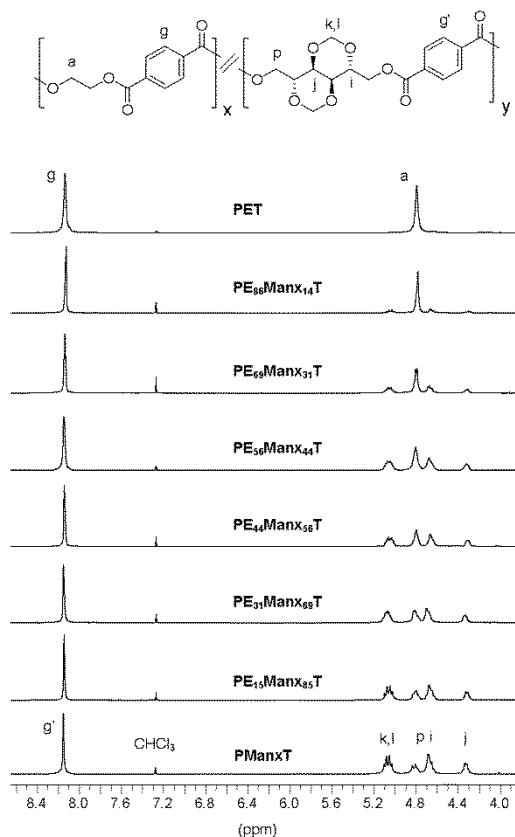


Figure 4.11. Compared ^1H NMR spectra of $\text{PE}_x\text{Man}_y\text{T}$ copolyesters in CDCl_3/TFA .

PE_xMan_xY_T copolyesters were obtained with weight-average molecular weights confined in the 33,000–41,000 g·mol⁻¹ interval, polydispersities between 2.3 and 2.5 and intrinsic viscosities of 0.6–0.8 dL·g⁻¹. Viscosimetric molecular weights were estimated by using the Mark-Houwink parameters reported for PET (Moore and Sanderson, 1968), and were found to be in the 14,000–26,000 g·mol⁻¹ range. The microstructure of PE_xMan_xY_T copolyesters was examined by means of ¹³C NMR spectroscopy taking benefit from the fact that the substituted aromatic carbons are sensitive to sequence distributions at the level of dyads. ¹³C NMR spectrum of PE₃₁Man₆₉T copolyester is depicted in Figure 4.12 for illustration. The changes taking place at the substituted aromatic carbon signals at 133–134 ppm with variation of the copolyester composition are illustrated in Figure 4.13. By integration of the peaks included in these signals, the EE, EManx/ManxE and ManxManx dyad contents were calculated. Based on these values, the number-average sequence lengths and the degree of randomness were estimated (Randal, 1977). Results are summarized in Table 4.6, which shows that the microstructure of PE_xMan_xY_T copolyesters was statistical, with randomness near unity in all cases.

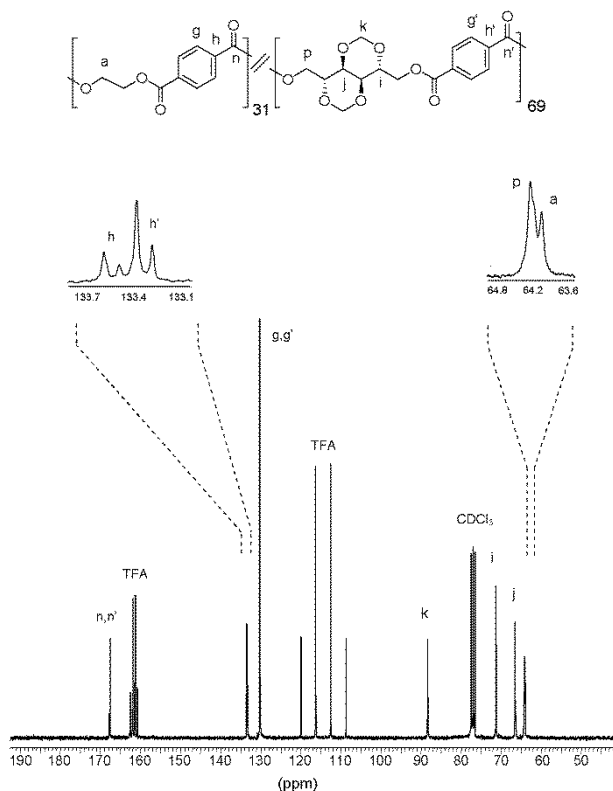


Figure 4.12. ¹³C NMR spectra of PE₃₁Man₆₉T copolyesters in CDCl₃/TFA.

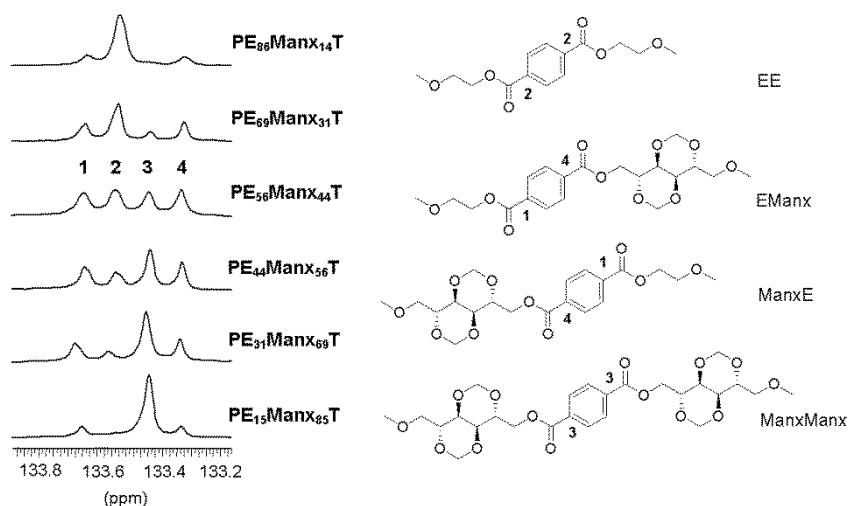


Figure 4.13. ^{13}C NMR signals used for the microstructure analysis of $\text{PE}_x\text{Manx}_y\text{T}$ copolyesters with indication of the dyads to which they are assigned.

4.3.3.2. Thermal and mechanical properties

The thermal behavior of $\text{PE}_x\text{Manx}_y\text{T}$ copolyesters was systematically studied by TGA and DSC taking as reference their parent homopolyesters containing exclusively Manx or ethylene glycol, and results are shown in Table 4.7. First, the thermal stability was evaluated by TGA under inert atmosphere. The remaining weight versus temperature plots are depicted in Figure 4.14. The thermal decomposition happens through one main step with a maximum rate T_d located in the 420–440 °C temperature range with values decreasing when increasing the content in Manx units. The final residue was about 11–13% of the initial weight, the greater amounts being left by copolyesters with higher contents in Manx units. The conclusion drawn from this TGA analysis is that in general the replacement of ethylene glycol by Manx units affects very slightly the thermal stability of the polyesters with the maximum decomposition temperature decreasing around 20 °C in the most detrimental case, which corresponds to PManxT homopolyester.

The DSC analyses revealed that the incorporation of Manx units in the chain of PET induced a significant increase in the glass-transition temperature of the polyester (Figure 4.15). The T_g steadily increased as ethylene glycol was replaced by Manx units going from 81 °C for PET up to 130 °C for $\text{PE}_{15}\text{Manx}_{85}\text{T}$ copolyester. These results are fully consistent with the T_g value of 137 °C observed for the PManxT homopolyester

provided that the microstructure of the copolyesters is random. As expected from its cyclic structure, the incorporation of Manx in PET copolyesters was more beneficial than that exerted by carbohydrate-based acyclic diols such as 2,3,4-tri-O-methyl- or benzyl pentitols and 2,3-di-O-methyl-L-threitol (Figure 4.16). In fact, the incorporation of Manx units in PET brings in an increasing of T_g similar to that attained in the copolymerization with isosorbide as far as the content in sugar-based units is less than 30%.

Table 4.7. Thermal and mechanical properties of PE_xMan_xT copolyesters.

Copolyester	TGA			DSC	Mechanical properties		
	$T_{5\%}^a$ (°C)	T_d^b (°C)	W^c (%)	T_g^d (°C)	Elastic modulus (MPa)	Tensile strength (MPa)	Elongation at break (%)
PET	384	442	11	81	1032±52	45±7	23±5
PE ₈₆ Man ₁₄ T	391	432	12	98	1038±48	45±6	11±4
PE ₆₉ Man ₃₁ T	390	432	12	109	1043±32	48±6	7±2
PE ₅₆ Man ₄₄ T	388	431	12	115	1047±41	48±7	5±2
PE ₄₄ Man ₅₆ T	389	431	13	121	1042±50	50±5	4±2
PE ₃₁ Man ₆₉ T	388	431	13	127	1055±37	55±5	2±1
PE ₁₅ Man ₈₅ T	382	427	13	130	1059±40	56±7	2±1
PManxT	378	421	13	137	1067±29	59±6	2±1

^aTemperature at which 5% weight loss was observed. ^bTemperature for maximum degradation rate. ^cRemaining weight at 600 °C. ^dGlass-transition temperature taken as the inflection point of the heating DSC traces of melt-quenched samples recorded at 20 °C·min⁻¹.

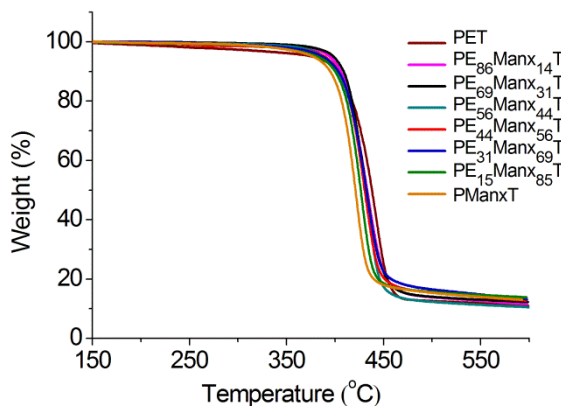


Figure 4.14. TGA traces of PE_xMan_xT copolyesters.

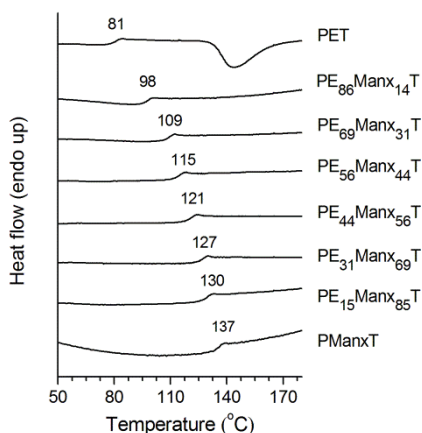


Figure 4.15. DSC heating traces of PE_xManx_yT copolyesters quenched from the melt.

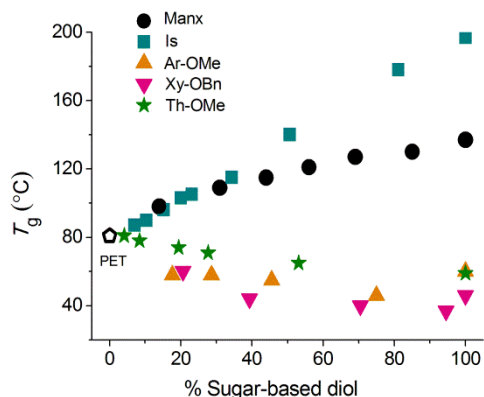


Figure 4.16. Glass-transition temperature vs. composition plot for PET copolyesters containing 2,4:3,5-di-O-methylene-D-mannitol (Manx), isosorbide (Is) (Storbeck and Ballauff, 1996; Quintana *et al.*, 2011); 2,3,4-tri-O-methyl-L-arabinitol (Ar-OMe) (Zamora *et al.*, 2005), 2,3,4-tri-O-benzylxylitol (Xy-OBn) (Zamora *et al.*, 2008), and 2,3-di-O-methyl-L-threitol (Th-OMe) (Kint *et al.*, 2001).

With regard to the melting and crystallization behavior, the heating DSC of the polyesters coming directly from synthesis showed qualitative differences. In general, the insertion of Manx units in minor amounts gave place to a noticeable decrease in both T_m and ΔH_m , showing the pronounced repressing effect of Manx on PET crystallinity. PET displayed both exothermic and endothermic peaks associated with cold crystallization ($T_{cc}= 123$ °C, $\Delta H_{cc}= 4.3$ J·g⁻¹) and melting ($T_m= 252$ °C, $\Delta H_m= 44.1$ J·g⁻¹), whereas the PE₈₆Manx₁₄T copolyester displayed a melting peak at 211 °C with a ΔH_m of 3.3 J·g⁻¹. All other copolyesters with higher content in Manx units as well as PManxT homopolyester appeared to be amorphous.

A preliminary evaluation of the mechanical properties of PE_xManx_yT copolyesters has been carried out. For comparison purposes, mechanical properties of PET and PManxT homopolyesters were also tested. The stress-strain curves resulting from tensile essays are depicted in Figure 4.17, and the mechanical parameters measured in these tests are compared in Table 4.7. The PE_xManx_yT copolyesters present a nearly steady trend with a continuous increase in both elastic modulus and tensile strength and a reduction in extensibility when increasing the content in Manx units. This behavior is in fully accordance with that displayed by PManxT as well as with what should be expected from the trend observed for glass-transition temperatures.

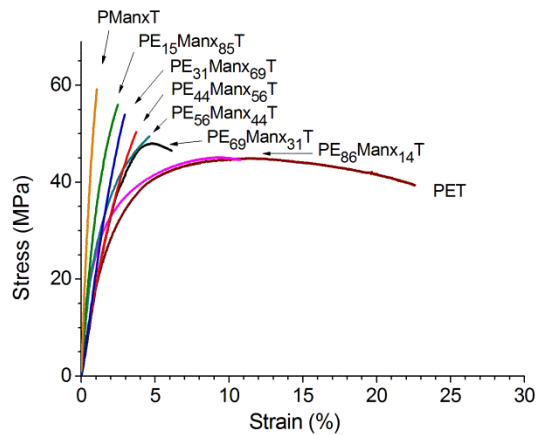


Figure 4.17. Stress-strain curves of PE_xManx_yT copolyesters.

4.3.3.3. Degradability

To investigate the influence of the incorporation of Manx on degradation of PET, a comparative study of the two homopolyesters PET and PManxT and $PE_{31}Manx_{69}T$ copolyester was carried out. The changes taking place in sample weight and molecular weight at increasing incubation times are depicted in Figure 4.18. According to the invariance observed in such parameters when these polyesters were incubated at pH 7.4 at 37 °C, it was concluded that none of them underwent significant degradation under physiological conditions. The same conclusion was reached when porcine pancreas lipase was added to the incubation medium. Conversely, the weight losses undergone by $PE_{31}Manx_{69}T$ and PManxT after 8 weeks of incubation at pH 2.0 at 80 °C were about 11% and 13%, respectively, and the decreases in the molecular weight were around 20-25% of the initial values. Furthermore, SEM analysis showed apparent physical alterations of the surfaces of $PE_{31}Manx_{69}T$ and PManxT after incubation corroborating the remarkable degrading action of the hot acidic buffer (Figure 4.19). The changes observed for PET in sample weight and molecular weight were much less noticeable and SEM observation revealed that alterations of the surface were practically negligible. These results demonstrate that the hydrolytic degradation of PET is significantly enhanced by the presence of Manx units.

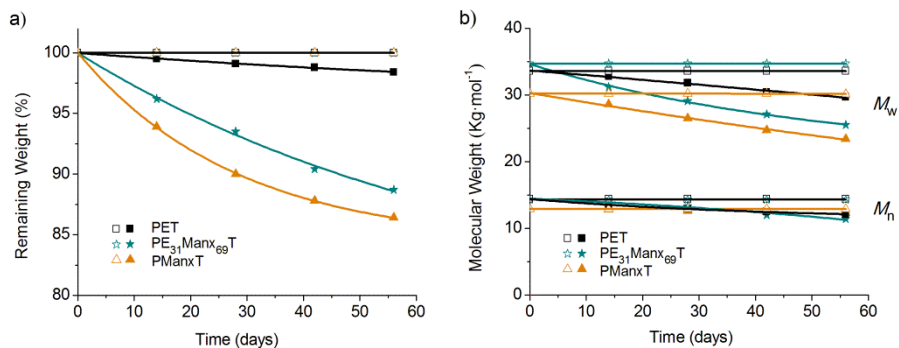


Figure 4.18. Degradation of PET, PE₃₁Man₆₉T and PManxT. Remaining weight (a) and molecular weight (b) versus degradation time at pH 7.4 at 37 °C with and without porcine pancreas lipase (empty symbols) and at pH 2.0 at 80 °C (solid symbols).

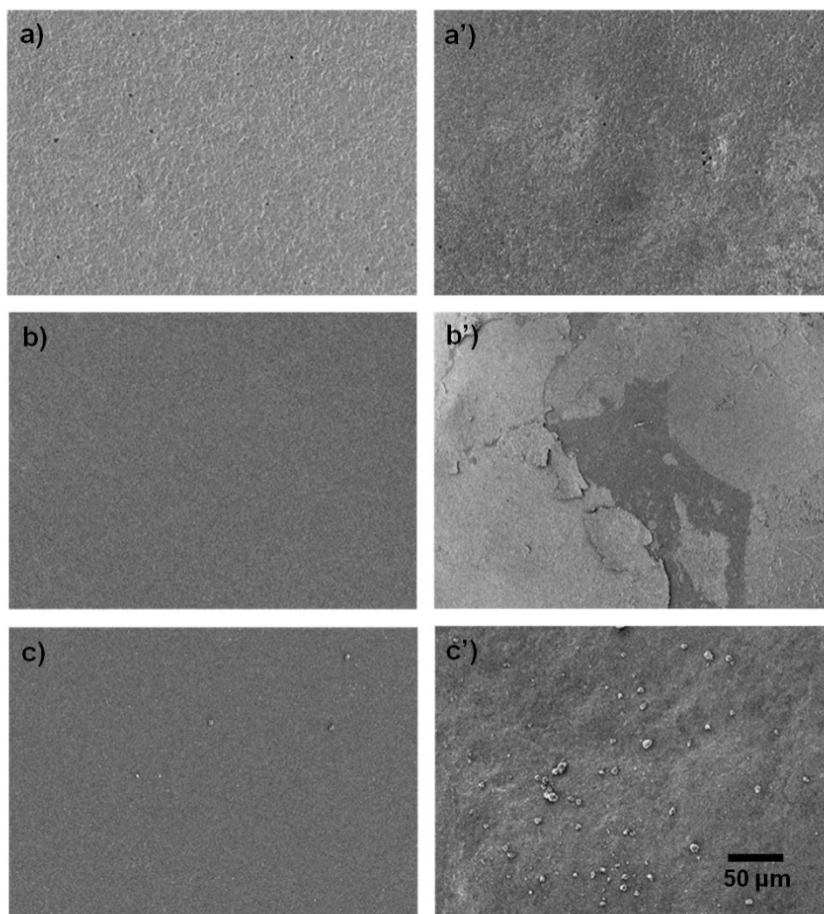


Figure 4.19. SEM micrographs of PET (top), PE₃₁Man₆₉T (center) and PManxT (bottom). (a,b,c) Initial sample. (a',b',c') After incubation at pH 2.0 at 80 °C for 56 days.

4.3.4. Conclusions

Bio-based PET copolyesters made from a bicyclic carbohydrate-based diol, Manx, obtained by internal acetalization of D-mannitol, have been successfully obtained by melt-polycondensation. These novel copolyesters have satisfactory molecular weights and a random microstructure. They are almost as thermally stable as PET with decomposition temperatures decreasing in 20 °C as maximum, which happens for the complete replacement of ethylene glycol by Manx. The crystallinity of PET is depressed by the presence of Manx to the point that it fully disappears for contents in Manx higher than ~15%. On the contrary, the glass-transition temperature of PET is raised by replacement of ethylene glycol units by Manx units. Depending on composition, glass-transition temperatures well above 100 °C can be reached. The relative higher T_g and low crystallizability of copolyesters points Manx as a bio-based comonomer suitable for obtaining amorphous PET products with enhanced glass-transition temperature, which is an optimum combination of properties for applications requiring thermal stability and transparency. Mechanical parameters such as tensile strength and elastic modulus also are increased with the introduction of Manx units, which also enhance the degradability of the resulting copolyesters.

4.3.5. References

- Bouma, K.; de Wit, G.; Lohmeijer, J.H.G.M.; Gaymans, R.J. *Polymer* **2000**, *41*, 3965-3974.
- Fenouillot, F.; Rousseau, A.; Colomines, G.; Saint-Loup, R.; Pascault, J.P. *Prog. Polym. Sci.* **2010**, *35*, 578-622.
- Gandini, A.; Coelho, D.; Gomes, M.; Reis, M.; Silvestre, A.J.D. *J. Mater. Chem.* **2009**, *19*, 8656-8664.
- Gomes, M.; Gandini, A.; Silvestre, A.J.D.; Reis, B. *J. Polym. Sci., Polym. Chem.* **2011**, *49*, 3759-3768.
- Hibbs, M.R.; Holtzclaw, J.; Collard, D.M.; Liu, R.Y.F.; Hiltner, A.; Baer, E.; Shiraldi, D.A. *J. Polym. Sci., Polym. Chem.* **2004**, *42*, 1668-1681.
- Japu, C.; Alla, A.; Martínez de Ilarduya, A.; García-Martín, M.G.; Benito, E.; Galbis, J.A.; Muñoz-Guerra, S. *Polym. Chem.* **2012**, *3*, 2092-2101.
- Kiely, D.E.; Chen, L.; Lin, T.H. *J. Am. Chem. Soc.* **1994**, *116*, 571-578.
- Kiely, D.E.; Chen, L.; Lin, T.H. *J. Polym. Sci., Polym. Chem.* **2000**, *38*, 594-603.

Kint, D.P.R.; Wigström, E.; Martínez de Ilarduya, A.; Alla, A.; Muñoz-Guerra, S. *J. Polym. Sci., Polym. Chem.* **2001**, *39*, 3250-3262.

Kondratowicz, F.I.; Ukielski, R. *Polym. Degrad. Stab.* **2009**, *94*, 375-382.

Kricheldorf, H.R.; Behnken, G.; Sell, M. *J. Macromol. Sci. Part A Pure Appl. Chem.* **2007**, *44*, 679-684.

Lavilla, C.; Alla, A.; Martínez de Ilarduya, A.; Benito, E.; García-Martín, M.G.; Galbis, J.A.; Muñoz-Guerra, S. *Biomacromolecules* **2011**, *12*, 2642-2652. **-Subchapter 3.2-**

Lavilla, C.; Alla, A.; Martínez de Ilarduya, A.; Benito, E.; García-Martín, M.G.; Galbis, J.A.; Muñoz-Guerra, S. *J. Polym. Sci., Polym. Chem.* **2012**, *50*, 1591-1604. (2012a) **-Subchapter 3.3-**

Lavilla, C.; Alla, A.; Martínez de Ilarduya, A.; Benito, E.; García-Martín, M.G.; Galbis, J.A.; Muñoz-Guerra, S. *J. Polym. Sci., Polym. Chem.* **2012**, *50*, 3393-3406. (2012b) **-Subchapter 4.2-**

Lavilla, C.; Alla, A.; Martínez de Ilarduya, A.; Benito, E.; García-Martín, M.G.; Galbis, J.A.; Muñoz-Guerra, S. *Polymer* **2012**, *53*, 3432-3445. (2012c) **-Subchapter 5.2-**

Lavilla, C.; Martínez de Ilarduya, A.; Alla, A.; García-Martín, M.G.; Galbis, J.A.; Muñoz-Guerra, S. *Macromolecules* **2012**, *45*, 8257-8266. (2012d) **-Subchapter 5.4-**

Lotti, N.; Colonna, M.; Fiorini, M.; Finelli, L.; Berti, C. *J. Appl. Polym. Sci.* **2013**, *128*, 416-423.

Metzke, M.; Guan, Z. *Biomacromolecules* **2008**, *9*, 208-215.

Moore, W.R.; Sanderson, D. *Polymer* **1968**, *9*, 153-158.

Okada, M. *Prog. Polym. Sci.* **2002**, *27*, 87-133.

Olewnik, E.; Czerwinski, W.; Nowaczyk, J.; Sepulchre, M.O.; Tessier, M.; Salhi, S.; Fradet, A. *Eur. Polym. J.* **2007**, *43*, 1009-1019.

Quintana, R.; Martínez de Ilarduya, A.; Alla, A.; Muñoz-Guerra, S. *J. Polym. Sci., Polym. Chem.* **2011**, *49*, 2252-2260.

Randal, J.C. *Polymer Sequence Determination*; Academic Press: New York, **1977**, pp. 41-69.

Sablong, R.; Duchateau, R.; Koning, C.E.; de Wit, G.; van Es, D.; Koelewijn, R.; van Haveren, J. *Biomacromolecules* **2008**, *9*, 3090-3097.

Salhi, S.; Tessier, M.; Blais, J.C.; Gharbi, R.E.; Fradet, A. *Macromol. Chem. Phys.* **2004**, *205*, 2391-2397.

Storbeck, R.; Ballauff, M. *J. Appl. Polym. Sci.* **1996**, *59*, 1199-1202.

Turner, S.R.; Seymour, R.W.; Dombroski, J.R. *Amorphous and Crystalline Polyesters based on 1,4-Cyclohexanedimethanol*. In: Scheirs, J.; Long, T.E.; Eds. *Modern*

Polyesters: Chemistry and Technology of Polyesters and Copolyesters; Wiley: Chichester, **2003**, pp. 267-292.

Williams, C.K. *Chem. Soc. Rev.* **2007**, *36*, 1573-1580.

Wu, J.; Eduard, P.; Thiyagarajan, S.; Jasinska-Walc, L.; Rozanski, A.; Fonseca Guerra, C.; Noordover, B.A.J.; van Haveren, J.; van Es, D.S.; Koning, C.E. *Macromolecules* **2012**, *45*, 5069-5080.

Zamora, F.; Hakkou, K.; Alla, A.; Espartero, J.L.; Muñoz-Guerra, S.; Galbis, J.A. *J. Polym. Sci., Polym. Chem.* **2005**, *43*, 6394-6410.

Zamora, F.; Hakkou, K.; Alla, A.; Marín-Bernabé, R.; de Paz, M.V.; Martínez de Ilarduya, A.; Muñoz-Guerra, S.; Galbis, J.A. *J. Polym. Sci., Polym. Chem.* **2008**, *46*, 5167-5179.

CHAPTER 5

POLY(BUTYLENE TEREPHTHALATE) COPOLYESTERS FROM CYCLIC ACETALIZED CARBOHYDRATE-BASED MONOMERS

5.1. Aim and scope of this Chapter

Poly(butylene terephthalate) (PBT) is a semicrystalline thermoplastic aromatic polyester used in a wide variety of engineering applications. PBT has a fairly high melting temperature of around 225 °C, and exhibits the property of crystallizing very fast from the melt. Its thermal behavior, together with its excellent mechanical properties, makes PBT the material of choice for most injection molding applications. Nevertheless, important shortcomings of this polyester are its non-renewable origin and its extremely high resistance to degradation by environmental and biological agents. In this regard, great attention has been given to incorporate bio-based units into PBT. The use of renewable sources as building-blocks for polymers not only contributes to reduce their dependence on petrochemicals but also increases the added-value of agriculture products and wastes.

The insertion of carbohydrate moieties in polycondensates as polyamides, polycarbonates and polyesters has been extensively explored in these last years. The use of carbohydrates as polymer building blocks is motivated by several reasons: they are easily available and even coming from agricultural wastes, they are found in a very rich variety of structures with great stereochemical diversity, and they constitute a truly renewable source. Moreover, carbohydrate-based polycondensates may typically display enhanced hydrophilicity, lower toxicity and higher susceptibility to degradation than those coming from petrochemical feedstocks. Nonetheless, hydrolytic and enzymatic degradation of carbohydrate-based PBT has been scarcely explored up to now. Among carbohydrate-based monomers, those with a bicyclic structure stand out for providing polycondensates with improved properties, especially those related to polymer chain stiffness. Furthermore, recent studies on aliphatic polyesters made from bicyclic acetalized galactaric acid have revealed the beneficial effect of these carbohydrate-based units regarding biodegradability (Chapter 3).

In this Chapter, the preparation by melt polycondensation and further characterization of PBT carbohydrate-based random copolyesters is reported. These copolyesters are obtained by replacing partially the diol or the diacidic monomers by bicyclic acetalized carbohydrate-based monomers derived from galactaric acid and D-mannitol, *i.e.* dimethyl 2,3:4,5-di-O-methylene-galactarate to replace dimethyl terephthalate, and 2,3:4,5-di-O-methylene-galactitol or 2,4:3,5-di-O-methylene-D-mannitol to replace 1,4-butanediol. The main aim of this study is to evaluate the influence of the

incorporation of the sugar-derived units on the thermal and mechanical properties of PBT, as well as on the enzymatic and hydrolytic degradability, taking into account whether the diol or the diacid unit is replaced.

5.2. Bio-based poly(butylene terephthalate) copolyesters containing bicyclic galactitol and galactaric acid: Influence of composition on properties

Summary: Copolyesters from 1,4-butanediol, dimethyl terephthalate and either 2,3:4,5-di-O-methylene-galactitol or dimethyl 2,3:4,5-di-O-methylene-galactarate with compositions of 10, 20, 30, 40 and 50% of either galactitol or galactarate units were prepared by melt-polycondensation. The copolyesters had M_w in the 32,000-41,000 $g \cdot mol^{-1}$ range and had a random microstructure. They displayed T_g from 20 to 70 °C with values steadily decreasing with the content in galactarate units but increasing with the content in galactitol units. All the copolyesters were semicrystalline with T_m between 115 and 210 °C and they adopted the crystal structure of PBT. Copolyesters containing up to 20% of galactitol units as well as all galactarate copolyesters were able to crystallize from the melt, at a crystallization rate that decreased with the content in carbohydrate-based units. Stress-strain essays revealed an increment in the tensile strength and elastic modulus with increasing contents in galactitol units whereas these parameters decreased when galactarate units were the replacing ones.

Publication derived from this work:

Lavilla, C.; Alla, A.; Martínez de Ilarduya, A.; Benito, E.; García-Martín, M.G.; Galbis, J.A.; Muñoz-Guerra, S. *Polymer* **2012**, 53, 3432-3445.

5.2.1. Introduction

Poly(butylene terephthalate) (PBT) is a well-known thermoplastic aromatic polyester that is used in a wide variety of engineering applications. PBT has a fairly high melting temperature of around 225 °C, and has the exceptional property of crystallizing very fast from the melt. Its thermal behavior, together with its excellent mechanical properties, makes PBT very suitable for injection molding applications (Gallucci and Patel, 2004). Nevertheless, despite being innocuous for humans, PBT is considered not to be an environmentally friendly material because its non-renewable origin and its great resistance to degradation by atmospheric and biological agents. In this regard, nowadays great efforts are being made to incorporate renewable and degradable units into PBT (Tripaty *et al.*, 2004; Marten *et al.*, 2005; Kijchavengkul *et al.*, 2010).

Carbohydrates constitute an interesting renewable source for being used as polymer building blocks; they are easily available, some even coming from agricultural wastes, and they are found in a very rich variety of structures with great stereochemical diversity. However, they possess an excess of functional groups that upon polycondensation would lead to undesirable cross-linking reactions unless special precautions are taken. Although some linear polyesters have been synthesized using carbohydrate-based monomers bearing free hydroxyl groups (Kietz *et al.*, 1994 and 2000), most synthesis have been carried out with derivatives in which the exceeding functional groups have been appropriately protected (Kricheldorf, 1997; Okada, 2002; Williams, 2007; Metzke and Guan, 2008). With regard to PBT, carbohydrate-derived acyclic monomers with secondary hydroxyl groups protected as methyl ether and benzyl ether, and with diol and diacid functionality, have been used to replace 1,4-butanediol and dimethyl terephthalate, respectively (Alla *et al.*, 2006; Zamora *et al.*, 2008 and 2009). These PBT copolyesters were semicrystalline for contents in sugar-derived units up to 30% and they retained the crystal structure of PBT. When 50% of dimethyl terephthalate was replaced by pentaaldrates, the glass-transition temperatures of copolyesters decreased in 17 °C respect to PBT homopolyester but they increased in 20 °C when 50% of 1,4-butanediol was replaced by pentalditols. Among carbohydrate-derived monomers, those with a cyclic structure stand out for providing polyesters and copolyesters with improved properties, especially those related to polymer chain stiffness. Thus 2,5-furandicarboxylic acid readily prepared from ubiquitous C5 and C6 carbohydrate precursors has been reported as a potential alternative to replace terephthalic acid for the preparation of aromatic polyesters based on renewable resources (Gandini *et al.*, 2009;

Gomes *et al.*, 2011). 1,4:3,6-Dianhydro-D-glucitol, known as isosorbide, is the only bicyclic carbohydrate-based monomer industrially available today. Isosorbide is prepared by dehydration of D-glucose coming from cereal starch, and its incorporation into aromatic polyesters has received a great deal of attention (Fenouillot *et al.*, 2010). PBT copolyesters containing 50% of isosorbide are amorphous and display a glass-transition temperature 65 °C higher than the PBT homopolyester; PBT copolyesters with contents of up to 30% in isosorbide are semicrystalline (Kricheldorf *et al.*, 2007). The two hydroxyl groups of isosorbide are secondary and, due to their different spatial position in the molecule, they display different reactivity. These features seriously hamper the polycondensation reaction in the melt so isosorbide copolyesters obtained by this method display rather limited molecular weights. Polymers with higher molecular weight could be obtained via polycondensation in solution, but due to the large use of solvents this method is not suitable to be applied at an industrial scale (Fradet and Tessier, 2003). Later, Sablong *et al.* investigated the incorporation of isosorbide into PBT via solid-state polymerization (Sablong *et al.*, 2008).

Another type of carbohydrate-based cyclic monomers are those obtained by internal acetalization (Kimura *et al.*, 1999; Iribarren *et al.*, 2000). Up to now, dimethyl 2,3:4,5-di-O-methylene-galactarate has been the only bicyclic acetalized carbohydrate-based monomer reported for obtaining polyesters and copolyesters. Aliphatic homopolyesters from dimethyl 2,3:4,5-di-O-methylene-galactarate and 1,*n*-alkanediols containing even numbers of methylenes (*n* from 6 to 12) and aliphatic copolyesters from dimethyl adipate, dimethyl 2,3:4,5-di-O-methylene-galactarate and 1,*n*-alkanediols were obtained from this bicyclic acetalized carbohydrate-based monomer (Lavilla *et al.*, 2011 -Subchapter 3.2- and 2012 -Subchapter 3.3-). An interesting characteristic of dimethyl 2,3:4,5-di-O-methylene-galactarate is that its incorporation in a polyester does not alter significantly the crystallizability in spite of being a bulky compound; which is in part due to the molecular symmetry displayed by this compound. In fact, the aliphatic copolyesters were found to be semicrystalline over the entire range of compositions.

In this paper we present an exploratory account of PBT copolyesters that are obtained by replacing partially the diol or the diacidic monomers by bicyclic acetalized carbohydrate-based monomers derived from galactaric acid, *i.e.* dimethyl 2,3:4,5-di-O-methylene-galactarate to replace dimethyl terephthalate, and 2,3:4,5-di-O-methylene-galactitol to replace 1,4-butanediol. These copolyesters will be called PB_xGal_xT and PBT_xGal_x, the abbreviation Gal_x standing for the sugar unit, in the former case as diol

and in the second as diacid, with the subscript y being their molar contents. The synthesis, microstructure, thermal properties, crystal structure and mechanical properties of the new copolyesters will be comparatively studied and discussed in detail. The main aim of this study is to evaluate the influence of the incorporation of the sugar-derived units on the basic properties of PBT taking into account whether the diol or the diacid unit is replaced.

5.2.2. Experimental section

5.2.2.1. Materials

Dimethyl 2,3:4,5-di-*O*-methylene-galactarate was synthesized following the procedure reported by Stacey *et al.* (Butler *et al.*, 1958). 2,3:4,5-di-*O*-methylene-galactitol was synthesized following the procedure reported by Burden *et al.* (Burden and Stoddart, 1975). The reagents 1,4-butanediol (99%) and dimethyl terephthalate (99+%), and the catalyst dibutyl tin oxide (DBTO, 98%) were purchased from Sigma-Aldrich. Solvents used for purification and characterization, such as chloroform and methanol, as well as solvents used in the solubility essays, were purchased from Panreac and they all were of either technical or high-purity grade. All the reagents and solvents were used as received without further purification.

5.2.2.2. General methods

^1H and ^{13}C NMR spectra were recorded on a Bruker AMX-300 spectrometer at 25.0 °C operating at 300.1 and 75.5 MHz, respectively. Polyesters and copolyesters were dissolved in a mixture of deuterated chloroform and trifluoroacetic acid (9:1), and spectra were internally referenced to tetramethylsilane (TMS). About 10 and 50 mg of sample dissolved in 1 mL of solvent were used for ^1H and ^{13}C NMR, respectively. Sixty-four scans were acquired for ^1H and 1,000-10,000 for ^{13}C with 32 and 64-K data points as well as relaxation delays of 1 and 2 s, respectively. Intrinsic viscosities of polymers dissolved in dichloroacetic acid were measured in an Ubbelohde viscosimeter thermostated at 25.0±0.1 °C. Gel permeation chromatograms were acquired at 35.0 °C with a Waters equipment provided with a refraction-index detector. The samples were chromatographed with 0.05 M sodium trifluoroacetate-hexafluoroisopropanol (NaTFA-HFIP) using a polystyrene-divinylbenzene packed linear column with a flow rate of 0.5 mL·min⁻¹. Chromatograms were calibrated against poly(methyl methacrylate) (PMMA)

monodisperse standards. The thermal behavior of polyesters was examined by DSC using a Perkin Elmer DSC Pyris 1. DSC data were obtained from 3 to 5 mg samples at heating/cooling rates of $10\text{ }^{\circ}\text{C}\cdot\text{min}^{-1}$ under a nitrogen flow of $20\text{ mL}\cdot\text{min}^{-1}$. Indium and zinc were used as standards for temperature and enthalpy calibration. The glass-transition temperatures were determined at a heating rate of $20\text{ }^{\circ}\text{C}\cdot\text{min}^{-1}$ from rapidly melt-quenched polymer samples. The treatment of the samples for isothermal crystallization experiments was the following: the thermal history was removed by heating the sample up to $250\text{ }^{\circ}\text{C}$ and left at this temperature for 5 min, and then it was cooled at $20\text{ }^{\circ}\text{C}\cdot\text{min}^{-1}$ to the selected crystallization temperature, where it was left to crystallize until saturation. For morphological study, isothermal crystallizations under the same conditions were carried out in an Olympus BX51 Polarizing Optical Microscope coupled to a THMS LINKAM heating plate and a cooling system LNP (Liquid Nitrogen Pump). Thermogravimetric analyses were performed under a nitrogen flow of $20\text{ mL}\cdot\text{min}^{-1}$ at a heating rate of $10\text{ }^{\circ}\text{C}\cdot\text{min}^{-1}$, within a temperature range of 30 to $600\text{ }^{\circ}\text{C}$, using a Perkin Elmer TGA 6 equipment. Sample weights of about 10-15 mg were used in these experiments. Films for mechanical testing measurements were prepared with a thickness of $\sim 200\text{ }\mu\text{m}$ by casting from solution ($100\text{ g}\cdot\text{L}^{-1}$) in either chloroform or a mixture of chloroform and hexafluoroisopropanol (5:1); the films were then cut into strips with a width of 3 mm while the distance between testing marks was 10 mm. The tensile strength, elongation at break and Young's modulus were measured at a stretching rate of $30\text{ mm}\cdot\text{min}^{-1}$ on a Zwick 2.5/TN1S testing machine coupled with a compressor Dalbe DR 150, at $23\text{ }^{\circ}\text{C}$. X-ray diffraction patterns were recorded on the PANalytical X'Pert PRO MPD θ/θ diffractometer using the $\text{Cu-K}\alpha$ radiation of wavelength 0.1542 nm from powdered samples coming directly from synthesis.

5.2.2.3. Polymer synthesis

$\text{PB}_x\text{Gal}_y\text{T}$ copolyesters were obtained from a mixture of 1,4-butanediol, 2,3:4,5-di-O-methylene-galactitol and dimethyl terephthalate with the selected composition. PBT_xGal_y copolyesters were obtained from a mixture of 1,4-butanediol, dimethyl terephthalate and dimethyl 2,3:4,5-di-O-methylene-galactarate with the selected composition. PBT homopolyester was obtained from 1,4-butanediol and dimethyl terephthalate. PGal_xT and PBGal_x homopolyesters were obtained from mixtures of 2,3:4,5-di-O-methylene-galactitol and dimethyl terephthalate, and 1,4-butanediol and dimethyl 2,3:4,5-di-O-methylene-galactarate, respectively. The reactions were performed in a three-necked, cylindrical-bottom flask equipped with a mechanical stirrer, a nitrogen

inlet and a vacuum distillation outlet. A 5-60% molar excess of diol mixture to the diester mixture, and dibutyl tin oxide (DBTO) as catalyst (0.6% molar respect to monomers) were used. The use of an excess of diol monomers in the polycondensation to polyesters is a common practice that is applied at both laboratory and industrial scales. Such excess ensures that diols do not become in defect due to uncontrolled volatilization, and that all methyl groups are replaced allowing the unlimited growing of the polymer chain. The remaining excess is removed under the high temperature and low vacuum applied at the last stage of the polycondensation reaction. The apparatus was vented with nitrogen several times at room temperature in order to remove the air and avoid oxidation during the polymerization. Transesterification reactions were carried out under a low nitrogen flow at the selected temperature. Polycondensation reactions were left to proceed at the selected temperature under a 0.03-0.06 mbar vacuum. Then, the reaction mixture was cooled to room temperature, and the atmospheric pressure was recovered with nitrogen to prevent degradation. The resulting polymers were dissolved in chloroform or in a mixture of chloroform and trifluoroacetic acid (9:1) and precipitated in excess of methanol in order to remove unreacted monomers and formed oligomers. Finally, the polymer was collected by filtration, extensively washed with methanol, and dried under vacuum.

PBT homopolymer. 60% molar excess of 1,4-butanediol to dimethyl terephthalate. Transesterification reactions at 180 °C for 1 h, at 200 °C for 1 h and at 240 °C for 0.5 h under a low nitrogen flow. Polycondensation reactions at 260 °C for 2 h under a 0.03-0.06 mbar vacuum. ¹H NMR (300.1 MHz, CDCl₃/TFA), δ (ppm): 8.13 (s, 4CH), 4.50 (t, 2CH₂), 2.02 (t, 2CH₂). ¹³C NMR (75.5 MHz, CDCl₃/TFA), δ (ppm): 168.0 (CO), 133.7, 129.9, 66.2, 25.1.

PB_xGal_yT copolyesters. ¹H NMR (300.1 MHz, CDCl₃/TFA), δ (ppm): 8.13 (s, B, Galx, 8CH), 5.20 and 5.15 (2s, Galx, 2CH₂), 4.69 (m, Galx, 2CH), 4.57 (m, Galx, 2CH₂), 4.50 (t, B, 2CH₂), 4.06 (m, Galx, 2CH), 2.02 (t, B, 2CH₂). ¹³C NMR (75.5 MHz, CDCl₃/TFA), δ (ppm): 168.3 (CO), 167.5 (CO), 134.2-134.0-133.7-133.4 (BGalx-BB-GalxGalx-GalxB dyads, h and h'), 130.4, 130.2, 95.7, 77.9, 76.7, 66.2, 65.3, 25.1.

PB₉₀Gal₁₀T and PB₈₀Gal₂₀T. 5% molar excess of the diol mixture to dimethyl terephthalate. Transesterification reactions at 160 °C for 1 h, at 200 °C for 1 h and at 240 °C for 0.5 h under a low nitrogen flow. Polycondensation reactions at 240 °C for 2.5 h under a 0.03-0.06 mbar vacuum.

PB₇₀Galx₃₀T. 5% molar excess of the diol mixture to dimethyl terephthalate. Transesterification reactions at 160 °C for 1 h, at 200 °C for 1 h and at 230 °C for 0.5 h under a low nitrogen flow. Polycondensation reactions at 230 °C for 3 h under a 0.03-0.06 mbar vacuum.

PB₆₀Galx₄₀T. 5% molar excess of the diol mixture to dimethyl terephthalate. Transesterification reactions at 160 °C for 1 h, at 200 °C for 1 h and at 220 °C for 0.5 h under a low nitrogen flow. Polycondensation reactions at 220 °C for 3.5 h under a 0.03-0.06 mbar vacuum.

PB₅₀Galx₅₀T. 5% molar excess of the diol mixture to dimethyl terephthalate. Transesterification reactions at 160 °C for 1 h, at 200 °C for 1 h and at 210 °C for 0.5 h under a low nitrogen flow. Polycondensation reactions at 210 °C for 4 h under a 0.03-0.06 mbar vacuum.

A detailed example: PB₇₀Galx₃₀T. 3.690 g dimethyl terephthalate (19.0 mmol), 1.262 g 1,4-butanediol (14.0 mmol), 1.236 g 2,3:4,5-di-*O*-methylene-galactitol (6.0 mmol) and 0.028 g dibutyl tin oxide (0.114 mmol) were placed in a three-necked, cylindrical-bottom flask equipped with a mechanical stirrer, a nitrogen inlet and a vacuum distillation outlet. The apparatus was vented with nitrogen several times at room temperature in order to remove the air and avoid oxidation during the polymerization. Transesterification reactions were carried out under a low nitrogen flow at 160 °C for 1 h, at 200 °C for 1 h and at 230 °C for 0.5 h. Polycondensation reactions were left to proceed at 230 °C for 3 h under a 0.03-0.06 mbar vacuum. Then, the reaction mixture was cooled to room temperature, and the atmospheric pressure was recovered with nitrogen to prevent degradation.

PBT_xGalx_y copolyesters. ¹H NMR (300.1 MHz, CDCl₃/TFA), δ (ppm): 8.13 (s, T, 4CH), 5.25 and 5.08 (2s, Galx, 2CH₂), 4.71 (m, Galx, 2CH), 4.51-4.45-4.34-4.30 (TT-TGalx-GalxT-GalxGalx dyads, a and a', 4CH₂), 4.36 (m, Galx, 2CH), 2.03-1.92-1.92-1.79 (TT-TGalx-GalxT-GalxGalx dyads, b and b', 4CH₂). ¹³C NMR (75.5 MHz, CDCl₃/TFA), δ (ppm): 172.3 (CO), 168.0 (CO), 133.7, 129.9, 96.9, 79.0, 75.5, 66.9-66.7-66.6-66.4 (GalxT-GalxGalx-TT-TGalx dyads, a and a'), 25.4-25.2-25.1-24.9 (TT-TGalx-GalxT-GalxGalx dyads, b and b').

PBT₉₀Galx₁₀ and PBT₈₀Galx₂₀. 60% molar excess of 1,4-butanediol to the diester mixture. Transesterification reactions at 180 °C for 1 h and at 200 °C for 2 h under a low

nitrogen flow. Polycondensation reactions at 230 °C for 3 h under a 0.03-0.06 mbar vacuum.

PBT₇₀Galx₃₀ and PBT₆₀Galx₄₀. 60% molar excess of 1,4-butanediol to the diester mixture. Transesterification reactions at 180 °C for 1 h and at 190 °C for 2 h under a low nitrogen flow. Polycondensation reactions at 220 °C for 3.5 h under a 0.03-0.06 mbar vacuum.

PBT₅₀Galx₅₀. 60% molar excess of 1,4-butanediol to the diester mixture. Transesterification reactions at 180 °C for 3 h under a low nitrogen flow. Polycondensation reactions at 210 °C for 4 h under a 0.03-0.06 mbar vacuum.

A detailed example: PBT₇₀Galx₃₀. 2.719 g dimethyl terephthalate (14.0 mmol), 1.572 g dimethyl 2,3:4,5-di-O-methylene-galactarate (6.0 mmol), 2.884 g 1,4-butanediol (32.0 mmol) and 0.030 g dibutyl tin oxide (0.120 mmol) were placed in a three-necked, cylindrical-bottom flask equipped with a mechanical stirrer, a nitrogen inlet and a vacuum distillation outlet. The apparatus was vented with nitrogen several times at room temperature in order to remove the air and avoid oxidation during the polymerization. Transesterification reactions were carried out under a low nitrogen flow at 180 °C for 1 h and at 190 °C for 2 h. Polycondensation reactions were left to proceed at 220 °C for 3.5 h under a 0.03-0.06 mbar vacuum. Then, the reaction mixture was cooled to room temperature, and the atmospheric pressure was recovered with nitrogen to prevent degradation.

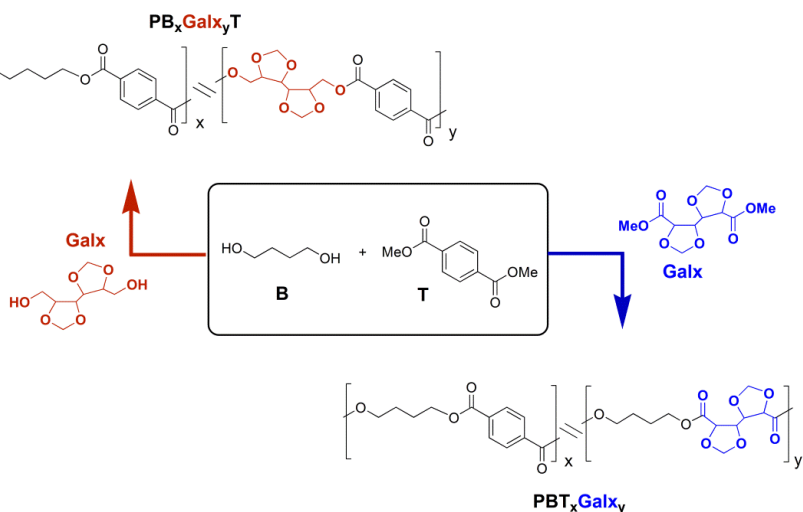
PGalxT homopolyester. 5% molar excess of 2,3:4,5-di-O-methylene-galactitol to dimethyl terephthalate. Transesterification reactions at 160 °C for 1 h and at 180 °C for 2 h under a low nitrogen flow. Polycondensation reactions at 180 °C for 5 h under a 0.03-0.06 mbar vacuum. ¹H NMR (300.1 MHz, CDCl₃/TFA), δ (ppm): 8.13 (s, 4CH), 5.20 and 5.15 (2s, 2CH₂), 4.69 (m, 2CH), 4.57 (m, 2CH₂), 4.06 (m, 2CH). ¹³C NMR (75.5 MHz, CDCl₃/TFA), δ (ppm): 167.5 (CO), 133.6, 130.3, 95.7, 77.9, 76.7, 65.3.

PBGalx homopolyester. 30% molar excess of 1,4-butanediol to dimethyl 2,3:4,5-di-O-methylene-galactarate. Transesterification reactions at 140 °C for 1 h and at 160 °C for 2 h under a low nitrogen flow. Polycondensation reactions at 160 °C for 5 h under a 0.03-0.06 mbar vacuum. ¹H NMR (300.1 MHz, CDCl₃/TFA), δ (ppm): 5.25 and 5.08 (2s, 2CH₂), 4.71 (m, 2CH), 4.36 (m, 2CH), 4.34 (t, 2CH₂), 1.79 (t, 2CH₂). ¹³C NMR (75.5 MHz, CDCl₃/TFA), δ (ppm): 172.3 (CO), 96.9, 79.0, 75.5, 66.7, 24.9.

5.2.3. Results and discussion

5.2.3.1. Synthesis and chemical structure

The synthesis of PB_xGal_xT copolyesters, from 1,4-butanediol, 2,3:4,5-di-O-methylene-galactitol and dimethyl terephthalate, and the synthesis of PBT_xGal_x copolyesters, from 1,4-butanediol, dimethyl terephthalate and dimethyl 2,3:4,5-di-O-methylene-galactarate (Scheme 5.1), were invariably performed in the melt and in the total absence of solvents in order to imitate as far as possible the conditions usually applied in the industrial practice. For comparison purposes, the parent PBT homopolymer was prepared from 1,4-butanediol and dimethyl terephthalate using the same polycondensation procedure; $PGalT$ homopolymer was obtained from 2,3:4,5-di-O-methylene-galactitol and dimethyl terephthalate and $PBGal$ homopolymer was prepared from 1,4-butanediol and dimethyl 2,3:4,5-di-O-methylene-galactarate.



Scheme 5.1. Polymerization reactions leading to PB_xGal_xT and PBT_xGal_x copolyesters.

In the preparation of PB_xGal_xT copolyesters, a 5% molar excess of the diol mixture to dimethyl terephthalate was used to control accurately the incorporation of the diols into the copolyesters; transesterification reactions were initiated at 160 °C in order to prevent volatilization of diols, and temperature was progressively increased to avoid crystallization of oligomers. Polycondensation reactions were performed under vacuum at temperatures in the 210-240 °C range; lower temperatures and longer reaction times

were used in copolyesters with higher contents in 2,3:4,5-di-*O*-methylene-galactitol to avoid the decomposition of this thermally sensitive compound. Regarding PBT_xGal_y copolyesters, a 60% molar excess of 1,4-butanediol to the diester mixture was used to promote the complete incorporation into copolyesters of dimethyl terephthalate and dimethyl 2,3:4,5-di-*O*-methylene-galactarate present in the feed. Transesterification reactions were initiated at 180 °C; polycondensation reactions were performed under vacuum to facilitate the removal of volatile by-products and at temperatures between 210 and 230 °C; lower temperatures and longer reaction times were used for copolyesters with higher contents in thermally sensitive dimethyl 2,3:4,5-di-*O*-methylene-galactarate. Thus, PB_xGal_yT and PBT_xGal_y copolyesters with intrinsic viscosities of 0.7-0.9 dL·g⁻¹, weight-average molecular weights between 32,000 and 41,000 g·mol⁻¹ and polydispersities in the 2.2-2.5 range were obtained as white powders with 85-90% of yield after purification. It is noteworthy that molecular weights slightly decay with the content in sugar units along the PB_xGal_yT series. This trend is commonly observed in the synthesis of copolyesters involving cyclic diol comonomers as 1,4-cyclohexylene dimethanol or isosorbide, and that has been interpreted as due to the higher difficulty of end chains to meet to each other because the diminished mobility of the polymer and therefore to react. The chemical constitution and composition of the resulting copolyesters were ascertained by ¹H NMR (Figure 5.1); for both PB_xGal_yT and PBT_xGal_y copolyesters, compositions were found to be very close to the feed ratio in all cases (Table 5.1).

The microstructure of PB_xGal_yT copolyesters was examined by means of ¹³C NMR spectroscopy taking benefit from the fact that the nonprotonated aromatic carbons are sensitive to sequence distributions at the level of dyads. ¹³C NMR spectrum of PB₇₀Gal₃₀T copolyester is depicted in Figure 5.2 for illustration. The changes taking place at the nonprotonated aromatic carbon signals at 133-135 ppm with variation of the polyester composition are illustrated in Figure 5.4. By integration of the peaks included in these signals, the BB, BGal_x/Gal_xB and Gal_xGal_x dyad contents were calculated. Based on these values, the number-average sequence lengths and the degree of randomness were estimated (Randal, 1977). Results are summarized in Table 5.2, which shows that the comonomer distribution in the PB_xGal_yT copolyesters was random for all studied compositions. With regard to PBT_xGal_y copolyesters, both ¹³C and ¹H spectra showed complex signals for the butanediol units, indicating that methylenes are sensitive to sequence effects. ¹³C NMR spectrum of PBT₇₀Gal₃₀ copolyester is depicted in Figure 5.3 for illustration, whereas the four signals in the 66-67 ppm carbon chemical shift interval corresponding to the four type of dyads (TT, Gal_xT/TGal_x, Gal_xGal_x) that are possible

along the copolyester chain are compared in Figure 5.4 for the whole set of PBT_xGal_y copolyesters. The plot of the content in each type of dyad as a function of the copolyester composition revealed that the microstructure of PBT_xGal_y copolyesters was also statistical, with randomness quite near unity in all cases.

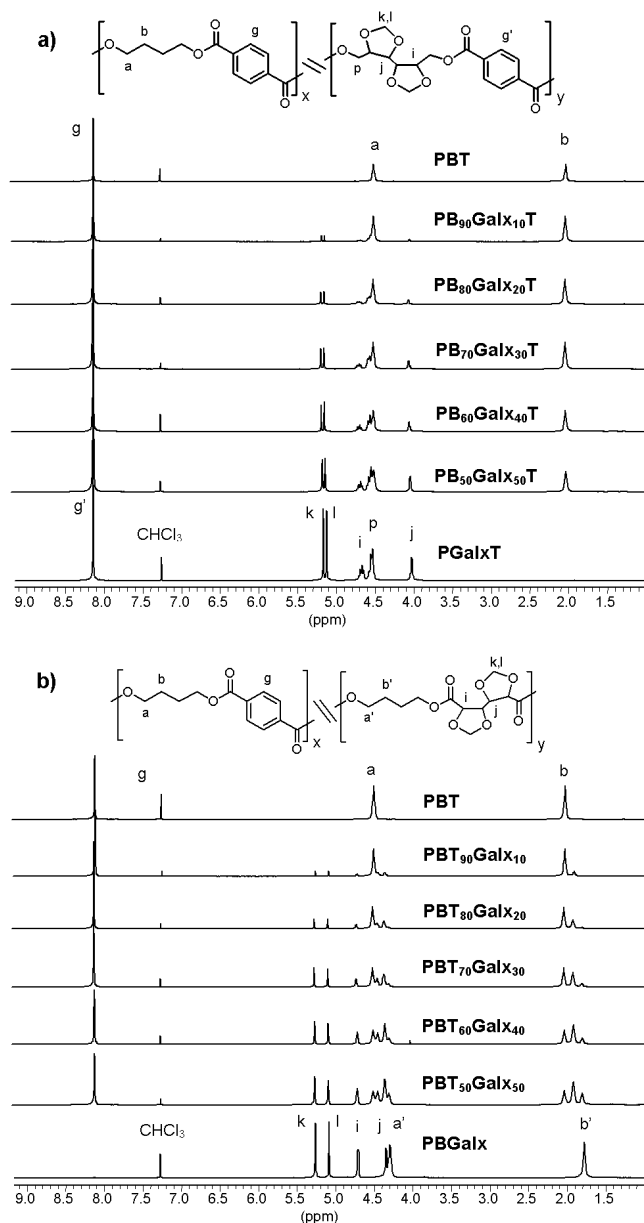


Figure 5.1. Compared ^1H NMR spectra of PB_xGal_xT (a) and PBT_xGal_xT (b) copolyesters.

Table 5.1. Molar composition, molecular weight and solubility of PB_xGal_xyT and PBT_xGal_xy copolyesters.

Copolyester	Yield (%)	Molar composition								Molecular weight				Solubility ^d					
		Feed				Copolyester ^a				$[\eta]^b$	M_n^c	M_w^c	\mathcal{D}^c	H ₂ O DMSO	DMF	THF	NMP	CHCl ₃	HFIP TFA
		Diol		Diacid		Diol		Diacid											
X _B	X _{Galx}	X _T	X _{Galx}	X _B	X _{Galx}	X _T	X _{Galx}												
PBT	90	100	0	100	0	100	0	100	0	0.93	17,100	41,300	2.4	-	-	-	-	-	+
PB ₉₀ Gal ₁₀ T	87	90	10	100	0	88.7	11.3	100	0	0.91	16,300	40,800	2.5	-	-	-	-	-	+
PB ₈₀ Gal ₂₀ T	89	80	20	100	0	78.9	21.1	100	0	0.90	16,800	40,300	2.4	-	-	-	-	+	+
PB ₇₀ Gal ₃₀ T	87	70	30	100	0	69.2	30.8	100	0	0.70	15,600	37,800	2.4	-	-	-	-	+	+
PB ₆₀ Gal ₄₀ T	88	60	40	100	0	61.3	38.7	100	0	0.65	14,400	36,500	2.5	-	-	-	+	+	+
PB ₅₀ Gal ₅₀ T	85	50	50	100	0	50.9	49.1	100	0	0.69	15,800	37,600	2.4	-	-	-	+	+	+
PBT ₉₀ Gal ₁₀	88	100	0	90	10	100	0	91.4	8.6	0.84	16,100	39,200	2.4	-	-	-	-	-	+
PBT ₈₀ Gal ₂₀	87	100	0	80	20	100	0	80.3	19.7	0.70	14,200	31,500	2.2	-	-	-	-	+	+
PBT ₇₀ Gal ₃₀	88	100	0	70	30	100	0	69.7	30.3	0.72	14,500	33,400	2.3	-	-	-	-	+	+
PBT ₆₀ Gal ₄₀	89	100	0	60	40	100	0	59.2	40.8	0.73	14,100	34,900	2.5	-	-	-	+	+	+
PBT ₅₀ Gal ₅₀	87	100	0	50	50	100	0	51.2	48.8	0.75	15,800	38,800	2.5	-	-	-	+	+	+
PGalxT	86	0	100	100	0	0	100	100	0	0.50	12,400	30,500	2.5	-	-	+	+	+	+
PBGalx	88	100	0	0	100	100	0	0	100	0.52	13,100	30,800	2.4	-	+	+	+	+	+

^a Molar composition determined by integration of the ¹H NMR spectra. ^b Intrinsic viscosity in dL·g⁻¹ measured in dichloroacetic acid at 25 °C. ^c Number and weight-average molecular weights in g·mol⁻¹ and dispersities measured by GPC in HFIP against PMMA standards. ^d (-) Insoluble, (+) soluble.

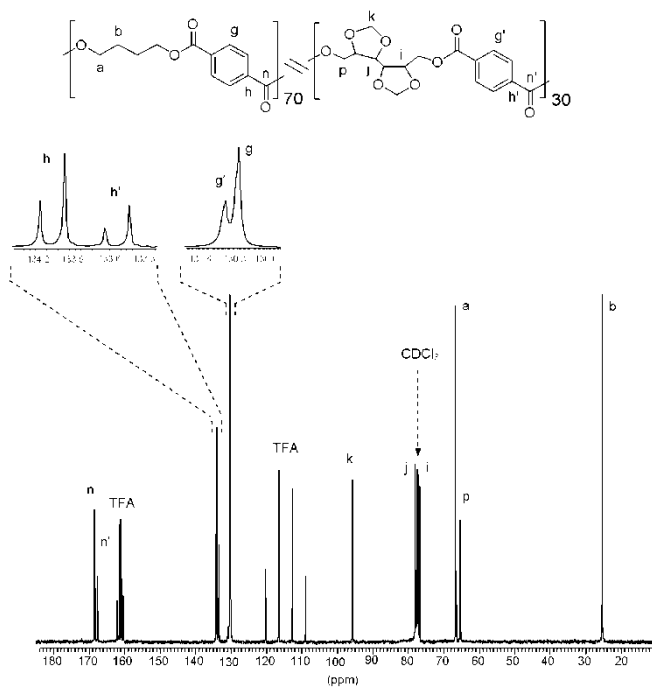


Figure 5.2. ^{13}C NMR spectrum of $\text{PB}_{70}\text{Gal}_{30}\text{T}$ copolyester.

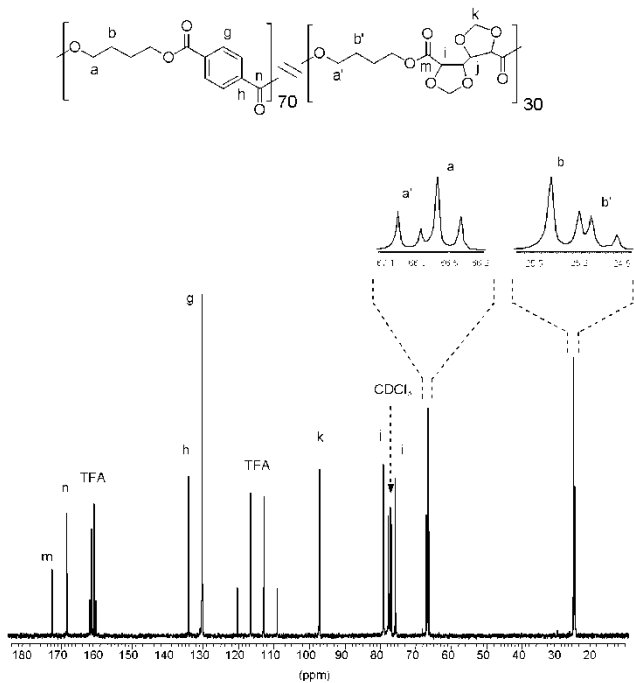


Figure 5.3. ^{13}C NMR spectrum of $\text{PBT}_{70}\text{Gal}_{30}$ copolyester.

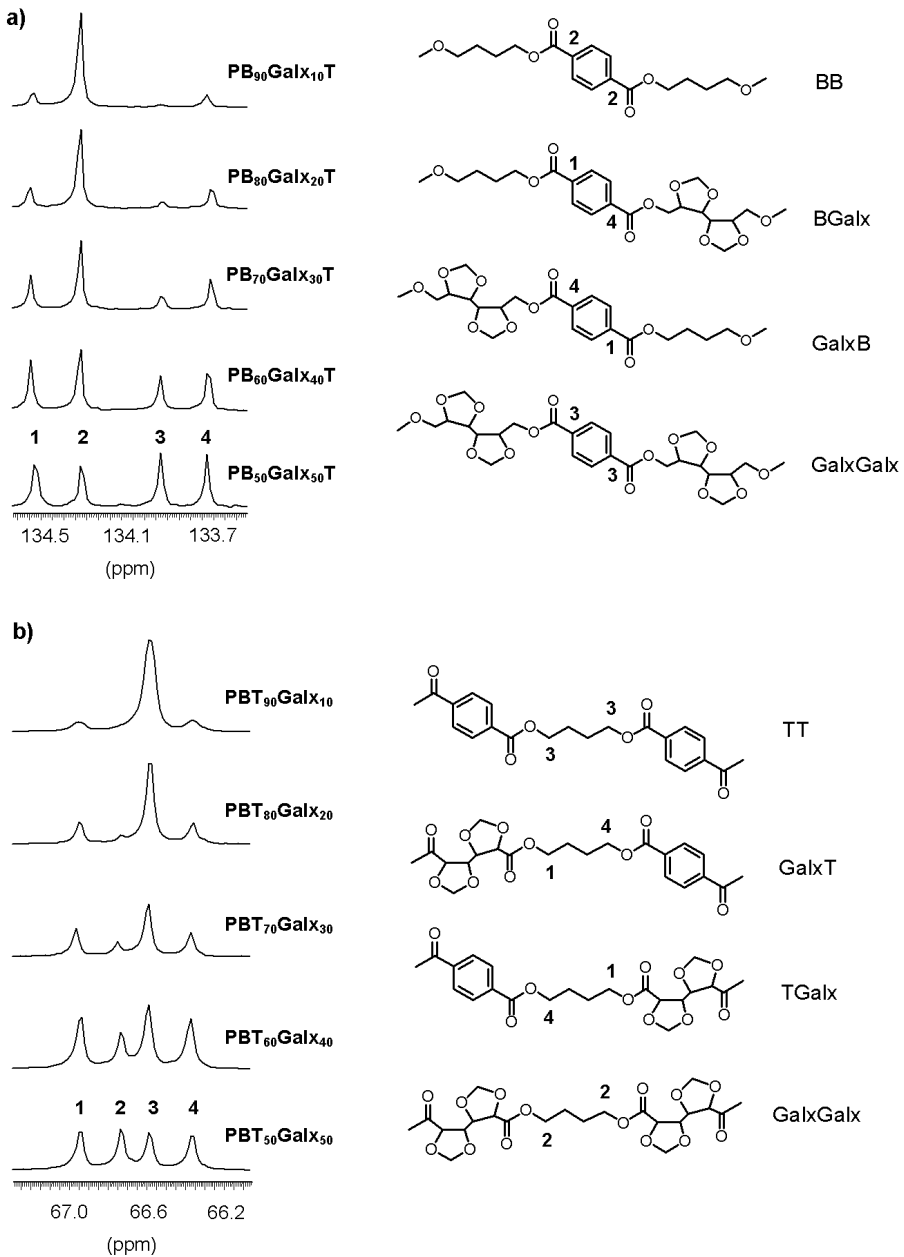


Figure 5.4. ^{13}C NMR signals used for the microstructure analysis of PB_xGal_xT (a) and PBT_xGal_x (b) copolyesters with indication of the dyads to which they are assigned.

Table 5.2. Microstructure analysis of PB_xGal_xyT and PBT_xGal_xy copolyesters.

Copolyester	Dyads (mol %)			Number Average Sequence Lengths		Randomness
	BB	BGalx/GalxB	GalxGalx	n_B	n_{Galx}	R
PB ₉₀ Gal ₁₀ T	71.8	25.1	3.1	6.7	1.2	0.95
PB ₈₀ Gal ₂₀ T	60.0	34.0	6.0	4.5	1.4	0.96
PB ₇₀ Gal ₃₀ T	44.9	44.3	10.8	3.0	1.5	1.00
PB ₆₀ Gal ₄₀ T	33.6	47.7	18.7	2.4	1.8	0.97
PB ₅₀ Gal ₅₀ T	22.5	50.5	27.0	1.9	2.1	1.01

Copolyester	Dyads (mol %)			Number Average Sequence Lengths		Randomness
	TT	TGalx/GalxT	GalxGalx	n_T	n_{Galx}	R
PBT ₉₀ Gal ₁₀	80.4	18.4	1.2	9.7	1.1	0.98
PBT ₈₀ Gal ₂₀	62.4	32.2	5.4	4.9	1.3	0.95
PBT ₇₀ Gal ₃₀	47.4	41.6	11.0	3.3	1.5	0.96
PBT ₆₀ Gal ₄₀	31.3	49.9	18.8	2.3	1.8	0.99
PBT ₅₀ Gal ₅₀	23.4	50.5	26.1	1.9	2.0	1.01

Solubilities of these polyesters in a variety of solvents were systematically evaluated, and the results are compared in Table 5.1. Whereas PBT is only soluble in trifluoroacetic acid and hexafluoroisopropanol, some PB_xGal_xyT and PBT_xGal_xy copolyesters as well as PGalxT and PBGalx homopolyesters could also be solubilized in chloroform and *N*-methyl-2-pyrrolidone. All homopolyesters and copolyesters studied were insoluble in water, methanol, ethanol, diethyl ether and dimethyl sulfoxide. In addition, PGalxT homopolyester was soluble in tetrahydrofuran, whereas PBGalx homopolyester was also soluble in tetrahydrofuran as well as in *N,N*-dimethylformamide.

5.2.3.2. Thermal properties

The thermal behavior of PB_xGal_xyT and PBT_xGal_xy copolyesters has been comparatively studied by TGA and DSC; the thermal parameters resulting from these analyses are given in Table 5.3, where the corresponding data for the parent homopolyesters PBT, PGalxT and PBGalx are also included for comparison.

Table 5.3. Thermal properties of PB_xGal_yT and PBT_xGal_y copolyesters.

Copolyester	TGA			DSC								
	$^{\circ}T_{5\%}^a$	T_d^b	W^c	T_g^d	First heating ^e		Cooling ^e		Second heating ^e			
					T_m	ΔH_m	T_c	ΔH_c	T_c	ΔH_c	T_m	ΔH_m
($^{\circ}C$)	($^{\circ}C$)	(%)	($^{\circ}C$)	($^{\circ}C$)	($^{\circ}C$)	($J \cdot g^{-1}$)	($^{\circ}C$)	($J \cdot g^{-1}$)	($^{\circ}C$)	($J \cdot g^{-1}$)	($^{\circ}C$)	($J \cdot g^{-1}$)
PBT	371	408	2	31	223	56.2	196	43.3	-	-	223	44.0
PB ₉₀ Gal ₁₀ T	372	409	5	46	197	37.2	162	25.8	-	-	199	26.1
PB ₈₀ Gal ₂₀ T	373	411	5	53	179	26.1	126	19.3	-	-	178	20.1
PB ₇₀ Gal ₃₀ T	375	414	6	57	151	21.9	-	-	-	-	-	-
PB ₆₀ Gal ₄₀ T	377	417	9	62	138	14.8	-	-	-	-	-	-
PB ₅₀ Gal ₅₀ T	379	418	10	70	119	8.7	-	-	-	-	-	-
PBT ₉₀ Gal ₁₀	368	405	4	29	210	43.1	181	30.1	-	-	210	30.3
PBT ₈₀ Gal ₂₀	361	404	7	27	189	28.8	163	23.5	-	-	188	23.8
PBT ₇₀ Gal ₃₀	347	403	9	25	166	22.4	127	16.2	-	-	165	17.0
PBT ₆₀ Gal ₄₀	336	402	9	23	129	15.9	68	2.7	75	10.2	129	13.5
PBT ₅₀ Gal ₅₀	333	400	10	22	115	10.0	64	2.1	81	4.2	117	7.2
PGalxT	382	436	12	87	-	-	-	-	-	-	-	-
PBGalx	328	379	12	18	122	35.1	-	-	81	13.6	125	14.7

^aTemperature at which 5% weight loss was observed. ^bTemperature for maximum degradation rate. ^cRemaining weight at 600 $^{\circ}C$. ^dGlass-transition temperature taken as the inflection point of the heating DSC traces of melt-quenched samples recorded at 20 $^{\circ}C \cdot min^{-1}$.

^eMelting (T_m) and crystallization (T_c) temperatures, and melting (ΔH_m) and crystallization (ΔH_c) enthalpies measured by DSC at heating/cooling rates of 10 $^{\circ}C \cdot min^{-1}$.

The TGA traces of PBT, PGalxT and PBGalx homopolyesters together with their derivative curves are shown in Figure 5.5, and those recorded from the whole sets of PB_xGal_yT and PBT_xGal_y copolyesters are comparatively depicted in Figure 5.6. Thermal decomposition of PBT occurs in a single stage with the maximum rate taking place at 408 °C ($^{max}T_d$). This polyester starts to decompose well above 300 °C with 5% of the initial weight being lost at 371 °C ($^{\circ}T_{5\%}$) and only 2% remaining at 600 °C. Decomposition of PB_xGal_yT copolyesters takes place also in one stage at temperatures steadily increasing as butanediol units are replaced by galactitol units achieving a $^{max}T_d$ of 418 °C for a 50% of substitution degree. The same trend is observed for $^{\circ}T_{5\%}$, corroborating that the introduction of galactitol units enhances the thermal stability of these polyesters. This result was in accordance with the high thermal stability observed for PGalxT homopolyester, with $^{\circ}T_{5\%}$ and $^{max}T_d$ of 382 and 436 °C, respectively. On the other hand, decomposition of PBT_xGal_y copolyesters also takes place mainly in one stage, but in this case with decomposition temperatures steadily decreasing as terephthalate units are replaced by galactarate units with $^{max}T_d$ falling to 400 °C for the $PBT_{50}Gal_{50}$ copolyester. These results were in accordance with those obtained for PBGalx homopolyester, in which the $^{max}T_d$ goes down to 379 °C. The residual weight left by both PB_xGal_yT and PBT_xGal_y copolyesters upon heating at 600 °C invariably increased with their content in sugar units, a trend that includes also the respective homopolyesters.

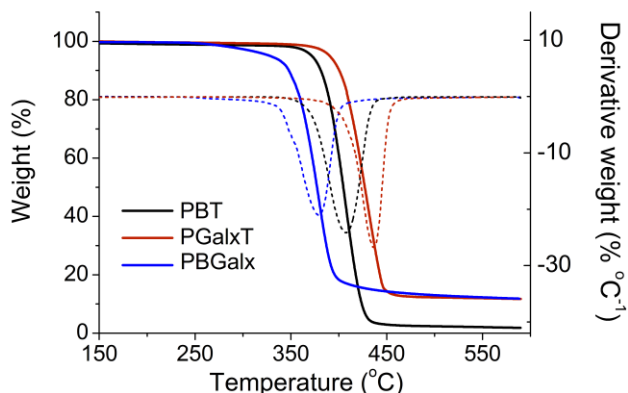


Figure 5.5. TGA traces (solid lines) and derivative curves (dashed lines) of PBT, PGalxT and PBGalx.

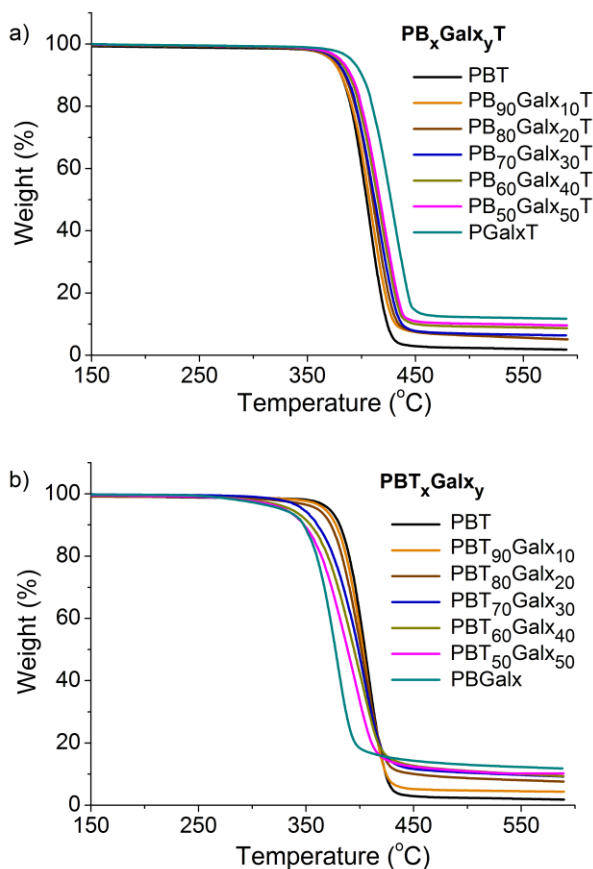


Figure 5.6. TGA traces of PB_xGal_xT (a) and PBT_xGal_x (b) copolyesters.

The DSC analyses revealed that the incorporation of sugar units in the chain of PBT induced significant changes in glass-transition of the parent polymer. In the PB_xGal_xT series, the glass-transition temperature (T_g) steadily increased as butanediol was replaced by galactitol units going from 31 °C for PBT up to 70 °C for the $PB_{50}Gal_{50}T$ copolyester. These results are fully consistent with the T_g value of 87 °C observed for the $PGal_xT$ homopolyester provided that the microstructure of the copolyesters is random. Conversely, the T_g in the PBT_xGal_x series decreased slightly with respect to PBT, in accordance with the T_g shown by the $PBGal_x$ homopolyester which is only 18 °C. The variation of T_g with the content of sugar units along the two series is plotted in Figure 5.7, showing vividly that the effect of galactitol on T_g is of opposite sign and stronger than that exerted by galactarate units. In fact, a replacement of 50% of diol units in PBT increased

the T_g in 39 °C, whereas the replacement of the diacid units in the same degree caused a decrease of T_g in 9 °C. The opposite effect on T_g observed for galactitol and galactarate units is reasonable taking into account the relative stiffness of the units implied in the replacement, *i.e.*, the flexibility of the bicyclic sugar units is in between the butylene and phenylene units to which they replace.

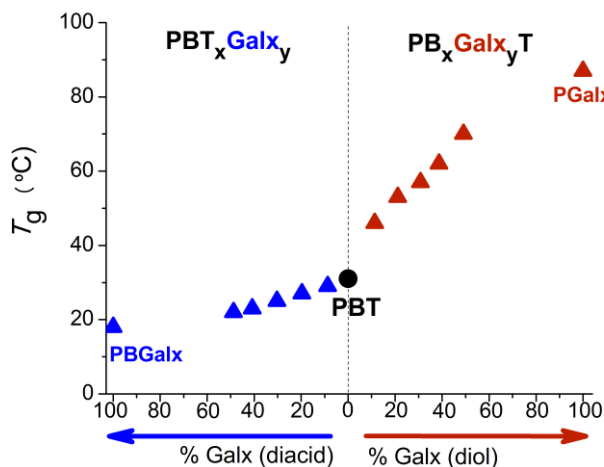


Figure 5.7. Glass-transition temperature vs. composition plot for PB_xGal_xT and PBT_xGal_x copolyesters.

DSC traces of PB_xGal_xT and PBT_xGal_x copolyesters, as well as PBT, PGalxT and PBGalx homopolyesters, registered at first heating are depicted in Figure 5.8. PBT and PBGalx homopolyesters are semicrystalline, with melting temperatures of 223 °C and 122 °C, respectively, whereas PGalxT homopolyester appears to be amorphous. Endothermic peaks characteristic of melting and indicative of the presence of a crystalline phase were observed for all PB_xGal_xT and PBT_xGal_x copolyesters. Comparison of melting temperatures and enthalpies of both PB_xGal_xT and PBT_xGal_x copolyesters with those of PBT homopolyester leads to the conclusion that the insertion of either galactitol or galactarate units gives place to a significant decrease in both T_m and ΔH_m . As it happened with T_g , the effect of copolymerization on crystallinity appears to be stronger when the diol units are the object of replacement.

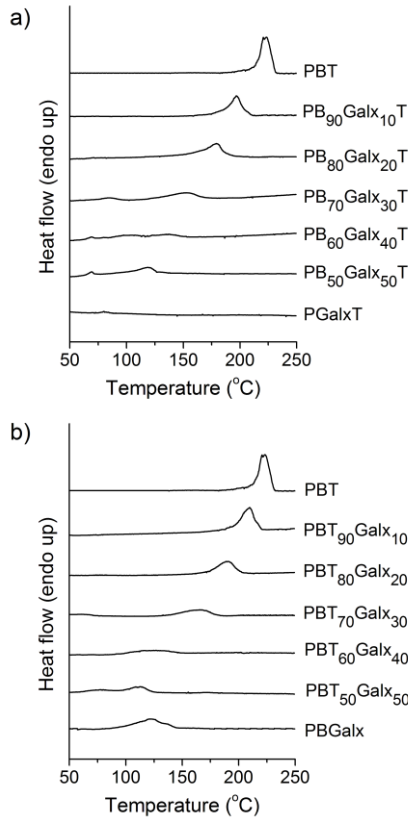


Figure 5.8. DSC melting traces of PB_xGal_xT (a) and PBT_xGal_x (b) coming directly from synthesis.

5.2.3.3. Isothermal crystallization

PBT has the property of crystallizing very fast from the melt. As far as PB_xGal_xT copolyesters are concerned, only $PB_{90}Gal_{10}T$ and $PB_{80}Gal_{20}T$ were able to crystallize upon cooling from the melt; on the contrary, all PBT_xGal_x copolyesters crystallized from the melt, whereas $PBGal_x$ homopolyester distinguished in undergoing cold crystallization. After crystallization from the melt, copolyesters recovered about 70-85% of their initial crystallinity and displayed almost the same melting temperatures.

To evaluate quantitatively the effect of galactitol and galactarate units on crystallizability, the isothermal crystallization of $PB_{90}Gal_{10}T$, $PB_{80}Gal_{20}T$, $PBT_{90}Gal_{10}$ and $PBT_{80}Gal_{20}$ copolyesters and PBT homopolyester was comparatively studied in the

150-210 °C interval. Unfortunately, not all the polymers could be compared at the same isothermal crystallization temperature due to large differences in their crystallization rates. However, crystallization temperatures were selected as close as possible so that meaningful conclusions could be drawn. The Hoffman-Weeks plot of T_m vs. T_c showed a good correlation (Figure 5.9) and provides the equilibrium melting temperatures of copolyesters, which display the same trend with composition as that observed for samples coming directly from synthesis.

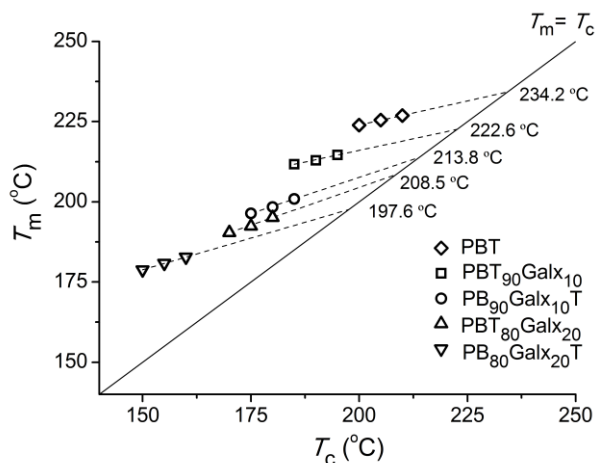


Figure 5.9. Hoffman-Weeks plot for isothermally crystallized copolyesters.

The evolution of the relative crystallinity, X_c , with crystallization time and the corresponding Avrami data plots $\log[-\ln(1-X_c)]$ vs. $\log(t-t_0)$ for some illustrative crystallization experiments are depicted in Figure 5.10. Kinetics data afforded by this study, which include the observed onset and half-crystallization times, as well as the corresponding Avrami parameters, are gathered in Table 5.4. An increasing delay in onset crystallization, as well as in the crystallization rate, with temperature was observed for all the studied polymers. Avrami exponents also increased with temperature and were not far from 2.5, which is consistent with a complex axialitic-spherulitic crystallization initiated by heterogeneous nucleation. In fact, parallel observation of the crystallization process under the polarizing optical microscope visually confirmed the instantaneous appearance of deficiently formed spherulites with some axialite reminiscences (Figure 5.11). The spherulitic growth rate measured by optical microscopy on thin films at cooling

from the melt for some illustrative experiments is shown in Figure 5.12. A linear radial growing is displayed by PBT and PBT₉₀Galx₁₀ and PBT₈₀Galx₂₀ with a slope decreasing with increasing amounts of Galx units in the copolyester. Although crystallizations had to be performed at different temperatures, the results are in full accordance with those obtained from isothermal crystallization in the bulk determined by DSC ascertaining that the depressing effect of copolymerization on crystallizability is operating at the primary crystallization regime.

Table 5.4. Isothermal crystallization data of PB_xGalx_yT and PBT_xGalx_y copolyesters.

Copolyester	T_c (°C)	t_0 (min)	$t_{1/2}$ (min)	n	$-\log k$	T_m (°C)
PBT	200	0.19	0.82	2.14	-0.25	223.9
	205	0.51	2.68	2.45	1.02	225.5
	210	2.33	12.83	2.56	2.78	226.9
PB ₉₀ Galx ₁₀ T	175	0.31	2.51	2.24	0.92	196.4
	180	0.58	4.80	2.57	1.74	198.4
	185	2.35	13.18	2.64	2.84	200.9
PBT ₉₀ Galx ₁₀	185	0.14	0.76	2.23	-0.31	211.7
	190	0.17	2.25	2.29	0.88	212.9
	195	0.67	6.83	2.53	2.08	214.6
PB ₈₀ Galx ₂₀ T	150	0.69	5.82	2.28	1.77	178.8
	155	1.21	9.17	2.33	2.24	180.9
	160	2.00	15.08	2.39	2.73	182.8
PBT ₈₀ Galx ₂₀	170	0.14	1.45	2.02	0.39	190.4
	175	0.35	2.89	2.11	0.99	192.4
	180	0.84	7.01	2.25	1.89	195.1

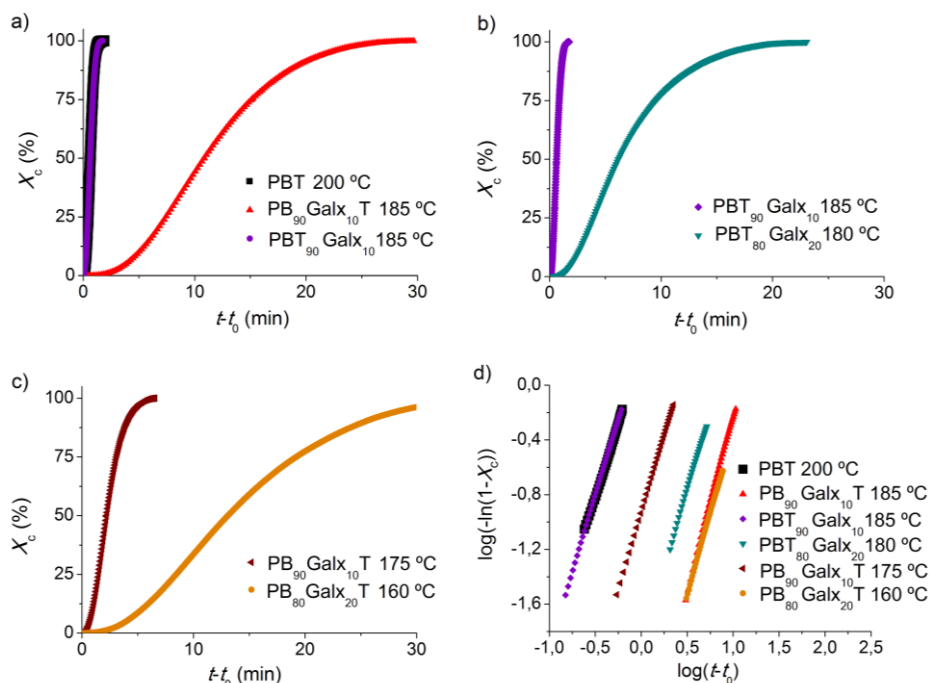


Figure 5.10. Isothermal crystallization of PBT, PB₉₀Gal_{x10}T, PBT₉₀Gal_{x10}, PB₈₀Gal_{x20}T, PBT₈₀Gal_{x20} at the indicated temperatures. Relative crystallinity vs. time plot (a,b,c) and log-log plot (d).

It was observed that the presence of galactitol or galactarate units in minor amounts depressed the crystallizability in PBT. Furthermore, comparison of crystallization data for PB₉₀Gal_{x10}T and PBT₉₀Gal_{x10} at 185 °C evidenced that crystallizability is more affected by the presence of galactitol than galactarate units. In fact, copolyesters containing more than 20% galactitol units were unable to crystallize upon cooling from the melt, whereas all the galactarate copolyesters studied in this work were capable of crystallizing from the melt. Comparison of crystallization data for PBT₉₀Gal_{x10} and PBT₈₀Gal_{x20} copolyesters revealed that crystallization is more repressed for higher contents in galactarate units. The valuable conclusion that can be drawn from this study is that PB_xGal_yT and PBT_xGal_y copolyesters containing minor amounts of either galactitol or galactarate units continue displaying the ability of crystallizing from the melt as their parent homopolymer PBT although at lower crystallization rates. Furthermore, it was learnt that the depressing effect on crystallizability is stronger when the diol is the replaced unit, which is in full agreement with the replacing effects on ΔH_m observed in the non-isothermal crystallization experiments described in the previous section.

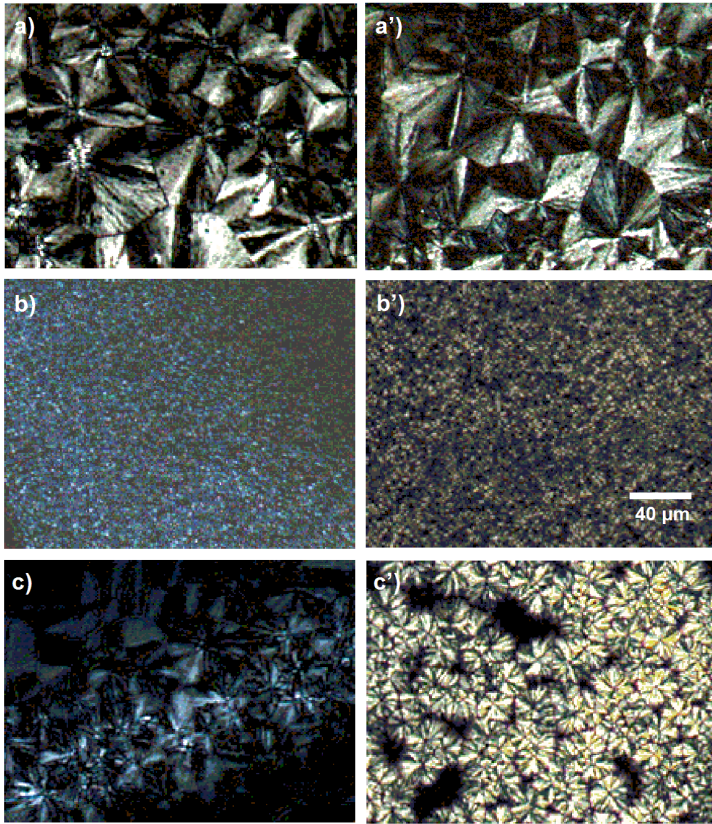


Figure 5.11. Polarized optical micrographs of samples isothermally crystallized at the indicated temperatures: (a) PBT at 210 °C; (a') PBT at 205 °C; (b) PB₉₀Galx₁₀T at 185 °C; (b') PB₈₀Galx₂₀T at 160 °C; (c) PBT₉₀Galx₁₀ at 195 °C; (c') PBT₈₀Galx₂₀ at 180 °C. The scale bar corresponds to 40 μm.

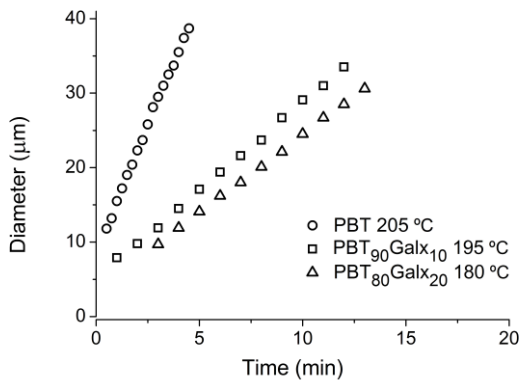


Figure 5.12. Spherulitic diameter vs. time plot for isothermally crystallized PBT, PBT₉₀Galx₁₀ and PBT₈₀Galx₂₀ at the indicated temperatures.

5.2.3.4. Crystal structure and stress-strain behavior

The data collected by X-ray diffraction analysis gave support to the DSC data corroborating that all PB_xGal_yT and PBT_xGal_y copolyesters, as well as PBT and PBGalx homopolyesters, are semicrystalline materials. The powder profiles obtained for PB_xGal_yT and PBT_xGal_y copolyesters are compared with that of PBT in Figure 5.13, and Bragg spacings present in such patterns are listed in Table 5.5.

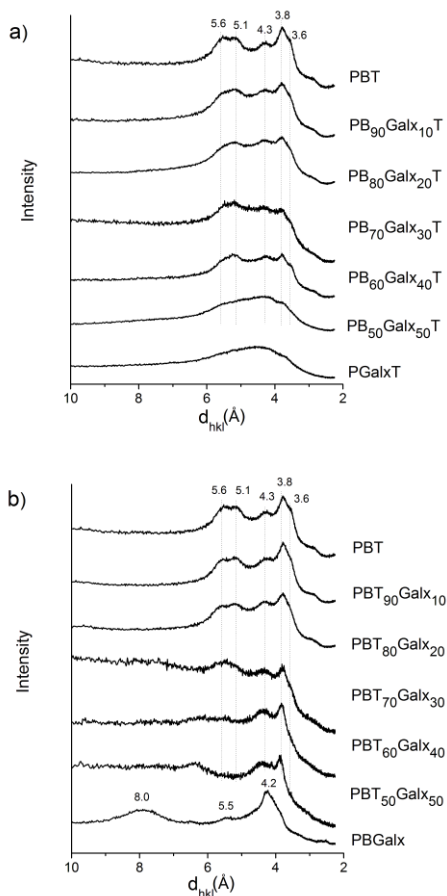


Figure 5.13. Powder WAXD profiles of PB_xGal_xT (a) and PBT_xGal_x (b) copolyesters.

Essentially the same pattern regarding both spacing and intensities is shared by PBT and all PB_xGal_yT and PBT_xGal_y copolyesters, revealing that the triclinic crystal structure of PBT (Hall, 1984) is retained in the copolyesters. Nevertheless, crystallinity decays with the content in sugar units, and it seems again to be more affected by the

introduction of galactitol than galactarate units. Conversely, the homopolyester PBGalx displayed a clearly dissimilar diffraction pattern, indicating that a different crystal structure must be adopted in this case. In agreement with DSC results, no discrete scattering characteristic of crystalline material was observed for the homopolyester PGalxT.

Table 5.5. Powder X-ray diffraction data and mechanical properties of PB_xGal_yT and PBT_xGal_y copolyesters.

Copolyester	X-ray diffraction data						Mechanical Properties		
	d^a (Å)						X_c^b	Elastic modulus (MPa)	Tensile strength (MPa)
PBT	5.6 s	5.1 s	4.3 s	3.8 s	3.6 m	0.48	841±15	42±5	14±3
PB ₉₀ Galx ₁₀ T	5.6 s	5.1 s	4.3 s	3.8 s	3.6 m	0.41	846±18	42±4	11±2
PB ₈₀ Galx ₂₀ T	5.6 m	5.1 m	4.3 m	3.8 s	3.6 w	0.34	850±23	44±6	10±3
PB ₇₀ Galx ₃₀ T	5.6 m	5.1 m	4.3 m	3.8 m	3.6 w	0.28	861±19	45±4	8±2
PB ₆₀ Galx ₄₀ T	5.6 m	5.1 m	4.3 m	3.8 m	3.6 w	0.17	865±25	47±5	7±1
PB ₅₀ Galx ₅₀ T	5.6 w	5.1 w	4.3 w	3.8 w	3.6 w	0.10	869±24	48±6	5±1
PBT ₉₀ Galx ₁₀	5.6 s	5.1 s	4.3 s	3.8 s	3.6 m	0.43	735±17	35±3	19±3
PBT ₈₀ Galx ₂₀	5.6 s	5.1 s	4.3 s	3.8 s	3.6 m	0.37	653±15	31±4	23±4
PBT ₇₀ Galx ₃₀	5.6 m	5.1 m	4.3 m	3.8 s	3.6 w	0.30	509±11	29±3	26±3
PBT ₆₀ Galx ₄₀	5.6 w	5.1 w	4.3 m	3.8 s	3.6 w	0.21	445±9	25±4	28±4
PBT ₅₀ Galx ₅₀			4.3 m	3.8 s	3.6 w	0.15	397±8	22±2	34±5
PGalxT						0	953±22	53±5	3±1
PBGalx	8.0 m	5.5 w	4.2 s			0.38	162±5	15±2	45±5

^a Bragg spacings measured in powder diffraction patterns for samples coming directly from synthesis. Intensities visually estimated as follows: m, medium; s, strong; w, weak. ^b Crystallinity index calculated as the quotient between crystalline area and total area. Crystalline and amorphous areas in the X-ray diffraction pattern were quantified using PeakFit v4.12 software.

A preliminary evaluation of the mechanical properties of PB_xGal_yT and PBT_xGal_y copolyesters has been carried out. For comparison purposes, mechanical properties of PBT, PGalxT and PBGalx homopolyesters were also tested. The stress-

strain curves resulting from tensile essays are depicted in Figure 5.14, and the mechanical parameters measured in these tests are compared in Table 5.5. PB_xGal_xT copolyesters present a nearly steady trend consisting of a continuous increase in both elastic modulus and tensile strength and a decrease in extensibility with the content in galactitol units, in accordance with the parameters obtained for $PGalT$ homopolyester. On the other hand, $PBGalx$ homopolyester displayed lower elastic modulus and tensile strength than PBT , and accordingly PBT_xGal_x copolyesters presented a steadily reduction in these parameters as the terephthalate units were replaced by galactarate units with values spanning between those of PBT and $PBGalx$ homopolyesters. It is worthy to note that variation of mechanical parameters for both PB_xGal_xT and PBT_xGal_x copolyesters was in accordance with what should be expected from the trend observed for glass-transition temperatures.

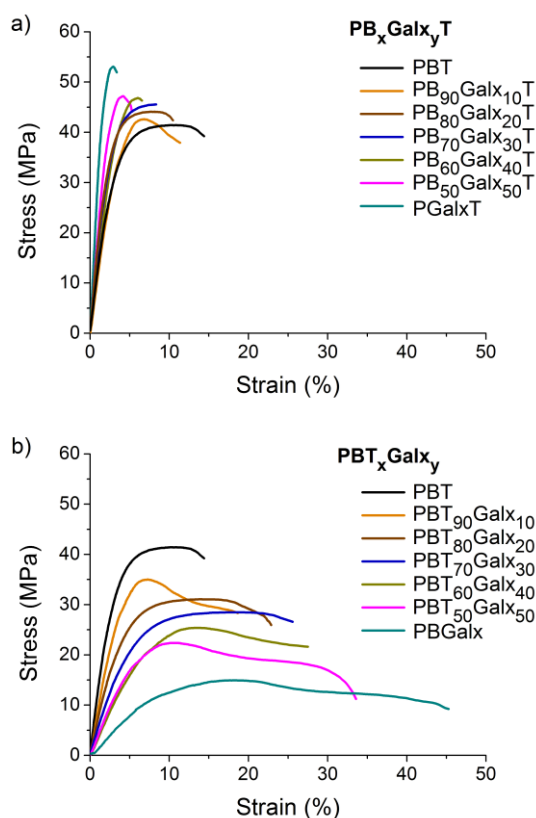


Figure 5.14. Stress-strain curves for PB_xGal_xT (a) and PBT_xGal_x (b) copolyesters.

5.2.4. Conclusions

Two sets of poly(butylene terephthalate) copolyesters containing up to 50 mol-% of bicyclic acetalized galactitol and galactarate units, respectively, have been successfully synthesized by polycondensation in the melt. The resulting copolyesters have compositions very close to those used in the feed and all they have a random microstructure. By taking special care of polycondensation conditions in order to prevent thermal degradation and volatilization of the diacetalized comonomers, copolyesters with pretty high molecular weight could be obtained in good yields. These copolyesters displayed enhanced solubility compared to PBT being remarkable in this regard their solubility in chloroform. The effect of the presence of the carbohydrate-based comonomer on thermal and mechanical properties of the polyesters was opposite according to which unit, the diol or the diacid, was replaced. The incorporation of acetalized galactitol units increased the thermal stability, the glass-transition temperature and the mechanical moduli. On the contrary, these parameters were diminished when the terephthalate units were the replaced units. All the copolyesters were semicrystalline and they tend to adopt the crystal structure of PBT. However, the crystallinity and crystallization rate of the copolyesters decreased with increasing content in bicyclic units irrespective of which unit was replaced. All the galactarate containing copolyesters were able to crystallize from the melt, a property only shared by copolyesters with contents in galactitol up to 20%. It is noteworthy the general observation that the effect exerted by copolymerization on properties was significantly stronger when the diol was the replacing unit.

5.2.5. References

- Alla, A.; Hakkou, K.; Zamora, F.; Martínez de Ilarduya, A.; Galbis, J.A.; Muñoz-Guerra, S. *Macromolecules* **2006**, *39*, 1410-1416.
- Burden, I.J.; Stoddart, J.F. *J. Chem. Soc. Perk. T. 1* **1975**, 675-682.
- Butler, K.; Lawrance, R.L.; Stacey, M. *J. Chem. Soc.* **1958**, 740-743.
- Fenouillot, F.; Rousseau, A.; Colomines, G.; Saint-Loup, R.; Pascault, J.-P. *Prog. Polym. Sci.* **2010**, *35*, 578-622.
- Fradet, A.; Tessier, M. *Polyesters*. In: Rogers, M.E.; Long, T.E.; Eds. *Synthetic Methods in Step-Growth Polymers*; John Wiley & Sons: Hoboken, **2003**, pp. 17-134.

Gallucci, R.R.; Patel, B.R. *Poly(butylene terephthalate)*. In: Scheirs, J.; Long, T.E.; Eds. *Modern Polyesters, Chemistry and Technology of Polyesters and Copolyesters*; John Wiley & Sons: Chichester, **2004**, pp. 293-321.

Gandini, A.; Coelho, D.; Gomes, M.; Reis, B.; Silvestre, A. *J. Mater. Chem.* **2009**, *19*, 8656-8664.

Gomes, M.; Gandini, A.; Silvestre, A.J.D.; Reis, B. *J. Polym. Sci., Polym. Chem.* **2011**, *49*, 3759-3768.

Hall, I.H. *The Determination of the Structures of Aromatic Polyesters from their Wide-angle X-Ray Diffraction Patterns*. In: Hall, I.H.; Ed. *Structure of Crystalline Polymers*; Elsevier Applied Science: UK, **1984**, pp. 39-78.

Iribarren, J. I.; Martínez de Ilarduya, A.; Alemán, C.; Oraison, J. M.; Rodríguez-Galán, A.; Muñoz-Guerra, S. *Polymer* **2000**, *41*, 4869-4879.

Kiely, D.E.; Chen, L.; Lin, T-H. *J. Am. Chem. Soc.* **1994**, *116*, 571-578.

Kiely, D.E.; Chen, L.; Lin, T-H. *J. Polym. Sci., Polym. Chem.* **2000**, *38*, 594-603.

Kijchavengkul, T.; Auras, R.; Rubino, M.; Selke, S.; Ngouajio, M.; Fernandez, R.T. *Polym. Degrad. Stabil.* **2010**, *95*, 2641-2647.

Kimura, H.; Yoshinari, T.; Takeishi, M. *Polym. J.* **1999**, *31*, 388-392.

Kricheldorf, H. R. *J. Macromol. Sci.* **1997**, *C37*, 599-631.

Kricheldorf, H.R.; Behnken, G.; Sell, M. *J. Macromol. Sci. Part A Pure Appl. Chem.* **2007**, *44*, 679-684.

Lavilla, C.; Alla, A.; Martínez de Ilarduya, A.; Benito, E.; García-Martín, M.G.; Galbis, J.A.; Muñoz-Guerra, S. *Biomacromolecules* **2011**, *12*, 2642-2652. **-Subchapter 3.2-**

Lavilla, C.; Alla, A.; Martínez de Ilarduya, A.; Benito, E.; García-Martín, M.G.; Galbis, J.A.; Muñoz-Guerra, S. *J. Polym. Sci., Polym. Chem.* **2012**, *50*, 1591-1604. **-Subchapter 3.3-**

Okada, M. *Prog. Polym. Sci.* **2002**, *27*, 87-133.

Marten, E.; Müller, R.J. Deckwer; W.-D. *Polym. Degrad. Stabil.* **2005**, *88*, 371-381.

Metzke, M.; Guan, Z. *Biomacromolecules* **2008**, *9*, 208-215.

Randal, J.C. *Polymer Sequence Determination*; Academic Press: New York, **1977**; pp 41-69.

Sablomg, R.; Duchateau, R.; Koning, C.E.; de Wit, G.; van Es, D.; Koelewijn, R.; van Haveren, J. *Biomacromolecules* **2008**, *9*, 3090-3097.

Tripathy, A.R.; MacKnight, W.J.; Kukureka, S.N. *Macromolecules* **2004**, *37*, 6793-6800.

Williams, C.K. *Chem. Soc. Rev.* **2007**, *36*, 1573-1580.

Chapter 5

Zamora, F.; Hakkou, K.; Alla, A.; Marín-Bernabé, R.; de Paz, M. V.; Martínez de Ilarduya, A.; Muñoz-Guerra, S.; Galbis, J.A. *J. Polym. Sci., Polym. Chem.* **2008**, *46*, 5167-5179.

Zamora, F.; Hakkou, K.; Alla, A.; Rivas, M.; Martínez de Ilarduya, A.; Muñoz-Guerra, S.; Galbis, J.A. *J. Polym. Sci., Polym. Chem.* **2009**, *47*, 1168-1177.

5.3. Biodegradation and hydrolytic degradation of poly(butylene terephthalate) copolyesters containing cyclic sugar units

Summary: *The hydrolytic and enzymatic degradation of PBT copolyesters obtained by replacing partially the diol or the diacidic monomers by bicyclic acetalized carbohydrate-based monomers from galactaric acid was studied. Changes taking place in sample weight, molecular weight, chemical constitution, crystallinity and morphology of the polyesters were evaluated. The partial replacement of 1,4-butanediol by 2,3:4,5-di-O-methylene-galactitol resulted in copolyesters with enhanced hydrodegradability compared to PBT. On the other hand, copolyesters obtained by partial replacement of dimethyl terephthalate by dimethyl 2,3:4,5-di-O-methylene-galactarate were biodegradable in the presence of lipases, and were hydrodegraded at a rate that increased with the content in galactarate units.*

Publication derived from this work:

Lavilla, C.; Muñoz-Guerra, S. *Polym. Degrad. Stabil.* **2012**, *97*, 1762-1771.

5.3.1. Introduction

Poly(butylene terephthalate) (PBT) is a semicrystalline aromatic polyester widely used in a variety of engineering applications, which has a melting temperature of around 225 °C and exhibits the property of crystallizing very fast from the melt. This exceptional thermal behavior and its excellent mechanical properties make PBT the material of choice for most injection molding applications (Gallucci and Patel, 2004). Nevertheless, important shortcomings of this polyester are its non-renewable origin and its extremely high resistance to degradation by environmental and biological agents. In this regard, great attention has been given to incorporate bio-based units into PBT (Tripathy *et al.*, 2004; Nakajima-Kambe *et al.*, 2009; Rychter *et al.*, 2010; Kijchavengkul *et al.*, 2010a and 2010b). The use of renewable sources as building-blocks for polymers not only contributes to reduce their dependence on petrochemicals but also increases the added-value of agriculture products and wastes. Furthermore, the incorporation of bio-based units in the polymer chain shall confer it higher hydrolytic degradability and biodegradability adding new application possibilities and favouring its chemical recycling and composting.

The insertion of carbohydrate moieties in polycondensates as polyamides (Kiely *et al.*, 2000; Zaliz and Varela, 2005), polycarbonates (Yokoe *et al.*, 2005; Galbis and García-Martín, 2008) and polyesters (Kulshrestha *et al.*, 2005; Gomes *et al.*, 2011) has been extensively explored in these last years. The use of carbohydrates as polymer building blocks is motivated by several reasons: they are easily available and even coming from agricultural wastes, they are found in a very rich variety of structures with great stereochemical diversity, and they constitute a truly renewable source. Moreover, carbohydrate-based polycondensates may typically display enhanced hydrophilicity, lower toxicity and higher susceptibility to degradation than those coming from petrochemical feedstocks. Nonetheless, hydrolytic and enzymatic degradation of carbohydrate-based PBT has been scarcely explored up to now. Alla *et al.* reported on the synthesis and hydrolytic degradation of PBT copolyesters containing up to 50% of trimethoxy pentitols derived from naturally occurring L-arabinose and D-xylose (Alla *et al.*, 2006). It was shown there that L-arabinitol- and D-xylitol-based PBT copolyesters were much more sensitive to hydrolysis than was PBT, whereas no significant differences in degradability were observed between the two copolyester series.

Among carbohydrate-based monomers, those with a bicyclic structure stand out for providing polycondensates with improved properties, especially those related to

polymer chain stiffness. 1,4:3,6-Dianhydro-D-glucitol, known as isosorbide, which is prepared by dehydration of D-glucose coming from cereal starch (Fenouillot *et al.*, 2010), is the only bicyclic carbohydrate-based monomer industrially available today. Another type of bicyclic carbohydrate-based monomers recently receiving attention consists of internal diacetal derivatives. Recent studies on aliphatic polyesters made from bicyclic acetalized galactaric acid have revealed the beneficial effect of these carbohydrate-based units regarding biodegradability (Lavilla *et al.*, 2011 -Subchapter 3.2-).

In this paper we study the hydrolytic and enzymatic degradation of PBT copolyesters that are obtained by replacing partially either the diol or the diacidic monomers by bicyclic acetalized galactose-based monomers, specifically 2,3:4,5-di-O-methylene-galactitol to replace 1,4-butanediol and dimethyl 2,3:4,5-di-O-methylene-galactarate to replace dimethyl terephthalate.

5.3.2. Experimental section

5.3.2.1. Materials

Polyesters were synthesized following the procedure recently reported by Lavilla *et al.* (Lavilla *et al.*, 2012 -Subchapter 5.2-). The sugar derived monomers used in this synthesis were 2,3:4,5-di-O-methylene-galactitol and dimethyl 2,3:4,5-di-O-methylene-galactarate. The latter was obtained by treating commercial galactaric acid with paraformaldehyde, concentrated sulphuric acid and methanol, following the procedure reported by Stacey *et al.* (Butler *et al.*, 1958). The treatment of this compound with a suspension of lithium aluminium hydride in dry tetrahydrofuran, following the procedure reported by Burden *et al.* (Burden and Stoddart, 1975) led to 2,3:4,5-di-O-methylene-galactitol. Commercial 1,4-butanediol and dimethyl terephthalate were used as respective comonomers. Polyesters and copolyesters were synthesized by a two-stage melt polycondensation process at temperatures between 160 and 240 °C and using dibutyl tin oxide (DBTO) as catalyst. The enzyme used in biodegradation experiments, lipase from porcine pancreas (activity 15-35 U·mg⁻¹, pH 8.0, 37 °C) was purchased from Sigma-Aldrich. One unit (U) was defined as that amount of enzyme which catalyzed the release of fatty acid from triglycerides at the rate of 1 μmol·min⁻¹. Solvents used for purification and characterization were purchased from Panreac and they all were of either technical or high-purity grade.

5.3.2.2. General methods

^1H and ^{13}C NMR spectra were recorded on a Bruker AMX-300 spectrometer at 25.0 °C operating at 300.1 and 75.5 MHz, respectively. Polyesters were dissolved in deuterated chloroform, in a mixture of deuterated chloroform and trifluoroacetic acid (9:1) or in deuterated water, and spectra were internally referenced to tetramethylsilane (TMS) or to 3-(trimethylsilyl)-propanesulfonic acid sodium salt. About 10 and 50 mg of sample dissolved in 1 mL of solvent were used for ^1H and ^{13}C NMR, respectively. Sixty-four scans were acquired for ^1H and 1,000-10,000 for ^{13}C with 32 and 64-K data points as well as relaxation delays of 1 and 2 s, respectively. Intrinsic viscosities of polymers dissolved in dichloroacetic acid were measured in an Ubbelohde viscosimeter thermostated at 25.0 \pm 0.1 °C. Gel permeation chromatograms were acquired at 35.0 °C with a Waters equipment provided with a refraction-index detector. The samples were chromatographed with 0.05 M sodium trifluoroacetate-hexafluoroisopropanol (NaTFA-HFIP) using a polystyrene-divinylbenzene packed linear column with a flow rate of 0.5 mL \cdot min $^{-1}$. Chromatograms were calibrated against poly(methyl methacrylate) (PMMA) monodisperse standards. The thermal behavior of polyesters was examined by DSC using a Perkin Elmer DSC Pyris 1. DSC data were obtained from 3 to 5 mg samples at heating/cooling rates of 10 °C \cdot min $^{-1}$ under a nitrogen flow of 20 mL \cdot min $^{-1}$. Indium and zinc were used as standards for temperature and enthalpy calibration. The glass-transition temperatures were determined at a heating rate of 20 °C \cdot min $^{-1}$ from rapidly melt-quenched polymer samples. Scanning electron microscopy (SEM) images were taken with a field-emission JEOL JSM-7001F instrument (JEOL, Japan) from Pt/Pd coated samples.

5.3.2.3. Hydrolytic and enzymatic degradation procedures

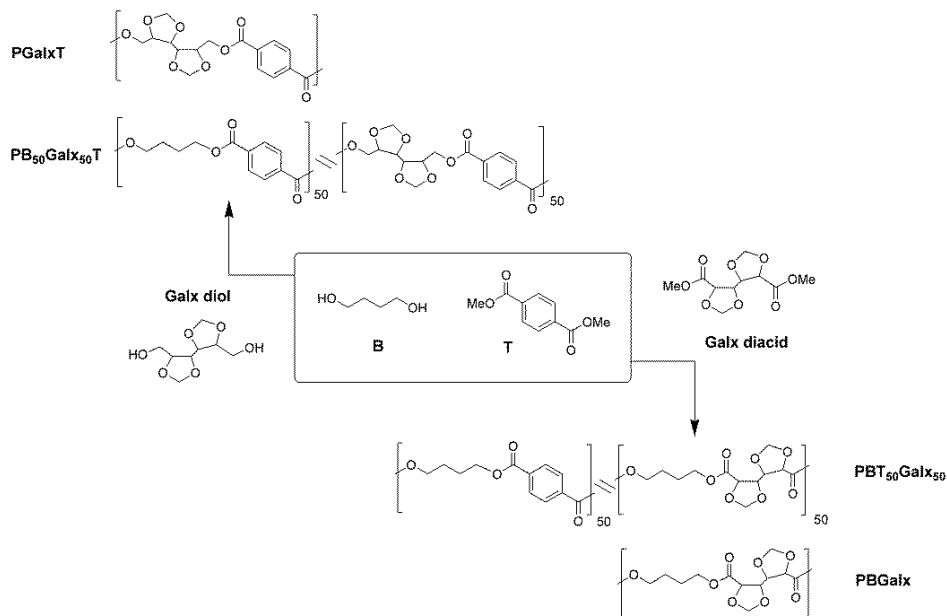
Films for polyester hydrolytic and enzymatic degradation studies were prepared with a thickness of \sim 200 μm by casting from solution (100 g \cdot L $^{-1}$) in either chloroform or a mixture of chloroform and hexafluoroisopropanol (5:1). The films were cut into 10-mm diameter, 20 to 30-mg weight disks and dried in vacuum to constant weight. For hydrolytic degradation, samples were immersed in vials containing 10 mL of citric acid buffer (pH 2.0) at 80 °C. After incubation for the scheduled period of time, the samples were rinsed thoroughly with distilled water and dried to constant weight. The enzymatic degradation was carried out at 37 °C in vials containing 10 mL of the enzymatic medium, consisting of a pH 7.4 buffered sodium phosphate solution containing lipase from porcine pancreas (10 mg). The buffered enzyme solution was replaced every 72 h to maintain the enzyme

activity. At the end of the scheduled incubation periods, the disks were withdrawn from the incubation medium, washed thoroughly with distilled water, dried to constant weight and analyzed by GPC chromatography, NMR spectroscopy and SEM microscopy.

For hydrolytic degradation studies of monomers, dimethyl 2,3:4,5-di-O-methylene-galactarate samples (100 mg) were immersed in vials containing 15 mL of citric acid buffer (pH 2.0), sodium phosphate buffer (pH 7.4) and sodium carbonate buffer (pH 10.5), respectively, and incubated at 23 °C for 12 weeks. Initially, the monomer was not soluble in the aqueous media in none of the studied pHs but solubilized completely after incubation. The residue left after evaporating water was analyzed by NMR spectroscopy.

5.3.3. Results and discussion

The sugar-based copolyesters and homopolyesters studied in this work were synthesized and characterized in detail as described in an earlier paper published by our group (Lavilla *et al.*, 2012 -Subchapter 5.2-). They are represented in Scheme 5.2, and the main features in connection with the degradation study carried out in this work are listed in Table 5.6.



Scheme 5.2. Chemical structure of PBT, PB₅₀Galx₅₀T, PGalxT, PBT₅₀Galx₅₀ and PBGalx polyesters.

Table 5.6. Molar composition, microstructure, molecular weight and thermal properties of polyesters.

	Molar composition ^a				Microstructure	Molecular weight				Thermal properties		
	Diol		Diacid			Randomness index ^b	$[\eta]^c$	M_n^d	M_w^d	\mathcal{D}^d	T_g^e (°C)	T_m^f (°C)
	X_B	X_{Galx}	X_T	X_{Galx}								
PBT	100	0	100	0	-	0.93	17,100	41,300	2.4	31	223	54
PB ₅₀ Galx ₅₀ T	51	49	100	0	1.01	0.69	15,800	37,600	2.4	70	106	9
PGalxT	0	100	100	0	-	0.50	12,400	30,500	2.5	87	174	17
PBT ₅₀ Galx ₅₀	100	0	51	49	1.01	0.75	15,800	38,800	2.5	22	122	24
PBGalx	100	0	0	100	-	0.52	13,100	30,800	2.4	18	142	28

^a Molar composition determined by ¹H NMR. ^b Randomness index of copolyesters statistically calculated on the basis of the ¹³C NMR analysis. ^c Intrinsic viscosity in dL·g⁻¹ measured in dichloroacetic acid at 25 °C.

^d Number and weight-average molecular weights in g·mol⁻¹ and dispersities measured by GPC in HFIP against PMMA standards. ^e Glass-transition temperature taken as the inflection point of the heating DSC traces of melt-quenched samples recorded at 20 °C·min⁻¹. ^f Melting temperatures (T_m) and enthalpies (ΔH_m) of samples from films measured by DSC at heating/cooling rates of 10 °C·min⁻¹.

The microstructure of PBT copolyesters containing either 50% of 2,3:4,5-di-O-methylene galactitol (PB₅₀Galx₅₀T) or 50% of dimethyl 2,3:4,5-di-O-methylene-galactarate (PBT₅₀Galx₅₀) was almost fully statistical, with randomness quite near unity. Both copolyesters, as well as their respective parent sugar-based homopolyesters PGalxT (100% of galactitol units) and PBGalx (100% of galactarate units) and PBT were semicrystalline, with melting enthalpies decreasing when introducing sugar-based units. Glass-transition temperatures steadily increased as butanediol was replaced by galactitol units going from 31 °C for PBT up to 70 °C for the PB₅₀Galx₅₀T copolyester, whereas a T_g value of 87 °C was observed for the PGalxT homopolyester. Conversely, the glass-transition temperatures of the galactarate-based polyesters and copolyesters were not far from that of PBT with values located within 18-31 °C range.

5.3.3.1. PBT copolyesters containing galactitol units

To evaluate the effects that the incorporation of 2,3:4,5-di-O-methylene galactitol unit exerts on degradation of PBT, a comparative study of PBT, PB₅₀Galx₅₀T and PGalxT was carried out.

5.3.3.1.1. Hydrolytic degradation and biodegradation at pH 7.4 at 37 °C

The variation in sample weight, M_w and M_n for PBT, PB₅₀Galx₅₀T and PGalxT upon incubation in aqueous pH 7.4 buffer at 37 °C, in the presence and in the absence of porcine pancreas lipase, is depicted in Figure 5.15. According to the invariance observed for these parameters it was concluded that none of them underwent significant degradation when incubated under physiological conditions. Furthermore, crystallinity of the incubated samples was nearly the same than that of the initial ones (Figure 5.16), and SEM micrographs revealed that no changes in morphology had taken place upon incubation (Figure 5.17 and Annex E).

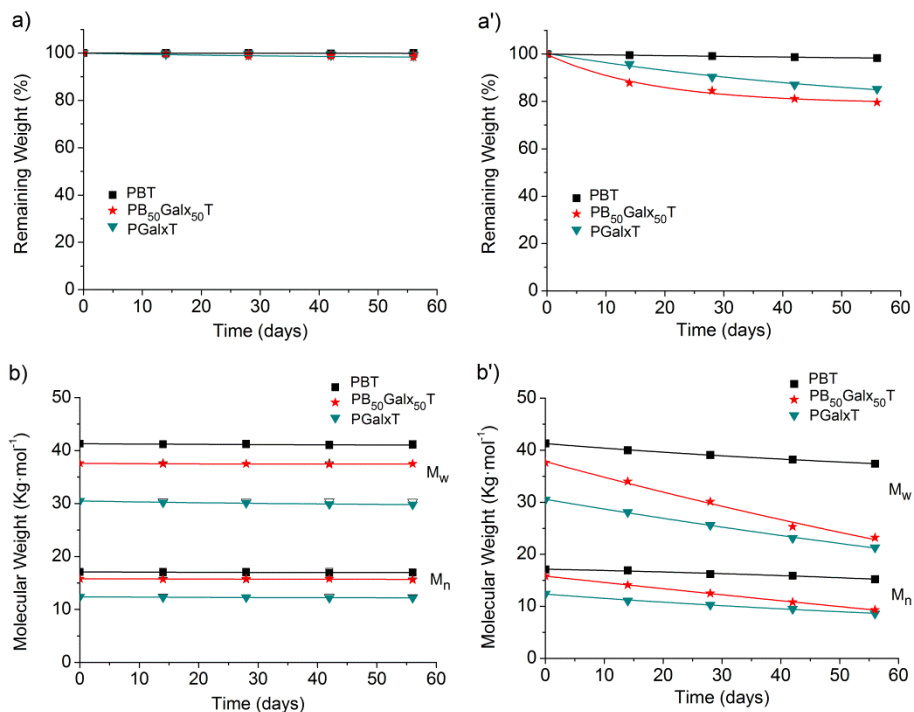


Figure 5.15. Degradation of PBT, PB₅₀Galx₅₀T and PGalxT. Remaining weight (a) and molecular weight (b) vs. degradation time with (solid symbols) and without (empty symbols) porcine pancreas lipase at pH 7.4 at 37 °C. Remaining weight (a') and molecular weight (b') vs. degradation time at pH 2.0 at 80 °C.

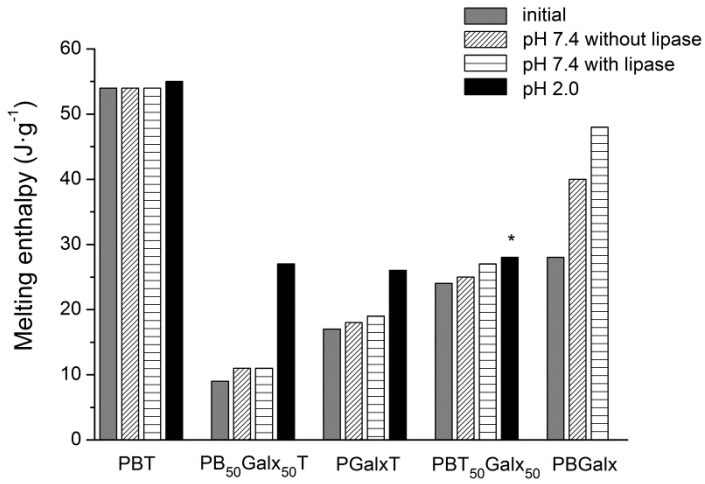


Figure 5.16. Melting enthalpies of polyesters after 56 days of incubation and initial samples. * After 14 days of incubation.

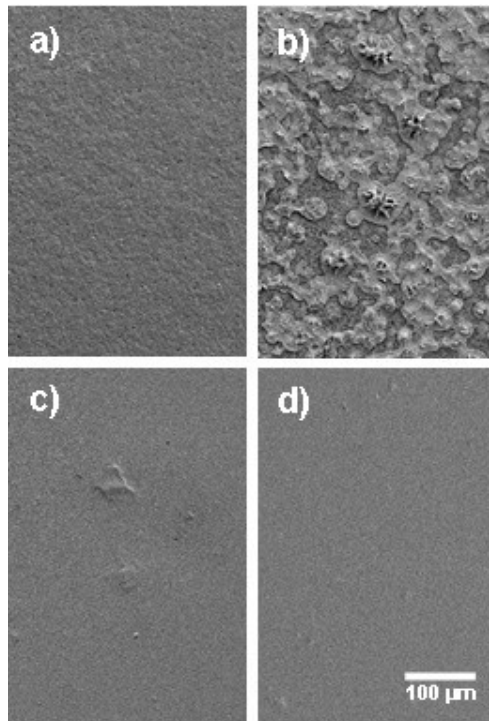


Figure 5.17. SEM micrographs of PB₅₀Gal₅₀T. Initial sample (a). After incubation at pH=2.0 at 80 °C for 56 days (b). After incubation at pH=7.4 at 37 °C for 56 days with (c) and without (d) lipase from porcine pancreas.

5.3.3.1.2. Hydrolytic degradation at pH 2.0 at 80 °C

PBT, PB₅₀Galx₅₀T and PGalxT were subjected in parallel to hydrolytic degradation experiments at pH 2.0 at 80 °C. The evolution of sample weight, M_w and M_n is depicted in Figure 5.15. The weight losses undergone by PB₅₀Galx₅₀T and PGalxT were about 18% and 12%, respectively, after 8 weeks of incubation; in accordance to changes taking place in sample weight, a decrease in M_w and an increase in the melting enthalpy were also observed. On the contrary, variations in sample weight, molecular weight, and melting enthalpy for PBT were practically negligible. ¹H NMR spectra of the residual material after incubation (Figures 5.18 and 5.19) did not show significant variations in the chemical constitution.

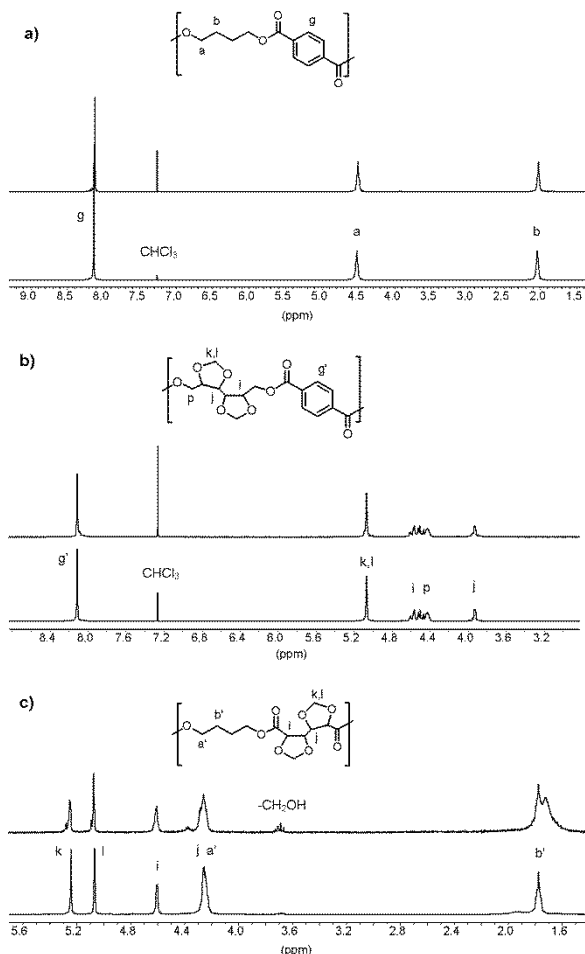


Figure 5.18. Compared ¹H NMR spectra of PBT (a), PGalxT (b) and PBGalx (c) homopolyesters after incubation (top) at pH 2.0 at 80 °C and initial (bottom).

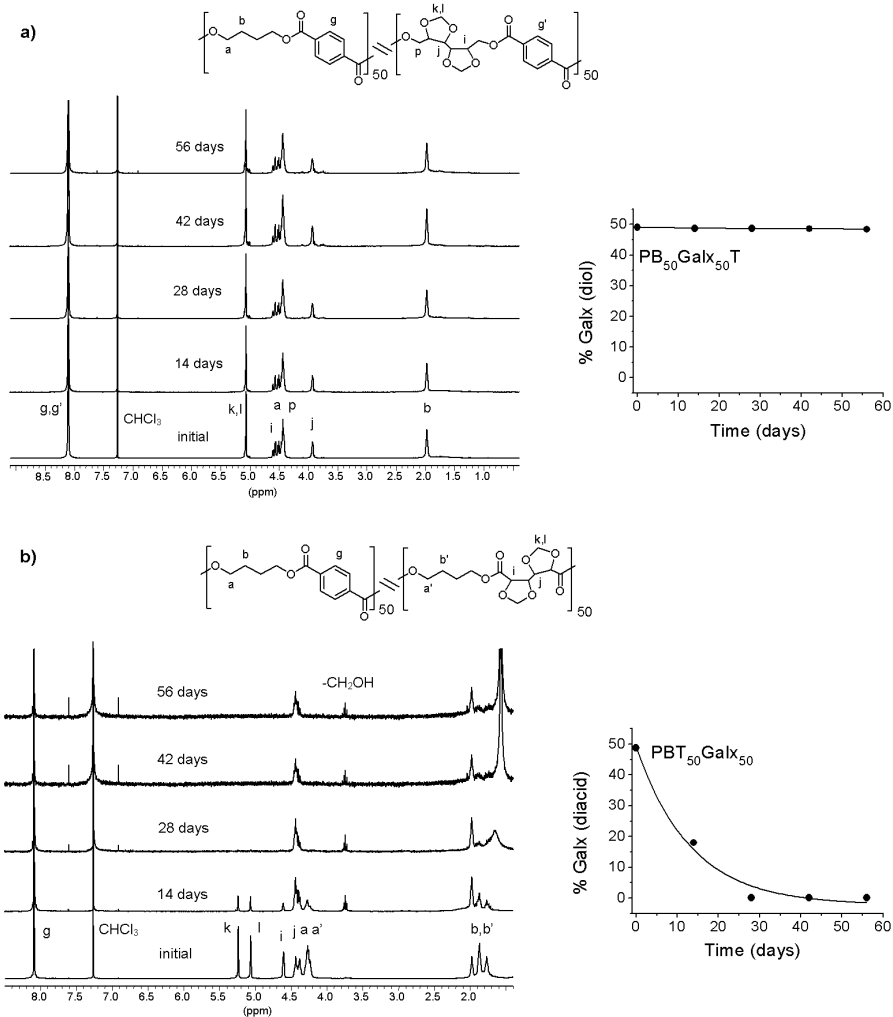


Figure 5.19. Compared ¹H NMR after incubation with water at pH 2.0 at 80 °C and initial spectra of PB₅₀Galx₅₀T (a) and PBT₅₀Galx₅₀ (b) copolyesters, and representation of Galx content vs. incubation time.

SEM analysis revealed that upon incubation PBT spherulites showed cracks in a low proportion whereas spherulites of incubated PGalxT homopolyester appeared frequently cracked (Annex E); with regard to PB₅₀Galx₅₀T copolyester, the initial surface displayed also very apparent physical alterations (Figure 5.17), showing that hydrolytic degradation was largely enhanced by the presence of galactitol units. Both sample weighting and SEM observations indicated that PB₅₀Galx₅₀T copolyester became

apparently degraded in a higher degree than PGalxT homopolyester despite its lesser content in galactitol. The reason for such behavior may be the lower glass-transition temperature displayed by the copolyester.

5.3.3.2. PBT copolyesters containing galactarate units

To investigate the influence of the incorporation of dimethyl 2,3:4,5-di-O-methylene-galactarate on degradation of PBT, a comparative study of the two homopolyesters PBT and PBGalx and the intermediate PBT₅₀Galx₅₀ copolyester was carried out under the same conditions used in the study of the PBT copolyesters containing galactitol units described above.

5.3.3.2.1. Hydrolytic degradation and biodegradation at pH 7.4 at 37 °C

The changes taking place in sample weight and molecular weight of PBT, PBT₅₀Galx₅₀ and PBGalx polyesters at increasing incubation times in aqueous pH 7.4 buffer at 37 °C, with and without porcine pancreas lipase, are presented in Figure 5.20. The weight that was lost upon 8 weeks of incubation in the presence of lipase was about 20% and 35% for PBT₅₀Galx₅₀ and PBGalx, respectively; whereas only 5% and 7% was lost upon incubation of the same polyesters in the absence of enzymes, respectively. However, the sample weight and molecular weight of PBT homopolyester was maintained unchangeable through the whole process. On the contrary, a slight decay in M_w and M_n was observed for both PBT₅₀Galx₅₀ and PBGalx polyesters when incubated in the absence of enzymes. Furthermore, when these two polyesters were incubated with lipase, M_w and M_n decayed substantially, the more pronounced change being observed for the homopolyester in agreement with the expected ability of galactarate units for making PBT biodegradable.

Melting enthalpies of PBT samples upon incubation were nearly the same than that of the initial sample according to the inexistence of degradation. However, it was noteworthy to observe that the crystallinity of both PBT₅₀Galx₅₀ and PBGalx increased as degradation proceeded, and that the raise in crystallinity was higher when samples were incubated in the presence of lipase (Figure 5.16). The SEM micrographs of PBT, PBT₅₀Galx₅₀ and PBGalx polyesters before and after incubation are shown in Figures 5.21 and 5.22 and in Annex E. This analysis confirmed that the surface of PBT remained unaltered after being incubated either in the presence or the absence of lipases. The results obtained in the parallel analysis carried out on PBT₅₀Galx₅₀ and PBGalx were

clearly different. SEM micrographs of PBT₅₀Galx₅₀ showed a certain grade of destruction of the polymer surface when it was incubated in the presence of lipase, a feature that was absent when incubation was carried out without enzymes. Regarding PBGalx, the initial surface did not display any feature of crystalline morphology, and after incubation with lipase, plenty of curved lines appeared delineating what seems to be a spherulitic texture. The conclusion derived from these observations is that degradation of PBT₅₀Galx₅₀ and PBGalx polyesters under physiological conditions was greatly enhanced by the action of enzymes, a property that points to dimethyl 2,3:4,5-di-O-methylene-galactarate as a potential comonomer for obtaining biodegradable PBT copolyesters.

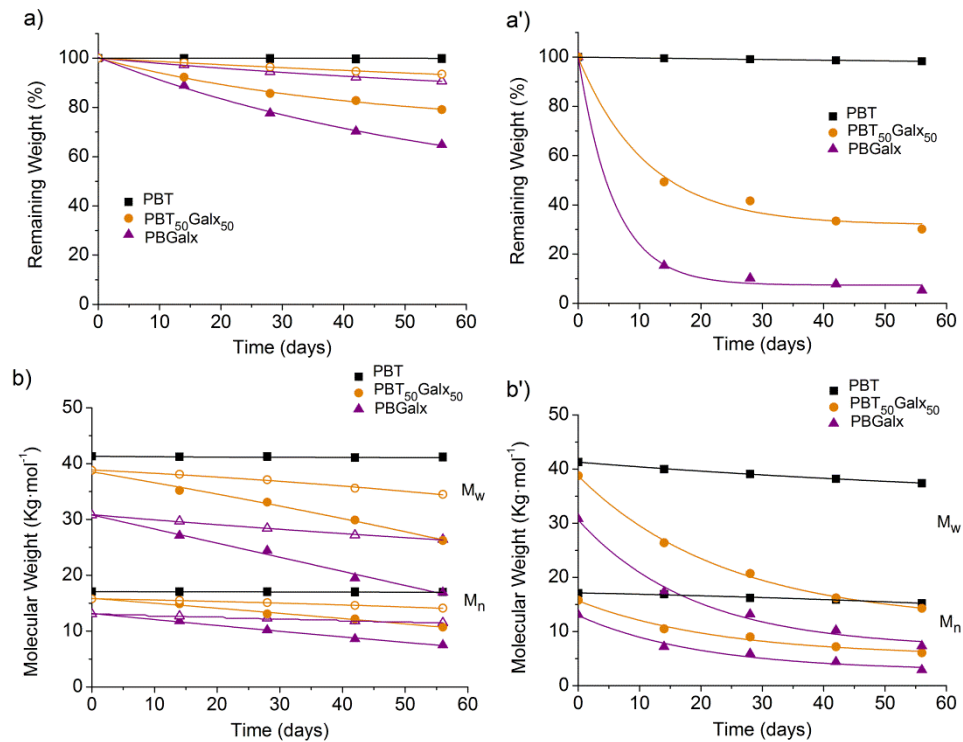


Figure 5.20. Degradation of PBT, PBT₅₀Galx₅₀ and PBGalx. Remaining weight (a) and molecular weight (b) vs. degradation time with (solid symbols) and without (empty symbols) porcine pancreas lipase at pH 7.4 at 37 °C. Remaining weight (a') and molecular weight (b') vs. degradation time at pH 2.0 at 80 °C.

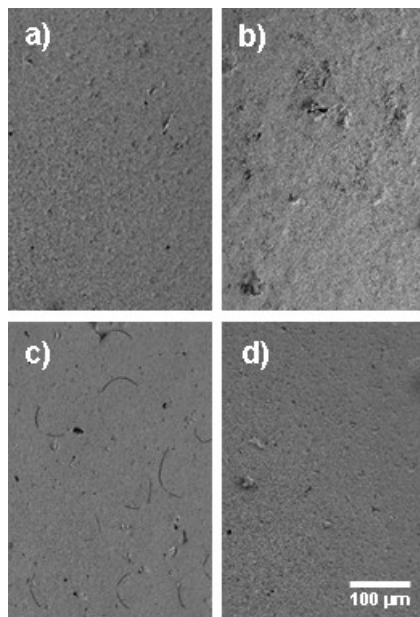


Figure 5.21. SEM micrographs of PBGalx. Initial sample (a). After incubation at pH=2.0 at 80 °C for 7 days (b). After incubation at pH=7.4 at 37 °C for 56 days with (c) and without (d) lipase from porcine pancreas.

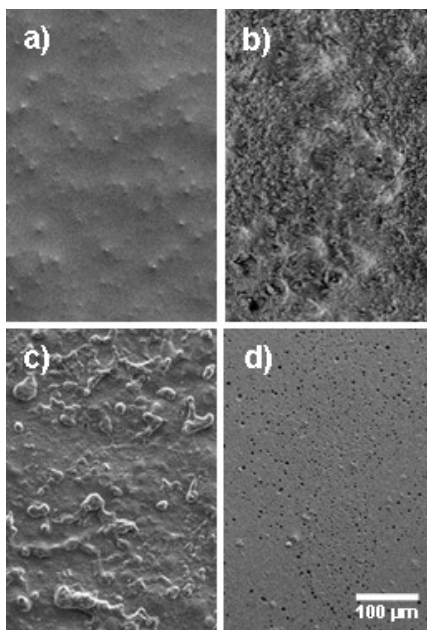


Figure 5.22. SEM micrographs of PBT₅₀Galx₅₀. Initial sample (a). After incubation at pH=2.0 at 80 °C for 56 days (b). After incubation at pH=7.4 at 37 °C for 56 days with (c) and without (d) lipase from porcine pancreas.

5.3.3.2.2. Hydrolytic degradation at pH 2.0 at 80 °C

The changes taking place in sample weight and molecular weight of PBT, PBT₅₀Galx₅₀ and PBGalx polyesters upon incubation at pH 2.0 at 80 °C are depicted in Figure 5.20. The profiles obtained for PBT indicate again that there was no loss of mass and that the decrease in molecular weight was practically negligible. Also the SEM analysis revealed that PBT remained almost unaltered after incubation, only showing very few small cracks and confirming the reluctance of this polyester to be hydrolyzed. On the contrary, PBGalx homopolyester showed a drastic loss of mass, about 85% upon only 2 weeks of incubation and achieving a total weight loss of almost 100% after 8 weeks, as well as a significant decrease in both M_w and M_n , which fell down to final values of 9,000 and 4,000 g·mol⁻¹, respectively. Neither SEM observations nor DSC measurements could be carried out after the whole period of incubation since no sample remained; however, SEM observations of PBGalx incubated for one week (Figure 5.21) confirmed that degradation of PBGalx under these conditions had already taken place in some extent in such a short period of time. PBT₅₀Galx₅₀ copolyester degradation results were intermediate between those of their respective two parent homopolyesters, losing about 70% of the initial mass and showing M_w and M_n values of 16,000 and 7,000 g·mol⁻¹ after 8 weeks of incubation. Furthermore, SEM micrographs (Figure 5.22) and DSC measurements (Figure 5.16 and Annex E) showed that the initial smooth surface of PBT₅₀Galx₅₀ was almost destroyed and crystallinity increased after incubation.

In order to deep insight the degradation of the polyester chain at the molecular level a NMR study was undertaken. ¹H NMR spectra of the products released to the aqueous medium and the residual material resulting after 8 weeks of incubation in acidic water are depicted in Figures 5.18, 5.19 and 5.23. As expected, PBT spectra of both the aqueous medium and the residual material did not show differences with the initial spectra. By contrast, the PBGalx spectrum of the incubation media showed signals corresponding to the released 2,3:4,5-di-O-methylene-galactaric acid and 1,4-butanediol, whereas the NMR spectrum of the residual material revealed no changes in the diacetal structure but showed -CH₂OH signals of terminal groups of the polyester, indicating a decrease in the molecular weight. On the other hand, the NMR analysis of the incubation medium of PBT₅₀Galx₅₀ showed only signals characteristic of 2,3:4,5-di-O-methylene-galactaric acid and 1,4-butanediol, whereas the spectrum of the residual polymer showed a progressive decrease in galactaric content. In fact, integration of galactaric and terephthalic signals indicated that the residual material contained only 18% of the

galactaric units after 2 weeks of incubation and almost nothing after 8 weeks. The spectrum showed also prominent $-\text{CH}_2\text{OH}$ signals due to a notable increase of terminal groups. It was concluded therefore that after the whole incubation period, the residual material of $\text{PBT}_{50}\text{Galx}_{50}$ copolyester essentially consisted of 1,4-butyleneterephthalate oligomers.

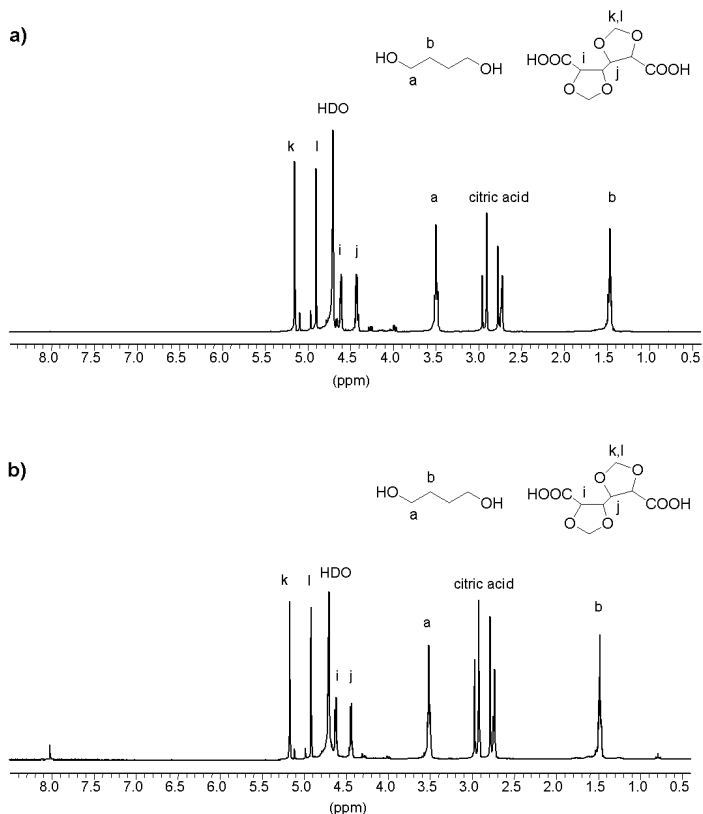
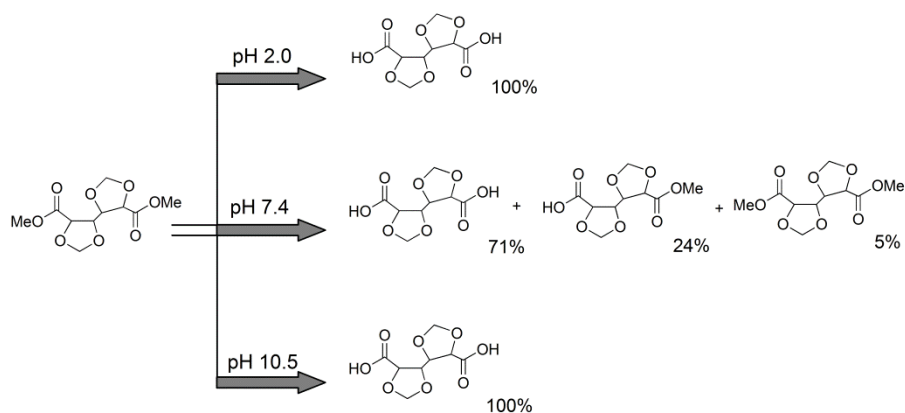


Figure 5.23. ^1H NMR spectra in D_2O of the products released to the aqueous medium after incubation of PBGalx (a) and $\text{PBT}_{50}\text{Galx}_{50}$ (b) at pH 2.0 at $80\text{ }^\circ\text{C}$ for 56 days.

5.3.3.3. Stability of the diacetal structure

PBT copolyesters containing bicyclic acetalized units, as well as their respective sugar-based homopolyesters, have shown to be degraded by water through splitting of the ester group whereas the acetal group remains stable against hydrolysis (Figures 5.18, 5.19 and 5.23). This result is rather striking because the acetal group is known to be sensitive to acidic conditions (Smith and March, 2007) and the opening of the dioxolane

rings might be expected to happen in some extent. A NMR study was undertaken in order to check the stability of the acetal groups of the bicyclic dioxolane structure, especially compared with the ester group. The dimethyl ester of the bicyclic acetalized galactaric acid was then incubated in aqueous buffer at pH 2.0, 7.4 and 10.5. The degradation products detected by NMR are depicted in Scheme 5.3 and the recorded spectra are provided in Annex E. After 12 weeks of incubation, degradation of the ester groups happened almost quantitatively in both acid and basic media. Upon incubation at pH 7.4, most of the bicyclic acetalized monomer was in the dicarboxylic form, a fourth part was as monoester form and only around 5% still remained as diester. What was really remarkable in this study is that the acetal structure stayed unchanged after the treatment under any applied conditions. Thus the stability against hydrolysis observed for the dioxolane rings of the sugar-based units contained in the PBT copolyesters was corroborated.



Scheme 5.3. Resulting products of the hydrolysis of dimethyl 2,3:4,5-di-O-methylene-galactarate at pH 2.0, pH 7.4 and pH 10.5 after 90 days.

5.3.4. Conclusions

PBT copolyesters in which the terephthalate units were replaced by dimethyl 2,3:4,5-di-O-methylene-galactarate appeared to be sensitive to enzymatic action showing a significant degradability under physiological conditions in the presence of lipases. When these polyesters were incubated at 80 °C in acidic medium, hydrolytic degradation occurred so fast that no sample remained after incubation for a few weeks. Conversely, PBT analogs based on 2,3:4,5-di-O-methylene-galactitol were not degraded under

physiological conditions either with or without the concurrence of enzymes, although they displayed enhanced hydrodegradability compared to PBT when incubated at 80 °C in acidic medium. In all cases, degradation proceeded by splitting of the relatively weak ester group associated to the sugar moiety and without modification of the diacetal structure. The outstanding conclusion derived from this study is that whereas the incorporation of 2,3:4,5-di-*O*-methylene-galactitol units in PBT leads to copolyesters with controlled hydrodegradability, the incorporation of 2,3:4,5-di-*O*-methylene-galactarate units is a suitable option for obtaining rapidly hydrodegradable and biodegradable PBT copolyesters.

5.3.5. References

- Alla, A.; Hakkou, K.; Zamora, F.; Martínez de Ilarduya, A.; Galbis, J.A.; Muñoz-Guerra, S. *Macromolecules* **2006**, *39*, 1410-1416.
- Burden, I.J.; Stoddart, J.F. *J. Chem. Soc. Perk. T. 1* **1975**, 675-682.
- Butler, K.; Lawrance, R.L.; Stacey, M. *J. Chem. Soc.* **1958**, 740-743.
- Fenouillot, F.; Rosseau, A.; Colomines, G.; Saint-Loup, R.; Pascault, J.-P. *Prog. Polym. Sci.* **2010**, *35*, 578-622.
- Gallucci, R.R.; Patel, B.R. *Poly(butylene terephthalate)*. In: Scheirs, J.; Long, T.E.; Eds. *Modern Polyesters, Chemistry and Technology of Polyesters and Copolyesters*; John Wiley & Sons: Chichester, **2004**, pp. 293-321.
- Galbis, J.A.; García-Martín, M.G. *Sugars as Monomers*. In: Belgacem, M.N.; Gandini, A.; Eds. *Monomers, Polymers and Composites from Renewable Resources*; Elsevier: Oxford, **2008**, 89-114.
- Gomes, M.; Gandini, A.; Silvestre, A.J.D.; Reis, B. *J. Polym. Sci., Polym. Chem.* **2011**, *49*, 3759-3768.
- Kiely, D.E.; Chen, L.; Lin, T.-H. *J. Polym. Sci., Polym. Chem.* **2000**, *38*, 594-603.
- Kijchavengkul, T.; Auras, R.; Rubino, M.; Alvarado, E.; Montero, J.C.R.; Rosales, J.M. *Polym. Degrad. Stabil.* **2010**, *95*, 99-107. (2010a)
- Kijchavengkul, T.; Auras, R.; Rubino, M.; Selke, S.; Ngouajio, M.; Fernandez, R.T. *Polym. Degrad. Stabil.* **2010**, *95*, 2641-2647. (2010b)
- Kulshrestha, A.S.; Gao, W.; Gross, R.A. *Macromolecules* **2005**, *38*, 3193-3204.
- Lavilla, C.; Alla, A.; Martínez de Ilarduya, A.; Benito, E.; García-Martín, M.G.; Galbis, J.A.; Muñoz-Guerra, S. *Biomacromolecules* **2011**, *12*, 2642-2652. **-Subchapter 3.2-**

Lavilla, C.; Alla, A.; Martínez de Ilarduya, A.; Benito, E.; García-Martín, M.G.; Galbis, J.A.; Muñoz-Guerra, S. *Polymer* **2012**, *53*, 3432-3445. **-Subchapter 5.2-**

Nakajima-Kambe, T.; Ichihashi, F.; Matsuzoe, R.; Kato, S.; Shintani, N. *Polym. Degrad. Stabil.* **2009**, *94*, 1901-1905.

Rychter, P.; Kawalec, M.; Sobota, M.; Kurcok, P.; Kowalczyk, M. *Biomacromolecules* **2010**, *11*, 839-847.

Smith, M.B.; March, J. *March's Advanced Organic Chemistry*; Wiley: Hoboken, **2007**, pp. 523,1270.

Tripathy, A.R.; MacKnight, W.J.; Kukuljick, S.N. *Macromolecules* **2004**, *37*, 6793-6800.

Yokoe, M.; Aoi, M.; Okada, M. *J. Polym. Sci., Polym. Chem.* **2005**, *43*, 3909-3919.

Zaliz, C.L.R.; Varela, O. *Tetrahedron Asymm.* **2005**, *16*, 97-103.

5.4. Bio-based aromatic polyesters from a bicyclic diol derived from D-mannitol

Summary: *2,4:3,5-di-O-methylene-D-mannitol, abbreviated as Manx, is a D-mannitol-derived compound with the secondary hydroxyl groups acetalized with formaldehyde. The bicyclic structure of Manx consists of two fused 1,3-dioxane rings, with two primary hydroxyl groups standing free for reaction. A homopolyester made of Manx and dimethyl terephthalate, as well as a set of copolyesters of poly(butylene terephthalate) (PBT) in which 1,4-butanediol was replaced by Manx up to 50% were synthesized and characterized. The polyesters had M_w in the 30,000-52,000 $\text{g}\cdot\text{mol}^{-1}$ range and a random microstructure, and were thermally stable up to nearly 370 °C. They displayed outstanding high T_g with values from 55 to 137 °C which steadily increased with the content in Manx. Copolyesters containing up to 40% of Manx were semicrystalline and adopted the crystal structure of PBT. Their stress-strain parameters were sensitively affected by the presence of carbohydrate-based units with elongation at break decreasing but tensile strength and elastic moduli steadily increasing with the degree of replacement.*

Publication derived from this work:

Lavilla, C.; Martínez de Ilarduya, A.; Alla, A.; García-Martín, M.G.; Galbis, J.A.; Muñoz-Guerra, S. *Macromolecules* **2012**, *45*, 8257-8266.

5.4.1. Introduction

Bio-based polymers are nowadays attracting a great deal of interest, not only for their potential to reduce the utilization of petrochemicals but also for increasing the added-value of agriculture products and wastes (Wool and Sun, 2005; Pillai, 2010; Gandini, 2011; Chen and Patel, 2012). Carbohydrates constitute an interesting renewable source for being used as polymer building blocks; they are the most abundant type of biomass feedstock and they are found in a very rich variety of structures displaying great stereochemical diversity. However, they possess an excess of functional groups that upon polycondensation would lead to undesirable cross-linking reactions unless special precautions are taken. Although some linear polycondensates have been synthesized using carbohydrate-based monomers bearing free hydroxyl groups (Kiely *et al.*, 1994 and 2000), most syntheses have been carried out with derivatives in which the exceeding functional groups have been appropriately protected (Kricheldorf, 1997; Okada, 2002; Williams, 2007; Metzke and Guan, 2008).

Among carbohydrate-derived monomers, those with a cyclic structure have achieved a privileged position because, in addition to their natural origin, they are able to provide polycondensates with improved properties, especially those related to polymer chain stiffness, as it is the case of the glass-transition temperature. A high T_g is nowadays a greatly appreciated property in polyesters that are addressed to packaging under heating or to the manufacture of containers for pressurized gaseous beverages. Thus 2,5-furandicarboxylic acid has been reported as a potential alternative to replace terephthalic acid for the preparation of aromatic polyesters based on renewable sources (Gandini *et al.*, 2009; Gomes *et al.*, 2011). 1,4:3,6-Dianhydro-D-glucitol, known as isosorbide, which is prepared by dehydration of D-glucose coming from cereal starch, is the only bicyclic carbohydrate-based monomer industrially available today. Isosorbide along with other less accessible dianhydrohexitols derivatives are receiving recently a great deal of attention as building blocks for the synthesis of aromatic copolyesters with increased T_g (Sablong *et al.*, 2008; Fenouillot *et al.*, 2010; Wu *et al.*, 2012). The two hydroxyl groups of isosorbide are secondary and, due to their different spatial position in the molecule, they display different reactivity. These features seriously hamper the polycondensation reaction in the melt, so isosorbide polyesters obtained by this method display rather limited molecular weights (Storbeck and Ballauff, 1996; Kricheldorf *et al.*, 2007). Another type of carbohydrate-based bicyclic monomers are those obtained by internal acetalization, which have been shown to be very suitable to prepare polyesters

by polycondensation in the melt since they are able to react at a rate similar to that of other acyclic conventional monomers (Lavilla *et al.*, 2011 -Subchapter 3.2-, 2012a -Subchapter 3.3- and 2012b -Subchapter 5.2-).

In this work we present a new bicyclic carbohydrate-based monomer useful for the preparation of linear polycondensates. 2,4:3,5-di-O-methylene-D-mannitol, abbreviated as Manx, is a D-mannitol-derived compound with the secondary hydroxyl groups acetalized with formaldehyde. A set of copolyesters of poly(butylene terephthalate) (PBT) in which the 1,4-butanediol has been replaced by Manx has been synthesized and characterized. PBT is a well-known thermoplastic aromatic polyester, with a melting temperature near 225 °C and a glass-transition temperature around 30 °C, which is used in a wide variety of engineering applications (Gallucci and Patel, 2004). Nevertheless, despite being innocuous for humans, PBT as well as other aromatic polyesters are considered not to be environmentally friendly materials due to their non-renewable origin (Tripathy *et al.*, 2004). In this work special attention is paid to study the effect of the introduction of renewable Manx on the glass-transition temperature, thermal stability and crystallizability of the resulting PBT copolyesters, because of the relevance that these properties have not only for the technical use of PBT but also for the potential application that this novel carbohydrate-based monomer may have in the synthesis of other polycondensates. Contrary to isosorbide, the two hydroxyl groups of Manx remaining free for reaction are primary and, since Manx possess a twofold axis of symmetry, they display the same reactivity. Moreover, the use of Manx as polycondensation monomer leads to regioregular polymer chains, provided that it is made to react with nondirectional monomers.

5.4.2. Experimental section

5.4.2.1. Materials

The reagents D-mannitol (ACS reagent grade), benzoyl chloride (99+%), paraformaldehyde (95%), 1,4-butanediol (99%) and dimethyl terephthalate (99+%), and the catalyst dibutyl tin oxide (DBTO, 98%) were purchased from Sigma-Aldrich. Solvents used for purification and characterization were purchased from Panreac and they all were of either technical or high-purity grade. All the reagents and solvents were used as received without further purification.

5.4.2.2. General methods

^1H and ^{13}C NMR spectra were recorded on a Bruker AMX-300 spectrometer at 25.0 °C operating at 300.1 and 75.5 MHz, respectively. Samples were dissolved either in deuterated chloroform, deuterated dimethyl sulfoxide or in a mixture of deuterated chloroform and trifluoroacetic acid (9:1), and spectra were internally referenced to tetramethylsilane (TMS). About 10 and 50 mg of sample dissolved in 1 mL of solvent were used for ^1H and ^{13}C NMR, respectively. Sixty-four scans were acquired for ^1H and 1,000-10,000 for ^{13}C with 32 K and 64 K data points as well as relaxation delays of 1 and 2 s, respectively. For conformational studies ^1H NMR spectra were recorded from 60 to -60 °C in the NMR spectrometer equipped with a variable-temperature unit. Temperatures were selected at 20 °C interval. For each temperature the sample was held for 10 min to reach thermal equilibrium. 2D NOE spectrum (NOESY) was recorded at a fixed temperature ($T = 298.1\text{ K}$) with a standard pulse sequence (noesytp) with a mixing time of 2 s over a sweep width of 1397 Hz using 2048 data points in the t_2 dimension and 256 increments in the t_1 dimension. The repetition delay was 2 s, and 256 scans were collected for each t_1 increment. ^1H NMR simulated spectra were obtained with SpinWorks 3.1.8 program (Kirk Marat, University of Manitoba). Intrinsic viscosities of polymers dissolved in dichloroacetic acid were measured in an Ubbelohde viscosimeter thermostated at 25.0 ± 0.1 °C. Gel permeation chromatograms were acquired at 35.0 °C using a Waters equipment provided with a refraction-index detector. The samples were chromatographed with 0.05 M sodium trifluoroacetate-hexafluoroisopropanol (NaTFA-HFIP) using a polystyrene-divinylbenzene packed linear column with a flow rate of $0.5\text{ mL}\cdot\text{min}^{-1}$. Chromatograms were calibrated against poly(methyl methacrylate) (PMMA) monodisperse standards. The thermal behavior of polyesters was examined by DSC using a Perkin Elmer DSC Pyris 1. DSC data were obtained from 3 to 5 mg samples at heating/cooling rates of $10\text{ }^\circ\text{C}\cdot\text{min}^{-1}$ under a nitrogen flow of $20\text{ mL}\cdot\text{min}^{-1}$. Indium and zinc were used as standards for temperature and enthalpy calibration. The glass-transition temperatures were determined at a heating rate of $20\text{ }^\circ\text{C}\cdot\text{min}^{-1}$ from rapidly melt-quenched polymer samples. The treatment of the samples for isothermal crystallization experiments was the following: the thermal history was removed by heating the sample up to 250 °C and left at this temperature for 5 min, and then it was cooled at $20\text{ }^\circ\text{C}\cdot\text{min}^{-1}$ to the selected crystallization temperature, where it was left to crystallize until saturation. For morphological study, isothermal crystallizations under the same conditions were carried out in an Olympus BX51 Polarizing Optical Microscope coupled to a THMS LINKAM heating plate and a cooling system LNP (Liquid Nitrogen Pump).

Thermogravimetric analyses were performed under a nitrogen flow of 20 mL·min⁻¹ at a heating rate of 10 °C·min⁻¹, within a temperature range of 30 to 600 °C, using a Perkin Elmer TGA 6 equipment. Sample weights of about 10-15 mg were used in these experiments. Films for mechanical testing measurements were prepared with a thickness of ~200 µm by casting from solution (100 g·L⁻¹) in either chloroform or a mixture of chloroform and hexafluoroisopropanol (5:1); the films were then cut into strips with a width of 3 mm while the distance between testing marks was 10 mm. The tensile strength, elongation at break and Young's modulus were measured at a stretching rate of 30 mm·min⁻¹ at 23 °C on a Zwick 2.5/TN1S testing machine coupled with a compressor Dalbe DR 150. X-ray diffraction patterns were recorded on the PANalytical X'Pert PRO MPD θ/θ diffractometer using the Cu-K α radiation of wavelength 0.1542 nm from powdered samples coming directly from synthesis.

5.4.2.3. Monomer synthesis

1,6-di-O-benzoyl-D-mannitol. A solution of 28.1 g of benzoyl chloride (200 mmol) in dry pyridine (70 mL) was added dropwise to a dispersion of 36.4 g of D-mannitol (200 mmol) in 70 mL of dry pyridine. The mixture was stirred at room temperature for 5 h and then poured into ice-water. The precipitated solid was filtered, washed with cold water and with chloroform, dried and recrystallized from ethanol. Yield: 36%. m.p. 189-193 °C [Lit. 188-192 °C (Brigl and Gruner, 1932)]. ¹H NMR (300.1 MHz, DMSO), δ (ppm): 8.1 (m, 4H, *o*-ArH), 7.6 (m, 2H, *p*-ArH), 7.5 (m, 4H, *m*-ArH), 5.1 (bs, 2H, OH), 4.7-4.3 (m, 6H, OCH₂, OH), 3.9 (m, 2H, CH₂CHOH), 3.7 (d, 2H, CH₂CHOHCHOH). ¹³C NMR (75.5 MHz, DMSO), δ (ppm): 166.0 (CO), 133.1, 130.1, 129.3, 128.6, 69.1, 68.3, 67.7.

1,6-di-O-benzoyl-2,4:3,5-di-O-methylene-D-mannitol. To a mixture of 28.0 g of 1,6-di-O-benzoyl-D-mannitol (72 mmol) and 28.0 g of paraformaldehyde (930 mmol), 22 mL of sulfuric acid 96% were added dropwise and the mixture was stirred for 3 h at room temperature. The reaction mixture was then repeatedly extracted with chloroform. The combined organic layers were washed with ammonia (12% w/w) and water, and dried over anhydrous sodium sulfate. The solution was evaporated to a solid residue, which was recrystallized from ethanol. Yield: 52%. m.p. 121-122 °C [Lit. 121 °C (Haworth and Wiggins, 1944)]. ¹H NMR (300.1 MHz, CDCl₃), δ (ppm): 8.1 (m, 4H, *o*-ArH), 7.6 (m, 2H, *p*-ArH), 7.4 (m, 4H, *m*-ArH), 5.0-4.8 (dd, 4H, OCH₂O), 4.8-4.3 (m, 4H, COOCH₂), 4.4 (m, 2H, OCH₂CH), 4.2 (m, 2H, OCH₂CHCH). ¹³C NMR (75.5 MHz, CDCl₃), δ (ppm): 166.3 (CO), 133.2, 129.7, 129.6, 128.4, 88.5, 71.1, 66.7, 63.7.

2,4:3,5-di-O-methylene-D-mannitol. A dispersion of 15.5 g of 1,6-di-O-benzoyl-2,4:3,5-di-O-methylene-D-mannitol (37 mmol) in 200 mL of dry methanol was stirred overnight with a small piece of sodium. The solution was treated with cation exchange resin, the resin was filtered and the filtrate concentrated to dryness. The resulting semisolid residue was washed with diethyl ether and recrystallized from ethanol. Yield: 72%. m.p. 139-140 °C [Lit. 139 °C (Haskins *et al.*, 1943)]. ^1H NMR (300.1 MHz, CDCl_3), δ (ppm): 5.0-4.8 (dd, 4H, OCH_2O), 4.2 (m, 2H, HOCH_2CH), 4.1 (m, 2H, HOCH_2CHCH), 4.0-3.7 (m, 4H, HOCH_2), 1.9 (bs, 2H, OH). ^{13}C NMR (75.5 MHz, CDCl_3), δ (ppm): 87.2, 73.5, 65.8, 59.6.

5.4.2.4. Polymer synthesis

$\text{PB}_x\text{Man}_y\text{T}$ copolyesters were obtained from a mixture of 1,4-butanediol, 2,4:3,5-di-O-methylene-D-mannitol and dimethyl terephthalate with the selected composition. PBT and PMan_xT homopolyesters were obtained by reacting dimethyl terephthalate with 1,4-butanediol and 2,4:3,5-di-O-methylene-D-mannitol, respectively. The reactions were performed in a three-necked, cylindrical-bottom flask equipped with a mechanical stirrer, a nitrogen inlet and a vacuum distillation outlet. An excess of diol mixture to dimethyl terephthalate was used and dibutyl tin oxide (DBTO, 0.6% molar respect to monomers) was the catalyst of choice. The apparatus was vented with nitrogen several times at room temperature in order to remove air and avoid oxidation during the polymerization. Transesterification reactions were carried out under a low nitrogen flow at the selected temperature. Polycondensation reactions were left to proceed at the selected temperature under a 0.03-0.06 mbar vacuum. Then, the reaction mixture was cooled to room temperature, and the atmospheric pressure was recovered with nitrogen to prevent degradation. The resulting polymers were dissolved in chloroform or in a mixture of chloroform and trifluoroacetic acid (9:1) and precipitated in excess of methanol in order to remove unreacted monomers and formed oligomers. Finally, the polymer was collected by filtration, extensively washed with methanol, and dried under vacuum.

PBT homopolyester. 60% molar excess of 1,4-butanediol to dimethyl terephthalate. Transesterification reactions at 180 °C for 1 h, at 200 °C for 1 h and at 240 °C for 0.5 h under a low nitrogen flow. Polycondensation reactions at 260 °C for 2 h under a 0.03-0.06 mbar vacuum. ^1H NMR (300.1 MHz, CDCl_3/TFA), δ (ppm): 8.13 (s, 4H, ArH), 4.50 (t, 4H OCH_2CH_2), 2.02 (t, 4H, OCH_2CH_2). ^{13}C NMR (75.5 MHz, CDCl_3/TFA), δ (ppm): 168.0 (CO), 133.7, 129.9, 66.2, 25.1.

PManxT homopolyester. 5% molar excess of 2,4:3,5-di-O-methylene-D-mannitol to dimethyl terephthalate. Transesterification reactions at 160 °C for 1 h and at 180 °C for 2 h under a low nitrogen flow. Polycondensation reactions at 180 °C for 5 h under a 0.03-0.06 mbar vacuum. ^1H NMR (300.1 MHz, CDCl_3/TFA), δ (ppm): 8.1 (s, 4H, ArH), 5.2-5.0 (m, 4H, OCH_2O), 4.9-4.5 (m, 4H, OCH_2CH), 4.7 (m, 2H, OCH_2CH), 4.3 (m, 2H, OCH_2CHCH). ^{13}C NMR (75.5 MHz, CDCl_3/TFA), δ (ppm): 167.5 (CO), 133.5, 130.3, 88.6, 71.4, 66.7, 64.4.

PB_xMan_yT copolyesters. The copolyesters were obtained by a similar procedure, with polymerization conditions slightly differing for each composition feed.

PB₉₀Man₁₀T and PB₈₀Man₂₀T. 5% molar excess of the diol mixture to dimethyl terephthalate. Transesterification reactions at 160 °C for 1 h, at 200 °C for 1 h and at 240 °C for 0.5 h under a low nitrogen flow. Polycondensation reactions at 240 °C for 2.5 h under a 0.03-0.06 mbar vacuum.

PB₇₀Man₃₀T. 5% molar excess of the diol mixture to dimethyl terephthalate. Transesterification reactions at 160 °C for 1 h, at 200 °C for 1 h and at 230 °C for 0.5 h under a low nitrogen flow. Polycondensation reactions at 230 °C for 3 h under a 0.03-0.06 mbar vacuum.

PB₆₀Man₄₀T. 5% molar excess of the diol mixture to dimethyl terephthalate. Transesterification reactions at 160 °C for 1 h, at 200 °C for 1 h and at 220 °C for 0.5 h under a low nitrogen flow. Polycondensation reactions at 220 °C for 3.5 h under a 0.03-0.06 mbar vacuum.

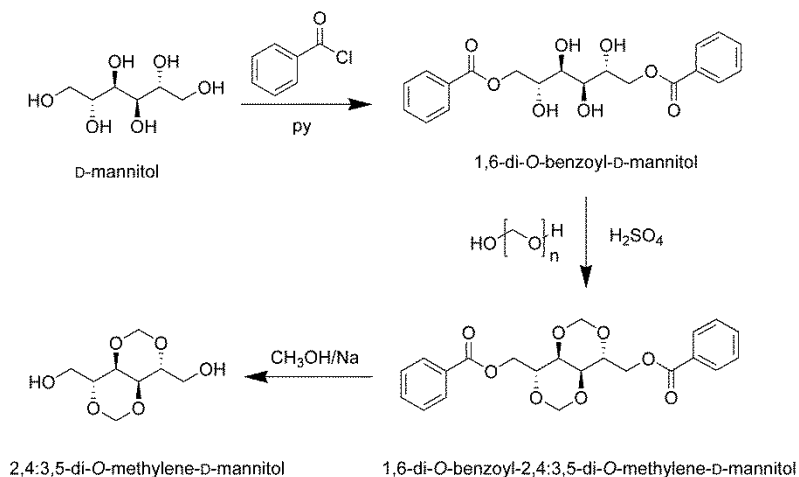
PB₅₀Man₅₀T. 5% molar excess of the diol mixture to dimethyl terephthalate. Transesterification reactions at 160 °C for 1 h, at 200 °C for 1 h and at 210 °C for 0.5 h under a low nitrogen flow. Polycondensation reactions at 210 °C for 4 h under a 0.03-0.06 mbar vacuum.

NMR characterization of PB_xMan_yT copolyesters. ^1H NMR (300.1 MHz, CDCl_3/TFA), δ (ppm): 8.1 (s, 4H, ArH), 5.2-5.0 (m, γ -4H, OCH_2O), 4.9-4.5 (m, γ -4H, OCH_2CH), 4.7 (m, γ -2H, OCH_2CH), 4.5 (t, α -4H, OCH_2CH_2), 4.3 (m, γ -2H, OCH_2CHCH), 2.0 (t, α -4H, OCH_2CH_2). ^{13}C NMR (75.5 MHz, CDCl_3/TFA), δ (ppm): 168.3 (CO), 167.5 (CO), 134.2-133.3, 130.4, 130.2, 88.6, 71.4, 66.7, 66.5, 64.4, 25.4.

5.4.3. Results and discussion

5.4.3.1. Monomer synthesis and conformation

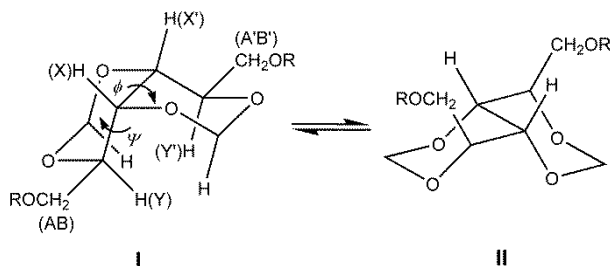
The bicyclic diol 2,4:3,5-di-O-methylene-D-mannitol (Manx) was prepared from D-mannitol following the chemical synthetic route depicted in Scheme 5.4. Primary hydroxyl groups of D-mannitol were first protected as benzoyl esters and then the addition of paraformaldehyde led to cyclic acetalization of the secondary hydroxyl groups in the 2,4:3,5 arrangement with the two fused 1,3-dioxane rings. ^1H and ^{13}C NMR spectra of Manx are shown in Annex F and detailed in Section 5.4.2. The coupling between the two protons of the methylene acetalic group with a $J = -6.2$ Hz confirms the presence of the two fused six membered rings and then the 2,4:3,5 arrangement of the bicyclic structure (Burden and Stoddart, 1975). It should be stressed that the synthesis route used for the preparation of Manx, although effective for the purpose of the work, is not environmentally friendly. Obviously, an alternative synthetic route or an improvement of the existing one will need to be developed to make this monomer of fully practical use and to render benefits to the environment.



Scheme 5.4. Synthesis of 2,4:3,5-di-O-methylene-D-mannitol.

This bicyclic diol Manx possesses a twofold axis of symmetry and therefore its two hydroxyl groups will display the same reactivity in the polycondensation reaction producing regioregular polymer chains. Since the two rings are fused, a fairly high degree of rigidity should be in principle expected for Manx although it could be largely relieved if

interconversion between possible conformers takes place. The rigidity of the monomer is critical for the preparation of polymers with improved thermal and mechanical properties. To appraise the effect that this novel diol monomer will have on the stiffness of the polyesters thence produced, a conformational analysis of 1,6-di-*O*-benzoyl-2,4:3,5-di-*O*-methylene-*D*-mannitol was undertaken. This diester is an adequate model compound for aromatic polyesters and copolyesters made from Manx. The two most probable conformations (Mills, 1955) for the 2,4:3,5-di-*O*-methylene-*D*-manno bicyclic structure are depicted in Scheme 5.5.



Scheme 5.5. Preferential conformers of 1,6-di-*O*-benzoyl-2,4:3,5-di-*O*-methylene-*D*-mannitol.

In order to assess the relative preference of Manx for these two conformations, a variable temperature ^1H NMR study was carried out in the +60 to -60 °C range, and 2D-NOESY spectra were recorded at room temperature. In the case that I and II conformers were present, two signals for each proton should appear in the ^1H NMR spectra at low temperatures since no interconversion is expected to take place under such conditions. On the contrary, single proton signals were observed along the whole interval and the only detected change was an upfield shift of the signals with heating (see Annex F). It can be concluded therefore that no conformational interconversion occurs and that only one conformer is present along the whole range of temperatures. The analysis of the coupling constants of the ^1H NMR spectra suggested that conformer I is the preferred one for Manx. In fact NMR spin simulation using the SpinWorks 3 program provided the *spin-spin* coupling constants (see Annex F) for the ABXY'X'A'B' system, in which small long range couplings between Y and X' protons were detected. The calculated coupling constants were:

$$J_{AB} = J_{A'B'} = -11.98 \text{ Hz}; J_{AY} = J_{A'Y'} = 2.91 \text{ Hz}; J_{BY} = J_{B'Y'} = 6.71 \text{ Hz}; J_{YY'} = J_{Y'Y} = 5.3 \text{ Hz}; J_{YX} = J_{Y'X'} = 8.60 \text{ Hz}; J_{YX'} = J_{Y'X} = -0.58 \text{ Hz}$$

Applying these coupling constants to the Karplus equation derived for alditols (Jardetzky and Roberts, 1981; Franks *et al.*, 1991), the torsional angles ψ and ϕ could be estimated. The values obtained were 160° and 48° respectively, which are very close to the angles measured for conformer I but very far from those of conformer II.

The identity of conformer I as the preferred one was strongly supported by 2D NOESY spectrum (Figure 5.24). As expected for conformation I, strong NOE signals were detected for H_Y and one of the acetal methylene protons, whereas no NOE signals were observed for H_X . In conformation II the short distances between H_X and one of the protons of the acetal methylene should be reflected in the 2D spectra with strong NOE signals, which is not the case. It is worthy to note that crystal structure studies on 2,4:3,5-di-*O*-methylene-*D*-mannitol-1,6-di-*trans*-cinnamate (Bernstein *et al.*, 1980) established a conformation in the solid state for the bicyclic unit similar to which is determined in this work. The conclusion derived from this conformational study is that the preferred conformation of Man_x is I and that this conformation is well stable; such features will confer to this monomer an enhancing stiffness effect on the polymer chain in which it is inserted.

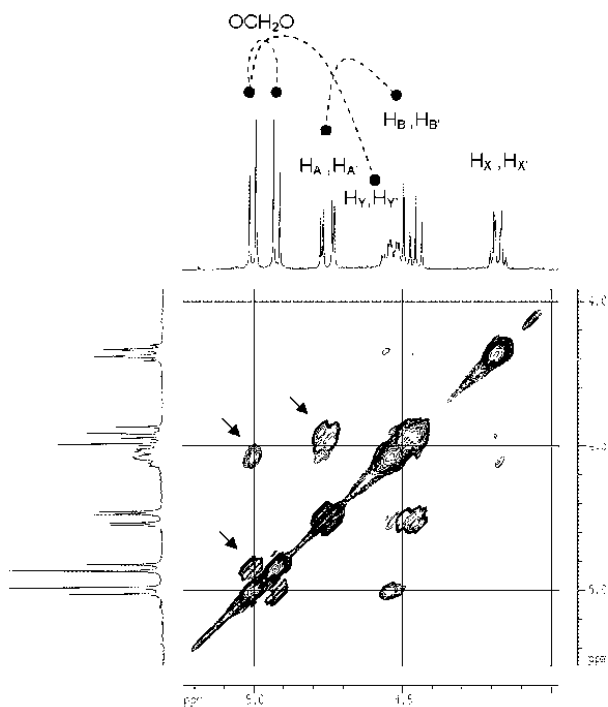
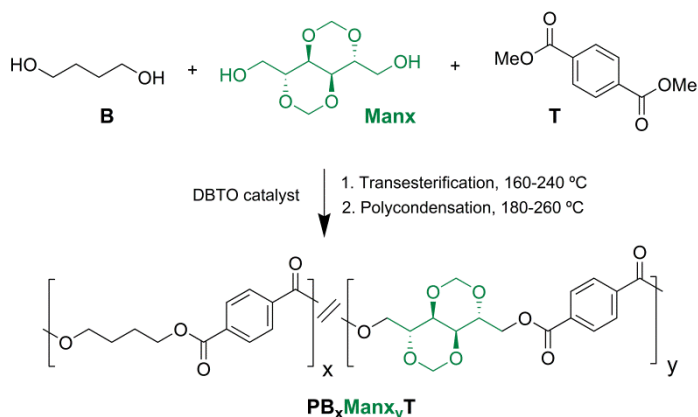


Figure 5.24. 2D NOESY spectrum of 1,6-di-*O*-benzoyl-2,4:3,5-di-*O*-methylene-*D*-mannitol. Small arrows indicate NOE signals.

5.4.3.2. Polymer synthesis and chemical structure

The polymerizations involving 2,4:3,5-di-O-methylene-D-mannitol were carried out in the total absence of solvents to imitate as far as possible the conditions usually applied in the industrial practice. PManxT homopolyester, from 2,4:3,5-di-O-methylene-D-mannitol and dimethyl terephthalate, as well as PB_xManx_yT copolyesters from 2,4:3,5-di-O-methylene-D-mannitol, 1,4-butanediol and dimethyl terephthalate, were prepared by a two-step melt-polycondensation process using DBTO as catalyst (Scheme 5.6). For comparison purposes, the parent PBT homopolyester was obtained from 1,4-butanediol and dimethyl terephthalate using the same polycondensation procedure. In the preparation of PB_xManx_yT copolyesters, the incorporation of the diols into the copolyesters was accurately controlled by using a 5% molar excess of the diol mixture to dimethyl terephthalate, and by initiating transesterification reactions at mild temperature to prevent volatilization of diols. Temperature was progressively increased to avoid crystallization of oligomers, and polycondensation reactions were performed at temperatures between 210 and 240 °C and under vacuum to facilitate the removal of volatile by-products; lower temperatures and longer reaction times were used in copolyesters with higher contents in Manx to minimize the decomposition of this sugar compound. When polymerizations were ended, the reaction mixtures were dissolved either in chloroform or in a mixture of chloroform and trifluoroacetic acid, and precipitated in methanol to obtain the polymers in yields close to 85-90%. The synthesis results obtained for sugar-based PManxT homopolyester and PB_xManx_yT copolyesters are gathered in Table 5.7 together with data for the parent PBT homopolyester.



Scheme 5.6. Polymerization reactions leading to PB_xManx_yT copolyesters.

Table 5.7. Molar composition, molecular weight and microstructure of PB_xMan_x_yT copolyesters.

Copolyester	Yield (%)	Molar composition				Molecular weight				Microstructure					
		Feed		Copolyester ^a		$[\eta]^b$	M_n^c	M_w^c	\mathcal{D}^c	Dyads			Number Average Sequence Lengths		Randomness ^d
		X_B	X_{Manx}	X_B	X_{Manx}					BB	BManx/ ManxB	ManxManx	n_B	n_{Manx}	
PBT	90	100	0	100	0	0.93	17,100 (11,800)	41,300 (40,500)	2.4 (3.4)						
PB ₉₀ Man _x ₁₀ T	86	90	10	91.0	9.0	1.18	20,300 (14,200)	51,200 (50,800)	2.5 (3.6)	75.6	21.7	2.7	8.0	1.3	0.92
PB ₈₀ Man _x ₂₀ T	87	80	20	80.3	19.7	0.84	16,500 (11,500)	41,000 (40,200)	2.5 (3.5)	59.9	34.0	6.1	4.5	1.4	0.96
PB ₇₀ Man _x ₃₀ T	86	70	30	69.2	30.8	0.75	16,600 (10,400)	38,500 (37,900)	2.3 (3.6)	44.9	44.0	11.1	3.0	1.5	0.99
PB ₆₀ Man _x ₄₀ T	85	60	40	59.2	40.8	0.83	16,400 (11,600)	40,100 (39,800)	2.4 (3.4)	35.0	47.8	17.2	2.5	1.7	0.99
PB ₅₀ Man _x ₅₀ T	88	50	50	49.0	51.0	0.77	16,300 (10,900)	38,900 (38,400)	2.4 (3.5)	23.1	48.4	28.5	2.0	2.2	0.97
PManxT	85	0	100	0	100	0.51	12,900 (8,100)	30,200 (29,300)	2.3 (3.6)						

^a Molar composition determined by integration of the ¹H NMR spectra. ^b Intrinsic viscosity in dL·g⁻¹ measured in dichloroacetic acid at 25 °C. ^c Number and weight-average molecular weights in g·mol⁻¹ and dispersities measured by GPC in HFIP against PMMA standards after (without parentheses) and before purification (in parentheses). ^d Randomness index of copolyesters statistically calculated on the basis of the ¹³C NMR analysis.

The precipitated PB_xMan_x_yT copolyesters were obtained with intrinsic viscosities between 0.8 and 1.2 dL·g⁻¹, weight-average molecular weights confined in the 38,000-52,000 g·mol⁻¹ interval, and dispersities in the 2.3-2.5 range. Molecular weights of PB_xMan_x_yT copolyesters slightly decay with the content in Man_x, in accordance with the values observed for PMan_xT homopolyester. The GPC analysis of the reaction product (without being subjected to any treatment) afforded weight-average molecular weights very close to those obtained for the precipitated product but with significantly higher dispersities. Such differences indicate the presence of minor amounts of oligomeric fractions or remaining monomers in the raw product that were then removed by precipitation. The ¹H NMR spectra corroborated the chemical structure of the copolyesters with all signals being correctly assigned to the different protons contained in their repeating units (Figure 5.25). Integration of the proton signals arising from B and Man_x units led to quantify the composition of the copolyesters in such units. Data provided by this analysis are given in Table 5.7, showing that all copolyesters had compositions very close to those of their corresponding feeds.

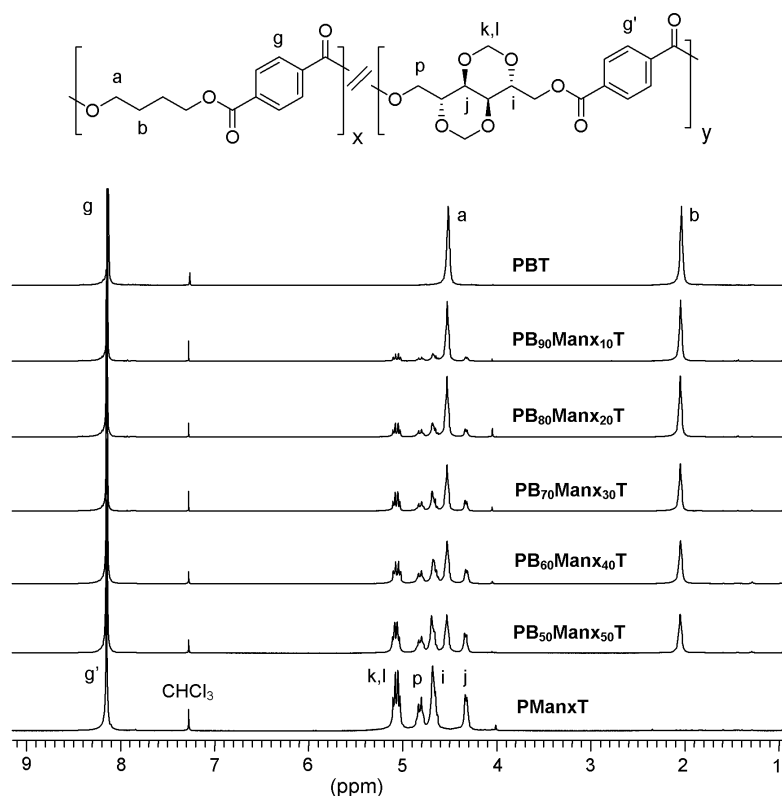


Figure 5.25. Compared ¹H NMR spectra of PB_xMan_x_yT copolyesters.

The microstructure of PB_xMan_xT copolyesters was determined by ^{13}C NMR analysis. The signals of all the magnetically different carbons contained in the repeating units of the copolyesters appear well resolved in the ^{13}C NMR spectra (see Annex F) and in particular those arising from the nonprotonated aromatic carbons, which come out to be sensitive to sequence effects at the dyad level. As shown in Figure 5.26 for the whole set of PB_xMan_xT copolyesters, each resonance of the nonprotonated aromatic carbons appears split so that four peaks are seen in the 133-135 ppm chemical shift interval corresponding to the three types of dyads (BB, BManx and ManxB, ManxManx) that are feasible along the copolyester chain. By integration of these peaks, the dyad contents, the number-average sequence lengths and the degree of randomness were estimated (Table 5.7), leading to the conclusion that the microstructure of the copolyesters was random in all cases.

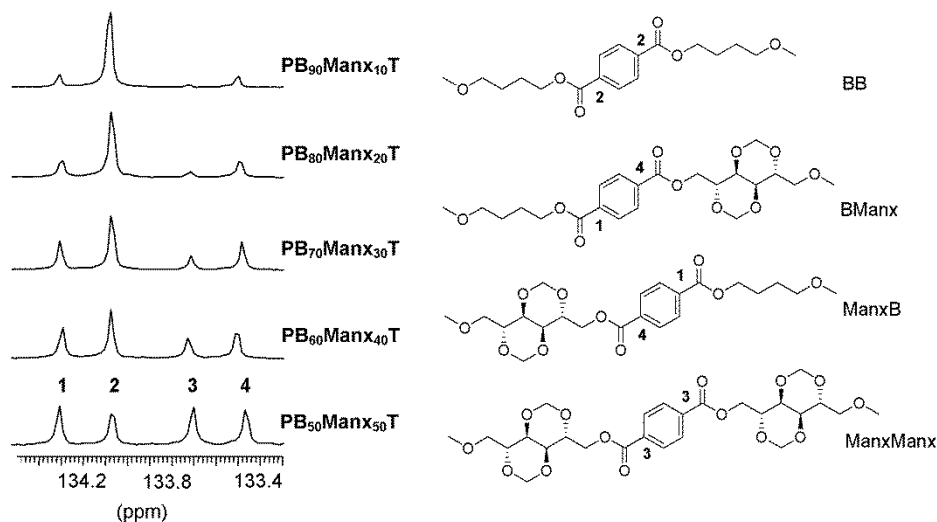


Figure 5.26. ^{13}C NMR signals used for the microstructure analysis of PB_xMan_xT copolyesters with indication of the dyads to which they are assigned.

5.4.3.3. Thermal properties

2,4:3,5-di-O-methylene-D-mannitol is a thermally fairly stable solid compound which starts to volatilize above 150 °C and displays a sublimation temperature of 280 °C without perceivable decomposition. The thermal stability of PManxT homopolyester and PB_xMan_xT copolyesters made from this compound was evaluated by thermogravimetry

under inert atmosphere and compared with that displayed by PBT. TGA traces are depicted in Figure 5.27, and thermal data provided by this analysis are presented in Table 5.8. The weight loss profiles generated reveal that all polyesters start to decompose well above 360 °C with a thermal degradation mechanism involving one main step with the maximum rate at temperatures steadily increasing with the content in Manx units. The same trend is observed for $^{\circ}T_{5\%}$, and these results are in accordance with the high thermal stability observed for PManxT homopolymer, with $^{\circ}T_{5\%}$ and $^{\max}T_d$ at 378 and 421 °C, respectively. The valuable conclusion drawn from this thermogravimetric study is that the insertion of Manx units in aromatic polyesters instead of reducing their thermal stability contributes to a significant increase in their decomposition temperatures. The fact of improving the thermal stability of commonly used aromatic polyesters such as PBT can broaden even more the application window of these materials.

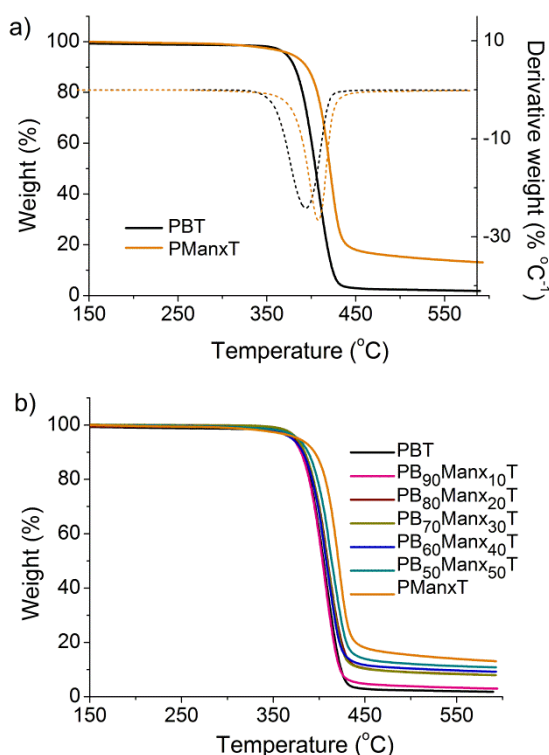


Figure 5.27. (a) TGA traces (solid lines) and derivative curves (dashed lines) of PBT and PManxT homopolymers. (b) TGA traces of PB_xManx_yT copolyesters.

Table 5.8. Thermal properties of PB_xMan_yT copolyesters.

Copolyester	TGA			DSC						
	^a T _{5%}	T _d ^b	W ^c	T _g ^d	First heating ^e		Cooling ^e		Second heating ^e	
					T _m	ΔH _m	T _c	ΔH _c	T _m	ΔH _m
(°C)	(°C)	(%)	(°C)	(°C)	(J·g ⁻¹)	(°C)	(J·g ⁻¹)	(°C)	(J·g ⁻¹)	
PBT	371	408	2	31	223 (223)	56.2 (54.3)	196	43.3	223	44.0
PB ₉₀ Man ₁₀ T	371	408	3	55	197 (196)	34.1 (33.0)	159	30.4	198	31.3
PB ₈₀ Man ₂₀ T	372	410	8	66	184 (183)	26.0 (27.0)	140	23.4	184	24.1
PB ₇₀ Man ₃₀ T	374	411	8	77	162 (162)	5.5 (16.6)	-	-	-	-
PB ₆₀ Man ₄₀ T	376	411	9	88	122 (119)	5.0 (9.8)	-	-	-	-
PB ₅₀ Man ₅₀ T	377	412	11	100	-	-	-	-	-	-
PManxT	378	421	13	137	-	-	-	-	-	-

^aTemperature at which 5% weight loss was observed. ^bTemperature for maximum degradation rate. ^cRemaining weight at 600 °C. ^dGlass-transition temperature taken as the inflection point of the heating DSC traces of melt-quenched samples recorded at 20 °C·min⁻¹. ^eMelting (T_m) and crystallization (T_c) temperatures, and melting (ΔH_m) and crystallization (ΔH_c) enthalpies measured by DSC at heating/cooling rates of 10 °C·min⁻¹ of precipitated samples (without parentheses) and of films (in parentheses).

Other thermal properties of prime importance in connection with the potential application of these polyesters are the glass-transition temperature (T_g) and the melting temperature (T_m). For instance, an increase in the T_g of these polyesters could open their use in the hot-filled and pasteurized-container fields. The glass-transition temperatures of the PManxT and PBT homopolyesters and PB_xMan_yT copolyesters were measured as the inflection point of the heating DSC traces of samples quenched from the melt. A remarkable feature of PManxT homopolyester is that it has a T_g more than 100 °C higher than the aromatic PBT homopolyester. Regarding PB_xMan_yT copolyesters, their T_g increase steadily with the content in Man_x units, with minimum and maximum values corresponding to their respective PBT and PManxT homopolyesters (Figure 5.28), as should be expected from their statistical microstructure. As expected from its cyclic stiff nature, the effect of Man_x on T_g of PBT is largely greater than that exerted by the

incorporation of acyclic sugar units such as trimethoxy xylitol or L-arabinitol (Alla *et al.*, 2006). It has even a much more pronounced effect than 2,3:4,5-di-O-methylene-galactitol, another acetalized sugar diol constituted by two non-fused dioxolane rings, which has been recently reported by us as capable of raising the T_g of PBT by near 30 °C when it replaces 1,4-butanediol in a 40% (Lavilla *et al.*, 2012b -Subchapter 5.2-). The effect of Manx turns to be similar to that of isosorbide; in fact, both PBT copolyesters containing 40% of either Manx or isosorbide (Kricheldorf *et al.*, 2007; Sablong *et al.*, 2008) display a T_g of around 90 °C. No doubt the fused bicyclic structure characteristic of both Manx and isosorbide is unique in providing the polyester chain with a degree of stiffness not achievable with the insertion of rotatable bicyclic units, as it is the case of the acetalized hexitol with *galacto* configuration.

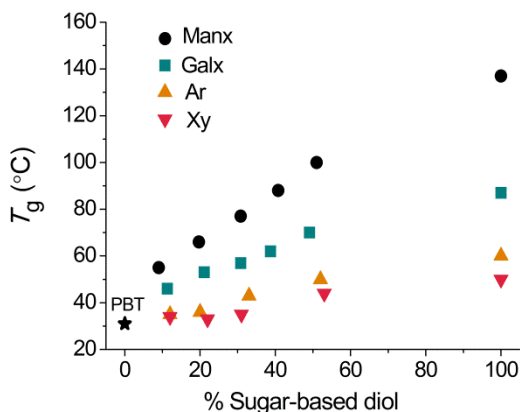


Figure 5.28. Glass-transition temperature versus composition plot for PBT copolyesters containing 2,4:3,5-di-O-methylene-D-mannitol (Manx), 2,3:4,5-di-O-methylene-galactitol (Galx) (Lavilla *et al.*, 2012b -Subchapter 5.2-), 2,3,4-tri-O-methyl-L-arabinitol (Ar) or 2,3,4-tri-O-methylxylitol (Xy) (Alla *et al.*, 2006).

DSC traces of polyesters in the powdered form registered at first heating are depicted in Figure 5.29. PB_xMan_xT copolyesters with molar contents in Manx below or equal to 40%, as well as PBT homopolyester, gave heating traces with melting endotherms indicating that they are semicrystalline. Comparison of melting temperatures and enthalpies of semicrystalline PB_xMan_xT copolyesters with that of PBT homopolyester leads to the conclusion that the insertion of Manx units gives place to a significant decrease in both T_m and ΔH_m (Table 5.8). $PB_{50}Man_{50}T$ copolyester as well as $PMan_xT$ homopolyester appear to be amorphous. DSC data recorded from polyester

films prepared by casting from solution are not far from those obtained from powders, the higher coincidence being found for lower contents in Manx units.

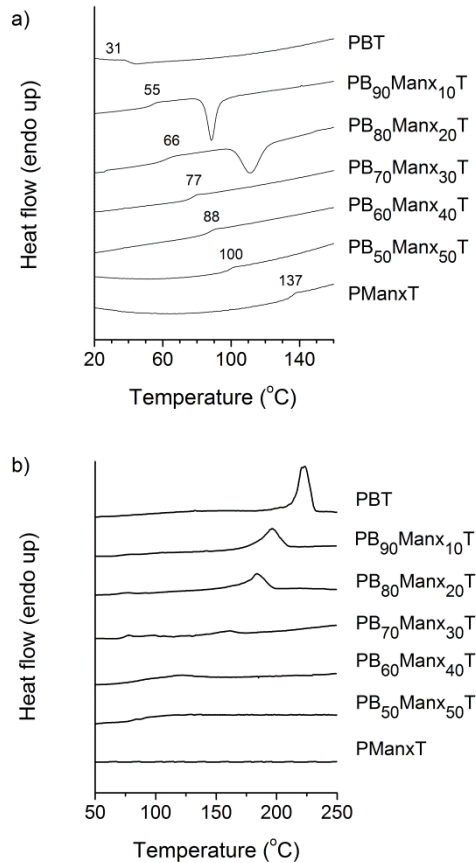


Figure 5.29. (a) DSC heating traces of PB_xMan_xT copolyesters quenched from the melt. (b) DSC melting traces of the PB_xMan_xT copolyesters without being subjected to any thermal treatment.

5.4.3.4. Isothermal crystallization

The cooling DSC traces obtained from molten samples revealed that PB_xMan_xT copolyesters with molar contents in Manx below or equal to 20%, as well as PBT homopolyester, were able to crystallize from the melt. After crystallization from the melt, these polyesters recovered about 75-95% of their initial crystallinity and displayed almost the same melting temperatures. Given the relevance of this property regarding polymer

processing, the isothermal crystallization of PB₉₀Man_{x10}T and PB₈₀Man_{x20}T copolyesters and PBT homopolyester was comparatively studied in the 150-210 °C interval. Unfortunately, not all of them could be compared at exactly the same isothermal crystallization temperature due to the large differences in crystallization rates displayed by them and to the short ranges of temperature in which crystallization evolution is measurable by DSC. Nevertheless, crystallization conditions were chosen as close as possible in order to be able to draw out meaningful conclusions. The Hoffman-Weeks plot of T_m versus T_c showed a good correlation (see Annex F) and provided the equilibrium melting temperatures, which as expected, continue to display the same trend with composition as was observed for the T_m measured for nonisothermally crystallized samples.

Table 5.9. Isothermal crystallization data of PB_xMan_yT copolyesters.

Copolyester	T_c (°C)	t_0 (min)	$t_{1/2}$ (min)	n	$-\log k$	T_m (°C)
PBT	200	0.19	0.82	2.14	-0.25	223.9
	205	0.51	2.68	2.45	1.02	225.5
	210	2.33	12.83	2.56	2.78	226.9
PB ₉₀ Man _{x10} T	165	0.15	1.13	2.01	0.15	194.5
	170	0.26	2.14	2.12	0.75	196.3
	175	0.31	4.37	2.43	1.64	198.0
	180	0.59	8.53	2.52	2.42	199.8
	185	1.93	19.43	2.57	3.34	202.1
PB ₈₀ Man _{x20} T	150	0.19	1.61	2.02	0.56	184.1
	155	0.23	2.45	2.04	0.93	185.3
	160	0.29	3.50	2.07	1.26	186.9
	165	0.44	5.60	2.13	1.74	188.8
	170	0.98	11.85	2.20	2.46	190.5

Kinetic data afforded by the Avrami analysis of the results obtained at the selected crystallization temperatures are gathered in Table 5.9. The evolution of the relative crystallinity, X_c , with crystallization time and the corresponding Avrami data plots $\log[-\ln(1-X_c)]$ versus $\log(t-t_0)$ for some illustrative crystallization experiments are depicted in Figure 5.30. The morphological appearance of the crystallized material observed by polarized optical microscopy is shown in Annex F. It is seen that for each polyester the crystallization half-time as well as the Avrami exponent n increase with temperature, the values of the latter being in the 2.0-2.6 range corresponding to a complex axialitic-spherulitic crystallization as was observed by polarizing optical microscopy. The double logarithmic plot indicates that only primary crystallization takes place in the selected time intervals, and that the presence of Manx units depresses the crystallizability in terephthalate copolyesters. The valuable conclusion that can be drawn from this study is that PB₉₀Manx₁₀T and PB₈₀Manx₂₀T copolyesters continue displaying the ability of crystallizing from the melt as their parent homopolymer PBT although at lower crystallization rates.

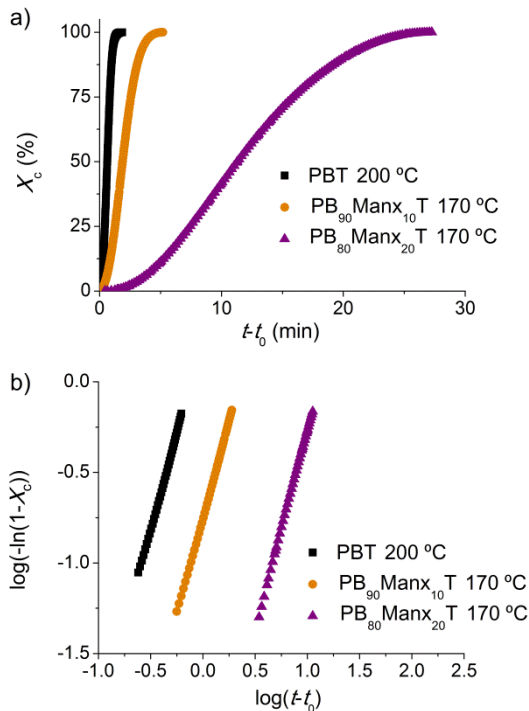


Figure 5.30. Isothermal crystallization of PBT, PB₉₀Manx₁₀T and PB₈₀Manx₂₀T at the indicated temperatures. Relative crystallinity versus time plot (a) and log-log plot (b).

5.4.3.5. Crystal structure and stress-strain behavior

Powder X-ray diffraction analyses were performed for all PB_xMan_yT copolyesters as well as PManxT and PBT homopolyesters. Powder X-ray diffraction profiles are presented in Figure 5.31, and Bragg spacings present in such patterns are listed in Table 5.10. In agreement with DSC results, copolyesters containing up to 40% of Manx produced discrete diffraction scattering distinctive of semicrystalline material whereas fully plain profiles characteristic of amorphous material were obtained from PB₅₀Man₅₀T as well as from the PManxT homopolyester. The PBT pattern is characterized by five prominent reflections at 5.6, 5.1, 4.3, 3.8 and 3.6 Å. Essentially the same pattern regarding both spacing and relative intensities is shared by PB_xMan_yT copolyesters with low content in Manx, revealing that the triclinic crystal structure of PBT (Hall, 1984) must be retained in these copolyesters. The crystallinity index was estimated as the quotient between crystalline area and total area of the X-ray diffraction pattern, showing that PB₉₀Man₁₀T, PB₈₀Man₂₀T, PB₇₀Man₃₀T and PB₆₀Man₄₀T were semicrystalline with crystalline indexes decreasing for increasing contents in Manx units. However, PB₅₀Man₅₀T copolyester and PManxT copolyester did not show any discrete reflection characteristic of crystalline material. These X-ray diffraction results are in full agreement with DSC results and confirmed that PB_xMan_yT copolyesters with molar contents in Manx below or equal to 40% are semicrystalline.

Table 5.10. Powder X-ray diffraction data and mechanical properties of PB_xMan_yT copolyesters.

Copolyester	X-ray diffraction data						Mechanical Properties		
	d^a (Å)					X_c^b	Elastic modulus (MPa)	Tensile strength (MPa)	Elongation at break (%)
PBT	5.6 s	5.1 s	4.3 s	3.8 s	3.6 m	0.48	841±15	42±5	14±3
PB ₉₀ Man ₁₀ T	5.6 s	5.1 s	4.3 m	3.8 s	3.6 m	0.39	852±13	44±6	12±3
PB ₈₀ Man ₂₀ T	5.6 m	5.1 m	4.3 m	3.8 m	3.6 w	0.32	871±25	45±7	9±2
PB ₇₀ Man ₃₀ T	5.6 w	5.1 w	4.3 w	3.8 w	3.6 w	0.11	888±17	46±5	8±3
PB ₆₀ Man ₄₀ T	5.6 w	5.1 w	4.3 w	3.8 w	3.6 w	0.10	891±19	50±7	5±2
PB ₅₀ Man ₅₀ T						0	909±26	52±5	3±1
PManxT						0	1067±29	59±6	2±1

^a Bragg spacings measured in powder diffraction patterns for samples coming directly from synthesis. Intensities visually estimated as follows: m, medium; s, strong; w, weak. ^b Crystallinity index calculated as the quotient between crystalline area and total area. Crystalline and amorphous areas in the X-ray diffraction pattern were quantified using PeakFit v4.12 software.

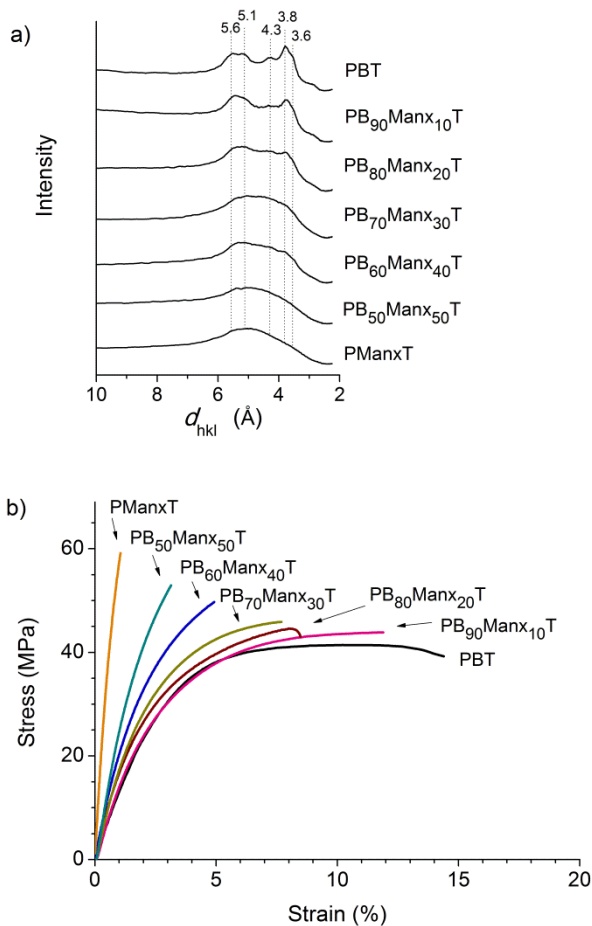


Figure 5.31. Powder WAXD profiles (a) and stress-strain curves (b) of PB_xMan_yT copolyesters.

To evaluate the influence of the presence of Manx in the mechanical properties of copolyesters, tensile assays of PManxT copolyester as well as PB_xMan_yT copolyesters were carried out using the films that were prepared by casting as described in Section 5.4.2. For comparison purposes, mechanical properties of PBT were also tested. According to enthalpy values (Table 5.8), the degree of crystallinity of these films must be close to that displayed by powders with X_c steadily decreasing with the increasing content of the copolyester in Manx units to become 0 for PB₅₀Man₅₀T and PManxT (Table 5.10). The stress-strain curves resulting from tensile essays are depicted in Figure 5.31, and the mechanical parameters measured in these tests are compared in

Table 5.10. PManxT homopolyester displayed higher elastic modulus and tensile strength than PBT, and accordingly PB_xMan_yT copolyesters present a nearly steady trend consisting of a continuous increase in both elastic modulus and tensile strength and a decrease in ductility when their content in Man_x units increases. The observed variations in the stress-strain behavior are fully consistent with the changes in T_g . Apparently, the mechanical moduli of these copolyesters are mainly determined by the mobility of the chains in the amorphous phase rather than by the structural stiffness induced by the presence of crystalline domains.

5.4.4. Conclusions

For the first time, polyesters from the bio-based 2,4:3,5-di-O-methylene-D-mannitol monomer, obtained by internal acetalization of the secondary hydroxyl groups of D-mannitol, have been successfully synthesized. By taking special care of polycondensation conditions, polyesters and statistical copolyesters with pretty high molecular weights were obtained in good yields. The incorporation of the sugar derived diol improved appreciably the thermal stability of the resulting polyesters. The most remarkable effect of copolymerization was however noticed on the glass-transition temperature which increased with the content in 2,4:3,5-di-O-methylene-D-mannitol almost linearly with a slope of about of 1 °C/%-mole allowing fine-tuning of T_g of PBT over a wide range. Consequently, the mechanical moduli of the copolyesters also increased significantly in the same sense. Although copolymerization depressed the crystallinity and crystallizability of PBT, those copolyesters containing up to 40% of sugar based units were semicrystalline and adopted the crystal structure of PBT, and those containing up to 20% were able to crystallize from the melt. The 50/50 copolyester as well as the polyester entirely made of Man_x units were amorphous, at least under the crystallization conditions used in this work. The bicyclic sugar based diol investigated in this work as monomer for polycondensation stands out not only for being a sustainable compound but also for providing polyesters with satisfactory molecular weights and with improved thermal and mechanical properties; nevertheless, the synthesis of this compound will need to be improved in order to make it simpler and to avoid the use of environmentally unfriendly reagents.

5.4.5. References

- Alla, A.; Hakkou, K.; Zamora, F.; Martínez de Ilarduya, A.; Galbis, J.A.; Muñoz-Guerra, S. *Macromolecules* **2006**, *39*, 1410-1416.
- Bernstein, J.; Green, B.S.; Rejtö, M. *J. Am. Chem. Soc.* **1980**, *102*, 323-328.
- Brigl, P.; Gruner, H. *Ber.* **1932**, *65B*, 641-645.
- Burden, I.J.; Stoddart, J.F. *J. Chem. Soc. Perk. T 1* **1975**, *7*, 666-674.
- Chen, G.Q.; Patel, M.K. *Chem. Rev.* **2012**, *112*, 2082-2099.
- Fenouillot, F.; Rousseau, A.; Colomines, G.; Saint-Loup, R.; Pascault, J.P. *Prog. Polym. Sci.* **2010**, *35*, 578-622.
- Franks, F.; Dadok, J.; Ying, S.; Kay, R.L.; Grigera, J.R. *J. Chem. Soc. Faraday Trans.* **1991**, *87*, 579-585.
- Gallucci, R.R.; Patel, B.R. *Poly(butylene terephthalate)*. In: Scheirs, J.; Long, T.E.; Eds. *Modern Polyesters, Chemistry and Technology of Polyesters and Copolyesters*; John Wiley & Sons: Chichester, **2004**, pp. 293-321.
- Gandini, A.; Coelho, D.; Gomes, M.; Reis, B.; Silvestre, A.J.D. *J. Mater. Chem.* **2009**, *19*, 8656-8664.
- Gandini, A. *Green Chem.* **2011**, *13*, 1061-1083.
- Gomes, M.; Gandini, A.; Silvestre, A.J.D.; Reis, B. *J. Polym. Sci. Polym. Chem.* **2011**, *49*, 3759-3768.
- Hall, I.H. *The Determination of the Structures of Aromatic Polyesters from their Wide-angle X-Ray Diffraction Patterns*. In: Hall, I.H.; Ed. *Structure of Crystalline Polymers*; Elsevier Applied Science: UK, **1984**, pp. 39-78.
- Haskins, W. T.; Hann, R. M.; Hudson, C. S. *J. Am. Chem. Soc.* **1943**, *65*, 67-70.
- Haworth, W. N.; Wiggins, L. F. *J. Chem. Soc.* **1944**, 58-61.
- Jardetzky, O.; Roberts, G.C.K. *Molecular Biology*; Academic Press: New York, **1981**. p. 201.
- Kiely, D.E.; Chen, L.; Lin, T.H. *J. Am. Chem. Soc.* **1994**, *116*, 571-578.
- Kiely, D.E.; Chen, L.; Lin, T.H. *J. Polym. Sci., Polym. Chem.* **2000**, *38*, 594-603.
- Kricheldorf, H.R.J. *Macromol. Sci.* **1997**, *C37*, 599-631.
- Kricheldorf, H.R.; Behnken, G.; Sell, M. *J. Macromol. Sci. Pure Appl. Chem.* **2007**, *44*, 679-684.
- Lavilla, C.; Alla, A.; Martínez de Ilarduya, A.; Benito, E.; García-Martín, M.G.; Galbis, J.A.; Muñoz-Guerra, S. *Biomacromolecules* **2011**, *12*, 2642-2652. -**Subchapter 3.2-**

Lavilla, C.; Alla, A.; Martínez de Ilarduya, A.; Benito, E.; García-Martín, M.G.; Galbis, J.A.; Muñoz-Guerra, S. *J. Polym. Sci. Polym. Chem.* **2012**, *50*, 1591-1604. (2012a)

-Subchapter 3.3-

Lavilla, C.; Alla, A.; Martínez de Ilarduya, A.; Benito, E.; García-Martín, M.G.; Galbis, J.A.; Muñoz-Guerra, S. *Polymer* **2012**, *53*, 3432-3445. (2012b) **-Subchapter 5.2-**

Metzke, M.; Guan, Z. *Biomacromolecules* **2008**, *9*, 208-215.

Mills, J.A. *Adv. Carbohydr. Chem.* **1955**, *10*, 1-53.

Okada, M. *Prog. Polym. Sci.* **2002**, *27*, 87-133.

Pillai, C.K.S. *Design. Monom. Polym.* **2010**, *13*, 87-121.

Sablong, R.; Duchateau, R.; Koning, C.E.; de Wit, G.; van Es, D.; Koelewijn, R.; van Haveren, J. *Biomacromolecules* **2008**, *9*, 3090-3097.

Storbeck, R.; Ballauff, M. *J. Appl. Polym. Sci.* **1996**, *59*, 1199-1202.

Tripathy, A.R.; MacKnight, W.J.; Kukureka, S.N. *Macromolecules* **2004**, *37*, 6793-6800.

Williams, C.K. *Chem. Soc. Rev.* **2007**, *36*, 1573-1580.

Wool, R.; Sun, S. *Biobased Polymers and Composites*; Academic Press: New York, **2005**.

Wu, J.; Eduard, P.; Thiyagarajan, S.; Jasinska-Walc, L.; Rozanski, A.; Fonseca Guerra, C.; Noordover, B.A.J.; van Haveren, J.; van Es, D.S.; Koning, C.E. *Macromolecules* **2012**, *45*, 5069-5080.

CHAPTER 6

SSM-PREPARED POLY(BUTYLENE TEREPHTHALATE) COPOLYESTERS FROM CYCLIC ACETALIZED CARBOHYDRATE- BASED MONOMERS

6.1. Aim and scope of this Chapter

Most of the approaches aimed at increasing the glass-transition temperature (T_g) of poly(butylene terephthalate) (PBT), such as reactive blending with more rigid polyesters and melt copolymerization with rigid comonomers, are successful in increasing the glass-transition temperature of PBT but at the same time severely compromise the melting and crystallization behavior. However, with solid-state modification (SSM) it is possible to exclusively modify the properties related to the amorphous phase (*i.e.* glass-transition temperature) while more or less retaining the crystallization behavior of the parent polyester.

SSM consists of making to react a comonomer with a semicrystalline polymer in the solid state, under an inert gas flow or vacuum at 20-30 °C below the T_m of the polymer but well above its T_g . SSM is based on the same principles as the commonly used solid-state polycondensation (SSP), which is usually employed to increase the molecular weight of semicrystalline polyesters and polyamides by transesterification and transamidation reactions, respectively, below the T_m but well above the T_g . Both techniques take advantage of the molecular mobility in the amorphous phase of the polymer above T_g .

During SSM, only chain segments present in the mobile amorphous fraction (MAF) of PBT are modified with the monomer. Mobility restrictions prevent the crystalline phase as well as the rigid amorphous fraction (RAF) from taking part in transesterification reactions occurring during the SSM process.

Among sugar-based monomers, especially those with a cyclic structure are of interest, due to their ability to add stiffness to the polymer backbone, resulting in enhanced T_g values. Recently, high molecular weight aromatic copolyesters containing isosorbide units have been prepared by solid-state modification of PBT. However, due to the relatively low reactivity of the secondary hydroxyl groups of isosorbide, the direct incorporation of this monomer into the polyester backbone using this technique was not possible. The synthesis of a macrodiol from isosorbide, terephthaloyl chloride and 1,4-butanediol was necessary to incorporate this bicyclic monomer into PBT via SSM.

In this Chapter, the sugar-based cyclic acetalized diols 2,3:4,5-di-O-methylene-galactitol (Galx), 2,4:3,5-di-O-methylene-D-mannitol (Manx) and 2,3-di-O-methylene-L-threitol will be directly incorporated into PBT. The chemical microstructure and thermal

properties of the resulting bio-based copolyesters will be discussed in detail, and compared to those of the melt polycondensation (MP)-prepared analogous copolyesters.

6.2. Solid-state modification of PBT with cyclic acetalized galactitol and D-mannitol: Influence of composition and chemical microstructure on thermal properties

Summary: Two bicyclic carbohydrate-based diols, 2,3:4,5-di-O-methylene-galactitol (Galx) or 2,4:3,5-di-O-methylene-D-mannitol (Manx), were introduced into the backbone of poly(butylene terephthalate) using the solid-state modification technique (SSM). The resulting copolyesters had a unique block-like chemical microstructure that endows them with superior thermal properties when compared with their random counterparts obtained by melt copolymerization. The materials prepared by SSM displayed higher melting points, crystallization temperatures and crystallinity, due to the presence of long PBT sequences in the copolyester. The glass-transition temperatures also increased upon incorporation of the bicyclic comonomers, this effect being more pronounced for Manx units. The melting points of these block-like copolyesters decreased after melting due to the occurrence of randomization but they remained higher than those of copolyesters prepared from the melt. SSM was demonstrated to be a very suitable technique for the incorporation of rigid monomers into the amorphous phase of PBT leading to bio-based non-random copolyesters with remarkable thermal properties.

Publication derived from this work:

Lavilla, C.; Gubbels, E.; Martínez de Ilarduya, A.; Noordover, B.A.J.; Koning, C.E.; Muñoz-Guerra, S. *Macromolecules* **2013**, *46*, 4335-4345.

6.2.1. Introduction

Poly(butylene terephthalate) (PBT) is a well-known semicrystalline aromatic polyester, characterized by a melting temperature near 225 °C and a high crystallization rate, which is nowadays used in a wide variety of engineering plastic applications (Gallucci and Patel, 2004). There is a current growing interest in increasing the glass-transition temperature (T_g) of PBT to extend its use to new demanding fields like manufacturing of containers for pressurized gaseous beverages. In this regard, various approaches such as reactive blending with more rigid polyesters and melt copolymerization with rigid comonomers have been explored in order to obtain PBT-based copolyesters with enhanced T_g (Denchev and Sarkissova, 1996; Kelsey *et al.*, 2000; Santos and Guthrie, 2006; Lotti *et al.*, 2011). However these copolyesters show a random or almost random chemical microstructure with shorter PBT sequences, and consequently they exhibit a lower melting temperature, crystallization rate and crystallinity with respect to pure PBT.

It would therefore be desirable to prepare PBT copolyesters having a higher T_g but with a crystallizability comparable to that of PBT. This may be achieved using the solid-state modification (SSM) technique, which derives from the solid-state polymerization (SSP) technique traditionally used as a post-polycondensation method for increasing the molecular weight of semicrystalline polymers (Chang, 1970; Fortunato *et al.*, 1981; Paspaspyrides and Vouyiouka, 2009). During SSM a comonomer is incorporated into the backbone of a semicrystalline polymer in the solid state, under an inert gas flow or vacuum at 20-30 °C below the melting temperature (T_m) of the polymer but well above its glass-transition temperature (T_g); under these relatively mild conditions, side or thermal degradation reactions are minimized or even effectively suppressed. The SSM technique takes benefit from the molecular mobility present at temperatures above T_g to insert the comonomer into the mobile amorphous phase of the polyester, whereas the chain segments in the rigid amorphous fraction and the crystalline phase do not participate in the transesterification reactions (Jansen *et al.*, 2005 and 2006). Thus, SSM allows for the exclusive modification of the properties concerning the amorphous phase and hence, the crystallization behavior of the resulting copolymers should be quite comparable with that of the starting material. Jansen *et al.* have reported on the incorporation of 2,2-bis-[4-(2-hydroxyethoxy)phenyl]propane, bis(2-hydroxyethyl)terephthalate and 2,2'-biphenyldimethanol into the amorphous phase of PBT by SSM leading to block-like copolyesters with unusual chemical microstructures

and morphologies (Jansen *et al.*, 2005, 2006, 2007 and 2008). Sablong *et al.* have recently used this innovative approach to successfully incorporate the heating sensitive isosorbide into PBT (Sablong *et al.*, 2008).

In order to reduce the use of petrochemicals and to increase the added value of agriculture waste streams, the development of bio-based monomers and polymers are receiving exceptional attention nowadays (Wool and Sun, 2005; Pillai, 2010; Chen and Patel, 2012). Carbohydrates are very prevalent and readily available compounds that may afford a wide variety of monomers suitable for making different classes of polymers (Galbis and García-Martín, 2010; Gandini, 2011). For example, 2,5-furandicarboxylate is regarded as the potential replacement for terephthalic acid in engineering, bottle or coating applications (Gandini *et al.*, 2009; Gomes *et al.*, 2011; Gubbels *et al.*, 2013). Carbohydrate-based difunctional compounds with a bicyclic molecular structure are receiving exceptional attention nowadays as comonomers for linear polycondensation because, in addition to their natural origin, they distinguish by their capacity to provide stiffness to the polymer backbone and to increase therefore the T_g . A well-known example is 1,4:3,6-dianhydro-D-glucitol, known as isosorbide, as well as other dianhydrohexitol derivatives used as monomers in the synthesis of polyesters with interesting properties and enhanced T_g (Sablong *et al.*, 2008; Kricheldorf *et al.*, 2007; Fenouillot *et al.*, 2010). Another family of carbohydrate-based bicyclic monomers, which have recently emerged in the polycondensation field, is that obtained by internal acetalization of carbohydrates. These monomers have shown to be very suitable for the preparation of copolyesters with enhanced T_g values by melt polycondensation (Lavilla *et al.*, 2011 -Subchapter 3.2-, 2012a -Subchapter 5.2-, 2012b -Subchapter 5.4-, 2013a -Subchapter 4.3- and 2013b -Subchapter 3.4-; Japu *et al.*, 2012).

In this work, two bicyclic acetalized carbohydrate-based diols, 2,3:4,5-di-O-methylene-galactitol (Galx) and 2,4:3,5-di-O-methylene-D-mannitol (Manx), have been incorporated into PBT via solid-state modification, leading to copolyesters with enhanced T_g values and a retained melting behavior. PBT appears to be a very convenient aromatic polyester to carry out the present study due to its relatively low T_m compared to PET, which allows the application of the SSM technique at lower temperatures. Galx is obtained by acetalization of galactaric acid with paraformaldehyde and subsequent reduction; the centrosymmetric structure of Galx consists of two non-fused 1,3-dioxolane rings with the two primary hydroxyl groups in *exo* positions. Manx is obtained by acetalization of 1,6-di-O-benzoyl-D-mannitol followed by hydrolysis of the benzoxy

groups; Manx consists of two fused 1,3-dioxane rings and possesses a twofold axis of symmetry, bearing two *exo* primary hydroxyl groups free for reaction. The synthesis, chemical microstructure and thermal properties of the copolyesters will be studied and discussed in detail. Moreover, their properties will be compared with those displayed by random copolyesters with similar compositions prepared by melt polycondensation (MP). We will show that SSM is a viable method for preparing copolyesters from carbohydrate-based monomers with unique chemical microstructures and superior thermal properties.

6.2.2. Experimental section

6.2.2.1. Materials

2,3:4,5-di-*O*-methylene-galactitol was synthesized following the procedure reported by Burden *et al.* (Burden *et al.*, 1975). 2,4:3,5-di-*O*-methylene-*D*-mannitol was synthesized following the procedure recently reported by Lavilla *et al.* (Lavilla *et al.*, 2012b -Subchapter 5.4-). PBT was a kind gift from DSM (Geleen, the Netherlands). The catalyst dibutyl tin oxide (DBTO, 98%) was purchased from Sigma-Aldrich. Deuterated chloroform (CDCl₃, 99.8% atom D) and deuterated trifluoroacetic acid (TFA-*d*, 99% atom D) were obtained from Cambridge Isotope Laboratories. Solvents used for purification and characterization were purchased from Biosolve (Valkenswaard, the Netherlands) and they all were of either technical or high-purity grade. All chemicals were used as received unless stated otherwise.

6.2.2.2. General methods

¹H and ¹³C NMR spectra were recorded on a Bruker AMX-300 spectrometer at 25.0 °C operating at 300.1 and 75.5 MHz, respectively. Samples were dissolved in a mixture of deuterated chloroform and trifluoroacetic acid (9:1), and spectra were internally referenced to tetramethylsilane (TMS). About 10 and 50 mg of sample dissolved in 1 mL of solvent were used for ¹H and ¹³C NMR, respectively. Sixty-four scans were acquired for ¹H and 1,000-10,000 for ¹³C with 32 and 64-K data points as well as relaxation delays of 1 and 2 s, respectively. Size-exclusion chromatography (SEC) was performed on a system equipped with a Waters 1515 Isocratic HPLC pump, a Waters 2414 refractive index detector (40 °C), a Waters 2707 autosampler, and a PSS PFG guard column followed by a 2PFG-linear-XL (7 μm, 8·300 mm) columns in series at 40 °C. HFIP with

potassium trifluoroacetate ($3 \text{ g}\cdot\text{L}^{-1}$) was used as eluent at a flow rate of $0.8 \text{ mL}\cdot\text{min}^{-1}$. The molecular weights were calculated against polymethyl methacrylate standards (Polymer Laboratories, $M_p= 580 \text{ Da}$ up to $M_p= 7.1\cdot 10^6 \text{ Da}$). Differential scanning calorimetry was performed using a DSC Q100 from TA-Instruments. DSC data were obtained from 4 to 6 mg samples at heating/cooling rates of $10 \text{ }^\circ\text{C}\cdot\text{min}^{-1}$ under a nitrogen flow of $50 \text{ mL}\cdot\text{min}^{-1}$. Indium was used as standard for temperature and enthalpy calibration. The glass-transition temperatures were determined at a heating rate of $20 \text{ }^\circ\text{C}\cdot\text{min}^{-1}$. Thermogravimetric analyses were performed under a nitrogen flow of $60 \text{ mL}\cdot\text{min}^{-1}$ at a heating rate of $10 \text{ }^\circ\text{C}\cdot\text{min}^{-1}$, within a temperature range of 25 to $600 \text{ }^\circ\text{C}$, using a TA Q500 equipment. Sample weights of about 5 mg were used in these experiments. X-Ray diffraction (XRD) measurements were performed on a Rigaku Geigerflex Bragg-Brentano Powder Diffractometer using Cu radiation, wavelength 1.54056 \AA , at 40 kV and 30 mA. The scans were performed with 0.02° steps and a dwell time of 3-6 s in the 2θ range from 10° till 35° . The analyses were performed on the crude copolyester samples.

6.2.2.3. Solution preparation of physical mixtures

Physical mixtures of PBT and 2,3:4,5-di-O-methylene-galactitol (Galx) or 2,4:3,5-di-O-methylene-D-mannitol (Manx) were prepared from solution using a common solvent approach. Prior to the preparation, the PBT was dissolved in a 3:1 (v/v) mixture of chloroform and HFIP and precipitated in excess of ethanol in order to remove any titanium-based catalysts. Calculated amounts of the purified PBT ($M_n= 23.3 \text{ kg}\cdot\text{mol}^{-1}$ and $M_w= 47.1 \text{ kg}\cdot\text{mol}^{-1}$, determined by SEC) and Galx or Manx were dissolved in HFIP and dibutyl tin oxide (DBTO, 0.36% molar with respect to PBT) was used as catalyst. As an example, the preparation of the physical mixture for the $^{SSM}\text{PB}_{86}\text{Galx}_{14}\text{T}$ copolyester (83.3/16.7 butanediol/Galx molar feed ratio) is described. 1.3640 g PBT (6.20 mmol), 0.2554 g Galx (1.24 mmol) and 0.0056 g DBTO (0.022 mmol) were dissolved in 10 mL HFIP at $55 \text{ }^\circ\text{C}$. After complete dissolution of all compounds the HFIP was distilled off. As soon as the material started to precipitate, a vacuum of 190-300 mbar was applied to complete the removal of HFIP. Finally, the obtained lump residue was dried under vacuum for 24 h, cooled in liquid nitrogen and subsequently ground into powder using an IKA A11 Basic Analytical mill. This powder was subsequently dried under vacuum for a period of 24 h. The molecular weight of the polymer in the mixture was then checked to ascertain that no undesirable reactions such as trans-esterification or degradation occurred during the preparation procedure. Different molar ratios of PBT and either Galx or Manx were used in order to obtain copolyesters with different compositions.

6.2.2.4. Solid-state modification (SSM) of PBT

The solid-state modification of PBT was performed in a reactor comprising a glass tube (inner diameter= 2.4 cm) with a sintered glass plate at the bottom. A heat exchange glass coil (inner diameter= 0.5 mm) surrounded the reactor and entered the inner glass tube at the bottom just below the glass plate (see Annex G). The nitrogen gas was heated by passing through this coil prior to entering the reactor. The nitrogen flow was controlled by a flow-meter. The procedure described below was used for both PBT/Galx and PBT/Manx mixtures. Typically, 0.4 g of a powdered PBT/diol mixture was placed on the sintered glass plate. The powder was fixed by addition of glass pearls (diameter= 2 mm) on top of the powder, and the reactor was purged with a nitrogen flow of $0.5 \text{ L}\cdot\text{min}^{-1}$ during 30 min. The SSM reactions were carried out at temperatures between 160 and 175 °C, and molecular weights were estimated as function of reaction time using SEC. After completion of the reaction, the reactor was gradually cooled down to room temperature by purging nitrogen through the reactor, and the obtained polymer was dried under vacuum. The Galx or Manx PBT copolyesters obtained via SSM are abbreviated as $^{\text{SSM}}\text{PB}_x\text{Gal}_y\text{T}$ and $^{\text{SSM}}\text{PB}_x\text{Man}_y\text{T}$, respectively, where x and y are the mole percentages (mol%) of 1,4-butanediol and either Galx or Manx, respectively, in the resulting copolyester.

$^{\text{SSM}}\text{PB}_x\text{Gal}_y\text{T}$ copolyesters recipe. All Galx-based copolyesters were obtained by a similar procedure, with experimental conditions slightly differing for each composition.

$^{\text{SSM}}\text{PB}_{91}\text{Gal}_9\text{T}$. 160 °C for 6 h and at 170 °C for 15 h under a $0.5 \text{ L}\cdot\text{min}^{-1}$ nitrogen flow.

$^{\text{SSM}}\text{PB}_{89}\text{Gal}_{11}\text{T}$. 160 °C for 6 h and at 170 °C for 15 h under a $0.5 \text{ L}\cdot\text{min}^{-1}$ nitrogen flow, and at 175 °C for 0.5 h under a $1 \text{ L}\cdot\text{min}^{-1}$ nitrogen flow.

$^{\text{SSM}}\text{PB}_{86}\text{Gal}_{14}\text{T}$. 160 °C for 6 h and at 170 °C for 15 h under a $0.5 \text{ L}\cdot\text{min}^{-1}$ nitrogen flow, and at 175 °C for 1 h under a $1 \text{ L}\cdot\text{min}^{-1}$ nitrogen flow.

$^{\text{SSM}}\text{PB}_{81}\text{Gal}_{19}\text{T}$. 160 °C for 6 h and at 170 °C for 15 h under a $0.5 \text{ L}\cdot\text{min}^{-1}$ nitrogen flow, and at 175 °C for 2 h under a $1 \text{ L}\cdot\text{min}^{-1}$ nitrogen flow.

$^{\text{SSM}}\text{PB}_{78}\text{Gal}_{22}\text{T}$. 160 °C for 6 h and at 170 °C for 15 h under a $0.5 \text{ L}\cdot\text{min}^{-1}$ nitrogen flow, and at 175 °C for 3 h under a $1 \text{ L}\cdot\text{min}^{-1}$ nitrogen flow.

***SSM* PB₇₁Galx₂₉T.** 160 °C for 6 h and at 170 °C for 15 h under a 0.5 L·min⁻¹ nitrogen flow, and at 175 °C for 4 h under a 1 L·min⁻¹ nitrogen flow.

NMR characterization of *SSM* PB_xGalx_yT copolyesters. ¹H NMR (300.1 MHz, CDCl₃/TFA), δ (ppm): 8.1 (s, 4H, ArH), 5.2 and 5.1 (2s, y·4H, OCH₂O), 4.7 (m, y·2H, OCH₂CH), 4.6 (m, y·4H, OCH₂CH), 4.5 (t, x·4H, OCH₂CH₂), 4.1 (m, y·2H, OCH₂CHCH), 2.0 (t, x·4H, OCH₂CH₂). ¹³C NMR (75.5 MHz, CDCl₃/TFA), δ (ppm): 168.3 (CO), 167.5 (CO), 134.2-133.4, 130.4, 130.2, 95.7, 77.9, 76.7, 66.2, 65.3, 25.1.

***SSM* PB_xManx_yT copolyesters recipe.** All Manx-based copolyesters were obtained by a similar procedure, with experimental conditions slightly differing for each composition.

***SSM* PB₉₂Manx₈T.** 160 °C for 6 h and at 170 °C for 15 h under a 0.5 L·min⁻¹ nitrogen flow, and at 175 °C for 1 h under a 1 L·min⁻¹ nitrogen flow.

***SSM* PB₈₈Manx₁₂T.** 160 °C for 6 h and at 170 °C for 15 h under a 0.5 L·min⁻¹ nitrogen flow, and at 175 °C for 2 h under a 1 L·min⁻¹ nitrogen flow.

***SSM* PB₈₆Manx₁₄T.** 160 °C for 6 h and at 170 °C for 15 h under a 0.5 L·min⁻¹ nitrogen flow, and at 175 °C for 2.5 h under a 1 L·min⁻¹ nitrogen flow.

***SSM* PB₈₂Manx₁₈T.** 160 °C for 6 h and at 170 °C for 15 h under a 0.5 L·min⁻¹ nitrogen flow, and at 175 °C for 3.5 h under a 1 L·min⁻¹ nitrogen flow.

***SSM* PB₇₇Manx₂₃T.** 160 °C for 6 h and at 170 °C for 15 h under a 0.5 L·min⁻¹ nitrogen flow, and at 175 °C for 4.5 h under a 1 L·min⁻¹ nitrogen flow.

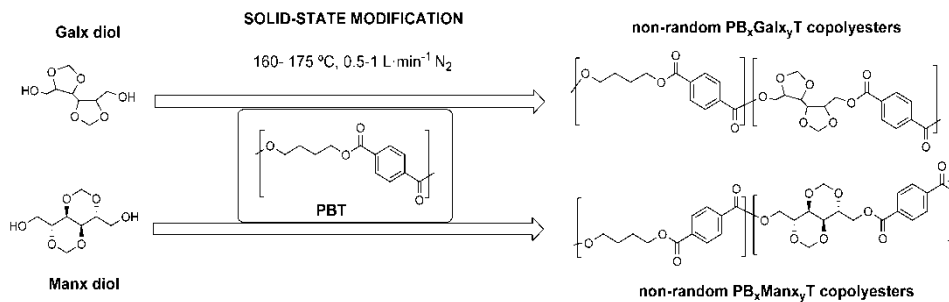
***SSM* PB₇₀Manx₃₀T.** 160 °C for 6 h and at 170 °C for 15 h under a 0.5 L·min⁻¹ nitrogen flow, and at 175 °C for 6 h under a 1 L·min⁻¹ nitrogen flow.

NMR characterization of *SSM* PB_xManx_yT copolyesters. ¹H NMR (300.1 MHz, CDCl₃/TFA), δ (ppm): 8.1 (s, 4H, ArH), 5.2-5.0 (m, y·4H, OCH₂O), 4.9-4.5 (m, y·4H, OCH₂CH), 4.7 (m, y·2H, OCH₂CH), 4.5 (t, x·4H, OCH₂CH₂), 4.3 (m, y·2H, OCH₂CHCH), 2.0 (t, x·4H, OCH₂CH₂). ¹³C NMR (75.5 MHz, CDCl₃/TFA), δ (ppm): 168.3 (CO), 167.5 (CO), 134.2-133.3, 130.4, 130.2, 88.6, 71.4, 66.7, 66.5, 64.4, 25.4.

6.2.3. Results and discussion

6.2.3.1. Polymer synthesis

The synthesis of the partially bio-based $^{SSM}PB_xGalx_yT$ and $^{SSM}PB_xManx_yT$ copolyesters was carried out by solid-state modification (SSM) of PBT with 2,3:4,5-di-O-methylene-galactitol (Galx) and 2,4:3,5-di-O-methylene-D-mannitol (Manx), respectively (Scheme 6.1). The SSM process was conducted at temperatures below the melting point of the PBT crystals, but far above the glass-transition temperature of PBT. At the used temperatures, the chains in the amorphous phase have sufficient mobility to take part in transesterification reactions with either Galx or Manx. Solid-state modification of a semicrystalline homopolyester is typically performed at temperatures 20-40 °C below its melting point and under a nitrogen flow of 2.5-3 L·min⁻¹ (Jansen *et al.*, 2005, 2006, 2007 and 2008; Sablong *et al.*, 2008). However, lower reaction temperatures (50-60 °C below the melting point of PBT) and reduced nitrogen flow (0.5 to 1 L·min⁻¹) were chosen in this study in order to minimize the volatilization of the sugar-based monomers. Although the SSM technique stands out as a copolymerization procedure of general interest, temperatures have to be kept at moderate values in order to avoid excessive volatilization of the entering comonomer and consequent deviation of the copolyester composition respect to the feed. Previous experiments carried out at higher temperatures and shorter reaction times led to copolyesters with lower amounts of the incorporated sugar-based comonomer.



Scheme 6.1. Solid-state modification of PBT leading to $^{SSM}PB_xGalx_yT$ and $^{SSM}PB_xManx_yT$ copolyesters.

Dibutyl tin oxide (DBTO) was the catalyst of choice as replacement of the commonly used titanium (IV) tetrabutoxide (TBT). Previously obtained results in the synthesis of polyesters from these particular sugar-derived bicyclic compounds by melt

polycondensation demonstrated a higher activity of DBTO compared to TBT (Lavilla *et al.*, 2011 -Subchapter 3.2-). This increase in reactivity allows to carry out the reaction at lower temperatures without needing to resort to longer reaction times. Initially, the reactions were left to proceed at 160 °C under a nitrogen flow of 0.5 L·min⁻¹ to incorporate the sugar-based diol into the PBT chain, and later the temperature and gas flow were augmented to 170-175 °C and 1 L·min⁻¹, respectively, to favor end-chain intermolecular reactions and increase the molecular weight of the resulting copolyesters. Longer reaction times at 175 °C were required for copolyesters made from higher amounts of sugar-based diol.

The molecular weight trend was studied as a function of the SSM reaction time (t_{SSM}) by size-exclusion chromatography (SEC). As an example of this trend, the SEC traces as a function of t_{SSM} for the ^{SSM}PB₇₇Man₂₃T copolyester are depicted in Figure 6.1a, whereas the M_n and \mathcal{D} of each chromatogram are plotted as a function of t_{SSM} in Figure 6.1b.

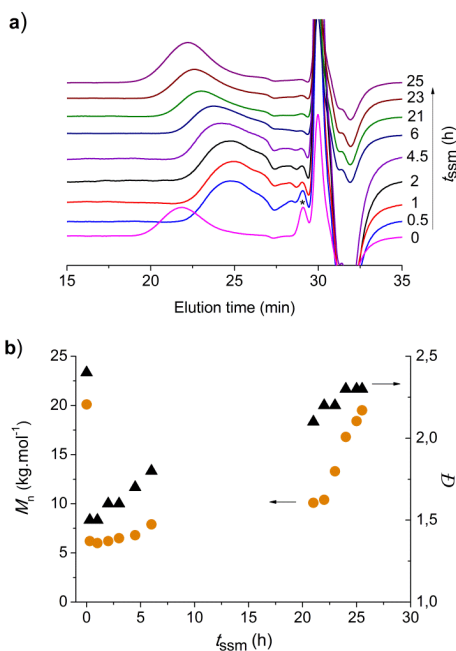


Figure 6.1. (a) SEC chromatograms of ^{SSM}PB₇₇Man₂₃T as function of t_{SSM} (b) Evolution of M_n (circle) and \mathcal{D} (triangle) as function of t_{SSM} . The symbols at $t_{SSM}=0$ correspond to the initial PBT sample.

The SEC chromatogram of the initial PBT/Manx diol mixture ($t_{SSM}=0$ h) shows the unreacted Manx monomer as a sharp peak (marked as * in Figure 6.1a) whereas the

broad peak going out at lower elution time corresponds to the unmodified PBT. After 0.5 h of transesterification, a clear decrease in intensity of the Manx peak was observed while the peak originating from PBT shifted to higher elution times. This shift is indicative for the chain scission of the PBT caused by the the transesterification reaction with Manx. At $t_{SSM} = 1$ h, the polymer was eluted at the highest elution time to subsequently shift back to lower values. Hence, recombination of the polymer chains takes place resulting in higher M_n and M_w values and liberation of 1,4-butanediol, which diffuses out of the polymer particles. All the SSM processes were followed using SEC, with the aim of obtaining $^{SSM}PB_xGal_xT$ and $^{SSM}PB_xMan_xT$ copolyesters with comparable molecular weights, and also similar to molecular weights of samples prepared by MP (abbreviated here as $^{MP}PB_xGal_xT$ and $^{MP}PB_xMan_xT$ copolyesters) (Lavilla *et al.*, 2012a -Subchapter 5.2- and 2012b -Subchapter 5.4-), in order to perform an accurate and reliable comparison of their crystallization behavior. All the SSM reactions were stopped when M_n and M_w values of about 17-20 and 40-44 $kg \cdot mol^{-1}$, respectively, were reached (Table 6.1).

The proton nuclear magnetic resonance (1H NMR) corroborated the expected chemical structure of the copolyesters (Figure 6.2), with all resonances being assigned to the various protons present in the copolyester backbone. Integration of the proton signals arising from 1,4-butanediol and sugar units led to the determination of the composition of the copolyesters. Data provided by this analysis is given in Table 6.1, where it can be seen that the bicyclic monomers Galx and Manx were successfully incorporated into the PBT by SSM. The final compositions of the copolyesters are comparable to the 1,4-butanediol:sugar feed compositions. This is in contrast to reported studies about the SSM of PBT using the sugar-based bicyclic diol isosorbide (Is). Experiments using SSM for the direct incorporation of Is into PBT were unsuccessful; isosorbide could not be incorporated under such conditions. The synthesis of a macrodiol from isosorbide, terephthaloyl chloride and 1,4-butanediol was necessary to incorporate this bicyclic monomer into PBT via SSM (Sabloug *et al.*, 2008). Nevertheless, in this present study the sugar-based diol was successfully incorporated without having to revert to the preparation of a sugar-based macrodiol. The reason for this difference is most probably that the primary hydroxyl groups of Galx and Manx have a much higher reactivity compared to the secondary hydroxyl groups of Is. By varying the PBT/Galx and PBT/Manx feed ratios, six copolyesters with various 1,4-butanediol:sugar ratios were obtained within each series (Table 6.1). The compositions and molecular weights of both SSM series are comparable and are also very similar to the fully random $^{MP}PB_xGal_xT$ and $^{MP}PB_xMan_xT$ copolyesters obtained by polycondensation in the melt.

Table 6.1. Molar composition, molecular weight and microstructure of $^{SSM}PB_xGalx_yT$ and $^{SSM}PB_xManx_yT$ copolyesters.

Copolyester	Molar composition				Molecular weight			Microstructure						
	Feed		Copolyester ^a		M_n^b	M_w^b	\mathcal{D}^b	Dyad content			Number Average Sequence Lengths		Randomness ^c	Randomness ^d
	X_B	X_{Sugar}	X_B	X_{Sugar}				N_{BB}	$N_{BS/SB}$	N_{SS}	n_B	n_S	R	R_c
PB ₉₁ Galx ₉ T	90.9	9.1	91.0	9.0	17,800	41,300	2.3	85.6	12.2	2.2	15.0	1.4	0.80	0.92
PB ₈₉ Galx ₁₁ T	87.0	13.0	88.7	11.3	19,800	43,600	2.2	80.3	16.2	3.5	10.9	1.4	0.79	0.93
PB ₈₆ Galx ₁₄ T	83.3	16.7	86.4	13.6	19,400	44,800	2.3	76.2	18.3	5.5	9.3	1.6	0.73	0.89
PB ₈₁ Galx ₁₉ T	80.0	20.0	80.6	19.4	17,900	43,100	2.4	65.6	24.6	9.8	6.3	1.8	0.71	0.89
PB ₇₈ Galx ₂₂ T	76.9	23.1	77.9	22.1	18,800	44,700	2.4	63.4	24.9	11.7	6.1	1.9	0.68	0.89
PB ₇₁ Galx ₂₉ T	71.4	28.6	71.0	29.0	18,500	44,000	2.4	52.9	29.3	17.8	4.6	2.2	0.67	0.85
PB ₉₂ Manx ₈ T	90.9	9.1	92.0	8.0	18,800	42,000	2.2	85.7	11.4	2.9	16.0	1.5	0.73	0.80
PB ₈₈ Manx ₁₂ T	87.0	13.0	88.2	11.8	17,600	41,300	2.3	78.8	15.4	5.8	11.2	1.7	0.66	0.77
PB ₈₆ Manx ₁₄ T	83.3	16.7	85.9	14.1	18,700	43,900	2.3	72.8	19.7	7.5	8.4	1.8	0.69	0.83
PB ₈₂ Manx ₁₈ T	80.0	20.0	81.5	18.5	17,100	40,800	2.4	66.4	23.1	10.5	6.7	1.9	0.67	0.83
PB ₇₇ Manx ₂₃ T	76.9	23.1	77.0	23.0	19,500	44,800	2.3	59.7	27.8	12.5	5.3	1.9	0.72	0.87
PB ₇₀ Manx ₃₀ T	71.4	28.6	69.7	30.3	17,700	40,700	2.3	52.1	29.2	18.7	4.6	2.3	0.66	0.82

^a Molar composition determined by integration of the ¹H NMR spectra. ^b Number and weight-average molecular weights in g·mol⁻¹ and dispersities measured by SEC in HFIP against PMMA standards. ^c Randomness index of copolyesters statistically calculated on the basis of the ¹³C NMR analysis. ^d Randomness index of the amorphous fraction of copolyesters, determined using the correction method reported by Jansen *et al.* (Jansen *et al.*, 2005)

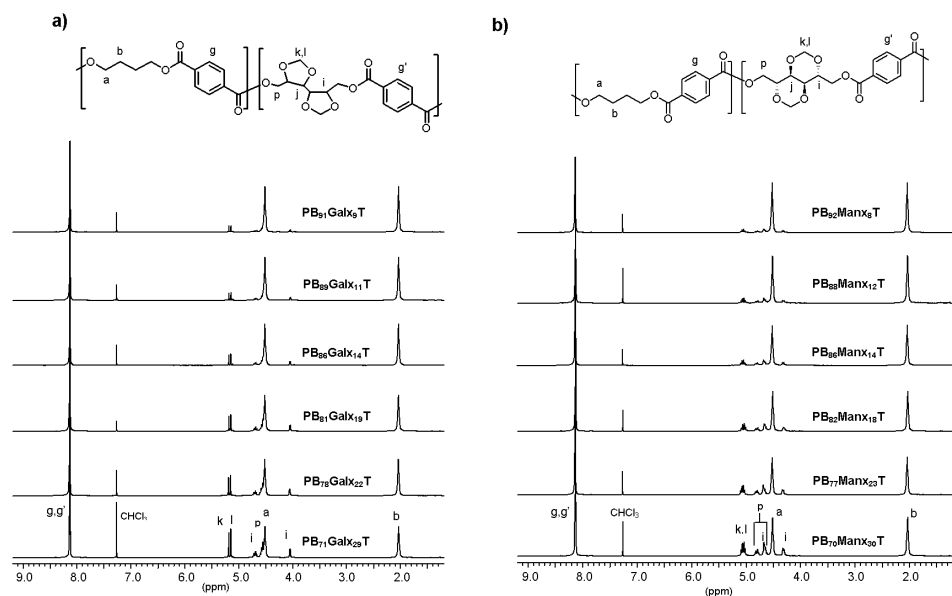


Figure 6.2. ^1H NMR spectra of $^{\text{SSM}}\text{PB}_x\text{Gal}_y\text{T}$ (a) and $^{\text{SSM}}\text{PB}_x\text{Man}_y\text{T}$ (b) copolyesters recorded in CDCl_3/TFA at room temperature.

6.2.3.2. Chemical microstructure

The chemical microstructure of $^{\text{SSM}}\text{PB}_x\text{Gal}_y\text{T}$ and $^{\text{SSM}}\text{PB}_x\text{Man}_y\text{T}$ copolyesters was elucidated using quantitative carbon nuclear magnetic resonance (^{13}C NMR) spectroscopy. The resonances of all magnetically different carbons present in the repeat units of the copolyesters are well resolved in the ^{13}C NMR spectra, which are shown in the Annex G. This is true in particular for the resonances arising from the non-protonated aromatic carbons, which prove to be sensitive to sequence distribution at the level of dyads (Kricheldorf, 1978; Newmark, 1980). The resonance of the quaternary carbon atom has split into four well resolved peaks which are observed in the 133–135 ppm chemical shift interval. These four resonances correspond to the different types of dyads (BB, BS and SB, SS) that are present along the copolyester backbone, and they display peak areas with a dependence on the copolyester composition (Figure 6.3).

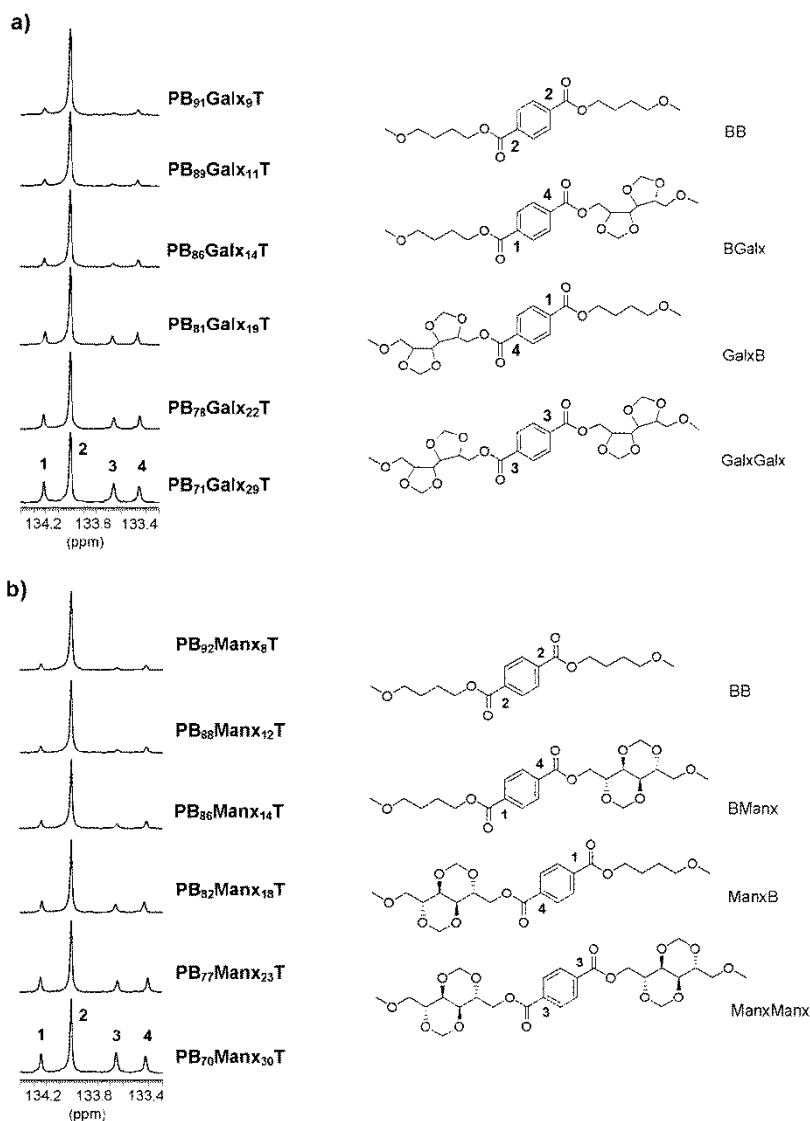


Figure 6.3. ^{13}C NMR signals used for the microstructure analysis of $^{\text{SSM}}\text{PB}_x\text{Gal}_y\text{T}$ (a) and $^{\text{SSM}}\text{PB}_x\text{Man}_y\text{T}$ (b) copolyesters with indication of the dyads to which they are assigned.

The molar fractions (N) of the different dyads in the copolyesters were determined by the integration of their corresponding resonances. Based on these results, the number average sequence lengths n of the butylene-terephthalate (B) and sugar-terephthalate (S) sequences, as well as the degree of randomness (R), are determined for each copolyester by using the equations given below (Yamadera and Murano, 1967;

Randall, 1977). When the R is determined to be in the order of unity the chemical microstructure is fully random. If the R value decreases towards zero, the chemical microstructure becomes more blocky.

$$n_B = (N_{BB} + 0.5 \cdot (N_{BS} + N_{SB})) / (0.5 \cdot (N_{BS} + N_{SB}))$$

$$n_S = (N_{SS} + 0.5 \cdot (N_{BS} + N_{SB})) / (0.5 \cdot (N_{BS} + N_{SB}))$$

$$R = (1/n_B) + (1/n_S)$$

Results from these calculations (Table 6.1) show that the overall sequence distribution in $^{SSM}PB_xGal_xT$ and $^{SSM}PB_xMan_xT$ copolyesters is non-random for the whole composition range used in this study. At low comonomer contents it was challenging to accurately determine the integral values for the comonomers. The R -values of copolyesters with medium to high content in sugar were all close to 0.70, indicating an overall non-random microstructure. Since the crystalline phase does not participate in the SSM process, long PBT sequences are expected to be retained in the copolyester, which probably lead to the observed deviation of the R -values from unity. In order to ascertain information about the chemical microstructure in the amorphous phase, a correction needs to be made for the crystalline phase. Jansen *et al.* have developed a calculation method to adjust the solution ^{13}C NMR peak integral values of the dyad sequences in such a way that only the amorphous fraction is accounted for (Jansen *et al.*, 2005). The chemical microstructures of the total amorphous phases of $^{SSM}PB_xGal_xT$ and $^{SSM}PB_xMan_xT$ copolyesters were determined by using this calculation method, implementing data obtained by differential scanning calorimetry, which will be discussed below. The calculated R -values of the amorphous phase are shown in Table 6.1. It can be observed that all the R -values increase after the correction. This can be easily understood because long PBT sequences have been excluded by this correction. The corrected R -values from the two series are similar, all of them being closer to unity, thus indicating a practically random chemical microstructure in the amorphous phase. The difference in the R -values between the two series before correction is most likely caused by the higher crystallinity of the Galx-based samples. The corrected R -values are depicted in Figure 6.4, together with overall SSM and MP R -values, showing that the chemical microstructures in the amorphous phases of copolyesters prepared by SSM are comparable to those of materials prepared by MP. Hence, by SSM Galx and Manx are incorporated into the mobile amorphous phase in a similar way as through melt polymerization, even though in SSM only the most mobile chain segments are participating in the transesterification reactions. The main conclusion of this study is that,

by using SSM, partially bio-based copolyesters with unique chemical microstructures have been obtained, consisting of a blocky overall microstructure formed by PBT homopolymer sequences in the crystalline phase and a practically random microstructure in the amorphous part.

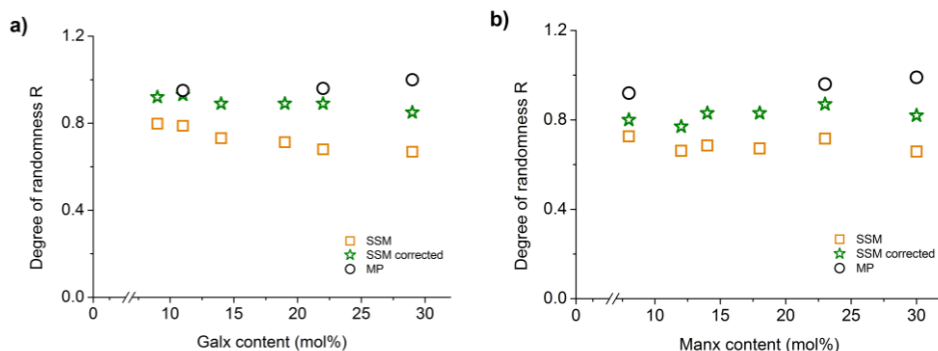


Figure 6.4. Comparison of the degrees of randomness of PB_xGal_xT (a) and PB_xMan_xT (b) copolyesters obtained by SSM and MP (Lavilla *et al.*, 2012a -Subchapter 5.2- and 2012b -Subchapter 5.4-).

6.2.3.3. Thermal properties

The thermal behavior of the PBT-based copolyesters prepared by SSM has been systematically studied by TGA and DSC (Table 6.2). The results obtained from the two series of copolyesters are compared with each other, with the parent homopolymer PBT, and with copolyesters prepared by MP. First, the thermal stability was evaluated by TGA under an inert atmosphere. The TGA traces of the complete sets of copolyesters are comparatively depicted in Annex G. The thermal properties derived from the shown thermograms, *viz.* onset decomposition temperatures ($^{\circ}T_{5\%}$) and temperatures for maximum degradation rate (T_d), are listed in Table 6.2. Decomposition of all $^{SSM}PB_xGal_xT$ and $^{SSM}PB_xMan_xT$ copolyesters takes place in one step, at higher temperatures with respect to neat PBT. Additionally, the residual weight left upon heating at 600 °C is about 3-7% of the initial weight. These results are in full accordance with the enhanced thermal stability observed for the copolyesters prepared by MP compared to PBT (Lavilla *et al.*, 2012a -Subchapter 5.2- and 2012b -Subchapter 5.4-). The valuable conclusion drawn from this comparative thermogravimetric study is that the insertion of sugar-based bicyclic Galx and Manx units into PBT by SSM increases the thermal stability of the PBT-based copolyesters.

Table 6.2. Thermal properties of ^{SSM}PB_xGal_xyT and ^{SSM}PB_xMan_xyT copolyesters.

Copolyester	TGA			DSC								
	°T _{5%} ^a (°C)	T _d ^b (°C)	W ^c (%)	T _g ^d (°C)	First heating ^e		Cooling ^e		Second heating ^e			
					T _m (°C)	ΔH _m (J·g ⁻¹)	T _c (°C)	ΔH _c (J·g ⁻¹)	T _c (°C)	ΔH _c (J·g ⁻¹)	T _m (°C)	ΔH _m (J·g ⁻¹)
PBT	348	385	0	45	225	60.5 ^f	193	52.0	-	-	224	49.0
PB ₉₁ Gal ₉ T	350	390	4	47	218	77.9	180	48.3	-	-	212	46.6
PB ₈₉ Gal ₁₁ T	360	399	3	49	209	71.6	176	43.8	-	-	209	38.3
PB ₈₆ Gal ₁₄ T	350	388	5	50	207	67.5	167	41.2	-	-	205	37.1
PB ₈₁ Gal ₁₉ T	354	391	5	54	208	56.5	143	37.5	-	-	191	26.9
PB ₇₈ Gal ₂₂ T	354	391	4	54	208	55.9	131	32.0	-	-	185	25.4
PB ₇₁ Gal ₂₉ T	354	391	6	57	205	41.1	-	-	121	9.6	169	11.9
PB ₉₂ Man ₈ T	363	399	4	56	211	67.3	183	41.5	-	-	212	41.4
PB ₈₈ Man ₁₂ T	349	388	7	62	210	64.8	170	39.0	-	-	205	32.3
PB ₈₆ Man ₁₄ T	364	401	6	67	208	63.5	158	38.3	-	-	200	30.3
PB ₈₂ Man ₁₈ T	351	389	5	68	207	56.0	140	27.3	-	-	190	27.0
PB ₇₇ Man ₂₃ T	362	402	6	70	206	45.4	121	2.6	139	5.1	181	8.8
PB ₇₀ Man ₃₀ T	354	392	7	76	205	37.7	-	-	-	-	-	-

^a Temperature at which 5% weight loss was observed. ^b Temperature for maximum degradation rate. ^c Remaining weight at 600 °C. ^d Glass-transition temperature taken as the inflection point of the heating DSC traces recorded at 20 °C·min⁻¹ during the 3rd heating run. ^e Melting (T_m) and crystallization (T_c) temperatures, and melting (ΔH_m) and crystallization (ΔH_c) enthalpies measured by DSC at heating/cooling rates of 10 °C·min⁻¹. ^f After applying a similar thermal treatment which was used for the copolyesters the ΔH_m increased to 74.4 J/g.

The DSC analysis revealed that the incorporation of the bicyclic Galx and Manx units by SSM induced significant changes in the glass-transition temperature (T_g) of PBT-based copolyesters (Table 6.2). In the $^{SSM}PB_xGalx_yT$ series, the T_g values steadily augmented as 1,4-butanediol was replaced by Galx units, reaching a value of 57 °C when 29 mol% of Galx was incorporated, and following a trend similar to that observed for $^{MP}PB_xGalx_yT$ copolyesters (Lavilla *et al.*, 2012a -Subchapter 5.2-). Regarding the $^{SSM}PB_xManx_yT$ series, the T_g also increased with increasing amount of incorporated comonomer; in this case the effect of the bicyclic diol on T_g was even more pronounced for all the compositions. A T_g value of 76 °C was reached for a Manx content of 30 mol%. Apparently, the fused bicyclic 1,3-dioxane structure of Manx has a more significant influence on the T_g values than the more flexible structure of Galx, a difference that has also been noticed in copolyesters prepared by MP (Lavilla *et al.*, 2012b -Subchapter 5.4-). These results evidence the effect that the rigid sugar-based comonomer exerts on restricting the mobility of the copolyester chain.

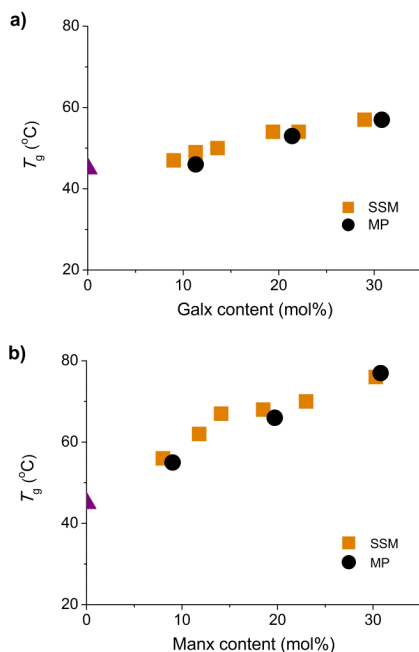


Figure 6.5. Glass-transition temperature versus composition plots for SSM and MP (Lavilla *et al.*, 2012a -Subchapter 5.2- and 2012b -Subchapter 5.4-) copolyesters. (a) PB_xGalx_yT and (b) PB_xManx_yT . The glass-transition temperatures were obtained from the third heating run. The triangle represents the T_g of the homopolymer PBT.

Melting temperatures (T_m) and enthalpies (ΔH_m), and crystallization temperatures (T_c) and enthalpies (ΔH_c) were measured using differential scanning calorimetry (DSC) and are listed in Table 6.2. For illustration, the DSC traces of ${}^{\text{SSM}}\text{PB}_{81}\text{Galx}_{19}\text{T}$, recorded upon heating and cooling, are depicted in Annex G. A decrease in T_m and ΔH_m can be seen when the first and second heating runs are compared, this behavior will be discussed later in this article. All the prepared ${}^{\text{SSM}}\text{PB}_x\text{Galx}_y\text{T}$ and ${}^{\text{SSM}}\text{PB}_x\text{Manx}_y\text{T}$ copolyesters are semicrystalline and exhibit a T_m value exceeding 205 °C in the first heating run. This T_m corresponds to the crystalline portion of the material which did not participate in the SSM reaction. Melting temperature versus composition plots for ${}^{\text{SSM}}\text{PB}_x\text{Galx}_y\text{T}$ and ${}^{\text{SSM}}\text{PB}_x\text{Manx}_y\text{T}$ copolyesters are comparatively depicted in Figure 6.6, together with data of the corresponding copolyesters obtained by MP. Whereas melting temperatures of ${}^{\text{MP}}\text{PB}_x\text{Galx}_y\text{T}$ and ${}^{\text{MP}}\text{PB}_x\text{Manx}_y\text{T}$ sharply decrease with increasing amounts of sugar-based units, the T_m of the copolyesters prepared by SSM did not present such a tendency. Moreover, the difference between the T_m values of materials prepared by SSM and MP is more pronounced as the sugar content increases. These results proved that, by means of SSM, it is possible to prepare sugar-based PBT copolyesters with only moderately decreasing melting temperatures.

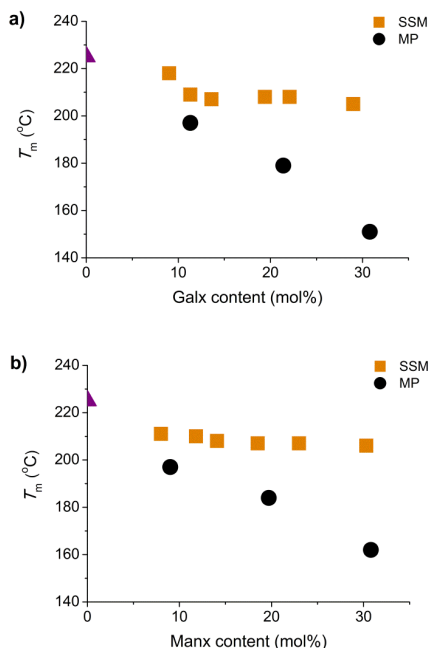


Figure 6.6. Melting temperature versus composition plots for SSM and MP (Lavilla *et al.*, 2012a -Subchapter 5.2- and 2012b -Subchapter 5.4-) copolyesters. (a) $\text{PB}_x\text{Galx}_y\text{T}$ and (b) $\text{PB}_x\text{Manx}_y\text{T}$. The triangle represents the melting temperature of the homopolymer PBT.

The copolyesters obtained by SSM have relatively high melting enthalpies (Table 6.2), especially compared to those prepared by MP (Lavilla *et al.*, 2012a - Subchapter 5.2- and 2012b -Subchapter 5.4-). This increase is due to annealing occurring during the SSM reaction. The results presented in Table 6.2 suggest that small amounts of the monomer present in the first SSM stages could act as a plasticizer, thus increasing the molecular mobility of the polymer chains and favoring annealing. However, a decrease in the melting enthalpy was observed when the amount of sugar-based comonomer was increased further. In order to determine the crystallinity of $^{SSM}PB_xGal_xT$ and $^{SSM}PB_xMan_xT$ copolyesters, to elucidate if co-crystallization is taking place and to complement the DSC data, wide-angle X-ray diffraction (WAXD) was performed on the two series of copolyesters as well as on neat PBT. The powder WAXD profiles are shown in Figure 6.7, and the most prominent Bragg spacings present therein are listed in Table 6.3.

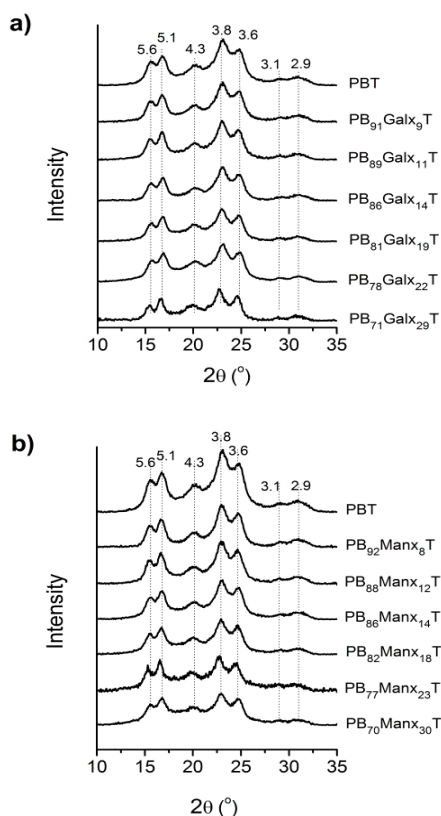


Figure 6.7. Powder WAXD profiles of $^{SSM}PB_xGal_xT$ (a) and $^{SSM}PB_xMan_xT$ (b) copolyesters with indication of d_{hkl} in Å.

Table 6.3. Powder X-ray diffraction data of ^{SSM}PB_xGal_yT and ^{SSM}PB_xMan_yT copolyesters.

Copolyester	d^a (Å)								X_c^b
PB ₉₁ Gal ₉ T	5.6 s	5.1 s	4.3 m	3.8 s	3.6 s	3.1 w	2.9 w	0.71	
PB ₈₉ Gal ₁₁ T	5.6 s	5.1 s	4.3 m	3.8 s	3.6 s	3.1 w	2.9 w	0.67	
PB ₈₆ Gal ₁₄ T	5.6 s	5.1 s	4.3 m	3.8 s	3.6 s	3.1 w	2.9 w	0.66	
PB ₈₁ Gal ₁₉ T	5.6 s	5.1 s	4.3 m	3.8 s	3.6 s	3.1 w	2.9 w	0.58	
PB ₇₈ Gal ₂₂ T	5.6 s	5.1 s	4.3 m	3.8 s	3.6 s	3.1 w	2.9 w	0.56	
PB ₇₁ Gal ₂₉ T	5.6 s	5.1 s	4.3 m	3.8 s	3.6 s	3.1 w	2.9 w	0.46	
PB ₉₂ Man ₈ T	5.6 s	5.1 s	4.3 m	3.8 s	3.6 s	3.1 w	2.9 w	0.66	
PB ₈₈ Man ₁₂ T	5.6 s	5.1 s	4.3 m	3.8 s	3.6 s	3.1 w	2.9 w	0.65	
PB ₈₆ Man ₁₄ T	5.6 s	5.1 s	4.3 m	3.8 s	3.6 s	3.1 w	2.9 w	0.64	
PB ₈₂ Man ₁₈ T	5.6 s	5.1 s	4.3 m	3.8 s	3.6 s	3.1 w	2.9 w	0.57	
PB ₇₇ Man ₂₃ T	5.6 s	5.1 s	4.3 m	3.8 s	3.6 s	3.1 w	2.9 w	0.49	
PB ₇₀ Man ₃₀ T	5.6 s	5.1 s	4.3 m	3.8 s	3.6 s	3.1 w	2.9 w	0.43	

^a Bragg spacings measured in powder diffraction patterns for samples coming directly from synthesis. Intensities visually estimated as follows: m, medium; s, strong; w, weak. ^b Crystallinity index calculated as the quotient of crystalline area and total area. Crystalline and amorphous areas in the X-ray diffraction pattern were quantified using PeakFit v4.12 software.

The PBT pattern is characterized by five prominent reflections at 5.6, 5.1, 4.3, 3.8 and 3.6 Å. Essentially the same pattern in terms of spacing and relative intensities is shared by all ^{SSM}PB_xGal_yT copolyesters, ^{SSM}PB_xMan_yT copolyesters and PBT. These results corroborate that all the copolyesters are semicrystalline, as observed by DSC, and they reveal that the triclinic crystal structure of PBT (Hall, 1984) has been retained in all copolyesters. Furthermore, it can be concluded that co-crystallization of GalxT or ManxT sequences in the PBT crystalline phase does not occur, which was also observed for the analogous PBT-based copolyesters prepared by MP (Lavilla *et al.*, 2012a -Subchapter 5.2- and 2012b -Subchapter 5.4-). The crystallinity index of ^{SSM}PB_xGal_yT and ^{SSM}PB_xMan_yT was estimated as the quotient between the crystalline area and the total area of the X-ray diffraction pattern (Table 6.3). It is clear from the data presented in Table 6.3 that the crystallinity index decreases with increasing sugar content. This decrease is remarkable because this would suggest that the crystalline fraction of the copolyester is not fully retained along the SSM process. It has been reported by Jansen

et al. that when the comonomer shows some affinity with the amorphous PBT this can lead to swelling of the amorphous phase (Jansen *et al.*, 2007). This swelling causes the rigid amorphous fraction (RAF) to become mobile enough to participate in the SSM process. Once all the RAF has become mobile, the swelling can also affect to the crystallites themselves, which also become available to the trans-reactions. This process would be favored by increasing concentration of the comonomer and would lead to a decrease in crystallinity, as observed.

For both $^{SSM}PB_xGal_xT$ and $^{SSM}PB_xMan_xT$ systems, crystallization temperatures (T_c) and enthalpies (ΔH_c) diminished when the amount of sugar-based comonomer was increased, so the copolyesters did not crystallize from the melt for sugar-contents above 23%. Nevertheless, when the results (Table 6.2) are compared with those obtained for copolyesters with similar compositions prepared by MP (Lavilla *et al.*, 2012a -Subchapter 5.2- and 2012b -Subchapter 5.4-), the materials obtained by SSM showed higher T_c and ΔH_c values. This was expected because the long PBT sequences still present after SSM facilitate the crystallizability of the materials. The aforementioned data clearly shows the good crystallizability of the two series of copolyesters prepared by SSM but it should be noted that the Galx-based copolyesters are more readily crystallizable than their Manx counterparts; the 'undercooling' (ΔT) values ($\Delta T = T_m - T_c$) required for crystallization are significantly lower for the formers. The fused bicyclic structure of Manx is much less flexible than the non-fused bicyclic skeleton of Galx and therefore subjected to more hindrance during the crystallization process. The main conclusion derived from these results is that by solid-state modification of PBT with the sugar-based bicyclic diols Galx and Manx, not only copolyesters with enhanced T_g values compared to pure PBT are obtained, reaching similar values to the MP ones, but also that these materials exhibit much higher T_m and T_c values than the copolyesters obtained by MP, clearly showing the advantage of using SSM as copolymerization method.

As mentioned above, when $^{SSM}PB_xGal_xT$ and $^{SSM}PB_xMan_xT$ samples were crystallized from the melt and were reheated, the melt crystallized polymers displayed lower T_m and ΔH_m values than the respective pristine samples (Table 6.2). Such incomplete recovery of the thermal properties suggests the occurrence of further transesterification reactions during the time in the melt, which lead to a more random chemical microstructure. In order to investigate this phenomenon, $^{SSM}PB_{82}Man_{18}T$ was subjected to a thermal treatment consisting of holding the copolyester in the melt at 260

°C for predetermined times (0, 10, 20, 30 min), and their chemical microstructure and thermal properties were then evaluated by ^{13}C NMR and DSC, respectively (Figure 6.8).

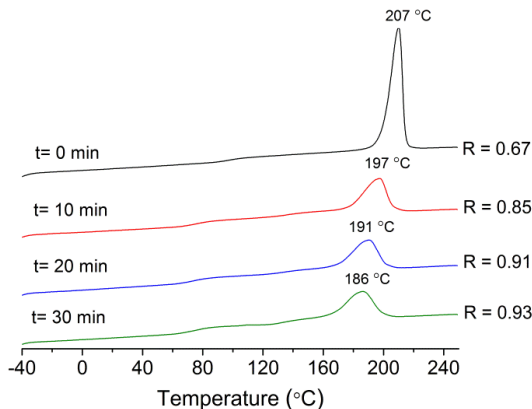


Figure 6.8. DSC traces from the first heating run of $^{\text{SSM}}\text{PB}_{82}\text{Manx}_{18}\text{T}$ copolyester as function of the residence time in the melt, with indication of their degrees of randomness R .

Upon the thermal treatment, the R values progressively increased indicating that copolyesters randomized by transesterification. This randomization process must be catalyzed by the DBTO, which was added to the PBT/sugar derivatives physical mixtures and was not removed from the material. The randomization phenomenon is therefore the reason for the difference in melting behavior observed during the first and second heating run in the DSC experiments. Nevertheless, it should be noticed that both T_m and ΔH_m recorded during the second heating run of the samples prepared by SSM are still higher than those obtained during first heating of PBT-based copolyesters prepared by MP with similar compositions. This means that although randomization of the blocky chemical microstructure of the SSM prepared copolyesters does occur to some extent during melting, it is not so extensive as to yield fully random copolyesters.

6.2.4. Conclusions

Two series of partially bio-based copolyesters were prepared by solid-state modification (SSM) of PBT with the sugar-based bicyclic diols 2,3:4,5-di-*O*-methylene-galactitol (Galx) or 2,4:3,5-di-*O*-methylene-*D*-mannitol (Manx). In contrast to other sugar-based diols used for SSM such as isosorbide, these diols could be inserted directly into the PBT chain without previous chemical modification. By taking special care of the

reaction conditions and by following the reaction evolution by SEC, PBT copolyesters with compositions similar to the corresponding feeds and with relatively high molecular weights were obtained. In this regard, these copolyesters are similar to those obtained by melt polycondensation (MP) using mixtures of comonomers. Since during the SSM the sugar comonomer is inserted specifically in the amorphous phase of PBT, the chemical microstructure of the SSM copolyesters consisted of a homogenous sequence of PBT attached to a more or less random sequence of butylene and sugar terephthalate units, which contrasts with the fully random microstructure displayed by copolyesters obtained by MP. However, the blocky microstructure of the SSM copolyesters randomized after melting in an extension dependable of the time at which the material was maintained in the melt.

As it is known to happen for MP copolyesters, the effect of inserting the bicyclic sugar-based diols into the PBT by SSM afforded copolyesters displaying higher thermal stability and also a noteworthy increase in T_g values, the effect being more pronounced for the fused Manx unit than for the non-fused Galx unit. Notwithstanding, the unique blocky microstructure generated by SSM provided the copolyesters obtained by this technique with remarkable thermal properties without parallelism in those prepared by MP. Specifically, SSM copolyesters displayed higher T_m and T_c values and a much higher crystallinity compared to MP copolyesters with similar chemical compositions.

6.2.5. References

- Burden, I.J.; Stoddart J.F. *J Chem Soc Perk T 1* **1975**, 675-682.
- Chang, T. *Polym. Eng. Sci.* **1970**, *10*, 364-368.
- Chen, G.Q.; Patel, M.K. *Chem. Rev.* **2012**, *112*, 2082-2099.
- Denchev, Z.; Sarkissova, M. *Macromol. Chem. Phys.* **1996**, *197*, 2869-2887.
- Fenouillot, F.; Rousseau, A.; Colomines, G.; Saint-Loup, R.; Pascault, J.P. *Prog. Polym. Sci.* **2010**, *35*, 578-622.
- Fortunato, B.; Pilati, F.; Manaresi, P. *Polymer* **1981**, *22*, 655-657.
- Galbis, J.A.; García-Martín, M.G. *Chem. Curr. Top.* **2010**, *295*, 147-176.

Gallucci, R.R.; Patel, B.R. *Poly(butylene terephthalate)*. In: Scheirs, J.; Long, T.E.; Eds. *Modern Polyesters, Chemistry and Technology of Polyesters and Copolyesters*; John Wiley & Sons: Chichester, **2004**, pp. 293-321.

Gandini, A.; Coelho, D.; Gomes, M.; Reis, B.; Silvestre, A.J.D. *J. Mater. Chem.* **2009**, *19*, 8656-8664.

Gandini, A. *Green Chem.* **2011**, *13*, 1061-1083.

Gomes, M.; Gandini, A.; Silvestre, A.J.D.; Reis, B. *J. Polym. Sci., Polym. Chem.* **2011**, *49*, 3759-3768.

Gubbels, E.; Jasinska-Walc, L.; Koning, C.E. *J. Polym. Sci., Polym. Chem.* **2013**, *51*, 890-898.

Hall, I.H. *The Determination of the Structures of Aromatic Polyesters from their Wide-angle X-Ray Diffraction Patterns*. In: Hall, I.H.; Ed. *Structure of Crystalline Polymers*; Elsevier Applied Science: UK, **1984**, pp. 39-78.

Jansen, M.A.G.; Goossens, J.G.P.; de Wit, G.; Bailly, C.; Schick, C.; Koning, C.E. *Macromolecules* **2005**, *38*, 10658-10666.

Jansen, M.A.G.; Goossens, J.G.P.; de Wit, G.; Bailly, C.; Koning, C.E. *Anal. Chim. Acta* **2006**, *557*, 19-30.

Jansen, M.A.G.; Wu, L.H.; Goossens, J.G.P.; de Wit, G.; Bailly, C.; Koning, C.E. *J. Polym. Sci., Polym. Chem.* **2007**, *45*, 882-899.

Jansen, M.A.G.; Wu, L.H.; Goossens, J.G.P.; de Wit, G.; Bailly, C.; Koning, C.E.; Portale, G. *J. Polym. Sci., Polym. Chem.* **2008**, *46*, 1203-1217.

Japu, C.; Alla, A.; Martínez de Ilarduya, A.; García-Martín, M.G.; Benito, E.; Galbis, J.A.; Muñoz-Guerra, S. *Polym. Chem.* **2012**, *3*, 2092-2101.

Kelsey, D.R.; Scardino, B.M.; Grebowicz, J.S.; Chuah, H.H. *Macromolecules* **2000**, *33*, 5810-5818.

Kricheldorf, H.R. *Makromol. Chem.* **1978**, *179*, 2133-2143.

Kricheldorf, H.R.; Behnken, G.; Sell, M. *J. Macromol. Sci. Pure Appl. Chem.* **2007**, *44*, 679-684.

Lavilla, C.; Alla, A.; Martínez de Ilarduya, A.; Benito, E.; García-Martín, M.G.; Galbis, J.A.; Muñoz-Guerra, S. *Biomacromolecules* **2011**, *12*, 2642-2652. **-Subchapter 3.2-**

Lavilla, C.; Alla, A.; Martínez de Ilarduya, A.; Benito, E.; García-Martín, M.G.; Galbis, J.A.; Muñoz-Guerra, S. *Polymer* **2012**, *53*, 3432-3445. (2012a) **-Subchapter 5.2-**

Lavilla, C.; Martínez de Ilarduya, A.; Alla, A.; García-Martín, M.G.; Galbis, J.A.; Muñoz-Guerra, S. *Macromolecules* **2012**, *45*, 8257-8266. (2012b) **-Subchapter 5.4-**

- Lavilla, C.; Martínez de Ilarduya, A.; Alla, A.; Muñoz-Guerra, S. *Polym. Chem.* **2013**, *4*, 282-289. (2013a) **-Subchapter 4.3-**
- Lavilla, C.; Alla, A.; Martínez de Ilarduya, A.; Muñoz-Guerra, S. *Biomacromolecules* **2013**, *14*, 781-793. (2013b) **-Subchapter 3.4-**
- Lotti, N.; Colonna, M.; Fiorini, M.; Finelli, L.; Berti, C. *Polymer* **2011**, *52*, 904-911.
- Newmark, R.A. *J. Polym. Sci.* **1980**, *18*, 559-563.
- Papaspyrides, C.D.; Vouyiouka, S.N. *Fundamentals of Solid State Polymerization*. In: Papaspyrides, C.D.; Vouyiouka, S.N.; Eds. *Solid State Polymerization*; John Wiley & sons: Hoboken, **2009**, pp 2-28.
- Pillai, C.K.S. *Design. Monom. Polym.* **2010**, *13*, 87-121.
- Randal, J.C. *Polymer Sequence Determination*; Academic Press: New York, **1977**, pp. 41-69.
- Sablong, R.; Duchateau, R.; Koning, C.E.; de Wit, G.; van Es, D.; Koelewijn, R.; van Haveren, J. *Biomacromolecules* **2008**, *9*, 3090-3097.
- Santos, J.M.R.C.A.; Guthrie, J.T. *J. Mater Chem.* **2006**, *16*, 237-245.
- Wool, R.; Sun, S. *Biobased Polymers and Composites*; Academic Press: New York, **2005**.
- Yamadera, Y.; Murano, M. *J. Polym. Sci., Polym. Chem.* **1967**, *5*, 2259-2268.

6.3. Carbohydrate-based PBT copolyesters from a cyclic diol derived from naturally occurring tartaric acid: A comparative study regarding melt polycondensation and solid-state modification

Summary: 2,3-di-O-methylene-L-threitol (Thx) is a cyclic carbohydrate-based diol prepared by acetalization and subsequent reduction of the naturally occurring tartaric acid. The structure of Thx consists of a 1,3-dioxolane ring with two attached primary hydroxyl groups. Two series of partially bio-based poly(butylene terephthalate) (PBT) copolyesters were prepared using Thx as comonomer by melt polycondensation (MP) and solid-state modification (SSM). Fully random copolyesters were obtained after MP using mixtures of Thx and 1,4-butanediol in the reaction with dimethyl terephthalate. Copolyesters with a unique block-like chemical microstructure were prepared by incorporation of Thx into the amorphous phase of PBT by SSM. The partial replacement of 1,4-butanediol units by Thx resulted in satisfactory thermal stabilities and gave rise to an increase in T_g values, and this effect was comparable for copolyesters prepared by MP and SSM. The partially bio-based materials prepared by SSM displayed higher melting points and easier crystallization from the melt, due to the presence of long PBT sequences in the backbone of the copolyester. The incorporation of Thx in the copolyester backbone enhanced the hydrolytic degradation of the materials with respect to the degradation of pure PBT.

Publication derived from this work:

Lavilla, C.; Gubbels, E.; Alla, A.; Martínez de Ilarduya, A.; Noordover, B.A.J.; Koning, C.E.; Muñoz-Guerra, S. (Submitted 2013)

6.3.1. Introduction

Nature produces approx. $140 \cdot 10^9$ tons of carbohydrates from carbon dioxide and water annually, making these compounds the most abundant organic materials on earth. Humanity only uses 4% of this feedstock for food and non-food purposes (Lichtenthaler, 2010). Therefore this class of compounds is an extraordinary source of chemicals, capable of providing a wide variety of building blocks for polycondensates (Wool and Sun, 2005; Galbis and García-Martín, 2008; Pillai, 2010). Thus, the development of carbohydrate-based polycondensates has the potential to significantly reduce the amount of petroleum consumed for polymer production. However, there are only a few examples of commercially available carbohydrate-derived polymers, which is mainly due to the relatively high price of these materials compared to their petroleum-based counterparts. Another limitation of carbohydrates as building blocks in the synthesis of linear polycondensates is their inherent multifunctionality. Although some linear polycondensates have been synthesized using carbohydrate-based monomers bearing pendant hydroxyl groups (Kiely *et al.*, 1994 and 2000), the most commonly used strategy is blocking them with stable protecting groups, and thus retaining only two reactive functions to carry out linear polycondensation (Galbis and García-Martín, 2010; Gandini, 2011).

Among carbohydrates, tartaric acid (2,3-dihydroxy-succinic acid) stands out by its easy accessibility and relative simplicity in terms of its molecular structure. This hydroxylated aldaric acid occurs in many plants and fermented grape juice (Blair and DeFratis, 2000). From tartaric acid, various monomers have been prepared and explored as carbohydrate-based building blocks in the synthesis of polycondensates, usually with the pendant hydroxyl groups protected in several forms (Alla *et al.*, 2000 and 2005; Kint *et al.*, 2001; Marín and Muñoz-Guerra, 2008; Japu *et al.*, 2013). Aromatic polyesters are used in a wide array of applications due to their high performance as thermoplastic materials with good thermal and mechanical properties (Gallucci and Patel, 2004). The properties of such aromatic polyesters can be adjusted by copolymerization, preferably with bio-based comonomers, in order to make these materials more environmentally friendly and more sustainable (Li *et al.*, 2012). However, the incorporation of bio-based acyclic monomers usually results in a lowered glass-transition temperature and reduced stiffness (Kint *et al.*, 2001; Zamora *et al.*, 2005; Li *et al.*, 2012). For example, 2,3-di-*O*-methyl-*L*-threitol, an acyclic diol with its secondary hydroxyl groups protected as methoxy ethers, has been employed in the preparation of aromatic

copolyesters (Kint *et al.*, 2001). On the other hand, carbohydrate-derived monomers with a cyclic structure distinguish themselves by providing polycondensates with improved properties, especially those related to polymer chain stiffness (Kricheldorf *et al.*, 2007; Gandini, 2009; Fenouillot *et al.*, 2010; Gubbels *et al.*, 2013a; Lavilla *et al.*, 2013a -Subchapter 4.3-). Two cyclic acetalized carbohydrate-based diols derived from tartaric acid, *i.e.* 2,3-di-*O*-isopropylidene-*L*-threitol and 2,3-di-*O*-methylene-*L*-threitol, with the pendant functional groups protected as isopropylidene acetal and methylene acetal, respectively, have been recently employed in the preparation of polyurethanes (Marín and Muñoz-Guerra, 2008).

In this work, the cyclic diol 2,3-di-*O*-methylene-*L*-threitol (Thx) is employed as building block for the preparation of poly(butylene terephthalate) (PBT) copolyesters. Whereas isopropylidene acetals are known to be unstable and easily removed in acidic media (Marín and Muñoz-Guerra, 2008; Gómez and Varela, 2009; Dhamaniya and Jacob, 2010), the protection by methylene acetal groups allows for the preparation of polycondensates with a satisfactory stability during processing and handling, since the methylene acetal rings are much more resistant to opening (Lavilla and Muñoz-Guerra, 2012 -Subchapter 5.3-; Lavilla *et al.*, 2013b -Subchapter 3.4-). Two different techniques, *i.e.* melt polycondensation (MP) and solid-state modification (SSM), will be used to prepare the novel bio-based copolyesters from the aforementioned Thx. The widely known MP technique consists of reacting the monomers Thx, 1,4-butanediol, and dimethyl terephthalate in the melt, *viz.* in two successive stages involving transesterification and polycondensation reactions. The SSM technique (Jansen *et al.*, 2006) is based on the same principles as the commonly used solid-state polycondensation (SSP), which is usually employed to increase the molecular weight of semicrystalline polyesters and polyamides by transesterification and transamidation reactions, respectively (Vouyiouka *et al.*, 2005; Papaspyrides and Vouyiouka, 2009). Both SSM and SSP techniques are carried out at a reaction temperature just (20-30 °C) below the melting temperature of the crystalline phase of the polymer, and they take advantage of the molecular mobility in the amorphous phase of the polymer relatively far above T_g . During the SSM process, the monomer Thx is inserted exclusively into the mobile amorphous fraction (MAF) of poly(butylene terephthalate); mobility restrictions prevent the crystalline phase and the rigid amorphous fraction (RAF) from taking part in transesterification reactions (Jansen *et al.*, 2005; Gubbels *et al.*, 2013b; Lavilla *et al.*, 2013c -Subchapter 6.2-). The synthesis, chemical microstructure and thermal properties of the resulting MP- and SSM-prepared bio-based copolyesters will be studied and

discussed in detail. Moreover, a hydrolytic degradation study will be carried out to evaluate the influence of the Thx units on the degradation of the copolyester, and to ascertain the stability of the acetal group forming part of the carbohydrate-based residues.

6.3.2. Experimental section

6.3.2.1. Materials

The cyclic diol 2,3-di-*O*-methylene-*L*-threitol (Thx) was synthesized from commercially available dimethyl *L*-tartrate, as described elsewhere (Marín and Muñoz-Guerra, 2008). The reagents 1,4-butanediol (99%), dimethyl terephthalate (99+%) and the catalyst dibutyl tin oxide (DBTO, 98%) were purchased from Sigma-Aldrich. PBT was a kind gift from DSM. Deuterated chloroform (CDCl_3 , 99.8% atom D) and deuterated trifluoroacetic acid (TFA-*d*, 99% atom D) were obtained from Cambridge Isotope Laboratories. Solvents used for purification and characterization were purchased from Panreac and Biosolve and these were all of either technical or high-purity grade. All chemicals were used as received unless stated otherwise.

6.3.2.2. General methods

^1H and ^{13}C NMR spectra were recorded on a Bruker AMX-300 spectrometer at 25.0 °C operating at 300.1 and 75.5 MHz, respectively. Samples were dissolved in a mixture of deuterated chloroform and deuterated trifluoroacetic acid (9:1), and spectra were internally referenced to tetramethylsilane (TMS). Approximately 10 and 50 mg of sample dissolved in 1 mL of the solvent mixture were used for ^1H and ^{13}C NMR, respectively. Sixty-four scans were acquired for ^1H and 1,000-10,000 for ^{13}C with 32 and 64-K data points as well as relaxation delays of 1 and 2 s, respectively. Size-exclusion chromatography (SEC) was performed on a system equipped with a Waters 1515 Isocratic HPLC pump, a Waters 2414 refractive index detector working at 40 °C, a Waters 2707 autosampler, and a PSS PFG guard column followed by a 2PFG-linear-XL (7 μm , 8·300 mm) columns in series at 40 °C. HFIP with potassium trifluoroacetate (3 $\text{g}\cdot\text{L}^{-1}$) was used as eluent at a flow rate of 0.8 $\text{mL}\cdot\text{min}^{-1}$. The molecular weights were calculated against polymethyl methacrylate standards (Polymer Laboratories, $M_p=$ 580 Da up to $M_p=$ 7.1·10⁶ Da). Differential scanning calorimetry (DSC) was performed using a Perkin Elmer DSC Pyris 1 equipment. DSC thermograms were obtained from 3 to 5 mg samples at

heating/cooling rates of $10\text{ }^{\circ}\text{C}\cdot\text{min}^{-1}$ under a nitrogen flow of $20\text{ mL}\cdot\text{min}^{-1}$. Indium and zinc were used as standards for temperature and enthalpy calibration. The glass-transition temperatures were determined from the third heating run at a heating rate of $20\text{ }^{\circ}\text{C}\cdot\text{min}^{-1}$ from rapidly melt-quenched polymer samples. The treatment of the samples for isothermal crystallization experiments was the following: the thermal history was removed by heating the sample up to $250\text{ }^{\circ}\text{C}$ and keeping the sample at this temperature for 5 min, subsequently it was cooled at $20\text{ }^{\circ}\text{C}\cdot\text{min}^{-1}$ to the selected crystallization temperature, where it was left to crystallize until saturation. Thermogravimetric analyses were performed under a nitrogen flow of $20\text{ mL}\cdot\text{min}^{-1}$ at a heating rate of $10\text{ }^{\circ}\text{C}\cdot\text{min}^{-1}$, within a temperature range of 30 to $600\text{ }^{\circ}\text{C}$, using a Perkin Elmer TGA 6 equipment. Sample weights of about 10-15 mg were used in these experiments. Wide-angle X-ray diffraction (WAXD) measurements were performed on a Rigaku Geigerflex Bragg-Brentano Powder Diffractometer using Cu radiation, wavelength 1.54056 \AA , at 40 kV and 30 mA. The scans were performed with 0.02 ° steps and a dwell time of 3 s in the 2θ range from 10 ° till 35 ° . The analyses were performed on the crude copolyester samples. Scanning electron microscopy (SEM) images were taken with a field-emission JEOL JSM-7001F instrument (JEOL, Japan) from platinum/palladium coated samples.

6.3.2.3. Polymer synthesis

6.3.2.3.1. Melt polycondensation (MP)

Thx-based copolyesters were obtained from a mixture of 1,4-butanediol, the cyclic diol 2,3-di-*O*-methylene-L-threitol (Thx) and dimethyl terephthalate (DMT) with a predetermined composition. PThxT homopolyester was obtained by reacting Thx with DMT. The reactions were performed in a three-necked, cylindrical-bottom flask equipped with a mechanical stirrer, a nitrogen inlet and a vacuum distillation outlet. A 5% molar excess of the diol mixture to DMT was used, and dibutyl tin oxide (DBTO, 0.6% molar with respect to monomers) was the catalyst of choice. The apparatus was purged with nitrogen several times at room temperature in order to remove the last traces of air. Transesterification reactions were carried out under a low nitrogen flow at the selected temperature. Polycondensation reactions were performed at a selected temperature under a 0.03-0.06 mbar vacuum. At the end of the reaction, the reaction mixture was cooled to room temperature under a nitrogen atmosphere. The resulting polymers were dissolved in a mixture of chloroform and trifluoroacetic acid (9:1) and precipitated in an excess of methanol. Finally, the polymer was collected by filtration, extensively washed with methanol and dried under vacuum. The detailed reaction conditions are given below.

The Thx-based copolyesters obtained via MP are abbreviated as $^{MP}PB_xThx_yT$, where x and y are the mole percentages (mol-%) of 1,4-butanediol and Thx, respectively, in the resulting copolyester.

PThxT homopolyester. Transesterification reactions were performed at 160 °C for 2 h and at 180 °C for 1 h under a low nitrogen flow. Polycondensation reactions were performed at 180 °C for 8 h under a 0.03-0.06 mbar vacuum. 1H NMR (300.1 MHz, $CDCl_3/TFA$), δ (ppm): 8.1 (s, 4H, ArH), 5.3 (s, 2H, OCH_2O), 4.6 (m, 4H, OCH_2CH), 4.5 (m, 2H, OCH_2CH). ^{13}C NMR (75.5 MHz, $CDCl_3/TFA$), δ (ppm): 167.0 (CO), 133.5, 130.3, 95.7, 75.9, 64.9.

$^{MP}PB_xThx_yT$ copolyesters. The copolyesters were obtained by a similar procedure, with polymerization conditions slightly differing for each composition feed.

$^{MP}PB_{96}Thx_4T$. Transesterification reactions were performed at 160 °C for 1 h, at 200 °C for 1 h and at 240 °C for 0.5 h under a low nitrogen flow. Polycondensation reactions were performed at 250 °C for 2.5 h under a 0.03-0.06 mbar vacuum.

$^{MP}PB_{91}Thx_9T$. Transesterification reactions were performed at 160 °C for 1 h, at 200 °C for 1 h and at 240 °C for 0.5 h under a low nitrogen flow. Polycondensation reactions were performed at 240 °C for 3 h under a 0.03-0.06 mbar vacuum.

$^{MP}PB_{84}Thx_{16}T$ and $^{MP}PB_{82}Thx_{18}T$. Transesterification reactions were performed at 160 °C for 1 h, at 200 °C for 1 h and at 230 °C for 0.5 h under a low nitrogen flow. Polycondensation reactions were performed at 230 °C for 3.5 h under a 0.03-0.06 mbar vacuum.

$^{MP}PB_{77}Thx_{23}T$ and $^{MP}PB_{71}Thx_{29}T$. Transesterification reactions were performed at 160 °C for 1 h, at 200 °C for 1 h and at 220 °C for 0.5 h under a low nitrogen flow. Polycondensation reactions were performed at 220 °C for 4 h under a 0.03-0.06 mbar vacuum.

NMR characterization of $^{MP}PB_xThx_yT$ copolyesters. 1H NMR (300.1 MHz, $CDCl_3/TFA$), δ (ppm): 8.1 (s, 4H, ArH), 5.3 (s, $y \cdot 2H$, OCH_2O), 4.6 (m, $y \cdot 4H$, OCH_2CH), 4.5 (t, $x \cdot 4H$, OCH_2CH_2), 4.5 (m, $y \cdot 2H$, OCH_2CH), 2.0 (t, $x \cdot 4H$, OCH_2CH_2). ^{13}C NMR (75.5 MHz, $CDCl_3/TFA$), δ (ppm): 168.0 (CO), 167.0 (CO), 134.2-133.2, 130.3, 130.1, 95.7, 75.9, 66.3, 64.9, 25.4.

6.3.2.3.2. Solid-state modification (SSM) of PBT

Physical mixtures of purified PBT ($M_n = 23.3 \text{ kg}\cdot\text{mol}^{-1}$ and $M_w = 47.1 \text{ kg}\cdot\text{mol}^{-1}$, determined by SEC), the cyclic diol Thx, and DBTO catalyst (0.36% molar with respect to PBT) were prepared from solution, using a common solvent approach as described elsewhere (Lavilla *et al.*, 2013c -Subchapter 6.2-), in which the PBT was first precipitated to remove any titanium-based catalysts. Different molar ratios of PBT and Thx were used in order to obtain copolyesters with varying compositions. The solid-state modification of PBT was performed in a reactor comprising a glass tube (inner diameter= 2.4 cm) with a sintered glass frit at the bottom. A heat exchange glass coil (inner diameter= 0.5 mm) surrounded the reactor and entered the inner glass tube at the bottom just below the glass frit. The nitrogen gas was heated by passing through this coil prior to entering the reactor, which was immersed in an oil bath kept at 160 °C. The nitrogen flow was controlled by a flow-meter. Typically, 0.4 g of the PBT/Thx physical mixture was placed on the sintered glass plate. The powder was fixed in place by addition of glass pearls (diameter= 2 mm) on top of the powder, and the reactor was purged with a nitrogen flow of $0.5 \text{ L}\cdot\text{min}^{-1}$ during 30 min prior to the reaction. Reactions were left to proceed at 160 °C under a $0.5 \text{ L}\cdot\text{min}^{-1}$ nitrogen flow until the desired molecular weights were attained, which were followed as function of reaction time using SEC. Reaction times were in the 4-20 h range. After completion of the reaction, the reactor was gradually cooled down to room temperature by removing the heat source and by continuing the purging of the reactor with nitrogen. Subsequently, the obtained polymer was dried under vacuum. The Thx copolyesters obtained via SSM are abbreviated as $^{\text{SSM}}\text{PB}_x\text{Thx}_y\text{T}$, where x and y are the mole percentages (mol-%) of 1,4-butanediol and Thx, respectively, in the resulting copolyester.

NMR characterization of $^{\text{SSM}}\text{PB}_x\text{Thx}_y\text{T}$ copolyesters. ^1H NMR (300.1 MHz, CDCl_3/TFA), δ (ppm): 8.1 (s, 4H, ArH), 5.3 (s, $y\cdot 2\text{H}$, OCH_2O), 4.6 (m, $y\cdot 4\text{H}$, OCH_2CH), 4.5 (t, $x\cdot 4\text{H}$, OCH_2CH_2), 4.5 (m, $y\cdot 2\text{H}$, OCH_2CH), 2.0 (t, $x\cdot 4\text{H}$, OCH_2CH_2). ^{13}C NMR (75.5 MHz, CDCl_3/TFA), δ (ppm): 168.0 (CO), 167.0 (CO), 134.2-133.2, 130.3, 130.1, 95.7, 75.9, 66.3, 64.9, 25.4.

6.3.2.4. Hydrolytic degradation procedures

Films for the hydrolytic degradation studies on the (co)polyesters were prepared with a thickness of approx. 200 μm by casting from solution ($100 \text{ g}\cdot\text{L}^{-1}$) in a mixture of chloroform and HFIP (5:1). The films were cut into disks with a diameter of 10 mm and a

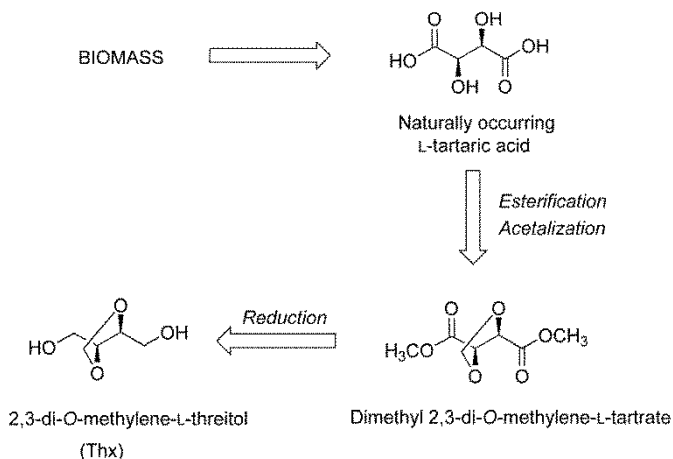
weight of 20 to 30 mg, which were subsequently dried under vacuum to constant weight. For the hydrolytic degradation, samples were immersed in vials containing 10 mL of citric acid buffer (pH 2.0) at 80 °C. After incubation for a predetermined period of time, the samples were rinsed thoroughly with distilled water, dried to constant weight and analyzed by SEC chromatography, NMR spectroscopy and SEM microscopy.

For hydrolytic degradation studies of the monomer 2,3-di-O-methylene-L-threitol, samples of this diol (80 mg) were immersed in NMR tubes containing 1 mL of citric acid buffer (pH 2.0), sodium phosphate buffer (pH 7.4) or sodium carbonate buffer (pH 10.5), all of them prepared in D₂O, and were incubated at 80 °C for 6 weeks. The residue left after incubation was analyzed by NMR spectroscopy.

6.3.3. Results and discussion

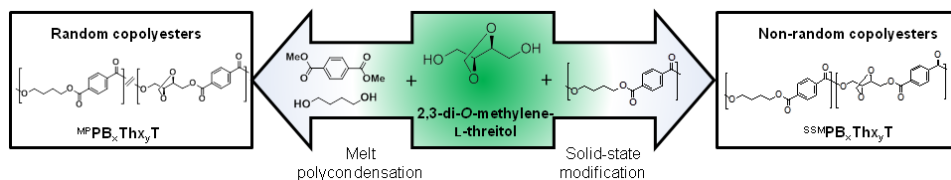
6.3.3.1. Polymer synthesis

The bio-based compound 2,3-di-O-methylene-L-threitol (Thx) was prepared following the route depicted in Scheme 6.2. The pendant hydroxyl groups from naturally occurring L-tartaric acid were protected by internal acetalization leading to the formation of a 1,3-dioxolane ring. The resulting product, dimethyl 2,3-di-O-methylene-L-tartrate, was subsequently reduced to obtain the desired Thx diol monomer. This cyclic diol possesses a 2-fold axis of symmetry, and therefore will produce stereoregular polymer chains and its two primary hydroxyl groups are expected to display the same reactivities towards a polycondensation reaction.



Scheme 6.2. Preparation of the bio-based 2,3-di-O-methylene-L-threitol.

Thx was used as diol comonomer in the synthesis of the bio-based copolyesters by two different approaches, *viz.* melt polycondensation (MP) and solid-state modification (SSM), as depicted in Scheme 6.3.



Scheme 6.3. Preparation of $^{\text{MP}}\text{PB}_x\text{Th}_y\text{T}$ and $^{\text{SSM}}\text{PB}_x\text{Th}_y\text{T}$ copolyesters.

$^{\text{MP}}\text{PB}_x\text{Th}_y\text{T}$ copolyesters were obtained by reacting dimethyl terephthalate (DMT) with mixtures with varying compositions of Thx and 1,4-butanediol in the melt. Transesterification reactions were initiated at 160 °C in order to prevent volatilization of the diols. As the reaction progressed the temperature was progressively increased to avoid crystallization of oligomers. The subsequent polycondensation reactions were performed under reduced pressure at temperatures in the range of 220-250 °C. Lower temperatures and longer reaction times were used for copolyesters with higher Thx contents, to avoid decomposition of this thermally sensitive compound. Dibutyl tin oxide (DBTO) was the catalyst of choice as replacement of the commonly used titanium (IV) tetrabutoxide (TBT). Results obtained from the synthesis of dimethyl 2,3:4,5-di-O-methylene-galactarate-based aliphatic polyesters by melt polycondensation demonstrated the higher activity of DBTO as catalyst compared to TBT (Lavilla *et al.*, 2011 -Subchapter 3.2-). $^{\text{MP}}\text{PB}_x\text{Th}_y\text{T}$ copolyesters were obtained with weight average molecular weights between 39 and 43 $\text{kg}\cdot\text{mol}^{-1}$ and polydispersity indices in the range of 2.1-2.4 (Table 6.4). Besides the copolyesters prepared by MP, solid-state modification (SSM) was used to prepare copolyesters with similar overall chemical compositions. Usually, SSM is performed at 20-30 °C below the melting point of a semicrystalline polymer (Jansen *et al.*, 2005 and 2006; Gubbels *et al.*, 2013b). However, in this present study the SSM of poly(butylene terephthalate) (PBT, $T_m = 225$ °C) with the cyclic diol Thx was conducted at 160 °C under a relatively low nitrogen flow, to minimize the volatilization of the carbohydrate-based monomer. DBTO was also used as catalyst for the SSM reactions, because of its high activity in the low temperature SSM processes (Lavilla *et al.*, 2013c -Subchapter 6.2-). All the SSM reactions were monitored using size-exclusion chromatography (SEC) to ensure that the $^{\text{SSM}}\text{PB}_x\text{Th}_y\text{T}$ copolyesters had similar molecular weights compared to their MP counterparts, in order to make a reliable

comparison of their thermal behavior. The SSM reactions were stopped when M_n and M_w values of 17-18 and 39-46 $\text{kg}\cdot\text{mol}^{-1}$ were reached, respectively (Table 6.4). The chemical composition and structure from both series of copolyesters were studied using proton NMR spectroscopy. The ^1H and ^{13}C NMR spectra of a representative Thx-based copolyester, in this case prepared by melt polycondensation, are presented in Figure 6.9.

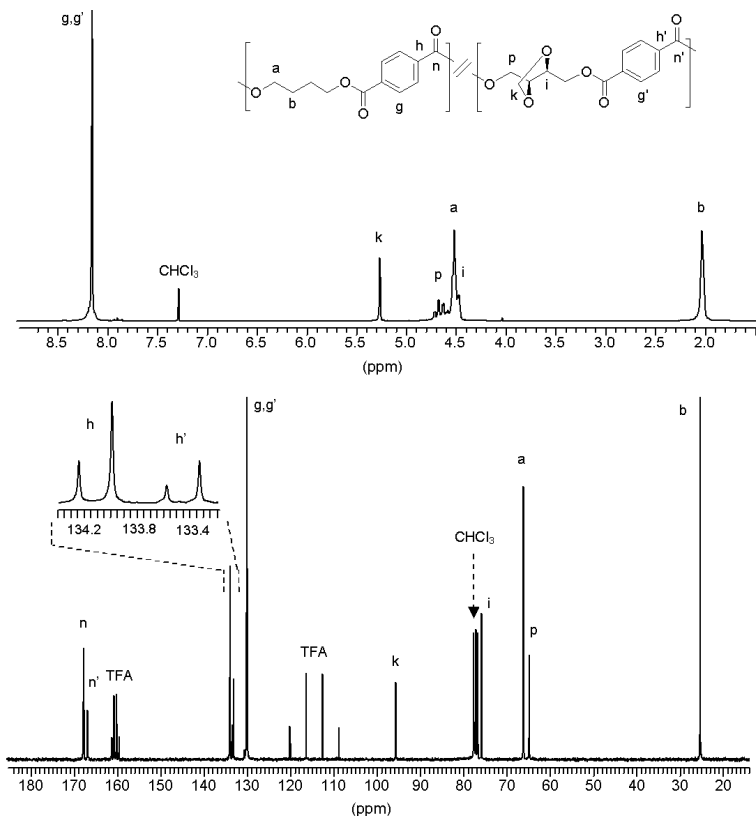


Figure 6.9. ^1H (top) and ^{13}C (bottom) NMR spectra of $^{\text{MP}}\text{PB}_{71}\text{Thx}_{29}\text{T}$ copolyester. A schematic representation of the copolyester backbone is also presented.

The ^1H NMR corroborated their expected chemical structure, and confirmed that Thx had successfully been incorporated into the backbone of the copolyesters, either by MP or SSM. The molar composition of the two series was determined by integration of the signals corresponding to 1,4-butanediol and Thx. The compositions of the copolyesters prepared by MP were found to be very close to the feed ratio (Table 6.4). However, the $^{\text{SSM}}\text{PB}_x\text{Thx}_y\text{T}$ copolyesters showed a significant deviation from their feed composition. Even though the SSM reaction conditions were very mild, a certain amount of comonomer was evaporated from the reactor during the SSM process.

Table 6.4. Molar composition, molecular weight and microstructure of the two series Thx-based copolyesters.

Copolyester	Molar composition				Molecular weight			Microstructure							
	Copolyester ^a		Feed		M_n^b	M_w^b	\mathcal{D}^b	Dyad content			Number Average Sequence Lengths		Randomness ^d	Randomness ^e	
	X_B	X_{Thx}	X_B	X_{Thx}				N_{BB}^c	$N_{BThx/ThxB}^c$	N_{ThxThx}^c	n_B	n_{Thx}			R
PBT	100	0	100	0	23,300	47,100	2.0								
^{MP} PB ₉₆ Thx ₄ T	95.9	4.1	95	5	18,700	42,500	2.3	83.8	15.3	0.9	11.9	1.1	0.98		
^{MP} PB ₉₁ Thx ₉ T	90.8	9.2	90	10	17,000	41,300	2.4	78.5	19.9	1.7	8.9	1.2	0.97		
^{MP} PB ₈₄ Thx ₁₆ T	84.2	15.8	85	15	16,800	40,500	2.4	70.7	26.2	3.1	6.4	1.2	0.97		
^{MP} PB ₈₂ Thx ₁₈ T	81.8	18.2	80	20	17,500	41,100	2.3	60.5	34.5	5.0	4.5	1.3	1.00		
^{MP} PB ₇₇ Thx ₂₃ T	76.7	23.3	75	25	16,600	40,300	2.4	57.4	36.1	6.5	4.2	1.4	0.98		
^{MP} PB ₇₁ Thx ₂₉ T	70.9	29.1	70	30	16,000	39,100	2.4	47.4	42.6	10.0	3.2	1.5	0.99		
^{SSM} PB ₉₆ Thx ₄ T	95.7	4.3	77	23	18,400	39,400	2.1	93.0	6.1	1.0	31.6	1.3	0.79		0.83
^{SSM} PB ₉₃ Thx ₇ T	92.6	7.4	83	17	17,800	46,200	2.4	88.2	10.0	1.8	18.6	1.4	0.79		0.86
^{SSM} PB ₉₁ Thx ₉ T	90.6	9.4	91	9	17,400	39,600	2.2	83.9	12.9	3.2	14.0	1.5	0.74		0.84
^{SSM} PB ₈₉ Thx ₁₁ T	88.7	11.3	67	33	17,200	41,000	2.4	76.3	18.1	5.6	9.4	1.6	0.72		0.84
^{SSM} PB ₈₂ Thx ₁₈ T	81.7	18.3	71	29	17,100	42,800	2.5	70.5	22.1	7.4	7.4	1.7	0.73		0.90
PThxT	0	100	0	100	3,800	8,800	2.3								

^a Molar composition determined by ¹H NMR spectroscopy. ^b Number and weight-average molecular weights in g·mol⁻¹ and dispersities measured by SEC in HFIP against PMMA standards. ^c N_{BB} , $N_{BThx/ThxB}$ and N_{ThxThx} indicate the relative molar amount of the dyads as obtained from ¹³C NMR. ^d Randomness index of copolyesters statistically calculated on the basis of the ¹³C NMR analysis. ^e Randomness index of the amorphous fraction of copolyesters, determined using the correction method reported by Jansen *et al.* (Jansen *et al.*, 2005).

6.3.3.2. Chemical microstructure

The chemical microstructure of the $^{MP}PB_xThx_yT$ and $^{SSM}PB_xThx_yT$ copolyesters was elucidated using quantitative ^{13}C NMR spectroscopy. As shown in Figure 6.9, the resonances of all magnetically different carbon atoms present in the backbone of the copolyesters are well resolved. The resonance arising from the non-protonated aromatic carbon atom proves to be sensitive to the sequence distribution of the units along the copolyester backbone at the level of dyads (Kricheldorf, 1978; Newmark, 1980). This resonance has split into four well-resolved peaks which are observed in the 133-135 ppm chemical shift interval. These four resonances correspond to the different types of dyads (BB, BThx and ThxB, ThxThx) which are present along the copolyester chain, and their peak areas display a dependence on the copolyester composition (Figure 6.10).

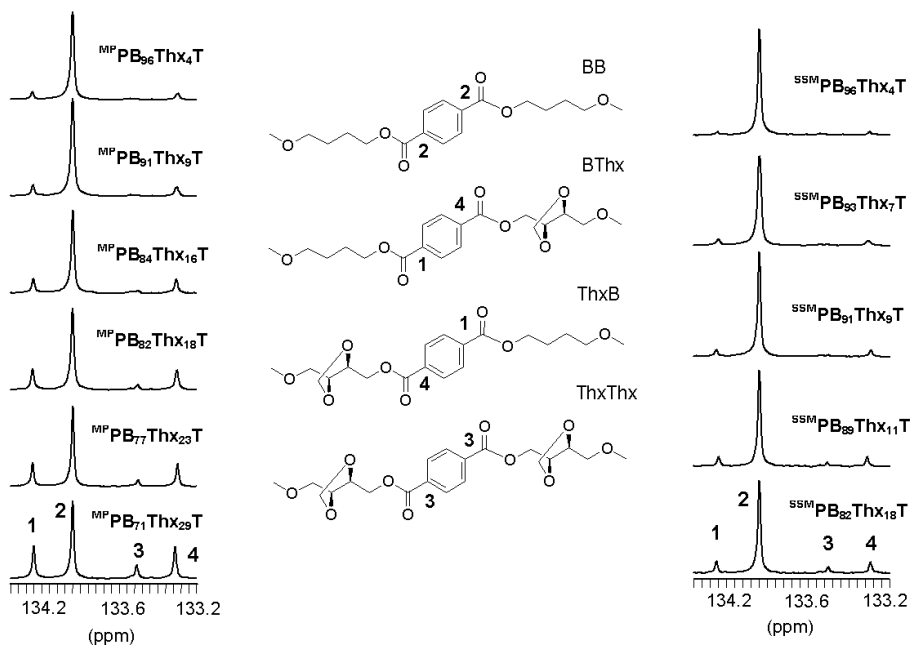


Figure 6.10. ^{13}C NMR signals used for the microstructure analysis of the $^{MP}PB_xThx_yT$ (left) and $^{SSM}PB_xThx_yT$ (right) copolyesters with schematic representation of the dyads to which they are assigned.

The molar fractions (M) of the different dyads in the copolyester chain were determined by integration of their corresponding resonances. Based on these results, the number-average sequence lengths n of the butylene-terephthalate (B) and threylene-terephthalate (Thx) sequences, as well as the degree of randomness (R), are determined

for each copolyester by using the equations given below (Yamadera and Murano, 1967; Randall, 1977).

$$n_B = (N_{BB} + 0.5 \cdot (N_{BThx} + N_{ThxB})) / (0.5 \cdot (N_{BThx} + N_{ThxB}))$$

$$n_{Thx} = (N_{ThxThx} + 0.5 \cdot (N_{BThx} + N_{ThxB})) / (0.5 \cdot (N_{BThx} + N_{ThxB}))$$

$$R = (1/n_B) + (1/n_{Thx})$$

R -values close to unity are indicative of a fully random chemical microstructure. When the R -value decreases towards zero or increases towards two, the chemical microstructure would be more blocky or alternating, respectively. Results from these calculations showed that the sequence distribution of the $^{MP}PB_xTh_xT$ copolyesters is essentially random for the whole range of compositions, with values of R near unity (Table 6.4). Conversely, the R -values for the $^{SSM}PB_xTh_xT$ copolyesters deviated significantly from unity, falling within the 0.72-0.79 range. These copolyesters possess therefore a block-like, non-random overall chemical microstructure, as reported for other copolyesters obtained by SSM (Jansen *et al.*, 2005; Gubbels *et al.*, 2013b; Lavilla *et al.*, 2013c -Subchapter 6.2-). Since the crystalline phase does not participate in the SSM process due to mobility restrictions, relatively long PBT sequences are expected to be retained in the $^{SSM}PB_xTh_xT$ copolyesters. These PBT sequences are included in the calculation of the overall chemical microstructure, since these values are determined from solution ^{13}C NMR data and both the random copolyester blocks and the relatively long PBT sequences of the copolyester macromolecules are dissolved for the NMR analysis. It is desirable to evaluate the chemical microstructure of the amorphous phase only, disregarding the contribution of the crystalline domains. To this end, Jansen *et al.* have developed a method to correct the R -values for the presence of the crystalline phase, yielding the randomness of the amorphous phase only (Jansen *et al.*, 2005). The chemical microstructure of the complete amorphous phase of the $^{SSM}PB_xTh_xT$ copolyesters was determined by using this calculation method, which implements data obtained by differential scanning calorimetry (DSC), as discussed below. The corrected R -values of the amorphous phase are shown in Table 6.4. These R -values are closer to unity, thus indicating that the amorphous phase would be practically random. Hence, by SSM the Thx is incorporated into the mobile amorphous fraction in a similar way as through melt polycondensation, even though in SSM only the most mobile chain segments are participating in the transesterification reactions. The main conclusion that can be drawn from this study is that, by using MP and SSM, partially bio-based copolyesters with different overall chemical microstructures can be prepared. MP leads to

fully random copolyesters, whereas the SSM-prepared copolyesters show a blocky overall microstructure, formed by long neat PBT sequences, originating from the crystalline phase present during SSM, and random copolyester segments that are located in the amorphous phase and that have participated in the transesterification reactions.

6.3.3.3. Thermal properties

The thermal behavior of both the $^{MP}PB_xTh_xT$ and the $^{SSM}PB_xTh_xT$ copolyesters has been comparatively studied by TGA and DSC. The thermal parameters resulting from these analyses are shown in Table 6.5, where the corresponding data for the parent homopolyesters PThxT and PBT are also included for comparison.

The thermal stability of the MP- and SSM-prepared copolyesters, as well as the homopolyester PThxT, were evaluated by TGA under inert atmosphere and compared with PBT. The TGA traces are depicted in Annex H. The thermal properties derived from the shown thermograms, *viz.* the onset decomposition temperature ($^{\circ}T_{5\%}$) and the temperature of maximum degradation rate (T_d), are listed in Table 6.5. The weight loss profiles obtained for the copolyesters reveal a thermal degradation mechanism involving one main degradation step and leaving a final residue of 2-10% of the initial weight. None of the polyesters show significant weight loss at temperatures below 360 °C. The $^{\circ}T_{5\%}$ and T_d of PBT are determined to be 371 and 408 °C, respectively. A higher thermal stability is observed for the PThxT homopolyester, which shows the aforementioned decomposition parameters at 387 and 441 °C, respectively. As expected, the $^{\circ}T_{5\%}$ and T_d for both the $^{MP}PB_xTh_xT$ and the $^{SSM}PB_xTh_xT$ copolyesters are found at intermediate values between those of their two parent homopolyesters. No noteworthy differences were detected in the thermal stability of the bio-based copolyesters prepared by MP and SSM containing similar amounts of Thx. The valuable conclusion drawn from this comparative thermogravimetric study is that the insertion of the carbohydrate-based cyclic Thx yields copolyesters with enhanced thermal stability with respect to pure PBT.

Table 6.5. Thermal properties of the two series of Thx-based copolyesters.

Copolyester	TGA			DSC								
	$^{\circ}T_{5\%}^a$ ($^{\circ}C$)	T_d^b ($^{\circ}C$)	W^c (%)	T_g^d ($^{\circ}C$)	First heating ^e		Cooling ^e		Second heating ^e			
					T_m ($^{\circ}C$)	ΔH_m ($J \cdot g^{-1}$)	T_c ($^{\circ}C$)	ΔH_c ($J \cdot g^{-1}$)	T_c ($^{\circ}C$)	ΔH_c ($J \cdot g^{-1}$)	T_m ($^{\circ}C$)	ΔH_m ($J \cdot g^{-1}$)
PBT	371	408	2	31	225	60.5	193	52.0	-	-	224	49.0
^{MP} PB ₉₆ Thx ₄ T	375	410	5	39	212	42.8	183	40.5	-	-	203/212 ^f	39.5
^{MP} PB ₉₁ Thx ₉ T	375	409	5	41	206	41.5	179	36.7	-	-	199/208 ^f	35.8
^{MP} PB ₈₄ Thx ₁₆ T	375	412	5	45	197	38.6	167	29.9	-	-	192/199 ^f	28.1
^{MP} PB ₈₂ Thx ₁₈ T	376	411	6	49	189	32.5	152	27.3	-	-	182/191 ^f	26.5
^{MP} PB ₇₇ Thx ₂₃ T	373	412	6	51	185	31.3	144	25.2	-	-	178/186 ^f	24.9
^{MP} PB ₇₁ Thx ₂₉ T	374	414	10	56	169	24.5	116	16.7	91.6	3.3	172	19.9
^{SSM} PB ₉₆ Thx ₄ T	372	408	5	35	214/222 ^f	76.2	188	47.9	-	-	209/219 ^f	47.6
^{SSM} PB ₉₃ Thx ₇ T	373	409	8	37	211/218 ^f	75.2	182	46.7	-	-	204/214 ^f	45.5
^{SSM} PB ₉₁ Thx ₉ T	372	410	6	38	210/218 ^f	74.3	181	46.1	-	-	202/213 ^f	42.9
^{SSM} PB ₈₉ Thx ₁₁ T	372	409	6	41	207/216 ^f	66.5	172	37.1	-	-	198/208 ^f	36.9
^{SSM} PB ₈₂ Thx ₁₈ T	372	409	8	44	209	63.2	167	35.8	-	-	194/203 ^f	35.4
PThxT	387	441	10	83	-	-	-	-	-	-	-	-

^a Temperature at which 5% weight loss was observed. ^b Temperature of the maximum degradation rate. ^c Remaining weight at 600 $^{\circ}C$. ^d Glass-transition temperature taken as the inflection point of the heating DSC traces recorded at 20 $^{\circ}C \cdot min^{-1}$ during the third heating run. ^e Melting (T_m) and crystallization (T_c) temperatures, and melting (ΔH_m) and crystallization (ΔH_c) enthalpies measured by DSC at heating/cooling rates of 10 $^{\circ}C \cdot min^{-1}$. ^f Multiple melting peaks.

The DSC analysis revealed that the incorporation of Thx into the backbone of PBT induced significant changes in the glass-transition temperature (T_g) when compared to neat PBT (Table 6.5). The dependence of the T_g values on the Thx content is plotted in Figure 6.11. Remarkably, PThxT has a T_g value 50 °C higher than PBT, proving a much more rigid main chain structure. Consequently, the partial replacement of the 1,4-butanediol units by Thx residues yields an increase in T_g , which shows no dependency on the copolyester preparation method (MP or SSM).

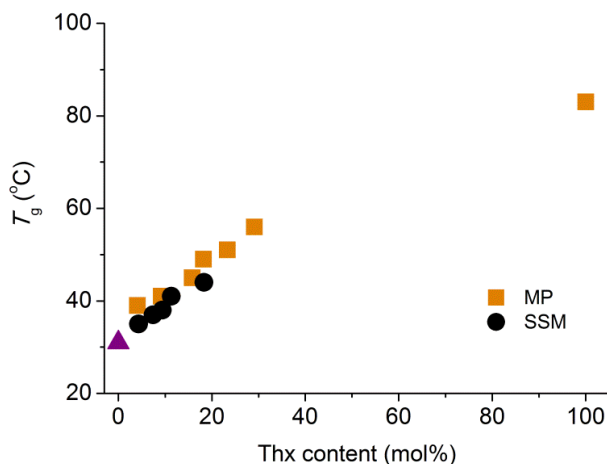


Figure 6.11. Glass-transition temperature versus composition plots for the $^{MP}PB_xTh_xT$ and the $^{SSM}PB_xTh_xT$ copolyesters. The triangle represents the T_g of the homopolyester PBT.

Melting temperatures (T_m) and enthalpies (ΔH_m) were measured by DSC and are listed in Table 6.5. PBT is a semicrystalline polyester with a melting temperature of 225 °C. Copolymerization of PBT with other compounds commonly affects the thermal properties significantly. Endothermic peaks, indicative for the presence of a crystalline phase, were observed for all $^{MP}PB_xTh_xT$ and $^{SSM}PB_xTh_xT$ copolyesters, whereas PThxT did not show such a behavior and proves to be fully amorphous. The T_m of the copolyesters proved to be dependent on the Thx content and also on the preparation method. Since in the first heating run the samples prepared by MP or SSM have a different thermal history, the SSM samples being annealed during the SSM treatment, a comparative analysis of the T_m will be performed on the results obtained from the second heating run, so after crystallization from the melt (discussed below). Melting and crystallization enthalpies of the MP and SSM copolyesters, however, will be compared for first heating, cooling and second heating.

From DSC analysis of the obtained copolyesters it is clear that the materials prepared by SSM exhibit higher first heating melting enthalpies compared to those prepared by MP exhibiting a similar overall chemical composition (Table 6.5). This higher enthalpy is due to the segmented nature of these SSM-prepared copolyesters and annealing of the copolyester during the SSM reaction. In order to determine the crystallinity of the Thx-based samples, to elucidate if co-crystallization had taken place and to complement the DSC data, wide-angle X-ray diffraction (WAXD) was performed on the two series of as synthesized copolyesters as well as on the PThxT and PBT homopolyesters. The WAXD profiles and the most important Bragg spacings present therein are shown Annex H. The pattern of PBT is characterized by five prominent reflections at 5.6, 5.1, 4.3, 3.8 and 3.6 Å. Essentially the same pattern, in terms of spacing and relative intensities, is shared by all $^{MP}PB_xThx_yT$ and $^{SSM}PB_xThx_yT$ copolyesters, revealing that the triclinic crystal structure of PBT (Hall, 1984) has been retained and that co-crystallization of ThxT repeat units in the PBT crystals does not occur. In agreement with DSC results, PThxT did not show any discrete reflections characteristic of crystalline material. The crystallinity index of the materials was estimated as the quotient between the crystalline and total area of the X-ray diffraction patterns (Annex H). A noticeable decrease in crystallinity with increasing Thx content was observed for the MP series, which was expected in view of the lack of co-crystallizability of the ThxT repeat units with BT repeat units. Regarding $^{SSM}PB_xThx_yT$ copolyesters, a slight decrease in crystallinity was also observed during first heating when the Thx content was increased, indicating that the crystalline phase was not completely retained during the SSM process. This phenomenon was observed before in other copolyesters prepared by SSM, and can be attributed to the participation of the outer side of the PBT crystallites in trans-reactions, thereby gradually dissolving part of the crystallites (Jansen *et al.*, 2008; Lavilla *et al.*, 2013c -Subchapter 6.2-).

From the data presented in Table 6.5, it can be noted that all the $^{MP}PB_xThx_yT$ and $^{SSM}PB_xThx_yT$ copolyesters were able to crystallize from the melt, and that the crystallization temperature (T_c) and the crystallization enthalpy (ΔH_c) both decrease with increasing Thx content. Besides the fact that Thx-based repeat units cannot (co)-crystallize (see earlier), the increasing amount of stiffer Thx containing segments makes crystallization from the melt more difficult. Nevertheless, when the results for the MP series are compared to those obtained for copolyesters prepared by SSM at similar compositions, the materials obtained by SSM showed higher T_c and ΔH_c values. This was expected, since longer PBT sequences are present in the SSM-prepared copolyesters,

which facilitate the crystallization of the materials. A further detailed crystallization study will be described below.

The thermal properties obtained from the second heating run of the MP- and SSM-prepared samples can be comparatively studied since they have similar thermal histories and have all been crystallized from the melt. After this melt-crystallization, ${}^{\text{MP}}\text{PB}_x\text{Th}_y\text{T}$ copolyesters recovered about 70-95% of their initial crystallinity and displayed no changes in their melting temperatures. However, when the SSM copolyesters were crystallized from the melt and reheated, there was a definite change in their melting behavior. Both the T_m and ΔH_m decreased significantly when the first and second heating were compared. A reason for this difference is the (partial) randomization of the chemical microstructure by transesterification reactions occurring in the melt. This randomization is an entropically driven process and is catalyzed by the presence of DBTO, which was added to the physical mixtures to facilitate the Thx incorporation. To study the randomization phenomenon, samples of ${}^{\text{SSM}}\text{PB}_{82}\text{Th}_{18}\text{T}$ were kept in the melt at 250 °C for predetermined times and after this treatment their chemical microstructure and thermal properties were studied using ${}^{13}\text{C}$ NMR and DSC, respectively (Annex H). A decrease of the melting temperature is observed as a function of the time during which the sample was kept in the melt, which was accompanied by an increase of the R -value from 0.73 to 0.92, showing that almost complete randomization of the chemical microstructure occurred after long residence times at 250 °C. Therefore, the changes in the thermal behavior between the first and second heating run are caused by the (at least partial) randomization of the chemical microstructure yielding shorter crystallizable PBT sequences. When the T_m values obtained from the second heating runs of the copolyesters prepared by SSM are compared to those prepared by MP, noticeable differences are observed and an overview is given in Figure 6.12. Interestingly, both T_m and ΔH_m recorded during the second heating run of the samples prepared by SSM are higher than those measured for the ${}^{\text{MP}}\text{PB}_x\text{Th}_y\text{T}$ series, the higher melting points of the SSM samples being related to the possible formation of thicker lamellae from the longer PBT sequences. This implies that even though randomization of the blocky chemical microstructure of the SSM-prepared copolyesters does occur to some extent during recording the DSC traces, it is not yet so extensive as to yield fully random copolyesters for which only relatively thin lamellae with low melting points can be formed.

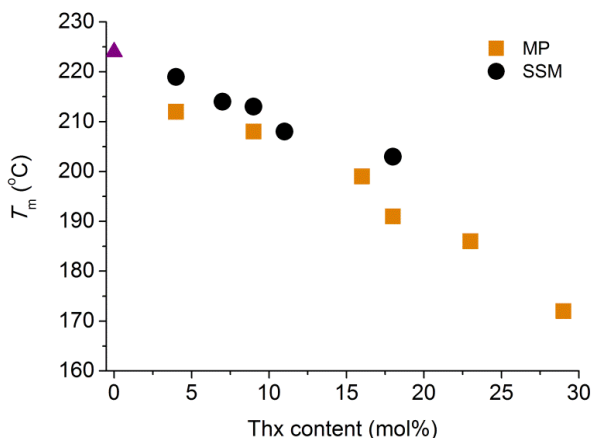


Figure 6.12. Overview of the melting temperature during the second heating run of the Thx-based copolyesters prepared by MP and SSM. The triangle represents the homopolymer PBT.

6.3.3.4. Isothermal crystallization

As mentioned above, all the ${}^{\text{MP}}\text{PB}_x\text{Thx}_y\text{T}$ and ${}^{\text{SSM}}\text{PB}_x\text{Thx}_y\text{T}$ copolyesters as well as PBT are able to crystallize from the melt. Since crystallization from the melt is relevant for processing, the isothermal crystallization of ${}^{\text{MP}}\text{PB}_{96}\text{Thx}_4\text{T}$, ${}^{\text{MP}}\text{PB}_{91}\text{Thx}_9\text{T}$, ${}^{\text{SSM}}\text{PB}_{96}\text{Thx}_4\text{T}$, ${}^{\text{SSM}}\text{PB}_{91}\text{Thx}_9\text{T}$ and PBT were comparatively studied in the 195–205 °C temperature interval. All the polyester materials could be isothermally crystallized at 200 °C. The evolution of the relative crystallinity, X_c , versus crystallization time is shown in Figure 6.13.

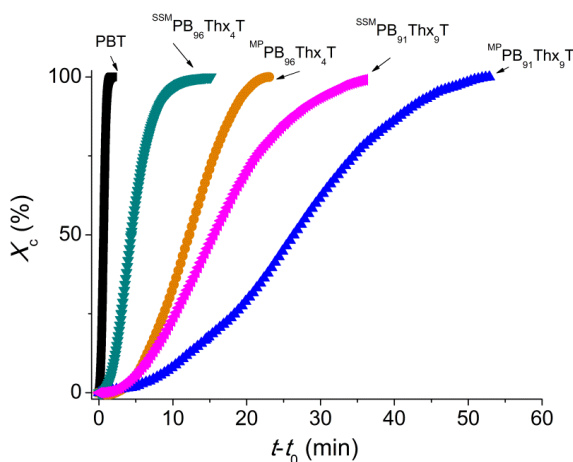


Figure 6.13. Relative crystallinity versus time plot of PBT, ${}^{\text{MP}}\text{PB}_{96}\text{Thx}_4\text{T}$, ${}^{\text{MP}}\text{PB}_{91}\text{Thx}_9\text{T}$, ${}^{\text{SSM}}\text{PB}_{96}\text{Thx}_4\text{T}$ and ${}^{\text{SSM}}\text{PB}_{91}\text{Thx}_9\text{T}$ isothermally crystallized at 200 °C.

Data obtained from the isothermal crystallization experiments are displayed in Table 6.6. The observed onset and half-crystallization times, as well as the corresponding calculated Avrami parameters, are given for each experiment. It can be noted that for all the copolyesters the Avrami exponent n increases with temperature, the values obtained being in the 2.0-2.6 range. The double-logarithmic plot of these data indicated that only primary crystallization takes place in the selected time interval (Annex H). An increase in crystallization temperature yielded a delay in the onset of crystallization besides the decrease in crystallization rate. Moreover, it was observed that the presence of minor amounts of Thx noticeably depressed the crystallizability of PBT. Furthermore, the comparison of crystallization data for $^{\text{MP}}\text{PB}_{96}\text{Thx}_4\text{T}$ and $^{\text{SSM}}\text{PB}_{96}\text{Thx}_4\text{T}$ evidenced that crystallizability is more repressed for a fully random copolyester prepared by MP than for the more blocky SSM-prepared copolyester. In accordance, $^{\text{SSM}}\text{PB}_{91}\text{Thx}_9\text{T}$ was found to crystallize at 200 °C with a higher crystallization rate than the analogous $^{\text{MP}}\text{PB}_{91}\text{Thx}_9\text{T}$ copolyester.

Table 6.6. Isothermal crystallization data.

Copolyester	T_c (°C)	t_0 (min)	$t_{1/2}$ (min)	N	$-\log k$	T_m (°C)
PBT	200	0.19	0.82	2.14	-0.25	223.9
	205	0.51	2.68	2.45	1.02	225.5
$^{\text{MP}}\text{PB}_{96}\text{Thx}_4\text{T}$	195	0.41	4.82	2.56	1.77	210.0
	200	0.55	12.77	2.61	2.99	212.1
$^{\text{MP}}\text{PB}_{91}\text{Thx}_9\text{T}$	195	1.58	9.52	2.06	2.04	207.0
	200	6.64	33.01	2.08	3.14	209.5
$^{\text{SSM}}\text{PB}_{96}\text{Thx}_4\text{T}$	195	0.19	1.54	2.31	0.48	215.8
	200	0.36	4.74	2.62	1.82	217.9
$^{\text{SSM}}\text{PB}_{91}\text{Thx}_9\text{T}$	195	0.23	5.95	2.01	1.68	213.0
	200	1.74	17.29	2.17	2.74	215.2

The conclusion that can be drawn from this comparative study is that the presence of Thx units depresses the crystallizability of terephthalate-based polyesters, and that the crystallization rate depends on the chemical microstructure of the polymeric material. SSM allows for the preparation of more readily crystallizable copolyesters, since long PBT sequences are retained during the SSM process.

6.3.3.5. Hydrolytic degradation

To investigate the influence of the incorporation of Thx on the hydrolytic degradation of PBT, a comparative study of the two homopolyesters PThxT and PBT in addition to the copolyesters with 18% Thx prepared by MP and SSM was carried out at pH 2.0 at 80 °C. Under these conditions, it is possible to study the degradation in a reasonable amount of time because of the relatively high hydrolysis rate. Changes in sample weight and molecular weight at increasing incubation times are depicted in Figure 6.14.

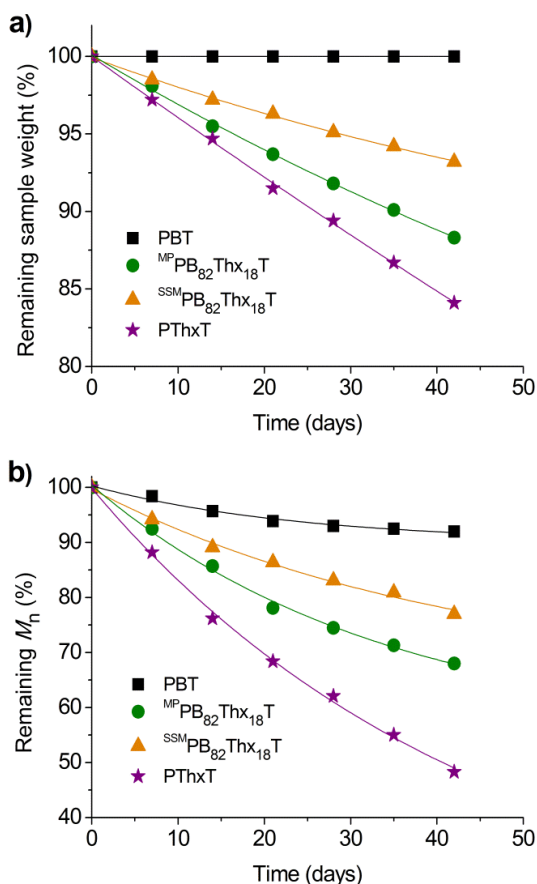


Figure 6.14. Degradation of PBT, $^{MP}PB_{82}Thx_{18}T$, $^{SSM}PB_{82}Thx_{18}T$ and PThxT at pH 2.0 at 80 °C. Remaining weight (a) and molecular weight (b) versus time.

PThxT underwent a weight loss of approx. 16% after six weeks of incubation time, which was accompanied by a decrease in the molecular weight of about 50%. This is in contrast to PBT, because the latter did not show any weight loss or significant decrease in molecular weights under these conditions. The decrease in the sample weight and the molecular weight were also noticeable for $^{MP}PB_{82}Thx_{18}T$ and $^{SSM}PB_{82}Thx_{18}T$, evidencing the positive effect of the Thx units on the hydrolytic degradability. Furthermore, SEM analysis showed more apparent physical degradation of the surfaces of $^{MP}PB_{82}Thx_{18}T$, $^{SSM}PB_{82}Thx_{18}T$ and PThxT compared to PBT (Annex H). The decreases in sample weight and molecular weight of the two copolyesters were found to be intermediate between those of PBT and PThxT homopolyesters, although the copolyesters prepared by MP showed more extensive hydrolytic degradation compared to the sample prepared by SSM. This can be explained by the higher crystallinity of $^{SSM}PB_{82}Thx_{18}T$ compared to $^{MP}PB_{82}Thx_{18}T$. The relatively long PBT sequences in the SSM sample do limit the degradation. The melting enthalpies of the initial SSM and MP samples obtained by solvent casting were 45.9 and 28.2 $J \cdot g^{-1}$, respectively. It is noteworthy to mention that the melting enthalpies of the remaining parts of both the copolyesters increased up to 59.3 and 46.6 $J \cdot g^{-1}$ after 6 weeks of incubation, respectively. Such an increase in crystallinity is indicative that hydrolysis has taken place preferably in the amorphous phase, as is usually observed in semicrystalline polymers.

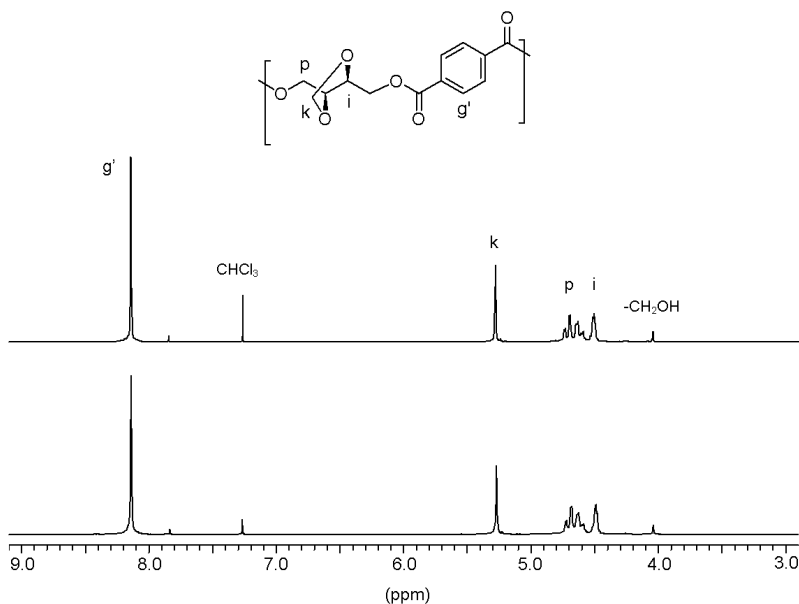


Figure 6.15. 1H NMR spectra in $CDCl_3/TFA$ of PThxT after incubation at pH 2.0 at 80 $^{\circ}C$ for 6 weeks (top) and initial sample (bottom).

To gain insight into the degradation mechanism of the polyester chain at the molecular level, ^1H NMR spectra were recorded for the polymer residues after incubation (Figure 6.15 and Annex H). The spectrum of the residue of PThxT displayed, in addition to the signals characteristic for the polymer, an increase in the signal arising from CH_2OH end groups. This is indicative of the reduced molecular weight, in full agreement with data provided by the SEC analysis. Furthermore, a full stability of the cyclic Thx structure against hydrolysis can be inferred from the total absence of any signal indicative of the hydrolysis of the acetal group in the $^{\text{MP}}\text{PB}_{82}\text{Thx}_{18}\text{T}$, $^{\text{SSM}}\text{PB}_{82}\text{Thx}_{18}\text{T}$ and PThxT spectra. This result is rather striking because acetal groups are known to be sensitive to acidic conditions (Smith and March, 2007), and the opening of the dioxolane ring might be therefore expected to happen to some extent. To corroborate the stability of the cyclic structure against hydrolysis, 2,3-di-O-methylene-L-threitol was incubated in aqueous buffer at pH 2.0, 7.4 and 10.5 at 80 °C for 6 weeks. The spectra recorded at the end of the incubation period are shown in Annex H; all spectra correspond to the structure of the original diol without any sign which would indicate hydrolysis of the acetal group taking place.

6.3.4. Conclusions

The cyclic diol 2,3-di-O-methylene-L-threitol (Thx), derived from naturally occurring tartaric acid, has been used as carbohydrate-based building block in the preparation of poly(butylene terephthalate) (PBT) copolyesters. Two series of partially bio-based copolyesters with comparable molecular weights were prepared by either melt polycondensation (MP) of Thx with dimethyl terephthalate and 1,4-butanediol, or by the solid-state modification (SSM) of PBT with Thx. Copolyesters with compositions very close to the feed ratio and a random chemical microstructure were obtained by MP. Conversely, SSM yielded only the partial incorporation of the Thx in the PBT backbone and led to a limited range of compositions. These copolyesters had a block-like overall chemical microstructure, formed by PBT sequences present in the crystalline phase during the SSM process and a practically random amorphous phase, which is taking part in the transesterification reactions. However, the blocky microstructure of the copolyesters prepared by SSM randomized after prolonged times in the melt.

The incorporation of the cyclic bio-based Thx afforded copolyesters displaying a satisfactory thermal stability and exhibiting increased T_g values. Furthermore, the unique

block-like chemical microstructure obtained after SSM yielded copolyesters with remarkable thermal properties. The SSM-prepared materials showed better crystallizability from the melt because of the long PBT sequences present in the backbone of these copolyesters. Furthermore, they displayed higher T_m values and a higher crystallinity compared to their MP counterparts, although these properties were not completely recovered after crystallizing from the melt as found for the MP-prepared samples.

The presence of the Thx significantly increased the hydrolytic degradability of PBT. This effect was more pronounced for the materials prepared by MP because of their lower crystallinity. The degradation of Thx-containing polyesters happened through hydrolysis of the main chain ester bonds without alteration of the acetal structure.

6.3.5. References

- Alla, A.; Rodríguez-Galán, A.; Muñoz-Guerra, S. *Polymer* **2000**, *41*, 6995-7002.
- Alla, A.; Oxelbark, J.; Rodríguez-Galán, A.; Muñoz-Guerra, S. *Polymer* **2005**, *46*, 2854-2861.
- Blair, G.T.; DeFraties, J.J. *Hydroxy Dicarboxylic Acids*. Kirk-Othmer Encyclopedia of Chemical Technology, **2000**. DOI: 10.1002/0471238961.0825041802120109.a01
- Dhamaniya, S.; Jacob, J. *Polymer* **2010**, *51*, 5392-5399.
- Fenouillot, F.; Rousseau, A.; Colomines, G.; Saint-Loup, R.; Pascault, J.P. *Prog. Polym. Sci.* **2010**, *35*, 578-622.
- Galbis, J.A.; García-Martín, M.G. *Sugars as Monomers*. In: Belgacem, M.N.; Gandini, A.; Eds. *Monomers, Polymers and Composites from Renewable Resources*; Elsevier: Oxford, **2008**, 89-114.
- Galbis, J.A.; García-Martín, M.G. *Chem. Curr. Top.* **2010**, *295*, 147-176.
- Gallucci, R.R.; Patel, B.R. *Poly(butylene terephthalate)*. In: Scheirs, J.; Long, T.E.; Eds. *Modern Polyesters, Chemistry and Technology of Polyesters and Copolyesters*; John Wiley & Sons: Chichester, **2004**, pp. 293-321.
- Gandini, A.; Coelho, D.; Gomes, M.; Reis, B.; Silvestre, A. *J. Mater. Chem.* **2009**, *19*, 8656-8664.
- Gandini, A. *Green Chem.* **2011**, *13*, 1061-1083.
- Gómez, R.; Varela, O. *Macromolecules* **2009**, *42*, 8112-8117.

Gubbels, E.; Jasinska-Walc, L.; Koning, C. *J. Polym. Sci., Polym. Chem.* **2013**, *51*, 890-898. (2013a)

Gubbels, E.; Jasinska-Walc, L.; Hermida Merino, D.; Goossens, H.; Koning, C. *Macromolecules* **2013**, *46*, 3975-3984. (2013b)

Hall, I.H. *The Determination of the Structures of Aromatic Polyesters from their Wide-angle X-Ray Diffraction Patterns*. In: Hall, I.H.; Ed. *Structure of Crystalline Polymers*; Elsevier Applied Science: UK, **1984**, pp. 39-78.

Jansen, M.A.G.; Goossens, J.G.P.; de Wit, G.; Bailly, C.; Schick, C.; Koning, C.E. *Macromolecules* **2005**, *38*, 10658-10666.

Jansen, M.A.G.; Goossens, J.G.P.; de Wit, G.; Bailly, C.; Koning, C.E. *Anal. Chim. Acta* **2006**, *557*, 19-30.

Jansen, M.A.G.; Wu, L.H.; Goossens, J.G.P.; de Wit, G.; Bailly, C.; Koning, C.E.; Portale, G. *J. Polym. Sci., Polym. Chem.* **2008**, *46*, 1203-1217.

Japu, C.; Martínez de Ilarduya, A.; Alla, A.; Muñoz-Guerra, S. *Polymer* **2013**, *54*, 1573-1582.

Kiely, D.E.; Chen, L.; Lin, T.-H. *J. Am. Chem. Soc.* **1994**, *116*, 571-578.

Kiely, D.E.; Chen, L.; Lin, T.-H. *J. Polym. Sci., Polym. Chem.* **2000**, *38*, 594-603.

Kint, D.P.R.; Wigstrom, E.; Martínez de Ilarduya, A.; Alla, A.; Muñoz-Guerra, S. *J. Polym. Sci., Polym. Chem.* **2001**, *39*, 3250-3262.

Kricheldorf, H.R. *Makromol. Chem.* **1978**, *179*, 2133-2143.

Kricheldorf, H.R.; Behnken, G.; Sell, M. *J. Macromol. Sci. Part A Pure Appl. Chem.* **2007**, *44*, 679-684.

Lavilla, C.; Alla, A.; Martínez de Ilarduya, A.; Benito, E.; García-Martín, M.G.; Galbis, J.A.; Muñoz-Guerra, S. *Biomacromolecules* **2011**, *12*, 2642-2652. **-Subchapter 3.2-**

Lavilla, C.; Muñoz-Guerra, S. *Polym. Degrad. Stabil.* **2012**, *97*, 1762-1771. **-Subchapter 5.3-**

Lavilla, C.; Martínez de Ilarduya, A.; Alla, A.; Muñoz-Guerra, S. *Polym. Chem.* **2013**, *4*, 282-289. (2013a) **-Subchapter 4.3-**

Lavilla, C.; Alla, A.; Martínez de Ilarduya, A.; Muñoz-Guerra, S. *Biomacromolecules* **2013**, *14*, 781-793. (2013b) **-Subchapter 3.4-**

Lavilla, C.; Gubbels, E.; Martínez de Ilarduya, A.; Noordover, B.A.J.; Koning, C.E.; Muñoz-Guerra, S. *Macromolecules* **2013**, *46*, 4335-4345. (2013c) **-Subchapter 6.2-**

Li, W.D.; Zeng, J.B.; Lou, X.L.; Zhang, J.J.; Wang, Y.Z. *Polym. Chem.* **2012**, *3*, 1344-1353.

Lichtenthaler, F.W. *Carbohydrates as Organic Raw Materials*. Ullmann's Encyclopedia of Industrial Chemistry, **2010**. DOI: 10.1002/14356007.n05_n07

Marín, R.; Muñoz-Guerra, S. *J. Polym. Sci., Polym. Chem.* **2008**, *46*, 7996-8012.

Newmark, R.A. *J. Polym. Sci.* **1980**, *18*, 559-563.

Papaspyrides, C.D.; Vouyiouka, S.N. *Fundamentals of Solid State Polymerization*. In: Papaspyrides, C.D.; Vouyiouka, S.N.; Eds. *Solid State Polymerization*; John Wiley & sons: Hoboken, **2009**, pp 2-28.

Pillai, C.K.S. *Design. Monom. Polym.* **2010**, *13*, 87-121.

Randal, J.C. *Polymer Sequence Determination*; Academic Press: New York, **1977**, pp. 41-69.

Smith, M.B.; March, J. *March's Advanced Organic Chemistry*; Wiley: Hoboken, **2007**, pp. 523,1270.

Vouyiouka, S.N.; Karakatsani, E.K.; Papaspyrides, C.D. *Prog. Polym. Sci.* **2005**, *30*, 10-37.

Wool, R.; Sun, S. *Biobased Polymers and Composites*; Academic Press: New York, **2005**.

Yamadera, Y.; Murano, M. *J. Polym. Sci., Polym. Chem.* **1967**, *5*, 2259-2268.

Zamora, F.; Hakkou, K.; Alla, A.; Rivas, M.; Roffé, I.; Mancera, M.; Muñoz-Guerra, S.; Galbis, J.A. *J. Polym. Sci., Polym. Chem.* **2005**, *43*, 4570-4577.

CHAPTER 7

CYCLIC ACETALIZED ALDITOLS COMPARED TO ISOSORBIDE AS COMONOMERS FOR TEREPHTHALATE COPOLYESTERS

7.1. Aim and scope of this Chapter

Aromatic polyesters, poly(ethylene terephthalate) (PET) and poly(butylene terephthalate) (PBT) in particular, are high performance thermoplastic materials that are massively used in a wide diversity of applications due to their excellent mechanical and thermal properties in addition to other more specific ones. However, an important shortcoming of these common aromatic polyesters is their non-renewable origin; due to the high price and future depletion of fossil fuel stocks, the development of bio-based polymers is attracting a great deal of interest nowadays.

Two approaches are currently followed for the preparation of bio-based aromatic polyesters, *viz.* the development of alternative routes from natural feedstock to produce monomers which are conventionally obtained from petrochemical source, and the synthesis of new monomers from natural sources to replace, either partially or totally, those of petrochemical origin used in the production of aromatic polyesters. The first approach entails no differences in terms of material properties between bio-based polyesters and their petrochemical counterparts since they share the same chemical structure. On the contrary, the latter approach affords novel polymers more or less different from the traditional ones according to the chemical structure of the bio-based monomer. Especially sugar-based monomers with a bicyclic structure are of interest, due to their ability to add stiffness to the polymer backbone, resulting in enhanced T_g values.

Many examples of polyesters containing 1,4:3,6-dianhydro-D-glucitol (isosorbide), a bicyclic diol prepared from D-glucose, have been described in the literature, and its incorporation into aromatic copolyesters has also been studied. The industrially relevant melt polycondensation technique, combined with the commonly used titanium (IV) tetrabutoxide (TBT) catalyst, have been reported to yield isosorbide-based copolyesters with very low molecular weights. The low and different reactivity of the two secondary hydroxyl groups of isosorbide is the reason for such behavior. Polymers with higher molecular weight could be obtained via polycondensation in solution, but due to the large use of solvents this method is not suitable to be applied at an industrial scale. Recently, the incorporation of isosorbide into PBT via solid-state modification (SSM) has been investigated. The direct incorporation of isosorbide into PBT was unsuccessful due to the low reactivity of this sugar-based diol. The synthesis of macrodiol bearing two primary hydroxyl groups, from isosorbide, terephthaloyl chloride and 1,4-butanediol was

necessary to incorporate isosorbide into the PBT chain, and yielded high molecular weight polymers.

In this Thesis it has been reported that internally diacetalized alditols with a bicyclic structure are also carbohydrate derivatives very suitable to prepare aromatic copolyesters displaying satisfactory general properties and enhanced T_g (Chapters 4-6). Furthermore, at difference with isosorbide, the more reactive primary hydroxyl groups of diacetalized alditols have allowed their direct incorporation into PBT by SSM (Chapter 6).

Given the structural proximity between isosorbide and diacetalized alditols, as well as their common potential use as polycondensation monomers, it is encouraging to make a comparative evaluation of their suitability for the synthesis of aromatic polyesters. Melt polycondensation will be the preparation technique chosen in this case since aromatic polyesters are commonly prepared by this method in the industry. In this Chapter, a comparative evaluation of the reactivity of isosorbide and two diacetalized alditols in the polycondensation with dimethyl terephthalate under the same polymerization conditions will be reported, and the influence that each monomer exerts on the glass-transition temperature and crystallinity of the polyesters will be studied.

7.2. Sugar-based aromatic copolyesters: A comparative study regarding isosorbide and diacetalized alditols as sustainable comonomers

Summary: Three carbohydrate-based bicyclic diols, 1,4:3,6-dianhydro-D-glucitol (isosorbide, *Is*), 2,3:4,5-di-O-methylene-galactitol (*Galx*) and 2,4:3,5-di-O-methylene-D-mannitol (*Manx*) were made to react in the melt and under the same conditions with dimethyl terephthalate and 1,4-butanediol to produce respectively three series of PB_xIs_yT , PB_xGalx_yT and PB_xManx_yT random copolyesters. Five different copolymerizations, with molar feed ratios of 1,4-butanediol to sugar-based diol of 90:10, 80:20, 70:30, 60:40 and 50:50, were carried out for each bicyclic diol in order to make a comparative study on their reactivity and properties of the resulting copolyesters. Molecular weights and compositions data of the copolyesters revealed the greater facility of diacetalized diols to react under these conditions compared to isosorbide. The three bicyclic diols contributed to increase the thermal stability and also the glass-transition temperature of PBT. The replacement of a 40% of 1,4-butanediol by sugar-based diol increased the glass-transition temperature of PBT from 31 °C to ~60 °C in the case of *Galx* and up to ~90 °C regarding *Is* and *Manx*. All PB_xGalx_yT copolyesters as well as PB_xIs_yT and PB_xManx_yT ones with contents of *Is* and *Manx* of up to 32% and 41%, respectively, were semicrystalline.

Publication derived from this work:

Lavilla, C.; Muñoz-Guerra, S. *Green Chem.* **2013**, *15*, 144-151.

7.2.1. Introduction

The urgent need to reduce the amount of petroleum consumed in the industry, as well as to minimize the impact of the use of plastics on the environment is attracting important efforts in research by following different approaches. Thus, significant increases in the recycling rates of polymers are taking place with facilities and changes in recent legislation that now permits even recycling of food contact polymers (Wool and Sun, 2005; Welle, 2011; Grause *et al.*, 2011). On the other side substitution of petroleum-based monomers by those coming from renewable sources has become one of the most important challenges in current polymer research (Belgacem and Gandini, 2008; Williams and Hillmyer, 2008). Among the renewable naturally occurring sources, carbohydrates stand out because they are hugely abundant, readily available and able to provide great functional diversity; an increasing activity in the research of carbohydrate-based polymers is reflected in the recently reported literature (Galbis and García-Martín, 2008; Narain, 2011; Gandini, 2011).

Aromatic polyesters, poly(ethylene terephthalate) (PET) and poly(butylene terephthalate) (PBT) in particular, are high performance thermoplastic materials that are massively used in a wide diversity of applications due to their excellent mechanical and thermal properties in addition to other more specific ones. The high resistance to atmospheric action and biological agents exhibited by these materials is an added value when they are intended to be used in long-term applications. On the contrary, they are considered unfriendly compounds when used in short-term applications because their non-renewable origin and great resistance to degradation (Müller *et al.*, 2001; Rychter *et al.*, 2010). In this regard, the development of aromatic polyesters from natural sources is currently drawing an enormous interest. To this purpose a really attractive approach is to unfold sustainable processes able to produce the traditional monomers implied in their synthesis. Thus ethylene glycol can be produced via oxidation and subsequent hydrolysis of bio-based ethylene (Chen and Patel, 2012), and 1,4-butanediol by hydrogenation of succinic acid obtained from corn (Delhomme *et al.*, 2009); also the production of terephthalic acid from limonene has been recently patented (Berti *et al.*, 2010). However the industrial application of these methods is still far from realization and monomers used today for the synthesis of industrial aromatic polyesters are almost entirely produced from petrochemical feedstocks. Another possibility of creating sustainable copolymers of PET and PBT is replacing either the diol or the diacid by other bio-based monomers. This is an

extremely appealing option provided that the properties of the original polymers are improved, or at least not significantly impoverished.

The high glass-transition temperature (T_g) is a greatly appreciated property in those polyesters addressed to packaging under heating or to the manufacture of containers for pressurized gaseous beverages; copolymerization with cyclic diols such as 1,4-cyclohexanedimethanol (Turner, 2004; González-Vidal *et al.*, 2009) or 1,3-ciclobutanediol (Booth *et al.*, 2006) has been a common strategy to obtain aromatic polyesters with enhanced T_g . Carbohydrate-derived monomers with a cyclic structure have achieved a privileged position because, in addition to their natural origin, they are able to provide polyesters with higher glass-transition temperatures while essentially retaining their original pattern of behavior. Thus, the olden known 2,5-furandicarboxylic acid is receiving in these last years a great deal of attention as a serious alternative to replace terephthalic acid in polyterephthalates (Gandini *et al.*, 2009; Gomes *et al.*, 2011). A decade ago, the bicyclic anhydride 1,4:3,6-dianhydro-D-glucitol, known as isosorbide, emerged with great pushing force as an adequate monomer for replacing aliphatic diols in PET and PBT (Storbeck and Ballauff, 1996; Kricheldorf, 1997). Very recently we have shown that internally diacetalized alditols with a bicyclic structure are also carbohydrate derivatives very suitable to prepare aromatic copolyesters displaying satisfactory general properties and enhanced T_g (Lavilla *et al.*, 2012a -Subchapter 5.2-, 2012b -Subchapter 5.4- and 2013 -Subchapter 4.3-; Japu *et al.*, 2012).

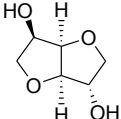
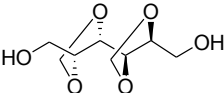
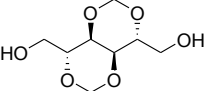
Given the structural proximity between isosorbide and diacetalized alditols, as well as their common potential use as polycondensation monomers, it is encouraging to make a comparative evaluation of their suitability for the synthesis of aromatic polyesters. This paper has been thought with such aim and it reports a comparative study of PBT polyesters and copolyesters obtained by replacing 1,4-butanediol by 1,4:3,6-dianhydro-D-glucitol (Is), 2,3:4,5-di-O-methylene-galactitol (Galx), and 2,4:3,5-di-O-methylene-D-mannitol (Manx). They will be called PB_xIs_yT , PB_xGal_xT and PB_xMan_xT , where x and y stand for the mole percentages (mol-%) of 1,4-butanediol and sugar-based bicyclic diol, respectively, in the resulting copolyester. The study examines the reactivity of the three bicyclic diols in the polycondensation with dimethyl terephthalate (DMT) under the same polymerization conditions and makes a comparative evaluation of the influence that each monomer exerts on the glass-transition temperature and crystallinity of the polyesters.

Compared structure and properties of Is, Galx and Manx

1,4:3,6-dianhydro-D-glucitol (Is) is the dianhydride generated in the dehydration of D-glucitol (sorbitol). Sorbitol is prepared by hydrogenation of D-glucose coming from cereal starch. Is is the only bicyclic carbohydrate-based monomer commercially available today at industrial level (Fenouillot *et al.*, 2010). It is composed of two *cis*-fused nearly planar tetrahydrofuran rings with a dihedral angle of 120° and the 2- and 5- hydroxyl groups in *endo* and *exo* positions, respectively. Since the two hydroxyl groups of Is are secondary, their accessibility to reagents is rather restricted, and due to their different spatial position in the molecule they will display different reactivity; in fact, a deficiency of the reactivity of the *endo* hydroxyl group has been detected in several polymerization studies recently reported (Noordover *et al.*, 2006 and 2007; Fenouillot *et al.*, 2010).

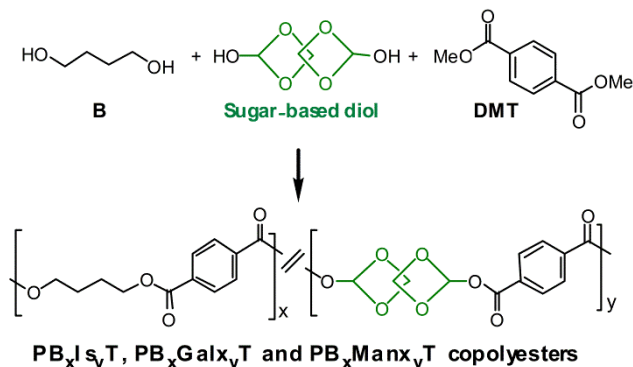
2,3:4,5-di-O-methylene-galactitol (Galx) is obtained from galactaric acid by acetalization of the four secondary hydroxyl groups with paraformaldehyde and subsequent reduction. The structure of Galx consists of two non-fused 1,3-dioxolane rings with the two primary hydroxyl groups in *exo* positions. Contrary to isosorbide, Galx is centrosymmetric so its two free hydroxyl groups display the same reactivity since they are spatially undistinguishable. 2,4:3,5-di-O-methylene-D-mannitol (Manx) is obtained by acetalization of 1,6-di-O-benzoyl-D-mannitol followed by hydrolysis of the benzyloxy groups. Manx consists of two fused 1,3-dioxane rings and possesses a twofold axis of symmetry and, similarly to Galx, the two primary hydroxyl groups are in *exo* positions and display the same reactivity. A comparative summary of the main features of Is, Galx and Manx of relevance to this study is given in Table 7.1.

Table 7.1. Main features of bicyclic diols.

Compound	Is	Galx	Manx
Chemical name	1,4:3,6-dianhydro-D-glucitol	2,3:4,5-di-O-methylene-galactitol	2,4:3,5-di-O-methylene-D-mannitol
Chemical structure			
Protecting group	dianhydride	diacetal	diacetal
OH groups	secondary	primary	primary
Cycle structure	tetrahydrofuran	1,3-dioxolane	1,3-dioxane
Symmetry	1	I	C ₂
OH stereo positions	<i>exo/endo</i>	<i>exo/exo</i>	<i>exo/exo</i>
Melting point	60-63 °C	100-102 °C	139-140 °C
Origin	D-glucose	D-galactose	D-fructose

7.2.2. Experimental section

The three series of polyesters, PB_xIs_yT , $PB_xGal_x_yT$ and $PB_xMan_x_yT$, subjected here to study were obtained according to the synthesis scheme depicted in Scheme 7.1.



Scheme 7.1. Polymerization reactions leading to PB_xIs_yT , $PB_xGal_x_yT$ and $PB_xMan_x_yT$ copolyesters.

Five different copolymerizations, with molar feed ratios of 1,4-butanediol to sugar-based diol of 90:10, 80:20, 70:30, 60:40 and 50:50, were carried out for each bicyclic diol. Exactly the same reaction conditions were used to prepare copolyesters of different series with the same molar feed ratio (1,4-butanediol to sugar-based diol) for the three series. Specific conditions were used for each molar feed ratio, as they are detailed in Annex I. The synthesis and characterization of $PB_xGal_x_yT$ and $PB_xMan_x_yT$ copolyesters and their parent homopolyesters has been reported previously in detail (Lavilla *et al.*, 2012a -Subchapter 5.2- and 2012b -Subchapter 5.4-). The synthesis of the PB_xIs_yT family has been carried out now with the purpose of providing the data necessary for the comparative study aimed in this work. The common synthetic procedure was the following: The polymerization feed was a mixture of dimethyl terephthalate, 1,4-butanediol and the sugar-based diol in the selected compositions. A molar excess of diol mixture to dimethyl terephthalate was used, and dibutyl tin oxide (DBTO) catalyst in 0.6% molar respect to monomers as well as antioxidants Irganox 1010 (0.1% w/w) and Irgafos 126 (0.3% w/w) were added. The reaction was performed in the melt along two steps in a three-necked, cylindrical-bottom flask equipped with a mechanical stirrer, a nitrogen inlet and a vacuum distillation outlet. Firstly the transesterification reaction was carried out

under a low nitrogen flow at temperatures in the 160-200 °C range depending on composition. The polycondensation reaction was left to proceed at a temperature between 210 and 240 °C under a 0.03-0.06 mbar vacuum. Then, the reaction mixture was cooled to room temperature, and the atmospheric pressure was recovered with nitrogen to prevent degradation. The resulting polymers were dissolved in chloroform or in a mixture of chloroform and trifluoroacetic acid (9:1), and precipitated in excess of methanol in order to remove unreacted monomers and formed oligomers. Finally, the polymer was collected by filtration, extensively washed with methanol, and dried under vacuum.

The resulting polymers were extensively characterized and their thermal properties accurately evaluated in parallel. The chemical constitution, composition and microstructure of polyesters and copolyesters were determined by NMR and their thermal stability measured by thermogravimetry under inert atmosphere. Their melting and glass-transition behavior were examined by DSC and temperatures and enthalpies measured at heating using exactly the same recording conditions.

The specific reaction conditions and results of the synthesis of the three series of polyesters as well as the technical and methodological details used in their characterization and properties evaluation are provided in Annex I.

7.2.3. Results and discussion

7.2.3.1. Synthesis: Molecular weight and composition

The polymerization conditions used in the synthesis of homopolyesters and copolyesters were selected to imitate as far as possible those usually applied in the industrial practice; reactions were performed in the melt with total absence of solvents, and they were left to proceed through a two-steps sequence of increasing temperature and vacuum. Transesterification reactions were started at 160 °C in order to prevent volatilization of diols, and left to proceed for 2-3 hours period along which temperature was progressively increased to avoid crystallization of early formed oligomers. Polycondensation reactions were carried out for 2-4 hours at temperatures in the 210-240 °C range and under vacuum to facilitate the removal of volatile by-products; lower temperatures and longer reaction times were used for copolyesters with higher contents in sugar-based monomers. Antioxidants additive were added in the synthesis of PB_xIs_yT

copolyesters to avoid discoloration, and dibutyl tin oxide (DBTO) was the catalyst of choice for the three series instead of the commonly used titanium (IV) tetrabutoxide (TBT). Our earlier results in the synthesis of aliphatic homopolyesters from the bicyclic diester dimethyl 2,3:4,5-di-O-methylene-galactarate and linear alkanediols demonstrated the higher activity of DBTO catalyst compared to TBT which allowed to proceed at lower reaction temperatures without increasing reaction times (Lavilla *et al.*, 2011 -Subchapter 3.2-). Under softer reaction conditions, decomposition of the thermally-sensitive sugar compounds was minimized and higher molecular weights could be attained. The synthesis results obtained for PBT, the three copolyester series, PB_xGal_yT, PB_xMan_yT and PB_xIs_yT, and their respective parent homopolyesters PGalxT, PManxT and PlsT are compared in Table 7.2.

PB_xGal_yT copolyesters were obtained from 1,4-butanediol, Galx and DMT with intrinsic viscosities of 0.7-0.9 dL·g⁻¹ and weight-average molecular weights between 36,000 and 41,000 g·mol⁻¹ (Lavilla *et al.*, 2012a -Subchapter 5.2-). Correspondingly, PB_xMan_yT copolyesters were obtained when Man_x was used as sugar-based comonomer instead (Lavilla *et al.*, 2012b -Subchapter 5.4-). In this case, relatively high molecular weight copolymers were also achieved, with intrinsic viscosities between 0.8 and 1.2 dL·g⁻¹ and weight-average molecular weights confined in the 38,000-52,000 g·mol⁻¹ interval. On the contrary, the results obtained in the copolymerizations based on Is were not as satisfactory as those based on Galx and Man_x; intrinsic viscosities and weight-average molecular weights of PB_xIs_yT copolyesters were in the 0.3-0.4 dL·g⁻¹ and 15,000-20,000 g·mol⁻¹ intervals, respectively. Although polycondensations in bulk involving Is have been usually carried out with TBT as catalyst (Noordover *et al.*, 2006 and 2007; Kricheldorf *et al.*, 2007; Inkinen *et al.*, 2010); it was here replaced by DBTO by the reasons indicated above. The molecular weights reported for Is containing copolyesters obtained by using TBT catalyst are even lower than those obtained here with DBTO. It is worthy to note that molecular weight values are very similar within each series (with the only exception of the homopolyester entirely made of sugar-based diol), and that essentially the same molecular weight dispersity is obtained for all the prepared polyesters regardless of which series is concerned. This satisfactory agreement adds confidence to the comparative analysis of thermal properties that is carried out below.

Table 7.2. Composition, molecular weights and thermal properties of sugar-based copolyesters.

Copolyester	Yield (%)	Molar composition X_B/X_{sugar}		Molecular weights				Thermal properties				
		Feed	Copolyester ^a	$[\eta]^b$	M_n^c	M_w^c	\mathcal{D}^c	$^{\circ}T_{5\%}^d$	T_d^e	T_g^f	T_m^g	ΔH_m^g
PBT	90	100/0	100/0	0.93	17,100	41,300	2.4	371	408	31	223	56.2
PB ₉₄ Is ₆ T	85	90/10	93.9/6.1	0.31	6,800	15,700	2.3	367	406	34	206	43.9
PB ₈₅ Is ₁₅ T	84	80/20	85.0/15.0	0.30	6,500	15,100	2.3	367	407	54	189	31.7
PB ₇₅ Is ₂₅ T	82	70/30	74.6/25.4	0.35	7,200	17,500	2.4	367	408	67	174	21.6
PB ₆₈ Is ₃₂ T	83	60/40	67.7/32.3	0.37	7,300	18,300	2.5	368	409	78	158	11.7
PB ₅₆ Is ₄₄ T	85	50/50	55.9/44.1	0.42	8,400	20,200	2.4	372	413	98	-	-
PIsT	80	0/100	0/100	0.20	2,300	5,400	2.3	374	424	148	-	-
PB ₈₉ Galx ₁₁ T	87	90/10	88.7/11.3	0.91	16,300	40,800	2.5	372	409	46	197	37.2
PB ₇₉ Galx ₂₁ T	89	80/20	78.9/21.1	0.90	16,800	40,300	2.4	373	411	53	179	26.1
PB ₆₉ Galx ₃₁ T	87	70/30	69.2/30.8	0.70	15,600	37,800	2.4	375	414	57	151	21.9
PB ₆₁ Galx ₃₉ T	88	60/40	61.3/38.7	0.65	14,400	36,500	2.5	377	417	62	138	14.8
PB ₅₁ Galx ₄₉ T	85	50/50	50.9/49.1	0.69	15,800	37,600	2.4	379	418	70	119	8.7
PGalxT	86	0/100	0/100	0.50	12,400	30,500	2.5	382	436	87	-	-
PB ₉₁ Manx ₉ T	86	90/10	91.0/9.0	1.18	20,300	51,200	2.5	371	408	55	197	34.1
PB ₈₀ Manx ₂₀ T	87	80/20	80.3/19.7	0.84	16,500	41,000	2.5	372	410	66	184	26.0
PB ₆₉ Manx ₃₁ T	86	70/30	69.2/30.8	0.75	16,600	38,500	2.3	374	411	77	162	5.5
PB ₅₉ Manx ₄₁ T	85	60/40	59.2/40.8	0.83	16,400	40,100	2.4	376	411	88	122	5.0
PB ₄₉ Manx ₅₁ T	88	50/50	49.0/51.0	0.77	16,300	38,900	2.4	377	412	100	-	-
PManxT	85	0/100	0/100	0.51	12,900	30,200	2.3	378	421	137	-	-

^a Molar composition determined by integration of the ¹H NMR spectra. ^b Intrinsic viscosity in dL·g⁻¹ measured in dichloroacetic acid at 25 °C.

^c Number-average and weight-average molecular weights in g·mol⁻¹ and dispersities measured by GPC in HFIP against PMMA standards.

^d Temperature at which 5% weight loss was observed. ^e Temperature for maximum degradation rate. ^f Glass-transition temperature taken as the inflection point of the heating DSC traces of melt-quenched samples recorded at 20 °C·min⁻¹. ^g Melting temperature (T_m) and enthalpy (ΔH_m) measured by DSC at a heating rate of 10 °C·min⁻¹.

A detailed comparison of the M_w attained for the three types of copolyesters for similar contents in the sugar-based comonomer is represented in Figure 7.1. The lower molecular weights attained for PB_xIs_yT compared to PB_xGal_xT and PB_xMan_xT when polymerized under the same polymerization conditions must be attributed to the lower reactivity of the secondary hydroxyl groups of Is compared to that of the primary ones present in both Galx and Manx. The limited reactivity of Is in melt polycondensation has been previously reported (Noordover *et al.*, 2006 and 2007; Kricheldorf *et al.*, 2007; Fenouillot *et al.*, 2010). Isosorbide copolyesters with higher molecular weight are achievable via polycondensation in solution (Kricheldorf *et al.*, 2007), but due to the large use of solvents, this method is not appropriate for industrial application (Fradet and Tessier, 2003). Recently, Sablong *et al.* investigated the incorporation of isosorbide into PBT via solid-state polymerization and reported the synthesis of higher molecular weight polymers by this method (Sablong *et al.*, 2008).

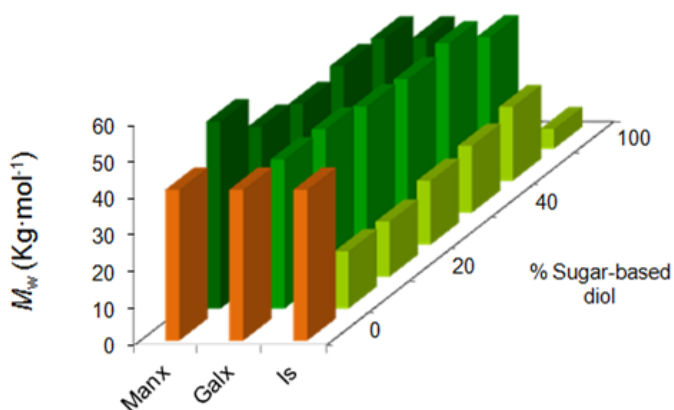


Figure 7.1. Weight-average molecular weight versus composition plot for PBT copolyesters containing isosorbide (Is), 2,3:4,5-di-O-methylene-galactitol (Galx) and 2,4:3,5-di-O-methylene-D-mannitol (Manx).

The chemical constitution and composition of the copolyesters were ascertained by NMR. A selection of spectra is provided in Annex I. The 1H NMR spectra corroborated the chemical structure of the copolyesters with all signals being properly assigned to the different protons contained in their repeating units. Integration of the proton signals arising from 1,4-butylene and sugar-based units led to quantify the composition of the copolyesters in such units. Five different experiences, with molar feed ratios of 1,4-butanediol and sugar-based diol of 90:10, 80:20, 70:30, 60:40 and 50:50, were carried

out within each series. The compositions of the resulting PB_xIs_yT , PB_xGalx_yT and PB_xManx_yT copolyesters are shown in Table 7.2. The correspondence between the comonomeric composition used in the feed and that present in the resulting copolyester depended on which sugar-based comonomer was involved. The fraction (%) of sugar-based diol (Is, Galx or Manx) that is incorporated in the PBT copolyester for the different feed compositions that have been studied in this work are depicted in Figure 7.2. The content of the copolyesters in Is units was found to be in all cases significantly lower than in their corresponding feeds, with losses of up to 40%; such discrepancy should be attributed to the higher reactivity of the hydroxyl groups of 1,4-butanediol compared to those of isosorbide. Conversely, no noteworthy differences in the relative incorporation of bicyclic acetalized diols and 1,4-butanediol were detected, suggesting that the primary hydroxyl groups of both Galx and Manx are able to react at a rate similar to those of 1,4-butanediol. Furthermore, the reactivity of the primary hydroxyl groups of Galx and Manx seems to be not affected by the presence of the neighboring acetalic cyclic structure, neither in the 2,3:4,5 nor in the 2,4:3,5 arrangement, since both PB_xGalx_yT and PB_xManx_yT copolyesters have compositions very close to those of their corresponding feeds.

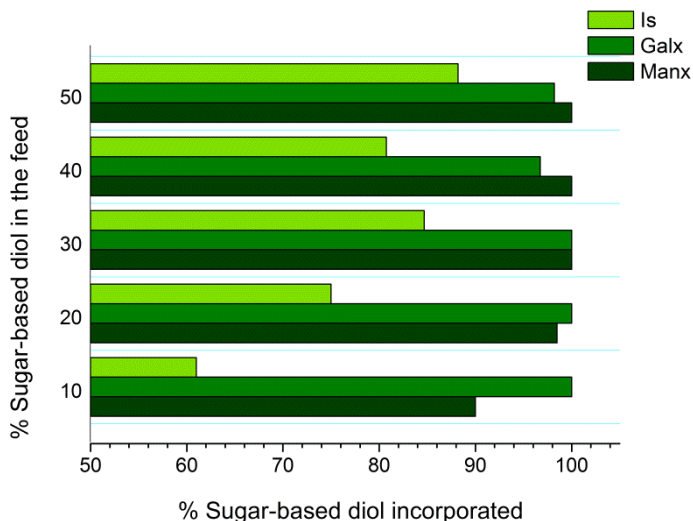


Figure 7.2. Fraction (%) of sugar-based diol (Is, Galx or Manx) that is incorporated in the PBT copolyester for the different feed compositions studied in this work.

The ^{13}C NMR spectra of $\text{PB}_x\text{Is}_y\text{T}$, $\text{PB}_x\text{Gal}_y\text{T}$ and $\text{PB}_x\text{Man}_y\text{T}$ copolyesters show the non-protonated aromatic carbon signal at 133-135 ppm with resolution enough (Figure 7.3) to estimate their degree of randomness (Randal, 1977), leading to the conclusion that the microstructure was random in the three series. Regarding $\text{PB}_x\text{Is}_y\text{T}$ copolyesters, each type of dyad consists of multiple peaks as a consequence of the two orientations possible for the non-symmetrical Is unit. Conversely, a single signal is detected for every dyad in $\text{PB}_x\text{Gal}_y\text{T}$ and $\text{PB}_x\text{Man}_y\text{T}$ copolyesters. Due to the symmetry of Galx and Manx units, only one orientation is feasible for these units when incorporated in the polymer chain. Consequently, copolyesters made from Galx and Manx should be expected to be stereoregular as it has been observed.

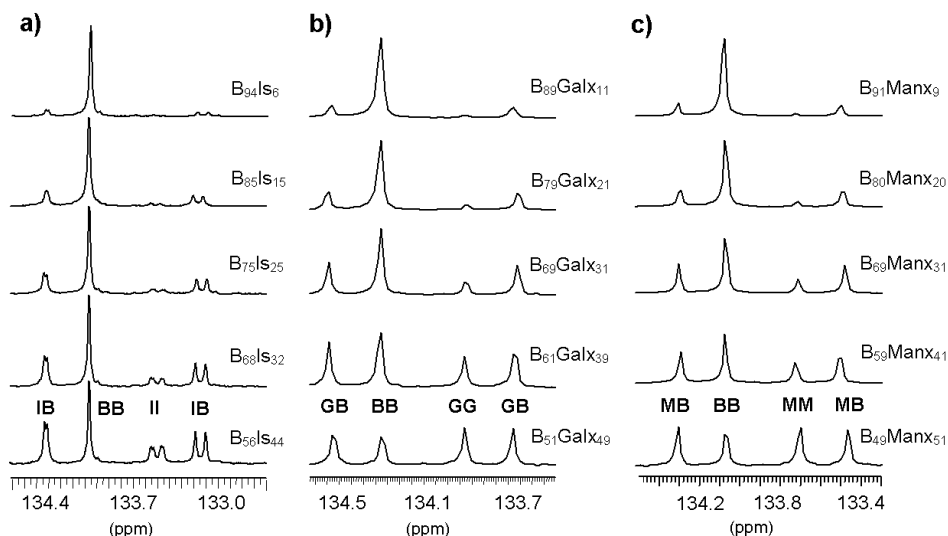


Figure 7.3. ^{13}C NMR signals of the non-protonated aromatic carbons of $\text{PB}_x\text{Is}_y\text{T}$ (a), $\text{PB}_x\text{Gal}_y\text{T}$ (b), and $\text{PB}_x\text{Man}_y\text{T}$ (c) copolyesters. The assignments correspond to terephthalic units attached to: B, butanediol; I, Isosorbide; G, Galx; M, Manx.

7.2.3.2. Thermal properties

The thermal behavior of $\text{PB}_x\text{Is}_y\text{T}$, $\text{PB}_x\text{Gal}_y\text{T}$ and $\text{PB}_x\text{Man}_y\text{T}$ copolyesters was systematically studied by TGA and DSC under inert atmosphere. The thermal parameters resulting from these analyses are given in Table 7.2, where the corresponding data for the parent homopolyesters PBT, PI_sT, PGalxT and PManxT are also included for comparison purposes. The thermal decomposition of all these polyesters occurs in a single stage leaving less than 10% of residue upon heating at 600 °C. PBT starts to

decompose well above 300 °C with 5% of the initial weight being lost at 371 °C ($^{\circ}T_{5\%}$) and with a maximum decomposition rate at 408 °C ($^{\max}T_d$). The onset decomposition temperatures of PB_xIs_yT , PB_xGal_xT and PB_xMan_xT copolyesters and their corresponding homopolyesters indicative of the thermal stability are comparatively depicted in Figure 7.4. In the PB_xIs_yT series, $^{\circ}T_{5\%}$ and $^{\max}T_d$ increase with the content in Is to reach values of 374 and 424 °C respectively in the PIsT homopolyester. Strangely copolyesters containing minor amounts of Is show values slightly below those of PBT; the low molecular weight of these copolyesters may be the reason for such behavior. Regarding PB_xGal_xT copolyesters, both $^{\circ}T_{5\%}$ and $^{\max}T_d$ steadily increase with the content in sugar units with values being comprised between those displayed by the two parent homopolyesters PBT and PGalxT. The same trend is observed for the PB_xMan_xT . These results are in full accordance with the high thermal stability observed for PGalxT and PManxT homopolyesters compared to PBT. The valuable conclusion drawn from this comparative thermogravimetric study is that the insertion of bicyclic sugar units in aromatic polyesters instead of reducing their decomposition temperatures contributes significantly to increasing their thermal stability. Since the melting temperature in these copolyesters decreases with composition, the gap between melting and decomposition temperatures becomes wider allowing a more comfortable melt processing. This is an issue of prime importance for the appraisal of these bio-based polymers as potential thermoplastic materials.

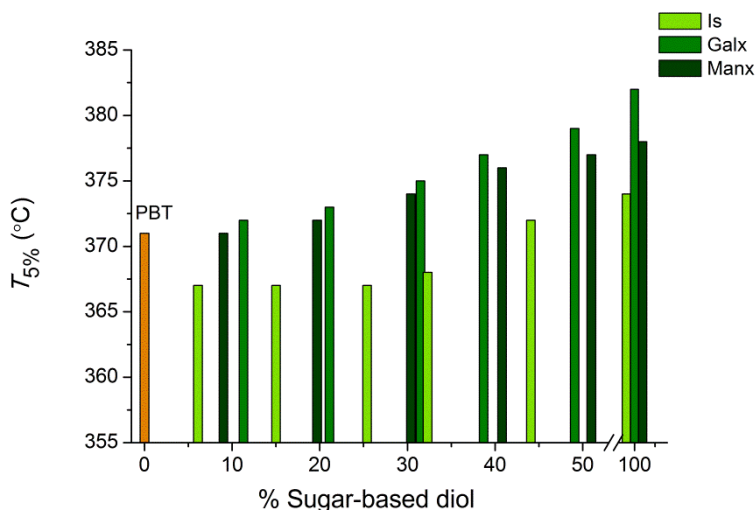


Figure 7.4. Temperature for 5% weight loss versus composition plot for PBT copolyesters containing Is, Galx and Manx.

The glass-transition temperatures (T_g) of PB_xIs_yT , PB_xGalx_yT and PB_xManx_yT copolyesters were measured as the inflection point of the heating DSC traces of samples quenched from the melt, and values are compared in Table 7.2 and depicted in Figure 7.5 together with those of their corresponding homopolyesters. The T_g of PB_xIs_yT copolyesters increased as butanediol was replaced by Is units, even at low Is contents despite the lower molecular weights of PB_xIs_yT copolyesters compared to that of PBT. Such behavior evidences the great positive effect that the fused bicyclic tetrahydrofuran structure exerts on restricting the mobility of the polyester chain. In the PB_xGalx_yT series the T_g also increased with the amount of replaced 1,4-butanediol with minimum and maximum values corresponding to their respective PBT and PGalxT homopolyesters. However the effect of Galx was less pronounced than that of Is for any composition with the difference becoming larger for higher degrees of replacement. Regarding PB_xManx_yT copolyesters, the T_g again increased as 1,4-butanediol was replaced by Manx units going from 31°C for PBT up to 137 °C for PManxT. The effect of Manx on T_g is also slightly weaker than that of Is but in this case differences almost fade away for low contents in bicyclic units; in fact, a similar increase in T_g was attained by incorporating either Is or Manx units as far as the content of 1,4-butanediol remained above 60%.

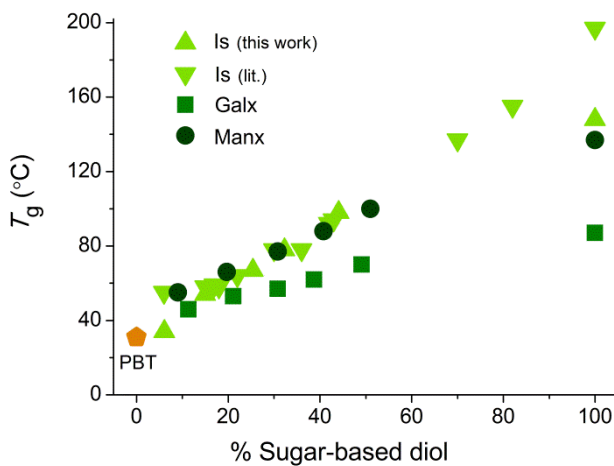


Figure 7.5. Glass-transition temperature versus composition plot for PBT copolyesters containing Is (data from this work and from literature: Kricheldorf *et al.*, 2007; Sablong *et al.*, 2008) Galx and Manx.

The conclusion drawn from this comparative study is that although the all three bicyclic carbohydrate-based diols, Is, Galx and Manx, are capable of raising the T_g of PBT, the effect is depending on the stiffness of the bicyclic structure inserted in the

copolyester chain. As expected, the fused rings of both Is and Manx exert an effect in the T_g more pronounced than the non-fused two 1,3-dioxolane rings present in Galx. Is appears to be the most effective T_g increasing comonomer because its bicyclic structure made of almost rigid tetrahydrofurane rings is more conformationally impeded than that of Manx made of 1,3-dioxanes. Nevertheless, an almost lineal increasing variation of T_g with the content in bicyclic units takes place in the three cases allowing a fine tuning of the property by proper adjusting of the copolyester composition.

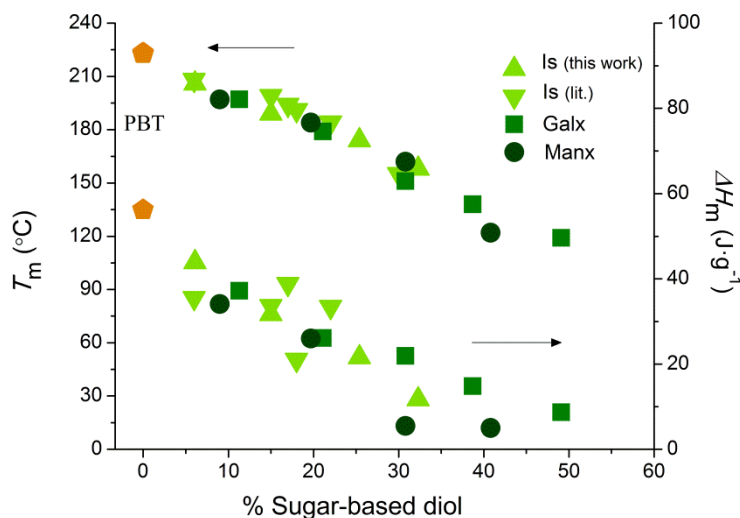


Figure 7.6. Melting temperature and enthalpy versus composition plot for PBT copolyesters containing Is (data from this work and from literature: Kricheldorf *et al.*, 2007; Sablong *et al.*, 2008) Galx and Manx.

With regard to the melting and crystallization behavior, the DSC analysis of the polyesters showed noteworthy qualitative and quantitative differences among the three series (Table 7.2). PBT is a semicrystalline polyester able to crystallize very fast and in a large degree under a wide variety of conditions, and it may serve as a reference. PB_xIs_yT and PB_xManx_yT copolyesters were found to be semicrystalline for low to medium contents in the bicyclic diol whereas PB_xGalx_yT were able to crystallize for the whole range of compositions. In fact, PB_xIs_yT copolyesters were semicrystalline up to 32% of Is, whereas PB_xManx_yT showed endothermic peaks characteristic of melting for Manx contents below or equal to 41%. Nevertheless, the insertion of Is, Galx and Manx units invariably gave place to a noticeable decrease in both T_m and ΔH_m (Figure 7.6), bringing into evidence

the repressing effect of the bicyclic diols on PBT crystallinity. The three homopolyesters PIsT, PGalxT and PManxT were amorphous, at least under the conditions here studied. The depressing effect of copolymerization on crystallinity appears to be stronger when bicyclic fused rings are incorporated into the polymer chain. The conclusion is that although the incorporation of the three bicyclic diols induced changes in the melting-crystallization behavior of PBT, the symmetric fused Manx unit seems to be capable of preserving the crystallinity more than the asymmetric fused Is, but less than the symmetric non-fused Galx.

7.2.4. Conclusions

Three different carbohydrate-based bicyclic diols, Is, which is a dianhydride derived from D-glucose, and Galx and Manx, which are internal diacetals derived from D-galactose and D-fructose, respectively, have been comparatively studied as comonomers of 1,4-butanediol in the preparation of PBT copolyesters by polycondensation in the melt. Exactly the same reaction conditions were used to prepare the three series of copolyesters and they were selected to afford high yields and molecular weights with a minimum degradation of the carbohydrate-based compounds. Copolyesters with pretty high molecular weights and compositions very close to their corresponding feeds have been obtained in the copolymerization with Galx and Manx whereas copolyesters made from Is displayed much lower molecular weights and losses in the sugar-derived comonomer of up to 40%. The three bicyclic monomers were able to enhance the thermal stability of PBT in a similar degree. Isosorbide is the bicyclic monomer that increases the glass-transition temperature of PBT most efficiently, although Manx is capable of affording almost the same effect as far as sugar-based contents are less than 40%. The three bicyclic sugar derived monomers depress the crystallinity of PBT in a degree that is depending on both symmetry and stiffness of the bicyclic structure; copolyesters of Is and Manx are semicrystalline for contents of up to 32% and 41% in these units, respectively, whereas those containing Galx preserve the crystallinity for all the studied compositions. The three homopolyesters entirely made of sugar-derived diols are amorphous.

7.2.3. References

Belgacem, M.N.; Gandini, A. *Monomers, Polymers and Composites from Renewable Resources*; Elsevier: Oxford, **2008**.

Berti, C.; Binassi, E.; Colonna, M.; Fiorini, M.; Kannan, G.; Karanam, S.; Mazzacurati, M.; Odeh, I.; Vannini, M. *US Pat. Appl. Publ.* 20100168371 (to SABIC-IP), **2010**.

Booth, C.J.; Kindinger, M.; McKenzie, H.R.; Handcock, J.; Bray, A.V.; Beall, G.W. *Polymer* **2006**, *47*, 6398-6405.

Chen, G.Q.; Patel, M.K. *Chem. Rev.* **2012**, *112*, 2082-2099.

Delhomme, C.; Weuster-Botz, D.; Kuhn, F.E. *Green Chem.* **2009**, *11*, 13-26.

Fenouillot, F.; Rousseau, A.; Colomines, G.; Saint-Loup, R.; Pascault, J.P. *Prog. Polym. Sci.* **2010**, *35*, 578-622.

Fradet, A.; Tessier, M. *Polyesters*. In: Rogers, M.E.; Long, T.E.; Eds. *Synthetic Methods in Step-Growth Polymers*; John Wiley & Sons: Hoboken, **2003**, pp. 17-134.

Galbis, J.A.; García-Martín, M.G. *Sugars as Monomers*. In: Belgacem, M.N.; Gandini, A.; Eds. *Monomers, Polymers and Composites from Renewable Resources*; Elsevier: Oxford, **2008**, 89-114.

Gandini, A.; Coelho, D.; Gomes, M.; Reis, B.; Silvestre, A. *J. Mater. Chem.* **2009**, *19*, 8656-8664.

Gandini, A. *Green Chem.* **2011**, *13*, 1061-1083.

Gomes, M.; Gandini, A.; Silvestre, A.J.D.; Reis, B. *J. Polym. Sci., Polym. Chem.* **2011**, *49*, 3759-3768.

González-Vidal, N.; Martínez de Ilarduya, A.; Muñoz-Guerra, S. *J. Polym. Sci., Polym. Chem.* **2009**, *47*, 5954-5966.

Grause, G.; Buekens, A.; Sakata, Y.; Okuwaki, A.; Yoshioka, T. *J. Mater. Cycles Waste* **2011**, *13*, 265-282.

Inkinen, S.; Stolt, M.; Södergard, A. *Biomacromolecules* **2010**, *11*, 1196-1201

Japu, C.; Alla, A.; Martínez de Ilarduya, A.; García-Martín, M.G.; Benito, E.; Galbis, J.A.; Muñoz-Guerra, S. *Polym. Chem.* **2012**, *3*, 2092-2101.

Kricheldorf, H.R. *J. Macromol. Sci. Rev. Macromol. Chem. Phys.* **1997**, *C37*, 599-631.

Kricheldorf, H.R.; Behnken, G.; Sell, M. *J. Macromol. Sci. Part A Pure Appl. Chem.* **2007**, *44*, 679-684.

Lavilla, C.; Alla, A.; Martínez de Ilarduya, A.; Benito, E.; García-Martín, M.G.; Galbis, J.A.; Muñoz-Guerra, S. *Biomacromolecules* **2011**, *12*, 2642-2652. **-Subchapter 3.2-**

Lavilla, C.; Alla, A.; Martínez de Ilarduya, A.; Benito, E.; García-Martín, M.G.; Galbis, J.A.; Muñoz-Guerra, S. *Polymer* **2012**, *53*, 3432-3445. (2012a) **-Subchapter 5.2-**

Lavilla, C.; Martínez de Ilarduya, A.; Alla, A.; García-Martín, M.G.; Galbis, J.A.; Muñoz-Guerra, S. *Macromolecules* **2012**, *45*, 8257-8266. (2012b) **-Subchapter 5.4-**

- Lavilla, C.; Martínez de Ilarduya, A.; Alla, A.; Muñoz-Guerra, S. *Polym. Chem.* **2013**, *4*, 282-289. **-Subchapter 4.3-**
- Müller, R.J.; Kleeberg, I.; Deckwer, W.D. *J. Biotechnol.* **2001**, *86*, 87-95.
- Narain, R. *Engineered Carbohydrate-Based Materials for Biomedical Applications: Polymers, Surfaces, Dendrimers, Nanoparticles and Hydrogels*; Wiley: Hoboken, **2011**.
- Noordover, B.A.J.; van Staalduinen, V.G.; Duchateau, R.; Koning, C.E.; van Benthem, R.A.T.M.; Mak, M. *Biomacromolecules* **2006**, *7*, 3406-3416.
- Noordover, B.A.J.; Duchateau, R.; van Benthem, R.A.T.M.; Ming, W.; Koning, C.E. *Biomacromolecules* **2007**, *8*, 3860-3870.
- Randal, J.C. *Polymer Sequence Determination*; Academic Press: New York, **1977**, pp. 41-69.
- Rychter, P.; Kawalec, M.; Sobota, M.; Kurcok, P.; Kowalczyk, M. *Biomacromolecules* **2010**, *11*, 839-847.
- Sablong, R.; Duchateau, R.; Koning, C.E.; de Wit, G.; van Es, D.; Koelewijn, R.; van Haveren, J. *Biomacromolecules* **2008**, *9*, 3090-3097.
- Storbeck, R.; Ballauff, M. *J. Appl. Polym. Sci.* **1996**, *59*, 1199-1202.
- Turner, S. R. *J. Polym. Sci., Polym. Chem.* **2004**, *42*, 5847-5852.
- Welle, F. *Resour. Conserv. Recy.* **2011**, *55*, 865-875.
- Williams, C.K.; Hillmyer, M.A. *Polym. Rev.* **2008**, *48*, 1-10.
- Wool, R.; Sun, S. *Biobased Polymers and Composites*; Academic Press: New York, **2005**.

GENERAL CONCLUSIONS

- Cyclic acetalized aldaric acids and alditols derived from D-galactose, D-mannose and L-tartaric acid with all the secondary hydroxyl groups protected as methylene acetals were used to obtain linear aliphatic and aromatic polyesters. Homopolyesters and random and block-like copolyesters were successfully prepared in high yields.
- In melt polycondensation (MP) polymerizations as well as in solid-state modification (SSM) procedures involving these sugar-based cyclic monomers, the experimental conditions were carefully adapted to the volatility of the sugar-based compounds. Mild temperatures were used for homopolyesters and copolyesters with higher contents in sugar. The use of dibutyl tin oxide (DBTO) instead of the commonly used titanium (IV) tetrabutoxide (TBT) as catalyst allowed to proceed at lower temperatures without increasing reaction times, which led to attaining higher molecular weights. Thus, DBTO was chosen as catalyst in all the MP carried out in this Thesis, and also was demonstrated to be very active in low temperature SSM processes.
- Aliphatic semicrystalline biodegradable homopolyesters from bicyclic acetalized dimethyl galactarate and linear alkanediols, and from bicyclic acetalized D-mannitol and dimethyl succinate were prepared in high yields with satisfactory molecular weights by polycondensation in the melt under mild conditions. Compared to the analogous aliphatic linear homopolyesters poly(alkylene adipate)s and poly(butylene succinate), the T_g was significantly increased by the presence of the bicyclic units in about 50-100 °C, reaching values in the -17 to 6 °C range for the non-fused bicyclic galactarate ones, whereas the fused bicyclic mannitol allowed to obtain a fully bio-based homopolyester with T_g = 68 °C. Thermal stability and mechanical modulus were notably augmented as well.
- When combined with linear alkanediols and dimethyl adipate or dimethyl succinate by MP, the symmetric galactarate-based and mannitol-based bicyclic units allowed to obtain aliphatic semicrystalline random copolyesters with glass-transition

temperatures, thermal stability and mechanical parameters intermediate between those of the parent homopolyesters.

- Random copolyesters from poly(ethylene terephthalate) (PET), poly(hexamethylene terephthalate) (PHT) or poly(dodecamethylene terephthalate) (PDT) with various cyclic acetalized monomers were successfully prepared by MP for the whole range of compositions. As expected, their properties were dependant on the alkanediol length and also on the stiffness of the cyclic unit incorporated. All PHT and PDT copolyesters were semicrystalline, and the variation of T_m with composition did fall into a minimum for intermediate compositions, according to the existence of two different crystal structures depending on which was the unit predominant in the copolyester. PET copolyesters were amorphous for contents higher than 15% of sugar-based units, and their T_g , mechanical modulus and hydrodegradability were significantly enhanced by the presence of mannitol-based bicyclic units.
- The effect of the carbohydrate-based comonomer on thermal and mechanical properties of poly(butylene terephthalate) (PBT) was opposite according to which unit, the diol or the diacid, was replaced. The incorporation of acetalized dimethyl galactarate by MP decreased the thermal stability, the glass-transition temperature and the mechanical moduli. On the contrary, these parameters were increased when the alkanediol units were the replaced ones. The effect of the presence of cyclic alditol units on T_g and T_m of the resulting random copolyesters was usually opposite. They favored an increase in T_g due to their stiffer nature, but also repressed partially the crystallizability of the polyesters and decreased T_m . Since the thermal stability usually increased with the content of cyclic alditols, a wider range of temperatures between melting and decomposition existed in the copolyesters, allowing a more comfortable melt processing.
- SSM-prepared PBT copolyesters from cyclic acetalized alditols displayed a unique block-like chemical microstructure, formed by long PBT sequences in the crystalline phase and a practically random amorphous part. At difference with isosorbide, which required the previous synthesis of a macromonomer, bicyclic acetalized alditols were capable of being incorporated directly into PBT by SSM. The unique chemical microstructure of the SSM-prepared copolyesters endowed them with superior thermal properties compared to their random counterparts prepared by MP. They displayed higher melting points, crystallization temperatures and crystallinity

although these properties were diminished after long times in the melt due to the occurrence of randomization processes. Incorporation of the cyclic acetalized alditols by SSM led to raises in T_g comparable to those of copolyesters prepared by MP.

- The presence of cyclic acetalized sugar-based units, both aldaric acids and alditols, enhanced significantly the hydrodegradability of aliphatic homopolyesters and copolyesters, and even made aromatic polyesters susceptible to water attack. In all cases, hydrolysis took place through the ester group without modification of the diacetal structure. The cyclic methylene acetal structures were resistant to hydrolysis in acidic, neutral or basic media. Degradation of sugar-based aliphatic polyesters under physiological conditions was clearly favored by the action of enzymes. Furthermore, cyclic acetalized aldaric acids made aromatic polyesters susceptible to biodegradation whereas this effect was not detected for the corresponding alditols.
- Compared to isosorbide, bicyclic acetalized alditols showed a greater facility to react under MP conditions. This was due to the higher reactivity of the primary hydroxyl groups of bicyclic acetalized galactitol or D-mannitol compared to isosorbide. Moreover, at difference with isosorbide, the two hydroxyl groups of these bicyclic acetalized symmetric alditols displayed the same reactivity.
- As expected from its cyclic stiff nature, the effect of the fused bicyclic acetalized D-mannitol on T_g of PBT was largely greater than that exerted by the incorporation of acyclic sugar units such as trimethoxy xylitol or L-arabinitol. It had a much more pronounced effect than the non-fused bicyclic galactitol, which was capable of raising the T_g of PBT by near 30 °C when it replaced 1,4-butanediol in a 40%. The effect of the D-mannitol-based units turned to be similar to that of isosorbide; both PBT copolyesters containing 40% of either Manx or isosorbide increased the T_g by near 60 °C.
- Isosorbide and bicyclic acetalized D-mannitol and galactitol depressed the crystallinity of random PBT copolyesters in a degree that depended on both symmetry and stiffness of the bicyclic structure; they were semicrystalline for contents of up to 32%, 41% and 50% in these units, respectively, whereas the three

homopolyesters entirely made of sugar-derived diols and terephthalate units were amorphous.

ANNEX A

MONOMER SYNTHESIS

Dimethyl 2,3:4,5-di-O-methylene-galactarate

To a mixture of 10.0 g of dimethyl galactarate (42 mmol) and 10.0 g of paraformaldehyde (332 mmol), 6 mL of sulfuric acid 96% were added dropwise and the mixture was set aside for 3 days at room temperature. Methanol (180 mL) was added and the mixture was refluxed for 2 h. After cooling, the solution was neutralized with barium carbonate. Methanol was removed under reduced pressure and the white residue was extracted with chloroform. Removal of chloroform gave the crude product, which was chromatographed on a silica gel column with ethyl acetate-light petroleum as eluant to give three fractions. The first fraction, on recrystallization from ethyl acetate-light petroleum, yielded dimethyl 2,3:4,5-di-O-methylene-galactarate. Yield: 20%

2,3:4,5-di-O-methylene-galactitol

Dimethyl 2,3:4,5-di-O-methylene-galactarate (560 mg, 2.1 mmol) was added to a suspension of lithium aluminium hydride (600 mg, 15.8 mmol) in dry tetrahydrofuran (50 mL) and the mixture was refluxed for 6 h. Excess of lithium aluminium hydride was destroyed by careful addition of water to the cooled mixture. The inorganic material was filtered off and the tetrahydrofuran was removed under reduced pressure to give the crude product, which was dissolved in chloroform, dried over anhydrous sodium sulfate and left to crystallize. Recrystallization from chloroform yielded 2,3:4,5-di-O-methylene-galactitol. Yield: 70%

2,4:3,5-di-O-methylene-D-mannitol

1,6-di-O-benzoyl-D-mannitol. A solution of 28.1 g of benzoyl chloride (200 mmol) in dry pyridine (70 mL) was added dropwise to a dispersion of 36.4 g of D-mannitol (200 mmol)

in 70 mL of dry pyridine. The mixture was stirred at room temperature for 5 h and then poured into ice-water. The precipitated solid was filtered, washed with cold water and with chloroform, dried and recrystallized from ethanol. Yield: 36%.

1,6-di-O-benzoyl-2,4:3,5-di-O-methylene-D-mannitol. To a mixture of 28.0 g of 1,6-di-O-benzoyl-D-mannitol (72 mmol) and 28.0 g of paraformaldehyde (930 mmol), 22 mL of sulfuric acid 96% were added dropwise and the mixture was stirred for 3 h at room temperature. The reaction mixture was then repeatedly extracted with chloroform. The combined organic layers were washed with ammonia (12% w/w) and water, and dried over anhydrous sodium sulfate. The solution was evaporated to a solid residue, which was recrystallized from ethanol. Yield: 52%.

2,4:3,5-di-O-methylene-D-mannitol. A dispersion of 15.5 g of 1,6-di-O-benzoyl-2,4:3,5-di-O-methylene-D-mannitol (37 mmol) in 200 mL of dry methanol was stirred overnight with a small piece of sodium. The solution was treated with cation exchange resin, the resin was filtered and the filtrate concentrated to dryness. The resulting semisolid residue was washed with diethyl ether and recrystallized from ethanol. Yield: 72%.

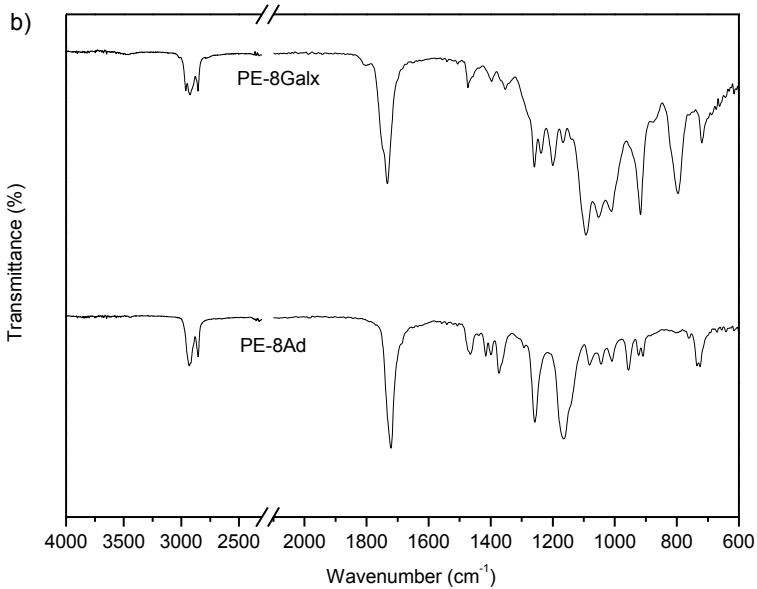
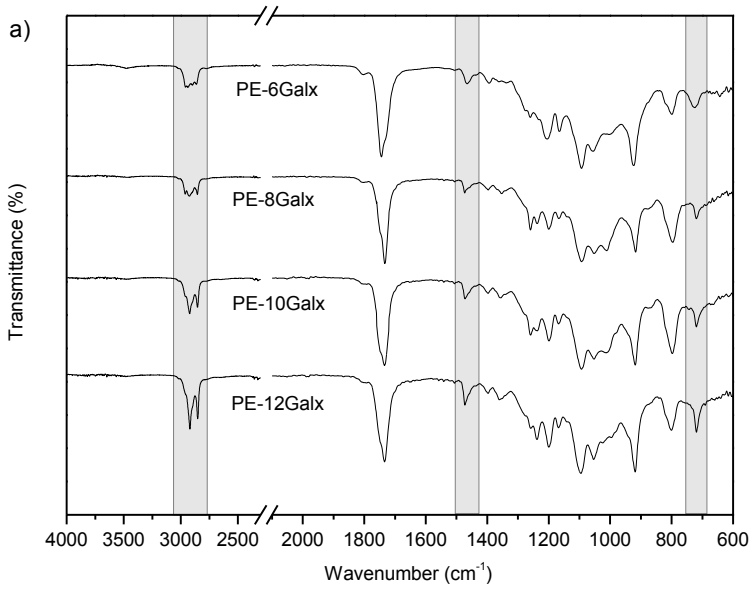
2,3-di-O-methylene-L-threitol

Dimethyl 2,3-di-O-methylene-L-tartrate. To a mixture of dimethyl L-tartrate (15 g, 84.3 mmol) and paraformaldehyde (15 g, 498 mmol) heated at 60 °C under stirring, was added dropwise 20 mL of sulfuric acid 98% and the mixture was stirred until complete dissolution. The reaction solution was then repeatedly extracted with chloroform. The combined organic layers were washed with ammonia (25% w/w) and water, and dried over anhydrous sodium sulfate. The solution was evaporated to dryness and purified by vacuum distillation to obtain an oily product. Yield: 60%.

2,3-di-O-methylene-L-threitol. To a cooled solution of 5 g of dimethyl 2,3-di-O-methylene-L-tartrate (26.3 mmol) in 40 mL of dry diethyl ether was added 2.67 g LiAlH₄ 97% (68.1 mmol) in 40 mL dry diethyl ether under nitrogen atmosphere. The mixture was stirred for 12 h, then cooled to 0 °C and sequentially and slowly added 7 mL H₂O, 8 mL NaOH (15% w/v), and 25 mL H₂O. Then, the mixture was filtrated and the solid extracted with hot acetone. The combined extracts were evaporated to dryness and purified by vacuum distillation, to obtain an oily product. Yield: 75%.

ANNEX B

Supporting information of Subchapter 3.2.



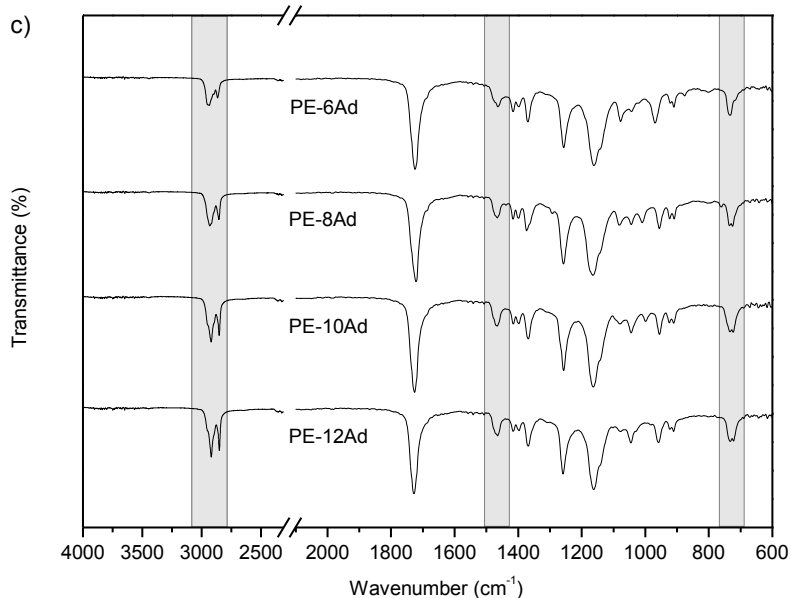


Figure B-1. (a) Compared FTIR spectra for PE-6Galx, PE-8Galx, PE-10Galx and PE-12Galx. In shadows, the absorptions which increase with polymethylene sequence length. (b) Compared FTIR spectra for PE-8Galx and PE-8Ad. (c) Compared FTIR spectra for PE-6Ad, PE-8Ad, PE-10Ad and PE-12Ad. In shadows, the absorptions which increase with polymethylene sequence length.

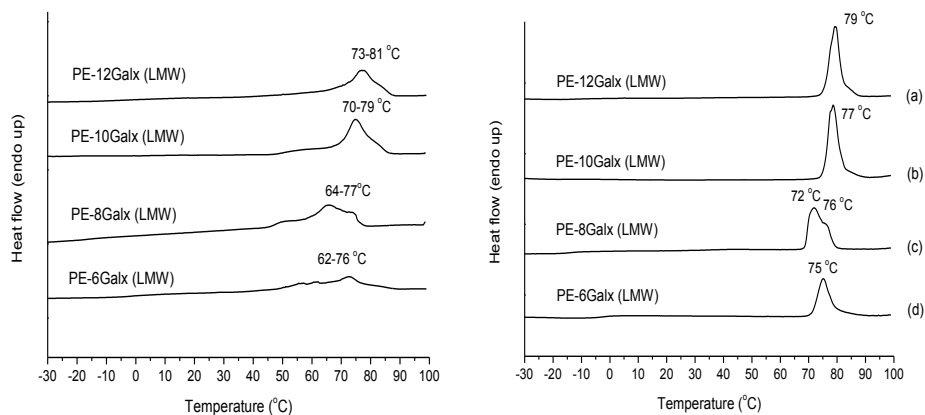


Figure B-2. DSC melting traces of samples of PE-*n*Galx (LMW) coming directly from synthesis (left) and annealed (right) at (a) 70 °C for 12 h, (b) 70 °C for 12 h, (c) 65 °C for 12 h, (d) 65 °C for 12 h.

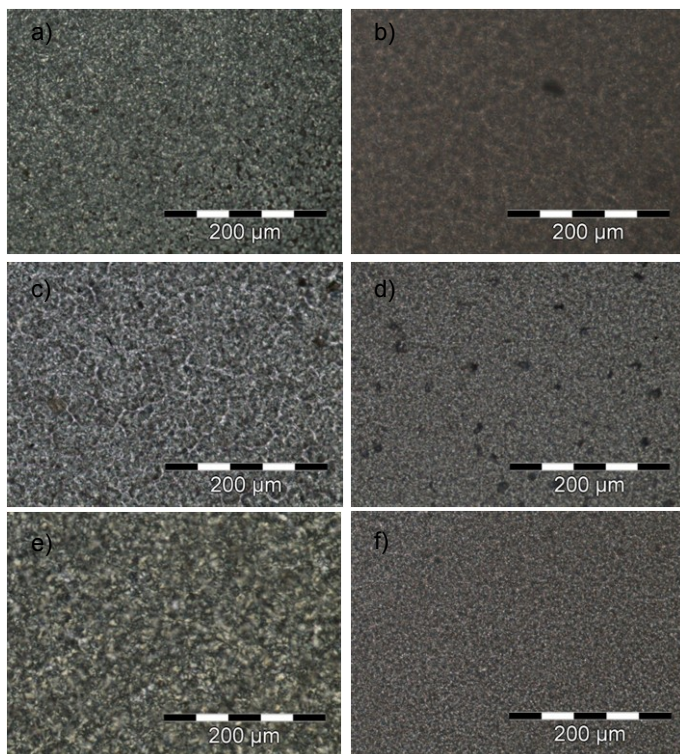


Figure B-3. Polarized optical micrographs of PE-12Galx isothermally crystallized at 50 °C (a) LMW, (b) HMW; 55 °C (c) LMW, (d) HMW; 60 °C (e) LMW, (f) HMW. The scale bar corresponds to 200 μm.

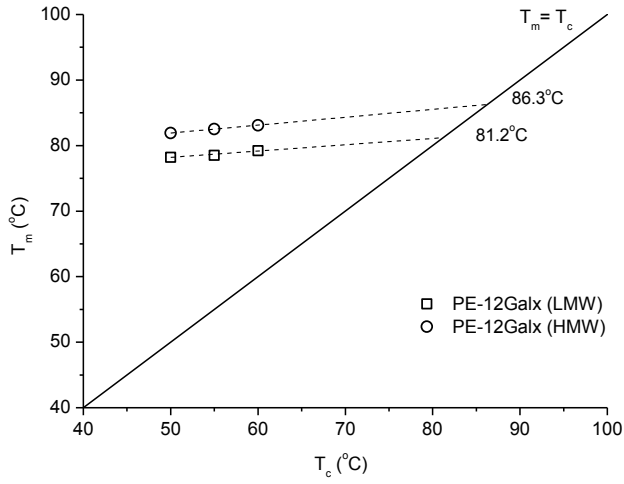


Figure B-4. Hoffman-Weeks plot for isothermally crystallized low and high-molecular weight PE-12Galx.

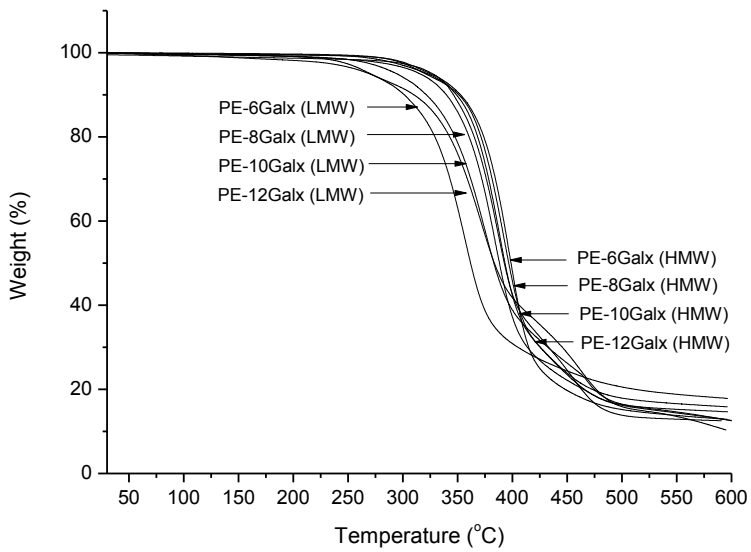


Figure B-5. TGA traces of low and high-molecular weight PE-*n*Galx.

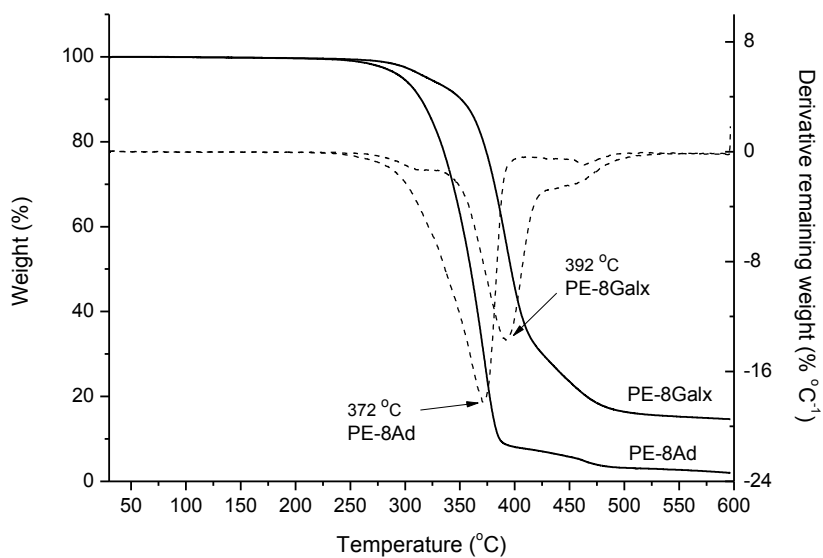


Figure B-6. TGA traces (solid lines) and derivative curves (dashed lines) of PE-8Ad and HMW PE-8Galx.

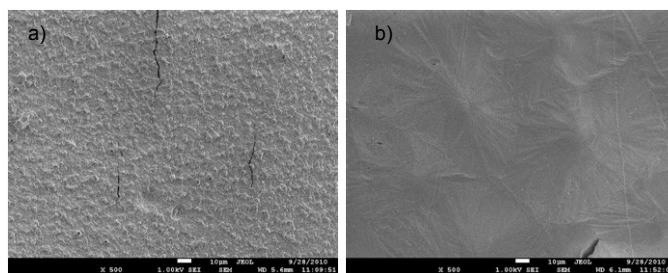


Figure B-7. SEM micrographs of PE-8Galx (a) and PE-8Ad (b) after hydrolytic degradation at pH=7.4 for 21 days.

ANNEX C

Supporting information of Subchapter 3.4.

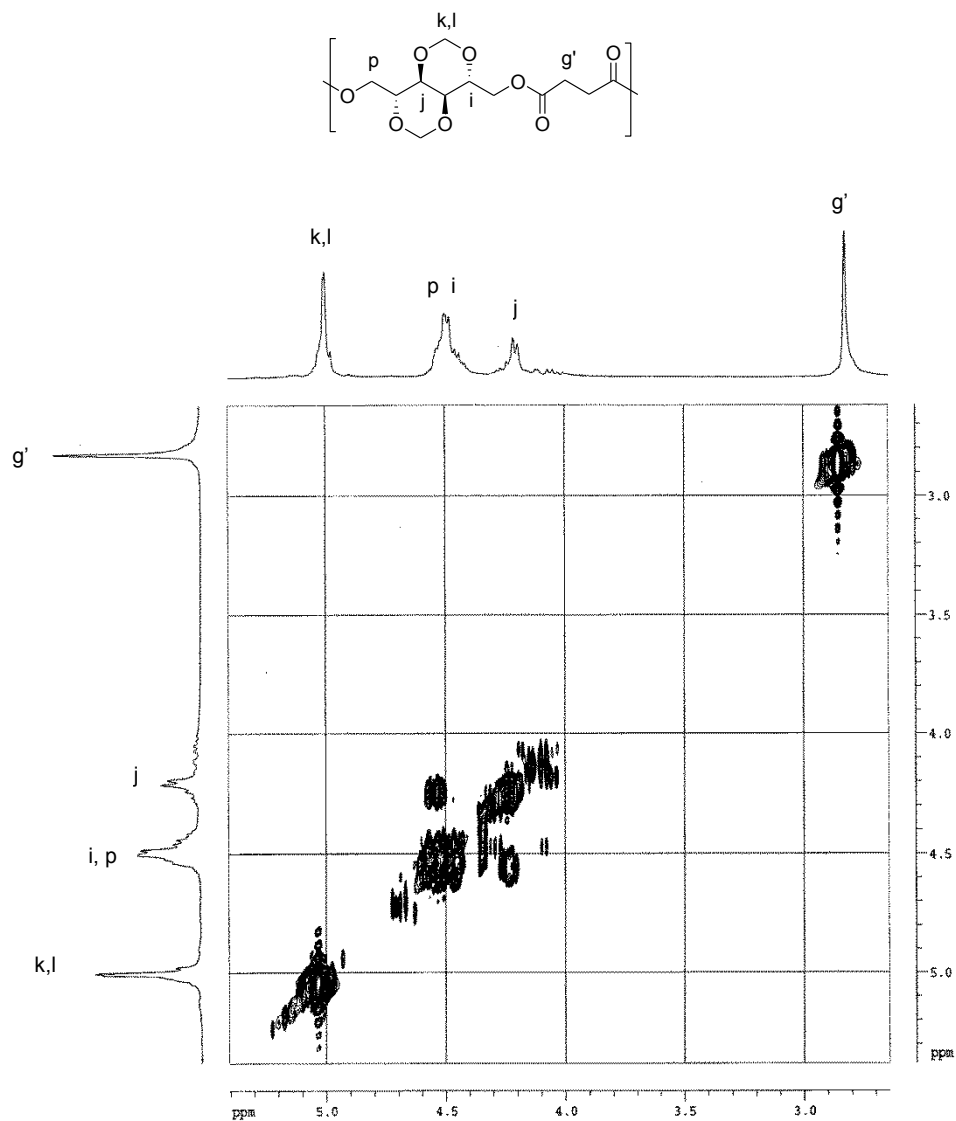


Figure C-1. COSY spectrum in CDCl₃/TFA of PManxS homopolyester.

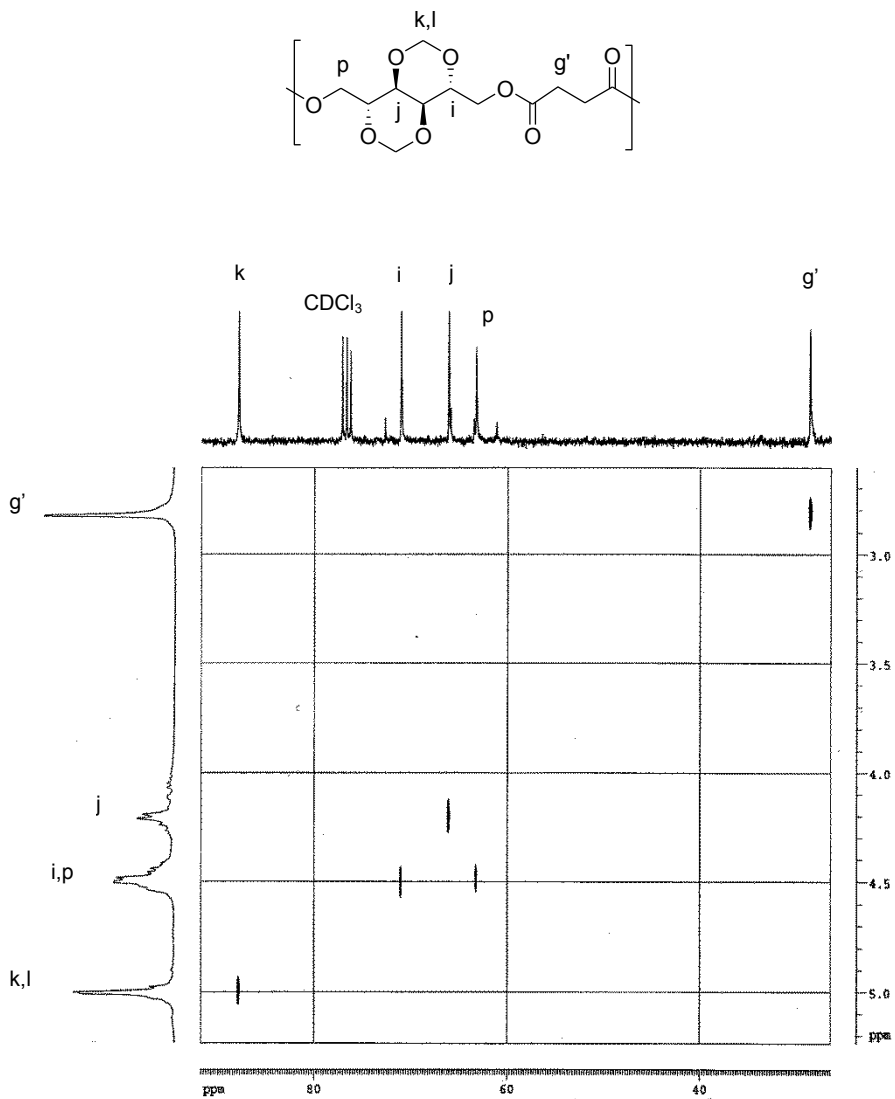


Figure C-2. ^1H - ^{13}C heteronuclear shift correlation spectrum (HETCOR) in CDCl_3/TFA of PManxS homopolymer.

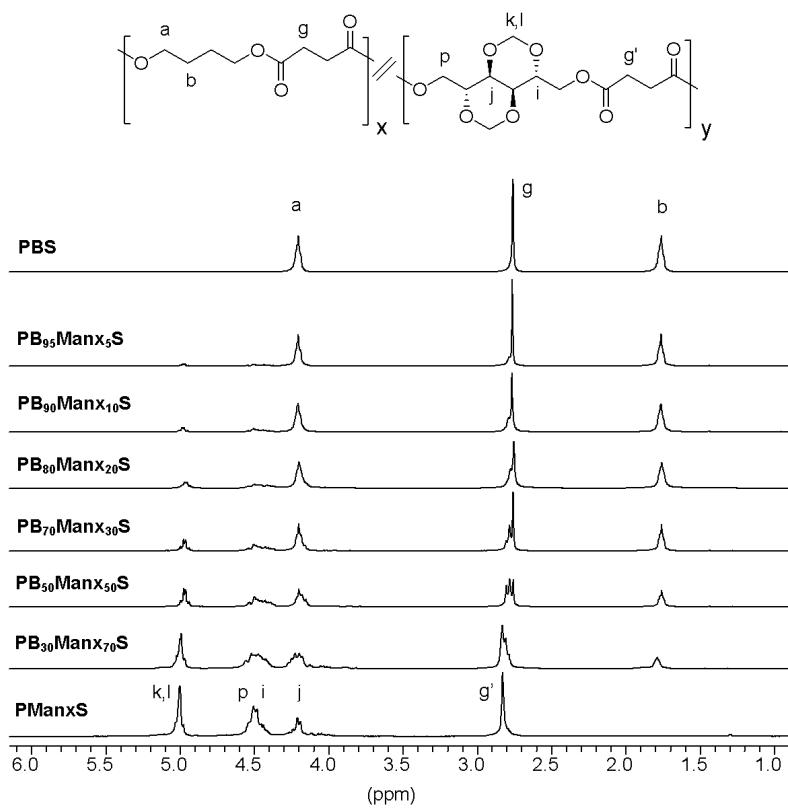


Figure C-3. Compared 1H NMR spectra in $CDCl_3/TFA$ of PB_xMan_xS copolyesters.

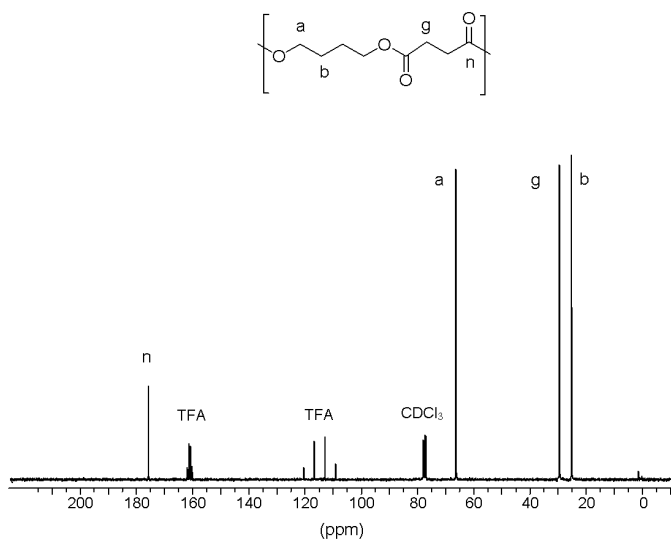


Figure C-4. ^{13}C NMR spectrum in CDCl_3/TFA of PBS homopolymer.

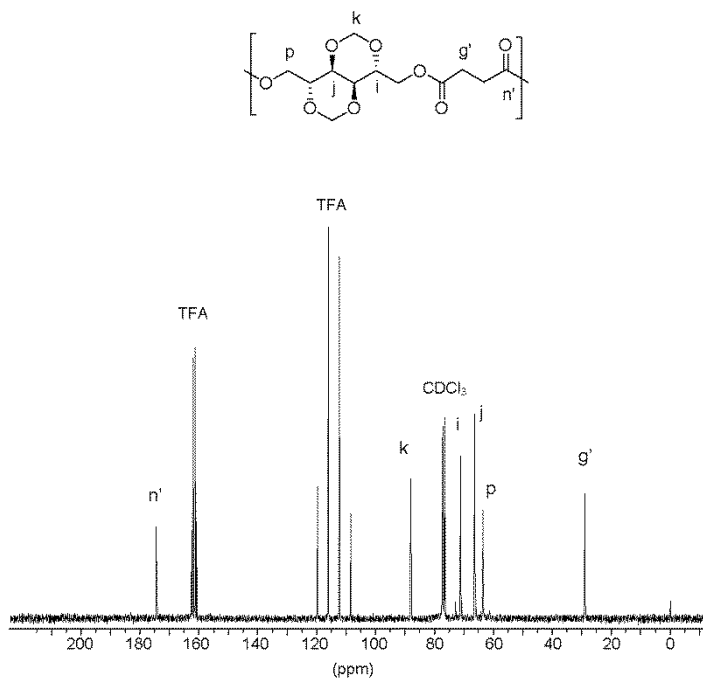


Figure C-5. ^{13}C NMR spectrum in CDCl_3/TFA of PManxS homopolymer.

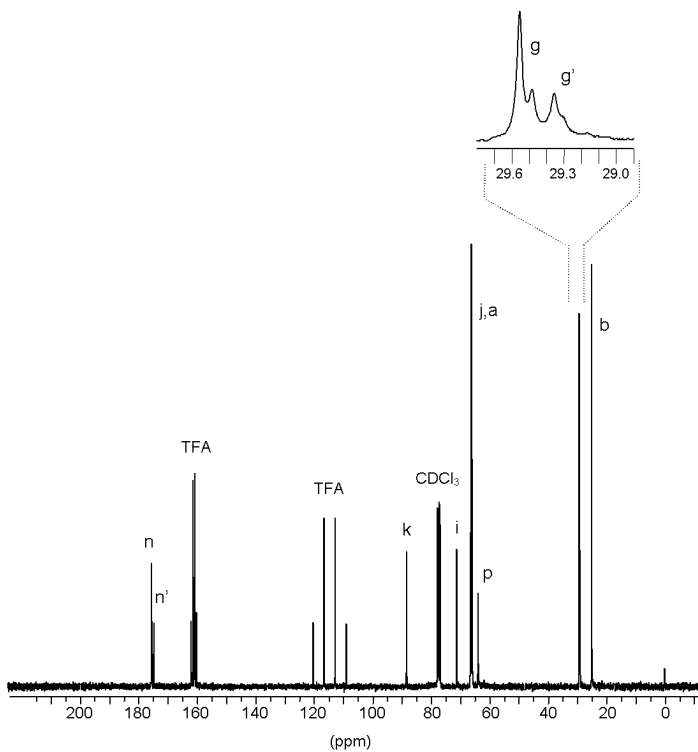
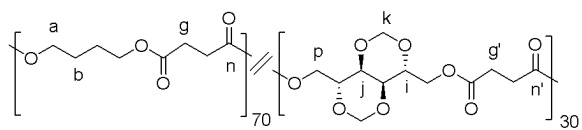


Figure C-6. ^{13}C NMR spectrum in CDCl_3/TFA of $\text{PB}_{70}\text{Man}_{30}\text{S}$ copolyester.

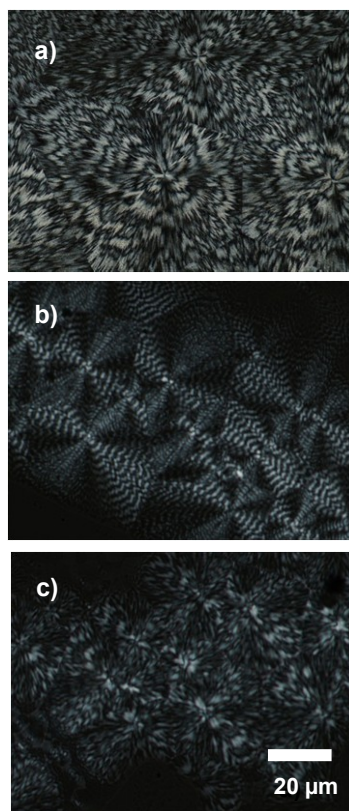


Figure C-7. Polarized optical micrographs of samples isothermally crystallized at the indicated temperatures: (a) PBS at 90 °C; (b) PB₉₅Man₅S at 75 °C; (c) PB₉₀Man₁₀S at 75 °C. The scale bar corresponds to 20 μm.

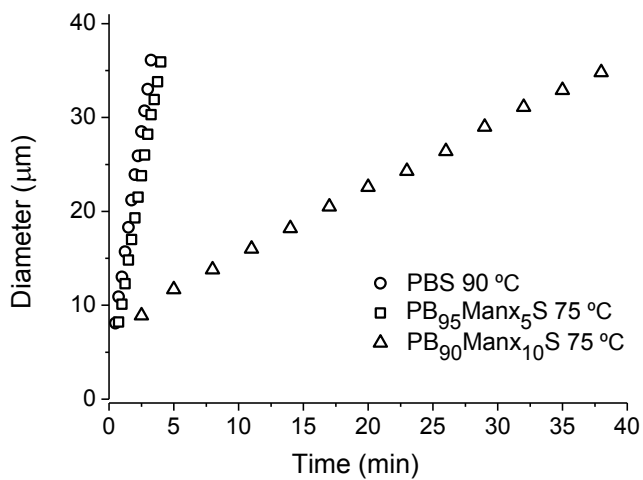


Figure C-8. Spherulitic diameter versus time plot for isothermally crystallized PBS, PB₉₅Man₅S and PB₉₀Man₁₀S at the indicated temperatures.

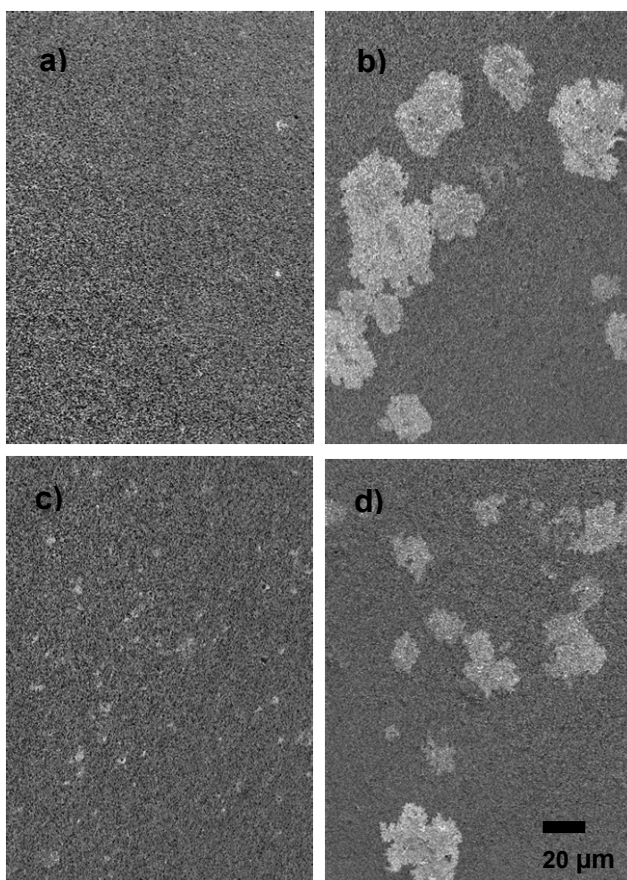


Figure C-9. SEM micrographs of PBS. Initial sample (a). After incubation at pH 2.0 (b), pH 7.4 without (c) and with (d) porcine pancreas lipase at 37 °C for 56 days.

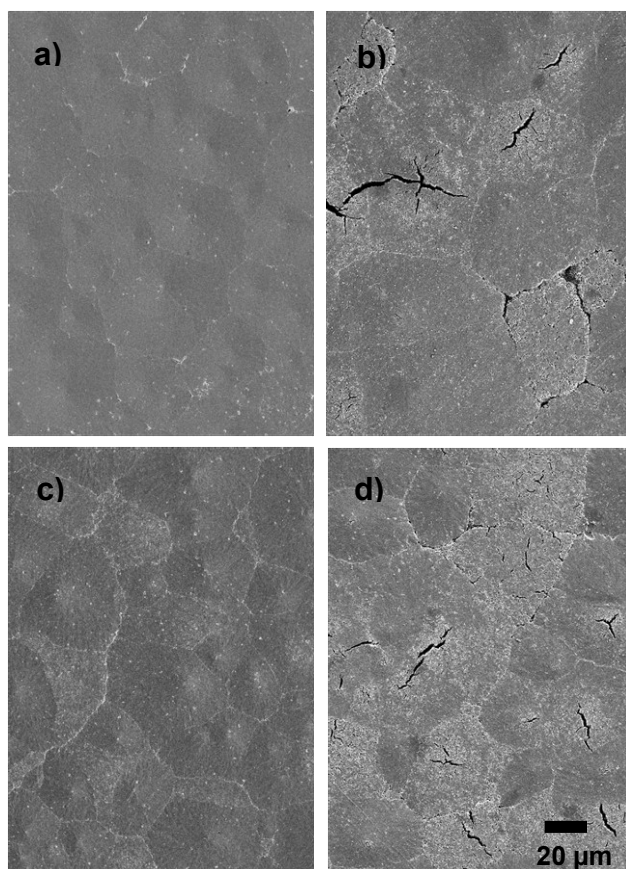


Figure C-10. SEM micrographs of $PB_{70}Man_{30}S$. Initial sample (a). After incubation at pH 2.0 (b), pH 7.4 without (c) and with (d) porcine pancreas lipase at 37 °C for 56 days.

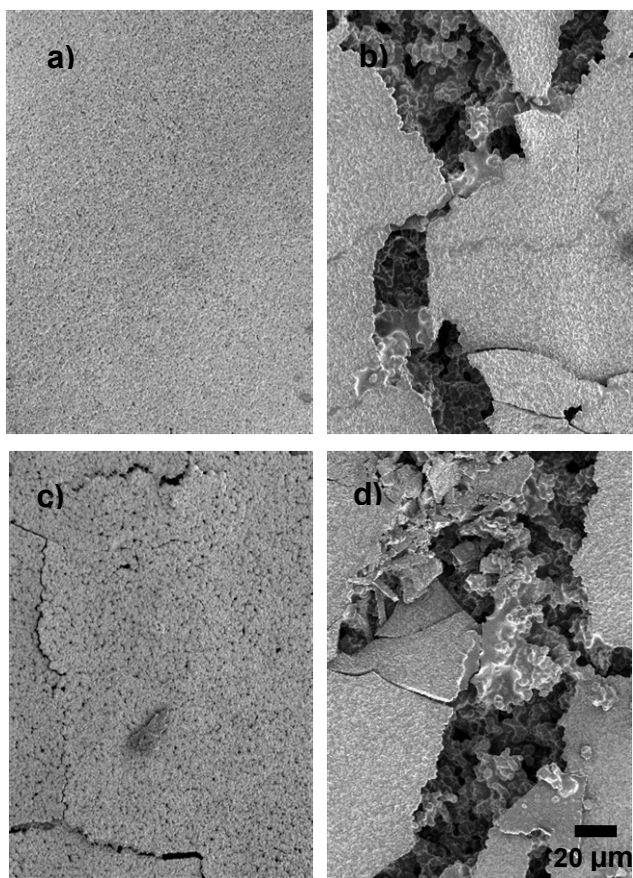


Figure C-11. SEM micrographs of PManxS. Initial sample (a). After incubation at pH 2.0 (b), pH 7.4 without (c) and with (d) porcine pancreas lipase at 37 °C for 56 days.

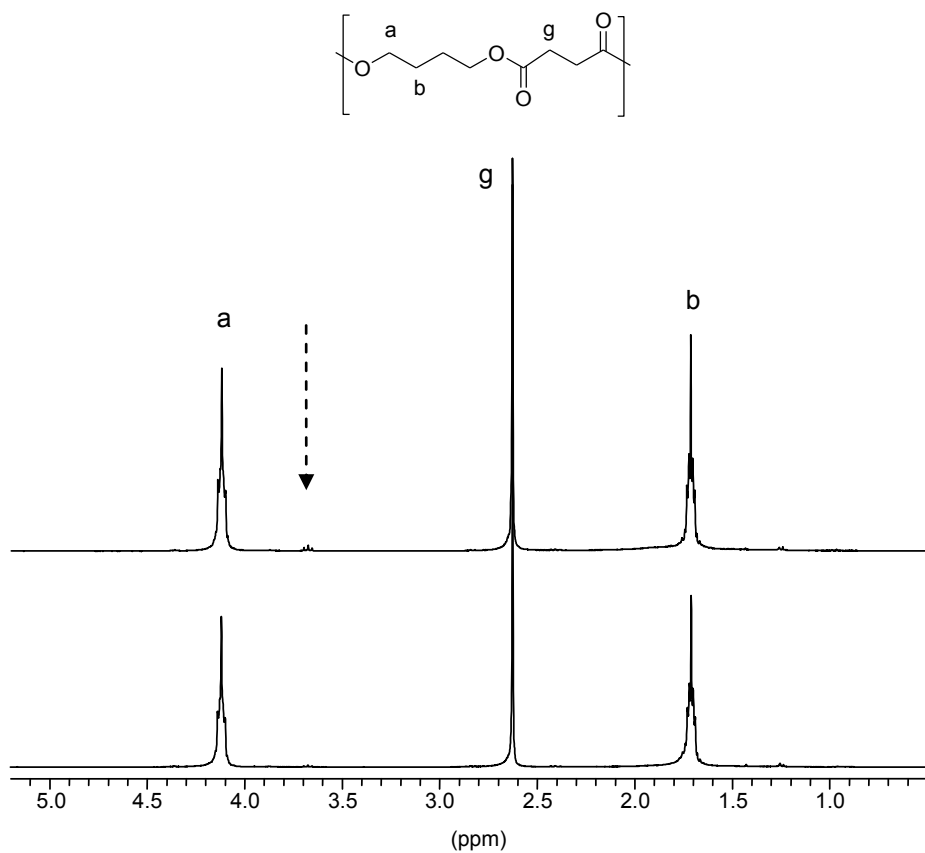


Figure C-12. Compared ^1H NMR spectra in CDCl_3 of PBS after incubation at pH 2.0 for 56 days (top) and initial sample (bottom). The arrow indicates the signal arising from $-\text{CH}_2\text{OH}$ end groups that appear upon hydrolysis of the main chain ester group.

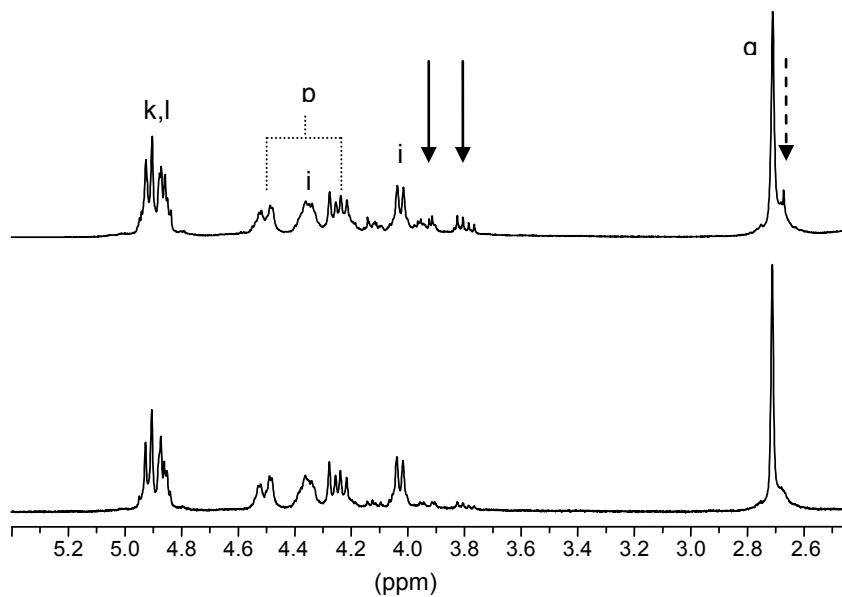
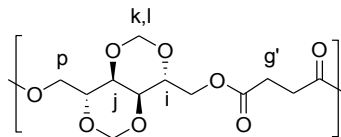


Figure C-13. Compared ^1H NMR spectra in CDCl_3 of PManxS after incubation at pH 2.0 for 56 days (top) and initial sample (bottom). The arrows indicate the signals arising from $-\text{CH}_2\text{OH}$ (solid line) and $-\text{CH}_2\text{COOH}$ (dashed line) end groups that appear upon hydrolysis of the main chain ester group.

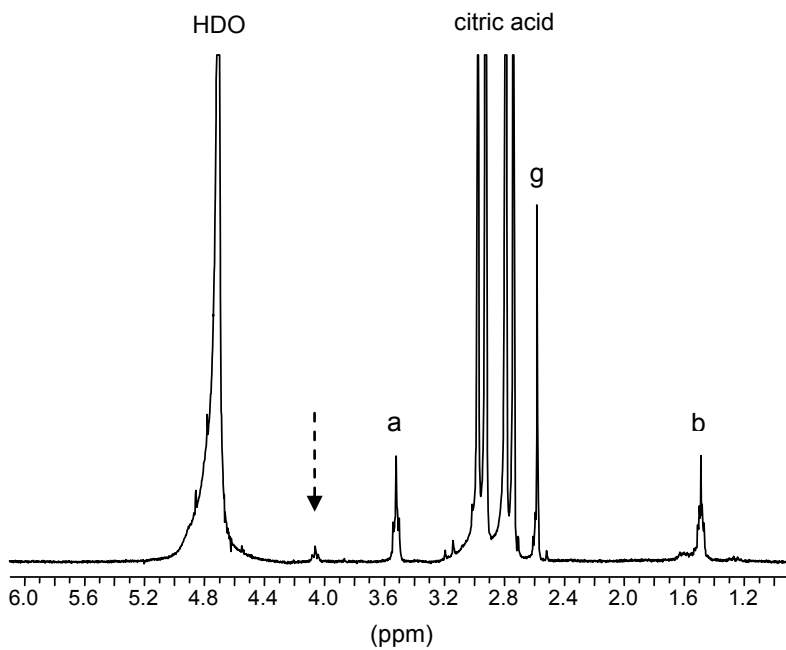
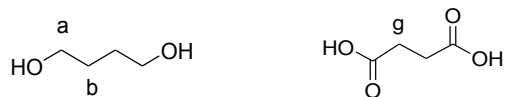


Figure C-14. ^1H NMR spectrum in D_2O of the products released to the aqueous medium after incubation of PBS at pH 2.0 for 56 days. The arrow indicates signals corresponding to oligomers that appear upon hydrolysis of the main chain ester group.

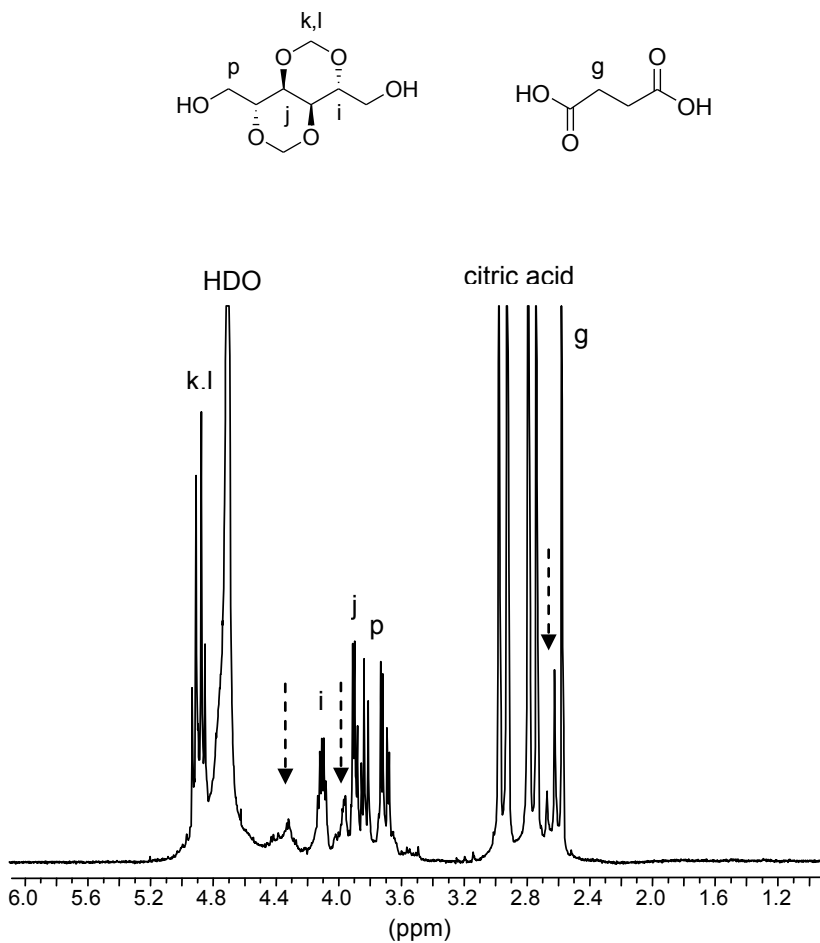


Figure C-15. ¹H NMR spectrum in D₂O of the products released to the aqueous medium after incubation of PManxS at pH 2.0 for 56 days. The arrows indicate signals corresponding to oligomers that appear upon hydrolysis of the main chain ester group.

ANNEX D

Supporting information of Subchapter 4.2.

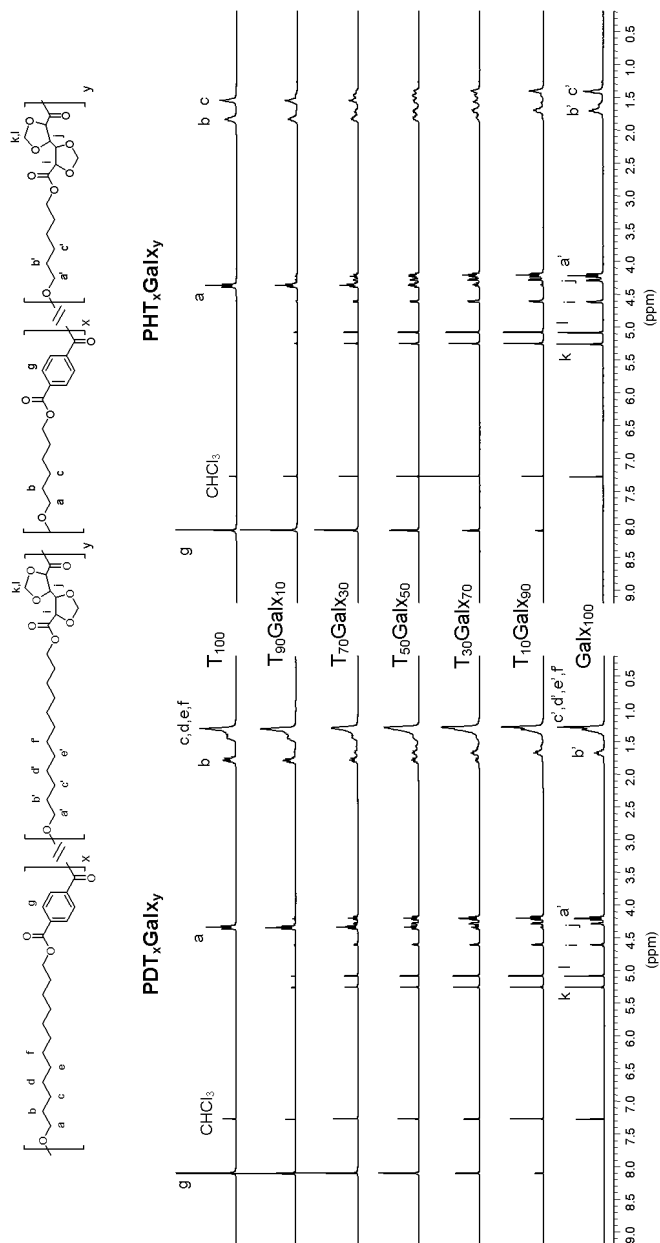


Figure D-1. Compared ^1H NMR spectra of PHT_xGal_y and PDT_xGal_y copolyesters.

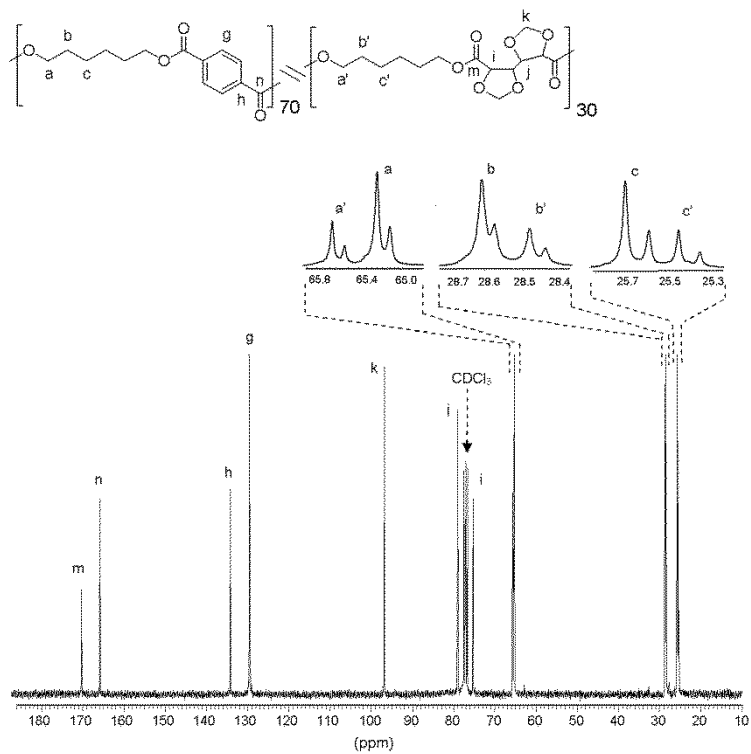


Figure D-2. ¹³C NMR spectrum of PHT₇₀Gal₃₀ copolyester.

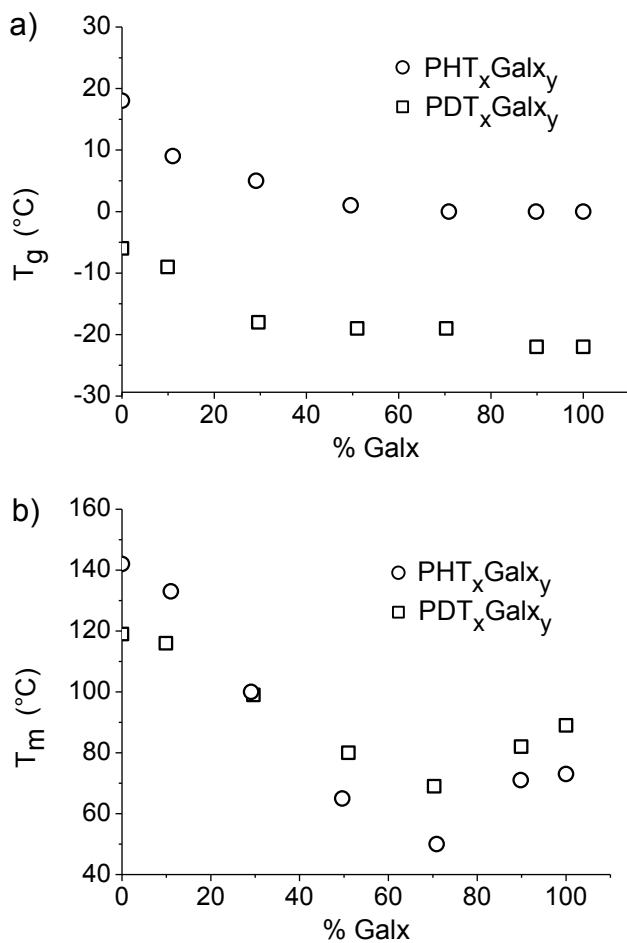


Figure D-3. Glass transition temperature (a) and melting temperature (b) vs. composition plots for PHT_xGal_y and PDT_xGal_y.

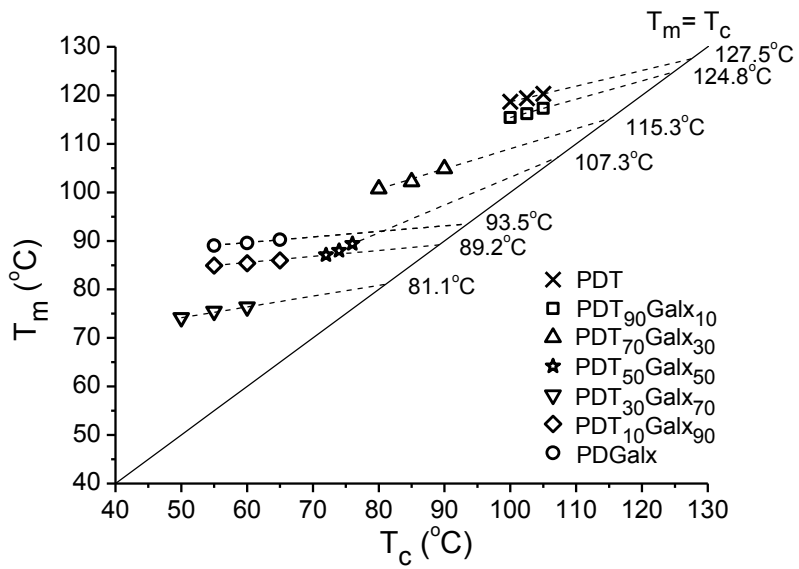


Figure D-4. Hoffman-Weeks plot for isothermally crystallized PDT_xGal_x_y copolyesters.

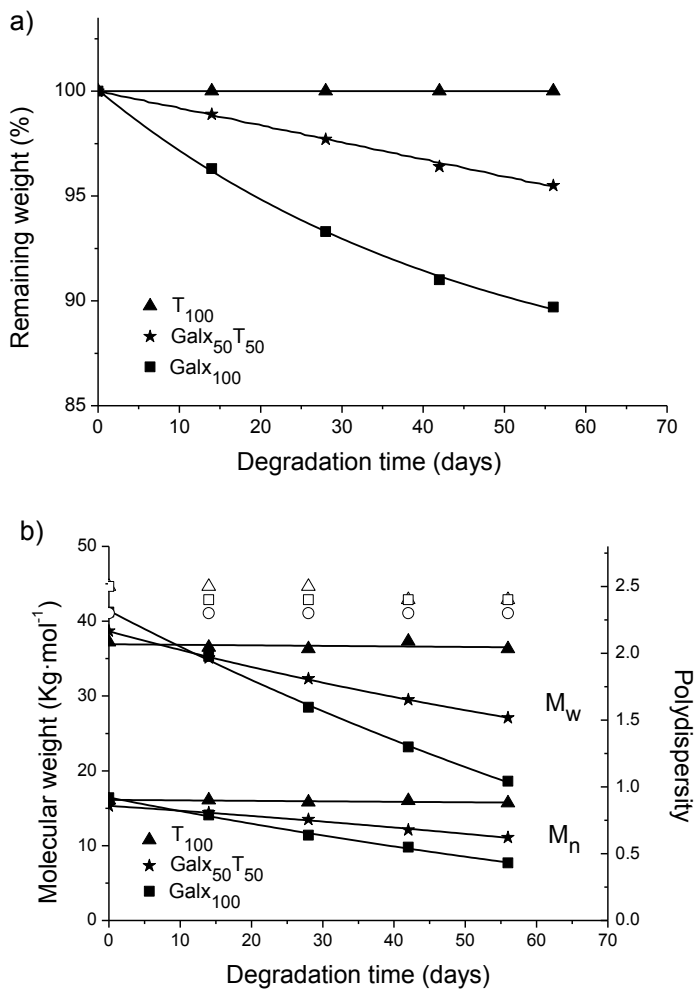


Figure D-5. Degradation of PDT, $PDT_{50}Galx_{50}$ and PDGal at pH 2.0 at 23°C. (a) Remaining weight vs. degradation time. (b) Changes in M_w and M_n (solid symbols) and polydispersity index (empty symbols) vs. incubation time.

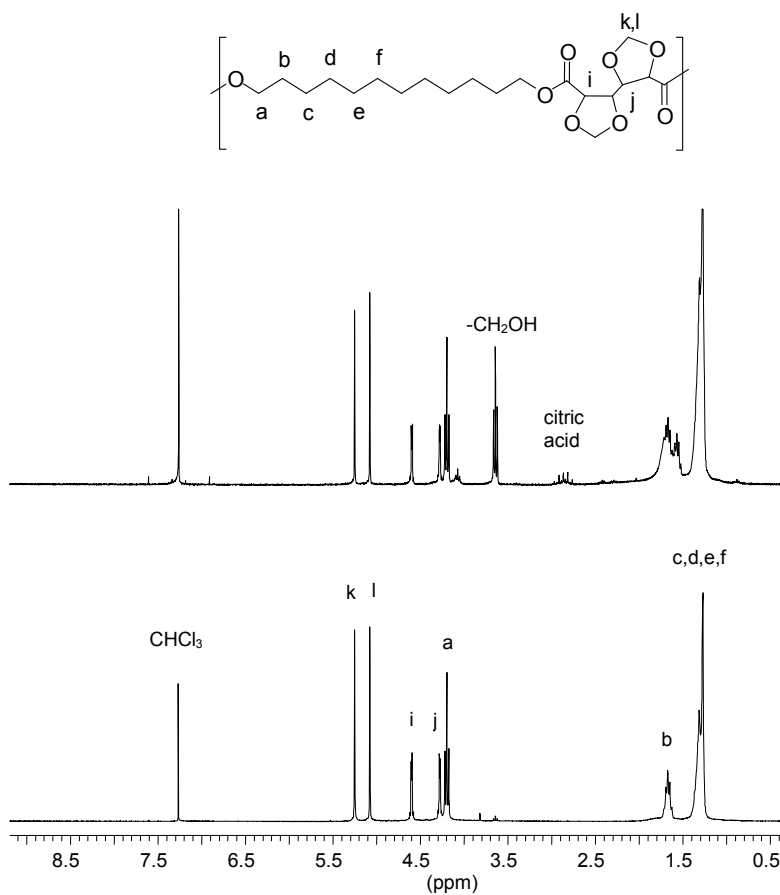


Figure D-6. Compared ^1H NMR spectra of PDGalx after incubation at pH=2.0 at 80 °C for 56 days (top) and initial sample (bottom).

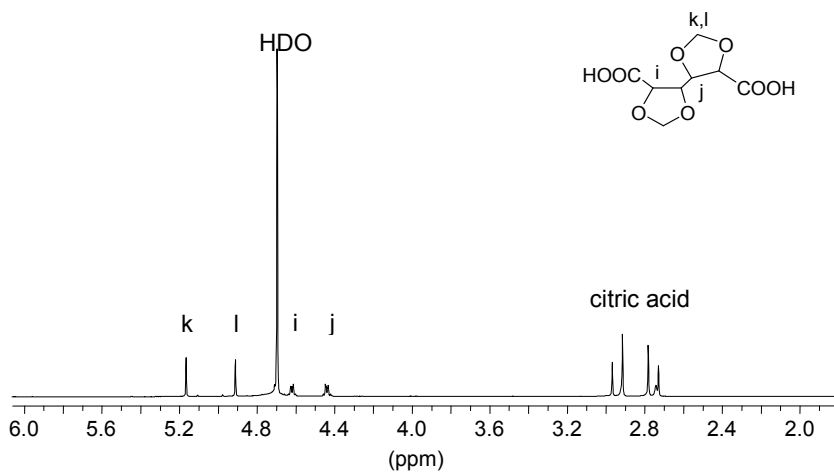


Figure D-7. ^1H NMR spectra in D_2O of the products released to the aqueous medium after incubation of PDGalx at 80°C in water at pH 2.0.

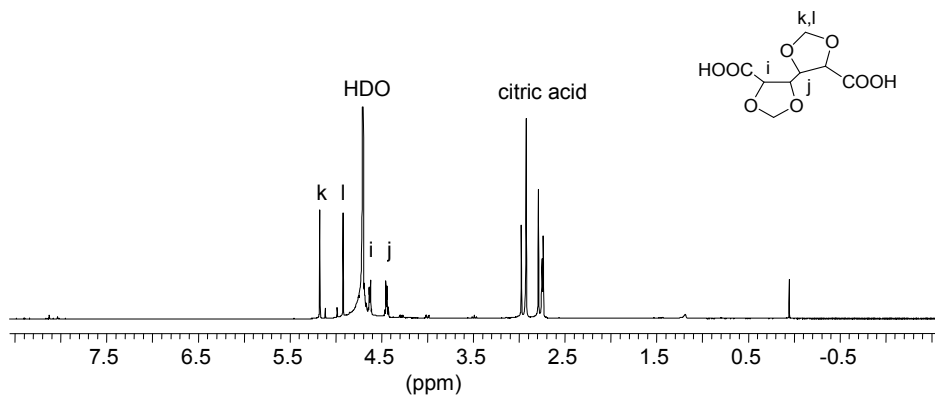


Figure D-8. ^1H NMR spectra in D_2O of the products released to the aqueous medium after incubation of PDT₅₀Galx₅₀ at 80°C in water at pH 2.0.

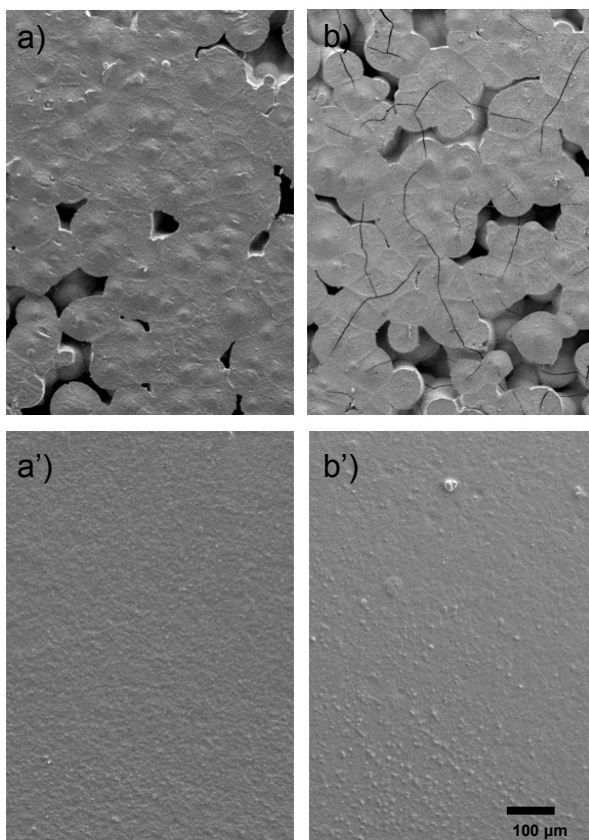


Figure D-9. SEM micrographs of PDGalx (top) and PDT₅₀Galx₅₀ (bottom). (a,a') After incubation without lipase at pH=7.4 at 37 °C for 21 days. (b,b') After incubation at pH=2.0 at 23 °C for 56 days.

ANNEX E

Supporting information of Subchapter 5.3.

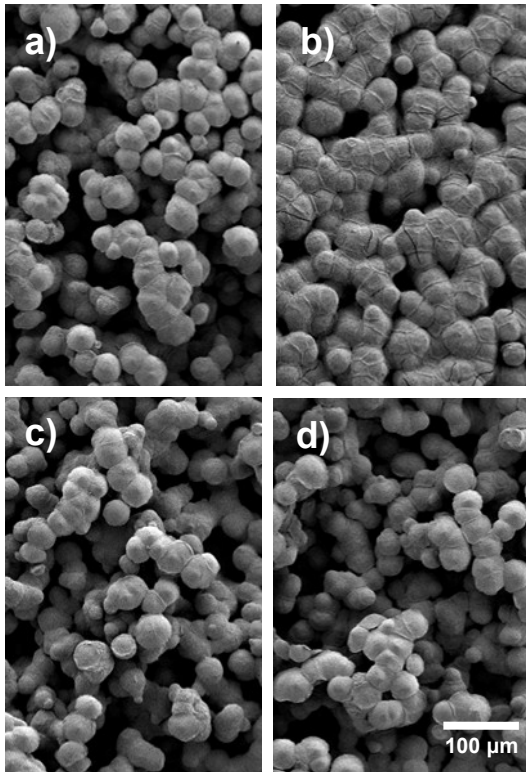


Figure E-1. SEM micrographs of PBT. Initial sample (a). After incubation at pH=2.0 at 80 °C for 56 days (b). After incubation at pH=7.4 at 37 °C for 56 days with (c) and without (d) lipase from porcine pancreas.

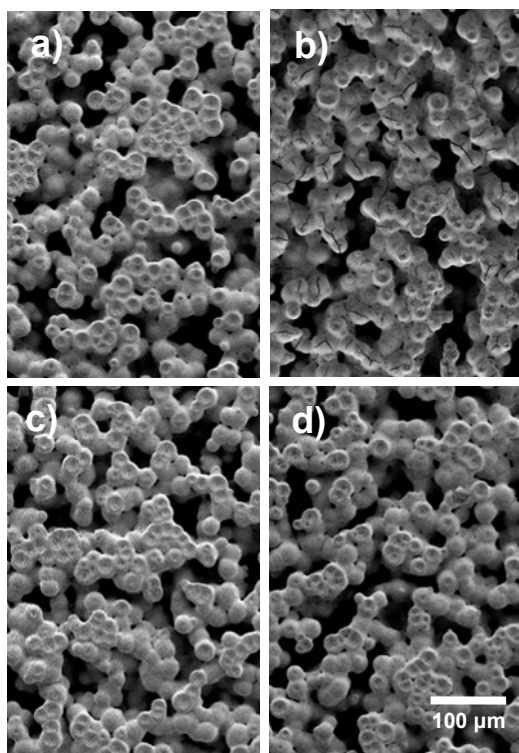


Figure E-2. SEM micrographs of PGalxT. Initial sample (a). After incubation at pH=2.0 at 80 °C for 56 days (b). After incubation at pH=7.4 at 37 °C for 56 days with (c) and without (d) lipase from porcine pancreas.

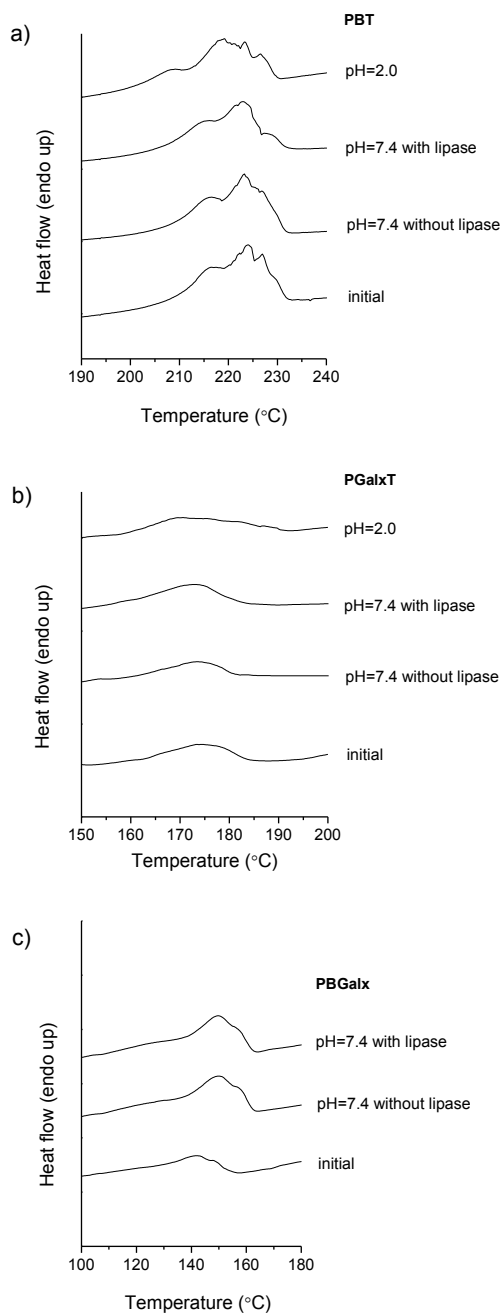


Figure E-3. DSC of PBT (a), PGalxT(b) and PBGalx (c) homopolymers upon incubation in pH=7.4 buffer with and without lipase from porcine pancreas, in pH=2.0 buffer and initial sample.

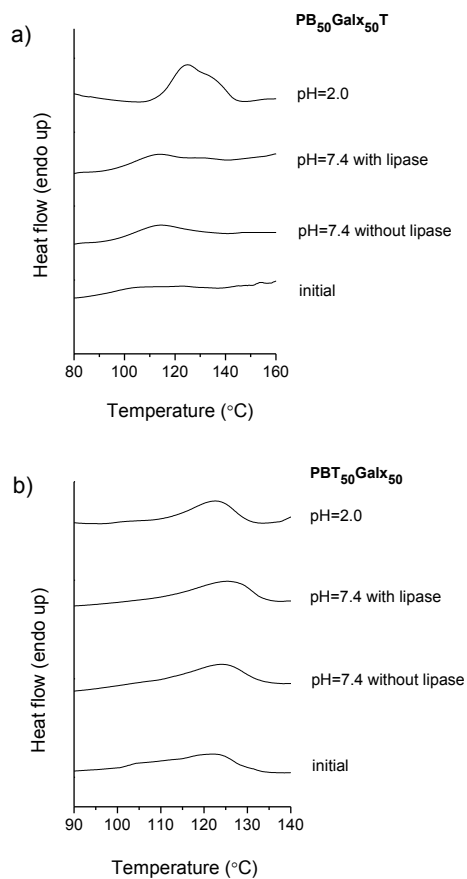


Figure E-4. DSC of $PB_{50}Galx_{50}T$ (a) and $PBT_{50}Galx_{50}$ (b) copolyesters upon incubation in pH=7.4 buffer with and without lipase from porcine pancreas, in pH=2.0 buffer and initial sample.

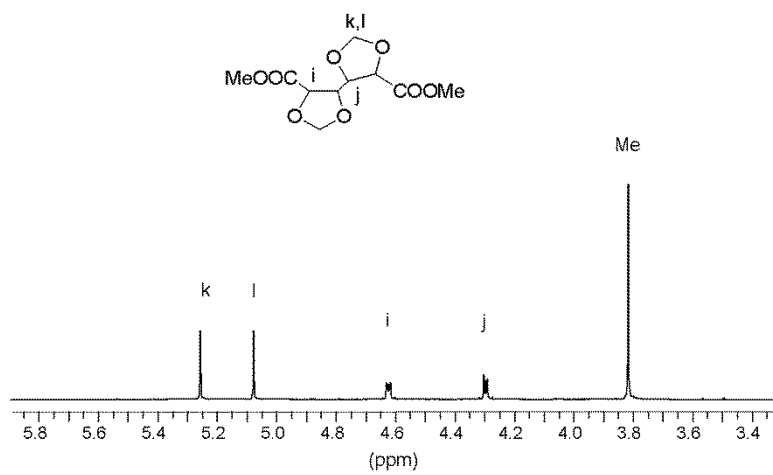


Figure E-5. ¹H NMR spectrum in CDCl₃ of dimethyl 2,3:4,5-di-O-methylene-galactarate.

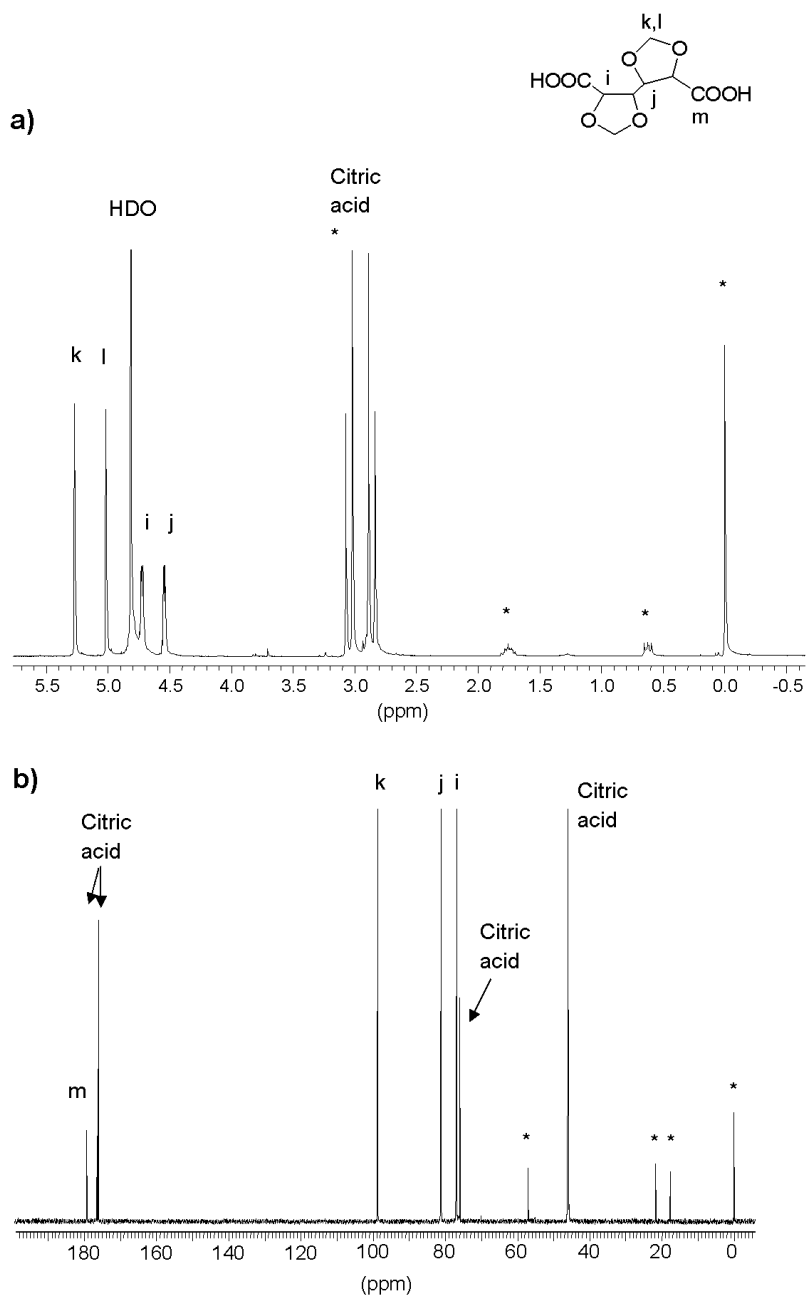


Figure E-6. ^1H (a) and ^{13}C (b) NMR spectrum in D_2O of the resulting product after incubation of dimethyl 2,3:4,5-di-O-methylene-galactarate at pH 2.0 for 12 weeks. * Reference: 3-(trimethylsilyl)-propanesulfonic acid sodium salt.

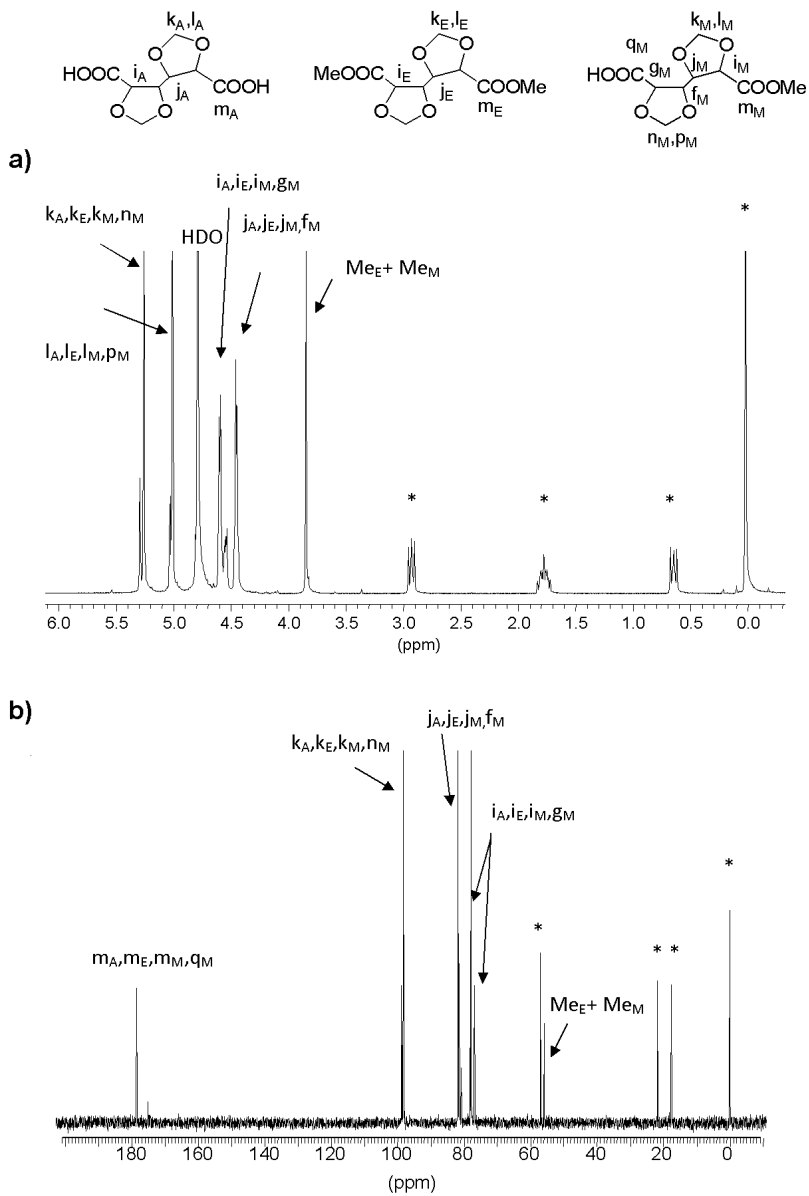


Figure E-7. ^1H (a) and ^{13}C (b) NMR spectrum in D_2O of the resulting product after incubation of dimethyl 2,3:4,5-di-O-methylene-galactarate at pH 7.4 for 12 weeks. * Reference: 3-(trimethylsilyl)propanesulfonic acid sodium salt.

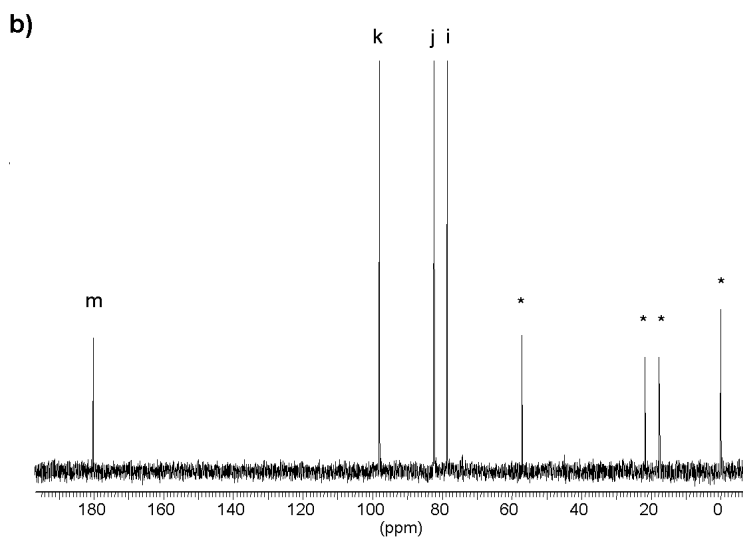
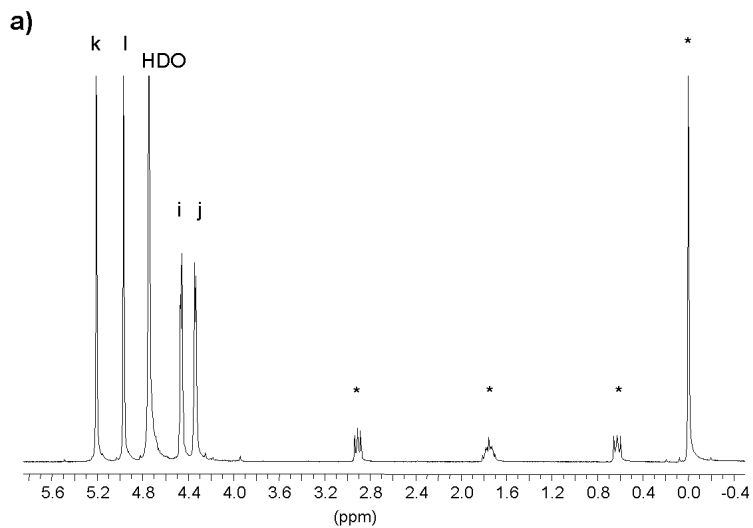
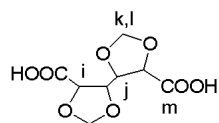


Figure E-8. ¹H (a) and ¹³C (b) NMR spectrum in D₂O of the resulting product after incubation of dimethyl 2,3:4,5-di-O-methylene-galactarate at pH 10.5 for 12 weeks. * Reference: 3-(trimethylsilyl)propanesulfonic acid sodium salt.

ANNEX F

Supporting information of Subchapter 5.4.

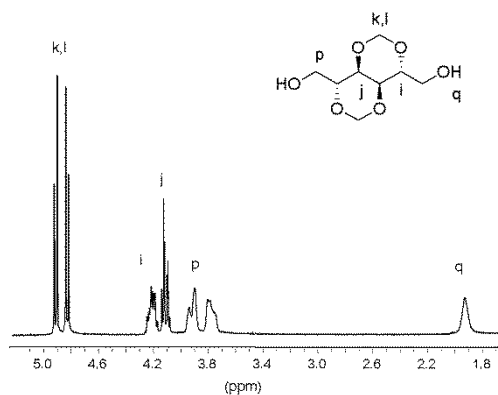


Figure F-1. ^1H NMR spectrum of 2,4:3,5-di-O-methylene-D-mannitol.

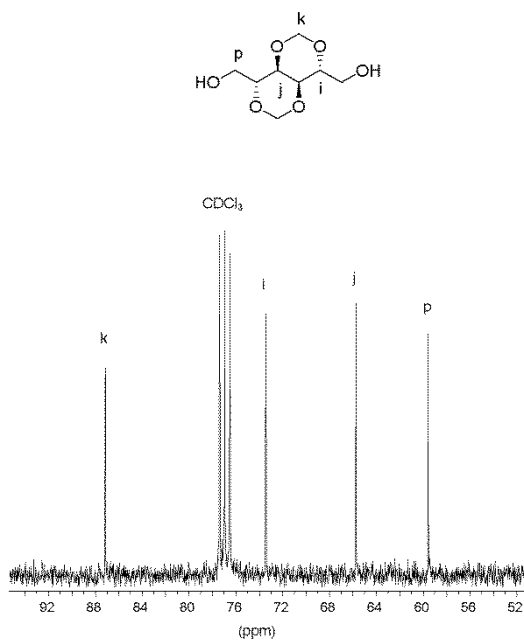


Figure F-2. ^{13}C NMR spectrum of 2,4:3,5-di-O-methylene-D-mannitol.

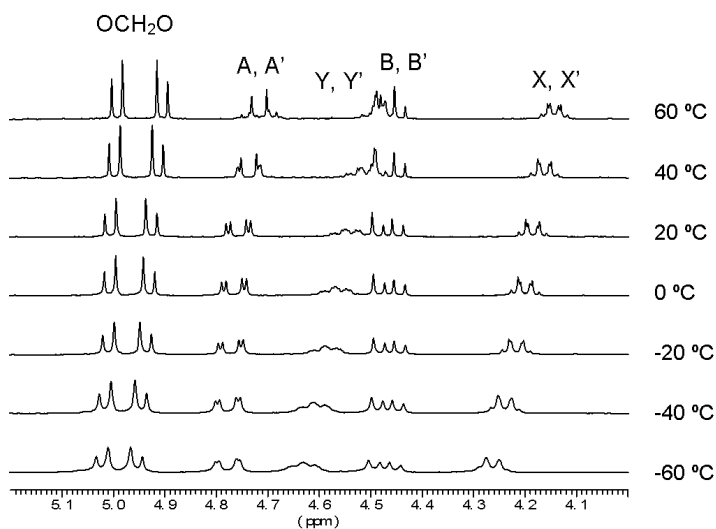


Figure F-3. ¹H NMR spectra of 1,6-di-O-benzoyl-2,4:3,5-di-O-methylene-D-mannitol at the indicated temperatures, with assignments corresponding to indications in Scheme 5.5.

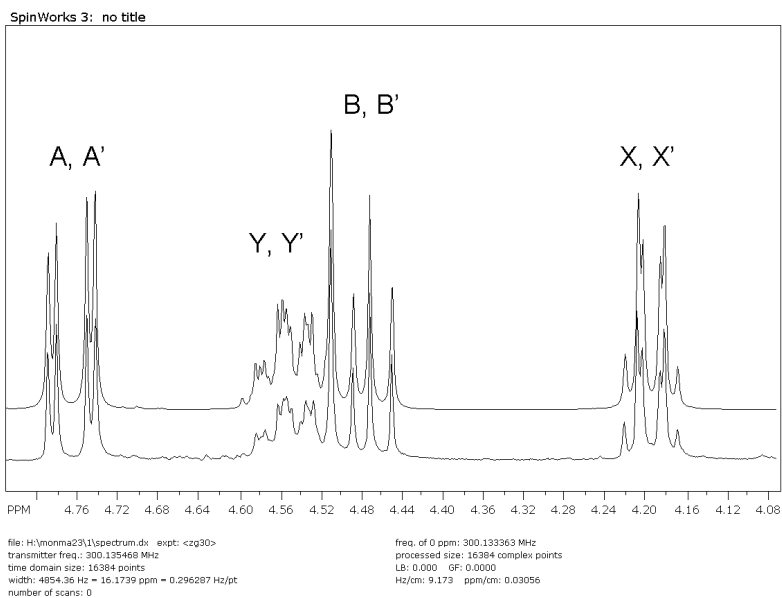


Figure F-4. Real (bottom) and simulated (top) ¹H NMR spectra of 1,6-di-O-benzoyl-2,4:3,5-di-O-methylene-D-mannitol in the region corresponding to the methyne and methylene protons.

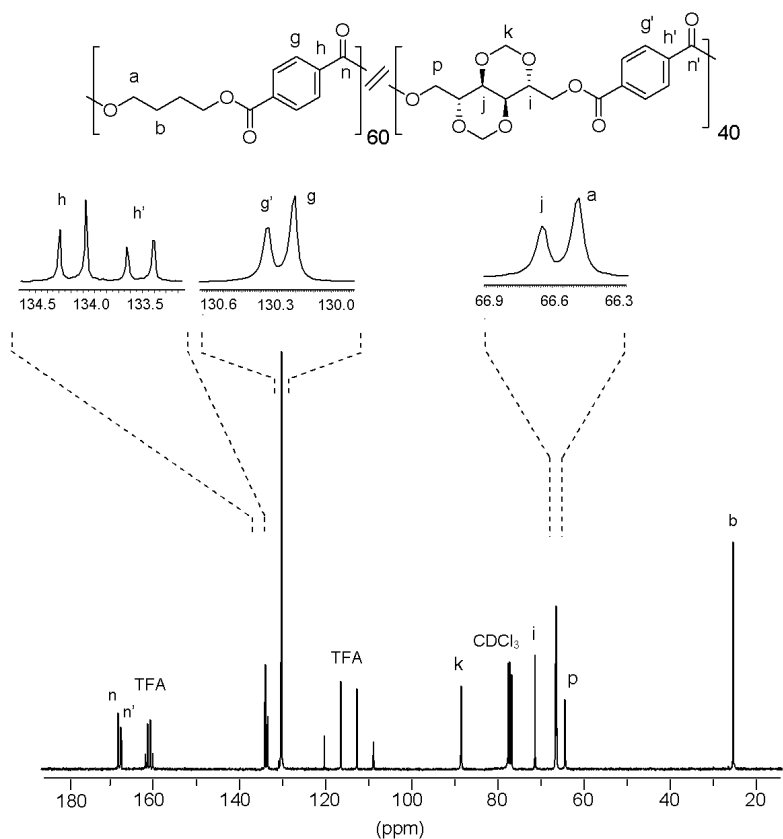


Figure F-5. ^{13}C NMR spectrum of $\text{PB}_{60}\text{Man}_{x40}\text{T}$ copolyester.

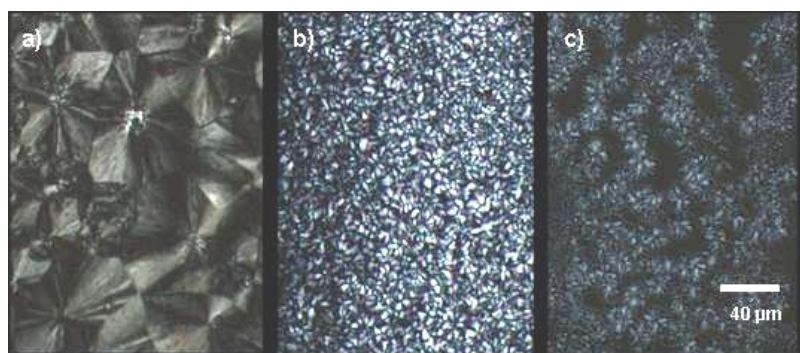


Figure F-6. Polarized optical micrographs of samples isothermally crystallized at the indicated temperatures: (a) PBT at 210 °C; (b) $\text{PB}_{90}\text{Man}_{x10}\text{T}$ at 185 °C; (c) $\text{PB}_{80}\text{Man}_{x20}\text{T}$ at 170 °C. The scale bar corresponds to 40 μm .

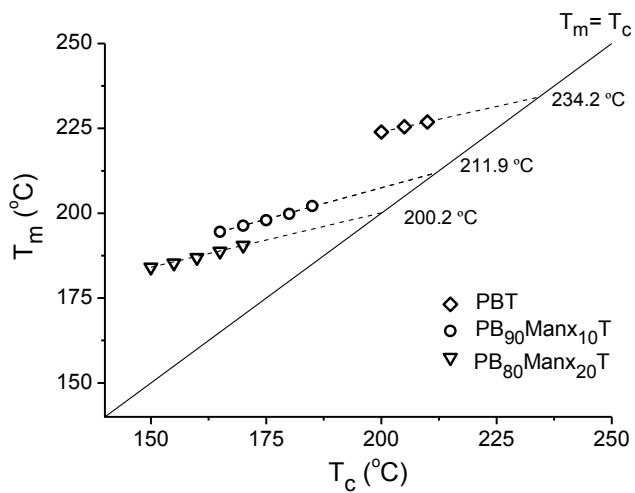


Figure F-7. Hoffman-Weeks plot for isothermally crystallized copolyesters.

ANNEX G

Supporting information of Subchapter 6.2.

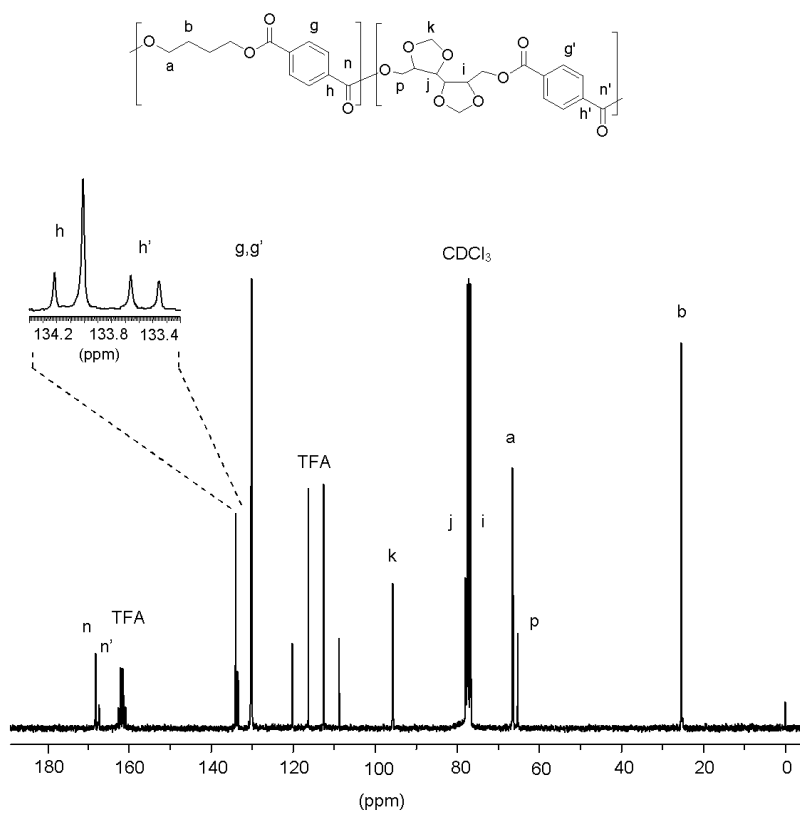


Figure G-1. ^{13}C NMR spectrum of $^{SSM}\text{PB}_{71}\text{Gal}_{29}\text{T}$ copolyester recorded in CDCl_3/TFA at room temperature.

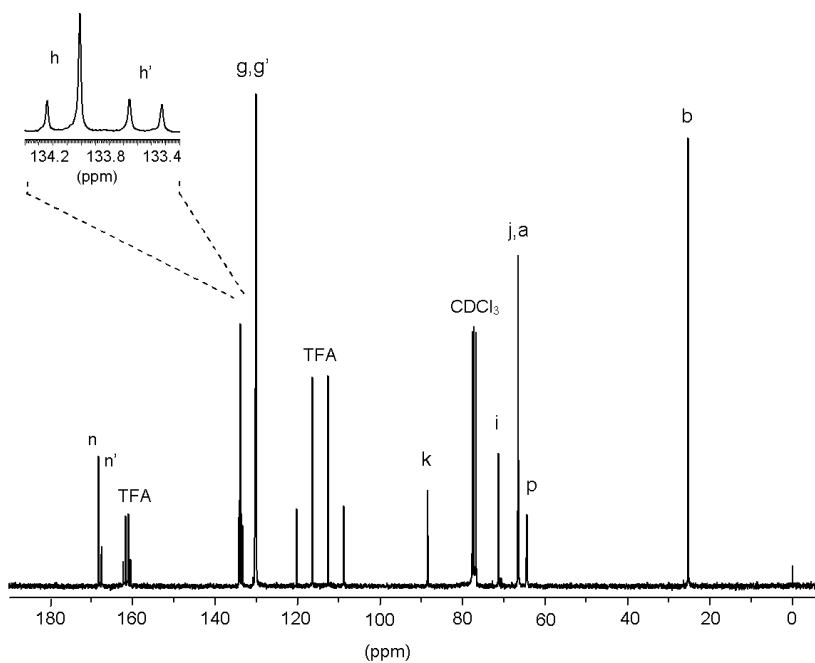
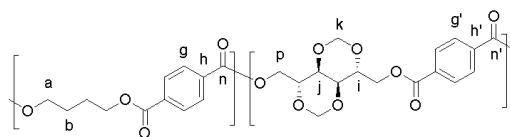


Figure G-2. ^{13}C NMR spectrum of ^{55}M PB₇₀Man₃₀T copolyester recorded in CDCl_3/TFA at room temperature.

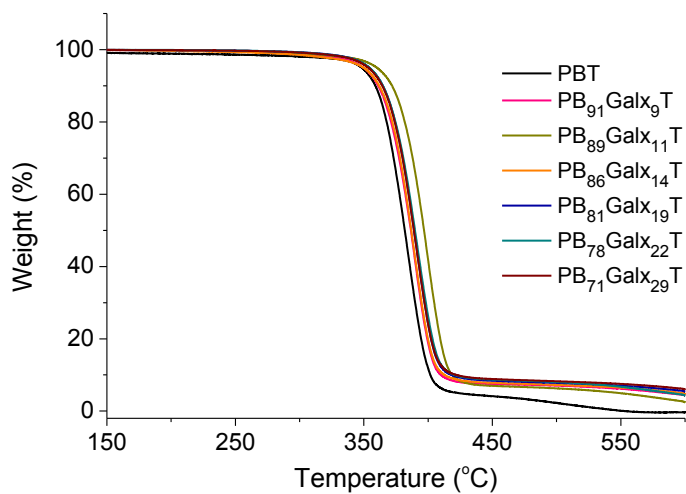


Figure G-3. TGA traces of ^{SSM}PB_xGal_yT copolyesters.

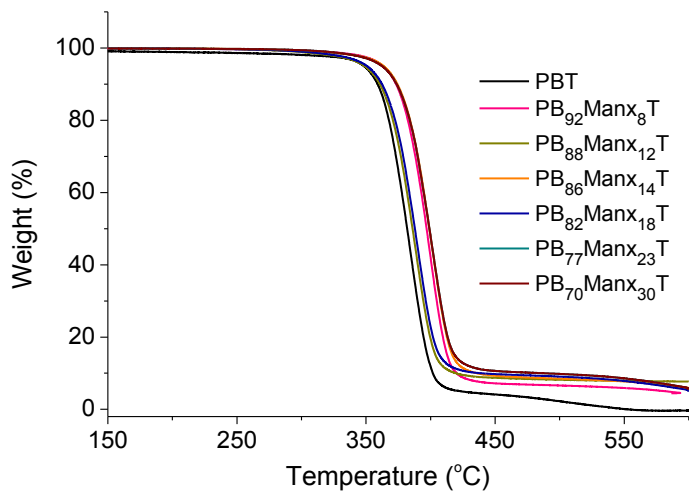


Figure G-4. TGA traces of ^{SSM}PB_xMan_yT copolyesters.

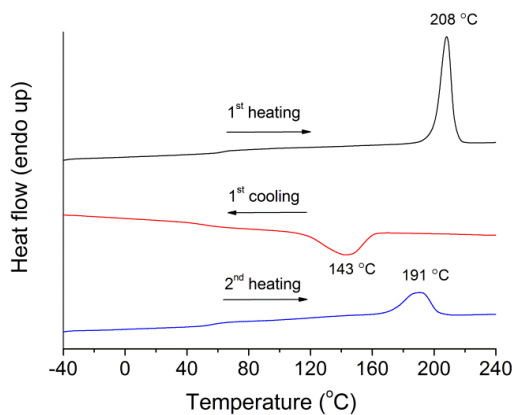


Figure G-5. DSC thermograms obtained for ^{SSM}PB₈₁Gal_{x19}T copolyester.

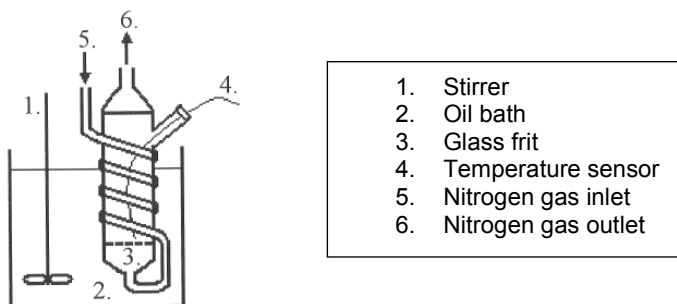


Figure G-6. Reactor used for SSM.

ANNEX H

Supporting information of Subchapter 6.3.

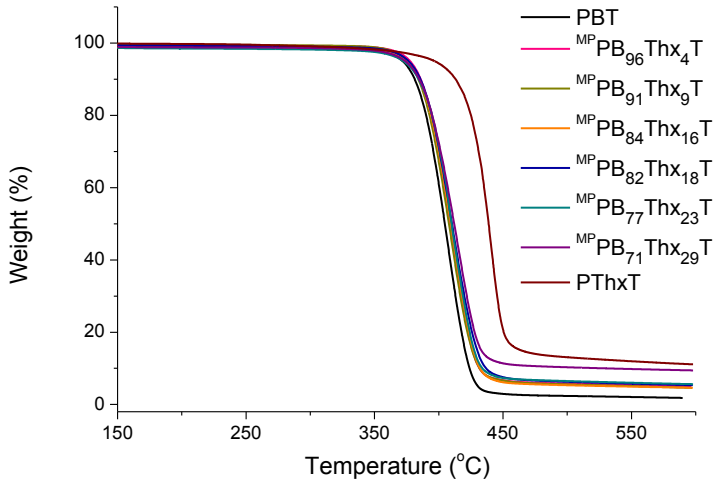


Figure H-1. TGA traces of ^{MP}PB_xThx_yT copolyesters.

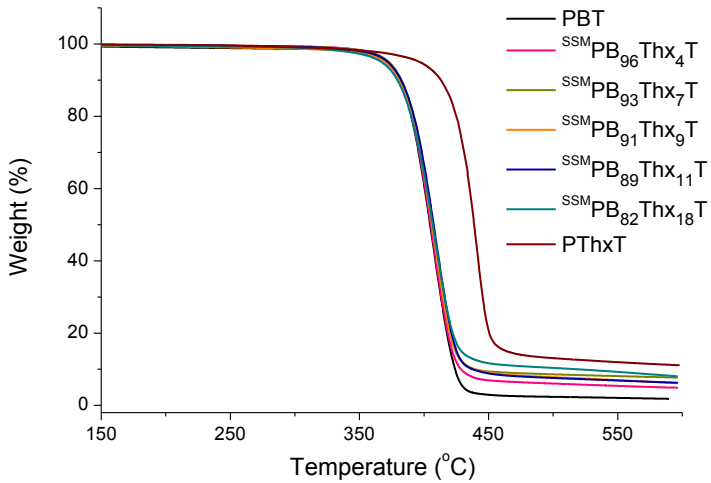


Figure H-2. TGA traces of ^{SSM}PB_xThx_yT copolyesters.

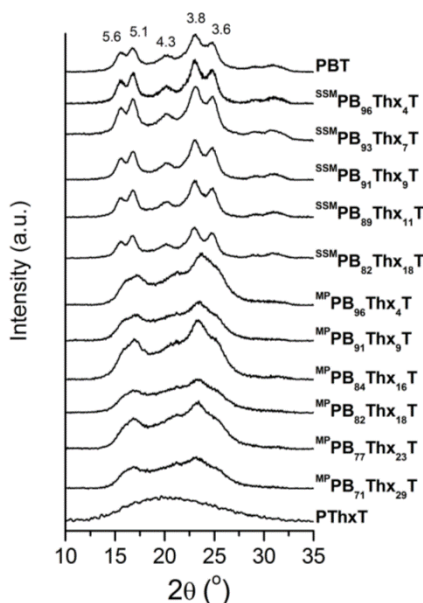


Figure H-3. WAXD profiles of $^{MP}PB_xThx_yT$ and $^{SSM}PB_xThx_yT$ copolyesters with indication of d_{hki} in Å.

Table H-1. Powder X-ray diffraction data.

Copolyester	d^a (Å)					χ_c^b
PBT	5.6 s	5.1 s	4.3 m	3.8 s	3.6 s	0.54
$^{MP}PB_{96}Thx_4T$	5.6 s	5.1 s	4.3 m	3.8 s	3.6 s	0.43
$^{MP}PB_{91}Thx_9T$	5.6 s	5.1 s	4.3 m	3.8 s	3.6 s	0.41
$^{MP}PB_{84}Thx_{16}T$	5.6 s	5.1 s	4.3 m	3.8 s	3.6 s	0.39
$^{MP}PB_{82}Thx_{18}T$	5.6 m	5.1 m	4.3 w	3.8 m	3.6 m	0.35
$^{MP}PB_{77}Thx_{23}T$	5.6 m	5.1 m	4.3 w	3.8 m	3.6 m	0.33
$^{MP}PB_{71}Thx_{29}T$	5.6 m	5.1 m	4.3 w	3.8 m	3.6 m	0.27
$^{SSM}PB_{96}Thx_4T$	5.6 s	5.1 s	4.3 m	3.8 s	3.6 s	0.64
$^{SSM}PB_{93}Thx_7T$	5.6 s	5.1 s	4.3 m	3.8 s	3.6 s	0.64
$^{SSM}PB_{91}Thx_9T$	5.6 s	5.1 s	4.3 m	3.8 s	3.6 s	0.62
$^{SSM}PB_{89}Thx_{11}T$	5.6 s	5.1 s	4.3 m	3.8 s	3.6 s	0.60
$^{SSM}PB_{82}Thx_{18}T$	5.6 s	5.1 s	4.3 m	3.8 s	3.6 s	0.57
PThxT						0

^a Bragg spacings measured in powder diffraction patterns for samples coming directly from synthesis. Intensities visually estimated as follows: m, medium; s, strong; w, weak. ^b Crystallinity index calculated as the quotient of crystalline area and total area. Crystalline and amorphous areas in the X-ray diffraction pattern were quantified using PeakFit v4.12 software.

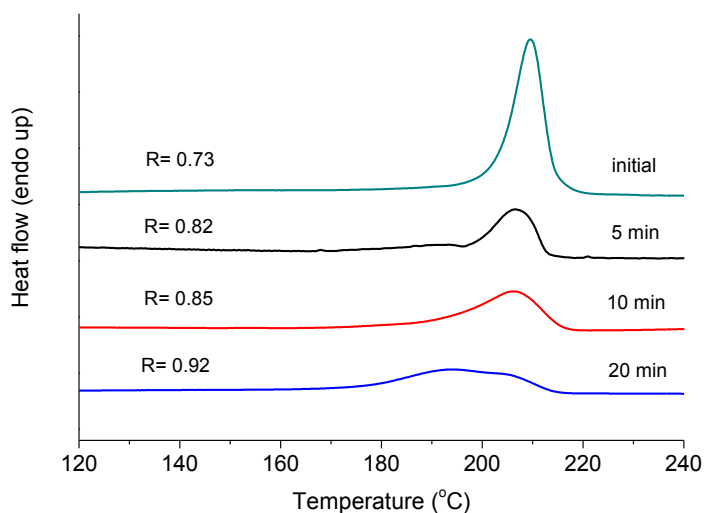


Figure H-4. DSC traces of the first heating run of $^{SSM}PB_{82}Th_{16}T$ copolyester as a function of the residence time in the melt, with indication of their degrees of randomness R .

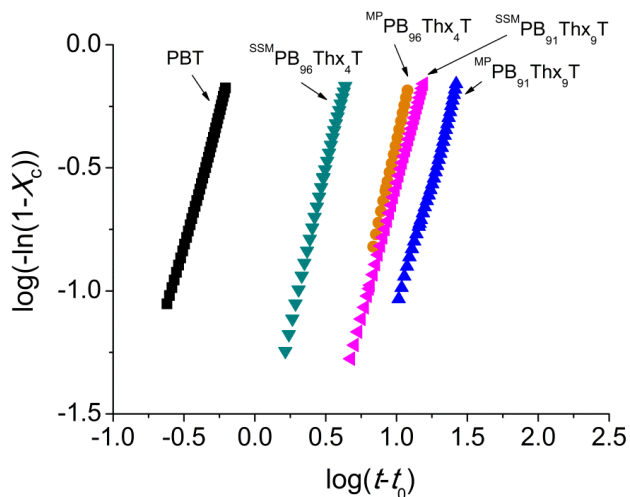


Figure H-5. Log-log plot of PBT, $^{MP}PB_{96}Th_{4}T$, $^{MP}PB_{91}Th_{9}T$, $^{SSM}PB_{96}Th_{4}T$ and $^{SSM}PB_{91}Th_{9}T$ isothermally crystallized at 200 °C.

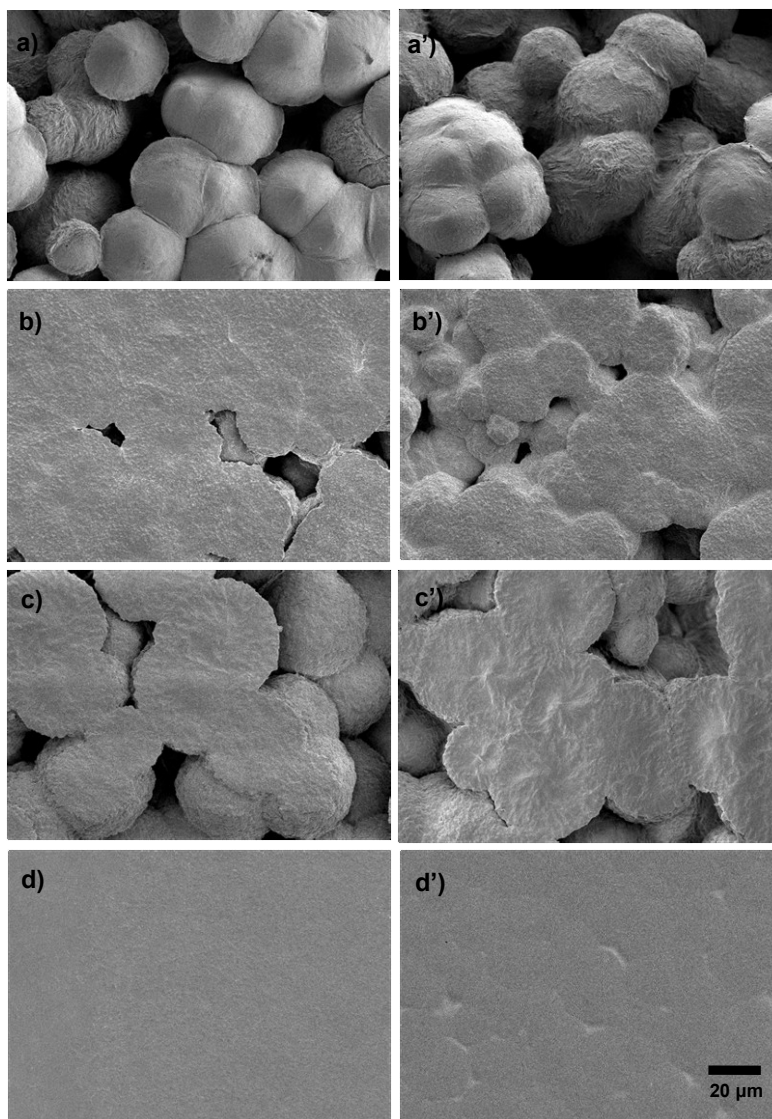


Figure H-6. SEM micrographs of PBT (a), $^{MP}PB_{82}Thx_{18}T$ (b), $^{SSM}PB_{82}Thx_{18}T$ (c) and PThxT (d): Initial sample (left) and after incubation at pH 2.0 at 80 °C for 6 weeks (right).

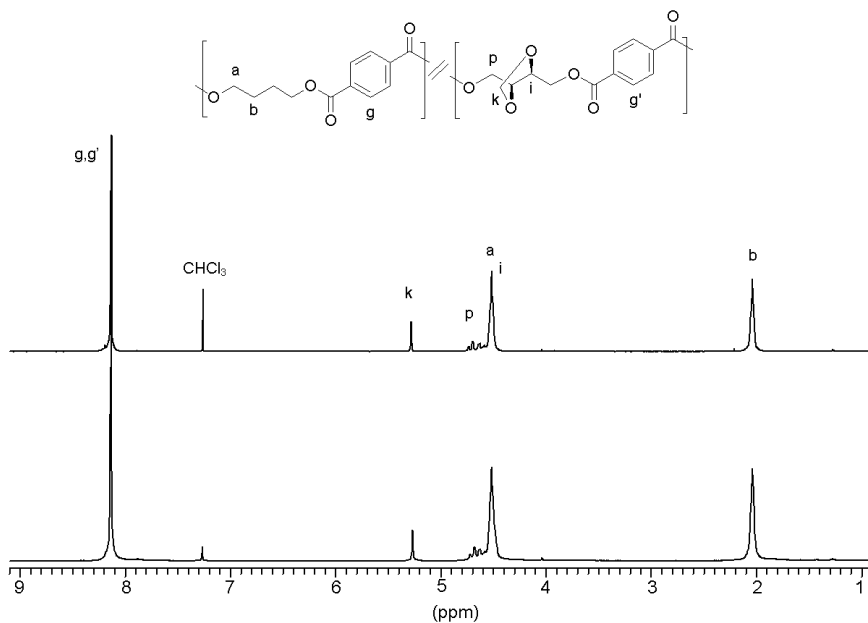


Figure H-7. Compared ^1H NMR spectra in CDCl_3/TFA of $^{\text{MP}}\text{PB}_{82}\text{Thx}_{18}\text{T}$ after incubation at pH 2.0 at 80°C for 6 weeks (top) and initial sample (bottom).

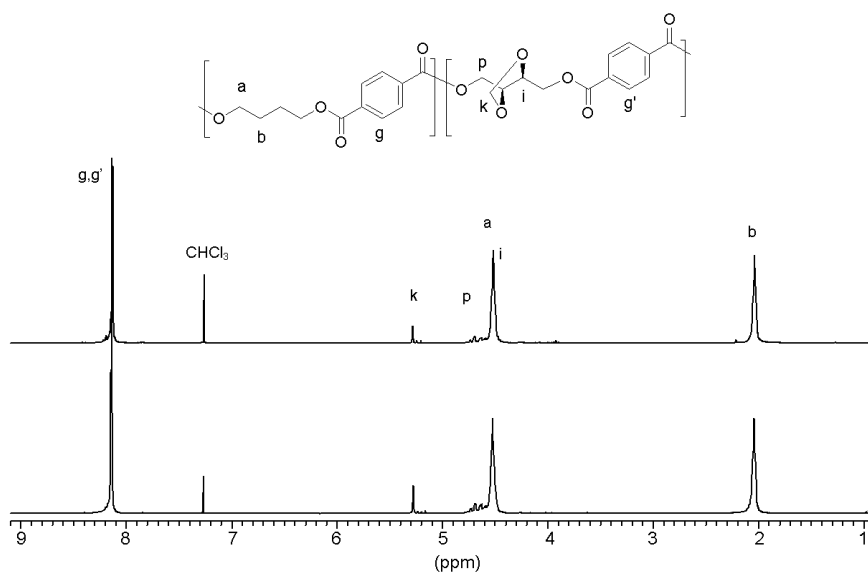


Figure H-8. Compared ^1H NMR spectra in CDCl_3/TFA of $^{\text{SSM}}\text{PB}_{82}\text{Thx}_{18}\text{T}$ after incubation at pH 2.0 at 80°C for 6 weeks (top) and initial sample (bottom).

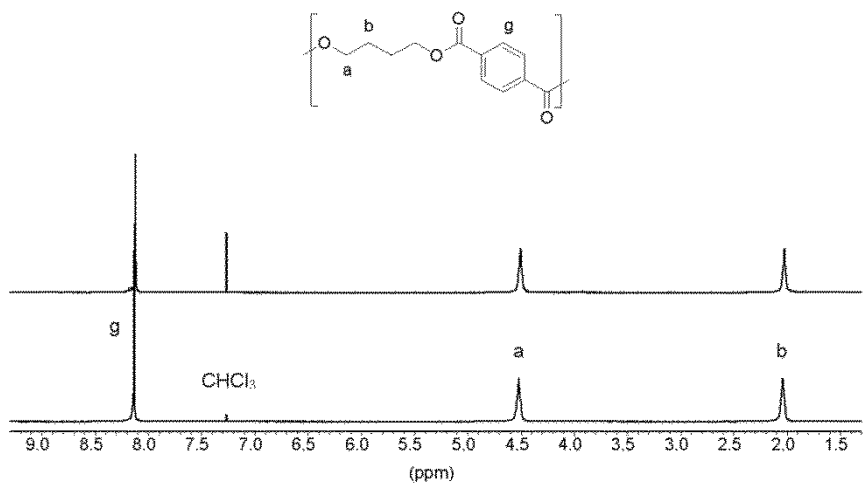


Figure H-9. Compared ¹H NMR spectra in CDCl₃/TFA of PBT after incubation at pH 2.0 at 80 °C for 6 weeks (top) and initial sample (bottom).

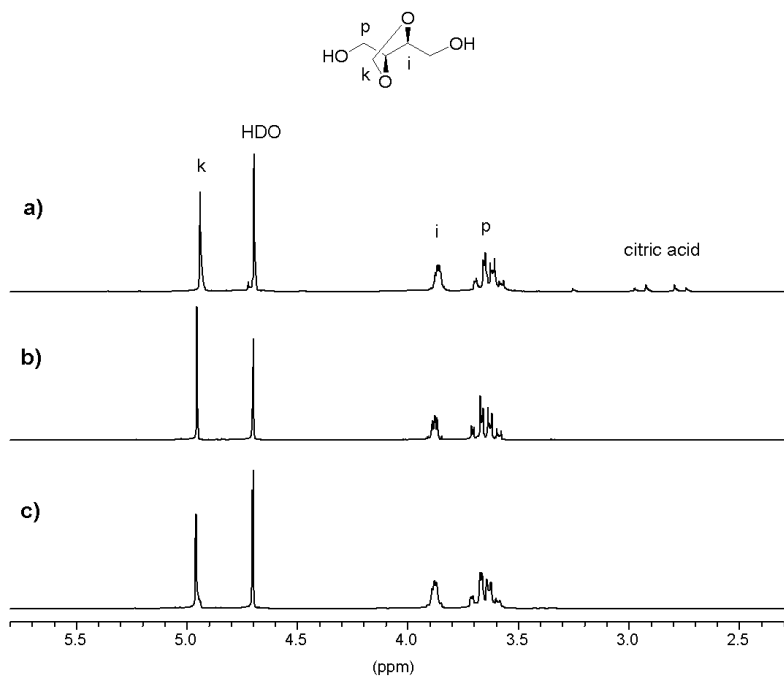


Figure H-10. Compared ¹H NMR spectra in D₂O of 2,3-di-O-methylene-L-threitol after incubation for 6 weeks at pH 2.0 (a), 7.4 (b) and 10.5 (c).

ANNEX I

Supporting information of Subchapter 7.2.

I.1. Detailed experimental procedure

I.1.1. Materials

The reagents 1,4-butanediol (99%), isosorbide (98%) and dimethyl terephthalate (99+%), and the catalyst dibutyl tin oxide (DBTO, 98%) were purchased from Sigma-Aldrich. Solvents used for purification and characterization, such as chloroform and methanol, were purchased from Panreac and they all were of either technical or high-purity grade. All the reagents and solvents were used as received without further purification.

I.1.2. General methods

^1H and ^{13}C NMR spectra were recorded on a Bruker AMX-300 spectrometer at 25.0 °C operating at 300.1 and 75.5 MHz, respectively. Polyesters and copolyesters were dissolved in a mixture of deuterated chloroform and trifluoroacetic acid (9:1), and spectra were internally referenced to tetramethylsilane (TMS). About 10 and 50 mg of sample dissolved in 1 mL of solvent were used for ^1H and ^{13}C NMR, respectively. Sixty-four scans were acquired for ^1H and 1,000-10,000 for ^{13}C with 32 and 64-K data points as well as relaxation delays of 1 and 2 s, respectively. Intrinsic viscosities of polymers dissolved in dichloroacetic acid were measured in an Ubbelohde viscosimeter thermostated at 25.0±0.1 °C. Gel permeation chromatograms were acquired at 35.0 °C with a Waters equipment provided with a refraction-index detector. The samples were chromatographed with 0.05 M sodium trifluoroacetate-hexafluoroisopropanol (NaTFA-HFIP) using a polystyrene-divinylbenzene packed linear column with a flow rate of 0.5 mL·min⁻¹. Chromatograms were calibrated against poly(methyl methacrylate) (PMMA) monodisperse standards. The thermal behavior of polyesters was examined by DSC using a Perkin Elmer DSC Pyris 1. DSC data were obtained from 3 to 5 mg samples at

heating/cooling rates of $10\text{ }^{\circ}\text{C}\cdot\text{min}^{-1}$ under a nitrogen flow of $20\text{ mL}\cdot\text{min}^{-1}$. Indium and zinc were used as standards for temperature and enthalpy calibration. The glass-transition temperatures were determined at a heating rate of $20\text{ }^{\circ}\text{C}\cdot\text{min}^{-1}$ from rapidly melt-quenched polymer samples. Thermogravimetric analyses were performed under a nitrogen flow of $20\text{ mL}\cdot\text{min}^{-1}$ at a heating rate of $10\text{ }^{\circ}\text{C}\cdot\text{min}^{-1}$, within a temperature range of 30 to $600\text{ }^{\circ}\text{C}$, using a Perkin Elmer TGA 6 equipment. Sample weights of about 10-15 mg were used in these experiments.

1.1.3. Polymer synthesis

PBT homopolyester. 60% molar excess of 1,4-butanediol to dimethyl terephthalate. Transesterification reactions at $180\text{ }^{\circ}\text{C}$ for 1 h, at $200\text{ }^{\circ}\text{C}$ for 1 h and at $240\text{ }^{\circ}\text{C}$ for 0.5 h under a low nitrogen flow. Polycondensation reactions at $260\text{ }^{\circ}\text{C}$ for 2 h under a 0.03-0.06 mbar vacuum.

PIsT, PGalxT and PManxT homopolyesters. 5% molar excess of sugar-based diol (Is, Galx or Manx) to dimethyl terephthalate. Transesterification reactions at $160\text{ }^{\circ}\text{C}$ for 1 h and at $180\text{ }^{\circ}\text{C}$ for 2 h under a low nitrogen flow. Polycondensation reactions at $180\text{ }^{\circ}\text{C}$ for 5 h under a 0.03-0.06 mbar vacuum.

PB_xIs_yT, PB_xGalx_yT and PB_xManx_yT copolyesters. The copolyesters were obtained by a similar method, with a procedure depending on each molar feed composition. The subscripts x and y are the mole percentages (mol-%) of 1,4-butanediol and sugar-based bicyclic diol, respectively, in the resulting copolyester determined by NMR.

PB₉₄Is₆T, PB₈₉Galx₁₁T and PB₉₁Manx₉T. The composition of the diol feed is 90 mol% of 1,4-butanediol and 10 mol% sugar-based diol. 5% molar excess of the diol mixture to dimethyl terephthalate. Transesterification reactions at $160\text{ }^{\circ}\text{C}$ for 1 h, at $200\text{ }^{\circ}\text{C}$ for 1 h and at $240\text{ }^{\circ}\text{C}$ for 0.5 h under a low nitrogen flow. Polycondensation reactions at $240\text{ }^{\circ}\text{C}$ for 2.5 h under a 0.03-0.06 mbar vacuum.

PB₈₅Is₁₅T, PB₇₉Galx₂₁T and PB₈₀Manx₂₀T. The composition of the diol feed is 80 mol% of 1,4-butanediol and 20 mol% sugar-based diol. 5% molar excess of the diol mixture to dimethyl terephthalate. Transesterification reactions at $160\text{ }^{\circ}\text{C}$ for 1 h, at $200\text{ }^{\circ}\text{C}$ for 1 h and at $240\text{ }^{\circ}\text{C}$ for 0.5 h under a low nitrogen flow. Polycondensation reactions at $240\text{ }^{\circ}\text{C}$ for 2.5 h under a 0.03-0.06 mbar vacuum.

PB₇₅Is₂₅T, PB₆₉Galx₃₁T and PB₆₉Manx₃₁T. The composition of the diol feed is 70 mol% of 1,4-butanediol and 30 mol% sugar-based diol. 5% molar excess of the diol mixture to dimethyl terephthalate. Transesterification reactions at 160 °C for 1 h, at 200 °C for 1 h and at 230 °C for 0.5 h under a low nitrogen flow. Polycondensation reactions at 230 °C for 3 h under a 0.03-0.06 mbar vacuum.

PB₆₈Is₃₂T, PB₆₁Galx₃₉T and PB₅₉Manx₄₁T. The composition of the diol feed is 60 mol% of 1,4-butanediol and 40 mol% sugar-based diol. 5% molar excess of the diol mixture to dimethyl terephthalate. Transesterification reactions at 160 °C for 1 h, at 200 °C for 1 h and at 220 °C for 0.5 h under a low nitrogen flow. Polycondensation reactions at 220 °C for 3.5 h under a 0.03-0.06 mbar vacuum.

PB₅₆Is₄₄T, PB₅₁Galx₄₉T and PB₄₉Manx₅₁T. The composition of the diol feed is 50 mol% of 1,4-butanediol and 50 mol% sugar-based diol. 5% molar excess of the diol mixture to dimethyl terephthalate. Transesterification reactions at 160 °C for 1 h, at 200 °C for 1 h and at 210 °C for 0.5 h under a low nitrogen flow. Polycondensation reactions at 210 °C for 4 h under a 0.03-0.06 mbar vacuum.

I.1.4. NMR characterization

PBT homopolyester. ¹H NMR (300.1 MHz, CDCl₃/TFA), δ (ppm): 8.1 (s, 4H, ArH), 4.5 (t, 4H, OCH₂CH₂), 2.0 (t, 4H, OCH₂CH₂). ¹³C NMR (75.5 MHz, CDCl₃/TFA), δ (ppm): 168.0 (CO), 133.7, 129.9, 66.2, 25.1.

PIsT homopolyester. ¹H NMR (300.1 MHz, CDCl₃/TFA), δ (ppm): 8.1 (m, 4H, ArH), 5.7 (m, 1H, CHO_{exo}), 5.6 (m, 1H, CHO_{endo}), 5.3 (m, 1H, CHCHO_{endo}), 4.9 (m, 1H, CHCHO_{exo}), 4.4-4.1 (m, 4H, CH₂CHO_{exo} and CH₂CHO_{endo}). ¹³C NMR (75.5 MHz, CDCl₃/TFA), δ (ppm): 166.3 (CO), 133.2, 130.2, 85.8, 81.3, 78.5, 75.0, 73.4, 70.8.

PGalxT homopolyester. ¹H NMR (300.1 MHz, CDCl₃/TFA), δ (ppm): 8.1 (s, 4H, ArH), 5.2 and 5.1 (2s, 4H, OCH₂O), 4.7 (m, 2H, OCH₂CH), 4.6 (m, 4H, OCH₂CH), 4.1 (m, 2H, OCH₂CHCH). ¹³C NMR (75.5 MHz, CDCl₃/TFA), δ (ppm): 167.5 (CO), 133.6, 130.3, 95.7, 77.9, 76.7, 65.3.

PManxT homopolyester. ¹H NMR (300.1 MHz, CDCl₃/TFA), δ (ppm): 8.1 (s, 4H, ArH), 5.2-5.0 (m, 4H, OCH₂O), 4.9-4.5 (m, 4H, OCH₂CH), 4.7 (m, 2H, OCH₂CH), 4.3 (m, 2H,

OCH₂CHCH). ¹³C NMR (75.5 MHz, CDCl₃/TFA), δ (ppm): 167.5 (CO), 133.5, 130.3, 88.6, 71.4, 66.7, 64.4.

PB_xIs_yT copolyesters. ¹H NMR (300.1 MHz, CDCl₃/TFA), δ (ppm): 8.1 (m, 4H, ArH), 5.7 (m, γ·1H, CHO_{exo}), 5.6 (m, γ·1H, CHO_{endo}), 5.3 (m, γ·1H, CHCHO_{endo}), 4.9 (m, γ·1H, CHCHO_{exo}), 4.5 (t, x·4H, OCH₂CH₂), 4.4-4.1 (m, γ·4H, CH₂CHO_{exo} and CH₂CHO_{endo}), 2.0 (t, x·4H, OCH₂CH₂). ¹³C NMR (75.5 MHz, CDCl₃/TFA), δ (ppm): 168.2 (CO), 166.3 (CO), 134.2, 133.2, 130.2, 85.8, 81.3, 78.5, 75.0, 73.4, 70.8, 66.2, 25.1.

PB_xGalx_yT copolyesters. ¹H NMR (300.1 MHz, CDCl₃/TFA), δ (ppm): 8.1 (s, 4H, ArH), 5.2 and 5.1 (2s, γ·4H, OCH₂O), 4.7 (m, γ·2H, OCH₂CH), 4.6 (m, γ·4H, OCH₂CH), 4.5 (t, x·4H, OCH₂CH₂), 4.1 (m, γ·2H, OCH₂CHCH), 2.0 (t, x·4H, OCH₂CH₂). ¹³C NMR (75.5 MHz, CDCl₃/TFA), δ (ppm): 168.3 (CO), 167.5 (CO), 134.2-133.4, 130.4, 130.2, 95.7, 77.9, 76.7, 66.2, 65.3, 25.1.

PB_xManx_yT copolyesters. ¹H NMR (300.1 MHz, CDCl₃/TFA), δ (ppm): 8.1 (s, 4H, ArH), 5.2-5.0 (m, γ·4H, OCH₂O), 4.9-4.5 (m, γ·4H, OCH₂CH), 4.7 (m, γ·2H, OCH₂CH), 4.5 (t, x·4H, OCH₂CH₂), 4.3 (m, γ·2H, OCH₂CHCH), 2.0 (t, x·4H, OCH₂CH₂). ¹³C NMR (75.5 MHz, CDCl₃/TFA), δ (ppm): 168.3 (CO), 167.5 (CO), 134.2-133.3, 130.4, 130.2, 88.6, 71.4, 66.7, 66.5, 64.4, 25.4.

I.2. NMR spectra

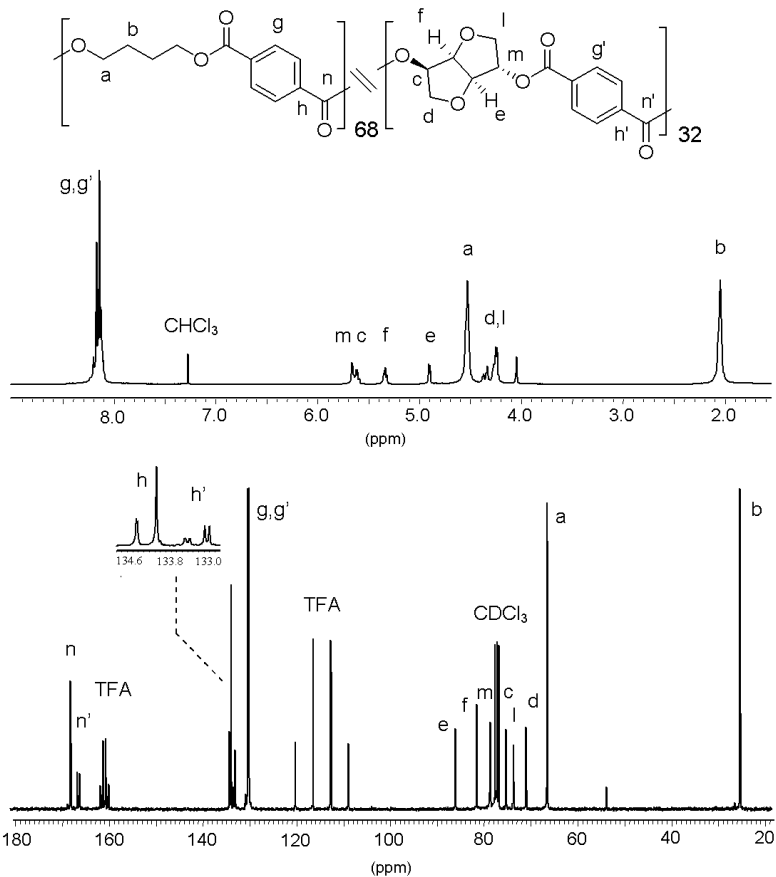


Figure I-1. ¹H (top) and ¹³C (bottom) NMR spectra of PB₆₈I₃₂T copolyester.

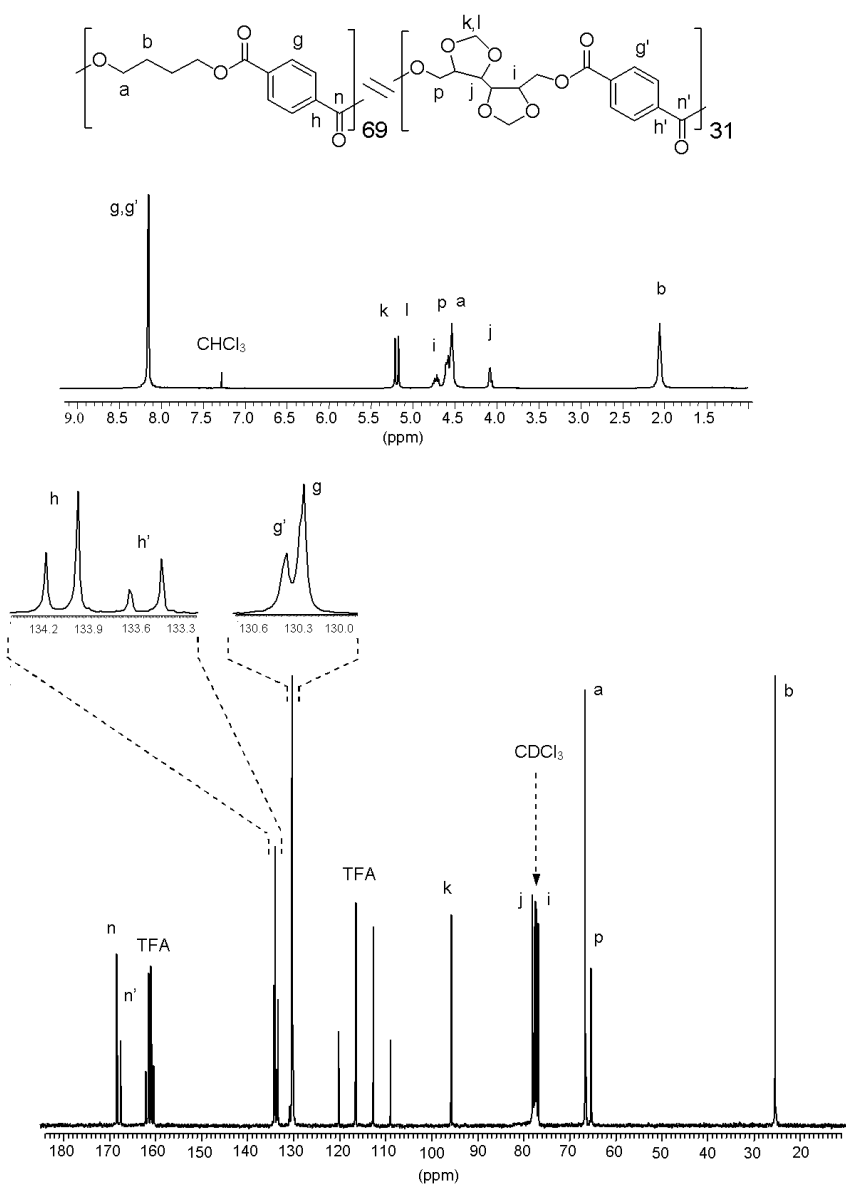


Figure I-2. ¹H (top) and ¹³C (bottom) NMR spectra of PB₆₉Gal_{x31}T copolyester.

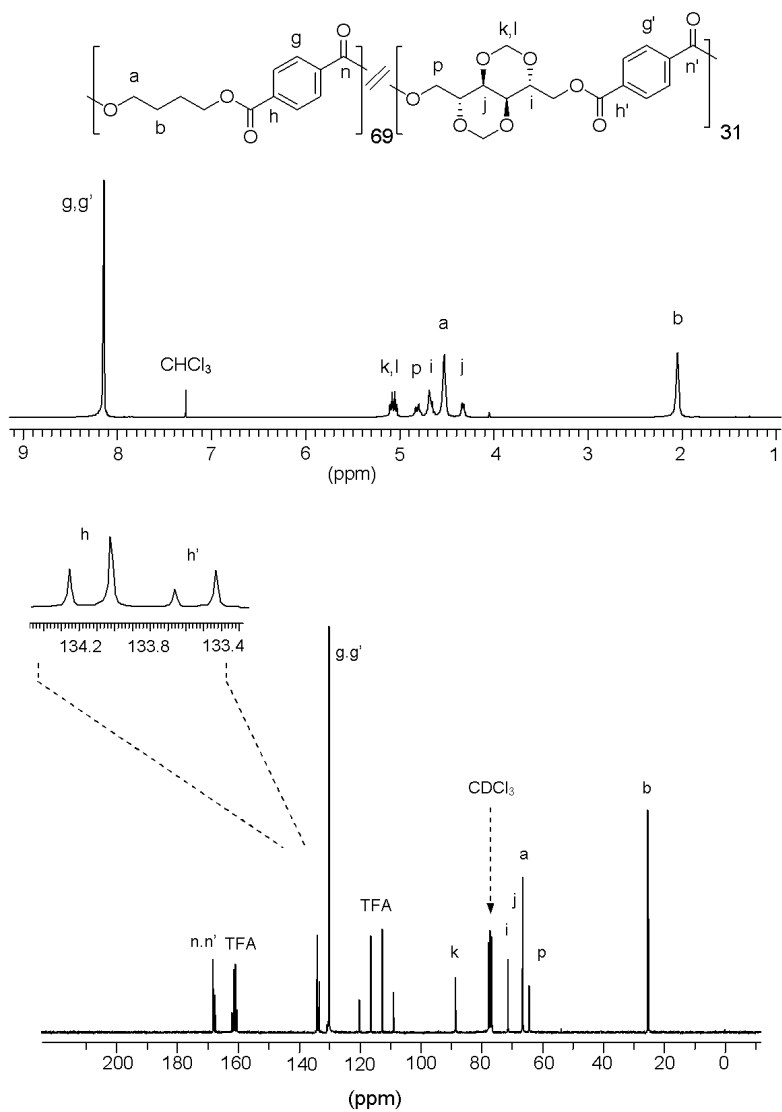


Figure I-3. ¹H (top) and ¹³C (bottom) NMR spectra of PB₆₉Man₃₁T copolyester.

I. 3. TGA

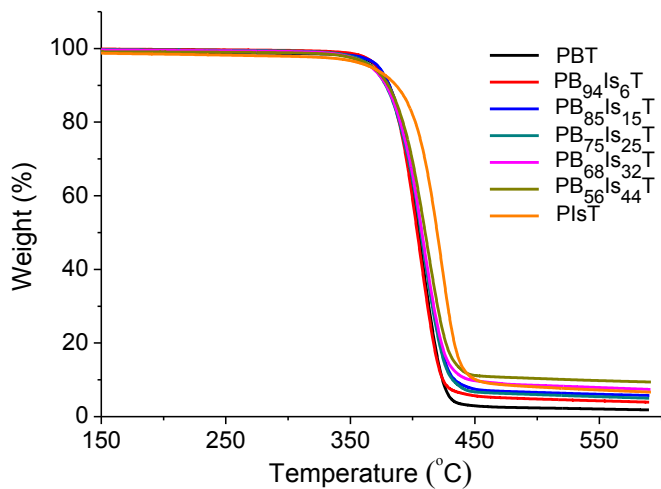


Figure I-4. TGA traces of PB_xIs_yT copolyesters.

I. 4. DSC

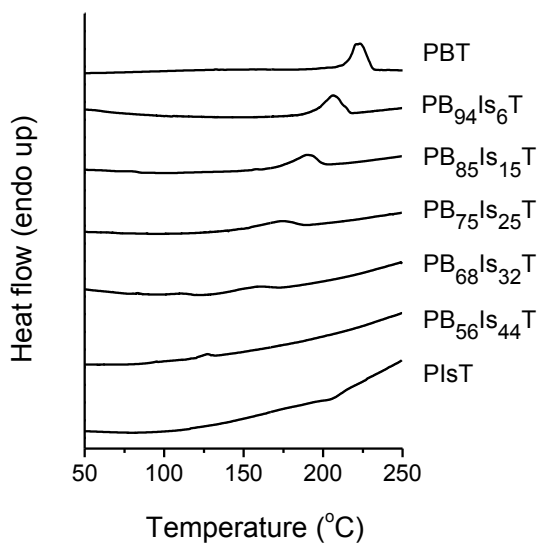


Figure I-5. DSC melting traces of PB_xIs_yT copolyesters coming directly from synthesis.

Acknowledgements

In the following section I would like to express my gratitude to all the people who supported me during this enriching experience, full of memories and challenges. Part of this section will be written in my mother tongues Spanish or Catalan, or in English, as I will express myself in the language I feel like when memories with each person come into my mind.

Mi especial agradecimiento al Prof. Sebastián Muñoz Guerra, por su labor como director de la presente tesis, y por su dedicación, apoyo y confianza durante todo este tiempo.

A toda la gente que forma parte del grupo, especialmente a los doctores Abdel Alla y Antxon Martínez de Ilarduya, por su amabilidad, ayuda, colaboración y por sus buenos consejos.

Al Prof. Juan Galbis, Dra. M. Gracia García-Martín y Dra. Elena Benito del grupo *Carbohidratos y Polímeros* de la Universidad de Sevilla, por su colaboración en este trabajo y su amabilidad.

I would like to thank Prof. Cor Koning and Dr. Bart Noordover for all their support and kindness during my stay at TU/e and further collaboration, which have been even better than I could expect. And to all SPM members, for making me enjoy my stay in Eindhoven. Special mention to Erik Gubbels, for the nice collaboration besides being a good friend.

A la Irene i la Francina, per la seva amabilitat i per ajudar-me amb els tràmits administratius.

A mis compañeros de laboratorio, por sus ánimos y por los buenos momentos que hemos pasado juntos. Mis compañeros de tesis Ainhoa, Cristina, Alberto, Mayka y Elena, y de máster Javier y Angélica. También a Yani, Sejin y Laura. Ainhoa y Javier, aquellas conversaciones surrealistas de las tardes 'se echan de menos'. Con todos vosotros no sólo he compartido mi trabajo sino una etapa de mi vida y también una buena amistad.

També al Guillem, el David, la Georgina, el Dani, l'Esther, la Mireia, el Frankie, la Mar i el Bruno, per la seva amistat i per fer de les hores de dinar quelcom agradable, animat i fins i tot surrealista a vegades.

A l'Anna, el Jordi i el Pere. Tot i que el món dels polímers els queda una mica llunyà, sempre s'han interessat per com m'anava aquesta tesi i tot en general. Que qualsevol 'novetat' o 'cotilleix' es pugui convertir en converses que durin fins i tot hores. I per la gran amistat que ens uneix des de fa molts anys.

A l'Amàlia, la Maria, la Rosa i el Víctor, els químics que ja portem uns quants anys compartint sopars, escapades, bon humor i una bona amistat. Tot i que sembla que va ser ahir quan començàvem junts la carrera a la UAB.

Als meus pares, pel seu afecte, comprensió, per l'educació que m'han donat i pel seu recolzament constant.

Als meus avis, per contribuir a la meva educació des que era ben petita i per estar sempre al meu costat.

A l'Ivan, per compartir la seva vida amb mi, per la seva comprensió i la seva incondicional ajuda. També per les bones idees per la portada d'aquesta tesi, i les útils suggerències des del punt de vista 'pràctic' que sempre el caracteritza.

A la Universitat Politècnica de Catalunya, per la beca de Formació de Personal Investigador (FPI-UPC, 2009-2011). Al Ministerio de Educación, por la beca de Formación de Profesorado Universitario (FPU-MEC, 2011-2013).

*A tots vosaltres, moltes gràcies.
A todos vosotros, muchas gracias.
To all of you, thank you.*

The Author

Cristina Lavilla Aguilar was born on the 12th of December 1985 in Terrassa, Spain. In 2003 she started her bachelor studies on Chemistry at the faculty of Science of the Universitat Autònoma de Barcelona (UAB, Spain). In 2007 she graduated with Honors and started her bachelor studies on Materials Engineering at the faculty of Engineering of the UAB, which successfully completed with Honors in 2009. In both bachelor degrees Cristina was further distinguished by the Spanish Ministry of Education with the *Premio Nacional Fin de Carrera* and the *Premio Nacional a la Excelencia en el Rendimiento Académico Universitario*, not only for being the best graduated student at UAB, but also for being one of the best in all Spanish universities.

In 2009 she started her master studies on Polymers and Biopolymers at the faculty of Industrial Engineering of the Universitat Politècnica de Catalunya (UPC, Spain). She worked as researcher on her master dissertation entitled 'Synthesis, characterization and biodegradability of aliphatic polyesters from cyclic diacetalized galactose' within the group 'Advanced and Biotechnological Industrial Polymers' under the supervision of Prof. Sebastián Muñoz Guerra, where she continued her research on her PhD project entitled 'Bio-based polyesters from cyclic monomers derived from carbohydrates'. During her PhD, Cristina acquired teaching experience in Organic Chemistry, Polymer Chemistry and Environmental Technology lessons and Polymers and Biopolymers practical courses, and she also performed an international stay at Technische Universiteit Eindhoven (TU/e, The Netherlands) for 3 months. The results of her studies are described in this Thesis.

List of publications

Scientific papers

1. Lavilla, C.; Alla, A.; Martínez de Ilarduya, A.; Benito, E.; García-Martín, M.G.; Galbis, J.A.; Muñoz-Guerra, S. 'Carbohydrate-based polyesters made from bicyclic acetalized galactaric acid'. *Biomacromolecules* **2011**, *12*, 2642-2652.
2. Lavilla, C.; Alla, A.; Martínez de Ilarduya, A.; Benito, E.; García-Martín, M.G.; Galbis, J.A.; Muñoz-Guerra, S. 'Carbohydrate-based copolyesters made from bicyclic acetalized galactaric acid'. *J. Polym. Sci., Polym. Chem.* **2012**, *50*, 1591-1604.
3. Lavilla, C.; Alla, A.; Martínez de Ilarduya, A.; Benito, E.; García-Martín, M.G.; Galbis, J.A.; Muñoz-Guerra, S. 'Biodegradable aromatic copolyesters made from bicyclic acetalized galactaric acid'. *J. Polym. Sci., Polym. Chem.* **2012**, *50*, 3393-3406.
4. Lavilla, C.; Alla, A.; Martínez de Ilarduya, A.; Benito, E.; García-Martín, M.G.; Galbis, J.A.; Muñoz-Guerra, S. 'Bio-based poly(butylene terephthalate) copolyesters containing bicyclic diacetalized galactitol and galactaric acid: Influence of composition on properties'. *Polymer* **2012**, *53*, 3432-3445.
5. Lavilla, C.; Muñoz-Guerra, S. 'Biodegradation and hydrolytic degradation of poly(butylene terephthalate) copolyesters containing cyclic sugar units'. *Polym. Degrad. Stabil.* **2012**, *97*, 1762-1771.
6. Lavilla, C.; Martínez de Ilarduya, A.; Alla, A.; García-Martín, M.G.; Galbis, J.A.; Muñoz-Guerra, S. 'Bio-based aromatic polyesters from a novel bicyclic diol derived from D-mannitol'. *Macromolecules* **2012**, *45*, 8257-8266.
7. Lavilla, C.; Martínez de Ilarduya, A.; Alla, A.; Muñoz-Guerra, S. 'PET copolyesters made from a D-mannitol derived bicyclic diol'. *Polym. Chem.* **2013**, *4*, 282-289.
8. Lavilla, C.; Muñoz-Guerra, S. 'Sugar-based aromatic copolyesters: A comparative study regarding isosorbide and diacetalized alditols as sustainable comonomers'. *Green Chem.* **2013**, *15*, 144-151.
9. Lavilla, C.; Alla, A.; Martínez de Ilarduya, A.; Muñoz-Guerra, S. 'High T_g bio-based aliphatic polyesters from bicyclic D-mannitol'. *Biomacromolecules* **2013**, *14*, 781-793.

10. Lavilla, C.; Gubbels, E.; Martínez de Ilarduya, A.; Noordover, B.A.J.; Koning, C.E.; Muñoz-Guerra, S. 'Solid-state modification of PBT with cyclic acetalized galactitol and D-mannitol: Influence of composition and chemical microstructure on thermal properties'. *Macromolecules* **2013**, *46*, 4335-4345.
11. Gubbels, E.; Lavilla, C.; Martínez de Ilarduya, A.; Noordover, B.A.J.; Koning, C.E.; Muñoz-Guerra, S. 'Partially renewable copolyesters prepared from acetalized D-glucitol by solid-state modification of PBT'. (Submitted to *J. Polym. Sci., Polym. Chem.*)
12. Lavilla, C.; Gubbels, E.; Alla, A.; Martínez de Ilarduya, A.; Noordover, B.A.J.; Koning, C.E.; Muñoz-Guerra, S. 'Carbohydrate-based PBT copolyesters from a cyclic diol derived from naturally occurring tartaric acid: A comparative study regarding melt polycondensation and solid-state modification'. (Submitted to *Green Chem.*)
13. Muñoz-Guerra, S.; Lavilla, C.; Japu, C.; Martínez de Ilarduya, A. 'Renewable terephthalate polyesters from carbohydrate-based bicyclic monomers'. (Submitted to *Green Chem.*)

Patents

1. Muñoz-Guerra, S.; Lavilla, C.; Japu, C.; García-Martín, M.G.; Alla, A.; Martínez de Ilarduya, A.; Benito, E.; Galbis, J.A. 'Homopoliésteres y copoliésteres derivados de alditoles y ácidos aldáricos diacetalizados'. Spanish Patent P201031709. (Patent application: 2010; Patent concession: 2013)

Conference proceedings

1. Lavilla, C.; Alla, A.; Martínez de Ilarduya, A.; Benito, E.; García-Martín, M.G.; Galbis, J.A.; Muñoz-Guerra, S. 'Aliphatic polyesters from cyclic diacetalized galactose'. Poster at the X Jornadas de Carbohidratos. Granada (Spain), 15th-18th September 2010.
2. Lavilla, C.; Alla, A.; Martínez de Ilarduya, A.; Benito, E.; García-Martín, M.G.; Galbis, J.A.; Muñoz-Guerra, S. 'Aliphatic polyesters from the carbohydrate-based bicyclic di-O-methylene-galactarate'. Oral Communication at the European Polymer Congress - XII GEP Congress. Granada (Spain), 26th June-1st July 2011.
3. Lavilla, C.; Japu, C.; García-Martín, M.G.; Galbis, J.A.; Muñoz-Guerra, S. 'Thermal and hydrolytic degradability of polyesters containing cyclic acetalized carbohydrate

- units'. Poster at the European Polymer Congress - XII GEP Congress. Granada (Spain), 26th June-1st July 2011.
4. Lavilla, C.; Alla, A.; Martínez de Ilarduya, A.; Benito, E.; García-Martín, M.G.; Galbis, J.A.; Muñoz-Guerra, S. 'Aliphatic copolyesters from the carbohydrate-based bicyclic di-O-methylene-galactarate'. Oral Communication at the Congreso de Jóvenes Investigadores en Polímeros. Islantilla (Spain), 22th-26th April 2012.
 5. Lavilla, C.; Alla, A.; Martínez de Ilarduya, A.; Muñoz-Guerra, S. 'Bio-based aliphatic polyesters from succinic acid and bicyclic D-mannitol'. Poster at the Frontiers in Polymer Science Congress, Sitges (Spain), 21th-23th May 2013.
 6. Lavilla, C.; Alla, A.; Martínez de Ilarduya, A.; Benito, E.; García-Martín, M.G.; Galbis, J.A.; Muñoz-Guerra, S. 'Sugar-based aromatic copolyesters from cyclic galactitol and galactaric acid derivatives'. Poster at the Frontiers in Polymer Science Congress, Sitges (Spain), 21th-23th May 2013.
 7. Lavilla, C.; Martínez de Ilarduya, A.; Alla, A.; García-Martín, M.G.; Galbis, J.A.; Muñoz-Guerra, S. 'Sugar-based aromatic copolyesters: A comparative study regarding isosorbide and diacetalized alditols as comonomers'. Oral Communication at the European Polymer Congress, Pisa (Italy), 16th-21th June 2013.
 8. Lavilla, C.; Alla, A.; Martínez de Ilarduya, A.; Muñoz-Guerra, S. 'Bio-based aliphatic polyesters from bicyclic D-mannitol'. Poster at the European Polymer Congress, Pisa (Italy), 16th-21th June 2013.
 9. Lavilla, C.; Martínez de Ilarduya, A.; Alla, A.; Muñoz-Guerra, S. 'Bio-based PET copolyesters from a D-mannitol-derived bicyclic diol'. Oral Communication at the Polymar 2013, Barcelona (Spain), 3rd-7th November 2013.

